

Durham E-Theses

Synthesis, structure and reactivity of [nido-CBH] ligands; group five and six metallocarborane complexes

Johnson, Andrew L.

How to cite:

Johnson, Andrew L. (2000) *Synthesis, structure and reactivity of [nido-CBH] ligands; group five and six metallocarborane complexes*, Durham theses, Durham University. Available at Durham E-Theses Online:
<http://etheses.dur.ac.uk/1162/>

Use policy

The full-text may be used and/or reproduced, and given to third parties in any format or medium, without prior permission or charge, for personal research or study, educational, or not-for-profit purposes provided that:

- a full bibliographic reference is made to the original source
- a [link](#) is made to the metadata record in Durham E-Theses
- the full-text is not changed in any way

The full-text must not be sold in any format or medium without the formal permission of the copyright holders.

Please consult the [full Durham E-Theses policy](#) for further details.

Academic Support Office, Durham University, University Office, Old Elvet, Durham DH1 3HP
e-mail: e-theses.admin@dur.ac.uk Tel: +44 0191 334 6107
<http://etheses.dur.ac.uk>

Synthesis, Structure and Reactivity of
***[nido-C₂B₉H₁₁]* Ligands;**
Group Five and Six Metallocarborane
Complexes

by

Andrew L. Johnson, B.Sc. (Dunelm)

Hatfield College, University of Durham

19 JUL 2000

The copyright of this thesis rests
with the author. No quotation
from it should be published
without the written consent of the
author and information derived
from it should be acknowledged.



A thesis submitted in part fulfilment of the requirements for the degree of
Doctor of Philosophy at the University of Durham

October 1999

Statement of Copyright

The copyright of this thesis rests with the author. No quotation from it should be published without his prior consent and information derived from it should be acknowledged.

Declaration

The work described in this thesis was carried out at the University of Durham, Department of Chemistry, between September 1994 and August 1999. All the work is my own unless stated otherwise, and it has not been submitted previously for a degree at this or any other university.

Financial Support

The Engineering and Physical Science Research Council (EPSRC) and Kværner Process Technology are gratefully acknowledged for providing funding for the work described herein.

To my parents and my grandparents, without whom this would not have
been possible.

*“Thus, the task is, not so much to see what no one has yet seen;
but to think what nobody has yet thought, about that which everybody sees.”*

- Erwin Schrödinger 1887-1961

*"The most exciting phrase to hear in science, the one that heralds new
discoveries, is not "Eureka!", but "That's funny..."*

- ISAAC ASIMOV (1920-1992, Science Fiction Writer.)

“Our results are, in fact, our true intentions”.

ANON.

ABSTRACT

Synthesis, Structure and Reactivity of [*nido*-C₂B₉H₁₁] ligands; Group

Five and Six Metallacarborane Complexes

This thesis describes exploratory synthetic and structural studies into the coordination chemistry of [*nido*-C₂B₉H₁₁] ligands in early transition metal organometallic chemistry. The chemistry of both group five and group six dicarbollide complexes has been investigated. The principle objective in these studies was to increase understanding of the chemistry involved, and to draw comparisons with the chemistry of related complexes.

Chapter One highlights the electronic and structural aspects of the ligand systems in this thesis, drawing attention to the similarities between the dicarbollide ligand [*nido*-C₂B₉H₁₁] and other “ $1\sigma 2\pi$ ” ligand systems such as cyclopentadienyl and imido ligands. The chemistry of early transition metal metallocarborane chemistry is also reviewed.

Chapter Two describes the synthesis, characterisation and structure of a series of *nido*-“C₂B₉” clusters. The formation of the two acidic *nido*-carborane clusters [*ortho*-C₂B₉H₁₃] and [*para*-C₂B₉H₁₃], and their reactions with bases, to form salts of the anionic *nido* clusters [*ortho*-C₂B₉H₁₂]⁻ and [*para*-C₂B₉H₁₂]⁻ are described. The molecular structures of the resulting salts are also presented. The alkane elimination reaction between the *nido* cluster [NHMe₃][*ortho*-C₂B₉H₁₂] and dimethyl zinc gives the macropolyhedral dimer [(7,8-C₂B₉H₁₁)ZnNMe₃]₂. The molecular structure of this dimer is presented and shows an unprecedented bonding motif with a planar diamond shaped Zn₂B₂ ring at its core.

Chapter Three describes the reactions between the group five amide complexes [M(NMe₂)₅] (M = Nb or Ta) and acidic *nido* carborane clusters. Characterisation and molecular structures for the resulting *ortho*- *meta*- and *para*-dicarbollide *tris*-amide complexes, of general formula [M(NMe₂)₃(C₂B₉H₁₁)] is also presented. The reactivity of these new metallacarborane complexes is investigated. The complex [Ta(NMe₂)₃(*ortho*-C₂B₉H₁₁)] is found to react with both dipolar multiply bonded compounds such as acetonitrile and CO₂ as well as cyclohexyl *iso*-nitrile, and protic acids such as phenols and thiophenols.

Chapter Four concentrates on the chemistry of the tungsten (VI) system [W(N^tBu)(NH^tBu)₂(C₂B₉H₁₁)] and its chemistry. The complex is formed by reacting the neutral *nido* carborane [*ortho*-C₂B₉H₁₃] with the tungsten complex [W(N^tBu)₂(NH^tBu)₂].

Focus is drawn to the relationship between this complex and its metallocene analogues. The tungsten dicarbollide complex reacts with both 2,6-dimethylphenol, to form $[\text{W}(\text{N}^t\text{Bu})(\text{NH}^t\text{Bu})(\text{OC}_6\text{H}_3\text{Me}_2)(\text{C}_2\text{B}_9\text{H}_{11})]$ and with water to form the oxo bridged species $[\{\text{W}(\text{N}^t\text{Bu})(\text{NH}^t\text{Bu})(\text{C}_2\text{B}_9\text{H}_{11})\}_2(\mu\text{-O})]$. The tungsten dicarbollide complex also undergoes an insertion with acetonitrile at room temperature to form the bis imido dicarbollide complex $[\text{W}(\text{N}^t\text{Bu})_2(\text{N}(\text{H})\text{CMeN}(\text{H})^t\text{Bu})(\text{C}_2\text{B}_9\text{H}_{11})]$.

Chapter Five gives experimental details and characterisation data for Chapter Two to Four.

Appendices list the data for X-ray structural determinations presented in this thesis.

Andrew Lee Johnson (October 1999)

Acknowledgements

Over the six years I have spent at Durham, I have been very lucky to work with many people to whom I owe a great deal. In particular I want to thank Andy Hughes and Ken Wade for giving me the opportunity to work with them. Both Ken and Andy have shown me great encouragement, and the enthusiasm that both of them have for chemistry (well most of the time anyway) has made working with them a pleasure. I have to give Andy special thanks for all of his help in the later stages of my time at Durham and for proof reading endless reams of verbal dribble.

I would also like to give a special thank-you to Judith Howard, who not only allowed me to infiltrate her group, but was able to provide me with a home at “Mother Howard’s Inn for the Poor and Needy”.

I should also like to thank all my friends at Durham past and present, and as I am sure to miss people out I must make my apologies now, sorry!

Thanks to Andy Kingsley, Brian Bridgwater, Melanie Thompson, Lynn Boyd, Graham Robertson, Alli Jones, Pat Gemmal, Marky Roden, Janet Maloney, Jan Kelly, Tom Hibbert, Sarah Lamb, Simon Crabtree, Nicky Moore, James Banister, Claire Wilson, Andres Goeta, Judith Howard, Mike Leach, Charlie Broder, Wendy Busby, Mark O’Halloran, Andy Hughes, Mark Fox, John Malget, Aileen Martin, Derek Tyers, Mark Wyatt, Dima Yufit, Horst Puschmann, Stephanie Blair, John Cowan, Rhodri Thomas and Jacquie Burke.

I am indebted to “some” of the technical staff at the department of chemistry, but special thanks must go to Jimmy, Joe and Tom as well as Val, who I will miss especially on the last Friday of every month.

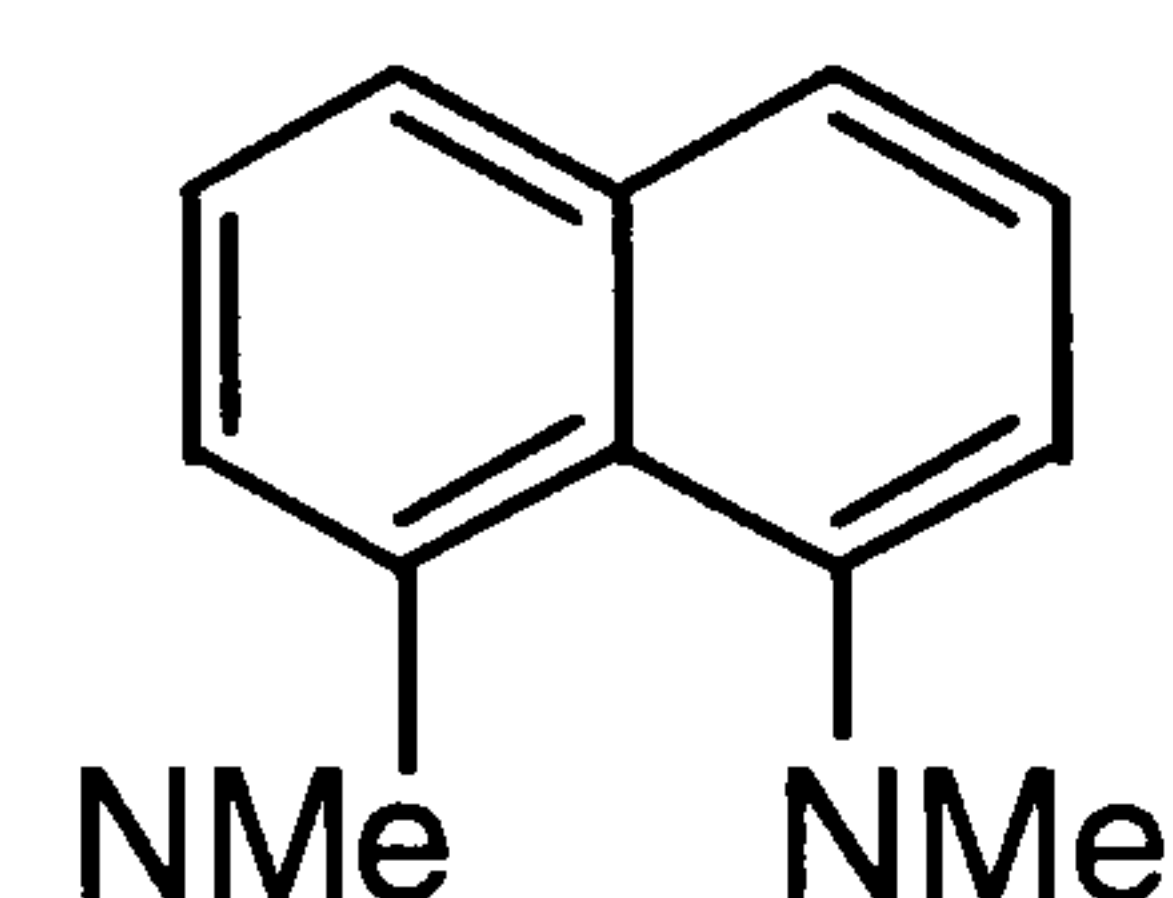
I have to give a big thank you to both Aileen Martin, who has diligently read all of this chapter in the hunt for “typos”, all for the reward of a bag of chocy balls, and Mark Fox, for all of his work and help in the lab.

I wish to thank Andy Kingsley and Jo Howson for being there when I’ve needed to whinge about my life, and for nodding and making sympathetic noises until I went away.

Finally I wish to thank my parents for their love support and encouragement.

ABBREVIATIONS

Ar	Aryl
AO	Atomic orbital
Bu	n-Butyl
^t Bu	tert-Butyl
CLF	Charged ligand formalism
Cp	Cyclopentadienyl
Cp*	Pentamethyl cyclopentadienyl
Cy	Cyclohexyl
DEPT	Distortionless enhancement by polarisation transfer
DMSO	Dimethyl sulphoxide
EHMO	Extended Hückel Molecular Orbital
Et	Ethyl
IR	Infra-red
L	General two-electron ligand
Me	Methyl
MO	Molecular Orbital
NLF	Neutral ligand formalism
NMR	Nuclear Magnetic Resonance
Ph	Phenyl
ⁱ Pr	iso-Propyl
Pr ⁿ	n-Propyl
PS	Proton sponge, 1,8-N,NN'N'-tetramethyl naphthalenediamine –
ppm	parts per million
THF	Tetrahydrofuran
TMSCl	Trimethyl silyl chloride
TMEDA	Tetremethylethylenediamine
TBDMS	<i>Tert</i> -butyldimethylsilyl
UV-vis	Electromagnetic radiation in the ultraviolet-visible region
X	General 1-electron ligand



KEY TO COMPOUND NUMBERING

- | | | | |
|----|------------------------------------------------------------------------------------------------------|----|-------------------------------------------------------------------------------------------------------------------------------------------------------------|
| 1 | <i>ortho</i> -C ₂ B ₁₀ H ₁₂ | 20 | [Ta(NMe ₂) ₃ (<i>para</i> -C ₂ B ₉ H ₁₁)] |
| 2 | <i>meta</i> -C ₂ B ₁₀ H ₁₂ | 21 | [Nb(O ₂ CNMe ₂) ₃ (<i>ortho</i> -C ₂ B ₉ H ₁₁)] |
| 3 | <i>para</i> -C ₂ B ₁₀ H ₁₂ | 22 | [Ta(O ₂ CNMe ₂) ₃ (<i>ortho</i> -C ₂ B ₉ H ₁₁)] |
| 4 | [<i>ortho</i> -C ₂ B ₉ H ₁₂] ⁻ | 23 | [Nb(S ₂ CNMe ₂) ₃ (<i>ortho</i> -C ₂ B ₉ H ₁₁)] |
| 5 | [<i>meta</i> -C ₂ B ₉ H ₁₂] ⁻ | 24 | [Ta(S ₂ CNMe ₂) ₃ (<i>ortho</i> -C ₂ B ₉ H ₁₁)] |
| 6 | [<i>para</i> -C ₂ B ₉ H ₁₂] ⁻ | 25 | [Ta(NC(Me)NMe ₂) ₃ (<i>ortho</i> -C ₂ B ₉ H ₁₁)] |
| 7 | [<i>ortho</i> -C ₂ B ₉ H ₁₃] | 26 | [Ta(NC(C ₆ H ₅ F)NMe ₂) ₂ Cl(<i>ortho</i> -C ₂ B ₉ H ₁₁)] |
| 8 | [<i>closo</i> -C ₂ B ₉ H ₁₁] | 27 | [Ta(NMe ₂) ₂ (Me ₂ NC-N(C ₆ H ₁₁))(<i>ortho</i> -C ₂ B ₉ H ₁₁)] |
| 9 | [<i>para</i> -C ₂ B ₉ H ₁₃] | 28 | [Ta(OC ₆ H ₃ Me ₂) ₃ (<i>ortho</i> -C ₂ B ₉ H ₁₁)] |
| 10 | [<i>ortho</i> -C ₂ B ₉ H ₁₁] ²⁻ | 29 | [Ta(SC ₆ H ₅) ₄ (10-Me ₂ NH- <i>ortho</i> -C ₂ B ₉ H ₁₀)] |
| 11 | [<i>meta</i> -C ₂ B ₉ H ₁₁] ²⁻ | 30 | [W(N ^t Bu) ₂ (NH ^t Bu) ₂] |
| 12 | [<i>para</i> -C ₂ B ₉ H ₁₁] ²⁻ | 31 | [W(N ^t Bu)(NH ^t Bu) ₂ (<i>ortho</i> -C ₂ B ₉ H ₁₁)] |
| 13 | [(<i>ortho</i> -C ₂ B ₉ H ₁₁)ZnNMe ₃] ₂ | 32 | [{W(N ^t Bu)(NH ^t Bu)(<i>ortho</i> -C ₂ B ₉ H ₁₁)} ₂ (μ-O)] |
| 14 | [Nb(NMe ₂) ₅] | 33 | [W(N ^t Bu)(NH ^t Bu)(OC ₆ H ₃ Me ₂)(<i>ortho</i> -C ₂ B ₉ H ₁₁)] |
| 15 | [Ta(NMe ₂) ₅] | 34 | [W(N ^t Bu)(NH ^t Bu)Cl(<i>ortho</i> -C ₂ B ₉ H ₁₁)] |
| 16 | [Nb(NMe ₂) ₃ (<i>ortho</i> -C ₂ B ₉ H ₁₁)] | 35 | [W(N ^t Bu) ₂ (N(H)CMeN(H) ^t Bu)(<i>ortho</i> -C ₂ B ₉ H ₁₁)] |
| 17 | [Ta(NMe ₂) ₃ (<i>ortho</i> -C ₂ B ₉ H ₁₁)] | | |
| 18 | [Nb(NMe ₂) ₃ (<i>meta</i> -C ₂ B ₉ H ₁₁)] | | |
| 19 | [[Ta(NMe ₂) ₃ (<i>meta</i> -C ₂ B ₉ H ₁₁)] | | |

TABLE OF CONTENTS

CHAPTER ONE

INTRODUCTION

1.1 Introduction and Historical Background	2
1.2 Carboranes.	2
<i>1.2.1 The Synthesis of Icosahedral Ortho-Carboranes</i>	<i>4</i>
<i>1.2.2 Bonding in Carboranes; Electron Deficient Clusters.</i>	<i>6</i>
<i>1.2.3 Deboronation of Carboranes</i>	<i>8</i>
1.3 Electronic and Structural Aspects of Metal Ligand Bonding.	11
<i>1.3.1 Imido Ligands, [NR].</i>	<i>11</i>
<i>1.3.1.1 Delocalised Bonding Approach</i>	<i>12</i>
<i>1.3.1.2 Nucleophilic Vs Electrophilic; A Rationale to Imido Reactivity</i>	<i>13</i>
<i>1.3.2 Alkoxo Ligands, [OR].</i>	<i>14</i>
<i>1.3.3 Metal Amido Ligands, [NR₂].</i>	<i>15</i>
<i>1.3.4 The Isolobal Analogy Between η^5-Cyclopentadienyl and Imido Ligands.</i>	<i>16</i>
<i>1.3.5 Carboranes as Ligands: Comparison with Other $1\sigma 2\pi$ Ligands.</i>	<i>20</i>
1.4 Metallocarboranes of the Early Transition Metal and f-Block Elements	23
<i>1.4.1 Metallocarboranes Containing Group 3 and Lanthanide Group Metals.</i>	<i>23</i>
<i>1.4.2 Metallocarboranes Containing Actinide Group Metals.</i>	<i>29</i>
<i>1.4.3 Metallocarboranes Containing Group 4 Transition Metals.</i>	<i>31</i>
<i>1.4.4 Metallocarboranes Containing Group 5 Transition Metals.</i>	<i>37</i>
<i>1.4.5 Metallocarboranes Containing Group 6 Transition Metals.</i>	<i>40</i>
<i>1.4.7 Metallocarboranes Containing Group 7 Transition Metals.</i>	<i>44</i>
1.5 References for Chapter One.	48

CHAPTER TWO

SYNTHESIS, STRUCTURE AND CHARACTERISATION OF *NIDO*- “C₂B₉” CLUSTERS

2.1 Introduction	57
2.2 Ortho-, Meta- and Para-C₂B₉ systems.	59
2.2.1 <i>Ortho</i> [C ₂ B ₉ H ₁₃]	59
2.2.2 <i>Meta</i> [C ₂ B ₉ H ₁₃]	61
2.2.3 <i>Para</i> -[C ₂ B ₉ H ₁₃]	63
2.3 Reaction of the carborane acids [<i>ortho</i>-C₂B₉H₁₃] and [<i>para</i>-C₂B₉H₁₃] with bases; structures of the [C₂B₉H₁₂]⁻ anion.	64
2.3.1 <i>Salts of [ortho-C₂B₉H₁₂]⁻</i>	64
2.3.2 <i>Salts of [para-C₂B₉H₁₂]⁻</i>	70
2.3.3 <i>Reactions With Basic Metal Alkyl Complexes.</i>	73
2.4 Summary	78
2.5 References for Chapter Two	80

CHAPTER THREE

DICARBOLLIDE COMPLEXES OF GROUP FIVE METALS; SYNTHESIS, STRUCTURE AND REACTIVITY

3.1 Introduction	87
3.1.1 <i>Metal Amide Complexes; Synthesis, Structure and Reactivity.</i>	88
3.1.1.1 <i>Transmetalation</i>	89

3.1.1.2 Elimination of Amine Hydrohalide	90
3.1.1.3 Transamination	91
3.1.1.4 Reactions of Metal Amides; Insertion Reactions	92
3.1.1.5 Reactions of Metal Amides; Reactions with Protic Acids.	95
3.1.2 Metal Amide Complexes of the Vanadium Group	97
3.2 Group 5 Metallocarborane Tris-Amide complexes.	98
3.2.1 Synthesis and Characterisation of Group 5 Dicarbolide Tris-Amide Complexes	98
3.2.2 Π Bonding in $[M(nido-C_2B_9H_{11})(NMe_2)_3]$ Complexes	108
3.3 Reactions of Group 5 Metallocarborane Tris-Amide complexes	111
3.3.1 Insertion of CO_2 and CS_2 into $[M(C_2B_9H_{11})(NMe_2)_3]$ Complexes	111
3.3.2 Insertion of Nitriles and Isonitriles into <i>ortho</i> - $[Ta(nido-C_2B_9H_{11})(NMe_2)_3]$ Complexes	118
3.3.3 Reactions of <i>ortho</i> - $[Ta(C_2B_9H_{11})(NMe_2)_3]$ with Protic Acids.	126
3.4 Summary	137
3.5 References for Chapter Three	138

CHAPTER FOUR

DICARBOLIDE COMPLEXES OF TUNGSTEN (VI); SYNTHESIS, STRUCTURE AND REACTIVITY

4.1 Introduction	150
4.2 Imido Complexes; General Introduction	151
4.2.1 ^{13}C NMR Spectroscopy	153
4.3 Tungsten (VI) Imido Dicarbolide Complexes.	154
4.3.1 Synthesis of $[W(N^iBu)(NH^iBu)_2(ortho-C_2B_9H_{11})]$	156

4.3.2 Reactions of $[W(N^tBu)(NH^tBu)_2(ortho-C_2B_9H_{11})]$ with Protic Acids.	162
4.3.3 Insertion Reactions with $[W(N^tBu)(NH^tBu)_2(ortho-C_2B_9H_{11})]$.	171
4.4 Summary	177
4.5 References for Chapter Four	178

CHAPTER FIVE

EXPERIMENTAL DETAILS

5.1 General Experimental Techniques	185
5.2 Experimental Details to Chapter Two	188
5.2.1 Synthesis of $[7,8-C_2B_9H_{13}]$, (7).	188
5.2.2 Acidification of $7,9-C_2B_9H_{12}^-$.	189
5.2.3 Synthesis of $[2,9-C_2B_9H_{13}]$, (9).	189
5.2.4 Synthesis of the Protonated Proton Sponge Salt of $7,8-C_2B_9H_{12}^-$, (4a).	190
5.2.5 Synthesis of the Triphenylmethyl Phosphonium Salt of $7,8-C_2B_9H_{12}^-$, (4b).	191
5.2.6 Synthesis of the Protonated Proton Sponge Salt of $2,9-C_2B_9H_{12}^-$, (9a).	192
5.2.7 Synthesis of $[{(nido-7,8-C_2B_9H_{11})ZnNMe_3}_2]$, (13).	193
5.3 Experimental Details to Chapter Three	194
5.3.1 Synthesis of $[3-Nb(NMe_2)_3(1,2-C_2B_9H_{11})]$, (16).	194
5.3.2 Synthesis of $[3-Ta(NMe_2)_3(1,2-C_2B_9H_{11})]$, (17).	195
5.3.3 Synthesis of $[2-Nb(NMe_2)_3(1,7-C_2B_9H_{11})]$, (18).	196
5.3.4 Synthesis of $[2-Ta(NMe_2)_3(1,7-C_2B_9H_{11})]$, (19).	197
5.3.5 Synthesis of $[2-Ta(NMe_2)_3(1,12-C_2B_9H_{11})]$, (20).	198
5.3.6 Synthesis of $[3-Nb(O_2C-NMe_2)_3(1,2-C_2B_9H_{11})]$, (21).	199
5.3.7 Synthesis of $[3-Ta(O_2C-NMe_2)_3(1,2-C_2B_9H_{11})]$, (22).	200

5.3.8 Synthesis of $[3\text{-Nb}(\text{S}_2\text{C-NMe}_2)_3(1,2\text{-C}_2\text{B}_9\text{H}_{11})]$, (23).	201
5.3.9 Synthesis of $[3\text{-Ta}(\text{S}_2\text{C-NMe}_2)_3(1,2\text{-C}_2\text{B}_9\text{H}_{11})]$, (24).	202
5.3.10 Synthesis of $[3\text{-Ta}(\text{NC}(\text{Me})\text{NMe}_2)_3(1,2\text{-C}_2\text{B}_9\text{H}_{11})]$, (25).	203
5.3.11 Synthesis of $[3\text{-Ta}(\text{NC}(\text{C}_6\text{H}_4\text{F})\text{NMe}_2)_2\text{Cl}(1,2\text{-C}_2\text{B}_9\text{H}_{11})]$, (26).	204
5.3.12 Synthesis of $[3\text{-Ta}(\text{NMe}_2)_2(\eta^2\text{-(Me}_2\text{N)C=N(C}_6\text{H}_{11})}(1,2\text{-C}_2\text{B}_9\text{H}_{11})]$, (27).	206
5.3.13 Synthesis of $[3\text{-Ta}(\text{OC}_6\text{H}_3\text{-2,6-Me}_2)_3(1,2\text{-C}_2\text{B}_9\text{H}_{11})]$, (28).	207
5.3.14 Synthesis of $[3\text{-Ta}(\text{SC}_6\text{H}_5)_4(9\text{-NHMe}_2\text{-1,2-C}_2\text{B}_9\text{H}_{10})]$, (29).	208
5.4 Experimental Details to Chapter Four	209
5.4.1 Synthesis of $[3\text{-W}(\text{N}^t\text{Bu})(\text{NH}^t\text{Bu})_2(1,2\text{-C}_2\text{B}_9\text{H}_{11})]$, (31).	209
5.4.2 Synthesis of $3,1,2\text{-}[\{3\text{-W}(\text{N}^t\text{Bu})(\text{NH}^t\text{Bu})(1,2\text{-C}_2\text{B}_9\text{H}_{11})\}_2(\mu\text{-O})]$, (32).	210
5.4.3 Synthesis of $[3\text{-W}(\text{N}^t\text{Bu})(\text{NH}^t\text{Bu})(\text{OC}_6\text{H}_3\text{Me}_2)(1,2\text{-C}_2\text{B}_9\text{H}_{11})]$, (33).	211
5.4.4 Synthesis of $[3\text{-W}(\text{N}^t\text{Bu})(\text{NH}^t\text{Bu})\text{Cl}(1,2\text{-C}_2\text{B}_9\text{H}_{11})]$, (34).	213
5.4.5 Synthesis of $[\text{W}(\text{N}^t\text{Bu})_2(\text{N}(\text{H})\text{C}(\text{CH}_3)\text{NH}^t\text{Bu})(1,2\text{-C}_2\text{B}_9\text{H}_{11})]$, (35).	214
5.5 References for Chapter 5	215

APPENDIX A

CRYSTAL DATA

A1 Crystal data for $[1,8\text{-(N(CH}_3)_2)(\text{NH(CH}_3)_2\text{C}_{10}\text{H}_8)][7,8\text{-C}_2\text{B}_9\text{H}_{12}]$; (4a).	218
A2 Crystal data for $[(\text{C}_6\text{H}_5)_3\text{PCH}_3][7,8\text{-C}_2\text{B}_9\text{H}_{12}]$; (4b).	225
A3 Crystal data for $[1,8\text{-(N(CH}_3)_2)(\text{NH(CH}_3)_2\text{C}_{10}\text{H}_8)][2,9\text{-C}_2\text{B}_9\text{H}_{12}]$; (6a).	232
A4 Crystal data for $[\{(7,8\text{-C}_2\text{B}_9\text{H}_{12})\text{ZnN(CH}_3)_3\}_2]:(\text{C}_7\text{H}_8)_{1.5}$; (13).	239
A5 Crystal data for $[3\text{-Nb}(\text{NMe}_2)_3(1,2\text{-C}_2\text{B}_9\text{H}_{11})]$; (16).	248

<i>A6 Crystal data for [3-Ta(NMe₂)₃(1,2-C₂B₉H₁₁)] ; (17).</i>	255
<i>A7 Crystal data for [2-Ta(NMe₂)₃(1,12-C₂B₉H₁₁)] ; (20).</i>	262
<i>A8 Crystal data for [3-Ta(O₂CNMe₂)₃(1,2-C₂B₉H₁₁)] : 1/2 C₇H₈ ; (22).</i>	268
<i>A9 Crystal data for [3-Nb(S₂CNMe₂)₃(1,2-C₂B₉H₁₁)] : CD₂Cl₂ ; (23).</i>	275
<i>A10 Crystal data for [3-Ta(N=C(C₆H₄F)NMe₂)₂Cl(1,2-C₂B₉H₁₁)] : 2CCl₂H₂ ; (26).</i>	282
<i>A11 Crystal data for [3-Ta(OC₆H₃-Me₂-2,6)₃(1,2-C₂B₉H₁₁)] ; (28).</i>	289
<i>A12 Crystal data for [3-Ta(SC₆H₅)₄(9-NHMe₂-1,2-C₂B₉H₁₀)] ; (29).</i>	300
<i>A13 Crystal data for [3-W(NC₄H₉)(NHC₄H₉)₂(1,2-C₂B₉H₁₁)] : [C₇H₈] ; (31).</i>	308
<i>A14 Crystal data for [{3-W(NC₄H₉)(NHC₄H₉)(1,2-C₂B₉H₁₁)}₂(μ-O)] : [C₇H₈] ; (32).</i>	315
<i>A15 Crystal data for [3-W(NC₄H₉)(NHC₄H₉)(OC₆H₃-Me₂)(1,2-C₂B₉H₁₁)] ; (33).</i>	317
<i>A16 Crystal data for [3-W(NC₄H₉)₂(N(H)C(CH₃)NH(C₄H₉)(1,2-C₂B₉H₁₁)] ; (35).</i>	324

APPENDIX B

COURSES, LECTURES AND CONFERENCES ATTENDED

<i>B1 FIRST YEAR INTRODUCTION COURSES: OCTOBER 1996</i>	333
<i>B2 EXAMINED LECTURE COURSES: OCTOBER 1996 TO APRIL 1994</i>	333
<i>B3 RESERCH COLLOQUIA, SEMINARS AND LECTURES ORGANISED BY THE DEPARTMENT OF CHEMISTRY</i>	334
<i>B4 Conferences and Symposia Attended</i>	340

Chapter One

Introduction

1.1 Introduction and Historical Background

The boron hydrides and the polyboranes were amongst the first cluster compounds to be recognised as well as the first known family of “electron deficient”*, i.e. non-classical covalent molecules.¹ The work of Stock² on the boranes in the early years of the twentieth century, actually preceded by several decades the discovery of an extensive series of metal clusters, although it was not until the 1950’s that the cage-like stereochemistry of the boranes was revealed by X-ray crystallography. In more recent years it has been shown that the boranes, metal clusters and many organometallics have a close electronic and structural relationship, and much of the experimental and theoretical work on boron cage systems can be used to great advantage when trying to understand other classes of molecular polyhedra.³

Because of the similarities between boron clusters and metal clusters it is not surprising to find species that contain both metal atoms and boron atoms in a cluster geometry. The enormous variety of such molecular structures that have evolved since the first of these compounds were described in 1965 is truly remarkable.⁴ One class of these metal-boron cluster compounds which contain at least one skeletal carbon atom are known as metallocarboranes.

This thesis describes the synthesis, structure and chemistry of selected early transition metallocarborane systems. In preparation for this, this introduction will discuss some previously reported metallocarborane species, and in a more general survey note selected organometallic compounds that have relevance to subsequent chapters. When necessary the synthesis structure and bonding of these complexes will also be discussed.

1.2 Carboranes.

Before we can discuss the chemistry of metallocarboranes it is necessary to provide a brief survey of carboranes in general, as the structure of the parent *closo*-carboranes is often maintained in the analogous metallocarborane. This section is not intended to be a full review of carborane chemistry as this would be a formidable task.

* The term “electron deficient” is a purely historical classification and a relic of an era that looked upon multi-centre bonding as a mode of bonding that only occurred in only a few unstable molecules. It is a very misleading term as most boranes have a closed shell electronic structures, and very few of these show any noticeable tendency to acquire electrons.

The term carborane is used for mixed hydrides of boron and carbon where the polyhedral skeleton contains at least one carbon atom.⁵ A large number of different carboranes exist and their derivative chemistry is well documented.⁶

At present the most extensively studied carborane derivatives in synthesis are the C- and B-substituted derivatives of $[nido-2,3-C_2B_4H_6]^{2-}$, $[nido-7,8-C_2B_9H_{11}]^{2-}$, and to a lesser extent $[nido-7,9-C_2B_{10}H_{12}]^{2-}$ (Figure 1.1).

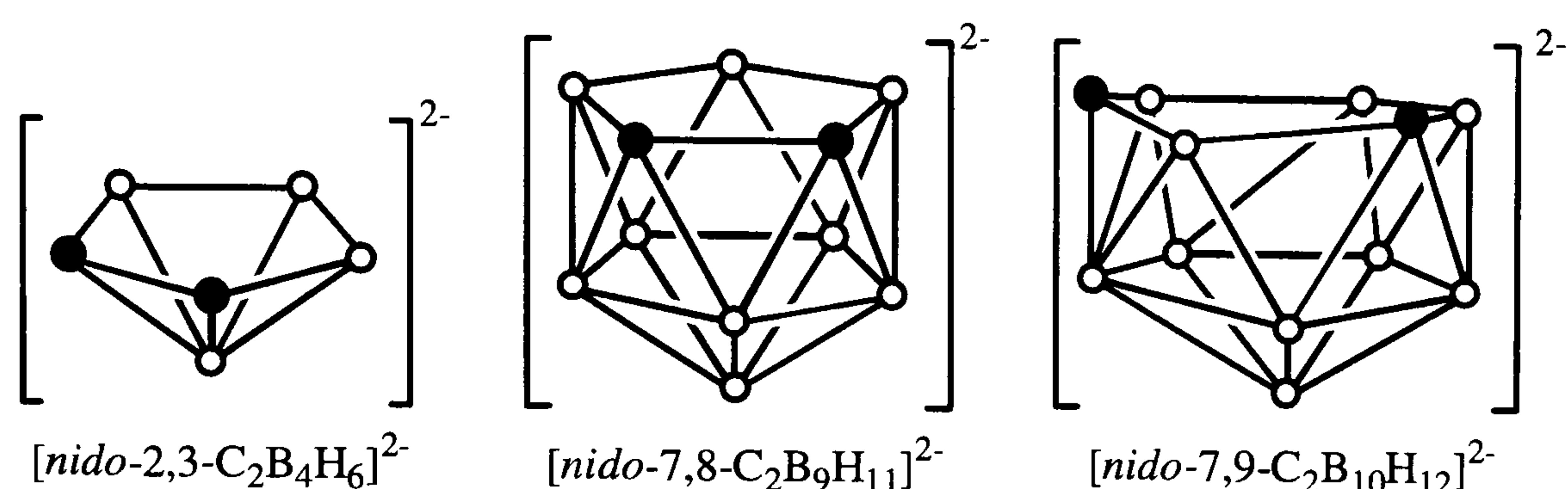


Figure 1.1 Structures of the $[nido-2,3C_2B_4H_6]^{2-}$, $[nido-7,8-C_2B_9H_{11}]^{2-}$ and the $[nido-7,9-C_2B_{10}H_{12}]^{2-}$ anions.

The work in this thesis is centred around the chemistry of the icosahedral dicarba-*closo*-decaboranes and their organometallic derivatives.

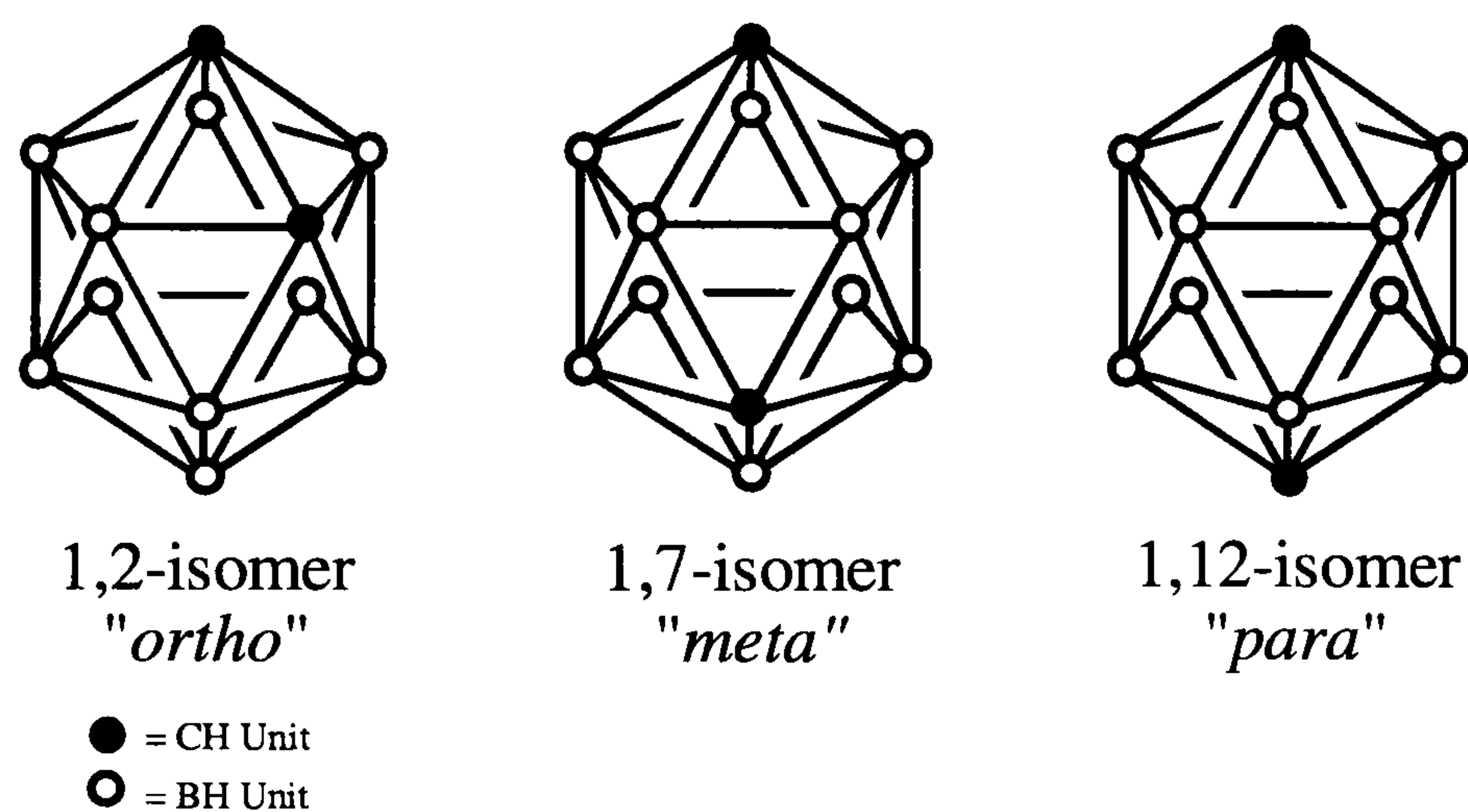


Figure 1.2 Isomers of $C_2B_{10}H_{12}$.

Three isomers of dicarba-*closo*-decaborane, $C_2B_{10}H_{12}$, exist (Figure 1.2): the 1,2-, 1,7- and 1,12- isomers, the numbers referring to the position of the carbons in the standard numbering scheme shown in Figure 1.3. The trivial names of the compounds are *ortho*-carborane, *meta*-carborane and *para*-carborane respectively.⁷

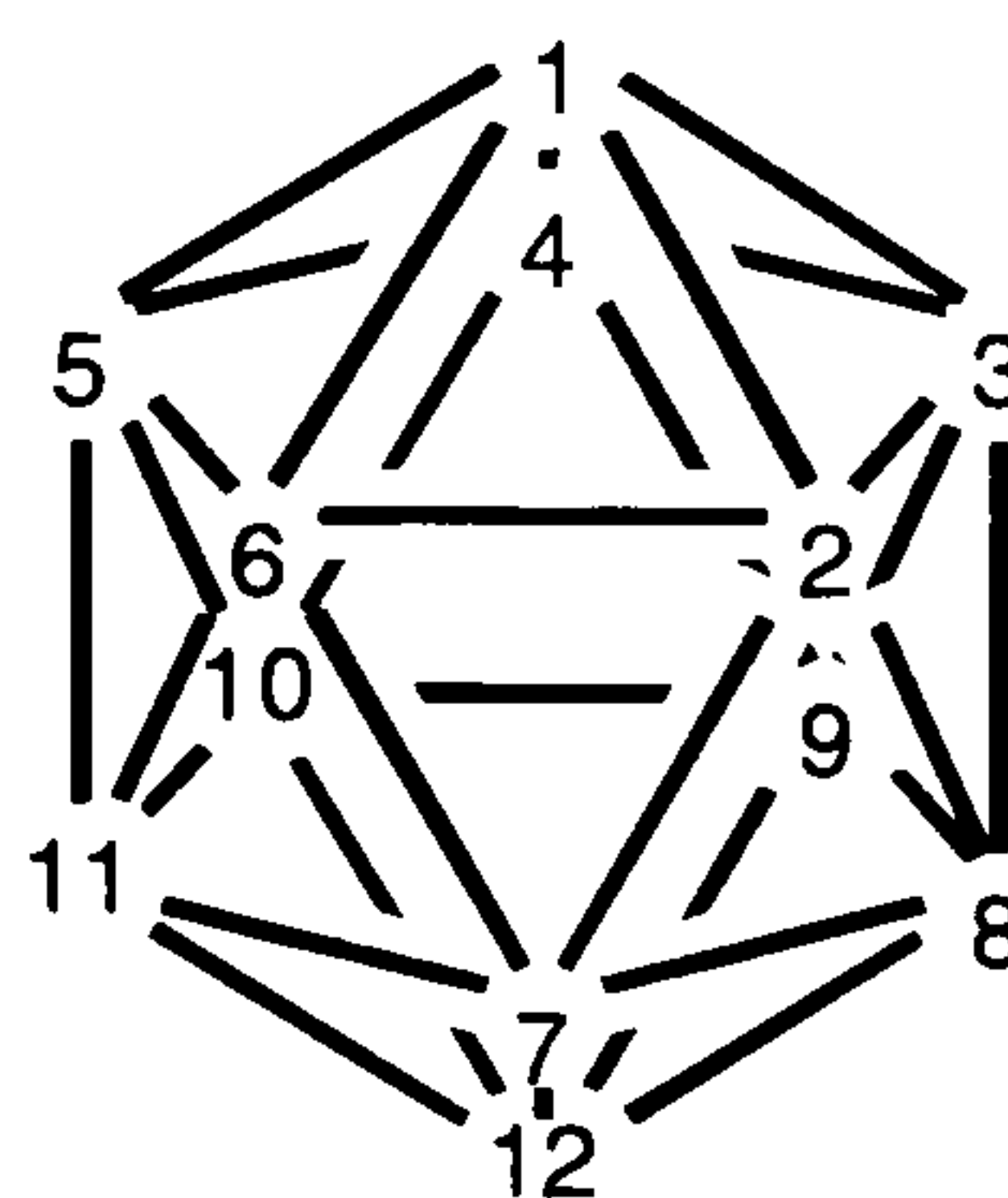
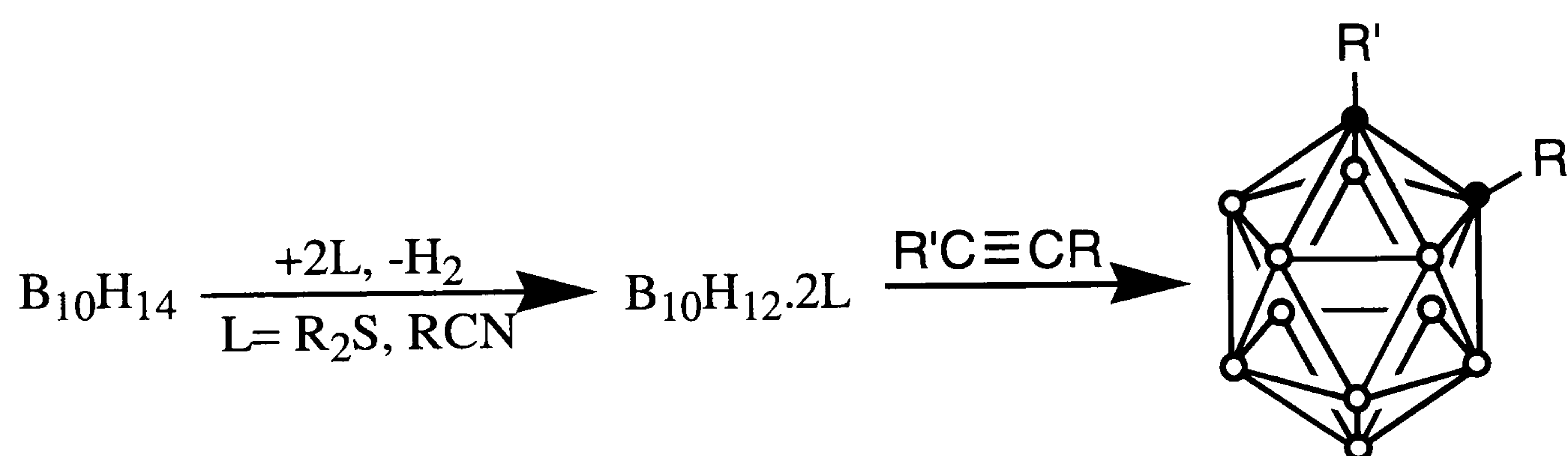


Figure 1.3 Standard Numbering Scheme

Decaborane(14), $B_{10}H_{14}$, is attacked by Lewis bases such as alkylamines, alkylsulfides, and acetonitrile, forming *bis*(ligand)derivatives of general formula $B_{10}H_{12}L_2$, which in turn react with ethyne to give the white *ortho*-carborane in high yields. The *meta*- and *para*- carboranes are synthesised from *ortho*-carborane by thermal isomerisation at 460°C and 620°C respectively.⁸ The formation of the *para*- isomer is accompanied by a large amount of decomposition resulting in a much higher cost for this isomer. This isomerisation (*ortho* → *meta* → *para*) occurs due to a tendency for similarly charged atoms (i.e. carbon) to adopt positions with the greatest separation in order to minimise the overall dipole effect,⁹ The *para*- isomer is of lower energy than the *meta*- isomer which in turn is lower than the *ortho*- isomer. The chemistry of these compounds is very similar in many ways to aromatic compounds such as benzene, and for this reason they are often given referred to as “*pseudo*-aromatic”. Unlike many of the smaller boranes, these clusters are stable to both oxygen and moisture, as well as being extremely stable to high temperatures. Because of its higher availability compared to the *meta*- and *para*- isomers, the *ortho*- isomer has received the most attention by synthetic chemists and a large number of derivatives are known.¹⁰

1.2.1 The Synthesis of Icosahedral Ortho-Carboranes

As stated above *ortho*-carborane is formed by the reaction of ethyne with Lewis base derivatives of decaborane(14). The use of functionalised ethynes, $RCCR'$, leads to the formation of substituted carboranes, $RCB_{10}H_{10}CR'$, although the number of substituents which are possible is limited to those that will tolerate the reaction conditions. (Equation 1.1).



Equation 1.1

Carborane alkyl and aryl compounds and the halogenated derivatives, e.g., CH_2X ($X = Br, Cl$), C_6H_5X ($X = F, Cl, Br$ and I) can be formed in this way and have been discussed elsewhere.⁵

Substituents can also be attached directly to the pre-formed cage. This procedure is often employed when the corresponding ethyne would either react with decaborane or the reaction results in low yields. The lithio derivatives, $\text{LiCCRB}_{10}\text{H}_{10}$, are most commonly used in such substitutions although magnesium and copper derivatives have been used in some cases.^{5,6} A strategy such as this relies on the acidity of the hydrogen atoms on the two carbon atoms. The acidic nature of these hydrogen atoms arise from the electron withdrawing effect of the cage. Treatment of ortho-carborane with n-butyl lithium removes this acidic proton to yield the lithio carborane.¹¹

In such metallation reactions, it is usual to employ a carborane with a substituent on the other carbon (e.g., phenyl or methyl) as this prevents unwanted disubstitution of the cage. TBDMS ($^t\text{BuMe}_2\text{Si}$) groups are sometimes used as protecting groups as they can be removed with ease to allow further substitution at the other carbon atom.¹² Disubstitution is readily achieved in the absence of such blocking groups. Figure 1.4 shows the structure of an isolated lithio carborane derivative.¹³

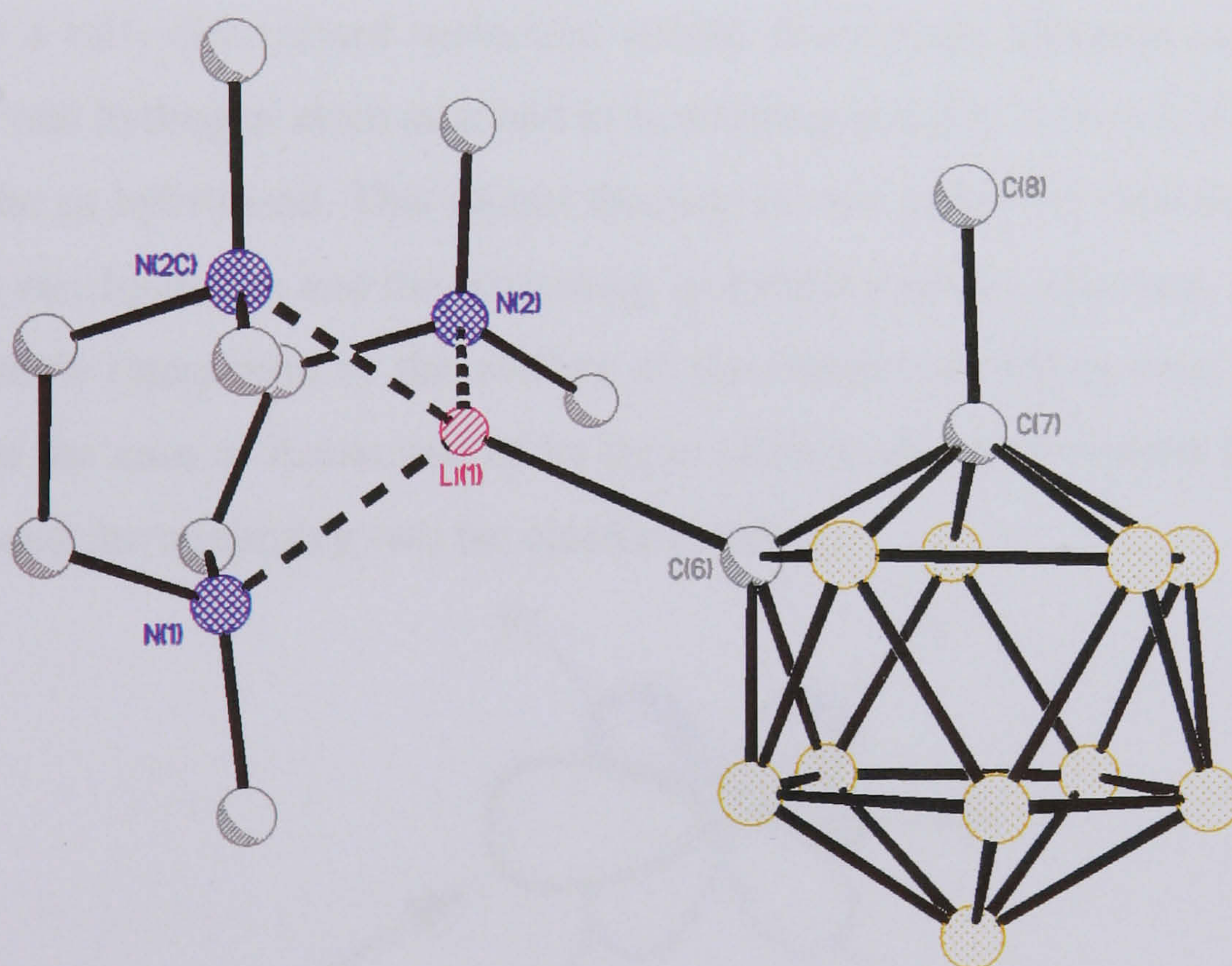


Figure 1.4 Molecular structure of the *mono* lithiated carborane complex $[(\text{Hexamethylenetriamine})\text{LiC}_2\text{B}_{10}\text{H}_{10}\text{Me}]$. Taken from ref. 13 (hydrogen atoms have been omitted for clarity).

The presence of a substituent on both carbon atoms is often an advantage for the characterisation of such carboranes by X-ray diffraction. Since both boron and carbon are adjacent elements, their number of electrons differs only by one, causing them to have similar X-ray scattering abilities, often leading to difficulties in distinguishing between BH and CH environments.

1.2.2 Bonding in Carboranes; Electron Deficient Clusters.

The term “electron deficient”, in this context, is used to describe situations in which electron counting reveals that there are too few electrons to allow the compound to be described in terms of the classical 2-centre 2-electron (2c2e) bond description.¹⁴ The atoms in such compounds aggregate and cluster to make best use of the available electrons with an electron pair being shared between more than two atoms, hence the term cluster.

The concept of the 3-centre 2-electron (3c2e) BHB bond was introduced by Longuet-Higgins¹⁵ to rationalise the bridged structure of diborane, and was later extended by Lipscomb to 3c2e BBB bonds. These concepts are used extensively to describe the bonding in the series of higher boranes in terms of 3c2e BBB and BHB bonds, as well as 2c2e BH and BB bonds.

The bonding in larger clusters such as $B_{12}H_{12}^{2-}$ can be described in terms of these localised bonds, but, as there are often a large number of canonical forms,¹ the bonding is better represented by a fully delocalised molecular orbital description. Because each boron atom in the cluster has one hydrogen atom attached to it, pointing radially outward, the boron atoms are considered to be *sp* hybridised. This means that one of two *sp*-hybrid orbitals is being used for bonding to the *exo*-hydrogen and the remaining *sp* hybrid (radial to the cage, pointing inwards) and two p orbitals (tangential to the surface of the cluster) are being used for cage bonding (Figure 1.5). In the case of boron one of its three valence electrons is used for bonding to the *exo*-hydrogen and the remaining two for cluster bonding.

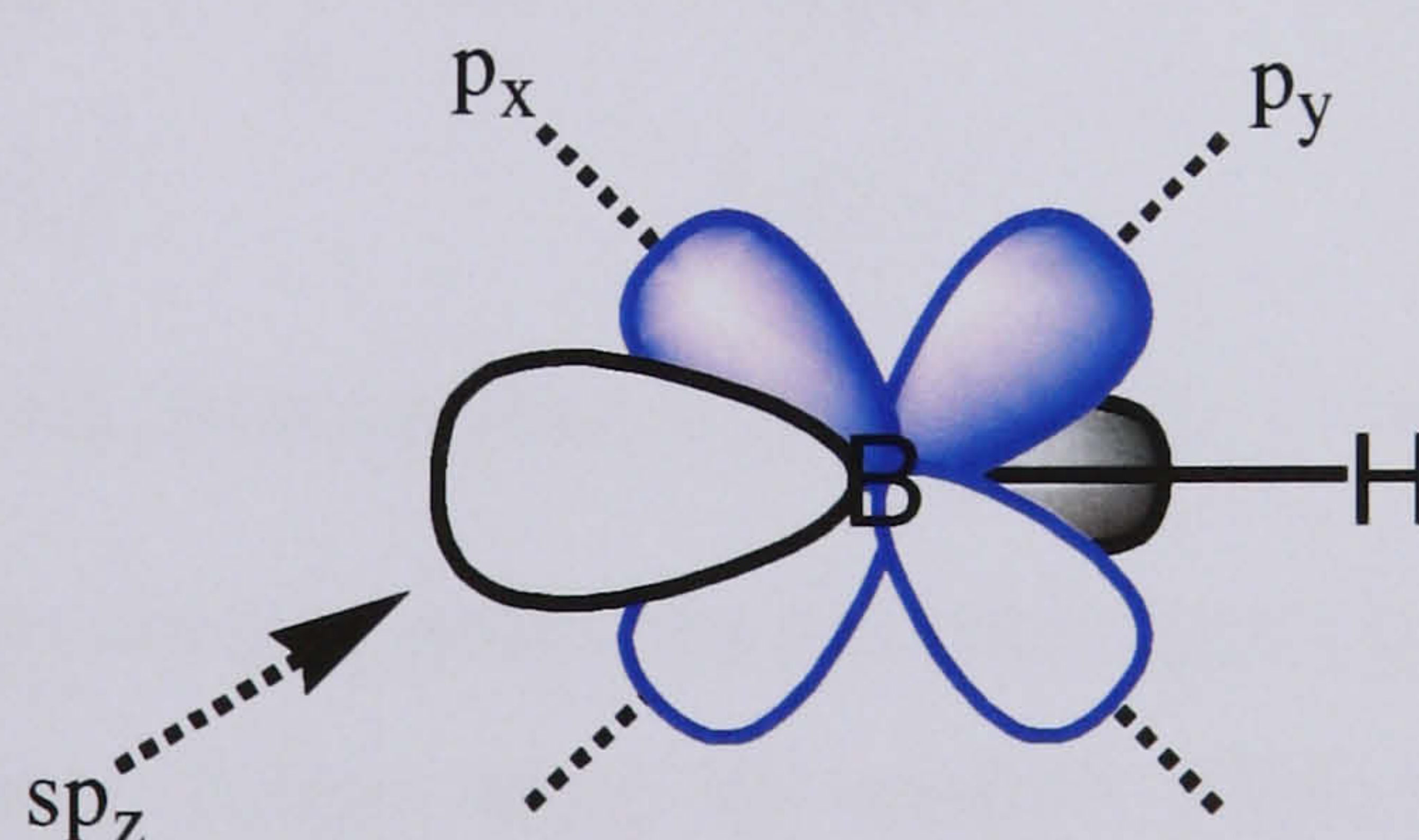


Figure 1.5 Tangential and Radial Orbitals of a BH cluster unit used for skeletal bonding.

The structures of such compounds can be rationalised in terms of the number of electrons involved in bonding the cluster's skeleton together. The atoms of the cluster are considered to occupy the vertices of a polyhedron with triangular faces. The number of vertices of the polyhedron will be one less than the total number of electron pairs used in the cluster bonding.^{3,16} This results in a cluster in which all the bonding MO's are filled.

e.g. $B_{12}H_{12}^{2-}$

12 x BH	= 12 x 2e ⁻	= 24e ⁻
Negative charge	= 2e ⁻	= 2e ⁻
Total skeletal electrons	= 26e ⁻	= 13e ⁻ pairs \Rightarrow 12 vertices

Hence $B_{12}H_{12}^{2-}$ has the structure of a twelve-vertex polyhedron, an icosahedron, with all vertices being occupied. This argument was originally used in reverse to show that an icosahedral cluster would require 13 filled MO's.¹⁷

As a consequence of the dependence of structure on the number of skeletal electrons available, if a vertex atom is removed from the cluster the structure will remain equivalent *if the number of skeletal electrons contributed by that vertex atom to the cluster bonding remain associated with the cluster*. Hence the clusters $B_{11}H_{11}^{4-}$ and $B_{10}H_{10}^{6-}$, can be considered to be derived from $B_{12}H_{12}^{2-}$ by the removal of $\{BH^{2+}\}$ units, both have 13 skeletal electron pairs and are therefore both based on the icosahedron with one and two vertices removed respectively (Figure 1.6). Clusters in which all the vertices are occupied are termed *closo*- (Greek meaning 'cage like'), those with one vertex unoccupied *nido*- ('net like') and those with two unoccupied *arachno*- ('web like').

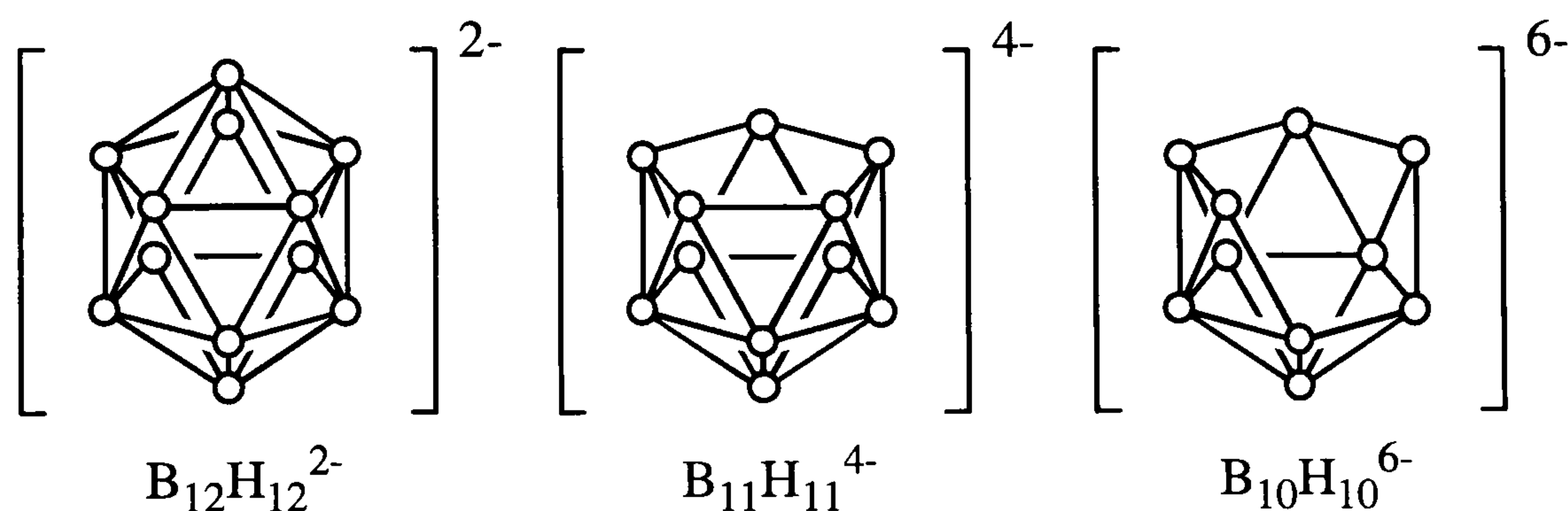


Figure 1.6 Structures of $B_{12}H_{12}^{2-}$, $B_{11}H_{11}^{4-}$ and $B_{10}H_{10}^{6-}$

By using the same principles we can retain the structure (and therefore the number of skeletal electron pairs) by replacing a vertex atom by another atom *providing that the number of skeletal electron pairs stays the same*. For example a BH^- (which supplies 3 electrons to the cage) unit can be replaced by an *iso*-lobal and *iso*-electronic CH (also supplying 3 electrons) (or in general a CR unit) with retention of the icosahedral structure.¹⁸ Hence $C_2B_{10}H_{12}$ has the same structure based on an icosahedron as $B_{12}H_{12}^{2-}$. These conclusions are clearly set out in Wade's rules.^{3,16,19}

With this in mind it is not a massive step to consider metal fragments that can supply the same number of electrons to the cluster being incorporated into the cluster framework. Like a BH

unit (supplying 2 electrons) a metal unit such as $M(CO)_3$ or $M'(\eta^5-C_5H_5)$ (where $M = Fe, Ru$ and Os and $M' = Co, Rh$ and Ir) can supply a pair of electrons and a set of three atomic orbitals of suitable symmetry for use in cluster bonding (Figure 1.7).²⁰

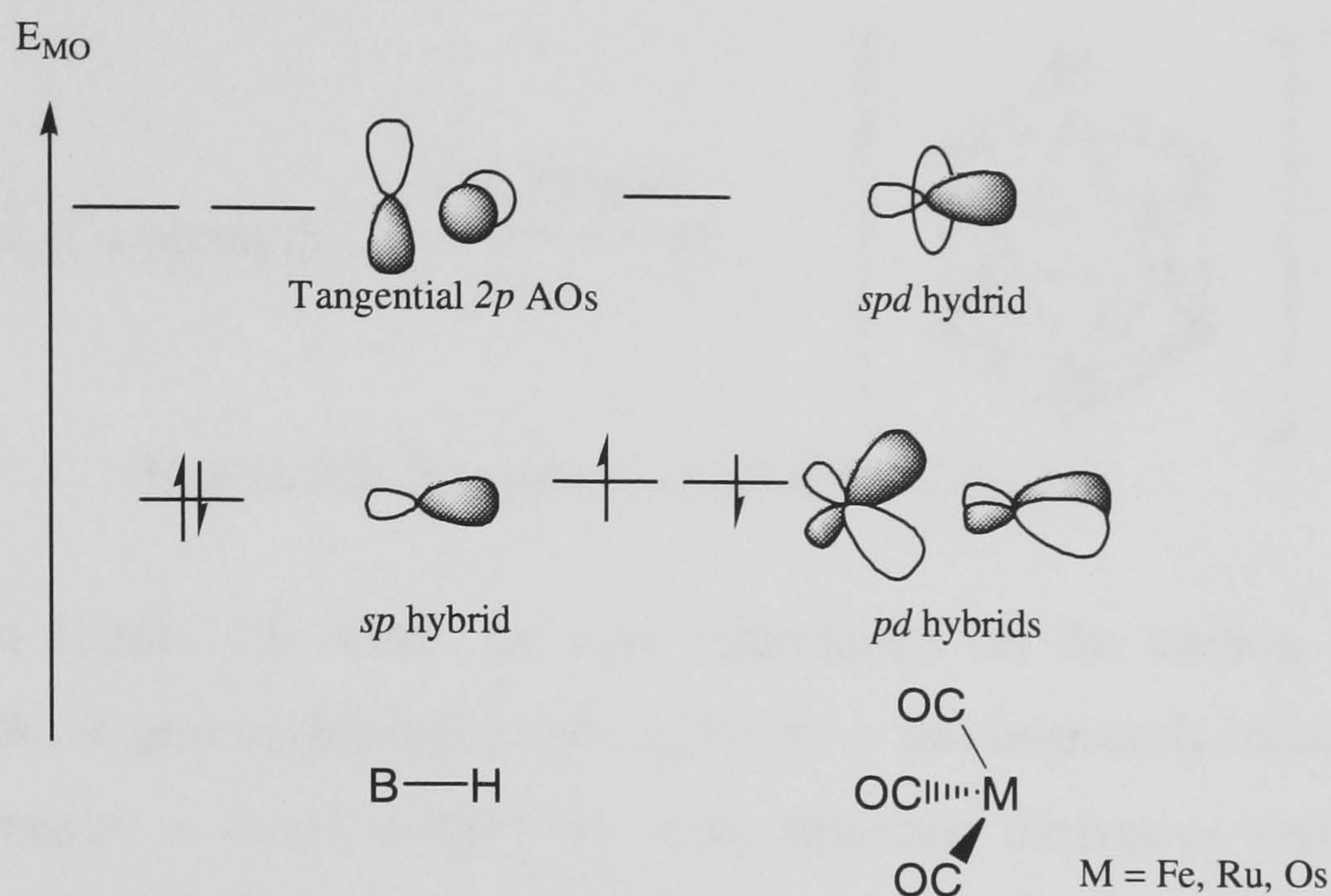


Figure 1.7 Comparison of the MO's of $[BH]^-$ and C_{3v} $[M(CO)_3]$ fragments ($M =$ group 8 metals). The fragments are *iso*-lobal because the number, symmetries and approximate energies of the orbitals are equal, and each set contains the same number of electrons. The order of MO's does not influence the bonding capacity of the fragment.

Such units are not rigorously *iso*-electronic with BH units (or CH^+ units in carboranes) but they are *iso*-lobal even if they do have considerable d character.²¹ For example we can see below that for the metallocarborane $[(C_2B_9H_{11})Fe(CO)_3]$, the $Fe(CO)_3$ unit replaces a BH unit in the parent carborane, $C_2B_{10}H_{12}$.

e.g. $[(C_2B_9H_{11})Fe(CO)_3]$

9 x BH	= 9 x $2e^-$	= $18e^-$
2 x CH	= 2 x $3e^-$	= $6e^-$
1 x $Fe(CO)_3$	= 1 x $2e^-$	= $2e^-$
Total skeletal electrons		= $26e^- = 13e^-$ pairs \Rightarrow 12 vertices

1.2.3 Deboronation of Carboranes

As mentioned earlier, the neutral *closo*-carboranes are far more stable than their borane analogues, for example they resist attack by strong acids. However, strong bases and strong nucleophiles may attack carboranes leading to degradation of the cluster.²² The selective

degradation of *ortho*-C₂B₁₀H₁₂ is achieved by using alcoholic base, leading to the formation of [*nido*-7,8-C₂B₉H₁₂]⁻ salts.²³ The reaction is selective due to the enhanced electrophilicity of the boron atoms adjacent to the two carbon atoms (Figure 1.8).

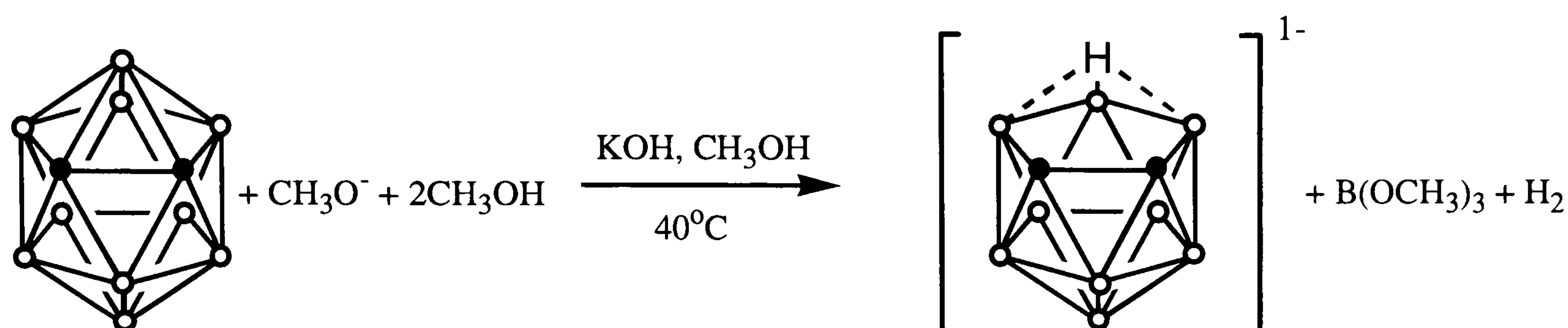


Figure 1.8 Deboronation of *ortho*-C₂B₁₀H₁₂.

As can be seen in Figure 1.9 when the two substituents on the carbon atoms are non-equivalent, although the parent *di*-substituted carborane is not inherently chiral (unless one of the substituents contains a chiral centre) the *nido*-carborane derivative can be one of two enantiomers, the product of the reaction usually being a racemic mixture.

The *meta*- and *para*-carboranes can also be deboronated, resulting in the formation of the [*nido*-1,7-C₂B₉H₁₂]⁻ and [*nido*-1,12-C₂B₉H₁₂]⁻ salts respectively. Figure 1.10 shows the numbering scheme for the resulting *nido*-carboranes. The exact location of the twelfth hydrogen atom in these anions is discussed in chapter 2 of this thesis along with the chemistry of these species.

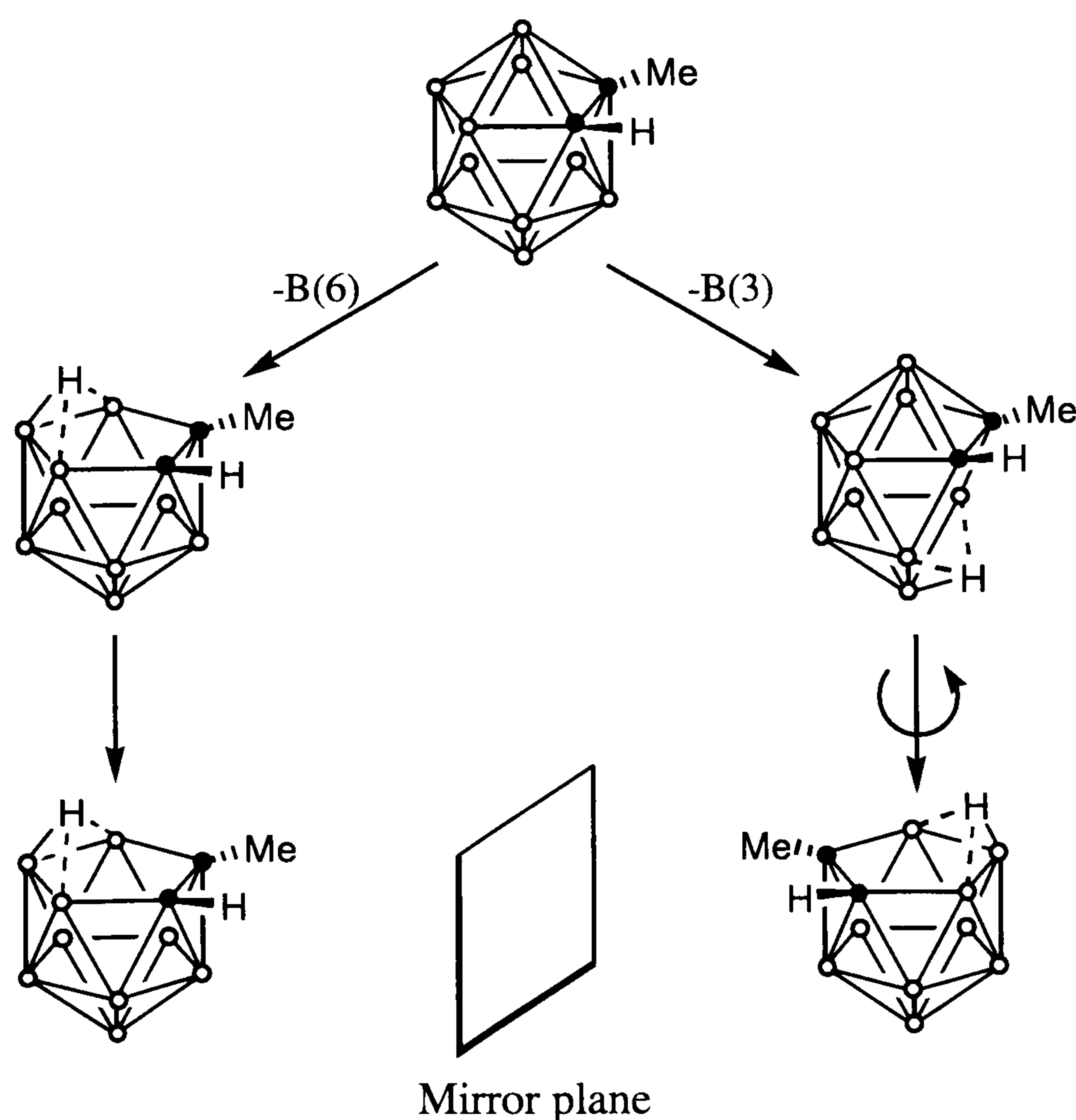


Figure 1.9 Scheme showing stereoisomerism in *nido*- substituted C₂B₉H₁₂⁻ ions.

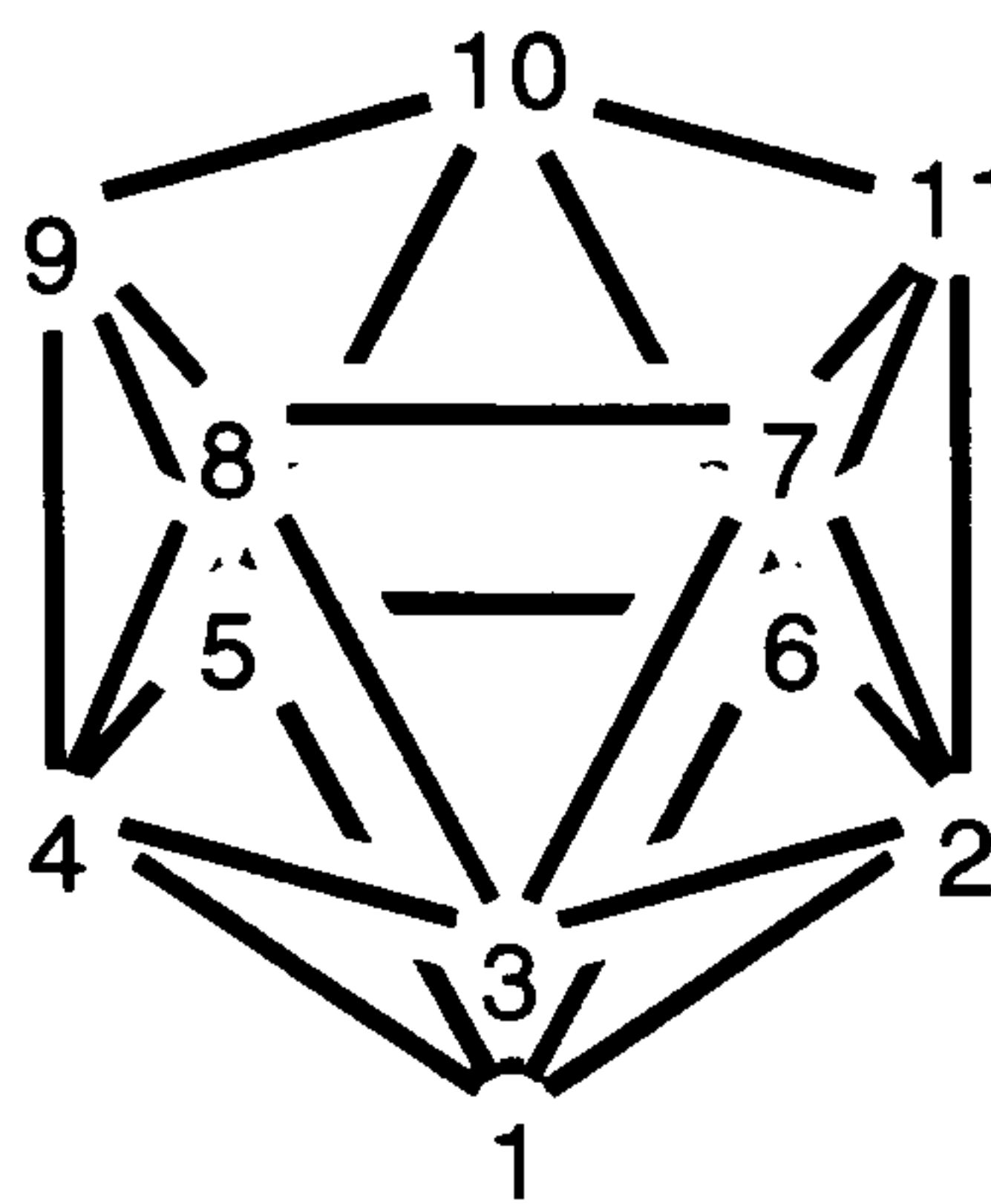
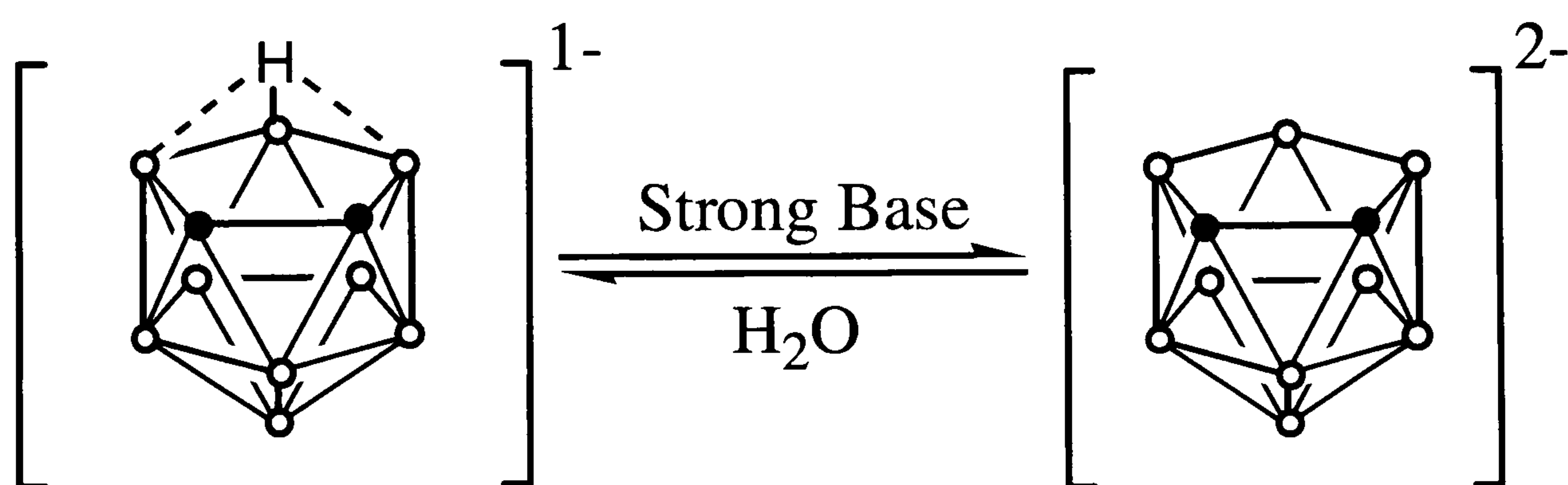


Figure 1.10 Standard numbering scheme for the nido-“C₂B₉” systems. Carbon atoms are given the lowest numbers possible, e.g. 7,8-, 7, 9-, and 2,9- respectively for the *ortho*- *meta*- and *para*- derivatives.

The mechanism of base degradation is not fully understood but it is thought to be a multi-step process initially involving nucleophilic attack of the base at the most electropositive boron atom.

The twelfth hydrogen atom in the [*nido*-C₂B₉H₁₂]⁻ ion can be reversibly removed from the cage by reactions with strong bases such as sodium metal,²⁴ sodium hydride²⁵ or butyl lithium²⁶ in ethereal solvents, forming the respective isomeric C₂B₉H₁₁²⁻. The same species has been shown to form in hot aqueous NaOH solution; the reversible equilibrium shown in equation 1.2 has been confirmed by the treatment of the *ortho*-C₂B₉H₁₁²⁻ with water to form the *ortho*-C₂B₉H₁₂⁻ salt and hydroxide ion.



Equation 1.2

These compounds are commonly referred to within the literature as dicarbollide anions, this name comes from the observation that the *nido*-11 particle icosahedral fragment resembles a spanish water jar called an “*olla*”. As a result Hawthorne and co-workers named the B₁₁H₁₁⁴⁻ ion the “*ollide ion*” and the CB₁₀H₁₁³⁻ and C₂B₉H₁₁²⁻ ions the “*carbollide*” and “*dicarbollide*”, (Cb²⁻), ions respectively.

1.3 Electronic and Structural Aspects of Metal Ligand Bonding.

This section describes the bonding modes commonly observed for a range of ligands that are found in organometallic chemistry and are of relevance to the chemistry in this thesis, concentrating mainly on the structural and electronic aspects of terminally bonded species, and noting the similarities between different ligands. The ligands described in this section will be discussed in terms of the neutral ligand formalism.²⁷

1.3.1 Imido Ligands, [NR].

Both terminal and bridging bonding modes are known for the imido ligand, [NR], of which the μ^2 -bridging mode is the one more commonly encountered.²⁸ Despite this there are a considerable number of terminally bound imido ligands which are particularly prevalent in sterically encumbered environments, or where the imido substituent is bulky.

The imido ligand can be considered to bond to a transition metal via one σ and either one or two π interactions. Limiting valence bond (VB) descriptions are shown in Figure 1.11, where the hybridisation about the nitrogen and the metal-ligand bond are suggested to impose certain structural parameters on the imido ligand.

Structure **A** depicts an sp^2 hybridised nitrogen atom leading to a M=N double bond ($1\sigma 1\pi$) and a bent M-N-R linkage with one lone pair residing in a $N(sp^2)$ orbital. In the neutral ligand formalism, the ‘bent’ imido ligand [NR] behaves as a 2 electron donor to the metal. Most structurally characterised M-N-R moieties are linear, suggesting sp hybridisation about the nitrogen, which results in the lone pair residing in a pure p -orbital. In structure **B** the M=N double bond ($1\sigma 1\pi$) is maintained if symmetry restrictions (or perhaps a severe energetic mismatch with available metal orbitals) do not allow lone-pair donation to the metal. However in most cases, the lone pair $p(\pi) \rightarrow M(d)$ donation is allowed, leading to the linear structure depicted in **C** and an M \equiv N bond order of 3. In this case, the imido ligand acts as a 4 electron donor to the metal, i.e. a $1\sigma, 2\pi$ ligand.

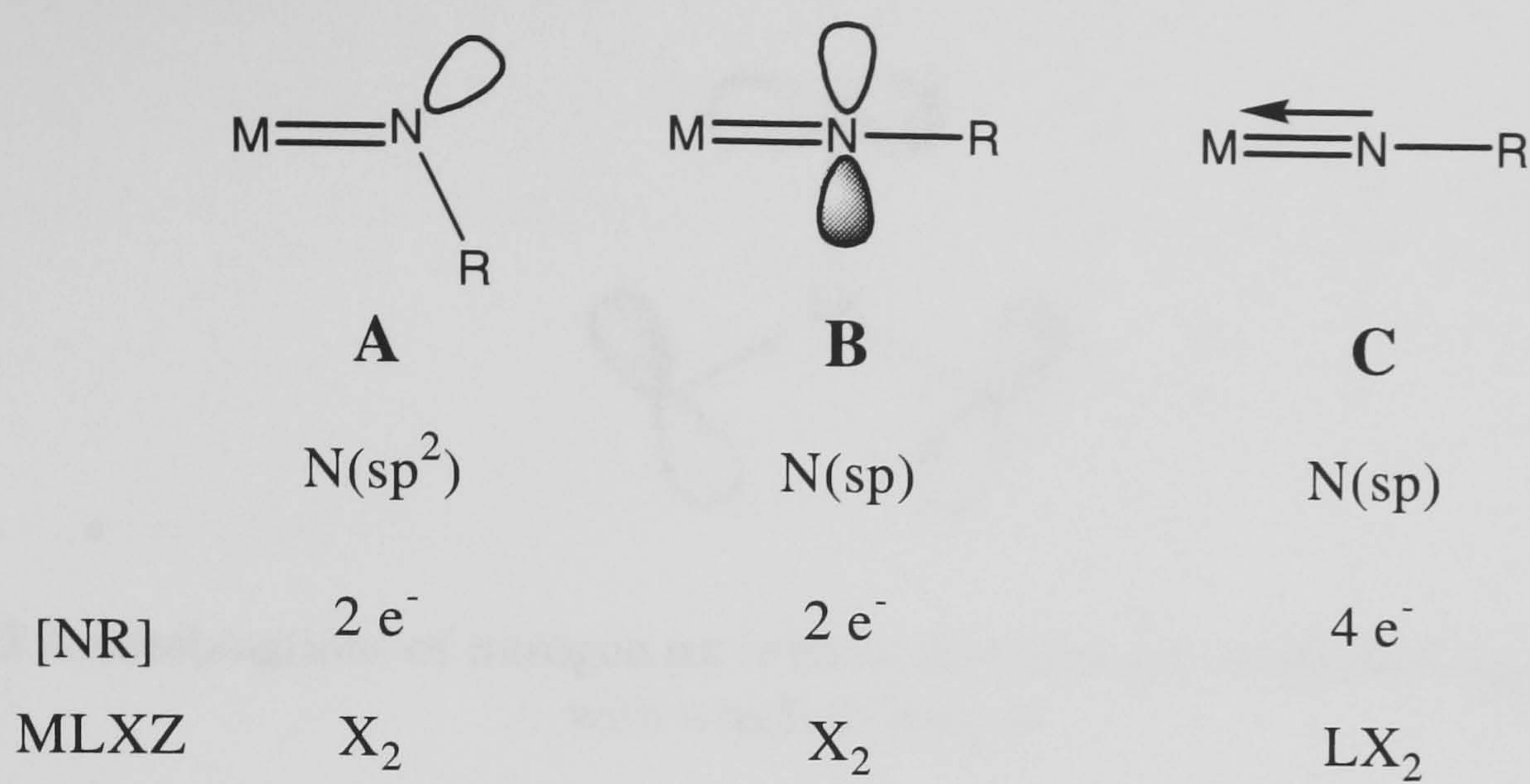


Figure 1.11 Limiting VB descriptions of metal-imido linkage.

1.3.1.1 Delocalised Bonding Approach

Lin and Hall have undertaken a group theoretical analysis of complexes containing metal-ligand multiple bonds, which provides a particularly useful framework for imido complexes. This study determines the maximum metal-ligand bond order for potentially triply bonded ligands “T” (such as [NR]) and the metal’s maximum d electron count for this maximum M-T bond order to be attained.²⁹

Consider the simpler example of the tetrahedral “MT₄” Os(N^tBu)₄ molecule, where, if the imido ligands donate their full complement of electrons to the metal, this would make a 24 electron complex. However, Table 1.1 shows that symmetry considerations reveal that a combination of three nitrogen pπ orbitals has t₁ symmetry, and therefore have no corresponding metal d orbital with which to interact (Figure 1.12). The molecule is therefore best considered an 18 electron complex and the maximum bond order in the molecule is therefore 2.25 [i.e. (4σ + 5π)/4], with three ligand-based π orbitals.

ligand σ	ligand π	metal s + p	metal d	max M-T bond order	max d electron for max bond order
a ₁ + t ₁	e + t ₂ + t ₁	a ₁ +t ₂	e + t ₂	2.25	0

Table 1.1

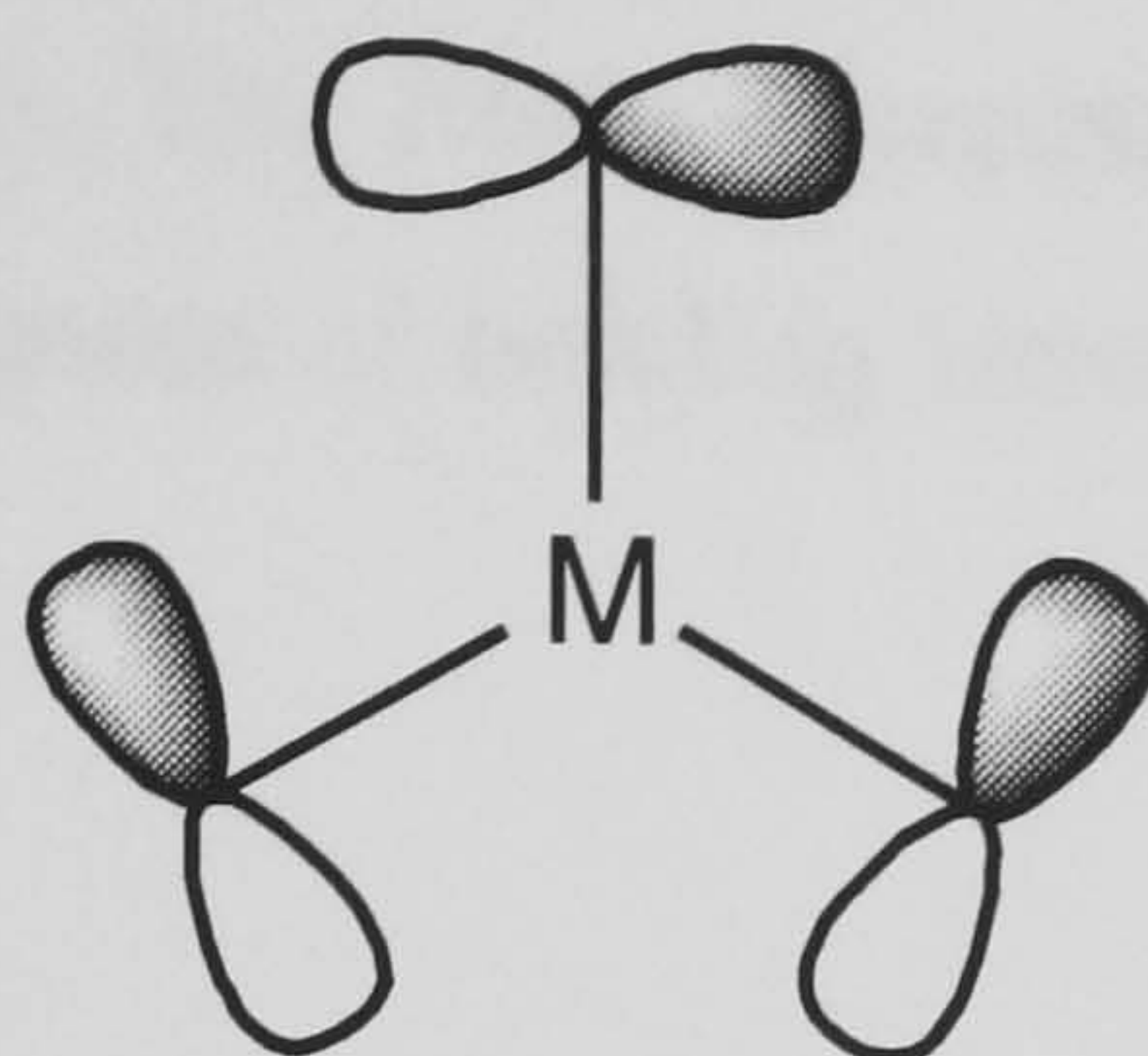


Figure 1.12 A combinations of nitrogen $p\pi$ orbitals that have no corresponding metal d orbital with which to interact

1.3.1.2 Nucleophilic Vs Electrophilic; A Rationale to Imido Reactivity

In a study by Nugent and co-workers,³⁰ using *ab-initio* calculations, a simple periodic trend for the reactive behaviour of imido ligands was uncovered. ‘*The charge on the imido group was found to decrease up and to the right of the periodic table*’. Figure 1.13 summarises this simple conceptual model. The changes in $N(p) \rightarrow M(d)$ interaction are a function of relative energies of the atomic orbitals involved.

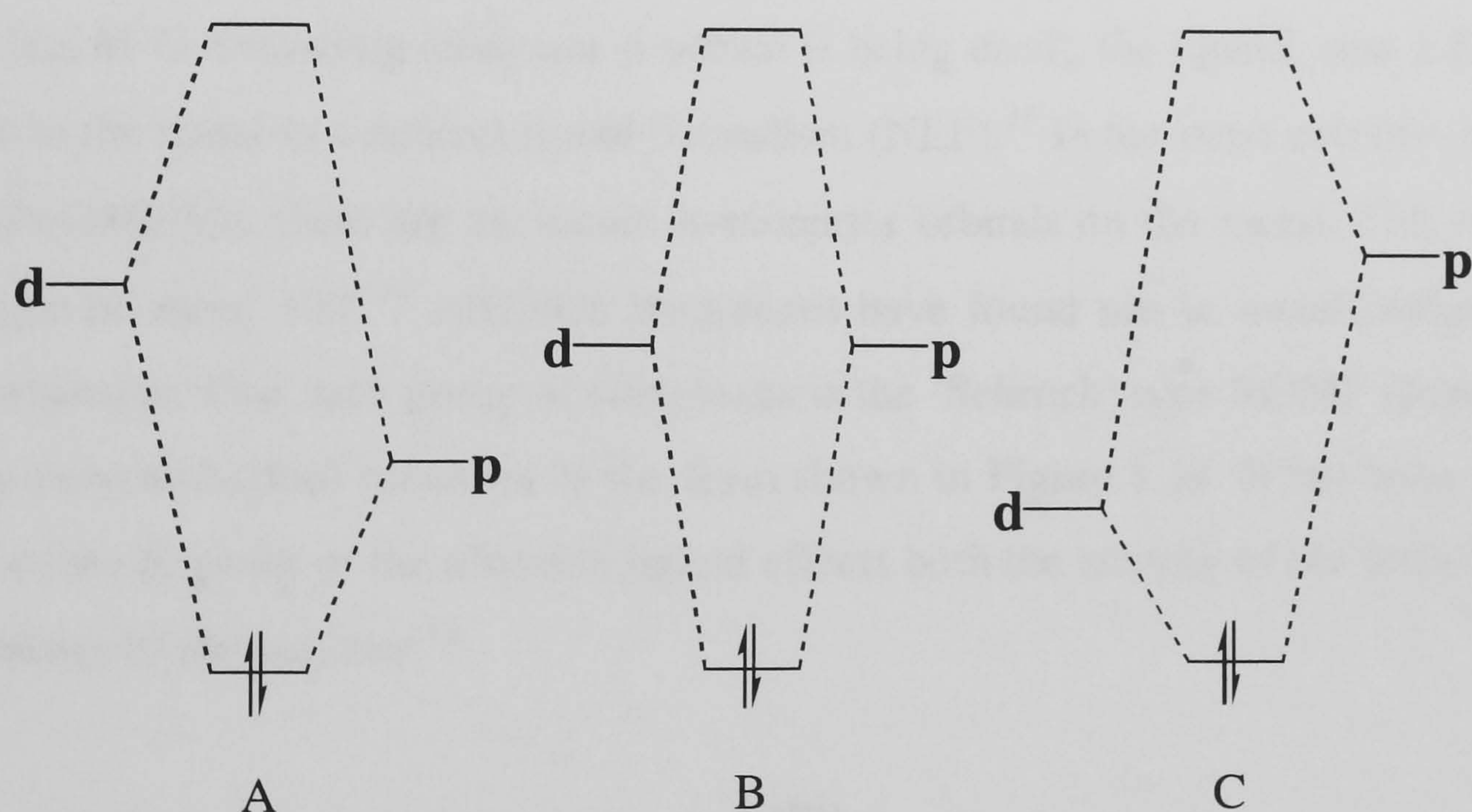


Figure 1.13 The reactivity of the imido ligand is a function of the relative energies of the atomic orbitals involved in the $N(p) \rightarrow M(d)$ interaction.

At one extreme, the ligand p orbitals are lower in energy than the metal d orbitals and the ligand acts as a π donor to the metal centre (A). The π -bonding molecular orbitals resemble ligand orbitals while the π^* orbitals are principally metal d; the ligand reacts with incoming substrates as a nucleophile. The other extreme case (C) considers the ligand orbitals empty and higher in energy than the metal d orbitals. The bonding MO's are principally metal in character

and the empty π^* levels are based largely on the ligand, giving rise to electrophilic behaviour. There is a continuum between the two extremes, which is partially traversed on moving from the early to the late transition metals. The imido compounds in this thesis fall in the range between **A** and **B**; **C** is a good description of bonding between metals and π -acid ligands such as carbonyls.

1.3.2 Alkoxo Ligands, [OR].

Alkoxo, [OR], ligands can be bridging or terminal, and the steric bulk of R will dictate which mode is preferred, bulky substituents preventing the formation of an alkoxide bridge.³¹ In terms of the neutral ligand formalism the alkoxo ligand [OR] is a L_2X ligand and donates up to 5 electrons to the metal centre, compared to the imido ligand which can only donate a total of 4 electrons to the metal centre, although both ligands are still thought of as being $1\sigma 2\pi$ ligands.

Only rarely are both lone pairs used for π -bonding to the metal. In the compound $(^t\text{Bu}_3\text{CO})_2\text{ZrMe}_2$ both lone pairs are used, resulting in a short M-O distance and a large M-O-C angle (almost 180°), with an *sp* hybridised O atom.³² More commonly M-O-C angles are about 140° with less M-O π -bonding (only one p orbital is being used), the ligand, now LX, donating 3 electrons to the metal in a neutral ligand formalism (NLF).³³ In the most extreme cases, such as $(\text{dppe})_2\text{Pt}(\text{OMe})\text{Me}$, there are no vacant π -acceptor orbitals on the metal. This results in a M-O-C angle of about 120° .³⁴ Alkoxide complexes have found use in metal complexes with catalytic behaviour. One such group of complexes is the ‘Schrock’ type ROMP (Ring Opening Metathesis Polymerisation) initiators of the form shown in Figure 1.14. It has been found that the nature of the R group of the alkoxide ligand effects both the activity of the initiator and the stereochemistry of the polymer.³⁵

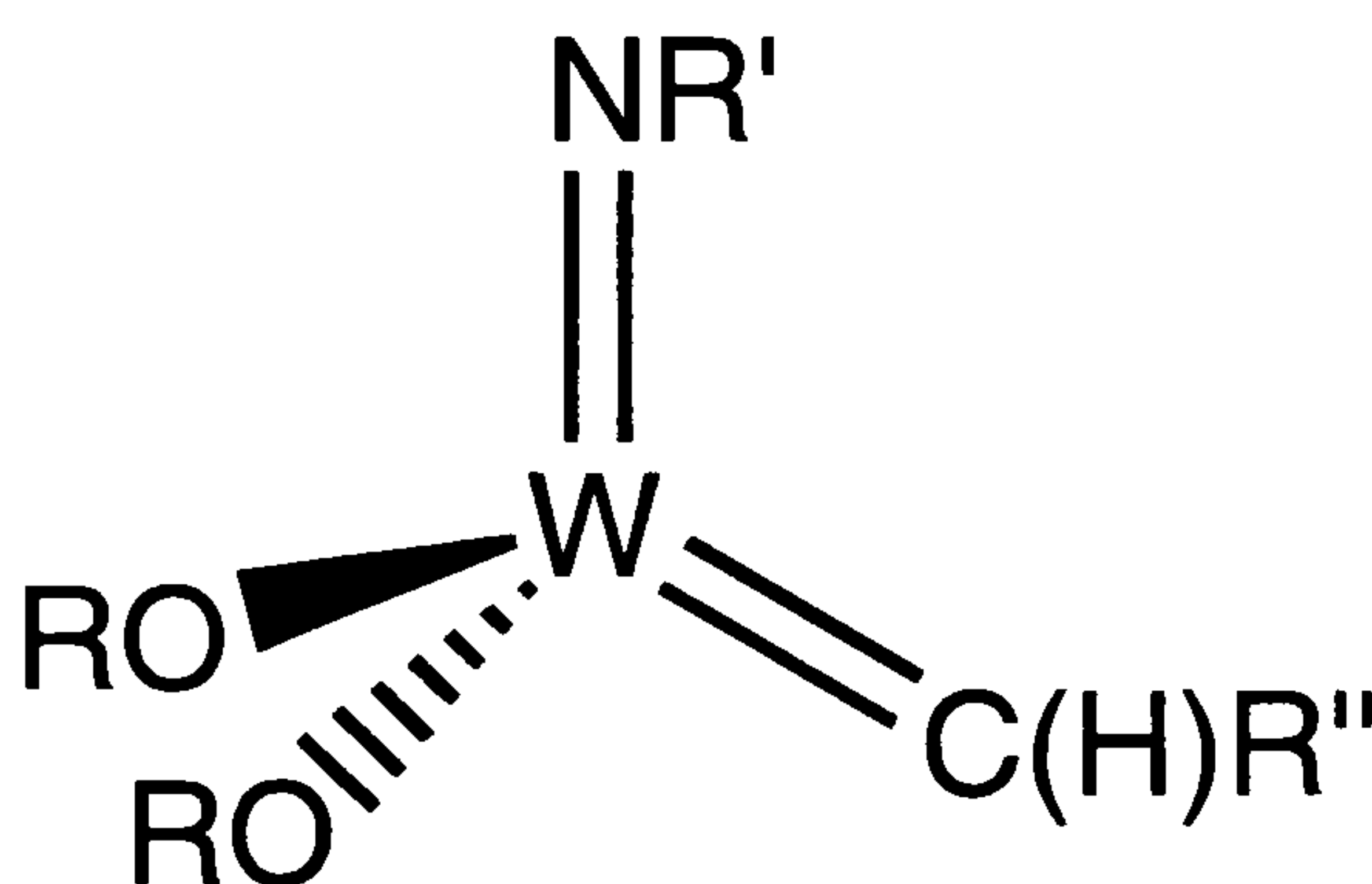


Figure 1.14 The general structure of ‘Schrock’ type ROMP catalysts.

1.3.3 Metal Amido Ligands, $[\text{NR}_2]$.

For a terminal metal alkyl amido complex there are two bonding possibilities, shown below.

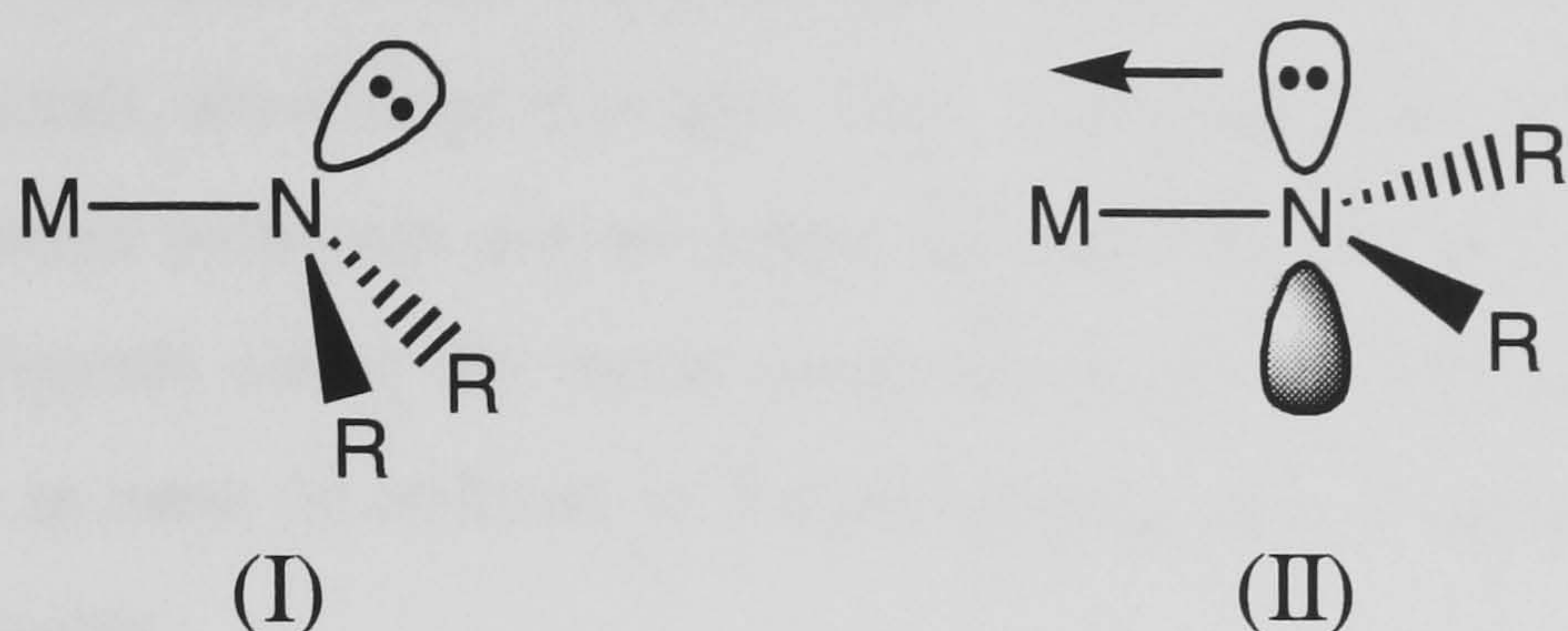


Figure 1.15 Diagram showing the principle bonding modes of the metal dialkylamido ligand.

Structure (I) shows a metal-nitrogen σ bond with a pyramidal sp^3 hybridised nitrogen. Structure (II) illustrates a situation in which π -bonding occurs from the p orbital orthogonal to the planar sp^2 hybridised nitrogen atom, and is predominantly found for high oxidation state early transition metal complexes (i.e. metals that have vacant d orbitals available for π -acceptance). The amide ligand can therefore act as both a one electron, X, ligand as shown in structure (I), or a three electron ligand, LX, structure (II). Structural data for transition metal amides show that the nitrogen atom of the amide ligand has a planar, or almost planar, three coordinate environment. In addition the M-N distance is usually shorter than the predicted single bond. These observations are usually interpreted as evidence for the presence of considerable $p\pi-d\pi$ bonding between the nitrogen and the metal atom.³⁶ However, the data are not unequivocal because the length of appropriate M-N single bonds are not known experimentally.³⁷

The tendency for metal amides to form bridged structures is less than in the case of alkoxides due to greater steric crowding at the nitrogen atom compared to that at the oxygen atom. The bridging group functions as a one electron, X, ligand to one metal centre using the lone pair on the nitrogen atom to form a bridging dative bond, L, to the other metal atom.

It has proven difficult to synthesise dialkyl amides of the later transition metals. This is attributed to the fact that the amide ligand can act as both a strong σ -donor and a strong π -donor and will therefore form strong bonds to the π -acceptor early transition metals but only weak bonds to the poorly π -accepting late transition metals. The use of the silylamide group $\text{N}(\text{SiMe}_3)_2$, has allowed the synthesis of such compounds for all the first row transition metals

and several of the lanthanides. An explanation for this may be that the nitrogen π -electrons are partially delocalised onto silicon, which thus allows the $\text{N}(\text{SiMe}_3)_2^-$ ligand to behave as a weak π -acceptor. However, the more significant factors which are applicable also for the rationalisation of the existence of low coordination number silylamides and dialkylamides of the early transition metals, are kinetic in origin. Thus, such amides are stable because normally accessible decomposition pathways are no longer energetically attractive. Also significant is the fact that bulky ligands cause the metal environment to be sterically hindered. Another factor is the absence in these complexes of β -hydrogens so that decomposition via β -hydride elimination is not possible.

1.3.4 The Isolobal Analogy Between η^5 -Cyclopentadienyl and Imido Ligands.

The symmetries of the partly or fully filled frontier orbitals of the η^5 -cyclopentadienyl ligand, Cp^- , and those of the imido ligand are similar, both possessing a σ and two degenerate π -orbitals, as shown in Figure 1.16. In this respect they may be regarded as being *pseudo*-isolobal, though not truly isolobal since η^5 -cyclopentadienyl ligand uses five atoms to coordinate to the metal centre and the imido only one. Another difference is that although in terms of the charged ligand formalism, both the Cp and NR^{2-} ligands are considered to contribute 6 electrons to the metal centre, but when thought of in terms of the preferred neutral ligand formalism, the Cp ligand is capable of donating a total of 5 electrons and the imido only 4 electrons.

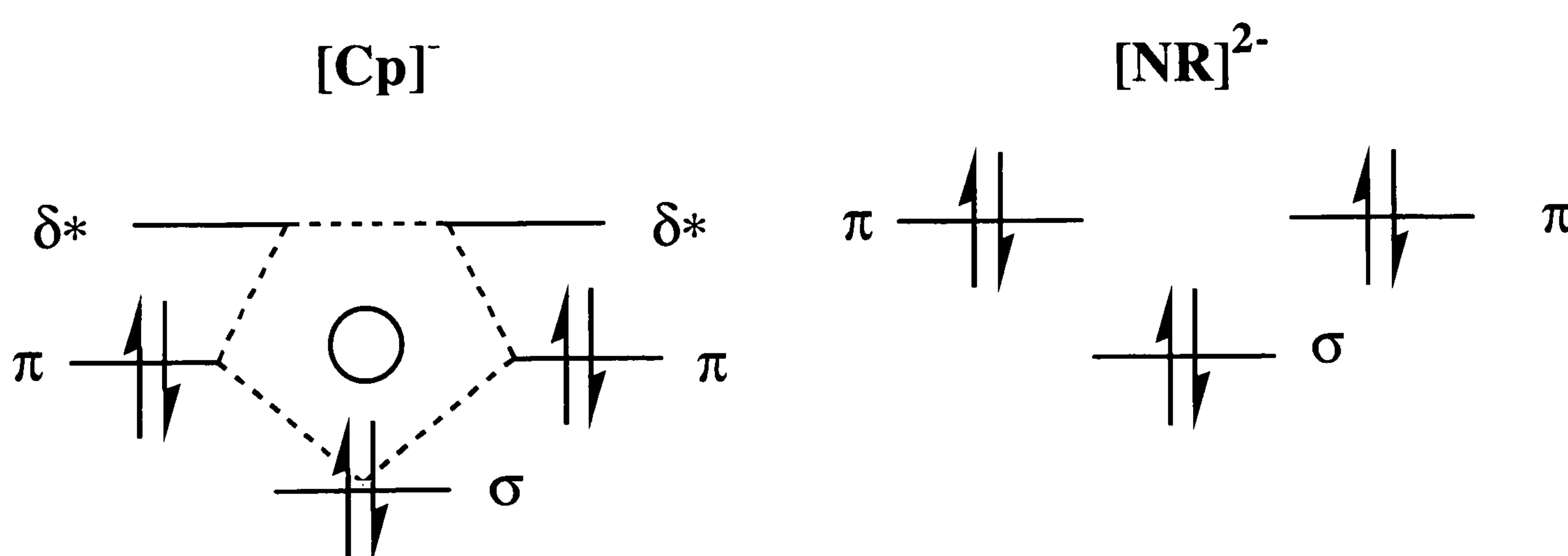


Figure 1.16 Representation of the frontier orbitals of the $[\text{C}_5\text{H}_5]^-$ and $[\text{NR}]^{2-}$ fragments. A comparison of the molecular orbitals of Cp^- and RN^{2-} show a number of similarities

Simple MO calculations of the π -molecular orbitals of the cyclopentadienyl anion (C_5H_5^-) reveal that it has a filled a_1 orbital of σ -symmetry and a set of occupied degenerate e_1 π -symmetry orbitals, in addition to two degenerate e_2 orbitals of δ -symmetry (Figure 1.17).

The early transition metals have no filled δ -symmetry orbitals on the metal that can donate into the e_2 pair of δ symmetry unoccupied acceptor orbitals, it is therefore unlikely that these levels (Figure 1.17) play a significant bonding role. The frontier orbitals of the imide dianion (NR^{2-}) in a terminal geometry (sp hybridised nitrogen) resemble those of the cyclopentadienyl unit, and thus also bond to the metal via one σ and two π interactions (Figure 1.16).³⁸

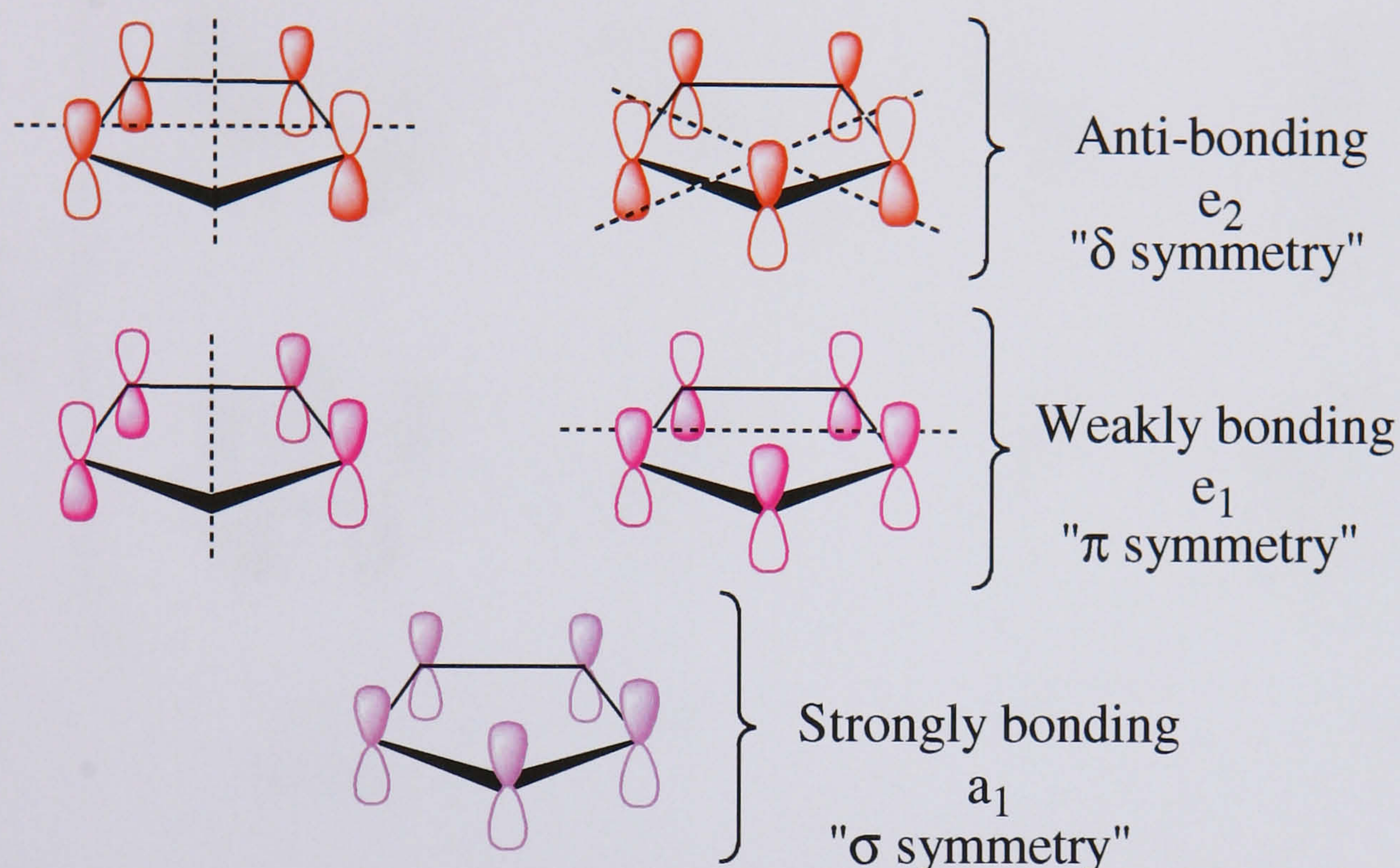


Figure 1.17 The atomic orbitals that form the p_π molecular orbitals of the C_5H_5 ring.

Figure 1.18 shows a pictographic comparison of the frontier orbitals of the $[\text{Cp}]$, $[\text{RN}]$, $[\text{RO}]$ and C_6R_6 fragments. All the ligands shown in Figure 1.18 have one common feature, that is they all possess one orbital of σ symmetry and two of π symmetry (this classification is based on their potential to bond to the metal), i.e., they are all $1\sigma 2\pi$ ligands. Simple energy level diagrams such as those shown in Figure 1.16 can be constructed for the arene, and alkoxide anions showing they are directly comparable with Cp^- and RN^{2-} .³⁹ It is useful to compare ligand fragments that are able to contribute the same number of electrons to the metal in this way. For example we can consider the alkoxo unit to be a 5-electron ligand (this is the maximum number of electrons it can potentially donate to the metal) and in this respect can be said to be iso-numeral to the η^5 cyclopentadienyl ligand, and as far as the symmetries of their filled or half filled frontier orbitals are concerned, the groups Cp and OR can be regarded as *pseudo-isolobal*. In the case of the imido ligand, this can supply one less electron to the metal than the five that OR or Cp can.

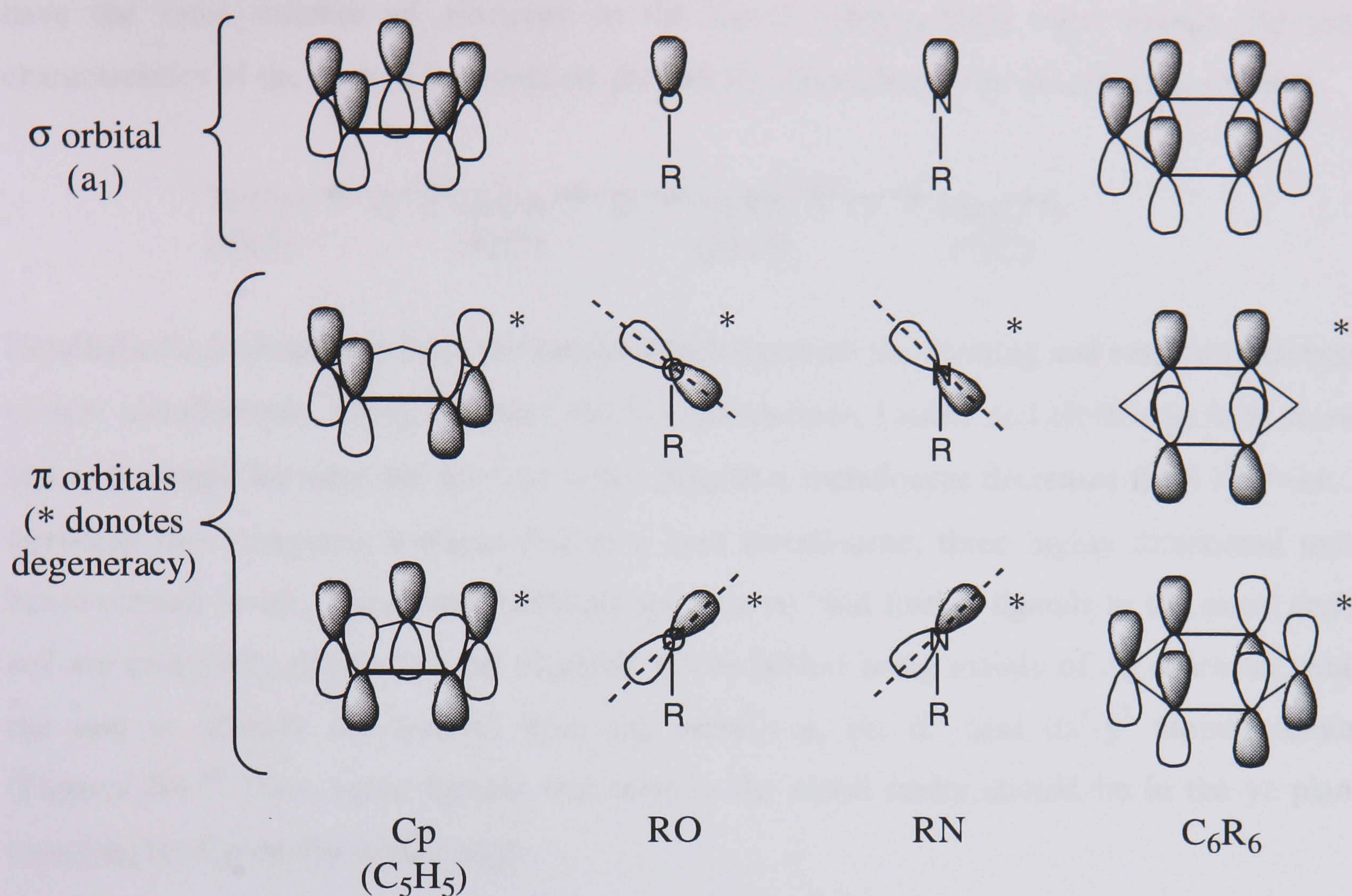


Figure 1.18 Pictographic representation of the σ and π orbitals of the [Cp], imido, alkoxo ligands and arene that can interact with metal orbitals on an early transition metal fragment (those orbitals marked with an asterix, *, are degenerate if the ligand possesses an overall symmetry greater than C_3).

Therefore, successive progressions along the transition series accompanied by sequential replacement of the cyclopentadienyl unit with an imido ligand leads to a series of isolobal and valence *iso*-electronic species as illustrated in Figure 1.19.

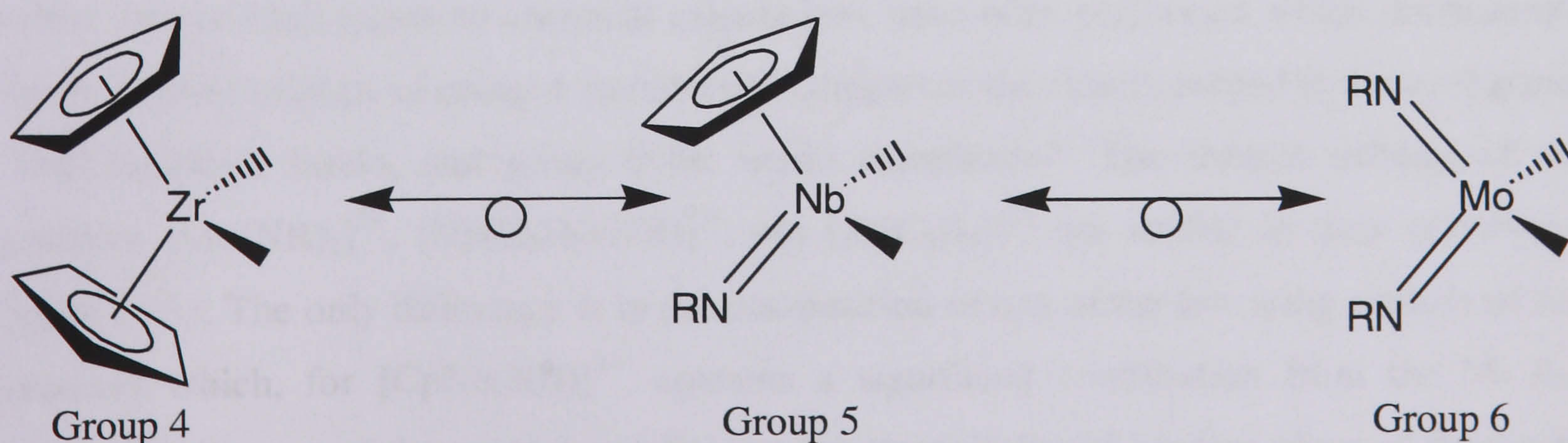
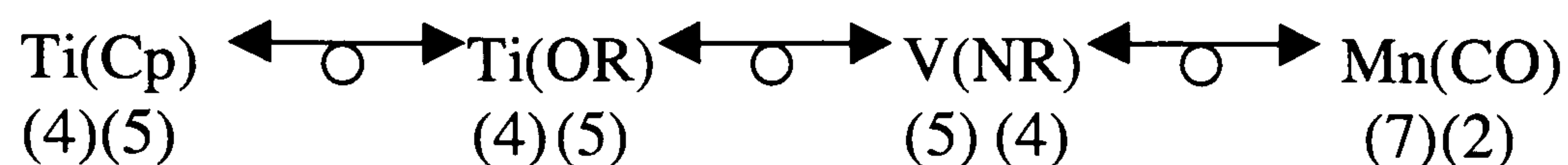


Figure 1.19 Successive progressions along the transition series accompanied by sequential replacement of the cyclopentadienyl unit with an imido ligand leads to a series of isolobal and valence *iso*-electronic species.

This relationship can be extended to metal-ligand fragments, such as those shown below, that have the same number of electrons in the metal valence shell even though the lobar characteristics of the ligands involved do not strictly allow them to be described as isolobal.



Detailed calculations have been performed which examine the bonding and resultant geometry of bent metallocenes. Using extended Hückel calculations, Lauher and Hoffmann have shown that as the angle between the normals to the rings in a metallocene decreases from 180° (i.e., a ferrocene-like structure), towards that of a bent metallocene, three highly directional metal based orbitals result. These ‘new’ orbitals are used to bind further ligands to the metal centre and are essentially directed in the yz plane, the b_2 orbital being mainly of d_{yz} character, while the two a_1 orbitals are formed from the metal’s s, p_z , d_{z^2} and dx^2-y^2 atomic orbitals (Figure 1.20).⁴⁰ Thus, other ligands that bind to the metal centre should lie in the yz plane, bisecting the Cp-M-Cp wedge angle.

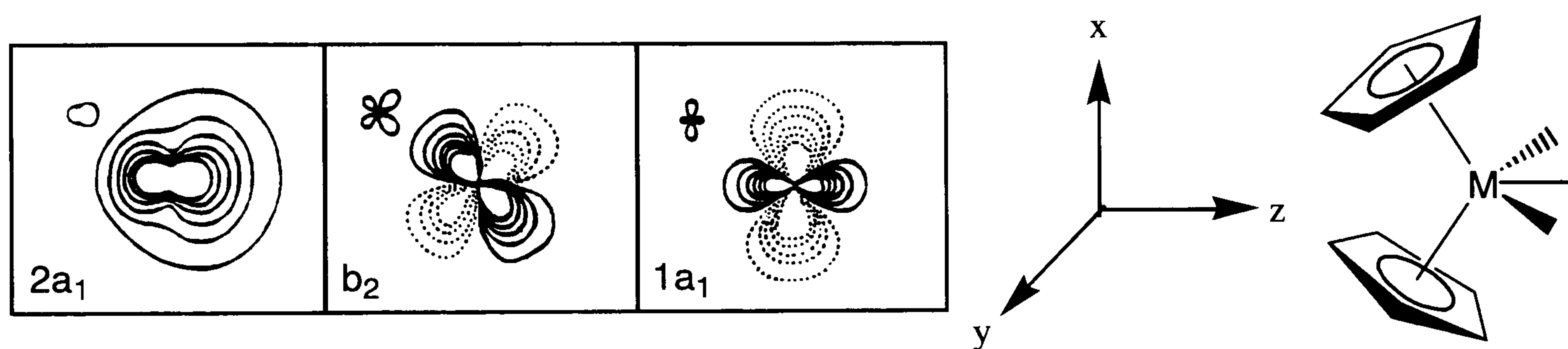


Figure 1.20 Contour diagrams of the three bonding orbitals in the bent metallocene fragment $[\text{Cp}_2\text{M}]$

Further Fenske-Hall quantum chemical calculations have been performed which demonstrate that the frontier orbitals of group 4 metallocene complexes are closely related to those of group 5 half sandwich imido, and group 6 bis imido complexes.⁴¹ The frontier orbitals of the fragments $[\text{Mo}(\text{NR})_2]^{2+}$, $[\text{Nb}(\text{C}_5\text{H}_5)(\text{NR})]^{2+}$ and $[\text{Zr}(\text{C}_5\text{H}_5)]^{2+}$ are similar in their orientation (Figure 1.21). The only difference is in the composition of one of the low lying orbitals of $2a_1$ symmetry which, for $[\text{CpNb}(\text{NR})]^{2+}$, contains a significant contribution from the Nb dx_z orbital. This lies out of the normal metallocene “equatorial” ligand binding plane of the Cp_2M and may account for the differences in the chemistry of Cp_2M and $\text{CpM}(\text{NR})$ fragments.

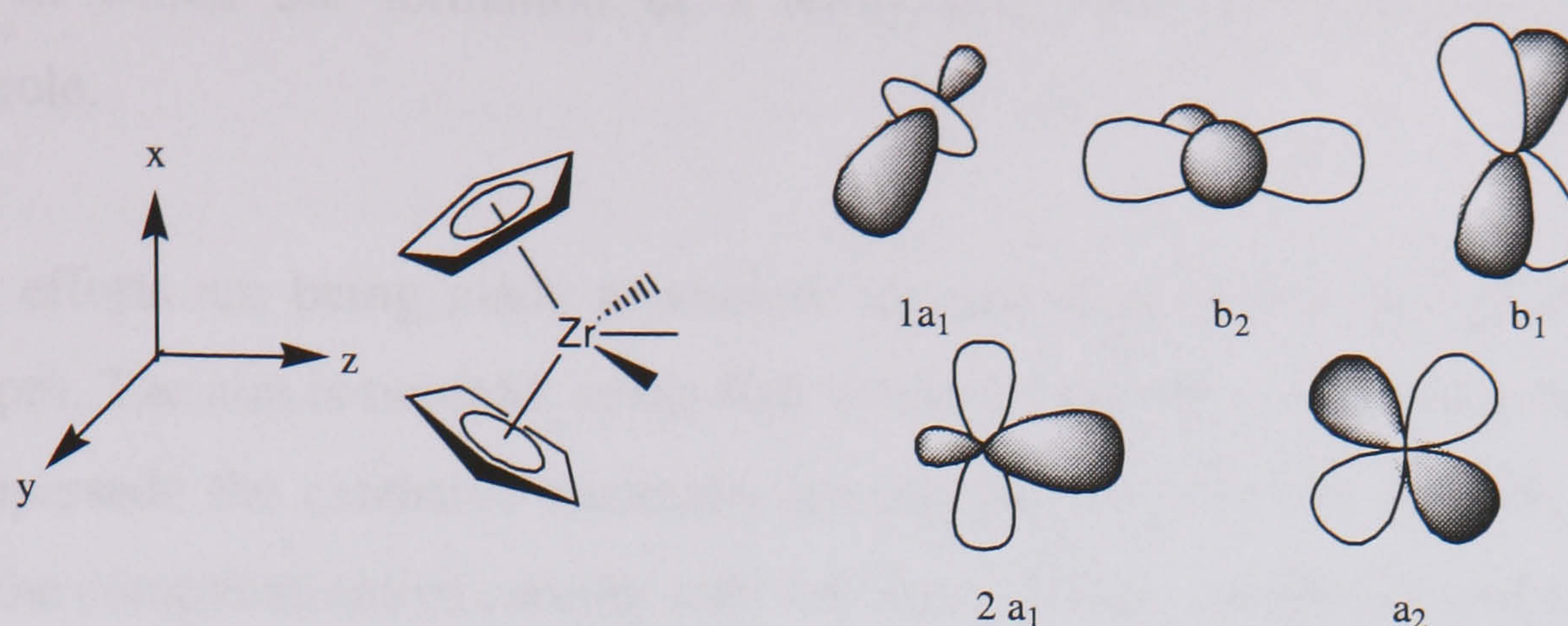


Figure 1.21 Frontier MO's of the $[\text{Zr}(\text{C}_5\text{H}_5)_2]^{2+}$ (most important contributions only)

1.3.5 Carboranes as Ligands : Comparison with Other $1\sigma 2\pi$ Ligands.

For a long time chemists have recognised the importance of the cyclopentadienyl ligand in organometallic chemistry, and the discovery and rationalisation of its structure and bonding of ferrocene in particular,⁴² as a turning point for organometallic chemistry. This new class of compounds served to form a bridge between the classical domains of inorganic and organic chemistry and the barriers between co-ordination chemistry and organometallic chemistry. The cyclopentadienyl ligand (C_5H_5^-), (Figure 1.16), is known to bind strongly to metals, generally being inert to both electrophiles and nucleophiles and, therefore, often regarded as a spectator ligand.

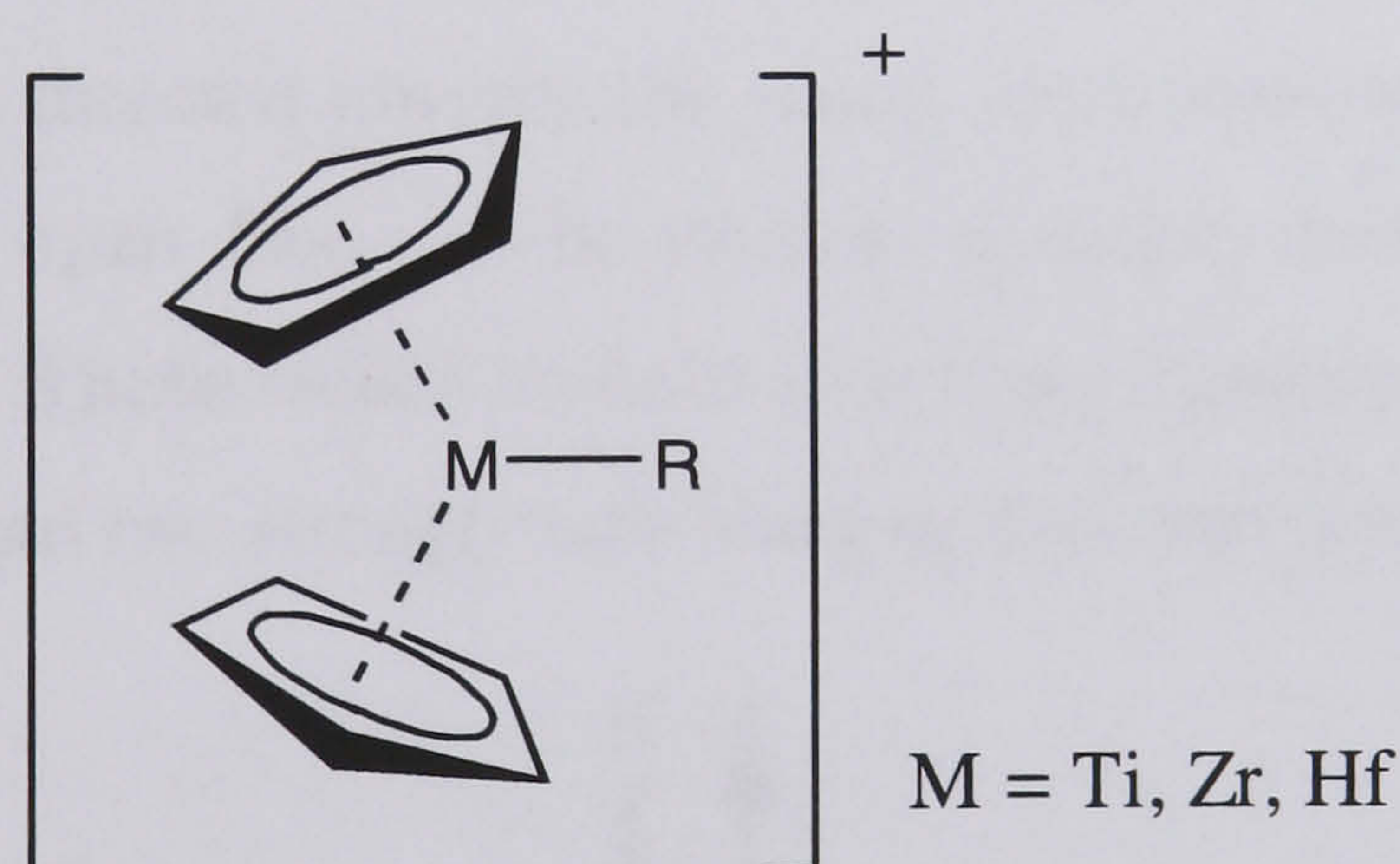


Figure 1.22 The cationic alkyl bis(cyclopentadienyl) complexes of group 4 metals of the type $[\text{Cp}_2\text{MR}]^+$ are thought to be intermediates in metallocene olefin polymerisation.

Since the discovery in 1957 that $[\text{Cp}_2\text{TiCl}_2]/\text{AlCl}_3$ can form a heterogeneous catalysis system for the polymerisation of ethylene, bis(cyclopentadienyl) complexes of group 4 metals have been under constant investigation. In later years it has been the cationic alkyl bis(cyclopentadienyl) complexes of group 4 metals of the type $[\text{Cp}_2\text{MR}]^+$ that have been recognised as the catalytically active species in metallocene based olefin polymerisation catalysts (Figure 1.22).⁴³ These highly electrophilic 14 electron species possess a very complex

chemistry in which the formation of a temporarily dormant stabilised adduct plays an important role.

Increasing efforts are being made to explore the potential of new ligand environments and catalyst types. The aim is twofold; in the first instance to develop a ligand system that can rival or even supersede the extensive chemistry already patented for Cp systems, and secondly to eliminate the complications of counter-ions for these cationic complexes and to develop neutral analogues. To this end, many groups have been interested in ligands other than cyclopentadienyl or its substituted derivatives as spectator ligands in the co-ordination environment of the early transition metal complexes. Examples of ligands that have attracted attention include imido,⁴⁴ alkoxides,⁴⁵ Schiff bases,⁴⁶ butadiene⁴⁷ and dicarbollide to name just a few.

In the late 1950s- early 1960s Lipscomb and co-workers, while discussing the bonding involved in boron hydride clusters, noted that in the cluster $B_{12}H_{12}^{2-}$ removal of a single apex as a $[BH]^{2+}$ would leave $B_{11}H_{11}^{4-}$, which is *iso*-electronic with $C_2B_9H_{11}^{2-}$, with five orbitals pointing towards the vacant apex (Figure 1.23).⁴⁸

This feature of the five membered face of $B_{11}H_{11}^{4-}$ is reminiscent of the molecular orbital diagrams of $C_5H_5^-$ shown in Figure 1.17. The bonding description for the ion $B_{11}H_{11}^{4-}$ places 6 electrons in the five orbitals directed towards the vacant apex position. In the $B_{11}H_{11}^{4-}$ ion the five atomic orbitals in the open face can be used to generate three bonding and two anti bonding molecular orbitals. These would include a strongly bonding a_1 orbital, two bonding and degenerate e_1 orbitals, and two strongly anti-bonding and degenerate e_2 orbitals.

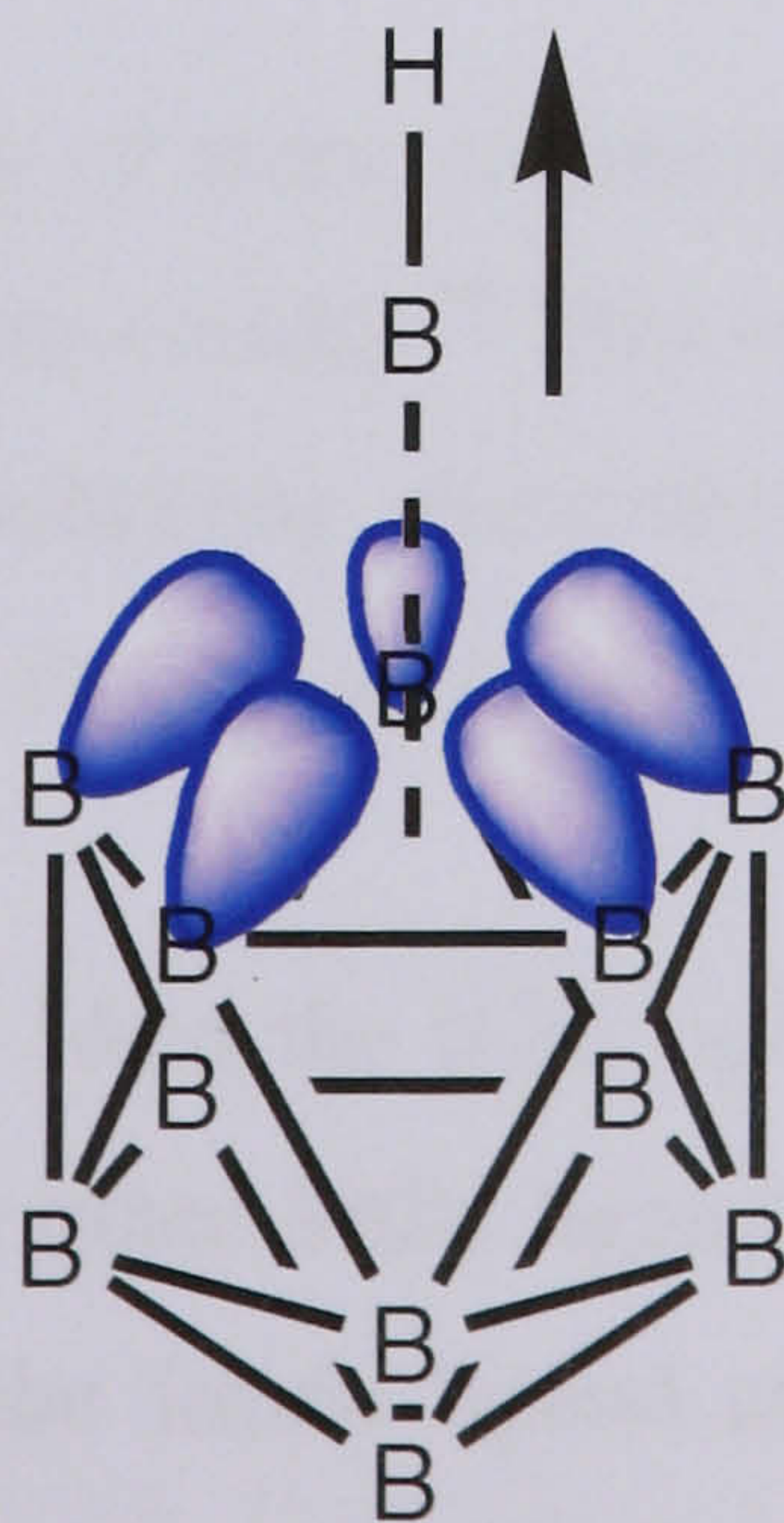


Figure 1.23 Removal of $\{BH\}^+$ from the anionic cluster $B_{12}H_{12}^{2-}$ leaves the cluster $B_{11}H_{11}^{4-}$, which has five radial sp^3 orbitals directed towards the vacant apical position. This is reminiscent of the frontier orbitals of Cp^- .

Chapter One - Introduction

In the case of the *ortho*-, *meta*- and *para*-C₂B₉H₁₁²⁻ ions, orbital degeneracy would be disrupted by the presence of carbon atoms in the open face of the cluster. However, this orbital non-degeneracy does not change the overall orbital energy or symmetry scheme. It was this rationale that led Hawthorne and co-workers to synthesise and characterise the first transition metal dicarbollide analogues of metallocenes.⁴⁹

Metallacarboranes of the type [(C₂B₉H₁₁)₂M]ⁿ⁻ or [(C₂B₉H₁₁)M(C₅H₅)]^{m-}, incorporating most of the transition metals were eventually synthesised, and a significant finding was that most of them are more stable than their metallocene analogues, and in some cases such as [(C₂B₉H₁₁)₂Cu(II)]²⁻ the metallocene analogue is not even known.⁵

The six electrons required for a filled-shell configuration are normally provided by the ligand anion, for example C₂B₉H₁₁²⁻. While the ligand can be regarded as a dianionic six-electron donor, as is conventional within the literature, it is more favourable here to think of the dicarbollide as a neutral four electron ligand.

Despite the acknowledged similarities between Cp⁻ and Cb²⁻ (C₂B₉H₁₁²⁻) as ligands, this analogy is flawed on several counts, and not only for those reasons stated above, i.e., non degeneracy of the 'π' orbitals of Cb²⁻, compared to Cp⁻, and increased electronic charge on Cb²⁻. The low electronegativity of boron compared to carbon, results in face-bonding interactions of the carborane with metal ions that are more covalent, hence stronger than the analogous metal-hydrocarbon sandwich bonds; this is the major reason for the typically higher chemical and thermal stability of the metallocarboranes compared to their metallocene and metal-arene cousins.

It has also been shown that in terms of steric requirements the pentamethyl-cyclopentadienyl ligand, [Me₅Cp], resembles [Cb] more closely.⁵⁰ This can be seen as an advantage for [Cb], as it has long been recognised in metallocene chemistry that sterically demanding ligands on metal centres can regulate activity at the metal centre.

In much the same way that we can liken the [Cp] ligand to the imido ligand, [NR], we can extend our arguments to incorporate other 1σ2π ligands such as the dicarbollide ligand, [Cb]. The apparent similarities between the imido ligand and the dicarbollide ligand (both are 4 electron 1σ2π donors to the metal centre, and both ligand systems are able to stabilise metals in high oxidation states) provide a handle by which the chemist can form a range of new and

interesting complexes that hopefully behave in a similar way to the traditional group 4 metallocenes and group 5 half sandwich imido complexes.

1.4 Metallocarboranes of the Early Transition Metal and f-Block Elements

This section reviews the known examples of early transition metals coordinated to carborane ligands. The discussion will be restricted to metallocarboranes in which the d-block elements are incorporated as an integral part of the polyhedral framework. No attempt will be made to incorporate those compounds that contain metal atoms involved solely as a member of a substituent group. Although subsequent chapters in this thesis will be concerned with the chemistry of “C₂B₉” metallocarborane derivatives, it is important to discuss some of the chemistry of C₂B₁₀H₁₂²⁻ and the smaller carborane C₂B₄H₆²⁻ as a ligand in this section as both ligands are capable of binding to the metal centre in an η^6 or η^5 fashion through a ‘C₂B₄’ or ‘C₂B₃’-face respectively.⁵¹ It should be noted that the metallocarborane complexes of C₂B₄H₆²⁻ possess a very different chemistry to their larger cousins, as has been documented in a recent review.⁵² Comprehensive reviews on metallocarborane complexes of the main group,⁵³ and transition metals have appeared elsewhere.^{51,54,55}

1.4.1 Metallocarboranes Containing Group 3 and Lanthanide Group Metals.

Although the cyclopentadienyl π -complexes of scandium have been known for some time,⁵⁶ analogous carborane complexes were not known until recently. In 1992 Bercaw *et al.* synthesised the first carborane containing scandium complex, which is a η^5 -permethylcyclopentadienyl η^5 -dicarbollide scandium alkyl complex, [Li(THF)₃]⁺ [Li[Sc(C₂B₉H₁₁)(Cp^{*})CH(SiMe₃)₂]₂]⁻.⁵⁷ The precursor to this complex, Cp^{*}Sc(C₂B₉H₁₁)(THF)₃, is formed by the elimination of methane from the reaction of [Cp^{*}ScMe₂]_x with C₂B₉H₁₃, followed by treatment with THF, or by the reaction between [Cp^{*}ScCl₂]_x and Na₂[C₂B₉H₁₁], followed by addition of THF.⁵⁸ Alkylation of the precursor with LiCH(SiMe₃)₂ yields the novel scandium complex shown below.

Figure 1.24 shows that each Sc atom is bonded in an η^5 -fashion to one Cp^{*} and one dicarbollide ligand. An interesting feature of this structure is that there is a lithium atom bridge between the two units, bonding loosely to three boron atoms of each dicarbollide ligand

resulting in a dimeric monoanion with a $[\text{Li}(\text{THF})_3]^+$ counter ion residing outside the coordination sphere to balance the charge.

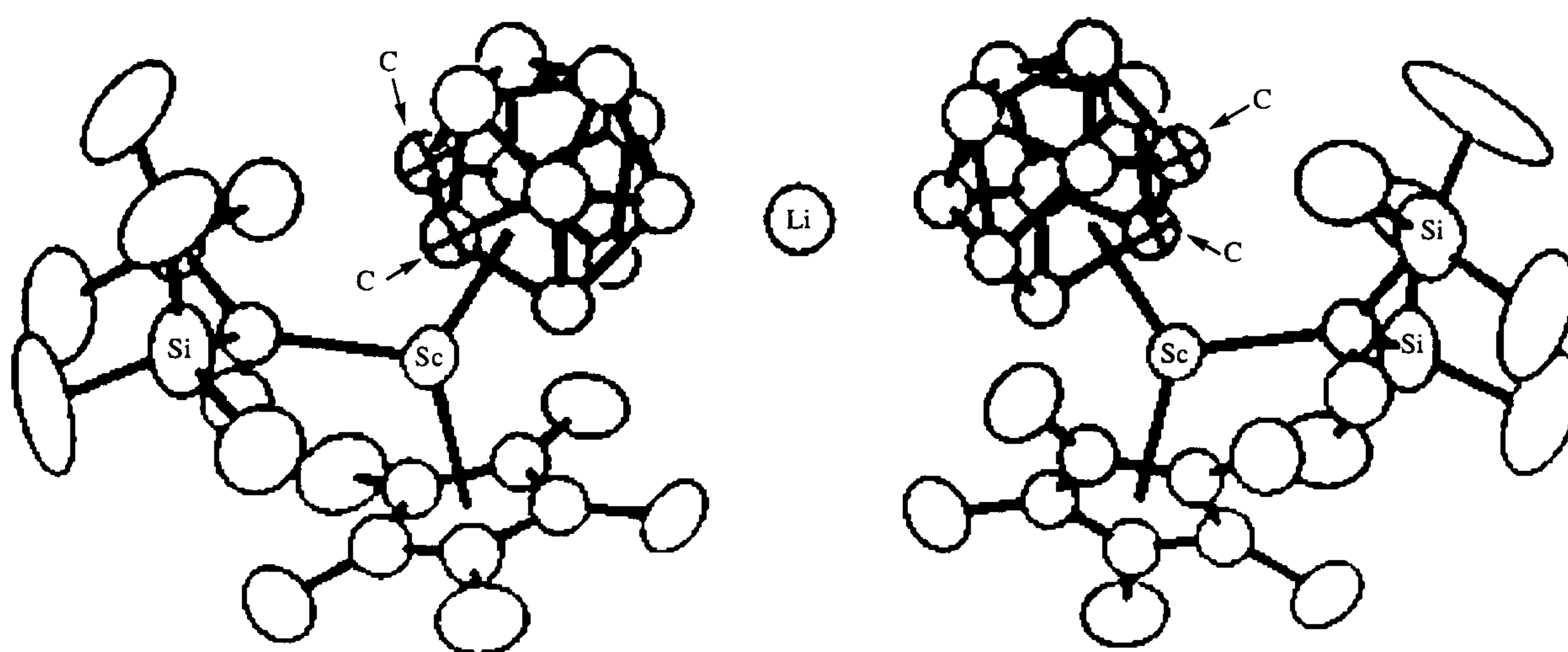


Figure 1.24 An ORTEP drawing of $\{[\text{Cp}^*(\text{C}_2\text{B}_9\text{H}_{11})\text{ScH}(\text{SiMe}_3)_2]_2\text{Li}\}(\text{Li}(\text{THF})_3)$ showing the two anions bridged by a lithium atom. Taken from ref. 58.

The alkylated derivative reacts slowly with H_2 to yield $[\text{Cp}^*(\text{C}_2\text{B}_9\text{H}_{11})\text{ScH}]_2[\text{Li}(\text{THF})_n]_2$. This dimer has been shown to be held together by reciprocal B-H dative bonds from the electron rich boron hydride bonds on the cage to the Lewis acidic scandium centre. NMR experiments show that these Sc-(B-H) interactions persist in the solution state. This interaction has shown to be strong enough to resist reaction with strong Lewis bases such as PMe_3 . The high stability of this dimer limits its use as an olefin polymerisation catalyst.

At the present time there exists no mixed ligand carborane complexes of yttrium, although the first carborane analogue of yttracene was made by Hosmane and co-workers in 1991.⁵⁹ The yttracarborane complex $[\text{Li}(\text{THF})_4][\text{Y}(\text{Cl})(\text{THF})\{\eta^5-(\text{SiMe}_3)_2\text{C}_2\text{B}_4\text{H}_4\}_2\text{Li}(\text{THF})]$ is formed by reaction of the dilithium salt of $[2,3-(\text{SiMe}_3)-2,3-\text{C}_2\text{B}_4\text{H}_4]^{2-}$ (see Figure 1.1) with YCl_3 in benzene followed by extraction into THF. The yttrium atom is bound in a η^5 -fashion to two C_2B_4 ligands as well as a chloride ion and a molecule of THF. The dianionic charge of the complex is balanced by the presence of an exo-polyhedral $\text{Li}(\text{THF})^+$ cation and a discrete $\text{Li}(\text{THF})_4^+$ cation outside the coordination sphere (Figure 1.25)

One limitation of the carborane ligand in group 3 metal chemistry (and lanthanide chemistry) is that, with two dianionic ligands and a 3^+ charge on the metal, there is little possibility of adding reactive anionic ligands, such as alkyls without forming a highly charged species. It is hoped that species such as those shown above for scandium and yttrium will support α -olefin polymerisation or oligomerisation catalytic activity.

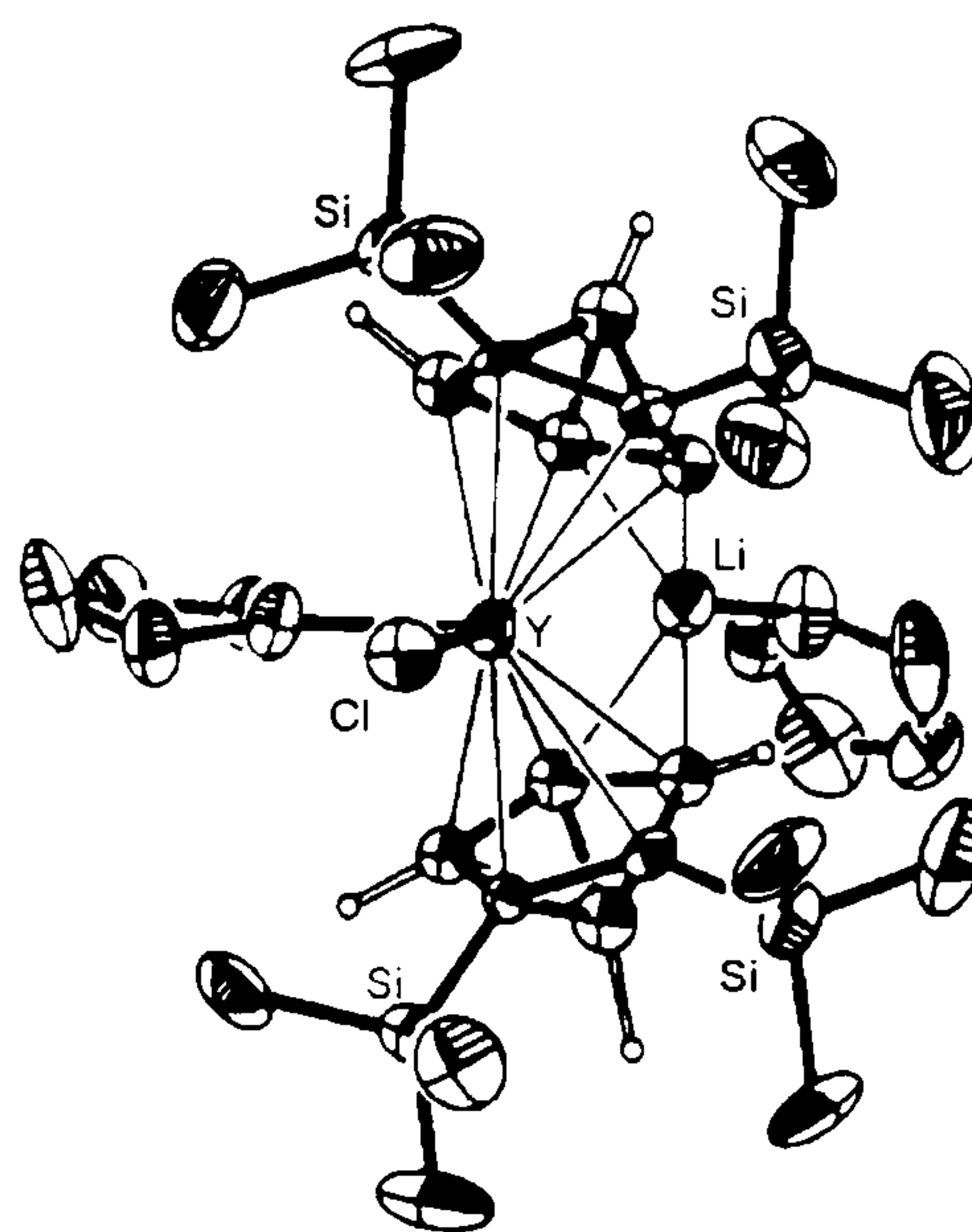


Figure 1.25 A perspective of the yttracarborane, $[\text{Li}(\text{THF})_4][\text{Y}(\text{Cl})(\text{THF})\{\eta^5\text{-(SiMe}_3)_2\text{C}_2\text{B}_4\text{H}_4\}_2\text{Li}(\text{THF})]$. Taken from ref. 59.

Although a variety of ligands have been established in organolanthanide systems, the cyclopentadienide anion and its C-substituted derivatives have been widely utilised.⁶⁰ The chemistry of lanthanide complexes of ‘C₂B₁₀’, ‘C₂B₉’ and ‘C₂B₄’ carborane ligand systems has only recently begun to be explored.

Hawthorne and co-workers have prepared a number of lanthanacarboranes during the last decade from the reaction of the Na salt of the dicarbollide anion with LnI₂ (Ln = Yb or Sm) in THF.⁶¹ These half sandwich complexes have the general formula [*closo*-Ln^(II)(C₂B₉H₁₁)(THF)₄] these compounds are found to be only sparingly soluble in THF and undergo ligand exchange in stronger donor solvents such as MeCN and DMF. The structure of the ytterbium DMF complex [*closo*-Yb^(II)(C₂B₉H₁₁)(DMF)₄] is shown in Figure 1.26. The structure reveals that the metal is essentially centred over the C₂B₃ face, and the coordination sphere of the Yb metal is completed by bonding to four DMF molecules (Figure 1.26).

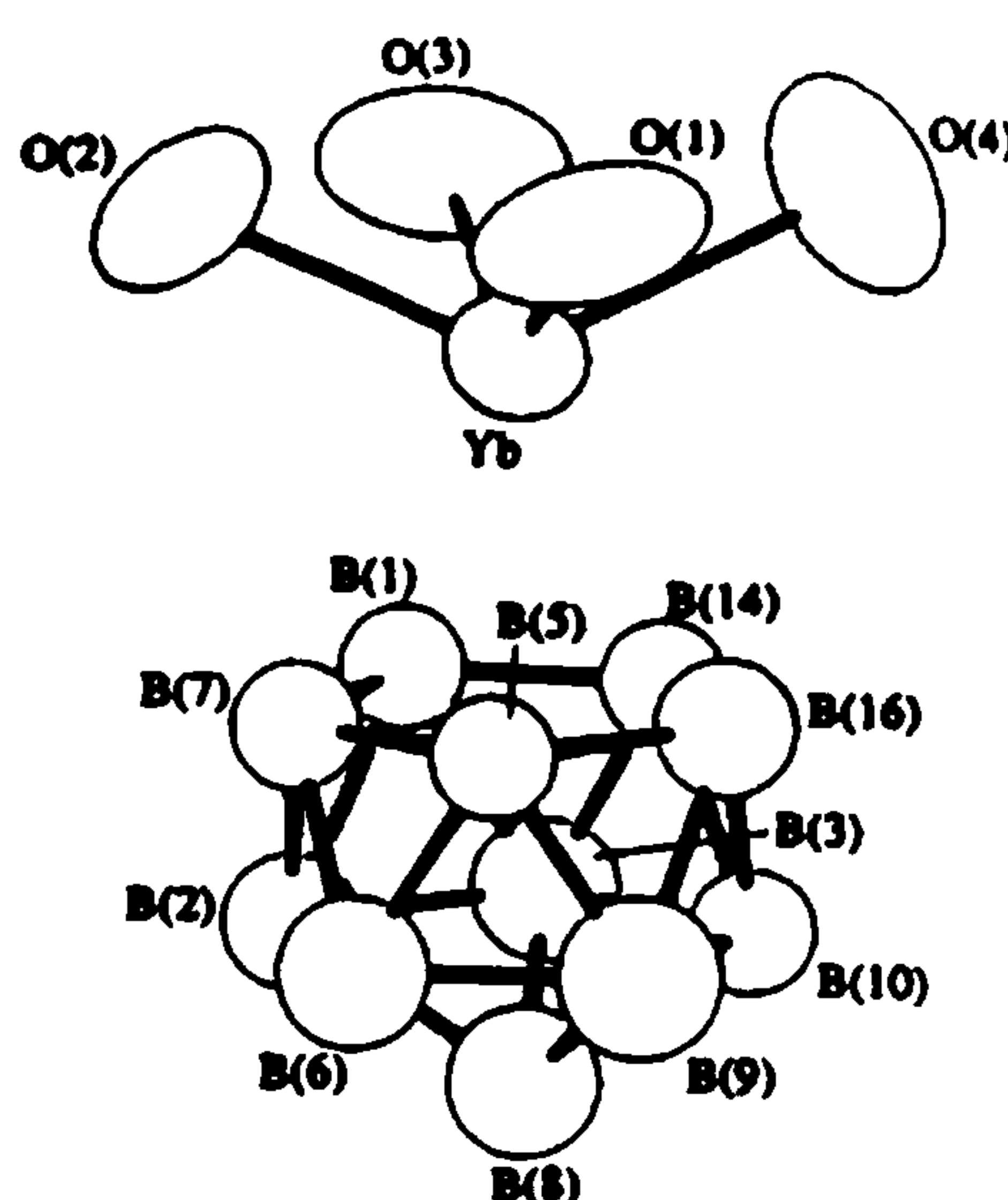


Figure 1.26 Molecular structure of [*closo*-Yb^(II)(C₂B₉H₁₁)(DMF)₄]. Only the oxygen atoms of the DMF ligands are shown. Due to disorder the cage carbon atoms could not be distinguished. Taken from ref. 61.

Further oxidation of these lanthanide (II) complexes is achieved by reacting the THF complexes with one equivalent of the thallacarborane salt [PPN] [*closo*-TlC₂B₉H₁₁] to form complexes of the general formula [PPN][*commo*-Ln^(III)(C₂B₉H₁₁)₂.(THF)₂] (Ln = Sm or Yb). The structure of the samarium derivative (Figure 1.27) shows a distorted tetrahedral geometry around the central metal with two carborane cages and two THF molecules filling the coordination sphere of the metal atom. The charge of the metal-bisdicarbollide anion is balanced by the presence of a discrete [PPN] cation.

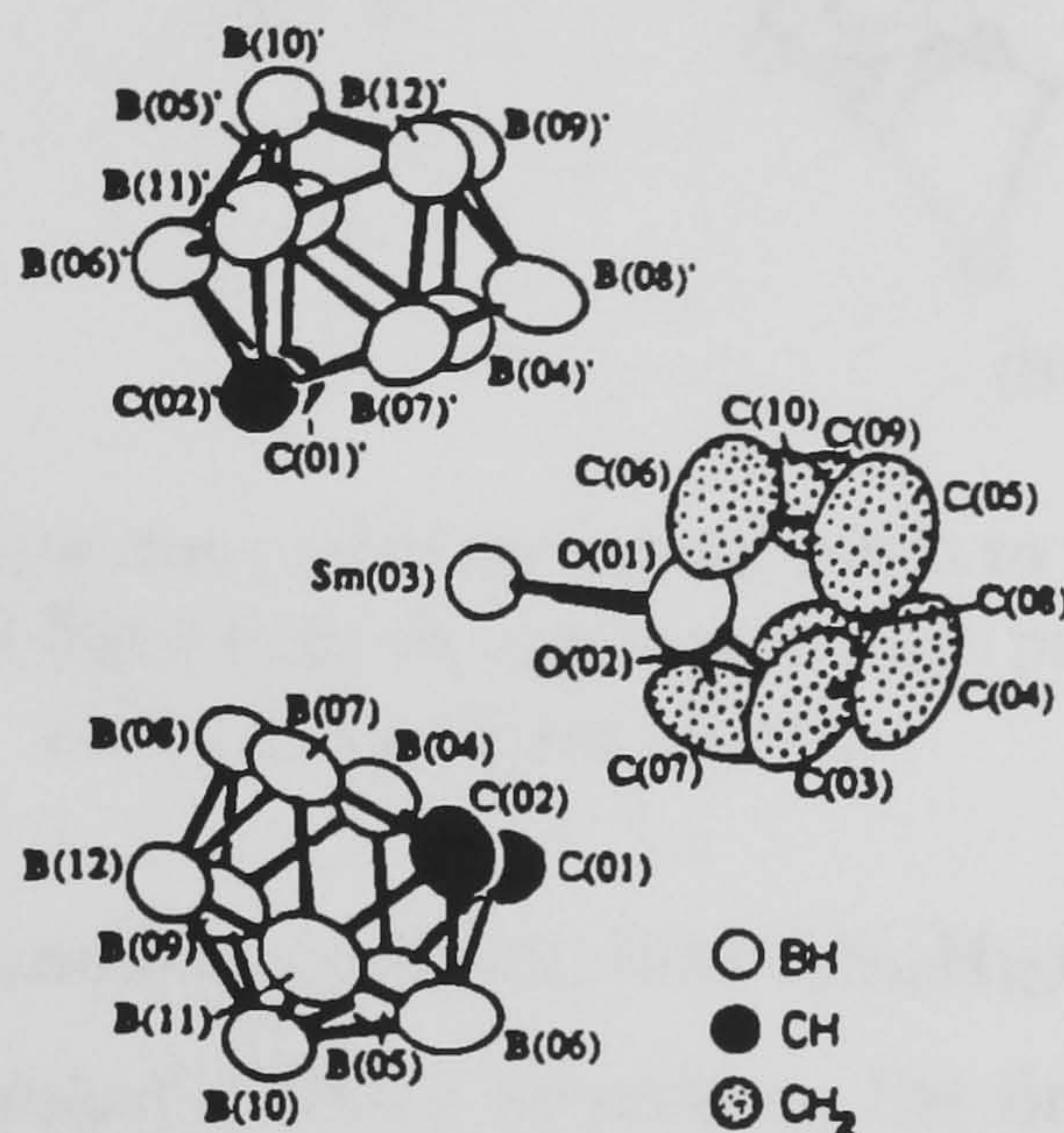


Figure 1.27 Molecular structure of the anion [*commo*-Sm^(III)(C₂B₉H₁₁)₂(THF)₂]⁻. The [PPN] cation is not shown. Taken from ref. 61.

Hawthorne *et al.* have also shown the utility of the dianion, [C₂B₁₀H₁₂]²⁻, in lanthanide chemistry.⁶² The reaction of LnI₂(THF)₂ (Ln = Sm, Eu, Yb) with one equivalent of Na₂[*nido*-C₂B₁₀H₁₂] in THF at room temperature results in the formation of lanthanide complexes which have been formulated as [Ln(C₂B₁₀H₁₂)(THF)_x]_n (x = 3, n = ∞, Ln = Sm or Eu; x = 4, n = 1, Ln = Yb). The ligand Na₂[*nido*-C₂B₁₀H₁₂] is formed by the reduction of 1,2-C₂B₁₀H₁₂ by sodium metal.⁶³ These metallacarboranes are found to be insoluble in THF but soluble in MeCN, thereby allowing the THF to be replaced by this solvent ligand.

The crystal structure of the europium derivative [Eu(C₂B₁₀H₁₂)(MeCN)₃]_∞ is composed of two crystallographically independent, but similar, spiral chains. Each carborane moiety serves as a ligand for two europium atoms, being bonded to one metal atom by a Eu-H-C interaction in the upper belt and a Eu-H-B in the lower belt, and to the other in an η⁶-fashion as shown in Figure 1.28. The coordination sphere about each europium atom is completed by three acetonitrile ligands to give a polymeric structure as in the strontium analogue.⁶³

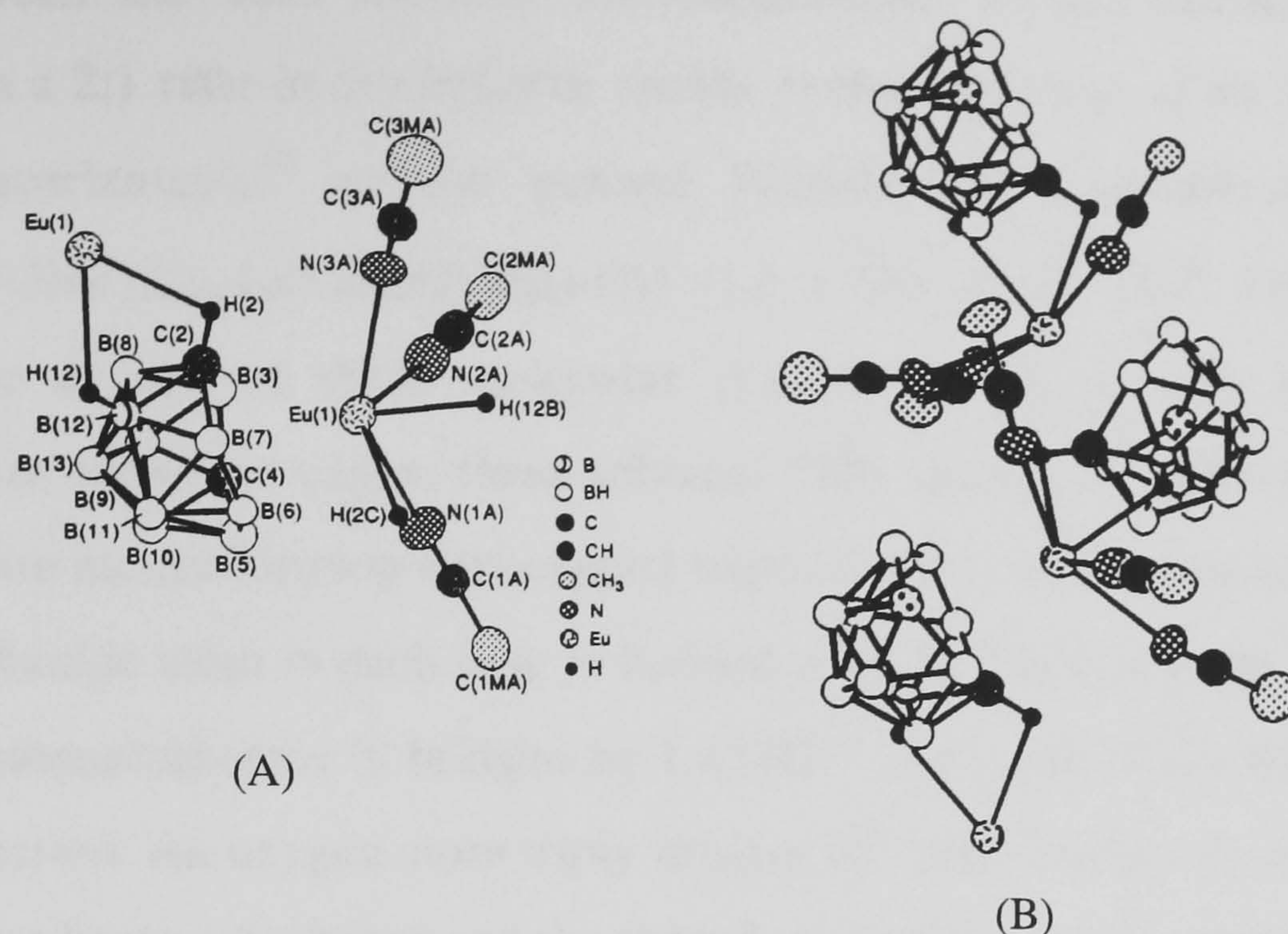


Figure 1.28 Picture (A) shows how one carborane ligand binds to two europium metal atoms. Picture (B) shows how three of these units fit together to form part of the spiral polymeric chain. Taken from ref. 62.

It was also found that the half sandwich complex, $[\text{Eu}(\text{C}_2\text{B}_{10}\text{H}_{12})(\text{THF})_3]_\infty$, will react further with another equivalent of $\text{Na}_2[\text{nido-C}_2\text{B}_{10}\text{H}_{12}]$ to produce the first structurally characterised lanthanacarborane to contain two $[\text{nido-7,9-C}_2\text{B}_{10}\text{H}_{12}]^{2-}$ ligands. Figure 1.29 shows the structure of the metal containing anion in the salt $[\text{NEt}_4]_2[\text{commo-Eu}(\text{C}_2\text{B}_{10}\text{H}_{12})(\text{THF})_2]^-$.

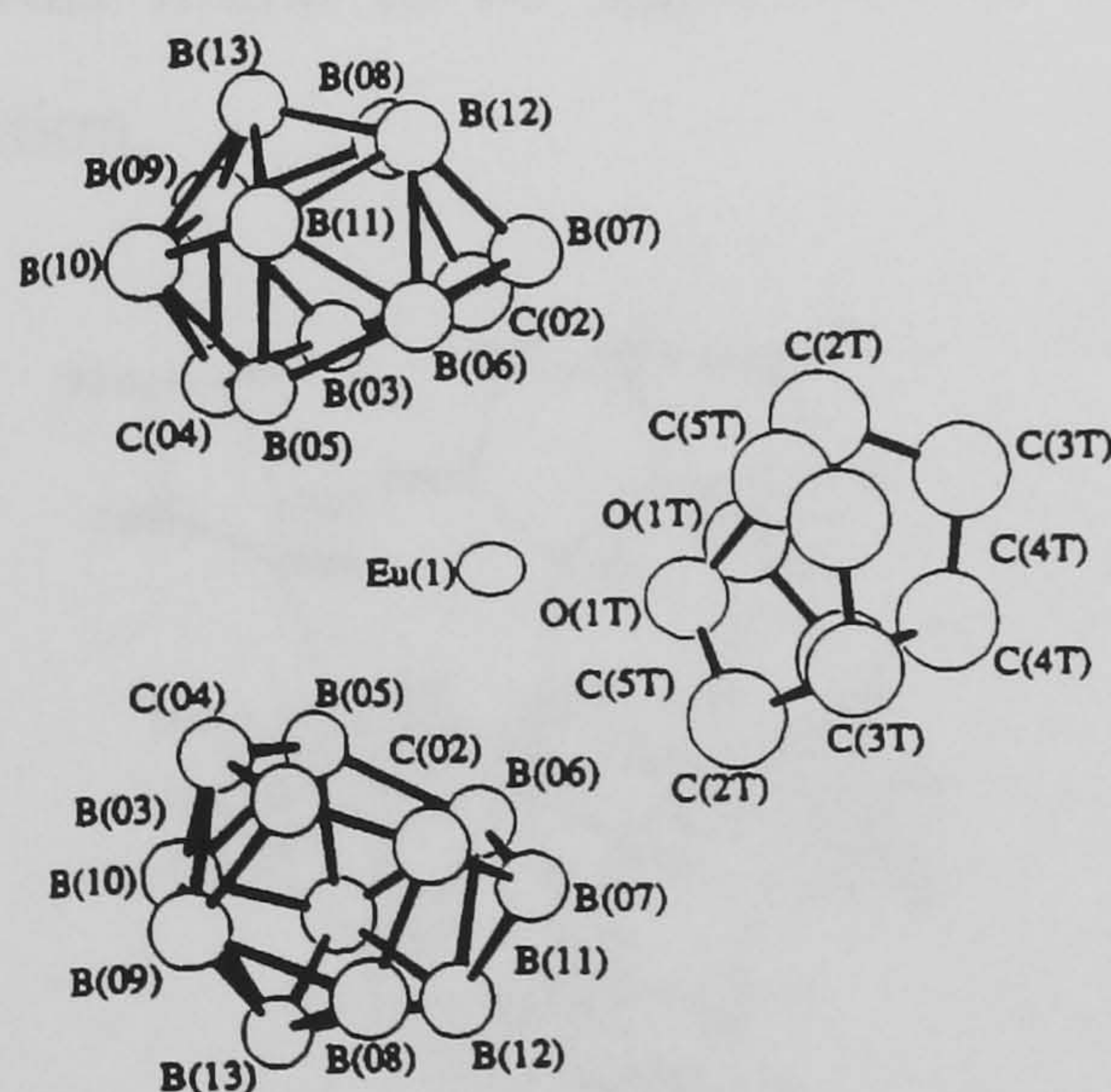


Figure 1.29 Molecular structure of the anion $[\text{commo-Eu}(\text{C}_2\text{B}_{10}\text{H}_{12})(\text{THF})_2]^-$. Taken from ref. 62.

Despite the successes in synthesising a number of half-sandwich and sandwich Sm(II), Sm(III), Yb(II) and Eu(II) complexes of both 'C₂B₉' and 'C₂B₁₀' carborane ligand systems, there have been no reports of analogous species incorporating other lanthanide metals. In comparison there are a larger number of publications of lanthanide-carborane complexes in which the carborane is the smaller 'C₂B₄' system.

The reaction between the THF solvated dilithiacarborane, $\text{Li}_2[2,3-(\text{SiMe}_3)_2\text{C}_2\text{B}_4\text{H}_4]$, and anhydrous LnCl_3 in a 2:1 ratio in dry benzene results in the formation of an unusual series of trinuclear lanthanacarboranes,⁶⁴ of the general formula $\{[\eta^5\text{-Ln}-(\text{SiMe}_3)_2\text{C}_2\text{B}_4]\}_3[(\mu_2\text{-Li}-(\text{SiMe}_3)_2\text{C}_2\text{B}_4)_3(\mu_3\text{-OMe})][\mu_2\text{-Li}(\text{C}_4\text{H}_8\text{O})]_3(\mu_3\text{-O})\}$ ($\text{Ln} = \text{Sm}, \text{Gd},^{65} \text{Tb},^{66} \text{Dy}$ and Ho). The molecular structure of one of these molecules ($\text{Ln} = \text{Sm}$) shows that the molecule is constructed from six carborane cages, three solvated-THF molecules, three lanthanide metal atoms and six lithium atoms, forming a tri-capped trigonal prism with Ln atoms in the capping positions. The lanthanide atom in each case is bonded in an η^5 -fashion to the carborane cage, while the *closo*-lanthanacarborane is bridged by $\text{Li}(\text{THF})^+$ and *closo*-lithiocarborane moieties, in the opposite direction. An oxygen atom triply bridges the three lanthanide metals since each of the six carboranes bears a 2^- charge and the three $\text{Ln}(\text{III})$ and six Li^+ metals are present. An additional $(\text{MeO})^-$ moiety is bound to the lower triangle of *closo* lithiocarboranes in a tetrahedral fashion. Hosmane suggests that the source of methoxide ion and oxygen is THF as this was the only oxygen containing substance in the synthetic scheme. The production of isostructural compounds from five independent syntheses with different lanthanide metals makes it unlikely that some chance oxygen-containing contaminant could be responsible for the course of the reaction. Since both $t\text{Bu-Li}$ and lanthanide compounds are known to degrade THF,^{67,68} and other oxygen containing compounds, and the THF-solvated dilithiacarboranes are known to decompose, it was found to be impossible to ascertain the exact reason for methoxide and oxide ion formation.

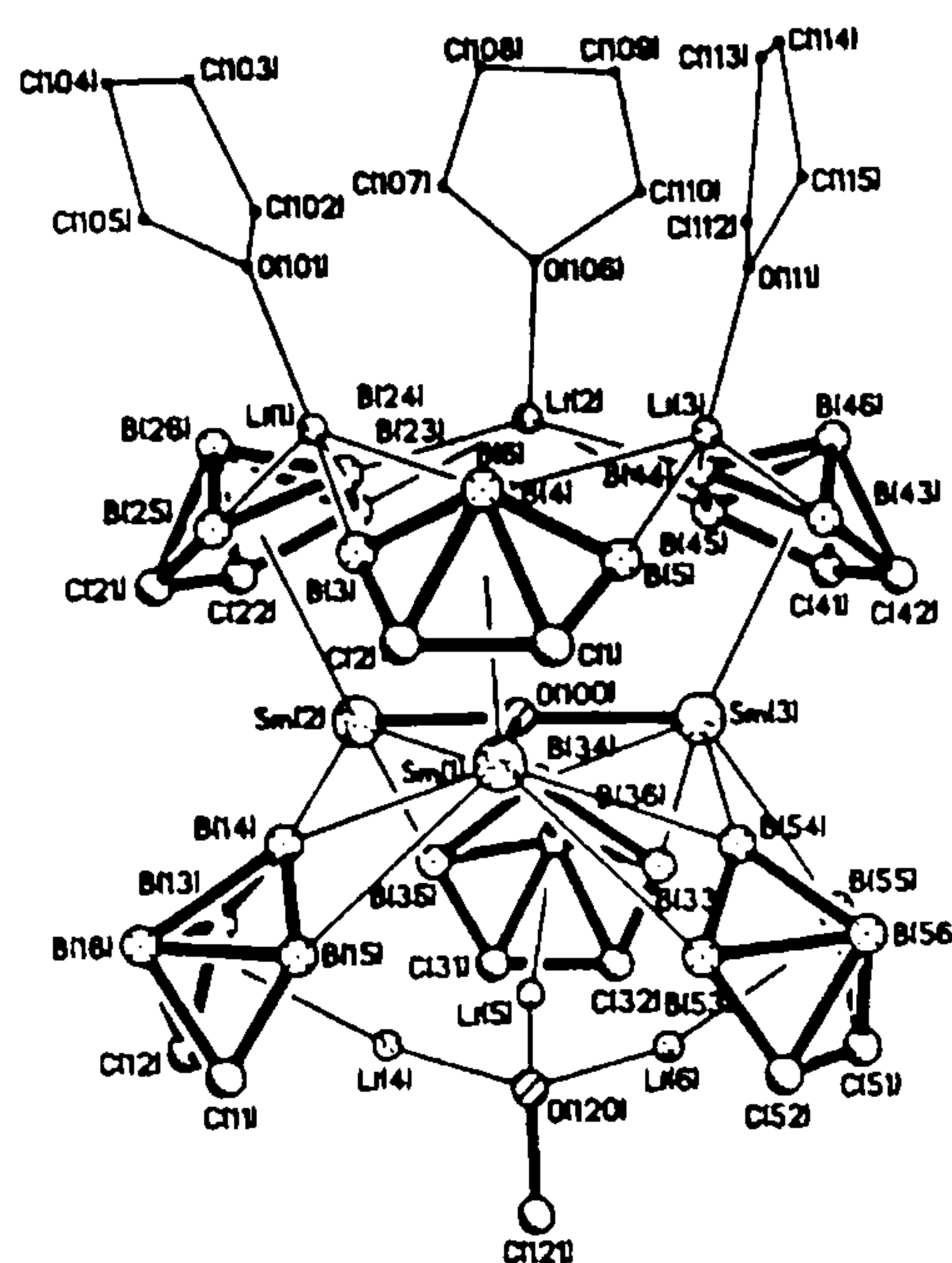


Figure 1.30 Molecular structure of the samarium complex $\{[\eta^5\text{-Sm}(\text{SiMe}_3)_2\text{C}_2\text{B}_4]\}_3[(\mu_2\text{-Li}(\text{SiMe}_3)_2\text{C}_2\text{B}_4)_3(\mu_3\text{-OMe})][\mu_2\text{-Li}(\text{C}_4\text{H}_8\text{O})]_3(\mu_3\text{-O})\}$. Taken from ref. 64.

In order to test this assumption Hosmane *et al.* have repeated these reactions using the TMEDA-solvated dilithiacarborane in place of the THF-solvated species, under reaction

conditions equivalent to those used in the synthesis of the tri-nuclear lanthanacarborane clusters.⁶⁹

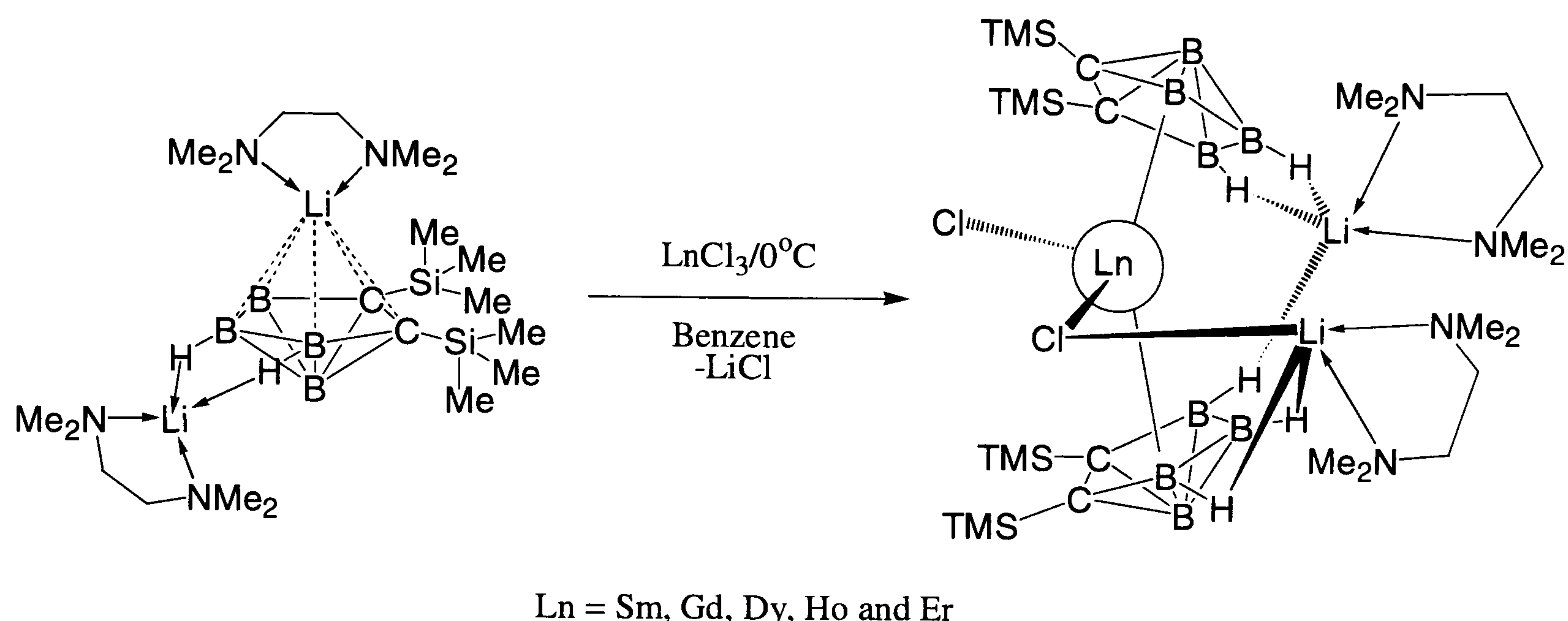


Figure 1.31 Scheme showing the reaction between the TMEDA-solvated dilithiacarborane and lanthanide trichlorides. Taken from ref. 69.

In the case where the TMEDA-solvated dilithiacarborane is used to react with lanthanide salts the products of the reaction are those that are expected, and all have similar structures to those found for the cyclopentadienide and larger 'C₂B₉' cages.⁷⁰ These results lend a great deal of weight to the assumption that THF is somehow degraded in the reaction scheme to form the tri-metallic systems.

1.4.2 Metallocarboranes Containing Actinide Group Metals.

The synthesis and reactivity of organoactinide complexes containing the dicarbollide ligand (C₂B₉H₁₁)²⁻, are remarkably unexplored.⁵¹ The uranium derivative [U(C₂B₉H₁₁)₂Cl₂]²⁻, was prepared and structurally characterised by Raymond almost 25 years ago.⁷¹ Since then not much work has appeared in the literature concerning the chemistry of actinacarboranes. Only in more recent times have similar anionic systems been made that are isostructural with the original uranium *bis*-dicarbollide. In 1996 and 1997 Abney and co workers have reported a series of compounds containing uranium(III), uranium (IV)⁷² and thorium (IV)⁷³. In general the actinide metal halide (Solvate), AcX_n(S)_m, was reacted with one (as in the case of UCl₃(THF)₄) or two equivalents (in the case of UBr₄(NCMe)₄ or ThCl₄) of the alkali dicarbollide salts M₂[C₂B₉H₁₁] (M = Li, Na and K) to form the half sandwich dicarbollide anionic complex [U(η⁵-C₂B₉H₁₁)I₂(THF)₂]⁻ and the anionic *bis*-dicarbollide complex [M(η⁵-C₂B₉H₁₁)₂X₂]²⁻ (M = U, X = Br; M = Th X = Cl). Examples of each structure are shown below. In the case of the

thorium complex, exchange of the chloride by bromide or iodide can be achieved by reacting the complex with the trimethylsilyl iodide or bromide respectively.

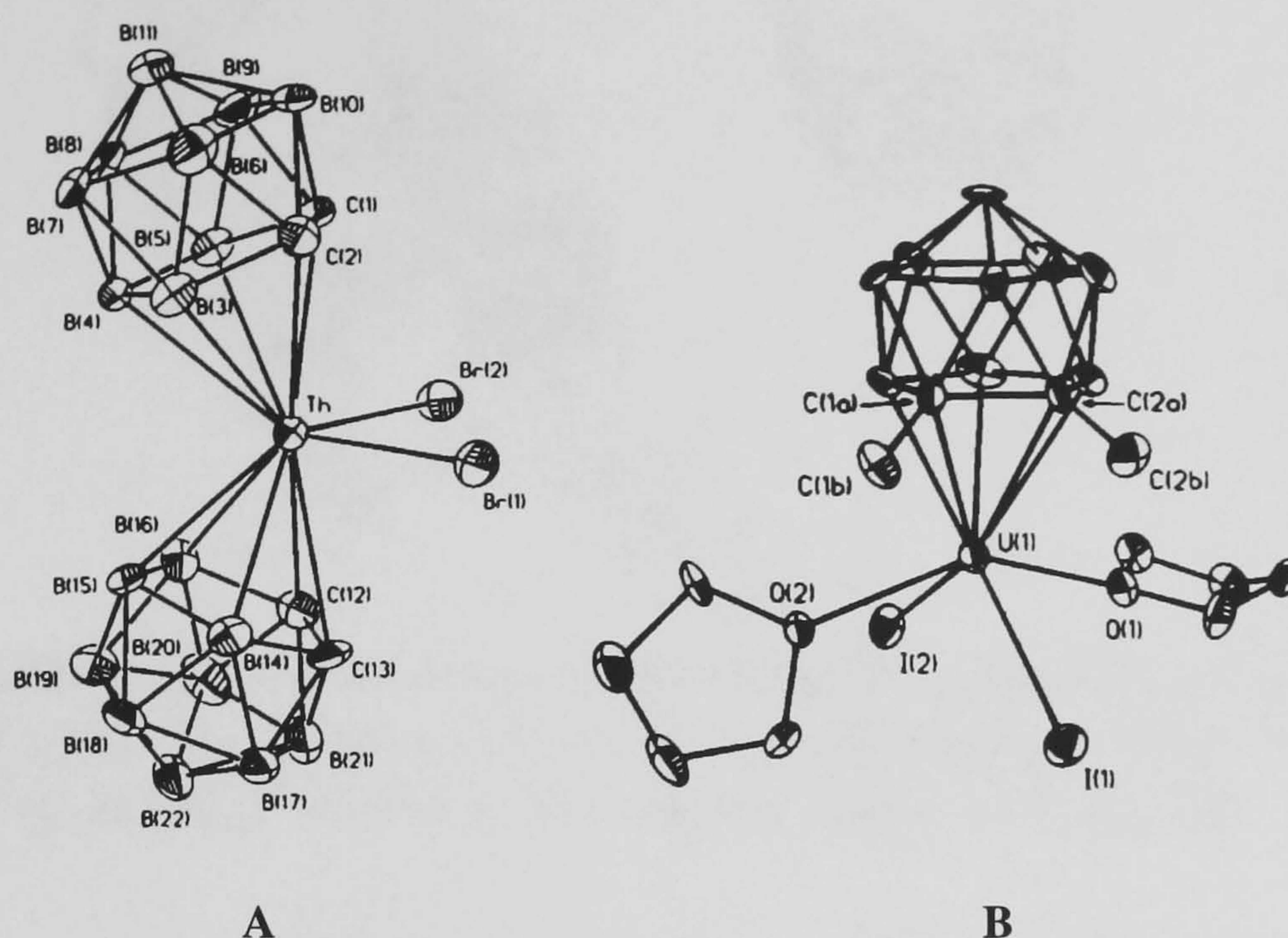


Figure 1.32 Diagram **A** shows the molecular structure of the dianion $[\text{Th}(\eta^5\text{-C}_2\text{B}_9\text{H}_{11})_2\text{Br}_2]^{2-}$, which is isostructural with the uranium derivatives. Taken from ref. 73. Diagram **B** shows the molecular structure of the mono anion $[\text{U}(\eta^5\text{-C}_2\text{B}_9\text{H}_{11})\text{I}_2(\text{THF})_2]^-$. Taken from ref. 72. In both cases the counter ion is PPN (not shown).

Welch and co-workers have also reported the synthesis of a uranium bis-dicarbollide complex.⁷⁴ The reaction between the diether-carborane $\text{Li}_2[7,8\text{-(CH}_2\text{OCH}_3)_2\text{-7,8-nido-C}_2\text{B}_9\text{H}_9]$ and UCl_4 in THF afforded the neutral bis carborane species $[\text{U}(\text{C}_2\text{B}_9\text{H}_9(\text{CH}_2\text{OCH}_3)_2)_2]$. Analysis of the complex showed that the complex can also be obtained as the bis (THF) adduct. It is thought that in the complex where there is no THF coordinated to the metal, simultaneous σ coordination of the pendent ether group to the metal centre occurs as the metal is considered to be relatively electron deficient, and a coordination sphere without such ligation is “*impossible to envisage*”.⁷⁴

More recently Xie and co-workers have explored the reaction of $\text{C}_2\text{B}_{10}\text{H}_{12}$ with UCl_4 in the presence of an excess of potassium metal.⁷⁵ It is well known that the *nido*- $\text{C}_2\text{B}_{10}\text{H}_{10}\text{R}_2^{2-}$ dianion, can bind to a transition metal in an η^6 -fashion.⁵¹ The reaction of *ortho*- $\text{C}_2\text{B}_{10}\text{H}_{12}$ and excess potassium metal in THF at room temperature followed by treatment with UCl_4 produced a compound that was shown by X-ray diffraction studies to be a centrosymmetric dimer with a bent sandwich structure. The molecular structure of the dimer comprises of two uranium atoms bound to one [*nido*- $\eta^6\text{-C}_2\text{B}_{10}\text{H}_{12}$]²⁻ ligand and one [*arachno*- $\eta^7\text{-C}_2\text{B}_{10}\text{H}_{12}$]⁴⁻ ligand.

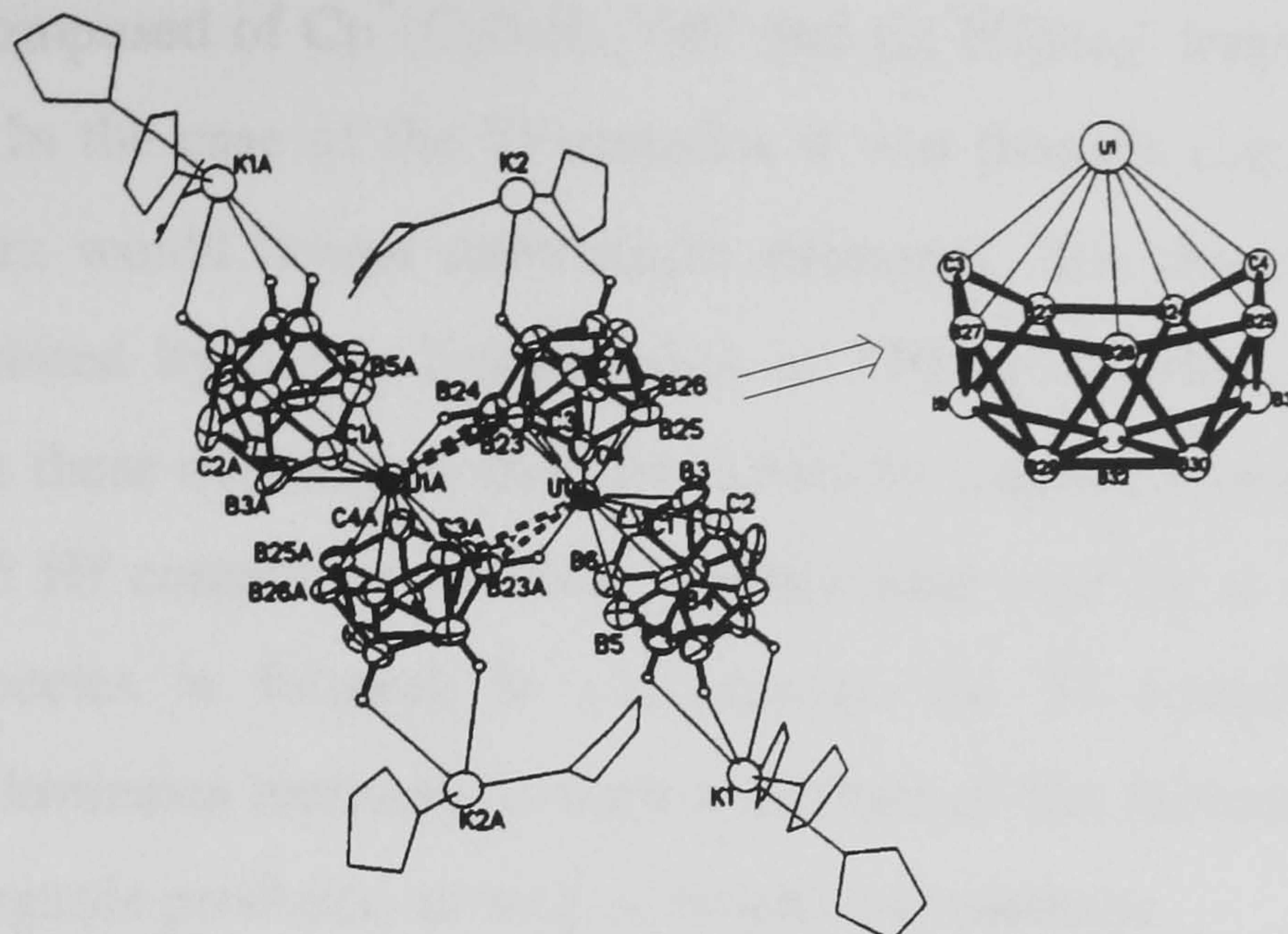


Figure 1.33. Molecular structure of the complex $[\{[(\eta^7\text{-C}_2\text{B}_{10}\text{H}_{12})(\eta^6\text{-C}_2\text{B}_{10}\text{H}_{12})\text{U}][\text{K}_2(\text{THF})_5]\}_2]$. The shape and coordination environment of the ‘C₂B₅’ face on the $(\eta^7\text{-C}_2\text{B}_{10}\text{H}_{12})^{4-}$ ligand is also shown. Taken from ref. 75.

The two sandwich complexes are held together by two B-H agostic interactions from the neighbouring ‘C₂B₅’ bonding face of the *arachno*-C₂B₁₀H₁₂⁴⁻ ligand. The overall charge of the dimer is balanced by coordination of a K(THF)₂⁺ moiety to both *arachno* ligands, and a K(THF)₃⁺ moiety to both *nido* ligands, as can be seen in the diagram above. This report is the first example of a metal complex containing the $\eta^7\text{-C}_2\text{B}_{10}\text{H}_{12}^{4-}$ ligand. The shape of the ‘C₂B₅’ face of the *arachno* ligand and the coordination environment of the *arachno* ligand are also shown in Figure 1.33.

1.4.3 Metallocarboranes Containing Group 4 Transition Metals.

Previous to the work of Bercaw *et al.* with the scandium dicarbollide systems, Jordan and co-workers investigated the reactions of C₂B₉H₁₃ with Cp^{*}MMe₃ to form complexes of the form $[(\text{Cp}^*)(\text{C}_2\text{B}_9\text{H}_{11})\text{M}(\text{Me})]_n$ (M = Ti,⁷⁶ n = 1; M = Zr⁷⁷ or Hf,⁷⁷ n = 2). The molecular structure of dimeric $[(\text{Cp}^*)(\text{C}_2\text{B}_9\text{H}_{11})\text{Hf}(\text{Me})]_2$ is shown in Figure 1.34.

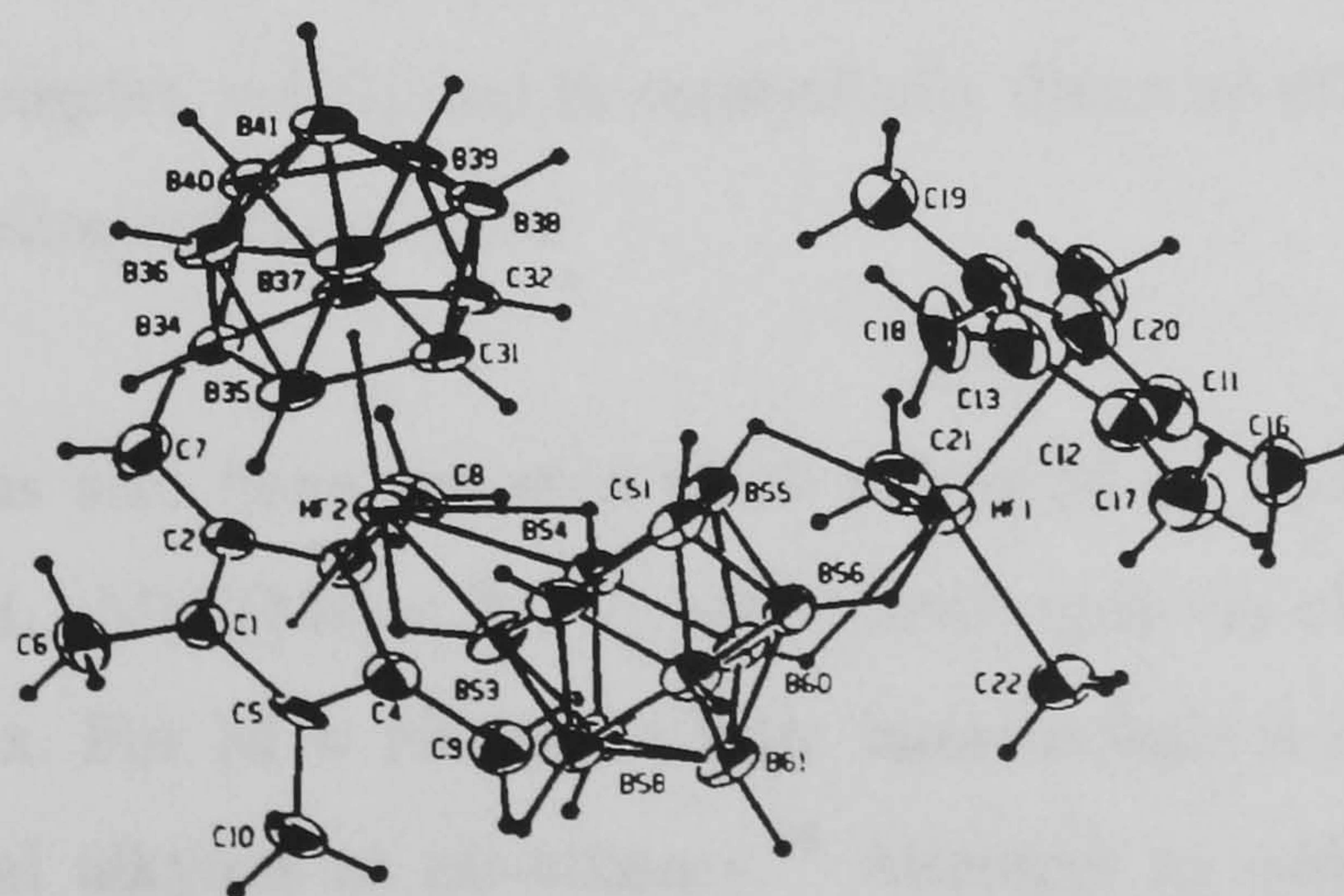


Figure 1.34 Molecular structure of the dimer $[(\text{Cp}^*)(\text{C}_2\text{B}_9\text{H}_{11})\text{Hf}(\text{Me})]_2$. Taken from ref. 77.

The structure is composed of $\text{Cp}^*(\text{C}_2\text{B}_9\text{H}_{11})\text{Hf}^+$ and $\text{Cp}^*\text{HfMe}_2^+$ fragments bridged by a single $\text{C}_2\text{B}_9\text{H}_{11}^{2-}$ ligand. In the case of the Ti complex it was thought that due to the smaller metal radius this complex would favour monomeric structures. The dimerisation of the Zr and Hf complexes is inhibited by donor ligands such as THF and PMe_3 coordinating to the metal centre. In all cases these complexes undergo thermally induced elimination of methane. In the case of the Zr and Hf complexes methane is eliminated over 2h at 45°C , and a methylene, $-\text{CH}_2-$, bridged species is formed. In comparison, the Ti complex is unstable at room temperature and eliminates methane to form a mixture of the fulvene ('tuck-in') complex and unidentifiable inorganic products, as well as ethane and methane.

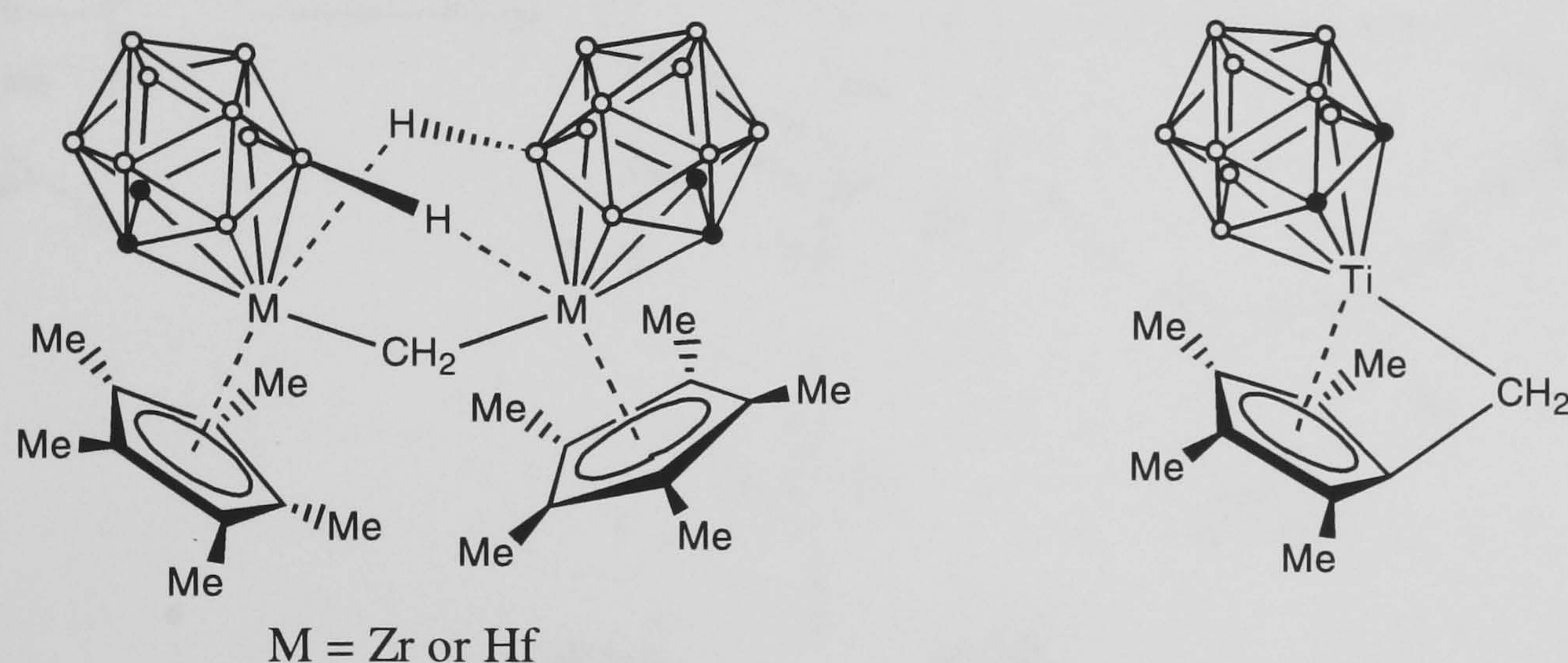


Figure 1.35 Structural diagram of the products from the thermal degradation of $[(\text{Cp}^*)(\text{C}_2\text{B}_9\text{H}_{11})\text{Ti}(\text{Me})]$ or $[(\text{Cp}^*)(\text{C}_2\text{B}_9\text{H}_{11})\text{M}(\text{Me})]_2$ ($\text{M} = \text{Zr or Hf}$). Taken from ref. 76 and 77 respectively.

All three methyl compounds $[(\text{Cp}^*)(\text{C}_2\text{B}_9\text{H}_{11})\text{M}(\text{Me})]_n$ insert 2-butyne into the metal methyl bonds to form monomeric alkenyl complexes $[(\text{Cp}^*)(\text{C}_2\text{B}_9\text{H}_{11})\text{M}[\text{C}(\text{Me})=\text{CMe}_2]]$. The Zr and Hf complexes are both moderately active ethylene polymerisation catalysts, as well as oligomerisation catalysts for propylene. The Ti complex also reacts with ethylene to form propene and $[(\text{Cp}^*)(\text{C}_2\text{B}_9\text{H}_{11})\text{M}(\text{CH}_2\text{CH}_3)]$ via ethylene insertion. β -hydride elimination and rapid insertion of the resulting hydride $[(\text{Cp}^*)(\text{C}_2\text{B}_9\text{H}_{11})\text{M}(\text{H})]$ was not observed. In a secondary process the complex was found to catalytically dimerise ethylene to 1-butene via an insertion and β -hydride elimination process.

The hydride complex has also been reported to be produced by reacting monomeric alkenyl complexes $[(\text{Cp}^*)(\text{C}_2\text{B}_9\text{H}_{11})\text{M}[\text{C}(\text{Me})=\text{CMe}_2]]$ with dihydrogen via elimination of 2-methyl-2-butene from the complex. For $\text{M} = \text{Hf}$ the hydride intermediate is capable of catalysing the hydrogenation of internal alkynes to *cis*-alkenes.⁷⁸ Attempts to isolate the hydride complex result in the isolation of the complex $(\text{Cp}^*)(\text{C}_2\text{B}_9\text{H}_{11})\text{Hf}(\mu\text{-}\eta^5\text{:}\eta^5\text{-C}_2\text{B}_9\text{H}_{10})\text{Hf}(\text{Cp}^*)(\text{H})$. The

complex has a dinuclear structure in which a $(\text{Cp}^*)(\text{C}_2\text{B}_9\text{H}_{10})\text{Hf}(\text{H})$ is bound to a second $(\text{Cp}^*)(\text{C}_2\text{B}_9\text{H}_{11})\text{Hf}$ via a dicarbollide carbon. This complex is formed by the reversible elimination of H_2 from two molecules of the hydride. The hafnium complex $[(\text{Cp}^*)(\text{C}_2\text{B}_9\text{H}_{11})\text{Hf}\{\text{C}(\text{Me})=\text{CMe}_2\}]$ has also been found to catalyse the regioselective dimerisation of terminal alkynes, $\text{RC}\equiv\text{CH}$, to 2,4-disubstituted 1-buten-3-yne, $\text{CH}_2=\text{CH}(\text{R})\text{C}\equiv\text{CR}$.⁷⁹

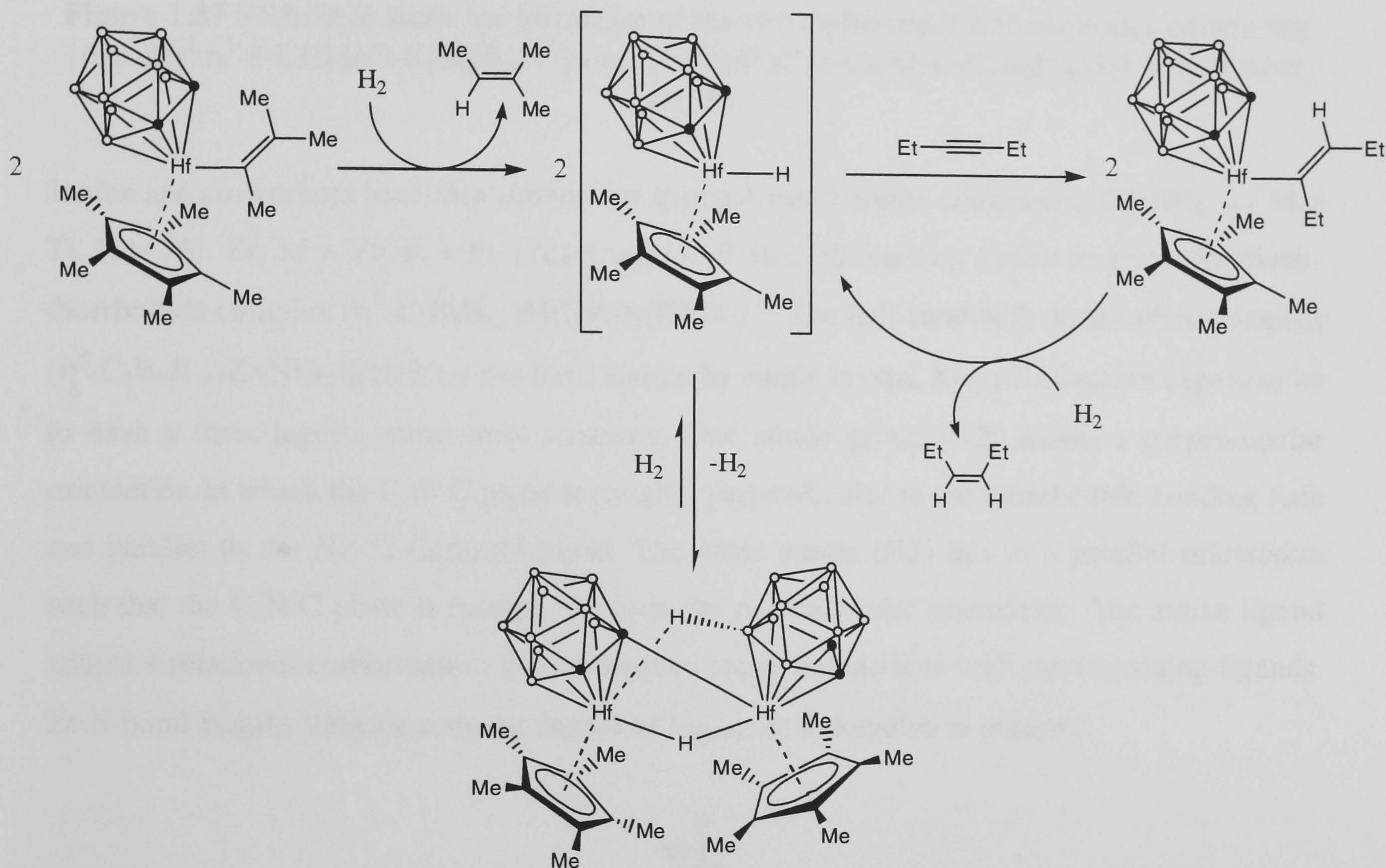


Figure 1.36 Scheme showing the formation of the hafnium dicarbollide hydride complex. The hydride intermediate is capable of forming the dinuclear complex $[(\text{Cp}^*)(\text{C}_2\text{B}_9\text{H}_{11})\text{Hf}(\mu\text{-}\eta^5\text{:}\eta^5\text{-C}_2\text{B}_9\text{H}_{10})\text{Hf}(\text{Cp}^*)(\text{H})]$ by loss of H_2 . The hydride intermediate is capable of catalysing the hydrogenation of internal alkynes to *cis*-alkenes. Taken from ref. 78.

The titanium complex $[(\text{Cp}^*)(\text{C}_2\text{B}_9\text{H}_{11})\text{Ti}(\text{Me})]$ has been shown to undergo insertion reactions with acetonitrile to form the azomethine and azomethine acetonitrile adduct complexes, $[(\text{Cp}^*)(\text{C}_2\text{B}_9\text{H}_{11})\text{Ti}(\text{NC}(\text{Me})\text{Me})]$ and $[(\text{Cp}^*)(\text{C}_2\text{B}_9\text{H}_{11})\text{Ti}(\text{NC}(\text{Me})\text{Me})(\text{NCMe})]$ respectively.⁷⁶ The Ti complex has more recently been shown to insert carbon monoxide into the Ti-Me bond to yield the two complexes $[(\text{Cp}^*)(\eta^5\text{:}\eta^1\text{-8-CHMeO-C}_2\text{B}_9\text{H}_{10})\text{Ti}]$ and $[(\text{Cp}^*)(\eta^5\text{:}\eta^1\text{-4-CHMeO-C}_2\text{B}_9\text{H}_{10})\text{Ti}]$.⁸⁰ Both carboranes contain a linked carborane-alkoxide ligand and differ only in the site of ligand attachment to the cage. NMR experiments performed by Jordan *et al.* have shown that the two complexes result from a common intermediate, as shown below.

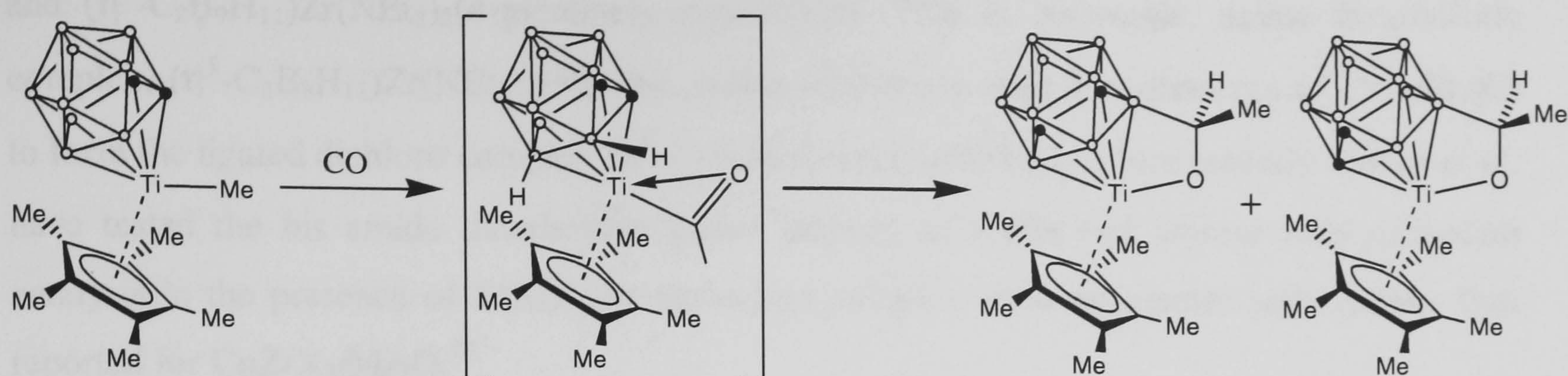


Figure 1.37 Scheme to show the formation of the two carborane linked alkoxides complexes $[(Cp^*)(\eta^5:\eta^1\text{-}8\text{-CHMeO-C}_2\text{B}_9\text{H}_{10})\text{Ti}]$ and $[(Cp^*)(\eta^5:\eta^1\text{-}4\text{-CHMeO-C}_2\text{B}_9\text{H}_{10})\text{Ti}]$. Taken from ref. 80

Jordan and co-workers have also shown that group 4 metal amide complexes, $[M(NR_2)_4]$ ($M = \text{Ti}, R = \text{Me}, \text{Et}; M = \text{Zr}, R = \text{Et}$) react with $C_2B_9H_{13}$, eliminating amine to yield the monodcarbollide complex $(\eta^5\text{-C}_2\text{B}_9\text{H}_{11})M(NR_2)_2(NHR_2)$.⁸¹ The half-sandwich dicarbollide complex $(\eta^5\text{-C}_2\text{B}_9\text{H}_{11})\text{Zr}(\text{NEt}_2)_2(\text{NHEt}_2)$ has been shown by single crystal X-ray diffraction experiments to have a three-legged piano stool structure. One amide group (N2) adopts a perpendicular orientation in which the C-N-C plane is roughly perpendicular to the dicarbollide bonding face and parallel to the N2-Zr-Centroid plane. The other amide (N3) lies in a parallel orientation such that the C-N-C plane is rotated 75° from the perpendicular orientation. The amine ligand adopts a rotational conformation that minimises steric interactions with the remaining ligands. Zr-N bond lengths indicate a strong degree of $N_{\text{amide}}\text{-Zr } \pi$ donation is present.

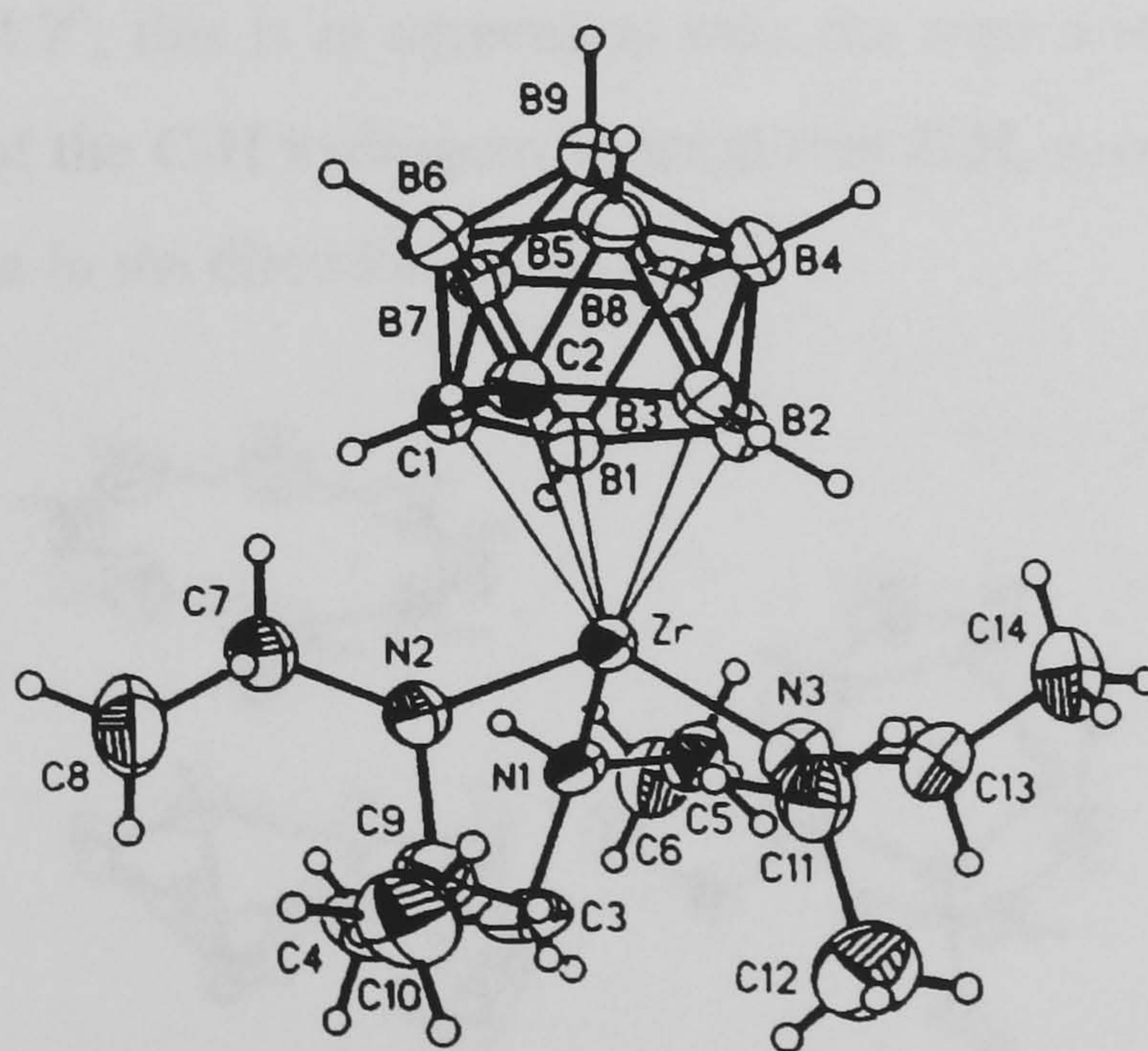


Figure 1.38 Molecular structure of $(\eta^5\text{-C}_2\text{B}_9\text{H}_{11})\text{Zr}(\text{NEt}_2)_2(\text{NHEt}_2)$. Taken from ref. 81.

The amine complex $(\eta^5\text{-C}_2\text{B}_9\text{H}_{11})\text{Zr}(\text{NEt}_2)_2(\text{NHEt}_2)$ has also been shown to undergo facile replacement of the amine ligand by THF and 4-picoline, yielding $(\eta^5\text{-C}_2\text{B}_9\text{H}_{11})\text{Zr}(\text{NEt}_2)_2(\text{THF})$

and $(\eta^5\text{-C}_2\text{B}_9\text{H}_{11})\text{Zr}(\text{NEt}_2)_2(4\text{-picoline})_2$ respectively. The Zr bis-amide, amine dicarbollide complex, $(\eta^5\text{-C}_2\text{B}_9\text{H}_{11})\text{Zr}(\text{NEt}_2)_2(\text{NHEt}_2)$, reacts selectively with 2 equivalents of $[\text{NH}_2\text{Et}_2]\text{Cl}$ to form the ligated dichloro complex $(\eta^5\text{-C}_2\text{B}_9\text{H}_{11})\text{Zr}(\text{Cl})_2(\text{NHEt}_2)_2$. More recently Jordan *et al.* have tested the bis amide dicarbollide amine adducts as olefin and styrene polymerisation catalysts in the presence of MAO, the zirconium complex showing greater activity than that reported for $\text{CpZrX}_3/\text{MAO}$.⁸²

Work from the groups of both M. F. Hawthorne⁸³ and Y. Do⁸⁴ has incorporated porphyrin ring systems into metallacarborane species with the synthesis of a zirconaporphyrin-dicarbollide complex. The reaction of $\text{Zr}(\text{OEP})\text{Cl}_2$, (OEP = dianion of octaethylporphyrin) with either the sodium⁸³ or thallium⁸⁴ dicarbollide salts, $\text{M}_2[\text{C}_2\text{B}_9\text{H}_{11}]$, yields the metallaporphyrin complex $(\eta^5\text{-C}_2\text{B}_9\text{H}_{11})\text{Zr}(\text{OEP})$. An interesting feature of this complex is that due to shielding of the CH hydrogens by the aromatic OEP ligand, ^1H NMR spectra shows a single resonance for this group at -2.84ppm , such resonances are typically found at 2-4ppm.

Group 4 complexes of the small carborane ' C_2B_4 ' have been known for some time and work in this area has been continued by several groups. The first complex of this type was the titanacarborane, $(\eta^8\text{-C}_8\text{H}_8)\text{Ti}[(\text{Et})_2\text{C}_2\text{B}_4\text{H}_4]$,⁸⁵ the solid state structure is shown in Figure 1.39. The cyclooctatetraene ring is planar within experimental error and is nearly parallel to the C_2B_3 ring of the carborane. The C_8H_8 ring hydrogen atoms are bent out of the C_8 plane towards the metal, by an average of 4.7° ; this is in agreement with the argument of Elian *et al.*,⁸⁶ which holds that the deflection of the C-H hydrogens in large ring C_nH_n π -complexes of the first row transition metals should be in the direction of the metal.

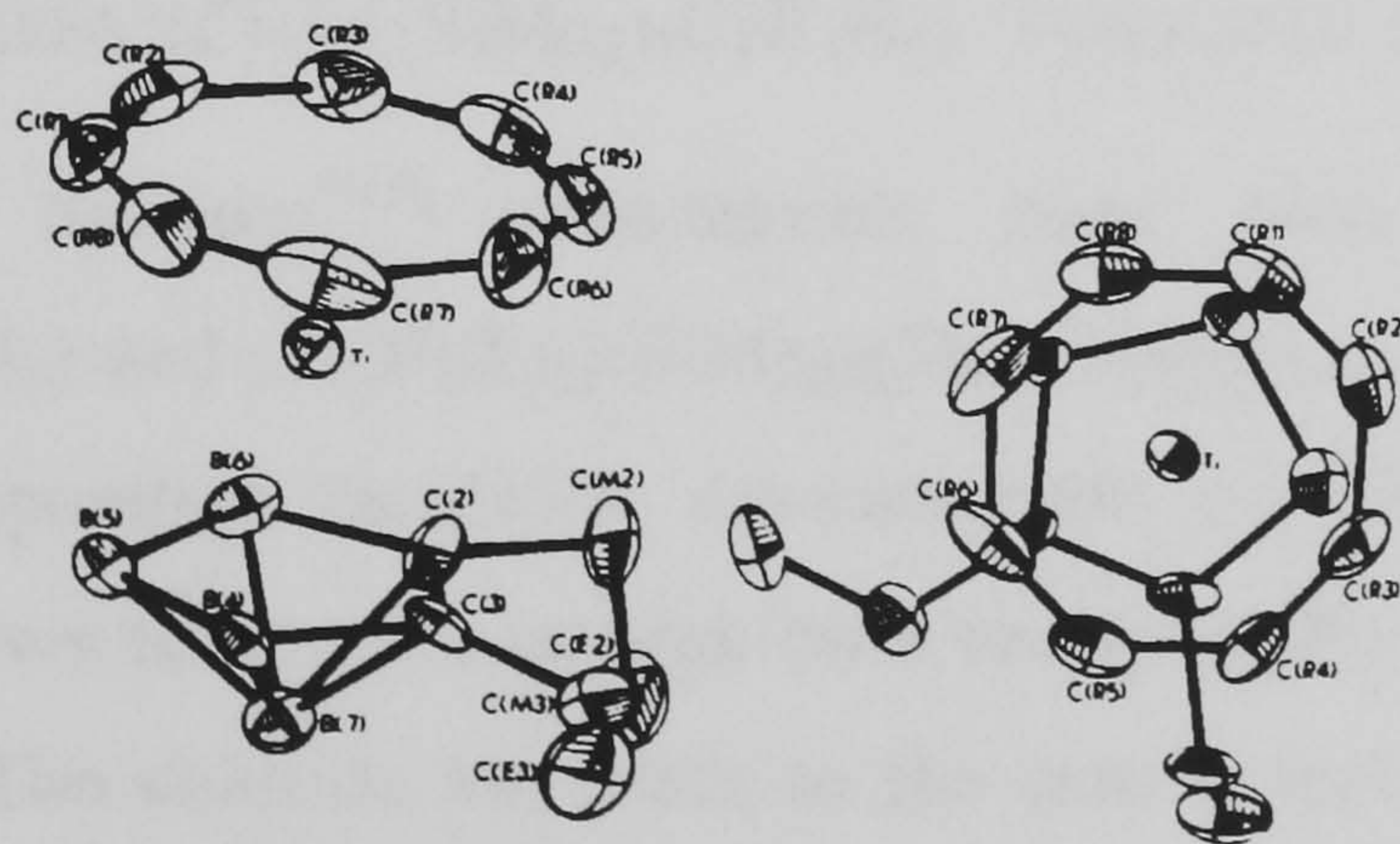


Figure 1.39 Molecular structure of $(\eta^8\text{-C}_8\text{H}_8)\text{Ti}[(\text{Et})_2\text{C}_2\text{B}_4\text{H}_4]$. In the right view the C_8 and C_2B_3 rings are projected onto the same plane, so that ring sizes are directly comparable. Taken from ref. 85.

Since then work with C_2B_4 carboranes and group 4 complexes has continued with the major contribution being from the group of Hosmane. Treatment of anhydrous Cp_2TiCl_2 with the

lithio carborane $\text{Li}_2[(\text{SiMe}_3)\text{C}_2\text{B}_4\text{H}_4]$ in a molar ratio of 1:1 produced dihydrofulvene $(\text{C}_5\text{H}_5)_2$ and a novel dimeric Ti(III) sandwich complex $[\text{commo-CpTi}\{(\text{SiMe}_3)_2\text{C}_2\text{B}_4\text{H}_4\}]_2$.⁸⁷ The molecular structure of this complex has been revealed to be a dimer coupled by direct interaction of the Ti(III) centres to the carborane face hydrogens. Chemical oxidation of this Ti(III) species is achieved by reacting the dimer with TiCl_4 . This results in the formation of a monomeric Ti(IV) metallocene, $\text{CpTi}[(\text{SiMe}_3)_2\text{C}_2\text{B}_4\text{H}_4](\text{Cl})(\text{THF})$. In a subsequent paper, Hosmane describes the chemistry of Ti(III) carborane complexes where the carborane is the unsymmetrical $[(\text{SiMe}_3)(\text{Me})\text{C}_2\text{B}_4\text{H}_4]$ ligand.⁸⁸ Reacting TiCl_3 with two equivalents of the TMEDA solvated dilithio carborane complex $(\text{TMEDA})_2\text{Li}_2[(\text{SiMe}_3)(\text{Me})\text{C}_2\text{B}_4\text{H}_4]$ or $(\text{TMEDA})_2\text{Li}_2[(\text{SiMe}_3)_2\text{C}_2\text{B}_4\text{H}_4]$ results in the formation of the dimeric Ti(III) species $[\text{Li}(\text{TMEDA})]_2[\text{Ti}\{(\text{SiMe}_3)(\text{Me})\text{C}_2\text{B}_4\text{H}_4\}_2]_2$ and the monomeric Ti(III) species $[\text{Li}(\text{TMEDA})]_2[(\text{Cl})\text{Ti}\{(\text{SiMe}_3)_2\text{C}_2\text{B}_4\text{H}_4\}_2]$ respectively. This is in contrast with the reaction between TiCl_3 and the 'carbons-apart' $(\text{TMEDA})_2\text{Li}_2[(\text{SiMe}_3)_2\text{C}_2\text{B}_4\text{H}_4]$, which yields the corresponding *mono-carborane* $(\text{TMEDA})(\text{Cl})\text{Ti}[(\text{SiMe}_3)_2\text{C}_2\text{B}_4\text{H}_4]$ (Figure 1.40).

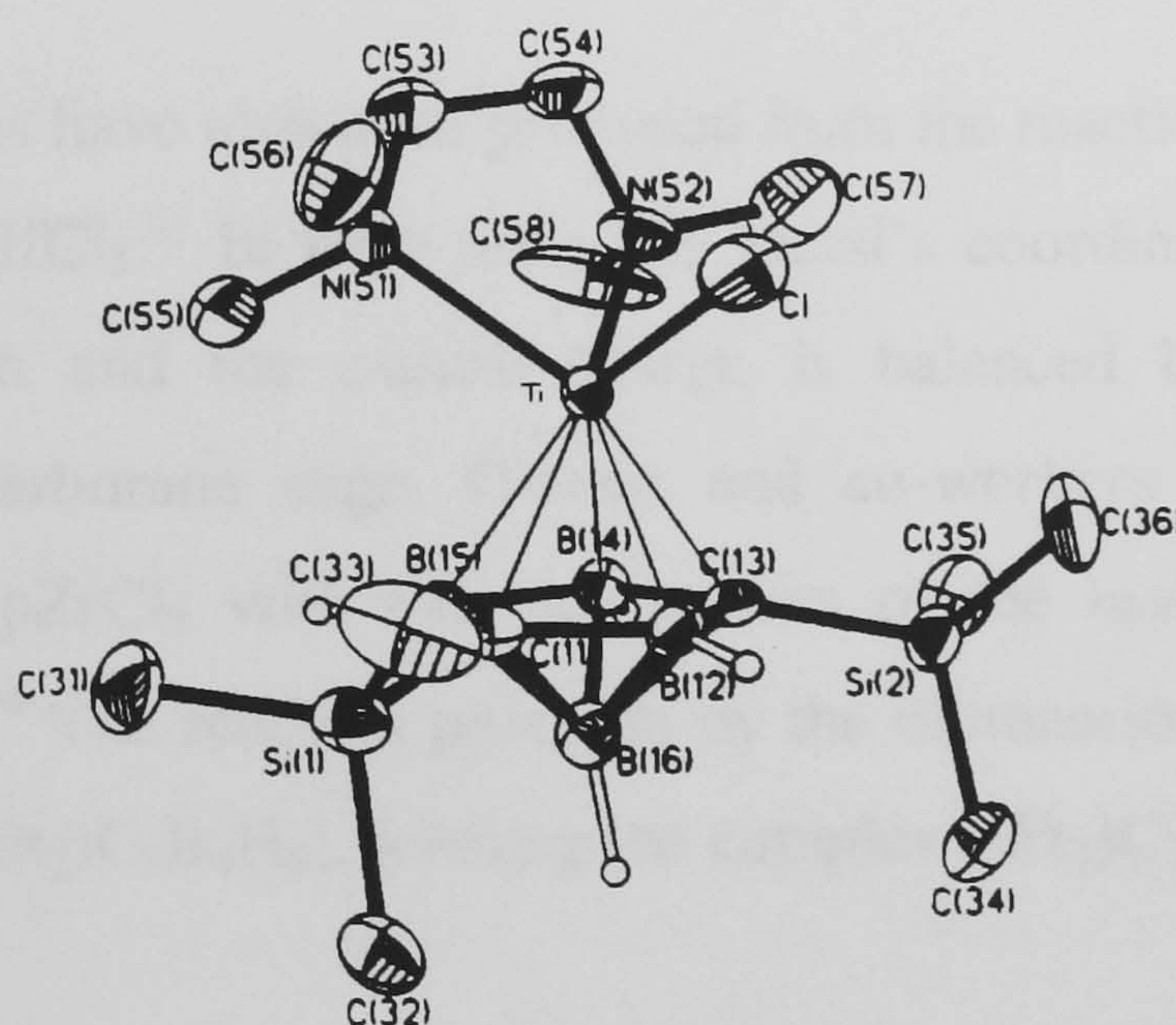


Figure 1.40 Molecular structure of the 'carbons-apart' complex $(\text{TMEDA})(\text{Cl})\text{Ti}[(\text{SiMe}_3)_2\text{C}_2\text{B}_4\text{H}_4]$. Taken from ref.88.

Both zirconium⁸⁹ and hafnium^{90,91} tetrachloride have been shown to react with $(\text{THF})_2\text{Li}_2[(\text{SiMe}_3)_2\text{C}_2\text{B}_4\text{H}_4]$ and $(\text{THF})_2\text{Li}_2[(\text{SiMe}_3)(\text{Me})\text{C}_2\text{B}_4\text{H}_4]$ in a 1:2 ratio resulting in the formation of the corresponding sandwich *bis-carborane* complexes. In both cases the complexes have been shown to be isostructural, both incorporating one equivalent of LiCl in the molecular structure. The chloride ion binds to the central metal atom as does one THF ligand, thus resulting in a *pseudo-tetrahedral* geometry around the metal. The lithium atom balances the charge of the molecule and coordinates to the two cages via B-H agostic interactions. The only difference between the two different types of complex i.e. $\text{Cl}(\text{THF})\text{M}[(\text{SiMe}_3)(\text{Me})\text{C}_2\text{B}_4\text{H}_4]_2\cdot[\text{Li}(\text{THF})_n]$ and $\text{Cl}(\text{THF})\text{M}[(\text{SiMe}_3)_2\text{C}_2\text{B}_4\text{H}_4]_2\cdot[\text{Li}(\text{THF})_n]$ is the value of n . When the carborane is $[(\text{SiMe}_3)(\text{Me})\text{C}_2\text{B}_4\text{H}_4]$ $n = 1$, and when the carborane

ligand is $[(\text{SiMe}_3)_2\text{C}_2\text{B}_4\text{H}_4]$, $n = 2$.⁹² Initial attempts to react the symmetrical zirconacarborane complex $\text{Cl}(\text{THF})\text{Zr}[(\text{SiMe}_3)_2\text{C}_2\text{B}_4\text{H}_4]_2 : [\text{Li}(\text{THF})_2]$ with one equivalent of the Grignard $\text{Me}_3\text{SiCH}_2\text{MgCl}$ resulted in the exchange of the coordinated $[\text{Li}(\text{THF})]^+$ by the non-coordinating $[\text{Mg}(\text{THF})_6]^{2+}$ and the formation of $\{\text{Cl}(\text{THF})\text{M}[(\text{SiMe}_3)_2\text{C}_2\text{B}_4\text{H}_4]\}_2 : [\text{Mg}(\text{THF})_6]$. Addition of excess Grignard results in the formation of the complex double salt shown in Figure 1.41.

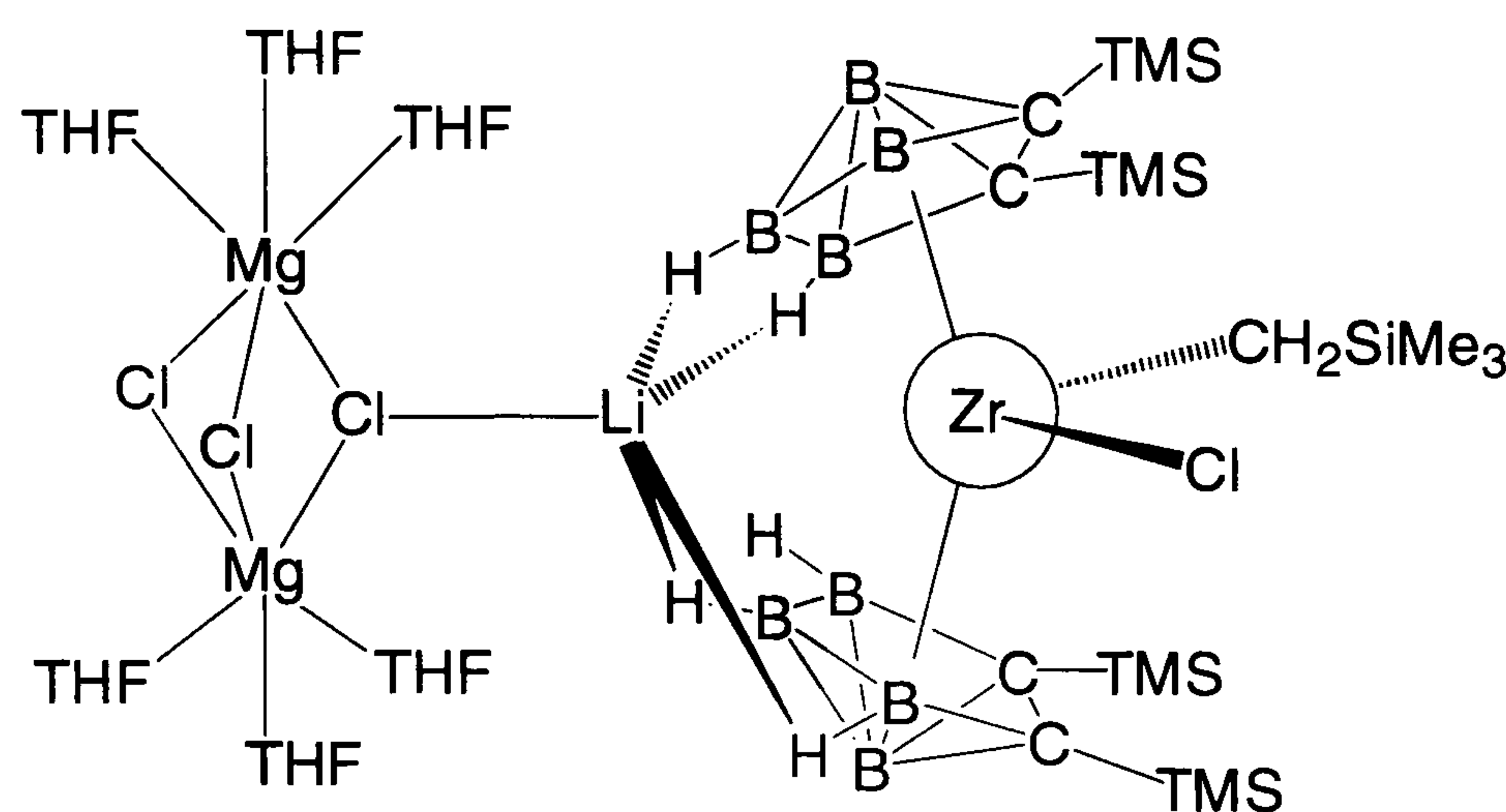


Figure 1.41 Diagram of the complex double salt. Taken from ref. 91.

Mixed sandwich complexes have also been produced from the reaction of the dilithiacarborane with Cp^*ZrCl_3 ⁹³ and Cp^*HfCl_3 .⁹¹ In both cases the metal's coordination is completed by the ligation of a chloride ion and the overall charge is balanced by the coordination of a $[\text{Li}(\text{THF})]^+$ unit to the carborane cage. Grimes and co-workers have synthesised similar complexes by reacting CpZrCl_3 with two equivalents of the *mono*-sodium carborane salt $\text{Na}[(\text{Et}_2)\text{C}_2\text{B}_4\text{H}_5]$ in THF.⁹⁴ The reaction proceeds by the elimination of NaCl and a molecule of the neutral carborane $[(\text{Et}_2)\text{C}_2\text{B}_4\text{H}_6]$, forming the complex $[(\text{Et}_2)\text{C}_2\text{B}_4\text{H}_4]\text{Zr}(\text{Cp}^*)\text{Cl}(\text{THF})$.

1.4.4 Metallocarboranes Containing Group 5 Transition Metals.

Compared to the chemistry of the group 4 metals, group 5 metal complexes of carboranes are less well documented. The only example of a vanadacarborane system is the complex $(\eta^8\text{-C}_8\text{H}_8)\text{V}[(\text{Et})_2\text{C}_2\text{B}_4\text{H}_4]$ ⁸⁵ which is iso-structural to the titanium complex $(\eta^8\text{-C}_8\text{H}_8)\text{Ti}[(\text{Et})_2\text{C}_2\text{B}_4\text{H}_4]$.⁸⁵ Work on tantalum and niobium carborane systems is also very sparse although complexes have been produced using both the ' C_2B_9 ' and ' C_2B_4 ' ligand systems.

Jordan *et al.* have reacted the dilithio carborane salt $\text{Li}_2[\text{C}_2\text{B}_9\text{H}_{11}]$ with TaCl_5 to form the three-legged piano stool complex $(\eta^5\text{-C}_2\text{B}_9\text{H}_{11})\text{TaCl}_3$,⁹⁵ which is shown in Figure 1.42. The dicarbollide is bound to the tantalum atom in a nearly symmetrical η^5 - fashion, and $\text{Cl}(3)$

eclipses B(8) of the dicarbollide ligand, while Cl(1) and Cl(2) eclipse the C-B bonds. As a result of this arrangement and the longer B-H bonds (vs. C-H distances), steric interaction between the cage and Cl(3) result in Cl(3) bending further away from the dicarbollide ligand. The structure of $(\eta^5\text{-C}_2\text{B}_9\text{H}_{11})\text{TaCl}_3$ is analogous to that of the iso-electronic complex CpTiCl_3 .⁹⁶

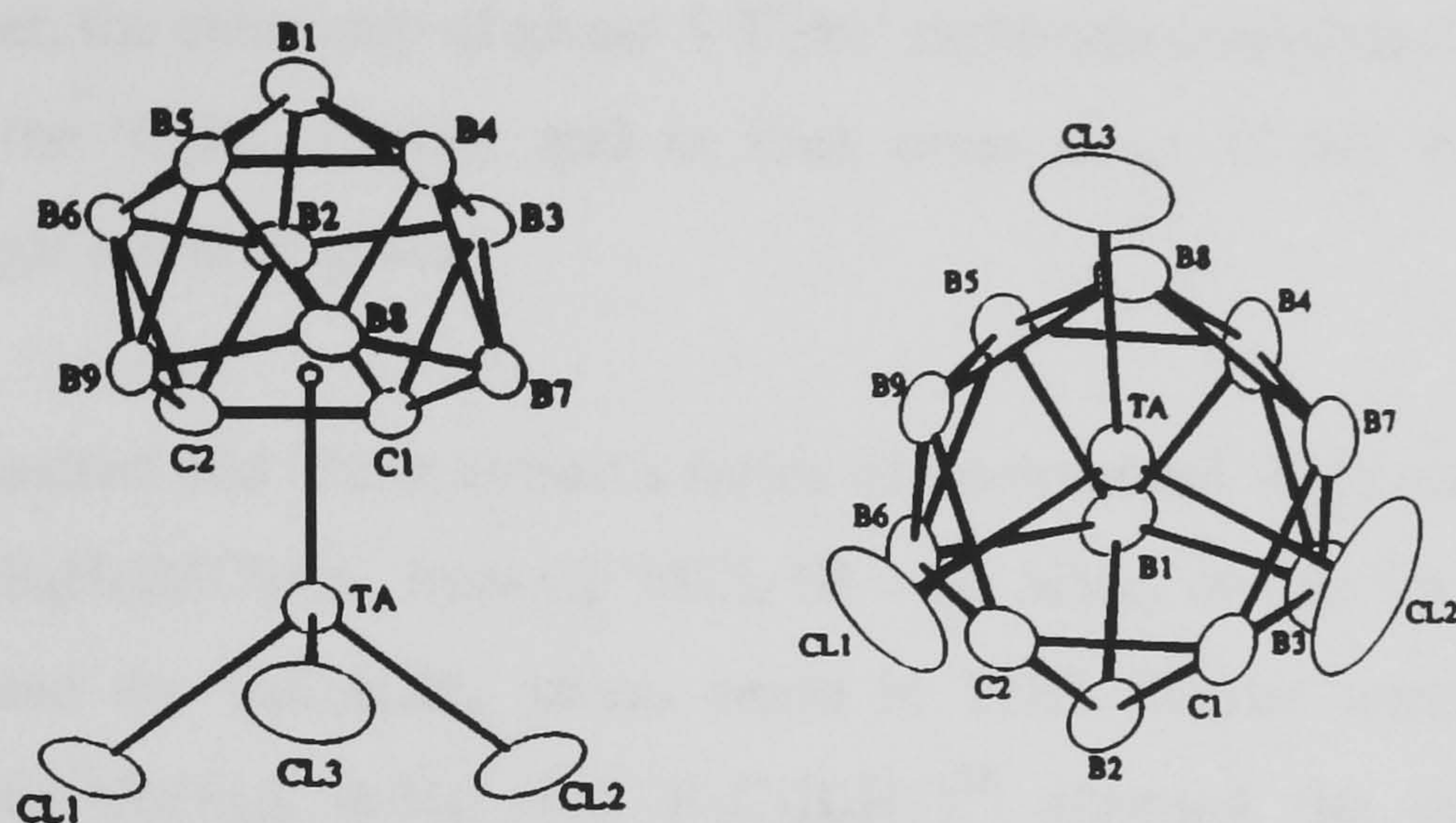


Figure 1.42. Structure of $(\eta^5\text{-C}_2\text{B}_9\text{H}_{11})\text{TaCl}_3$, viewed parallel to and along the Ta-dicarbollide_{centroid} axis. Taken from ref. 95

The trichloro- complex shown above reacts with $\text{Tl}(\text{MeC}_5\text{H}_4)$ to eliminate TlCl and form the mixed metallocene complex $(\eta^5\text{-C}_2\text{B}_9\text{H}_{11})(\text{Me-Cp})\text{TaCl}_2$. This compound can also be formed from the reaction of CpTaCl_4 with $\text{Li}_2[\text{C}_2\text{B}_9\text{H}_{11}]$. Both the tri-chloro tantalum dicarbollide and the methyl-Cp complex react with methyl magnesium iodide to form the corresponding tri- and di-methyl complexes, $(\eta^5\text{-C}_2\text{B}_9\text{H}_{11})\text{TaMe}_3$ and $(\eta^5\text{-C}_2\text{B}_9\text{H}_{11})(\text{Me-Cp})\text{TaMe}_2$ respectively. The trichloro complex was subsequently shown to react with $[\text{PPN}][\text{Tl}(\text{C}_2\text{B}_9\text{H}_{11})]$ to yield the *bis*-dicarbollide complex $[(\text{C}_2\text{B}_9\text{H}_{11})_2\text{Ta}(\text{Cl})_2][\text{PPN}]$.⁹⁷ As with the neutral Cp tantalum carborane complex, the anionic *bis*-carborane complex can be methylated to form the tantalum dimethyl species $[(\text{C}_2\text{B}_9\text{H}_{11})_2\text{Ta}(\text{Me})_2]^-$, the structure of which is shown in Figure 1.43.

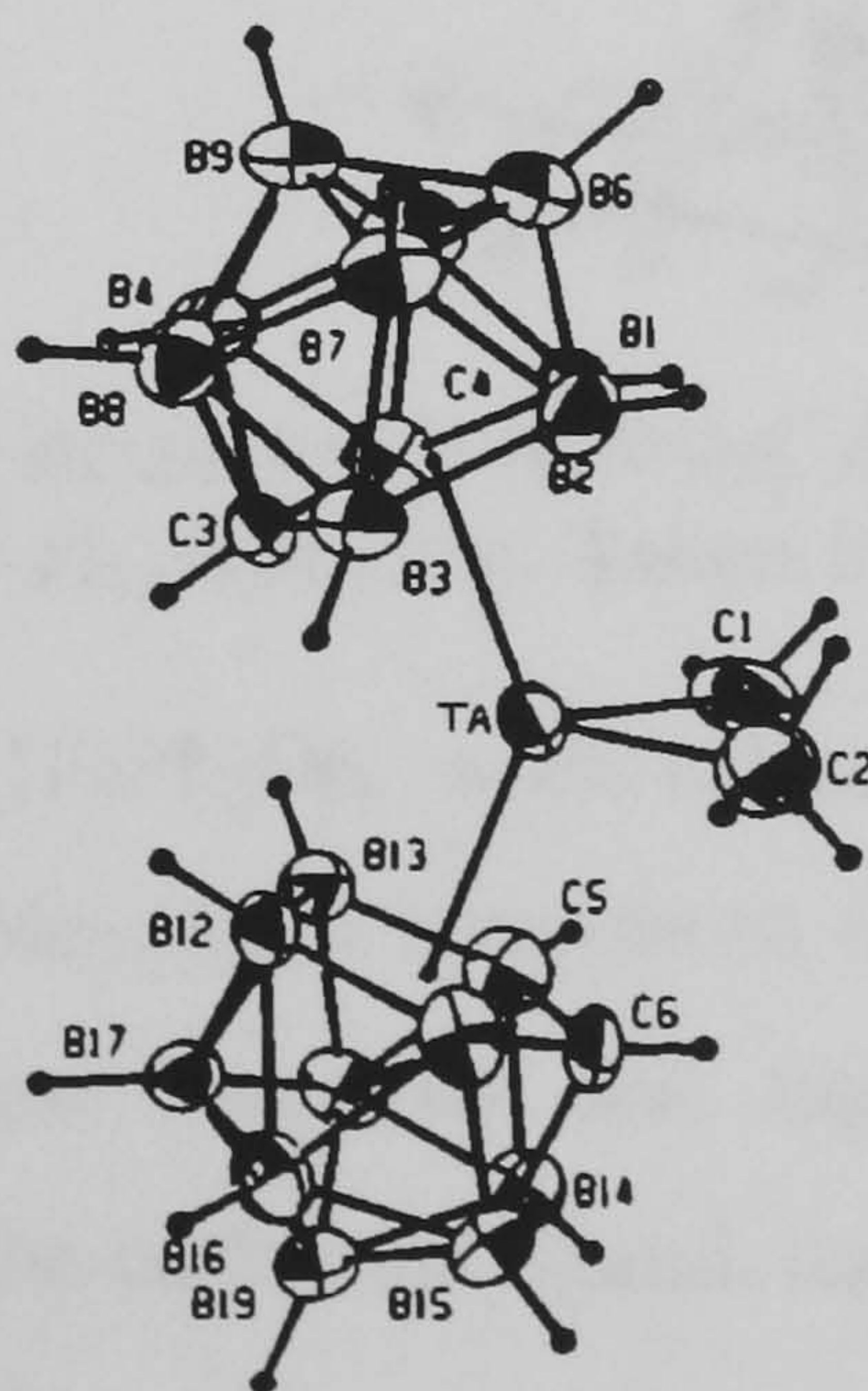


Figure 1.43 Molecular structure of the anion $[(\text{C}_2\text{B}_9\text{H}_{11})_2\text{Ta}(\text{Me})_2]^-$. Taken from ref. 97.

In an attempt to synthesise the neutral *bis*-dicarbollide species, $[(C_2B_9H_{11})_2Ta(Cl)]$, Jordan *et al.* attempted a chloride abstraction using $Ag[PF_6]$; due to the highly electrophilic nature of the neutral species such as $[(C_2B_9H_{11})_2Ta(X)]$, abstraction of F^- from PF_6^- and the formation of PF_5 produced $[(C_2B_9H_{11})_2Ta(F)_2]^-$ as the tantalum containing species.⁹⁷

As mentioned earlier, the chemistry of group 5 ' C_2B_4 ' carborane complexes is marginally more extensive than that of the ' C_2B_9 ' system, and as with other areas of this chemistry has been dominated by a single research group.

Grimes *et al.* synthesised and characterised a series of isostructural sandwich complexes of the general type $(R_2C_2B_4H_4)MCl_2Cp'$ from $Cp'MCl_4$ ($R = Et, SiMe_3$ or Me ; $Cp' = C_5H_5$ or C_5Me_5 ; $M = Ta$ or Nb) and the $R_2C_2B_4H_5^-$ mono anion in THF. Similar treatment of the *nido*-metallacarborane $Cp^*Co(Et_2C_2B_3H_4)^-$ (cf. $R_2C_2B_4H_5^-$)⁹⁸ afforded the novel triple decker complexes $[Cp^*Co(Et_2C_2B_3H_3)]MCl_2Cp'$ (examples of both types of complex are shown in figure 1.44).⁹⁴ For both families of compounds, treatment with a range of alkylating agents yields the mono or disubstituted compounds $(R_2C_2B_4H_4)TaCl(L)Cp'$ or $(R_2C_2B_4H_4)M(L)_2Cp'$ and the corresponding triple-decker complexes $[Cp^*Co(Et_2C_2B_3H_3)]TaCl(L)Cp'$ and $[Cp^*Co(Et_2C_2B_3H_3)]M(L)_2Cp'$ ($M = Ta$ or Nb ; $L = Me, Et, Ph, CH_2Ph, CH_2CMe_3$ or OPh).

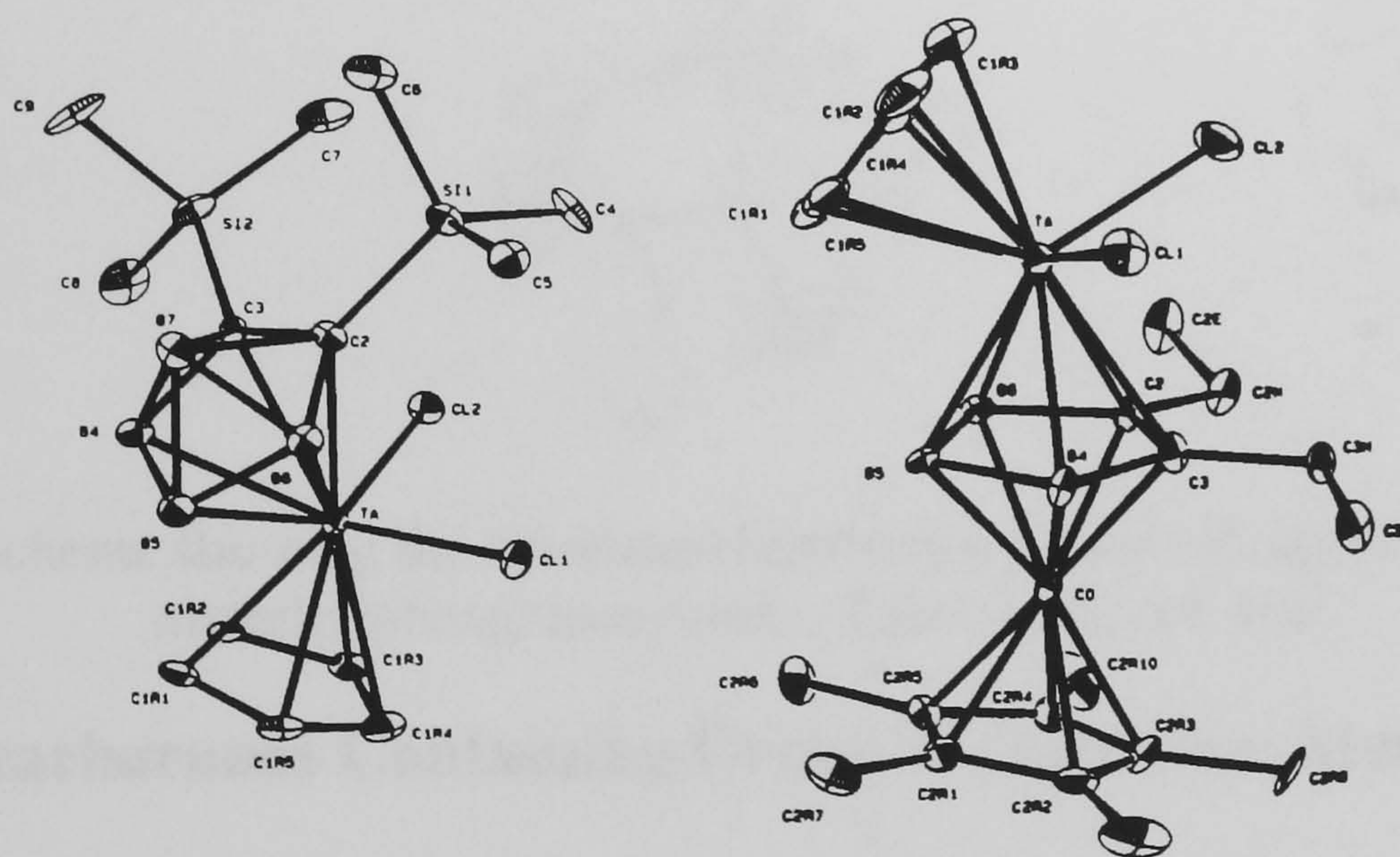


Figure 1.44 Molecular structures $[(SiMe_3)_2C_2B_4H_4]TaCl_2Cp$ and $[Cp^*Co(Et_2C_2B_3H_3)]TaCl_2Cp$. Taken from ref. 94.

The di-phenyl derivative $[Et_2C_2B_4H_4]TaPh_2Cp$, when subjected to high temperatures in the presence of a donor ligand such as PMe_3 , loses benzene to afford the metal benzyne complex $[Et_2C_2B_4H_4]Ta(\eta^2-C_6H_4)Cp$.⁹⁹ The low reactivity and high stability of this complex is attributed to the stabilising power of the carborane ligand, due to the electron delocalisation in the metallacarborane cluster framework.

Both the di-methyl and di-phenyl complexes, $[(Et_2C_2B_4H_4)]TaMe_2Cp$, and $[(Et_2C_2B_4H_4)]TaPh_2Cp$, undergo insertion reactions with nitriles and isocyanides under conditions that differ from the formally iso-electronic metallocene compounds of group 4 metals.¹⁰⁰ The insertion of nitriles into the metal methyl bonds is achieved using UV-vis irradiation. Insertion into the diphenyltantalum system is achieved at elevated temperatures.

In contrast, isocyanides such as t-butyl isocyanide and 2,6-dimethylphenyl isocyanide produce mixtures of the 'in' and 'out' η^2 -iminoacyl complexes shown in Figure 1.45. Both the 'in' and 'out' tantalum phenyl complex $[Et_2C_2B_4H_4]Ta(Ph)(\eta^2-C(Ph)N(2,6-Me_2C_6H_3)Cp)$ undergo further insertion with another equivalent of either tert-butyl isocyanide or 2,6-dimethylphenyl isocyanide, resulting in a cage insertion reaction.

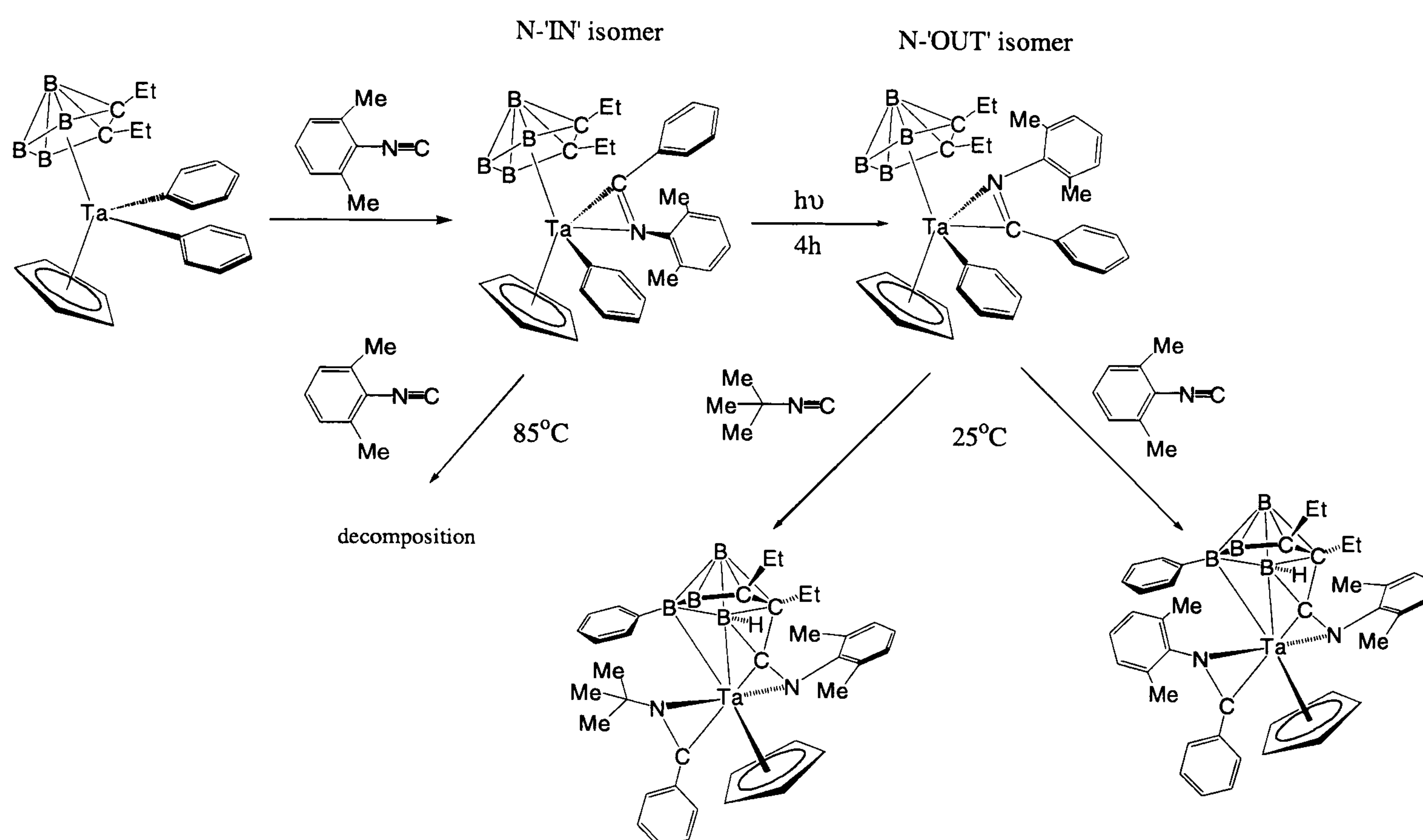


Figure 1.45 Scheme showing the insertion chemistry of $[(Et_2C_2B_4H_4)]TaPh_2Cp$, with 2,6-dimethylphenyl isocyanide. Taken from ref. 100.

1.4.5 Metallocarboranes Containing Group 6 Transition Metals.

It can be clearly seen that both the dicarbollide ligand, and carborane ligands in general, have assumed a significant role in organometallic chemistry. Nowhere is this more illustrated than in the work of Stone in the area of alkylidyne complexes and metallocarboranes with both bridging carbene and carbyne ligands.^{101,102} The alkylidyne work centres on the ability of the $[\eta^5-R_2C_2B_9H_9]^{2-}$ unit to replace its isoelectronic analogue $[\eta^5-C_5R_5]^-$ ($R = H$ or Me) in moieties such as $[W(\equiv CR)(CO)_2(\eta^5-C_5R_5)]$. Protonation of such carborane alkylidyne complexes of tungsten or molybdenum induces migration of the CR unit to a boron atom on the carborane ligand;¹⁰³ when protonation is conducted in the presence of other reagents, bimetallic

compounds are produced via alkylidyne-ligand coupling.¹⁰⁴ In the presence of $[\text{Mo}(\equiv\text{CC}_6\text{H}_4\text{Me})(\text{CO})_2(\eta^5\text{-C}_5\text{H}_5)]$, protonation of $[\text{NEt}_4][\text{W}(\equiv\text{CR})(\text{CO})_2(\eta^5\text{-C}_2\text{B}_9\text{H}_{11})]$ with $\text{HBF}_4\cdot\text{Et}_2\text{O}$ gave the molybdenum-tungsten species shown in Figure 1.46. A vast range of products have been produced by variation of the added substrate, the acid employed for protonation and metallocarborane salt used. The stereochemistry and other aspects of this chemistry have been commented upon elsewhere.^{51,101,105}

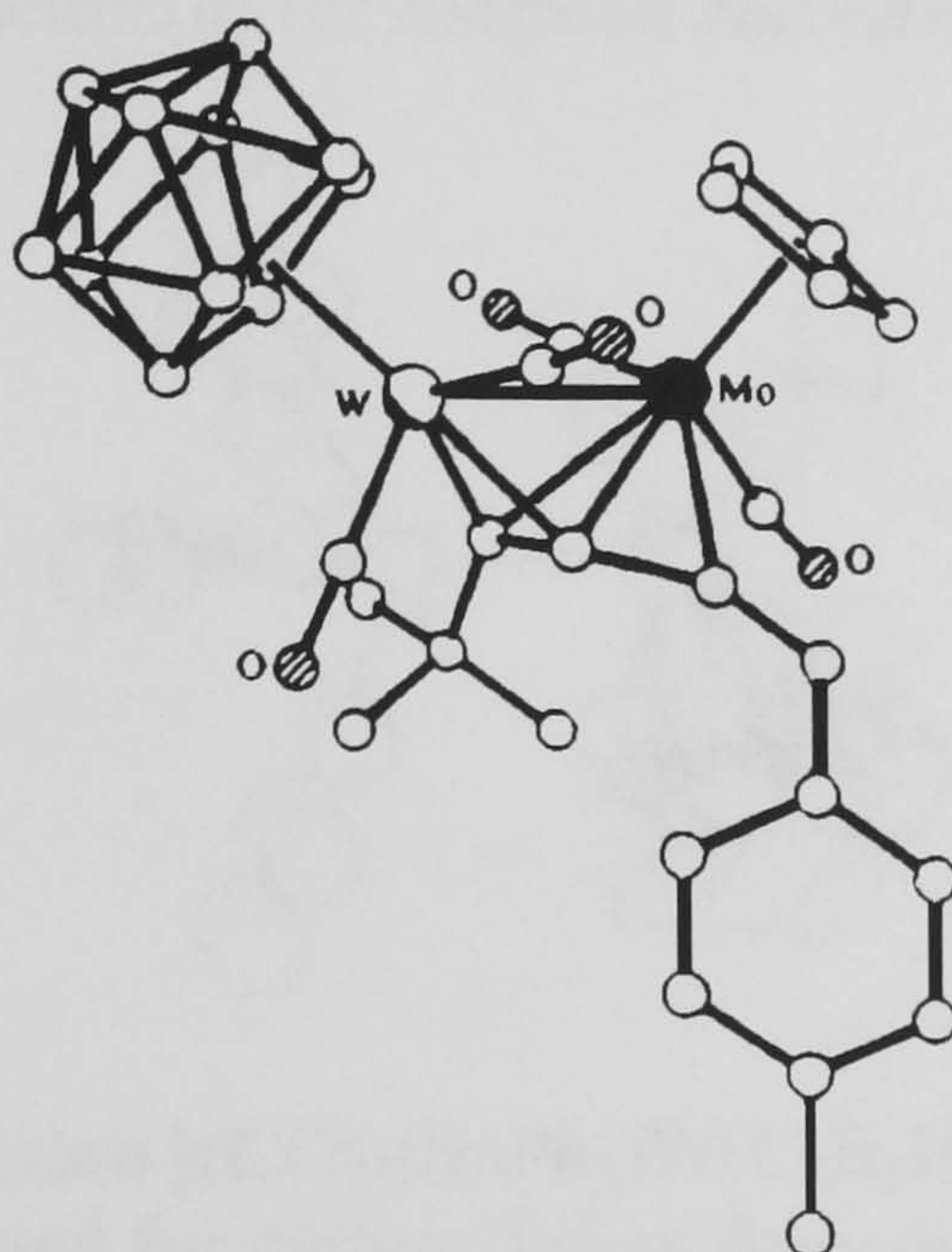


Figure 1.46 Structure of 3,1,2-[MeC₆H₄CH=C₃(^tBu)CpMo(CO)₂](CO)₂W(C₂B₉H₁₁). Taken from ref. 104.

The research on tungsten and molybdenum has also been extended to mixed metal clusters without the migration of alkylidyne moieties. Molecules containing unsaturated metal-carbon or unsaturated metal-metal bonds, complex with other metal ligand systems, as do alkenes or alkynes, provided that the metal centre is electron rich yet has a vacant coordination site. Treatment of the complex $[\text{NEt}_4][\text{W}(\equiv\text{CR})(\text{CO})_2(\eta^5\text{-C}_2\text{B}_9\text{H}_{11})]$ with $[\text{AuCl}(\text{PPh}_3)]$ or $[\text{Pt}(\text{COD})_2]$ generates the two complexes (*vide infra*).¹⁰¹

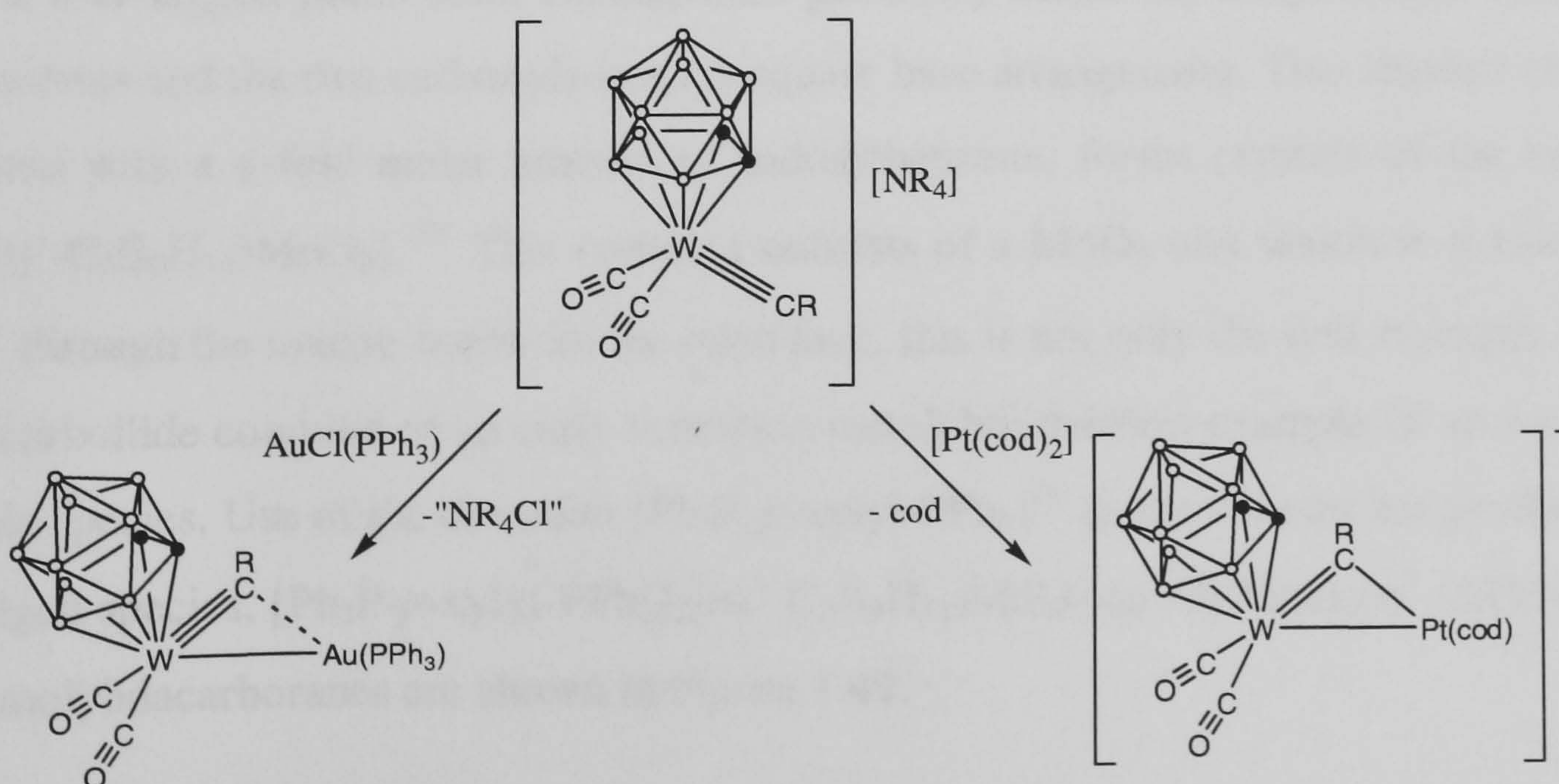


Figure 1.47 Examples of polynuclear metal complexes having exo-polyhedral carbene or carbyne bridges. Taken from ref. 101.

A vast range of heteropolynuclear metallocarboranes of both Mo and W have been synthesised containing *exo* polyhedral bonds to iron, cobalt, copper, molybdenum, ruthenium, rhodium, tungsten, iridium, platinum and gold.⁵⁵

A somewhat different series of heterodinuclear complexes of the type $[(\text{CO})_3(\text{SnPh}_3)\text{M}(\text{C}_2\text{B}_9\text{H}_{11})]^-$ having a Sn-M bond (M = Cr, Mo and W) have been prepared in the group of Hawthorne; the structure of the tungsten derivative is shown below.¹⁰⁶

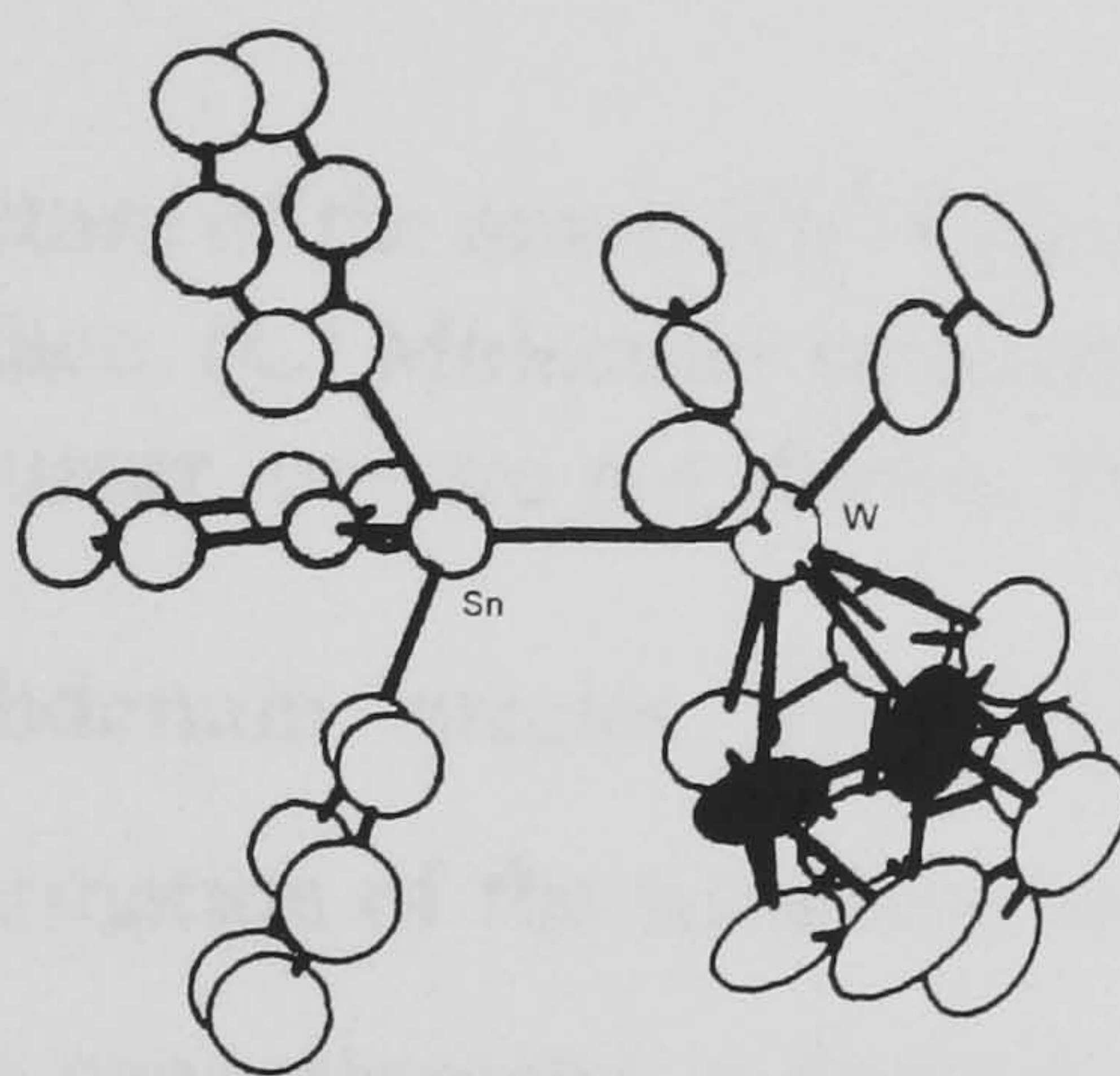


Figure 1.48 Structure of the anion $[(\text{CO})_3(\text{SnPh}_3)\text{W}(\text{C}_2\text{B}_9\text{H}_{11})]^-$. The counter ion $[\text{PPN}]^+$ is omitted for clarity. Taken from ref. 106

It is noteworthy that the majority of the complexes that contain metals from group six are not in their highest oxidation state, especially as carboranes are reputed to stabilise the higher oxidation state metals.

One example of a metallocarborane with the metal in the highest oxidation state comes from the lab of Y. Do. The molybdacarborane complex $[\text{NMe}_4]_2[(\eta^5\text{-C}_2\text{B}_9\text{H}_{11})\text{Mo}(\text{CO})_3]$ reacts with phenyldisulphide to form the dithiolate complex $[\text{NMe}_4]_2[(\eta^5\text{-C}_2\text{B}_9\text{H}_{11})\text{Mo}(\text{CO})_2(\text{SPh})_2]$ which possesses a four-legged piano stool coordination geometry about the molybdenum atom with the two thiolates and the two carbonyls in a *cis*-square base arrangement. This thiolate complex when treated with a 4-fold molar amount of iodosylbenzene, forms crystals of the complex $[\text{NMe}_4]_2[(\eta^1\text{-C}_2\text{B}_9\text{H}_{11})\text{MoO}_3]$.¹⁰⁷ This complex consists of a MoO_3 unit which is σ -bonded to the ' C_2B_9 ' through the unique boron on the open face, this is not only the first example of a σ -bonded dicarbollide complex of an early transition metal, but the first example of an *oxo*-metal dicarbollide species. Use of the di-cation $[\text{Ph}_3\text{P-}p\text{-xylyl-PPh}_3]^{2+}$ as the counter ion produces the μ -*oxo* bridged species, $[\text{Ph}_3\text{P-}p\text{-xylyl-PPh}_3]_2[(\eta^5\text{-C}_2\text{B}_9\text{H}_{11})\text{MoO}_2-(\mu\text{-O})\text{-MoO}_2(\eta^5\text{-C}_2\text{B}_9\text{H}_{11})]$.¹⁰⁷ Both *oxo*-molybdacarboranes are shown in Figure 1.49.

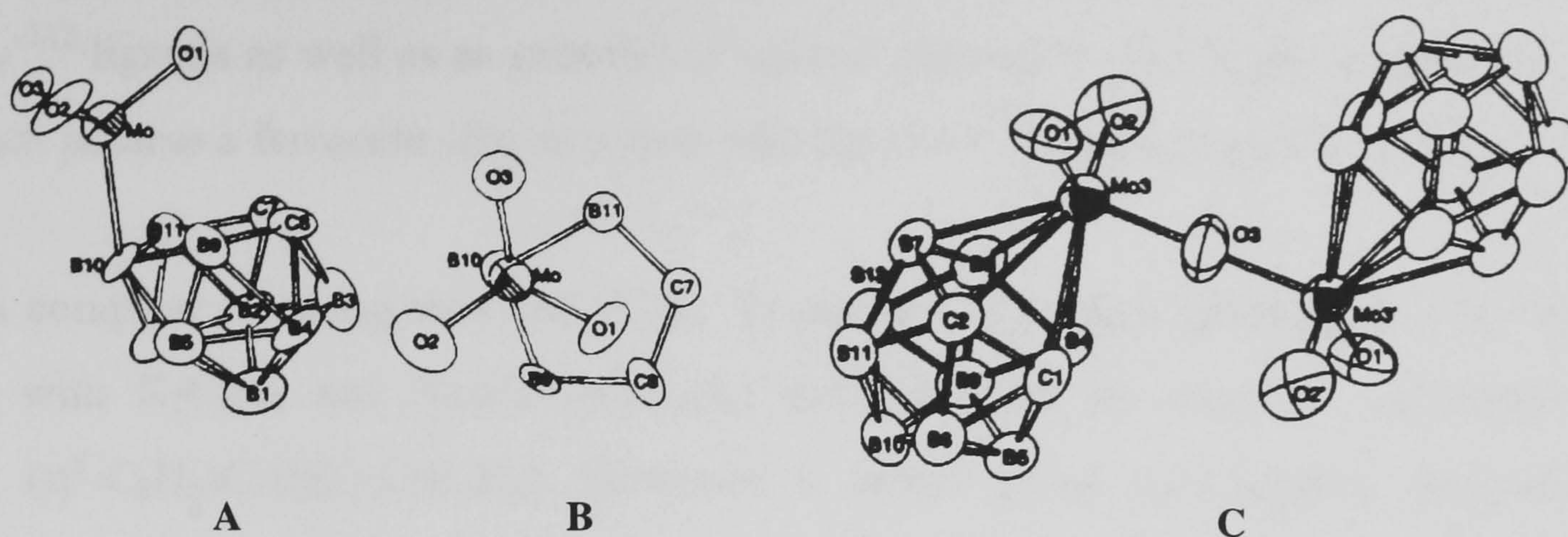


Figure 1.49 (A) Molecular structure of the anion $[(\eta^1\text{-C}_2\text{B}_9\text{H}_{11})\text{MoO}_3]^-$. (B) Projection of the MoO_3 fragment onto the C_2B_3 face. (C) Molecular structure of $[(\eta^5\text{-C}_2\text{B}_9\text{H}_{11})\text{MoO}_2-(\mu\text{-O})\text{-MoO}_2(\eta^5\text{-C}_2\text{B}_9\text{H}_{11})]^-$. Counter ions are not shown. Taken from ref. 107 above.

Further oxidation of the molybdenum species $[\text{NMe}_4]_2[(\eta^5\text{-C}_2\text{B}_9\text{H}_{11})\text{Mo}(\text{CO})_2(\text{SPh})_2]$ by phenyldisulphide results in the formation of the tetrathiolate-bridged complex $[\text{N}(\text{PPh}_3)_2][(\eta^5\text{-C}_2\text{B}_9\text{H}_{11})\text{Mo}(\text{SPh})_2]_2$ in which the cage geometry is derived from the scission of the C-C bond and a concomitant movement of the unique B in the *nido*-face towards the molybdenum atom. Treatment with either Br_2 or PhIO affords the complex $[\text{NMe}_4][(\eta^5\text{-C}_2\text{B}_9\text{H}_{11})\text{Mo}(\text{CO})_2(\text{SPh})_2]$. The *closo*- MoC_2B_9 icosahedral framework in this complex is reformed, which is thought to be consistent with the expected mixed Mo(III)Mo(IV) paramagnetism.¹⁰⁸

A system of substantial interest is the Mo(IV) complex $[\text{Mo}(\eta^5\text{-C}_5\text{H}_5)(\eta^3:\eta^2\text{-C}_3\text{H}_3)\text{C}_2\text{B}_9\text{H}_9]$ which is formed by the oligomerisation of $\text{BH}_3\text{:THF}$ in the presence of $[\text{MoH}_2(\eta^5\text{-C}_5\text{H}_5)_2]$.¹⁰⁹ The complex was characterised by single crystal X-ray crystallography. The most noticeable feature of the complex is the partial incorporation of a Cp ring into the metallacarborane, with both parts of the ligand interacting with the metal centre. The carborane ligand acts as an $\eta^5\text{-C}_2\text{B}_9$ ligand as well as a η^3 -allyl to the metal centre.

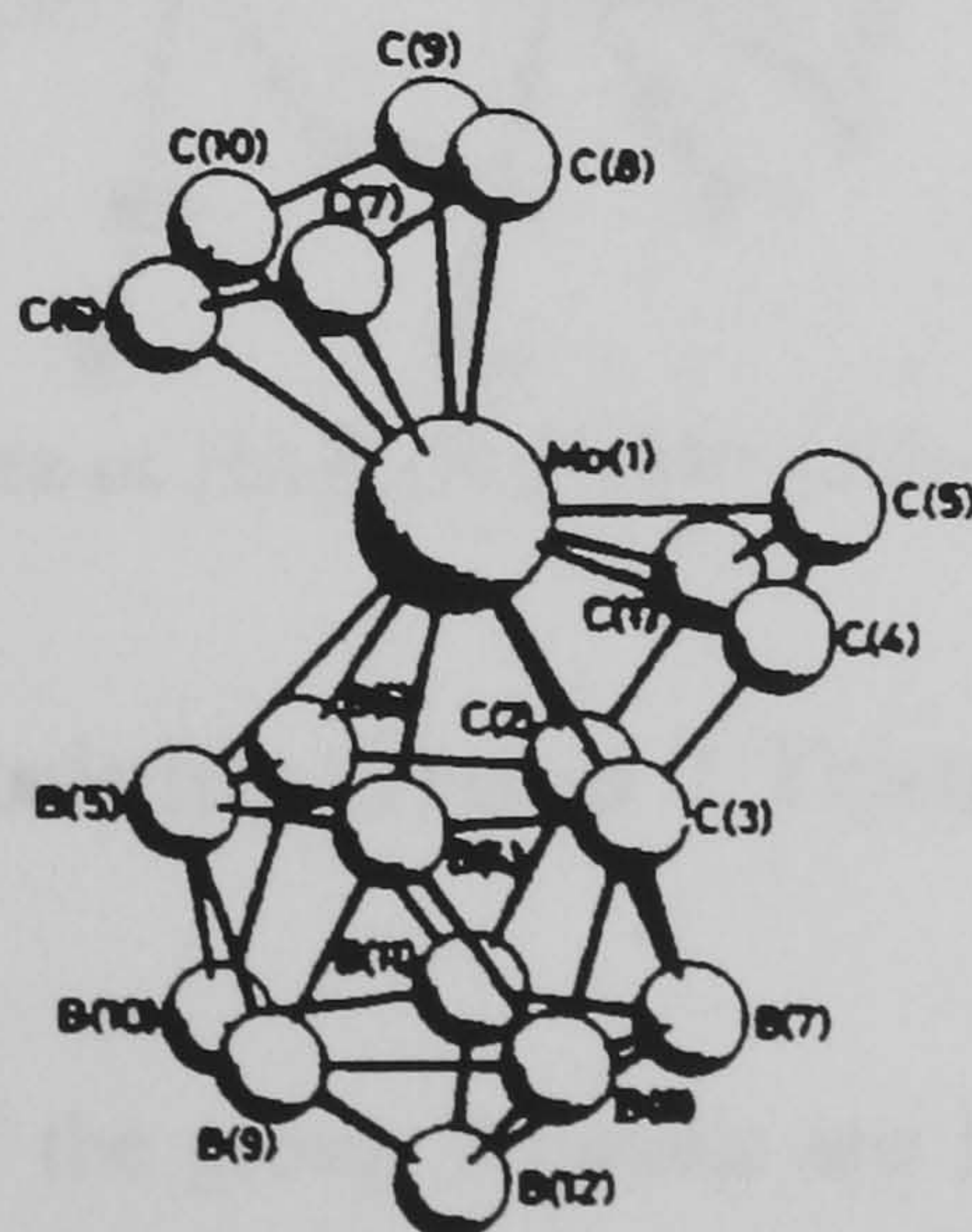
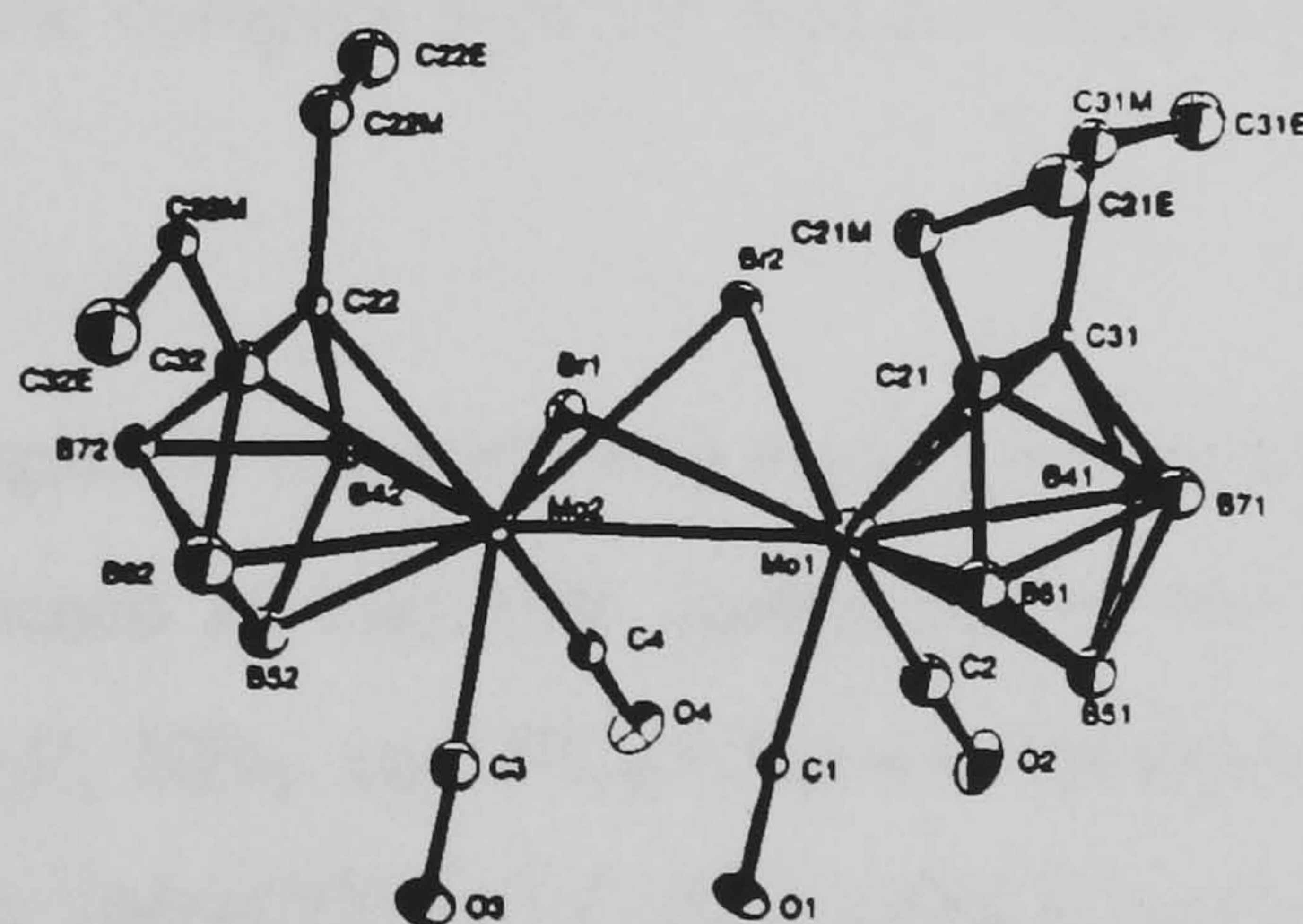


Figure 1.50 Molecular structure of $[\text{Mo(IV)}(\eta\text{-C}_5\text{H}_5)(\eta^3:\eta^2\text{-C}_3\text{H}_3)\text{C}_2\text{B}_9\text{H}_9]$. Taken from ref. 109.

There are several examples of anionic Cr(III) bis carborane complexes of both the 'C₂B₉'^{110,111} and 'C₂B₄'¹¹² ligands as well as an example of neutral chromium (IV) 'C₂B₉' complexes,^{112,113} all of which possess a ferrocene like structure with the two C₂B₃ faces parallel.

Group six complexes bearing only one 'C₂B₄' ligand have also been synthesised. The reaction of CrCl₃ with K₂C₈H₈ and Na₂[(Et)₂C₂B₄H₄] did not yield the expected chromium (III) complex, (η⁸-C₈H₈)Cr[(Et)₂C₂B₄H₄]. However, a yellow-green paramagnetic product was isolated in very low yield, and characterised as [(η⁷-C₇H₇)Cr{(Et)₂C₂B₄H₄}]. The product, [(η⁷-C₇H₇)Cr{(Et)₂C₂B₄H₄}], is structurally similar to the vanadium(III) and titanium(III) cyclooctatetraene complexes mentioned previously, except for substitution of the [cot] ligand for the tropylium ligand [η⁷-C₇H₇].⁸⁵

More recently Grimes and co-workers have produced the first Mo and W complexes bearing small carborane ligands. Treatment of the tricarbonyl complexes [(MeCN)₃M(CO)₃] (M = Mo or W) with the di-lithium salt of [(Et)₂C₂B₄H₄]²⁻ yields the monocarborane tricarbonyl anions of the form [{(Et)₂C₂B₄H₄}M(CO)₃]⁻. These complexes form the dimeric products [{Et₂C₂B₄H₄}M(CO)₂]₂(μ-X₂) (M= Mo or W, X = Cl, Br or I) upon treatment with Ph₄X (X = Cl, Br or I) and triflic acid.¹¹⁴ The molecular structure of the molybdenum complex [{Et₂C₂B₄H₄}Mo(CO)₂]₂(μ-Br₂), shown in Figure 1.51, shows that the two MC₂B₄ units are linked by a direct metal-metal bond which is bridged by two Br atoms. The coordination sphere of the metal atoms is completed by ligation of two carbonyl ligands per metal.



Only relatively few complexes have a *closo*-MnC₂B₉ cage framework and in all these species the manganese is ligated by three carbonyl groups. Stone *et al.* have produced a zwitterionic, or charge compensated, manganese system from the reaction of C₂B₉H₁₃ with [MnMe(CO)₅] in THF.¹¹⁶ The reaction proceeds by the evolution of methane and by some unknown mechanism to form the complex [Mn(CO)₃{ η^5 -C₂B₉H₁₀-O(CH₂)₄}]. A similar reaction of the anionic ligand C₂B₉H₁₁²⁻ with BrMn(CO)₅ results in the formation of the expected anionic species [Mn(CO)₃{ η^5 -C₂B₉H₁₁}]⁻.⁴⁹ The molecular structure of the charge compensated complex is shown in Figure 1.52.

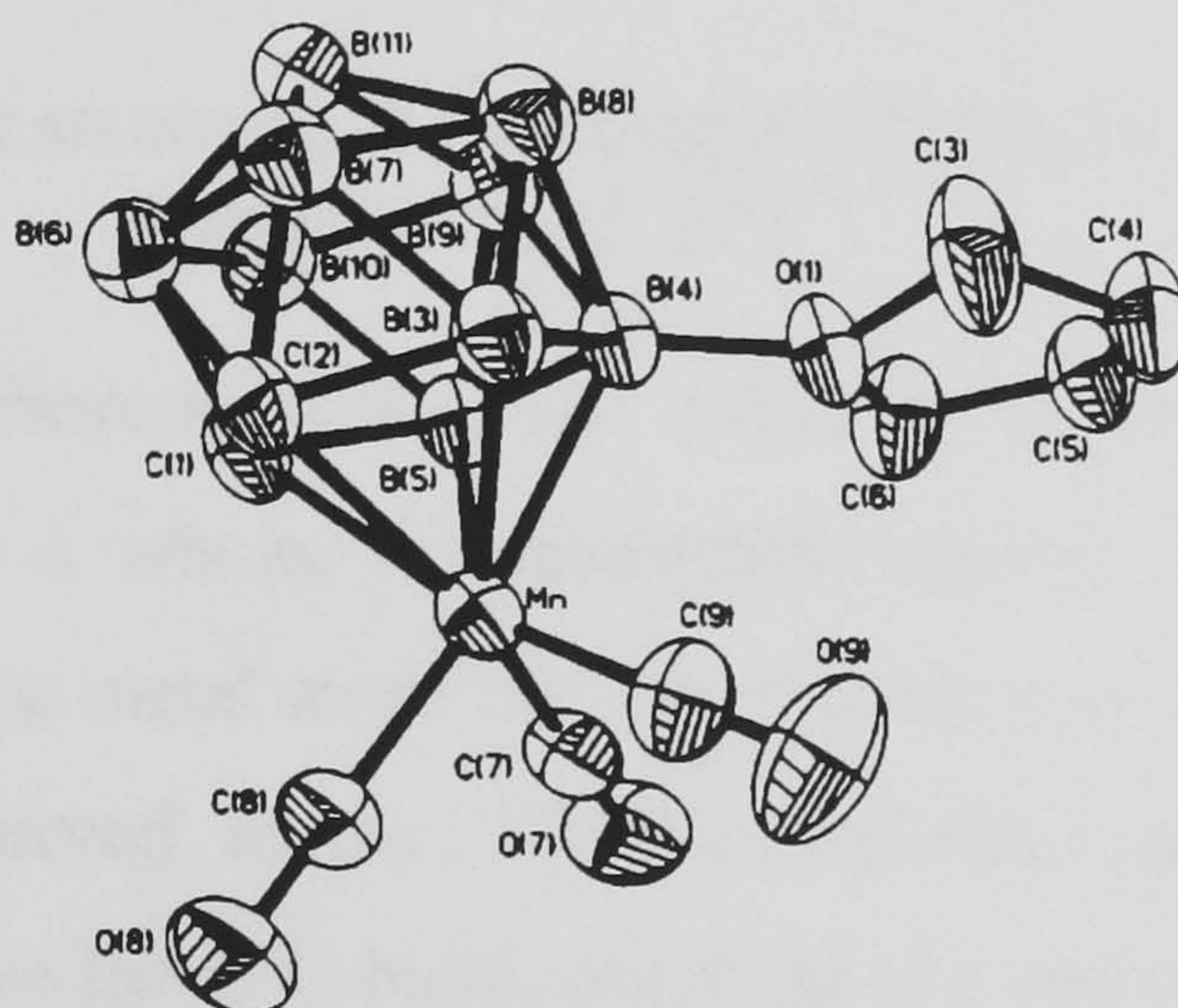


Figure 1.52 The molecular structure of the complex [Mn(CO)₃{ η^5 -C₂B₉H₁₀-O(CH₂)₄}]. Taken from ref. 116

The complex consists of a Mn(CO)₃ unit bonded in an η^5 -fashion to the carborane cage. The C₂B₉ cage itself is substituted at the unique boron atom in the C₂B₃ face by a (OC₄H₈) unit. The ‘THF’ unit bears a single positive charge on the oxygen atom, thus rendering the ligand, as a whole monoanionic (cf. the complex with the non substituted cage is anionic, [Mn(CO)₃{ η^5 -C₂B₉H₁₁}]⁻).⁴⁹

The ‘THF’ ring in this complex is susceptible to nucleophilic attack and on addition of a strong nucleophile forms ring-opened zwitterionic complexes of the form [Mn(CO)₃{ η^5 -C₂B₉H₁₀-O(CH₂)₃CH₂L}]. (L = Ph₃P, NEt₃ and NC₅H₄Me-4). Treatment with [NEt₄]I results in the formation of the complex [Mn(CO)₃{ η^5 -C₂B₉H₁₀-O(CH₂)₄I}][NEt₄], which involves halide cleavage of a C-O⁺ bond. Welch and co-workers have previously produced another manganese charge compensated system from the reaction of the K[9-SMe₂-7,8-C₂B₉H₁₁] with [Mn(CO)₃(NCMe)₃][BF₄].¹¹⁷ The molecular structure of the resulting complex [Mn(CO)₃{SMe₂-C₂B₉H₁₁}] is shown in Figure 1.53.

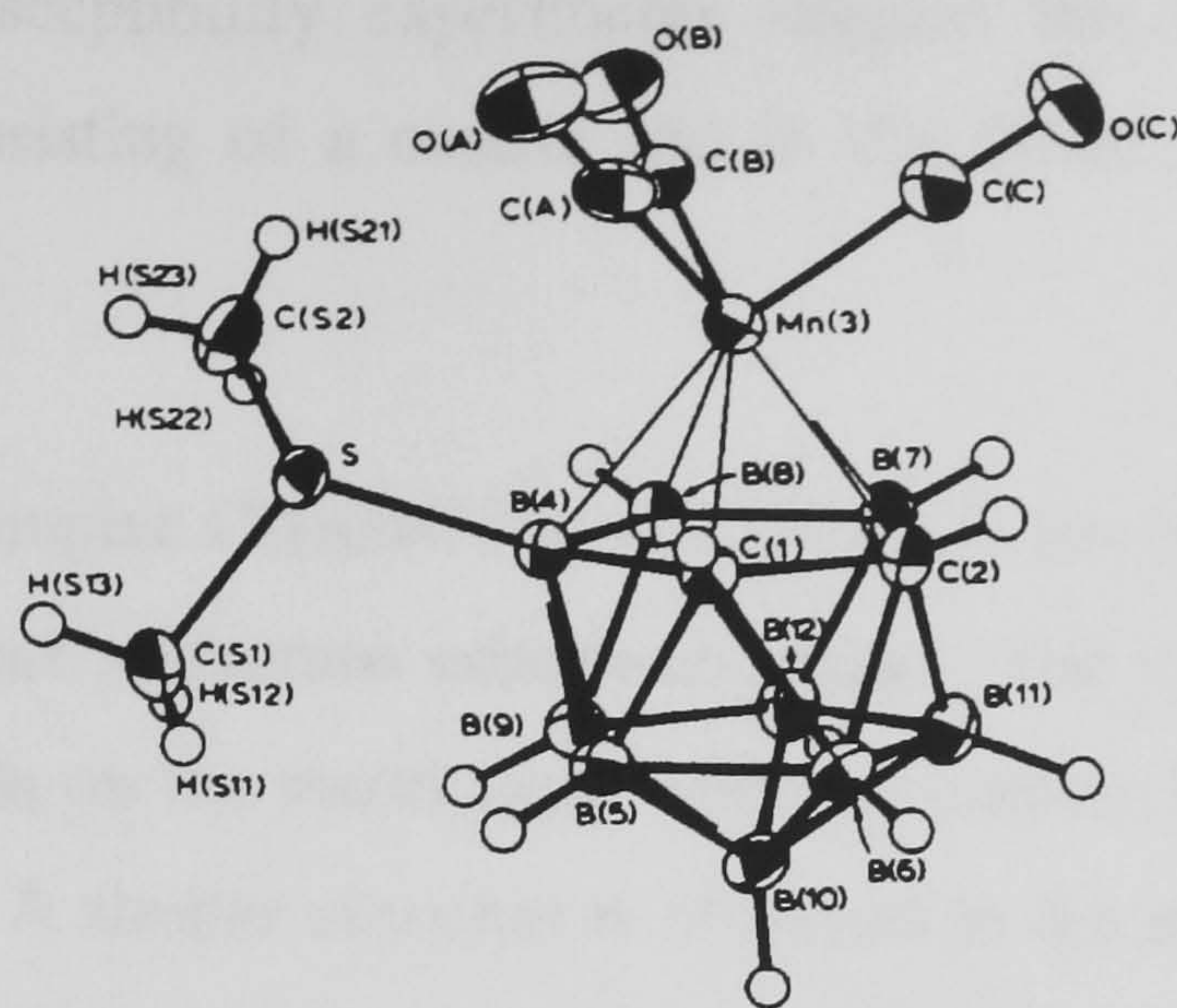


Figure 1.53. The molecular structure of the complex $[\text{Mn}(\text{CO})_3\{\text{SMe}_2\text{-C}_2\text{B}_9\text{H}_{11}\}]$.
Taken from ref. 117

As in the case of the ‘THF’-carborane system the sulfur atom bears a uni-positive charge making the carborane ligand, as a whole, a monoanionic ligand. In the “ SMe_2 ” carborane system one of the carbonyls on the metal atom lies directly *trans* to the C-C bond in the C_2B_3 face. This geometry is not observed in the ‘THF’-carborane complex where one of the carbonyl ligands lies directly above the C-C bond, resulting in a molecular C_s symmetry.

Manganese has also been shown to form stable complexes with the smaller C_2B_4 carboranes. Reaction of MnCl_2 with the mixed metal carborane $[\text{Na}(\text{THF})][\text{LiC}_2(\text{SiMe}_3)_2\text{B}_4\text{H}_4]$ results in the formation the complex shown in Figure 1.54.¹¹⁸ The molecule consists of a *commo*- $[\text{Mn}(\text{C}_2\text{B}_4)_2]$ unit symmetrically bonded to the Mn atoms of two $[\text{Mn}(\text{C}_2\text{B}_4)]$ units. Each $[\text{Mn}(\text{C}_2\text{B}_4)]$ unit in turn is linked to a lithium atom via B-H interactions. The two $[\text{Mn}(\text{C}_2\text{B}_4)]$ units are then subsequently bridged by a $[\text{Li}(\text{THF})]$ unit (the THF molecule and SiMe_3 units on the cage carbons are not shown in Figure 1.54).

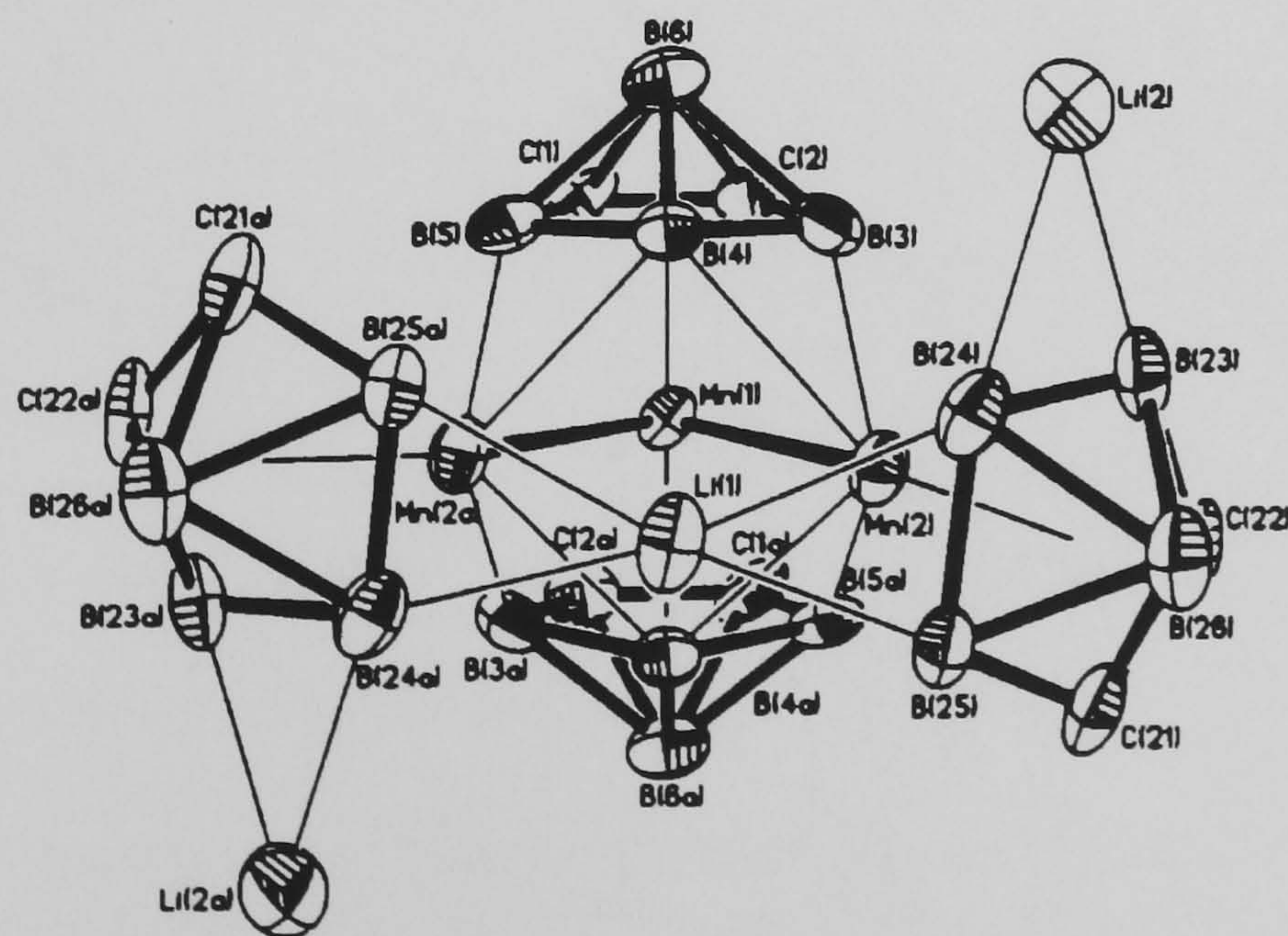


Figure 1.54 The molecular structure of the complex $[\text{Mn}_3(\text{C}_2(\text{SiMe}_3)_2\text{B}_4\text{H}_4)_4\text{Li}_2(\text{Li}(\text{THF}))]$.
Taken from ref. 118.

Data from magnetic susceptibility experiments suggest that the Mn_3 system is a mixed oxidation state triad consisting of a central Mn in the formal 3+ state and bonded to two terminal Mn(I) atoms.

Although the rhenium complex $\text{Cs}[\text{Re}(\text{CO})_3\{\eta^5\text{-C}_2\text{B}_9\text{H}_{11}\}]$ has been known since 1966¹¹⁹ very little chemistry of rhenium carborane complexes exists. The structure of the rhenium anion shows the three carbonyls on the metal atom with one carbonyl almost *trans* to C-C bond in 'C₂B₃' face of the cage. A similar situation is observed in the more recently formed complex $[\text{NEt}_3(\text{CH}_2\text{Ph})]_2[\text{Re}(\text{CO})_3\{\eta^5\text{-CB}_{10}\text{H}_{11}\}]$, which contains the mono carbon carborane ligand.¹²⁰ The three carbonyl ligands on the metal atom are orientated in such a way in the solid state that one carbonyl ligand lies directly *trans* to the carbon atom in the 'CB₄' face (Figure 1.55).

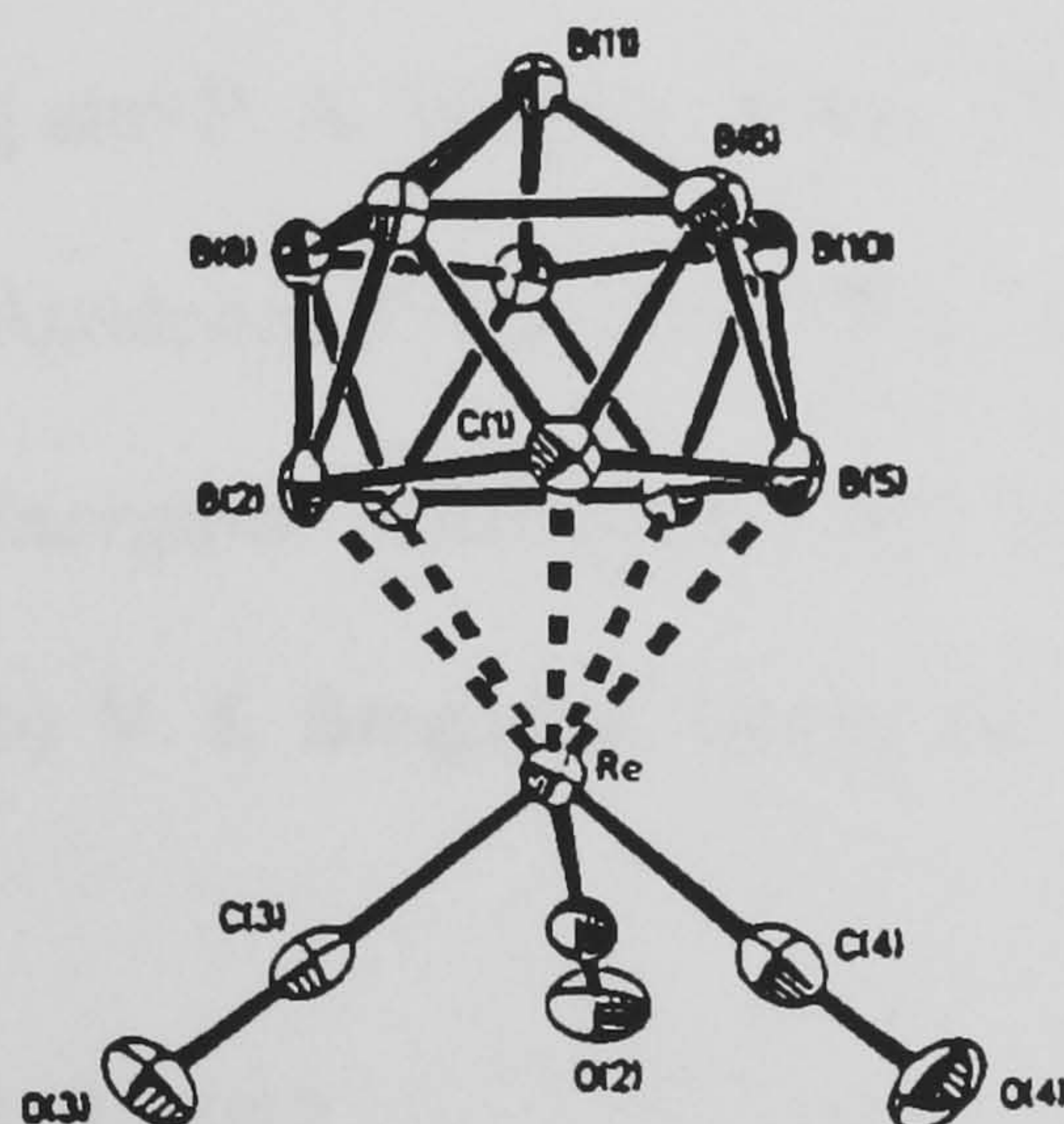


Figure 1.55 Molecular structure of the anion $[\text{Re}(\text{CO})_3\{\eta^5\text{-CB}_{10}\text{H}_{11}\}]^{2-}$. Taken from ref. 120.

The monoanionic complexes of manganese and rhenium $[\text{M}(\text{CO})_3\{\eta^5\text{-C}_2\text{B}_9\text{H}_{11}\}]^-$ ($\text{M} = \text{Mn}$ or Re) have also been complexed with cyclodextrins to form novel inclusion complexes.¹²¹

1.5 References for Chapter One.

- 1 (a) W.N. Lipscomb, *"Boron Hydrides"*, Benjamin, New York, 1963; (b) *"Boron Hydride Chemistry"* Ed. E.L. Muetteries, Academic Press, New York, 1975; (c) N. N. Greenwood and B. S. Thomas, *"The Chemistry of Boron"*, Pergamon Press, Oxford, 1973; (d) K. Wade, *"Electron Deficient Compounds"*, Nelson, Oxford, 1971.
- 2 A. Stock, *"Hydrides of Boron and Silicon"*, Cornell University Press, Ithaca, New York, 1933.
- 3 K. Wade, *Adv. Inorg. Chem. Radiochem.*, 1976, **18**, 1, and references therein.
- 4 M. F. Hawthorne, D. C. Young and P. A. Wegner, *J. Am. Chem. Soc.*, 1965, **87**, 1818.
- 5 R. N. Grimes, *"Carboranes"*, Academic Press, New York, 1970.
- 6 (a) *"Gmelin Handbook of Inorganic Chemistry"*, 8th Ed., Springer-Verlag, Berlin, 3rd Supplement, Vol. 4, 1988; (b) V. I. Bregadze, *Chem. Rev.*, 1992, **92**, 209, and references therein.
- 7 R. Adams, *Inorg. Chem.*, 1963, **2**, 1087.
- 8 (a) D. Grafstein and J. Dvöřak, *Inorg. Chem.*, 1963, **2**, 1128; (b) S. Papetti and T. L. Heying, *J. Am. Chem. Soc.*, 1964, **86**, 2295.
- 9 R. E. Williams in *"Electron Deficient Boron and Carbon Clusters"*, G. A. Olah, K. Wade and R. E. Williams, John Wiley & Sons Inc., New York, 1991.
- 10 (a) P. Kasynski, *Coll. Czech. Chem. Commun.*, 1999, **64**, 859; (b) O. A. Melnik, A. A. Sakharova, T. M. Frunze, *Uspekhi. Khimii*, 1988, **57**, 1529.
- 11 T. L. Heying and S. Papetti, *Inorg. Chem.*, 1963, **2**, 1097.
- 12 F. A. Gómez, S. E. Johnson and M. F. Hawthorne, *J. Am. Chem. Soc.*, 1991, **113**, 5915.
- 13 W. Clegg, D. A. Brown, S. J. Bryan and K. Wade, *Polyhedron*, 1984, **3**, 307.
- 14 L. Pauling, *"The Nature of the Chemical Bond"*, Cornell University Press, Ithaca, New York, 1939.

- 15 H. C. Longuet-Higgins, *J. Chem. Phys.*, 1949, **46**, 275.
- 16 K. Wade, *Chem. Commun.*, 1971, 791.
- 17 H. C. Longuet-Higgins and M de V. Roberts, *Proc. Roy. Soc. London., Ser A*, 1955, **230**, 110.
- 18 A. A. Ardi and T. P. Fehlner, *Adv. Organomet. Chem.*, 1990, **30**, 189.
- 19 K. Wade, *Chem. Brit.*, 1975, **11**, 177.
- 20 It is worth noting that the cyclopentadienyl ligand occupies three coordination sites and is iso-lobal with the $\text{Fe}(\text{CO})_3$ unit. See R. Hoffmann, *Angew. Chem., Int. Ed. Engl.*, 1982, **21**, 711.
- 21 M. Eliañ and R. Hoffmann, *Inorg. Chem.*, 1975, **15**, 1058.
- 22 M. G. Davidson, M. A. Fox, T. G. Hibbert, J. A. K. Howard, A. Mackinnon, I. S. Neratin and K. Wade, *Chem. Comm.*, 1999, 1649.
- 23 J. Plešek, S. Heřmánek and B. Štíbr, *Inorg. Synth.*, 1985, **22**, 231.
- 24 M. F. Hawthorne, D. C. Young and P. A. Wegner, *J. Am. Chem. Soc.*, 1965, **87**, 1818.
- 25 L. I. Zakharkin, E. I. Kukulina and L. S. Podvisotskaya, *Izv. Akad. Nauk SSSR, Ser. Kim.*, 1966, 1866.
- 26 J. S. Roscoe, S. Kongpricha and S. Papetti, *Inorg. Chem.*, 1970, **9**, 1561.
- 27 M. L. H. Green, *J. Organomet. Chem.*, 1995, **500**, 127.
- 28 (a) C. T. Vroegop, J. H. Teuben, F. Van Bolhuis and J. G. M. Van der Linden, *J. Chem. Soc., Chem. Comm.*, 1983, 550; (b) W.A. Nugent, R. L. Harlow, *Inorg. Chem.*, 1979, **18**, 2030; (c) W. A. Nugent and R. L. Harlow, *J. Am. Chem. Soc.*, 1980, **102**, 1759.
- 29 Z. Lin and M. B. Hall, *Coord. Chem. Rev.*, 1993, **123**, 149.
- 30 W. A. Nugent, R. J. McKinny, R. V. Kasowski and F. A. Van-Catledge, *Inorg. Chim. Acta*, 1982, **65**, L91.
- 31 D. C. Bradley, *J. Organomet. Chem.*, 1982, **239**, 17.

- 32 H. Weingold, P. C. Wailes and A. P. Bell, *J. Organomet. Chem.*, 1972, **34**, 155.
- 33 M. H. Chisholm, I. P. Rothwell, “*Comprehensive Coordination Chemistry*” Vol. II, pg. 336-364, Pergamon Press, Oxford, 1987.
- 34 M. H. Chisholm, D. M. Hoffman, and J. C. Huffman, *Inorg. Chem.*, 1984, **23**, 3683.
- 35 W. J. Feast, V. C. Gibson and E. L. Marshall, *J. Chem. Soc., Chem. Commun.*, 1992, 1157.
- 36 M. F. Lappert, P. P. Power, A. R. Sanger, and R. C. Sirivastava, “*Metal and Metalloid Amides*”, Halsted Press/Wiley, New York, 1980.
- 37 R. A. Andreson, D. B. Beach and W. L. Jolly, *Inorg. Chem.*, 1985, **24**, 4741.
- 38 (a) D. S. Williams, J. T. Anhaus, M. H. Schofield, R. R. Schrock and W. M. Davis, *J. Am. Chem. Soc.*, 1991, **113**, 5480; (b) D. S. Glueck, J. C. Green, R. I. Michelman, and I. N. Wright, *Organometallics*, 1992, **11**, 4221.
- 39 V. C. Gibson, *J. Chem. Soc., Dalton Trans.*, 1994, 1607.
- 40 J. W. Lauher and R. Hoffmann, *J. Am. Chem. Soc.*, 1976, **98**, 1729.
- 41 D. N. Williams, J. P. Mitchell, A. D. Poole, U. Siemeling, W. Clegg, D. C. R. Hockless, P. A. O'Neill and V. C. Gibson, *J. Chem. Soc., Dalton Trans.*, 1992, 739.
- 42 G. Wilkinson, *J. Organomet. Chem.*, 1975, **100**, 273.
- 43 M. Bochmann, *J. Chem. Soc., Dalton Trans.*, 1996, 255.
- 44 (a) C. T. Jekel-Vroegop, J. H. Teuben, *Organomet. Chem.* 1985, **286**, 309; (b) M. L. H. Green, P. C. Konidaris, P. Mountford, S. J. Simpson, *J. Chem. Soc., Chem Commun.*, 1992, 256.
- 45 A. Recknagel, A. Steiner, S. Brooker, D. Stalke and T. F. Eldermann, *J. Organomet. Chem.*, 1991, **415**, 315.
- 46 E. Solari, C. Floriani, A. Chiesi-Villa and C. Rizzoli, *J. Chem. Soc., Dalton Trans.*, 1992, 367.
- 47 G. E. Herberich, U. Englert, K. Linn, P. Roos and J. Runsink, *Chem. Ber.*, 1991, **124**, 975.

Chapter One - Introduction

- 48 E. B. Moore, L. Lohr and W. N. Lipscomb, *J. Chem. Phys.*, 1961, **35**, 1329.
- 49 M. F. Hawthorne, D. C. Young, T. D. Andrews, D. V. Howe, R. L. Pilling, A. D. Pitts, M. Reintjes, L. F. Warren and P. A. Wegner, *J. Am. Chem. Soc.*, 1968, **90**, 879.
- 50 T. P. Hanusa, *Polyhedron*, 1982, **1**, 663.
- 51 A. K. Saxena and N. S. Hosmane, *Chem. Rev.*, 1993, **93**, 1081.
- 52 R. N. Grimes, *Chem. Rev.*, 1992, **92**, 251; and references therein.
- 53 A. K. Saxena, J. A. Maguire and N. S. Hosmane, *Chem. Rev.*, 1997, **97**, 2421.
- 54 R. N. Grimes in “*Comprehensive Organometallic Chemistry*”, Eds.; G. Wilkinson, F. G. A. Stone and E. W. Abel, Pergamon Press, New York, 1982.
- 55 R. N. Grimes in “*Comprehensive Organometallic Chemistry*”, Eds.; G. Wilkinson, F. G. A. Stone, E. W. Abel, Pergamon Press, New York, 1995.
- 56 Various authors in *Comprehensive Organometallic Chemistry*; G. Wilkinson, Eds. F.G.A. Stone and E.W. Able, Pergamon Press, New York, 1982.
- 57 R. E. Marsh, W. P. Schaefer, G. C. Bazan and J. E. Bercaw, *Acta Cryst.*, 1992, **C48**, 1416.
- 58 G. C. Bazan, W. P. Schaefer and J. E. Bercaw, *Organometallics*, 1993, **12**, 2126.
- 59 A. R. Oki, H. Zhang and N. S. Hosmane, *Organometallics*, 1991, **10**, 3966.
- 60 W. J. Evans, *Adv. Organomet. Chem.*, 1985, **24**, 131.
- 61 M. J. Manning, C. B. Knobler, R. Khattar and M. F. Hawthorne, *Inorg. Chem.*, 1991, **30**, 2009.
- 62 R. Khattar, M. J. Manning, C. B. Knobler, S. E. Johnson and M. F. Hawthorne, *Inorg. Chem.*, 1992, **31**, 268.
- 63 R. Khattar, C. B. Knobler and M. F. Hawthorne, *Inorg. Chem.*, 1990, **29**, 2191.
- 64 N. S. Hosmane, Y. Wang, A. R. Oki, H. Zhang and J. A. Maguire, *Organometallics*, 1996, **15**, 626.
- 65 A. R. Oki, H. Zhang and N. S. Hosmane, *Angew. Chem., Int. Ed. Engl.*, 1992, **31**, 432.

- 66 H. Zhang, A. R. Oki, Y. Wang, J. A. Maguire and N. S. Hosmane, *Acta Cryst.*, 1995, **C51**, 635.
- 67 (a) M. E. Jung and R. B. Blum, *Tetrahedron Lett.*, 1977, 3791; (b) A. Maercker and W. Theysohn, *J. Leibigs Ann. Chem.*, 1971, **70**, 747; (c) K. Kamata and M. Terashima, *Heterocycles*, 1980, **14**, 205.
- 68 H. Schumann, E. Plamidis and J. Loebel, *J. Organomet. Chem.*, 1990, **384**, C49.
- 69 N. S. Hosmane, Y. Wang, H. Zhang, J. A. Maguire, M. McInnis, T. G. Grey and J. D. Collins, *Organometallics*, 1996, **15**, 1006.
- 70 K. Prout, S. T. Cameron, R. A. Forder, S. R. Denton and V. G. Rees, *Acta Cryst.*, 1974, **B51**, 2290.
- 71 (a) F. R. Fronczek, G. W. Halstead and K. N. Raymond, *J Chem. Soc., Chem. Commun.*, 1976, 279; (b) F. R. Fronczek, G.W. Halstead and K. N. Raymond, *J. Am. Chem. Soc.*, 1977, **99**, 1769.
- 72 D. Rabinovich, C. M. Haswell, B. L. Scott, R. L. Miller, J. B. Nielson and K. D. Abney, *Inorg. Chem.*, 1996, **35**, 1425.
- 73 D. Rabinovich, R. M. Chamberlin, B. L. Scott, R. L. Miller, J. B. Nielson and K. D. Abney, *Inorg. Chem.*, 1997, **36**, 4216.
- 74 K. Shaw, B. D. Reid and A. J. Welch, *J. Organomet. Chem.*, 1994, **482**, 207.
- 75 Z. Xie, C. Yan, Q. Yang and T. C. W. Mak, *Angew. Chem., Int. Ed. Engl.*, 1999, **38**, 1761.
- 76 C. Keruder, R. F. Jordan and H. Zhang, *Organometallics*, 1995, **14**, 2993.
- 77 D. J. Crowther, D. C. Swenson and R. F. Jordan, *J. Am. Chem. Soc.*, 1995, **117**, 10403.
- 78 M. Yoshida, D. J. Crowther and R. F. Jordan, *Organometallics*, 1997, **16**, 1349.
- 79 M. Yoshida and R. F. Jordan, *Organometallics*, 1997, **16**, 4508.
- 80 X. Bei, C. Kreuder, D. C. Swenson, R. F. Jordan and V. G. Young, *Organometallics*, 1998, **17**, 1085.

- 81 D. E. Bowen, R. F. Jordan and R. D. Rogers, *Organometallics*, 1995, **14**, 3630.
- 82 S. Saccheo, G. Gioia, A. Grassi, D. E. Bowen and R. F. Jordan, *J. Mol. Catal., A: Chemical*, 1998, **128**, 111.
- 83 S. E. Johnson, C. B. Knobler and M. F. Hawthorne, *J. Am. Chem. Soc.*, 1992, **114**, 3996.
- 84 H. Kim, D. Whang, K. Kim and Y. Do, *Inorg. Chem.*, 1993, **32**, 360.
- 85 R. G. Swisher, E. Sinn and R. N. Grimes, *Organometallics*, 1984, **3**, 599.
- 86 M. Elia, M. M. L. Chen, D. M. P. Mingos and R. Hoffmann, *Inorg. Chem.*, 1976, **15**, 1148.
- 87 N. S. Hosmane, Y. Wang, H. Zhang, J. A. Maguire, E. Waldhör, W. Kaim, H. Binder and R. K. Kremer, *Organometallics*, 1994, **13**, 4156.
- 88 N. S. Hosmane, Y. Wang, H. Zhang, K. J. Lu, J. A. Maguire, T. G. Grey, K. A. Brooks, E. Waldhör, W. Kaim and R. K. Kremer, *Organometallics*, 1997, **16**, 1365.
- 89 U. Siriwardane, H. Zhang and N. S. Hosmane, *J. Am. Chem. Soc.*, 1990, **112**, 9637.
- 90 H. Zhang, L. Jia and N. S. Hosmane, *Acta Cryst.*, 1993, **C49**, 453.
- 91 N. S. Hosmane, H. Zhang, H. Zhang, L. Jia, T. J. Colacot, J. A. Maguire, X. Wang, S. N. Hosmane and K. A. Brooks, *Organometallics*, 1999, **18**, 516.
- 92 C. J. Thomas, L. Jia, H. Zhang, U. Siriwardane, J. A. Maguire, Y. Wang, K. A. Brooks, V. P. Weiss and N. S. Hosmane, *Organometallics*, 1995, **14**, 1365.
- 93 S. S. H. Mao, T. D. Tilley, A. L. Rheingold and N. S. Hosmane, *J. Organomet. Chem.*, 1997, **533**, 257.
- 94 K. E. Stockman, K. L. Houseknecht, E. A. Boring, M. Sabat, M. G. Finn and R. N. Grimes, *Organometallics*, 1995, **14**, 3014.
- 95 R. Uhrhammer, D. J. Crowther, J. D. Olson, D. C. Swenson and R. F. Jordan, *Organometallics*, 1992, **11**, 3098.

Chapter One - Introduction

- 96 L. M. Engelhardt, R. I. Papasergio, C. L. Ranson and A. H. White, *Organometallics*, 1984, **3**, 18.
- 97 R. Uhrhammer, Y. X. Su, D. C. Swenson and R. F. Jordan, *Inorg. Chem.*, 1994, **33**, 4398.
- 98 R. N. Grimes, *Chem. Rev.*, 1992, **92**, 251.
- 99 K. L. Houseknecht, K. E. Stockman, M. Sabat, M. G. Finn and R. N. Grimes, *J. Am. Chem. Soc.*, 1995, **117**, 1163.
- 100 E. Boring, M. Sabat, M. G. Finn and R. N. Grimes, *Organometallics*, 1997, **16**, 3993.
- 101 F. G. A. Stone, *Adv. Organomet. Chem.*, 1990, **31**, 53.
- 102 S. A. Brew and F. G. A. Stone, *Adv. Organomet. Chem.*, 1993, **35**, 135.
- 103 S. A. Brew, D. D. Devore, P. D. Jenkins, M. U. Pilotti and F. G. A. Stone, *J. Chem. Soc., Dalton Trans.*, 1992, 393.
- 104 G. C. Bruce, D. F. Mullica, E. L. Sappenfield and F. G. A. Stone, *J. Chem. Soc., Dalton Trans.*, 1992, 2685.
- 105 F. G. A. Stone, *Pure and Appl. Chem.*, 1986, **58**, 529.
- 106 J. Kim, Y. Do, Y. S. Sohn, C. B. Knobler and M. F Hawthorne, *J. Organomet. Chem.*, 1991, **418**, C1.
- 107 J. H. Kim, E. Hong, J. Kim and Y. Do, *Inorg. Chem.*, 1996, **35**, 5112.
- 108 J. H. Kim, M. Lamrani, J.W. Hwang, and Y. Do, *J. Chem. Soc., Chem. Commun.*, 1997, 1761.
- 109 P. D. Grebenick, M. L. H. Green, M. A. Kelland, J. B. Leach and P. Mountford, *J. Chem. Soc., Chem. Commun.*, 1989, 1397.
- 110 D. StClair, A. Zalkin and D. H. Tempelton, *Inor. Chem.*, 1971, **10**, 2587
- 111 F. A. Gómez, S. E. Johnson, C. B. Knobler and M. F. Hawthorne, *Inorg. Chem.*, 1992, **31**, 3558.

- 112 A. R. Oki, H. Zhang, J. A. Maguire, N. S. Hosmane, H. Ro, W. E. Hatfield, M. Moscherosch and W. Kaim, *Organometallics*, 1992, **11**, 4202.
- 113 A. Oki, H. Zhang, J. A. Maguire, N. S. Hosmane, H. Ro and W. E. Hatfield, *Organometallics*, 1991, **10**, 2996.
- 114 M. A. Curtis, E. J. Houser, M. Sabat and R. N. Grimes, *Inorg. Chem.*, 1998, **37**, 102.
- 115 N. N. Greenwood and A. Earnshaw, in “*Chemistry of the Elements*”, Pergamon Press Ltd., Oxford, 1994.
- 116 M. Gómez-Saso, D. F. Mullica, E. Sappenfield and F. G. A. Stone, *Polyhedron*, 1996, **15**, 793.
- 117 J. Crowe, E. J. M. Hamilton, J. C. V. Laurie and A. J. Welch, *J. Organomet. Chem.*, 1990, **394**, 1.
- 118 A. R. Oki, H. Zhang and N. S. Hosmane, *J. Am. Chem. Soc.*, 1991, **113**, 8531.
- 119 A. Zalkin, T. E. Hopkins and D. H. Templeton, *Inorg. Chem.*, 1966, **5**, 1189.
- 120 I. Blandford, J. C. Jeffery, P. A. Jelliss and F. G. A. Stone, *Organometallics*, 1998, **17**, 1402.
- 121 P. A. Chetcuti, P. Moser and G. Rihs, *Organometallics*, 1991, **10**, 2895.

Chapter Two

Synthesis Structure and Characterisation Of *Nido*-“C₂B₉” Clusters

2.1 Introduction

All three icosahedral carboranes 1,2-C₂B₁₀H₁₂ (**1**), 1,7-C₂B₁₀H₁₂ (**2**) and 1,12-C₂B₁₀H₁₂ (**3**), commonly known as *ortho*-, *meta*- and *para*-carborane respectively, are highly resistant to thermal and chemical attack, a fact that has allowed the development of a large derivative chemistry in which the cage system remains intact.¹ Nevertheless, Wiesboeck and Hawthorne discovered, almost 35 years ago, that *ortho*-carborane can be selectively degraded by strong bases,² to remove one boron atom from the cage and form salts of *nido*-7,8-dicarbaundecaboranate (1-), and this is arguably the most important reaction of these systems.³

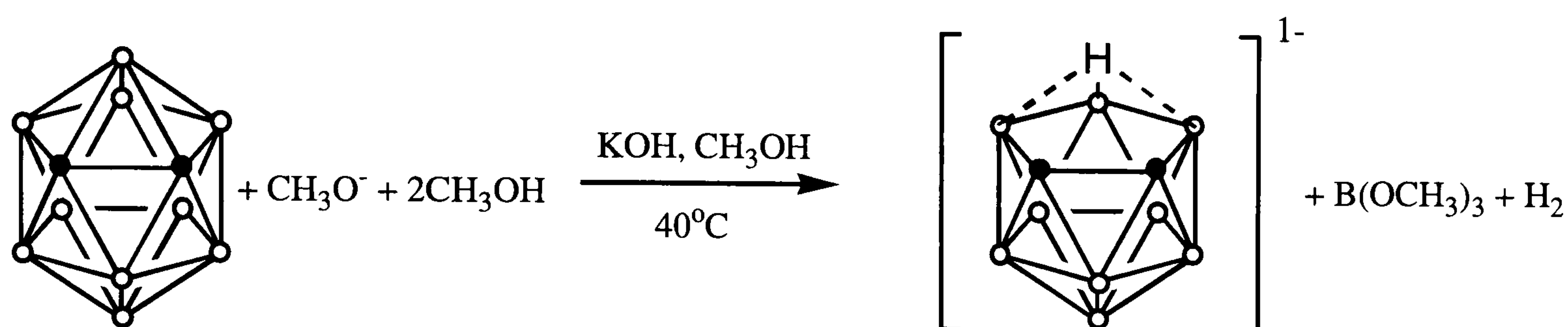


Figure 2.1 Deboronation of *ortho*-carborane (1,2-C₂B₁₀H₁₂) (**1**) by methoxide ion to form the *nido*- anion [7,8-C₂B₉H₁₂]⁻ (**5**).

Both the *ortho*- and *meta*-carboranes (or their substituted derivatives) are readily degraded by base under controlled conditions to the corresponding *nido*-carborane anions, [7,8-C₂B₉H₁₂]⁻ (**4**) and [7,9-C₂B₉H₁₂]⁻ (**5**) respectively. In both cases the boron atom removed is the one that is adjacent to both electronegative carbon atoms, since these boron atoms are more susceptible to nucleophilic attack.⁴

Early attempts to degrade the third isomer 1,12-C₂B₁₀H₁₂ (**3**) using ethanolic KOH failed, presumably because no boron atom is adjacent to both carbon atoms. More recently, Busby and Hawthorne used crown ether promoted base degradation in aprotic solvents at high temperature to degrade *para*-carborane in a much higher yield (95%).^{5,6}

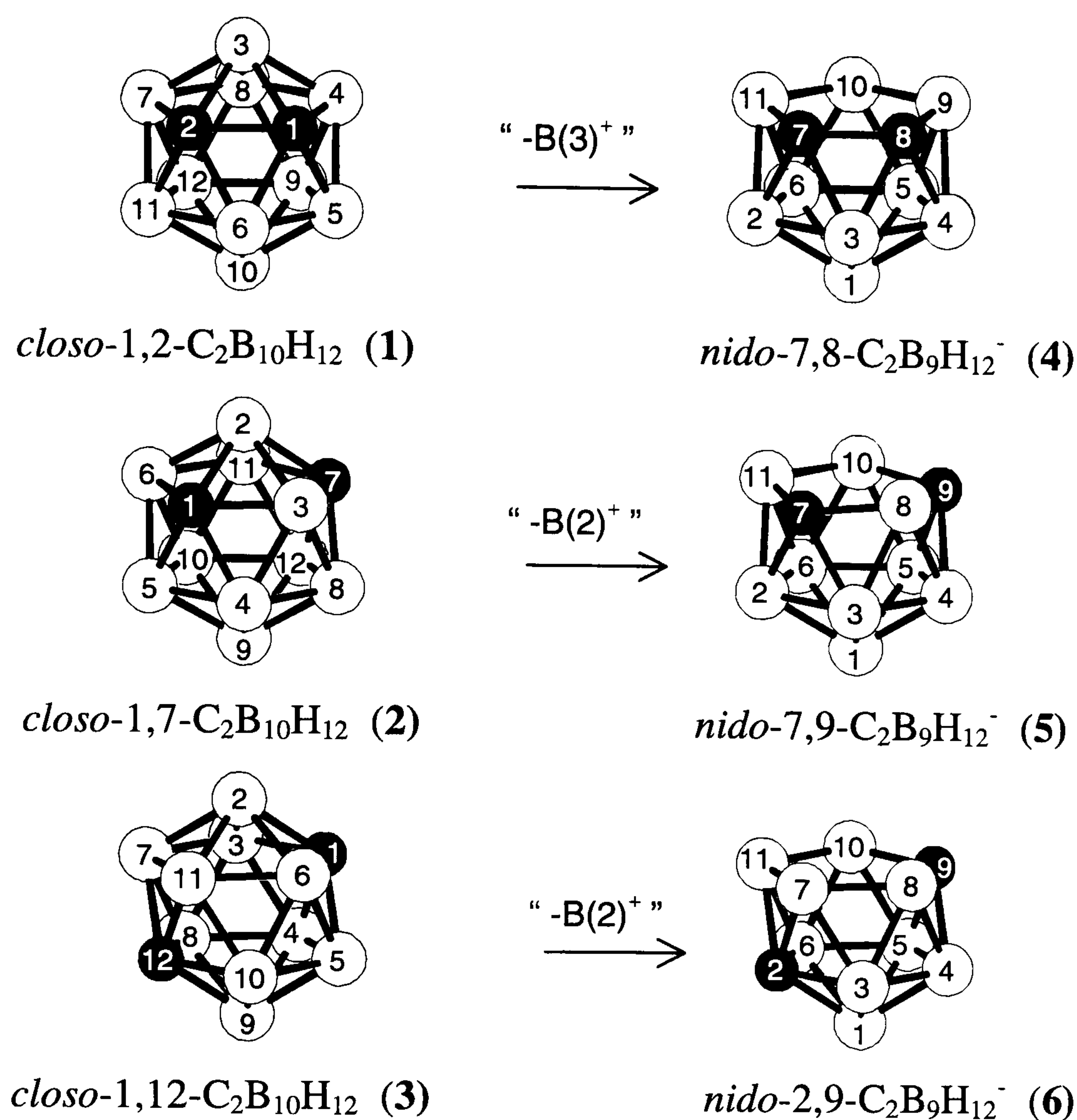


Figure 2.2 Deboronation of the parent *closo*-[C₂B₉H₁₂] systems to form the monoanion nido-[C₂B₉H₁₂]⁻. Numbering schemes for the *closo*- and *nido*- compounds are also shown.

The acidification of 7,8- (4), 7,9- (5) and 2,9-C₂B₉H₁₂⁻ (6) anions affords the neutral carboranes 7,8-, 7,9- and 2,9-C₂B₉H₁₃ (7-9) respectively.^{4,6} However we shall report, in this thesis, new evidence that disputes the existence of 7,9-C₂B₉H₁₃.

Deprotonation of the *nido*-[C₂B₉H₁₂]⁻ mono anions by strong bases leads to the formation of the dianionic *nido*-carboranes, *nido*-[7,8-C₂B₉H₁₁]²⁻ (10), *nido*-[7,9-C₂B₉H₁₁]²⁻ (11) and *nido*-[2,9-C₂B₉H₁₁]²⁻ (12). These compounds have the ability to bind to metal atoms in a η⁵-fashion, and this discovery led to the development of the field of metallocarborane chemistry.^{7,8}

As mentioned in chapter one, these dianions, (10), (11) and (12), are commonly referred to within the literature as dicarbollide anions. This name comes from the observation that the *nido*-11 particle icosahedral fragment resembles a spanish water jar called an “olla”. As a result Hawthorne and co-workers named the B₁₁H₁₁⁴⁻ ion the “ollide ion” and the CB₁₀H₁₁³⁻ and C₂B₉H₁₁²⁻ ions the “carbollide” and “dicarbollide”, (Cb²⁻), ions respectively.

Throughout the rest of this chapter we shall refer to the *nido*- anions using the trivial names of the parent *closo*-carborane species. This means that the *nido*-7,8-“C₂B₉” cage systems will be referred to as *ortho*-“C₂B₉”, 7,9-“C₂B₉” as *meta*-“C₂B₉” and 2,9-C₂B₉ as *para*-“C₂B₉” respectively.

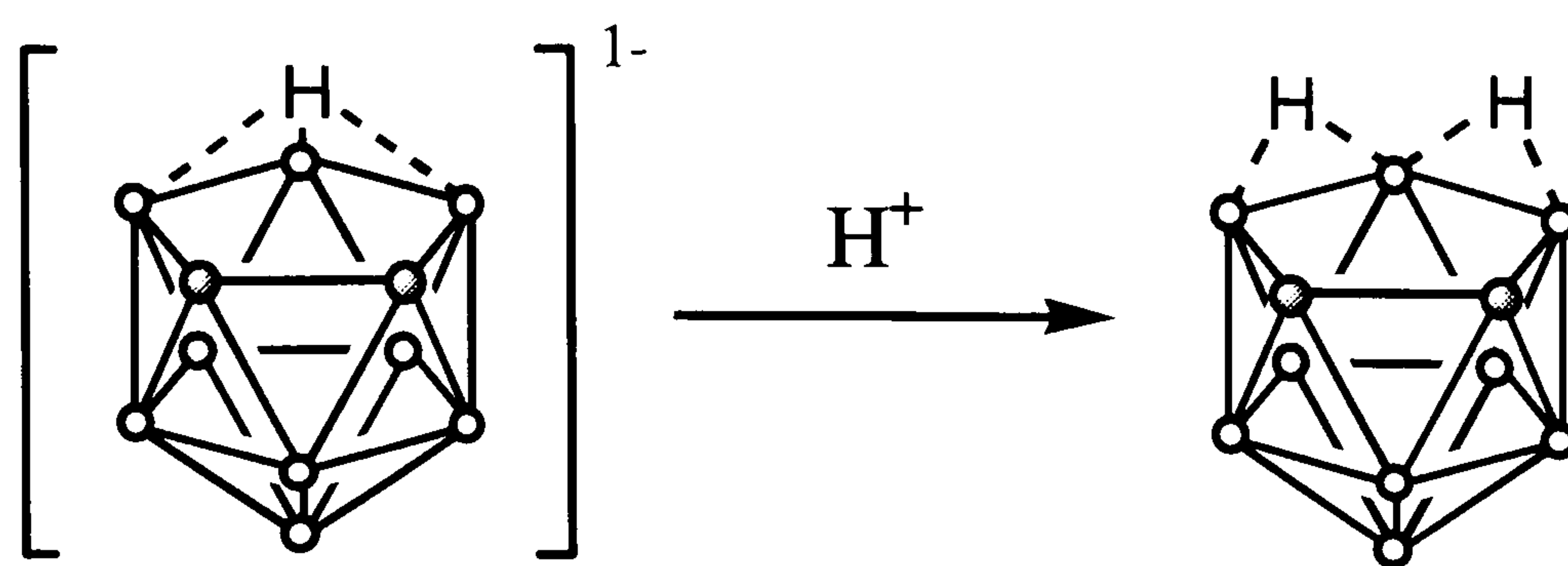
2.2 Ortho-, Meta- and Para-C₂B₉ systems.

As discussed in the introduction and chapter one, the *nido*-C₂B₉H₁₂⁻ anions are formed by the selective base degradation of the parent *closo*-C₂B₁₀H₁₂ carborane. The reaction is selective due to the enhanced electrophilicity of the boron atoms adjacent to the carbon atoms. As the carbon atoms move apart this inductive effect decreases, resulting in the reduced susceptibility of both *meta*- and *para*-carborane to attack by strong base compared to that of the *ortho*-derivative. For this reason, increasingly harsh conditions are used to decapitate the *closo*- cage as we go from *ortho*- to *meta*- to *para*-C₂B₁₀H₁₂.

2.2.1 Ortho-[C₂B₉H₁₃]

Ortho-carborane is decapitated in almost quantitative yields by the action of potassium hydroxide in methanol over a period of hours. The resulting methanolic solution of K[*ortho*-C₂B₉H₁₂] and excess KOH is then stripped of solvent. Remaining water is removed from the resulting white slurry by performing an azeotropic distillation. The dry carborane and excess potassium hydroxide are mixed with dry benzene to form a suspension to which excess 80% H₃PO₄ is added; this both neutralises the excess hydroxide and acidifies the *nido*- anion [*ortho*-C₂B₉H₁₂]⁻ to the neutral carborane [*ortho*-C₂B₉H₁₃].

Upon the addition of the acid, the white suspension disappears and the reaction mixture forms a biphasic mixture. The benzene layer is removed from the acid layer and is pumped to dryness; the resulting off-white solid can be purified by vacuum sublimation.⁹



Scheme 2.1 Synthesis of [*ortho*-C₂B₉H₁₃], (7).

The ¹¹B NMR spectrum for (7) shows the presence of 5 boron resonances in a 2:2:1:1:3 ratio. These as well as the ¹H and ¹³C resonances are in almost complete agreement with those discussed elsewhere.¹⁰

Although *ortho*-C₂B₉H₁₃, (7), has been known for some 35 years, it has received very little attention and to our knowledge no molecular structure, determined by X-ray crystallography, of either the parent complex or a substituted derivative has been reported.¹¹ While the compound forms colourless crystalline material in the absence of atmospheric moisture, attempts to isolate crystals suitable for X-ray diffraction have, to-date, been unsuccessful, the material being both soluble in hydrocarbon solvents and very moisture sensitive. It was for this reason that samples of the complex were sent to the E.P.S.R.C. electron diffraction service in Edinburgh. Work on this compound is ongoing.

As part of the work towards experimentally determining the structure of *ortho*-C₂B₉H₁₃, the geometry of the complex was optimised by Dr. Mark Fox of this department using the Gaussian 94 package, at the MP2/6-31G* level and is shown below in Figure 2.3.¹²

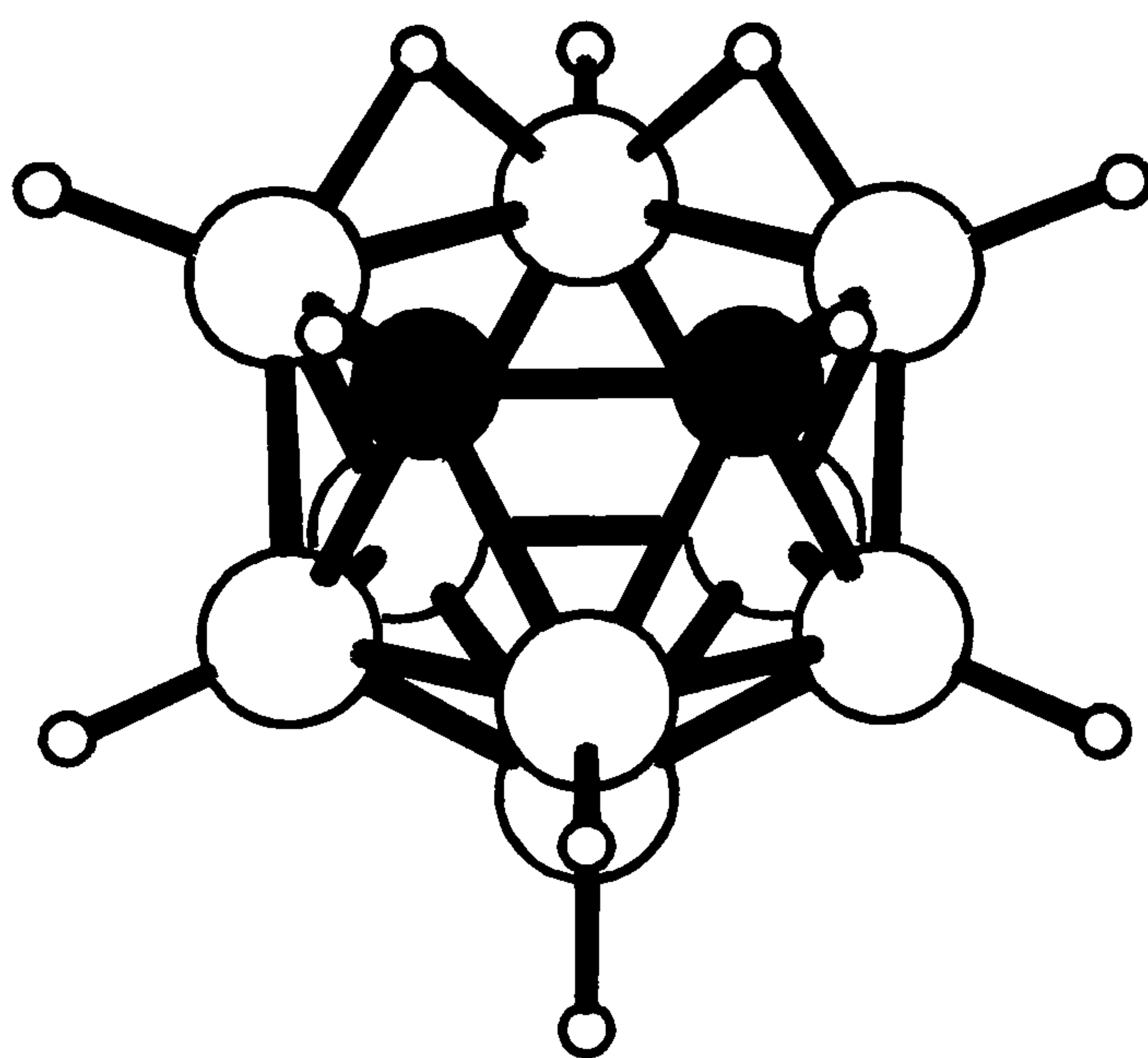


Figure 2.3 Pictographic representation of the geometry optimised structure of the neutral carborane *ortho*-C₂B₉H₁₃ (7).

The optimised geometry of (7) is consistent with the previously proposed structures, with a plane of symmetry running through the molecule and the two bridging hydrogens occupying two equivalent positions between B(9) and B(10) and B(11) and B(10). Theoretically calculated ¹¹B NMR shifts are in very close agreement to those found experimentally.¹³

Although there are no derivatives of [*ortho*-C₂B₉H₁₃] that have been structurally characterised,^{14,15} the structure of the double cluster 11-vertex:11-vertex tetracarborane [C₄B₁₈H₂₂], shown in Figure 2.4, has recently been determined by single crystal X-ray diffraction.¹⁶ The cluster can be perceived as two *nido*-C₂B₉ sub-clusters, the geometry of which is close to that predicted for the neutral carborane (7).

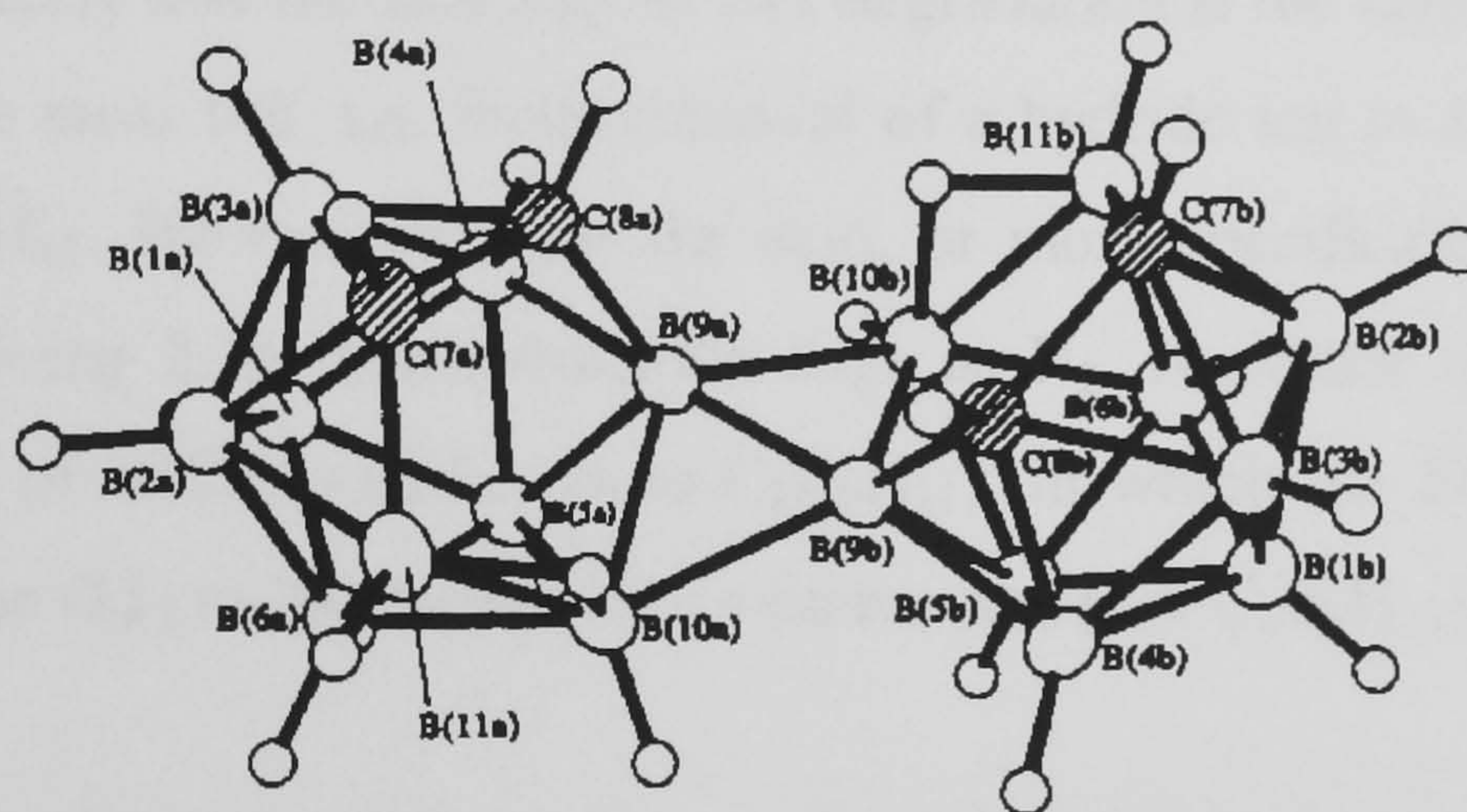


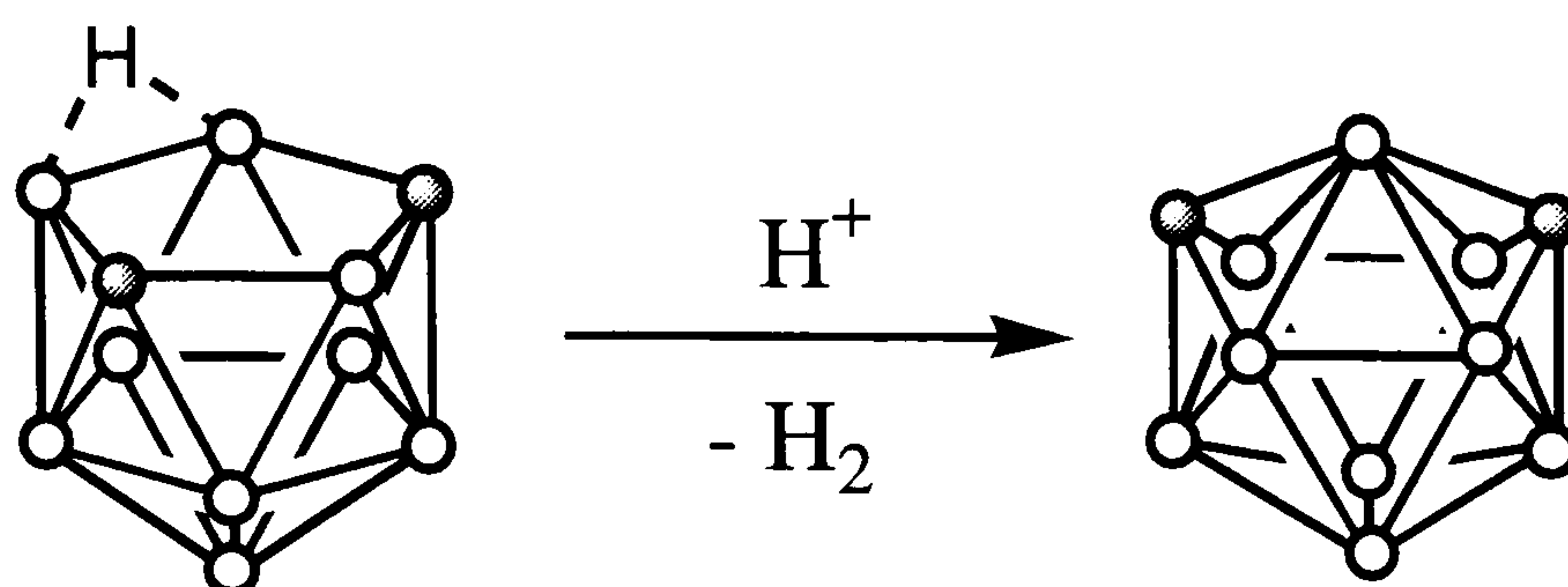
Figure 2.4. Molecular structure of the tetracarborane [C₄B₁₈H₂₂], Taken from ref. 16. The geometry of the {C₂B₉}-subunits is very similar to that calculated for [*ortho*-C₂B₉H₁₃].¹³

2.2.2 Meta-[C₂B₉H₁₃]

Both Hawthorne^{4b} and Rudolph¹⁷ have previously reported the reaction of the salt K[*meta*-C₂B₉H₁₂] with acid, and reported the production of the dibasic acid [*meta*-C₂B₉H₁₃]. Hawthorne also reports that this compound is not stable enough to allow chemical characterisation and rapidly forms the smaller *closo* carborane [2,3-C₂B₉H₁₁] (13).^{4b}

In our study we have found no evidence to support the claim that [*meta*-C₂B₉H₁₃] is formed in the reaction between its salts and acid. In fact in a typical reaction between a slurry of N^tBu₄ [7,9-C₂B₉H₁₂] in benzene and concentrated sulphuric acid at 0°C, gas, identified as H₂, was observed to be evolved immediately. The reaction was repeated several times at lower temperatures, and monitored by ¹¹B NMR spectroscopy, and the product of the reaction being identified as [*closo*-2,3-C₂B₉H₁₁].¹⁸ The studies revealed that this product was formed in near

quantitative yields with no evidence of peaks corresponding to an intermediate, such as C₂B₉H₁₃.



Scheme 2.2 Reaction of [*meta*-C₂B₉H₁₂][−] salts with acid. Formation of the *closo* carborane [2,3-C₂B₉H₁₁].

Salts of the *nido* carborane [*meta*-C₂B₉H₁₂][−] are known to be air sensitive, degrading quickly to boric acid. It is most likely that the first step in this degradation is the same as that observed in the acidification of the *meta* salt, i.e. facile removal of a hydride ion to form the air sensitive *closo*-carborane C₂B₉H₁₁. We can consider the acid, or more specifically the H⁺ ions, to be oxidising agents removing 2 electrons from the cage as H₂. A similar observation has been made for the reaction of SnCl₂ with Li₂[*meta*-C₂B₉H₁₁], in which the Sn(II) oxidises the 26 electron *nido*-carborane (**11**) to 24 electron *closo* carborane, [2,4-C₂B₉H₁₁].¹⁹

This ease with which salts of the *nido* carborane [*meta*-C₂B₉H₁₂][−] degrade is possibly a result of the geometry of the cluster. The *meta* relationship of the carbons in the only known isomer of *closo*-[C₂B₉H₁₁] places them at the lowest order vertices of the dodecahedron, in accordance with the empirical observation of the “preferred” placement of the “electron rich” heteroatoms.²⁰ The relationship of the carbons in [*meta*-C₂B₉H₁₁]^{2−} renders the closure of the cage a much lower energy process, compared to [*ortho*-C₂B₉H₁₁]^{2−} where closure of the cage would not place the carbon at low order vertices without rearrangement of the polyhedron.^{19,21}

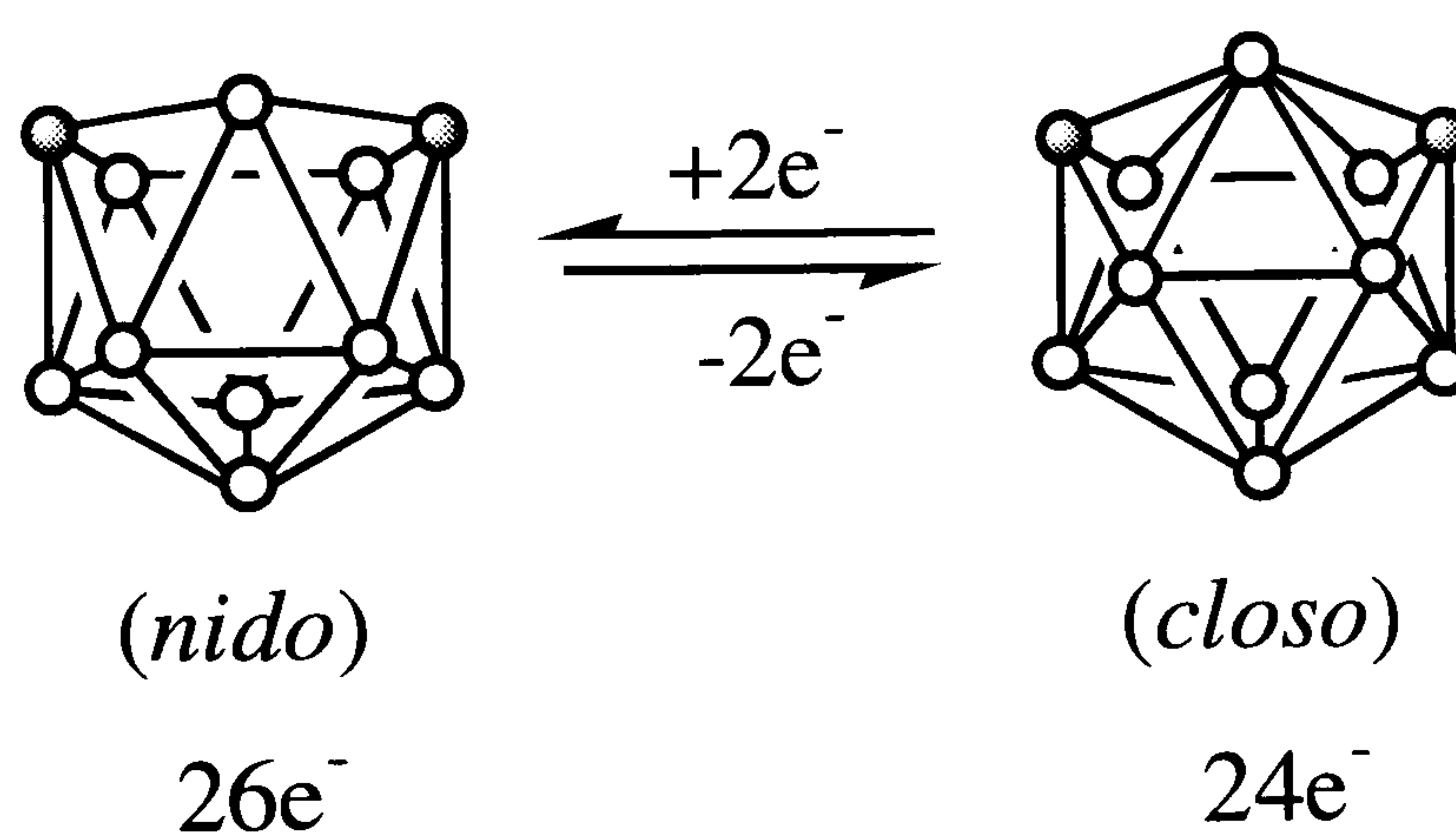
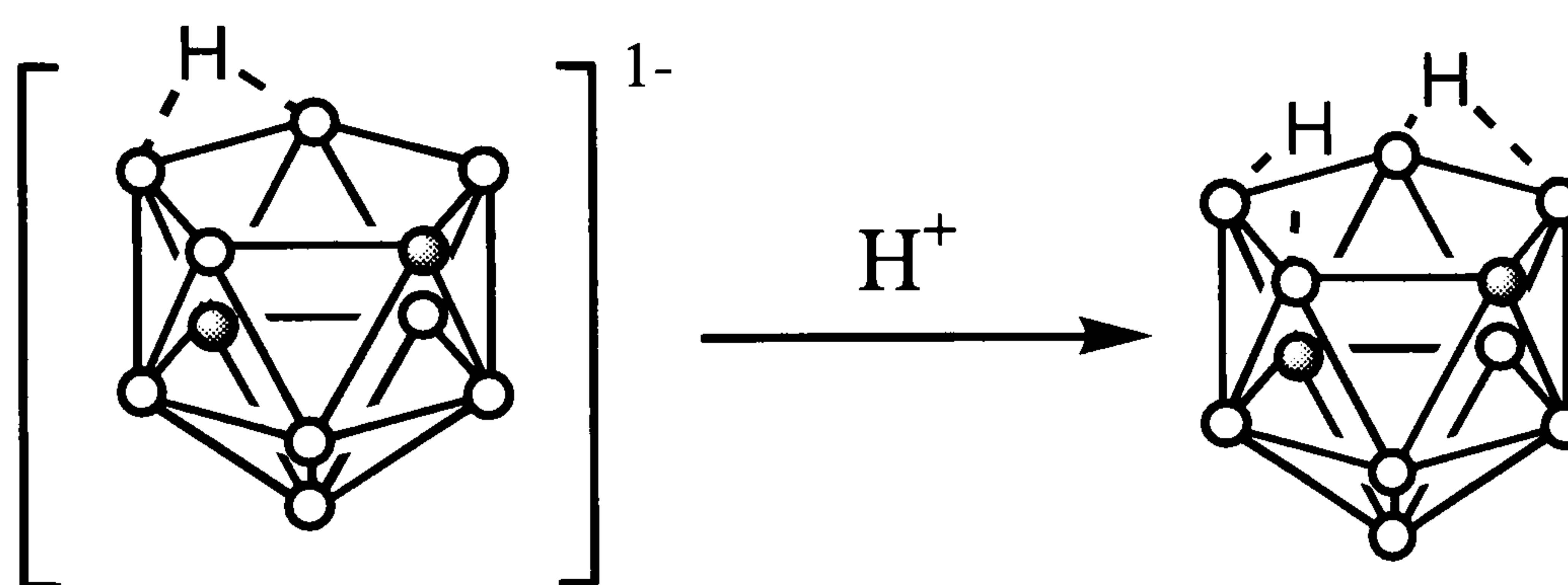


Figure 2.5 The interconversion of *nido* and *closo* 11 atom frameworks.

2.2.3 Para-[C₂B₉H₁₃]

The deboronation of *para*-carborane has previously been achieved on small scales using very harsh conditions.^{5,6} The slow deboronation of *para*-carborane in toluene at 120°C in the presence of tetraglyme and anhydrous potassium hydroxide was found to be preferable to either of the two alternative methods.

Anhydrous potassium hydroxide powder was found to be soluble in 1:1 (by volume) mixture of toluene and tetraglyme. *Para*-C₂B₁₀H₁₂ was then added to the mixture and refluxed for 18 hours, over which time the deboronated salt [K(tetraglyme)][*para*-C₂B₉H₁₂] precipitated from the solution as a white powder. The reaction mixture containing excess hydroxide and unused *para*-carborane was removed from the precipitate by cannula filtration and the solid residue washed with toluene. The anhydrous solid was then slurried in benzene and acidified with 80% H₃PO₄. The benzene layer was separated and the benzene removed under reduced pressure. The resulting pungent white solid was then sublimed under reduced pressure at room temperature to provide pure [*para*-C₂B₉H₁₃].



Scheme 2.3 Synthesis of [*para*-C₂B₉H₁₃], (9).

As with the carborane [*ortho*-C₂B₉H₁₃], the optimised geometry of the cluster was calculated using the Gaussian 94 package, at the MP2/6-31G* level (Figure 2.6).¹² The structure is in agreement with that predicted by Heřmánek in 1973, with two hydrogens bridging the open “CB₄” face in a symmetrical fashion, as predicted by NMR studies. Calculated theoretical ¹¹B NMR data are also in good agreement with those found experimentally.¹³

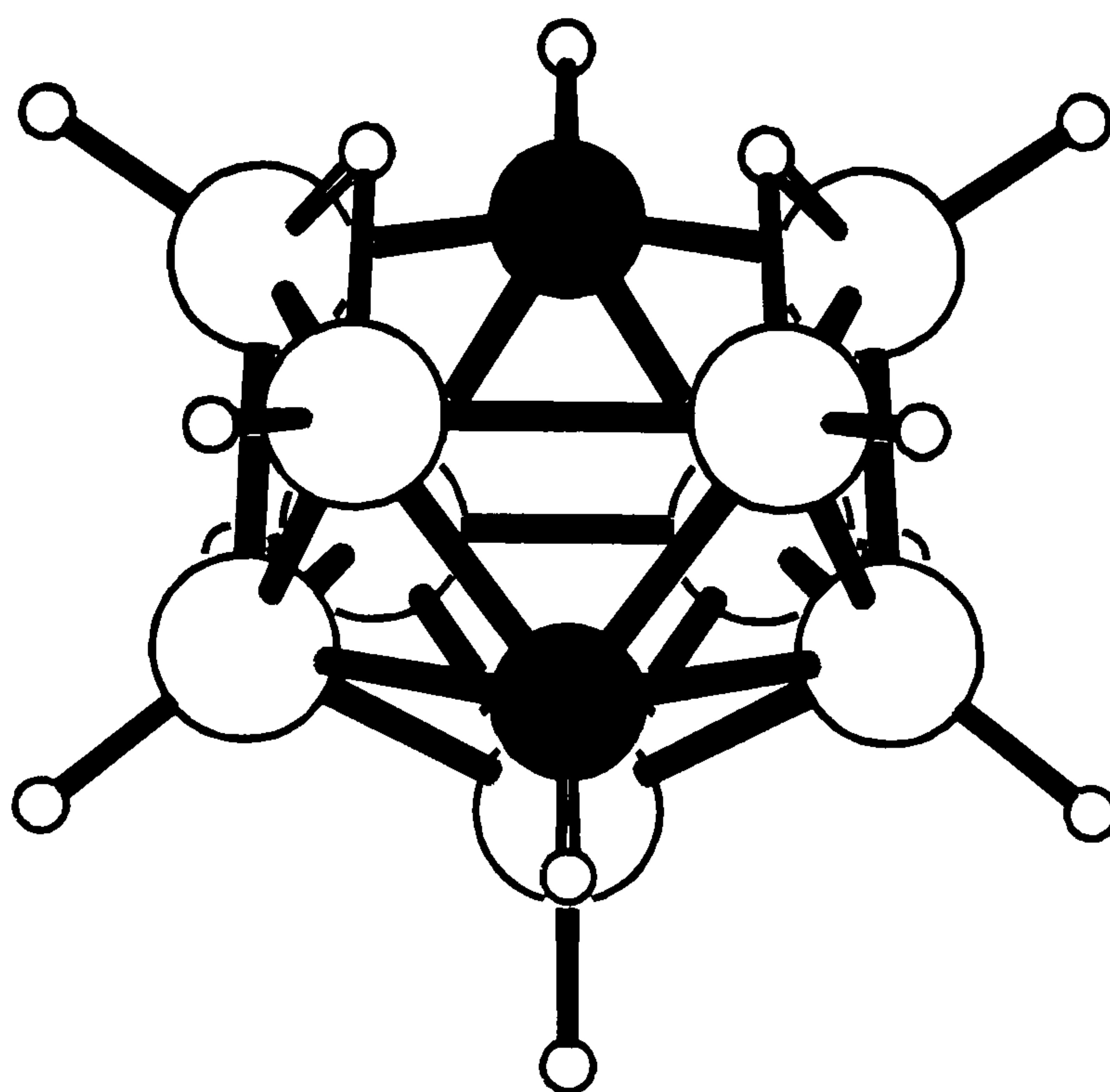


Figure 2.6 Pictographic representation of the geometry optimised structure of the neutral carborane *para*-C₂B₉H₁₃ (**9**).

2.3 Reaction of the carborane acids [*ortho*-C₂B₉H₁₃] and [*para*-C₂B₉H₁₃] with bases; structures of the [C₂B₉H₁₂][−] anion.

The two carborane acids, [*ortho*-C₂B₉H₁₃] (**7**) and [*para*-C₂B₉H₁₃] (**9**), both react with bases such as 1,8-N,N,N',N'-tetramethylnaphthalenediamine, proton sponge (PS), or simple amines. With bases such as amines only one of the bridging protons is removed, to form salts of the carborane of the form [BH]⁺[C₂B₉H₁₂][−], where B is a base such as NMe₃. Systems such as these can be thought of as conjugate acid and conjugate base salts, where the protonated base becomes the conjugate acid and the carborane anion the conjugate base.

2.3.1 Salts of [*ortho*-C₂B₉H₁₂][−]

The neutral carborane, [*ortho*-C₂B₉H₁₃], reacts in a 1:1 ratio with a solution of proton sponge in toluene to form the [*ortho*-C₂B₉H₁₂][−] salt as a white precipitate. After removal of solvent and washing of the salts with toluene, crystals of the hygroscopic salt, suitable for single crystal X-ray diffraction were grown from CH₂Cl₂ layered with pentane. The molecular structure of the carborane salt [(N(Me)₂H)(N(Me)₂)(C₁₀H₆)]⁺[*nido*-7,8-C₂B₉H₁₂][−] ([PSH]⁺[*nido*-7,8-C₂B₉H₁₂][−]) (**4a**) is shown in Figure 2.7.

The nitrogen base 1,8-bis(dimethylamino)naphthalene, [PS], is regarded as one of the strongest nitrogen bases known, with the protonated form having the highest pK_a value in aqueous solution of all the aromatic amines,²² and has been used as a proton abstractor in the synthesis of metallocarborane, carborane and borane complexes.^{10b,23} Studies on a series of salts containing the cation [PSH⁺] have shown that the N...N distance in the [PSH⁺] cation is generally very short, i.e. between 2.55 Å and 2.65 Å,²⁴ (N...N in this study is 2.599(3) Å) which is comparable with the lower limit (2.60 ± 0.05 Å) for the N...N distance in the N...H...N hydrogen bonds).²⁵

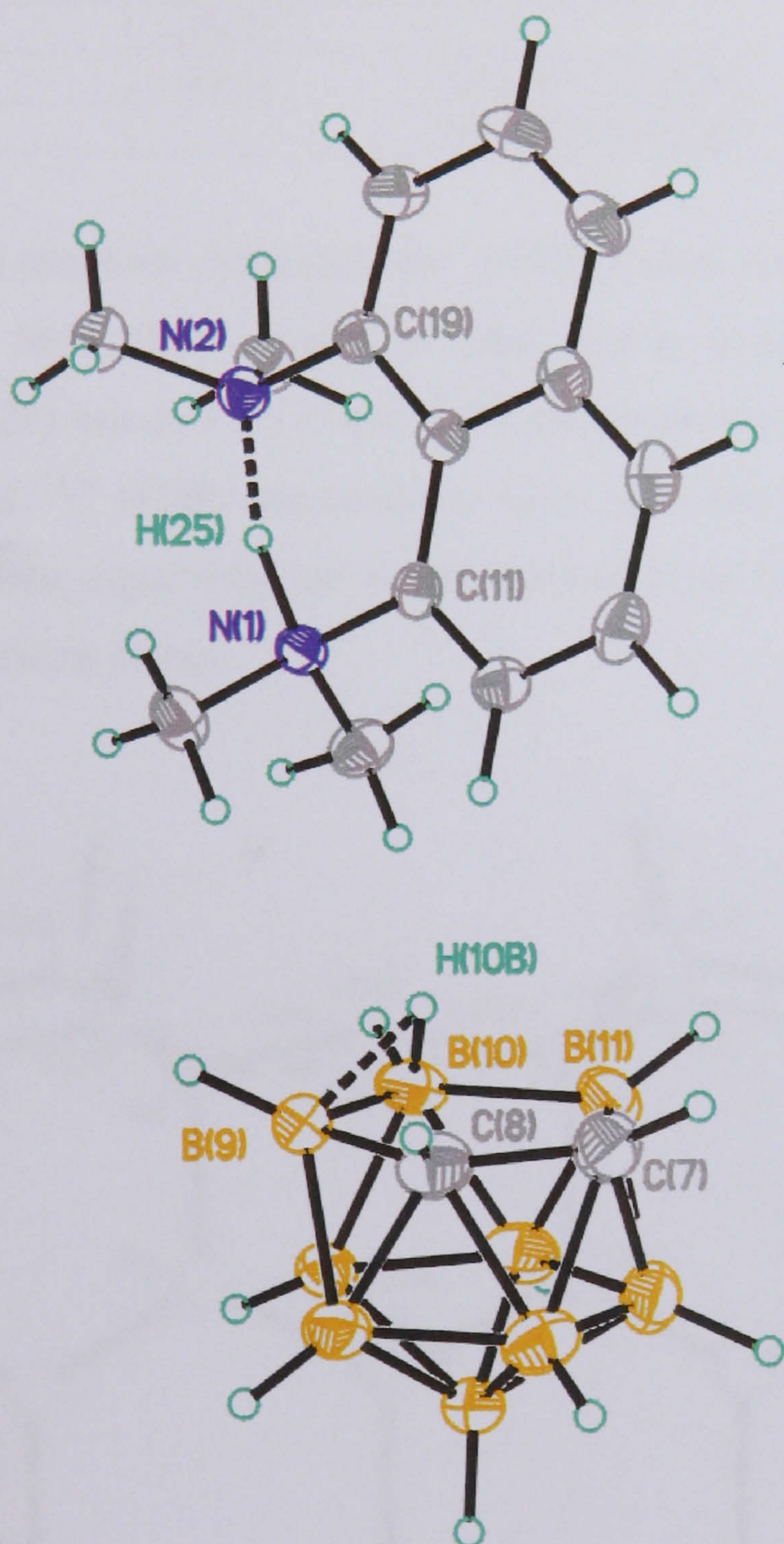


Figure 2.7 Molecular structure of [PSH]⁺[nido-7,8-C₂B₉H₁₂]⁻ (**4a**). Thermal ellipsoids of non hydrogen atoms are shown at 50% probability. Hydrogen atoms are shown as hollow circles.

Table 2.1 Selected bond distances (Å), and bond angles (°) for (4a).

B(10)-H(10B)	1.16(4)	H(25)-N(1)-C(11)	100.9(16)
B(9)-H(10B)	1.54(4)	H(25)-N(2)-C(19)	99.4(15)
C(7)-C(8)	1.560(4)	C(11)-N(1)	1.476(3)
C(7)-B(11)	1.622(5)	N(1)-C(23)	1.496(3)
C(8)-B(9)	1.621(4)	N(1)-C(24)	1.494(3)
B(9)-B(10)	1.842(5)		
B(10)-B(11)	1.812(4)	C(19)-N(2)	1.469(3)
		N(2)-C(21)	1.489(3)
N(1)---N(2)	2.599(4)	N(2)-C(22)	1.492(3)
N(1)-H(25)	1.25(4)		
N(2)-H(25)	1.40(4)	N(1)-C(11)-C(20)	118.1(2)
		N(2)-C(19)-C(20)	118.6(2)

By contrast with several previous structures, the [PSH⁺] cation does not possess molecular C₂ symmetry,²⁴ with the N(1)···H(25) bond in (4a) being considerably shorter than the corresponding N(2)···H(25) bond (1.25(4) and 1.40(4)Å respectively); this is shown clearly in Figure 2.8. Both ¹H and ¹³C NMR spectroscopy have show the [PSH⁺] cation to posses C₂ symmetry in solution, thus suggesting the unsymmetrical bond lengths observed in the solid state is due to crystal packing forces.

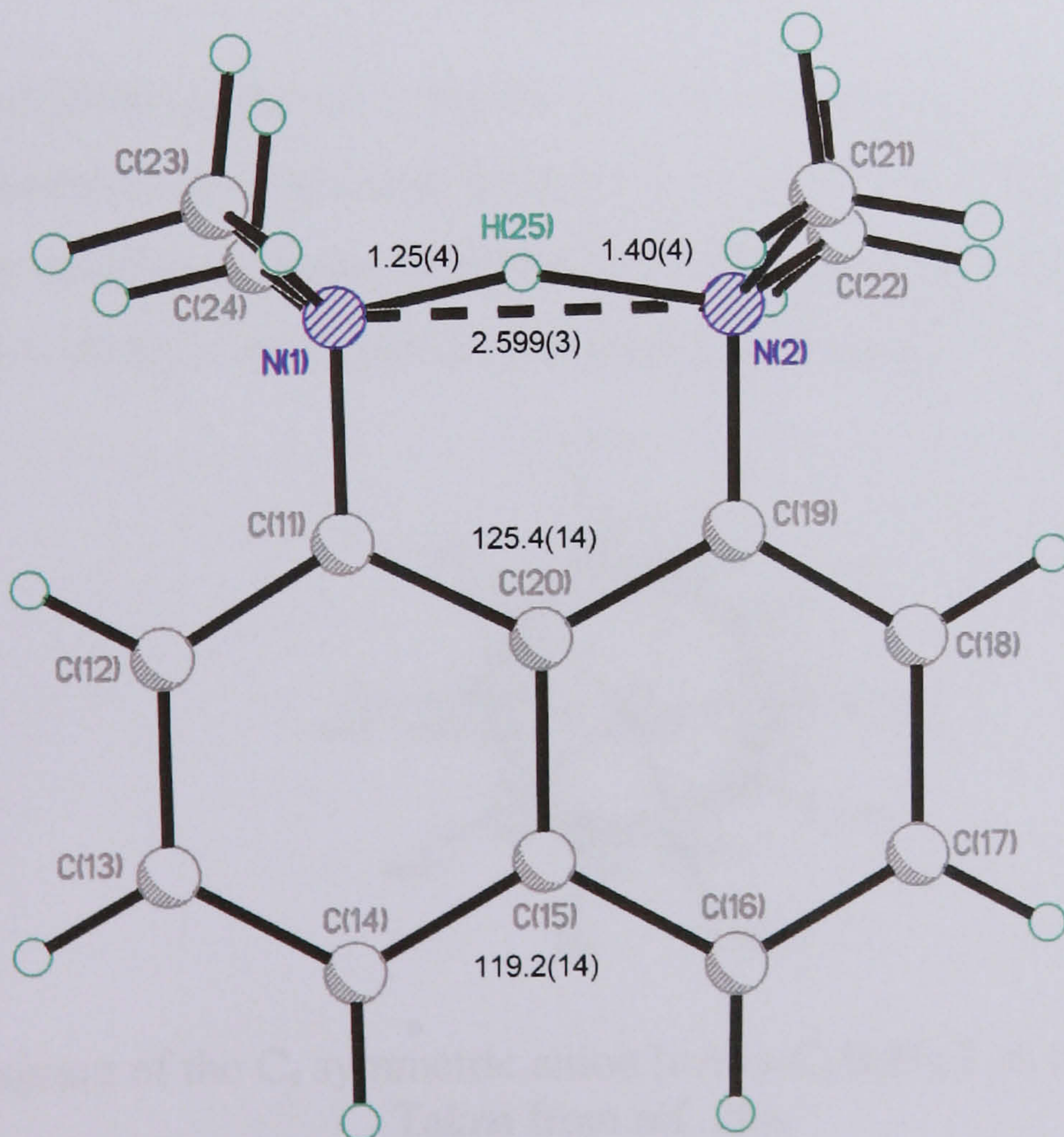


Figure 2.8 Representation of the cation, [PSH⁺], including the N···N, N···H bond distances (Å) and the C(14)-(C15)-C(16) and C(11)-C(20)-C(19) angles(°).

Although the two nitrogen atoms lie in the same plane as the naphthalene ring system, the molecule experiences a considerable amount of strain, with the deformation of the naphthalene ring being similar to that found in other 1,8-disubstituted naphthalenes.²⁴ The C(11)-C(20)-C(19) angle is larger than the C(14)-C(15)-C(16) angle, Figure 2.8, resulting in a longer C(11)···C(19) distance compared to C(14)···C(16) (2.546(4)Å and 2.471(4)Å respectively).

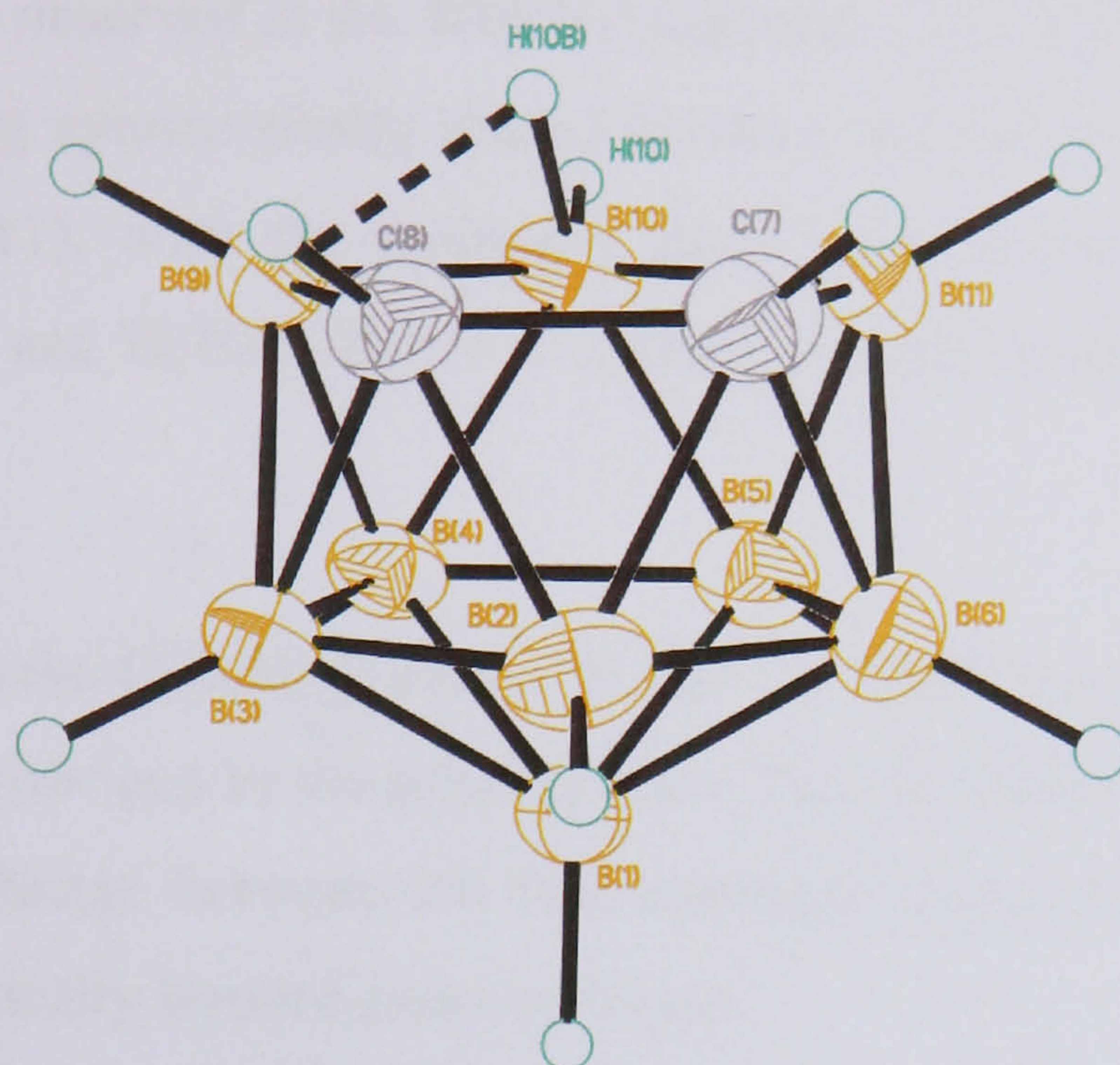


Figure 2.9 Molecular structure of the anion [*ortho*-C₂B₉H₁₂]⁻ as the PSH⁺ salt. All non hydrogen atoms are shown with 50% thermal ellipsoids, all hydrogen atoms are shown as hollow circles.

The anion [*ortho*-C₂B₉H₁₂]⁻, shown in Figure 2.9, has the expected *nido*-icosahedral geometry with an *exo*-polyhedral H atom terminal to each B or C cage atom. The open face is not planar, but is folded in an envelope fashion, about the B(9)···B(11) vector, similar to that seen in other salts of the [*ortho*-C₂B₉H₁₂]⁻ anion and its substituted derivatives.^{15,26}

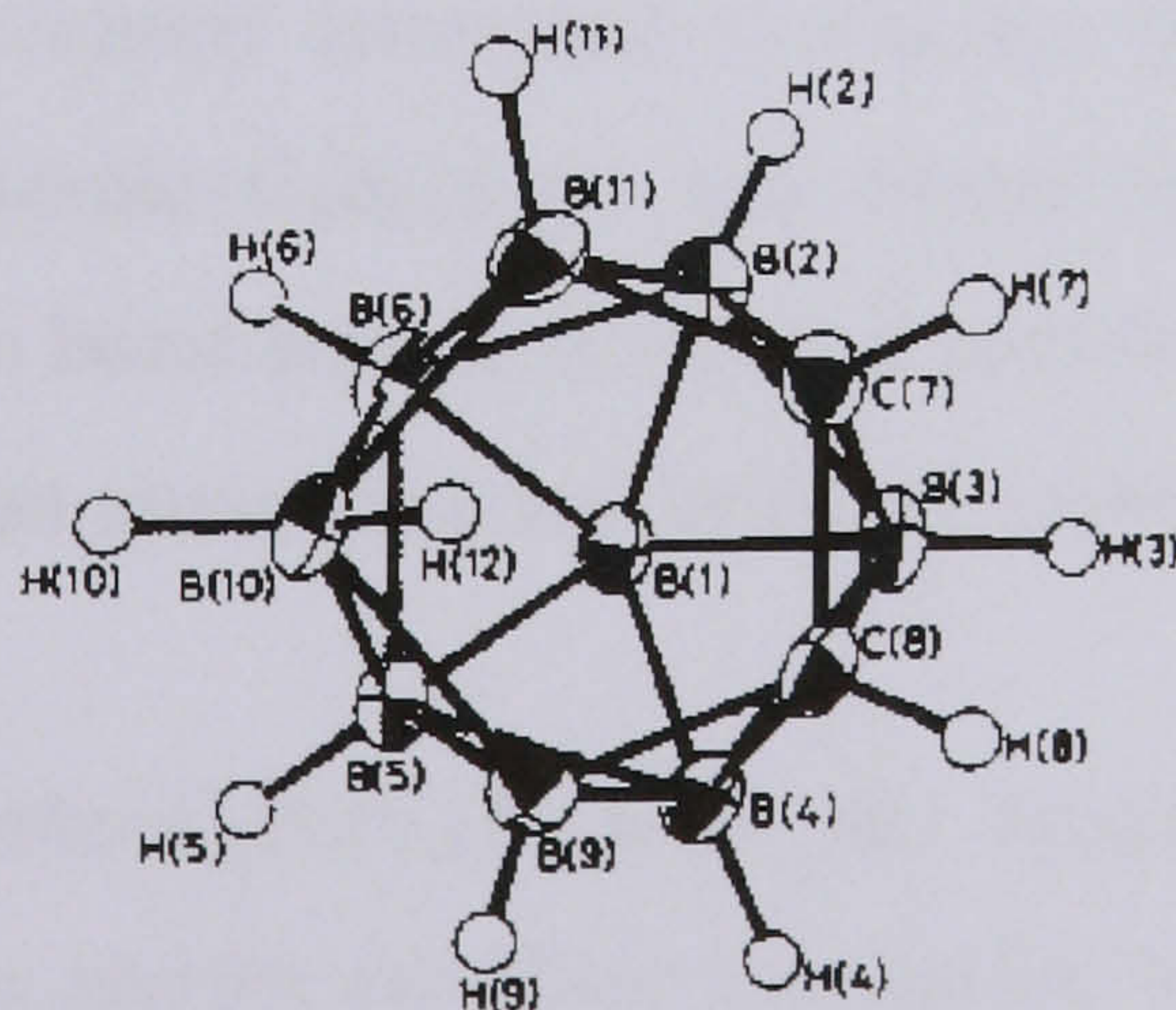


Figure 2.10 Diagram of the C_s symmetric anion [*ortho*-C₂B₉H₁₂]⁻ as the [(DMSO)₂H]⁺ salt. Taken from ref. 26a.

The molecular structure (Figure 2.9) clearly shows that the twelfth H (H(10B)) atom of (4a) occupies a non symmetric *endo*-terminal position on B(10). This is in direct contrast to the

structure of [(DMSO)₂H]⁺[*ortho*-7,8-C₂B₉H₁₂]⁻ determined by Welch in which the twelfth hydrogen occupies a symmetric position on B(10) affording the anion, as a whole, molecular C_s symmetry (Figure 2.10).^{26a}

The bond between H(10B) and B(10) is as expected longer than the *exo*-B-H bonds as observed in similar studies.²⁷ The H(10)-B(10)-H(10B) angle, 112.2(22)^o is slightly longer than the ideal tetrahedral angle observed in the Welch compound. This difference is possibly caused by the hydrogen not being symmetrically placed between the two boron atoms either side of B(10), i.e. B(9) and B(11), with the hydrogen atom lying towards the B(10)-B(9) bond (H(10B)-B(9) = 1.54(4)^o and H(10B)-B(11) = 1.85(4)^o, cf. H(12)-B(10)/B(110) = 1.71(3)^o in the symmetric case).

As with the symmetric [*ortho*-C₂B₉H₁₂]⁻ anion, ¹H and ¹¹B NMR spectra are unable to confirm the position of the *endo*-hydrogen in the solution state. The ¹H NMR data can be considered to arise from the fast interchange between the two canonical forms of the anion (4) shown in Figure 2.11, or a symmetrically bonded *endo*-hydrogen.

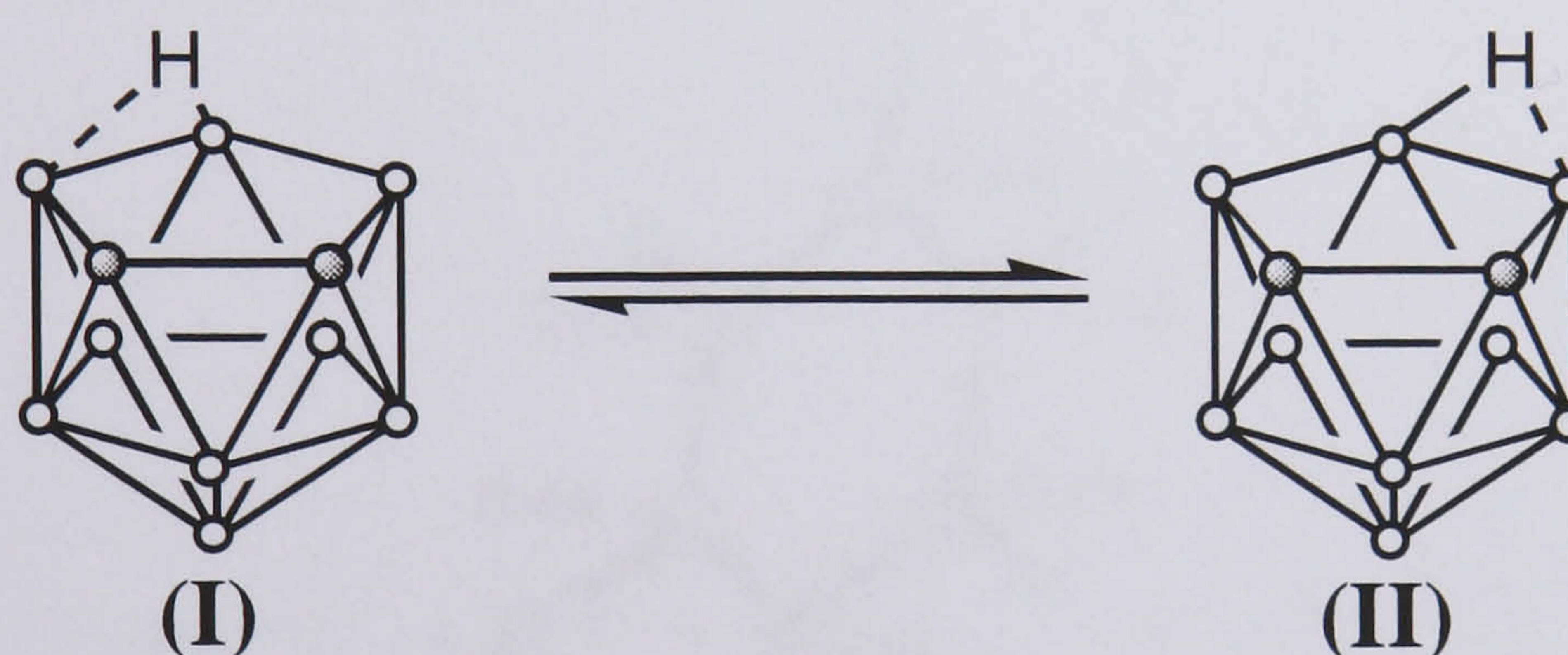


Figure 2.11 Interchange of the two canonical forms of the anion [*ortho*-C₂B₉H₁₂]⁻.

Onak and co-workers have previously attempted to resolve the dispute over the preferred geometry of the mono anion [*ortho*-C₂B₉H₁₂]⁻, and found better correlation between the experimentally found heavy atom bond lengths (C-C, C-B and B-B),^{26a} and those calculated for the anion [*ortho*-C₂B₉H₁₂]⁻ with an unsymmetrical bridging hydrogen atom (II).²⁸

Geometry optimisation of [*ortho*-C₂B₉H₁₂]⁻ with an unsymmetric bridging hydrogen, performed by Dr. Mark Fox, has shown excellent correlation with the structure of the anion found experimentally in this study, (4a). The study also reveals that the previously determined symmetric structure,^{26a} is in good agreement with the optimised geometry of the symmetric anion.

Although calculations show the unsymmetrical structure to be of lower energy, the difference in energy between the two optimised structures (unsymmetrical and symmetrical) is very small

(0.3 kcal mol⁻¹).¹³ These results indicate a fine balance between the preference for either geometry.

In an attempt to vary the cation in these complexes, a reaction between the neutral carborane (7) and the phosphonium ylide Ph₃PCH₂ was attempted. The ylide reacted with the carborane in a 1:1 ratio in an analogous reaction to that described for the proton sponge reaction. Crystals were grown slowly from a concentrated solution of dichloromethane layered with pentane at –30°C.

Analysis of the resulting salt [Ph₃PCH₃]⁺[*ortho*-C₂B₉H₁₂]⁻ by both ¹H and ¹¹B NMR spectroscopy indicated, as with the [PSH]⁺ salt, that the [Ph₃PCH₃]⁺ salt was comprised of two discrete ions, with the carborane anion exhibiting very similar chemical shifts to those shown for the [PSH]⁺ salt (4a). The molecular structure determined by X-ray diffraction (shown in Figure 2.12) confirms this observation with no evidence of inter-molecular contacts between the phosphonium cation and the [*ortho*-C₂B₉H₁₂]⁻ anion.

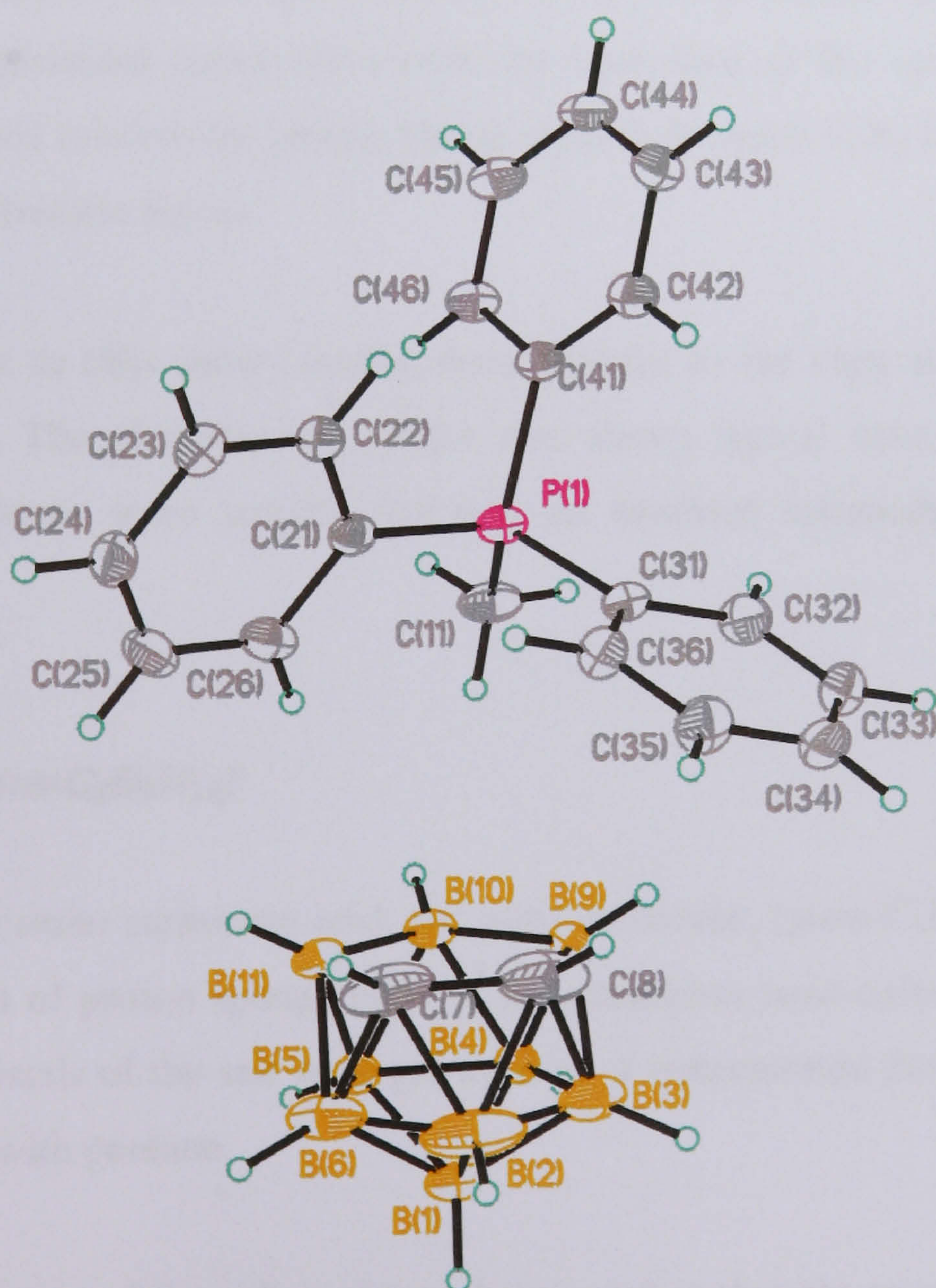


Figure 2.12 Molecular structure of [Ph₃PCH₃]⁺[C₂B₉H₁₂]⁻ (4b). Thermal ellipsoids of non hydrogen atoms are shown at 50% probability. Hydrogen atoms are shown as hollow circles.

Table 2.2 Selected bond distances (Å), and bond angles (°) for (4b).

C(7)-C(8)	1.630(4)		
C(7)-B(11)	1.612(3)		
C(8)-B(9)	1.658(4)	C(11)-P(1)-C(21)	110.67(10)
B(9)-B(10)	1.764(3)	C(11)-P(1)-C(31)	108.47(9)
B(10)-B(11)	1.756(3)	C(11)-P(1)-C(41)	108.88(9)
		C(21)-P(1)-C(31)	108.75(8)
P(1)-C(11)	1.790(2)	C(21)-P(1)-C(41)	109.01(8)
P(1)-C(21)	1.794(2)	C(31)-P(1)-C(41)	111.06(8)
P(1)-C(31)	1.792(2)		
P(1)-C(41)	1.499(2)		

Unfortunately the twelfth hydrogen on the carborane anion could not be located in the difference Fourier map, although NMR spectroscopy suggests a similar environment for the hydrogen atom on the cage to that observed in (4a).

Although there are thought to be no C-H···B interactions in the structure shown in Figure 2.12, with the closest contacts being between H(11C) on the phosphonium methyl group and B(10), at 2.73Å, the phosphonium cation rides over the open face of the carborane cage, with its methyl group directed towards the unique boron atom in the open C₂B₃ face. This is thought to be an effect of electrostatic forces.

The carborane cage in (4b) shows similar bond lengths to the cage anion in (4a) to within experimental error. The phosphonium cation also shows typical behaviour with the angles around the phosphorus atom tending towards an idealised tetrahedral geometry as seen elsewhere.²⁹

2.3.2 Salts of [para-C₂B₉H₁₂]

As with the neutral *ortho* carborane acid, the *para* carborane, [para-C₂B₉H₁₃], (9) reacts with only one equivalent of proton sponge to form the analogous *para* carborane salt [PSH]⁺[2,9-C₂B₉H₁₂]⁻ (6a). Crystals of the salt were grown from a concentrated dichloromethane solution which was layered with pentane.

The molecular structure of the salt is shown below and is thought to be the first structurally characterised example of a [para-C₂B₉H₁₂]⁻ anion.

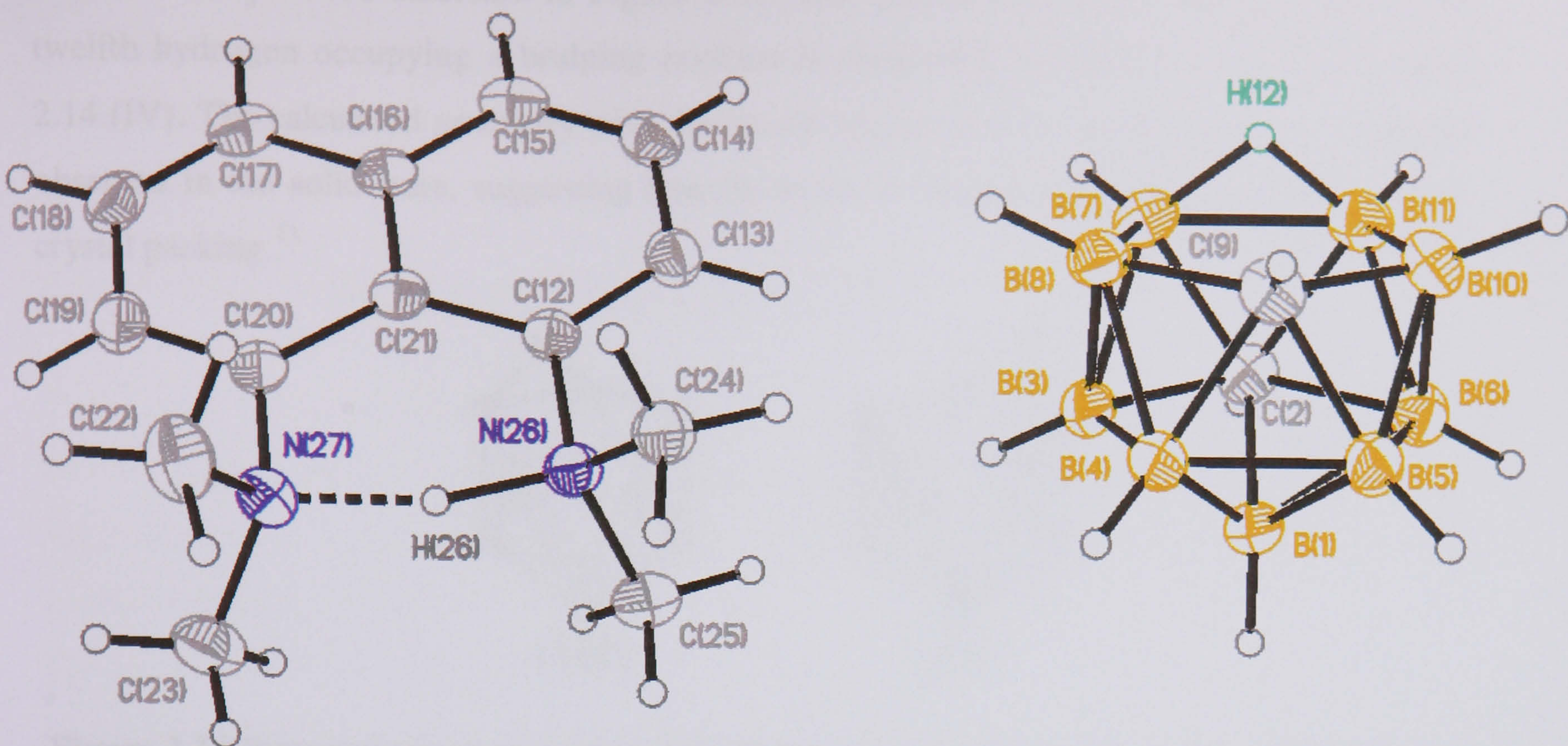


Figure 2.13 Molecular structure of [PSH]⁺[2,9-C₂B₉H₁₂]⁻ (**6a**). Thermal ellipsoids of non hydrogen atoms are shown at 50% probability. Hydrogen atoms are shown as hollow circles.

Table 2.3 Selected bond distances (Å), and bond angles (°) for (**6a**).

B(7)-H(12)	1.293(17)	H(26)-N(26)-C(12)	99.9(8)
B(11)-H(12)	1.261(16)	H(26)-N(27)-C(20)	98.4(7)
B(1)-C(2)	1.719(2)	C(12)-N(26)	1.4772(2)
B(1)-B(3)	1.771(2)	N(26)-C(24)	1.4919(18)
B(1)-B(4)	1.780(2)	N(26)-C(25)	1.4950(18)
B(1)-B(5)	1.772(2)		
C(2)-B(3)	1.743(2)	C(20)-N(27)	1.495(17)
C(2)-C(3)	1.742(2)	N(27)-C(22)	1.4830(19)
B(3)-B(4)	1.732(2)	N(27)-C(23)	1.4848(19)
B(4)-B(5)	1.794(2)		
B(5)-B(6)	1.733(2)	N(26)-C(12)-C(21)	117.84(11)
B(7)-B(8)	1.772(2)	N(27)-C(20)-C(21)	118.10(11)
B(7)-B(11)	1.891(2)		
B(8)-C(9)	1.644(2)	N(26)···N(27)	2.587(2)
C(9)-B(10)	1.642(2)	N(26)-H(26)	1.212(18)
B(10)-B(11)	1.768(2)	N(27)···H(26)	1.415(18)

In contrast to reports of the 7,8- and 7,9-C₂B₉H₁₂⁻ there are very few reports on the [nido-2,9-C₂B₉H₁₂]⁻ anion ([*para*-C₂B₉H₁₂]⁻) and the position of the twelfth hydrogen atom has not been discussed. Here the X-ray crystal structure of the proton sponge salt of [*para*-C₂B₉H₁₂]⁻ shows a bridging hydrogen atom located between B(7) and B(11). Geometry optimisation of the *para*-anion (**6a**) by Dr. Mark Fox of this department has located two minima in the geometries of the anion. The first, and lower energy, geometry, has a bridging hydrogen at B(7) and B(11) as

seen in the molecular structure in Figure 2.13. The second structural minimum having the twelfth hydrogen occupying a bridging position between B(7) and B(8), is shown in Figure 2.14 (IV). The calculated geometry with the lowest energy is in excellent agreement with that observed in the solid state, suggesting that the anion in (6a) is unaffected by forces such as crystal packing.¹³

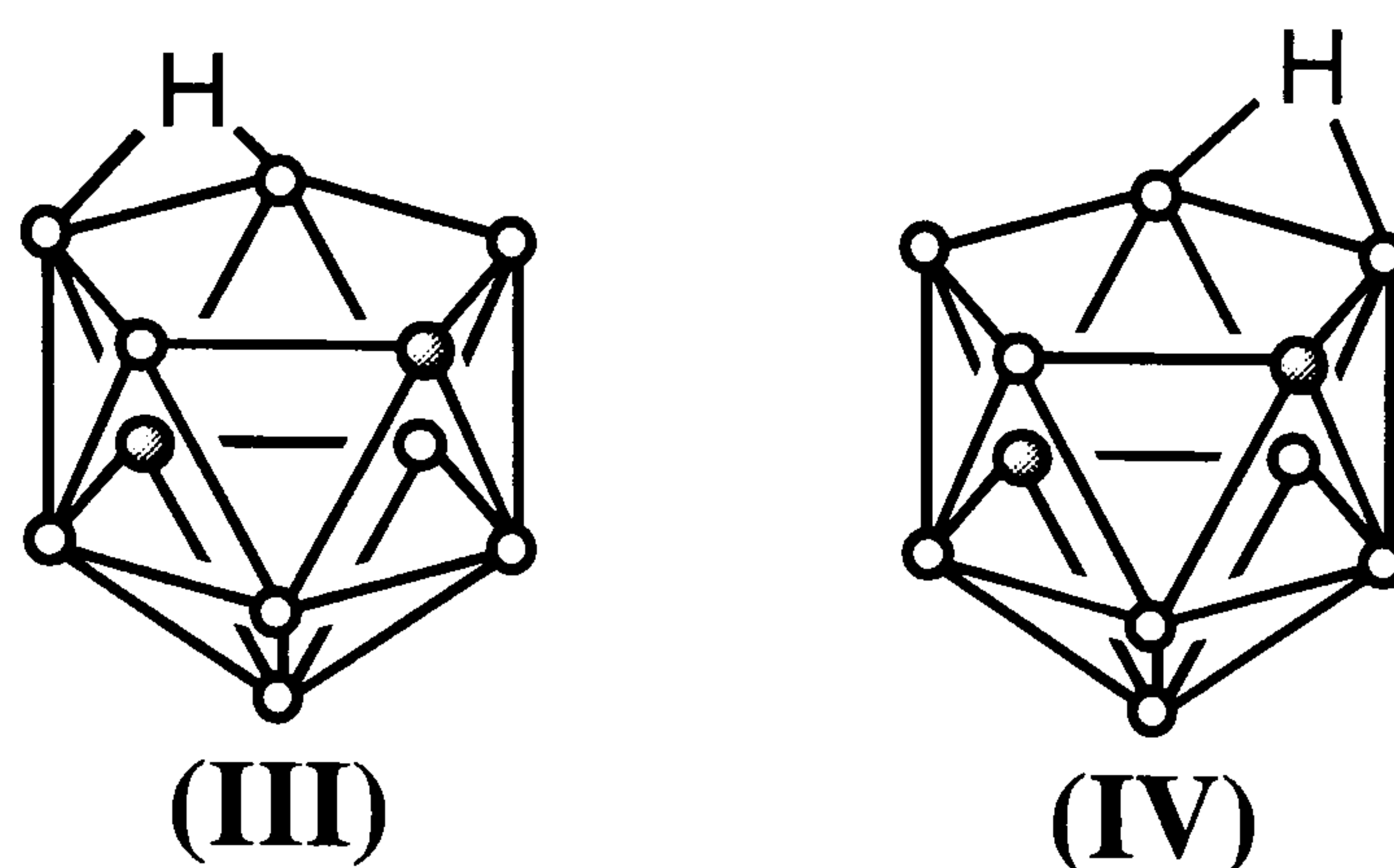


Figure 2.14 Representations of the two minima found for the geometry of the *para*-carborane anion [*nido*-2,9-C₂B₉H₁₂]⁻. Structure (III) is found to be the lower in energy of the two minima, and the geometry is in almost perfect agreement with that found by X-ray diffraction experiments.

The [PSH⁺] cation in (6a) has very similar bond lengths and angles to the cation observed in (4a), with the nitrogen atoms lying in the same plane as the naphthalene ring system.

Bond lengths and bond angles in the anion are very similar to those found in the parent *closo para*-carborane,³⁰ except for the expected lengthening of the bonds about the open “CB₄” face.

Both the neutral [*ortho*-C₂B₉H₁₃] and [*para*-C₂B₉H₁₃] carboranes react with bases because the bridging hydrides are acidic and the reactions discussed above can be thought of as simple acid base reactions. The p*K*_as of both carboranes have been previously discussed by both Hawthorne and Heřmánek, with reported p*K*_a values of 2.95 (in 33% by volume methanol water) and 3.15 (in 50% ethanol) for the neutral carboranes (7) and (9) respectively, thus placing these complexes on the same relative p*K*_a range as HF and HSO₄⁻.³¹

The acidity of the second hydrogen on the face of the carborane ligand is less well documented with only the p*K*_a value of the potassium salt of [*ortho*-C₂B₉H₁₂]⁻ recorded. Shatenshtein found the p*K*_a of the second hydrogen to be 21.3, and comparable to the acidity of both organic systems such as phenyl acetylene, indene or fluorene,³¹ and with the p*K*_as for the *closo*-carboranes 1-phenyl-*ortho*-carborane, 1-methyl-*ortho*-carborane, *ortho*-carborane and 1-isopropyl-*ortho*-carborane.³² The *ortho* anion is, therefore, a relatively strong acid for an anionic species.³³ A possible reason for this is the electron withdrawing nature of the carborane

cage making the anion a stronger acid than first expected. This enables the *endo*-hydrogens on the neutral carboranes to be removed by strong bases such as butyl lithium to form complexes of the dianionic carborane, [C₂B₉H₁₁]²⁻.

2.3.3 Reactions With Basic Metal Alkyl Complexes.

The capacity of the *nido*-carborane anion [C₂B₉H₁₁]²⁻ to bond cationic metallic units at sites on its open pentagonal face that reflect the frontier orbital characteristics of the metallic cations has long been recognised.^{1a,1c,7,8} As previously discussed in chapter one, the arrangement of the frontier orbitals of [C₂B₉H₁₁]²⁻ is similar to those of the cyclopentadienyl, (C₅H₅⁻), and imido, RN²⁻, ligands.³⁴ Both [C₂B₉H₁₁]²⁻ and RN²⁻ act as 4 electron LX₂ ligands.³⁵ Metallic residues that are isolobal with BH²⁺ can bond η⁵ to the face, and so effectively complete the *closo*-metallacarborane. It has been recognised that metal fragments with full, or almost full, d shells tend to occupy "slipped" positions over the open face, even though the metal fragment formally has the three vacant orbitals of a BH²⁺ unit (one radially, two tangentially oriented).³⁶ Coordination in an η¹ mode is also observed when the metal fragment has fewer than 3 vacant orbitals, as is the case in the complex [(η¹-C₂B₉H₁₁)SnPh₃]⁻.³⁷ Other alternative cluster geometries may also be observed even when the metal fragment is not isolobal with HB²⁺, but has three vacant orbitals available for M-Cb bonding.³⁸

Alkyl metal complexes such as [Cp*ScMe₂]_x,³⁹ Cp*MMe₃,⁴⁰ AlR₃ (R = Me and Et)⁴¹ and BeMe₂⁴² have previously been shown to react with the dibasic neutral carborane acids, such as [*ortho*-C₂B₉H₁₃]. In a similar fashion dimethyl zinc, [ZnMe₂], was found to react with the acidic carborane salt [(Me₃NH)⁺(*ortho*-C₂B₉H₁₂)⁻]^{*} which, by loss of two moles of methane, was expected to afford a monomeric icosahedral metallacarborane [Me₃N-ZnC₂B₉H₁₁], Figure 2.16.⁴³ The units Me₃N-Zn²⁺ and HB²⁺ are formally isolobal, and so in principle HB²⁺ units of borane clusters might be expected to be replaced by Me₃N-Zn²⁺ units.

The analogous beryllium complex, [Me₃N-BeC₂B₉H₁₁], shown in Figure 2.15, is believed to be isostructural and isoelectronic with *closo*-C₂B₁₀H₁₂.⁴² The ¹H NMR spectrum of this beryllium complex is reported to contain two peaks in a 2:9 ratio at δ 2.55 and δ 2.90 ppm, and assigned to the carborane C-H and the methyl groups of the NMe₃ unit respectively. The ¹¹B NMR

* The salt [(Me₃NH)⁺(*ortho*-C₂B₉H₁₂)⁻] can be considered the conjugate acid and conjugate base salt formed from the reaction of the parent carborane acid (7) and trimethyl amine.

spectrum of this complex is reported to show 5 unresolved resonances, although, relative intensity ratios are not reported.⁴⁴

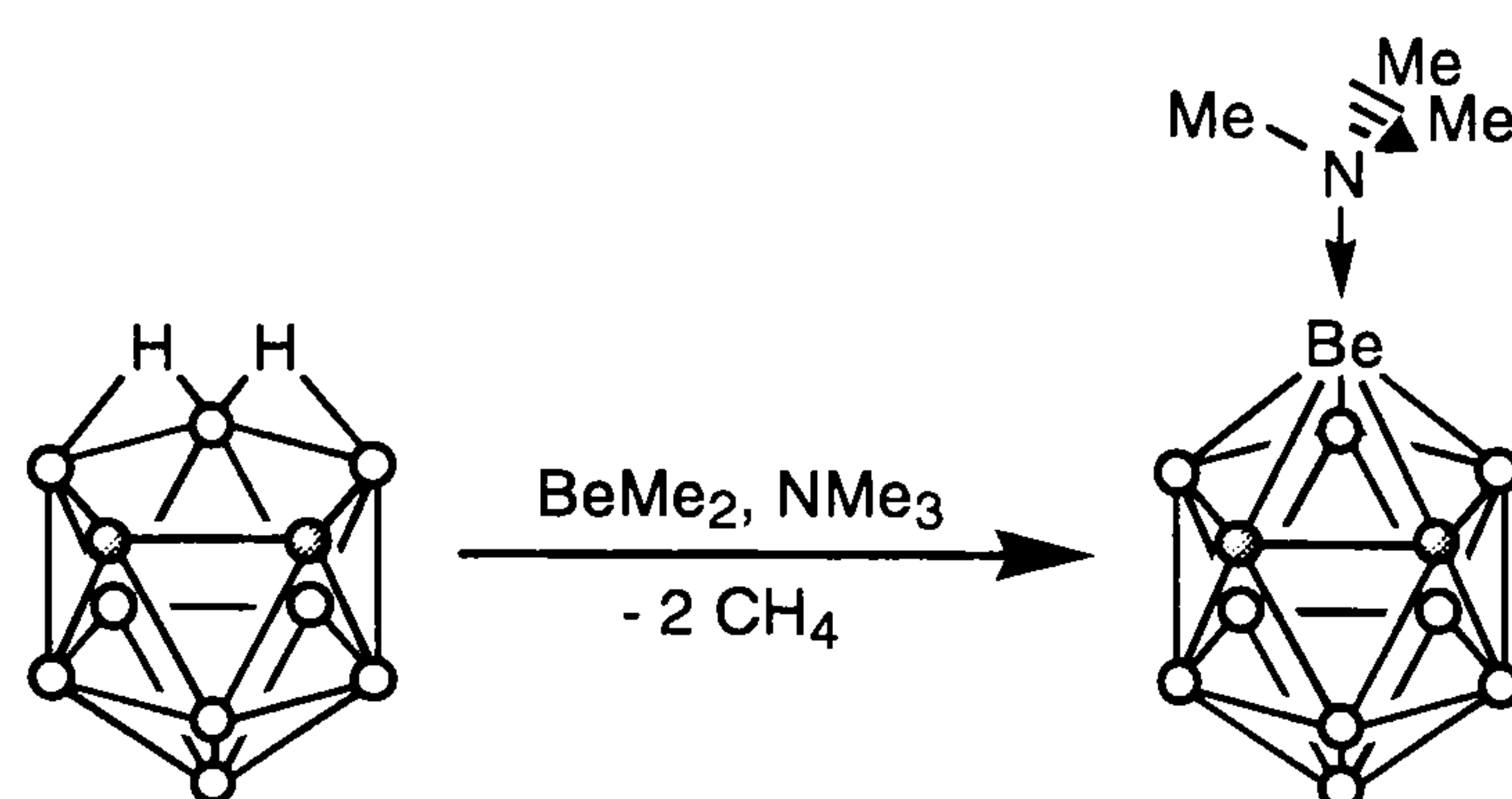


Figure 2.15 Reaction of *ortho*-C₂B₉H₁₃ with BeMe₂ in the presence of trimethyl amine, forms the *closo*-metallacarborane complex, [Me₃N-Bec₂B₉H₁₁]. Taken from ref. 42.

The ¹H NMR spectrum, in *d*⁵-pyridine, of the product isolated from the reaction between [(Me₃NH)⁺(*ortho*-C₂B₉H₁₂)⁻], (**4c**) and ZnMe₂ in toluene showed two resonances in the expected 2:9 intensity ratio at δ_H 1.24 and δ_H 2.07 ppm respectively. The ¹¹B NMR spectrum also shows a likeness to that observed in the case of the beryllium complex with 4 peaks in a 5:2:1:1 intensity ratio at -16.3, -21.5, -32.3 and -38.5 ppm respectively.

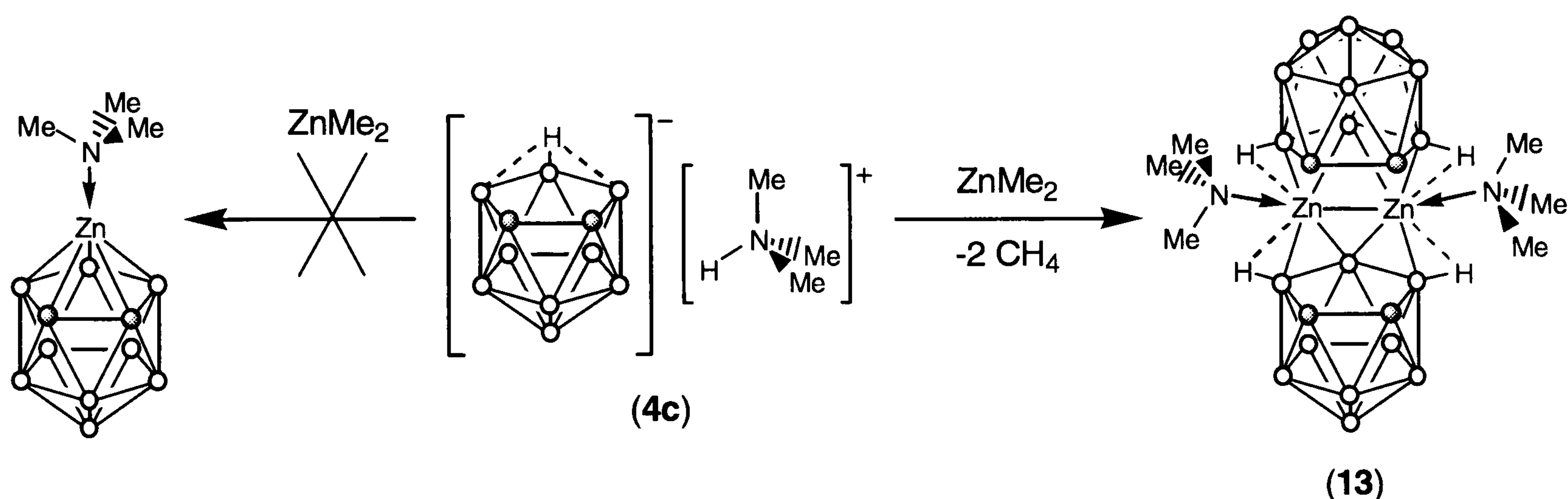


Figure 2.16 Anticipated and isolated products from the reaction of [(Me₃NH)⁺(*ortho*-C₂B₉H₁₂)⁻] and ZnMe₂.

The stoichiometry of the product was as expected; however, an X-ray crystallographic study has shown the product to have an alternative remarkable macropolyhedral dimeric structure, [(*ortho*-C₂B₉H₁₁)ZnNMe₃]₂ (**13**), shown in Fig. 2.17.

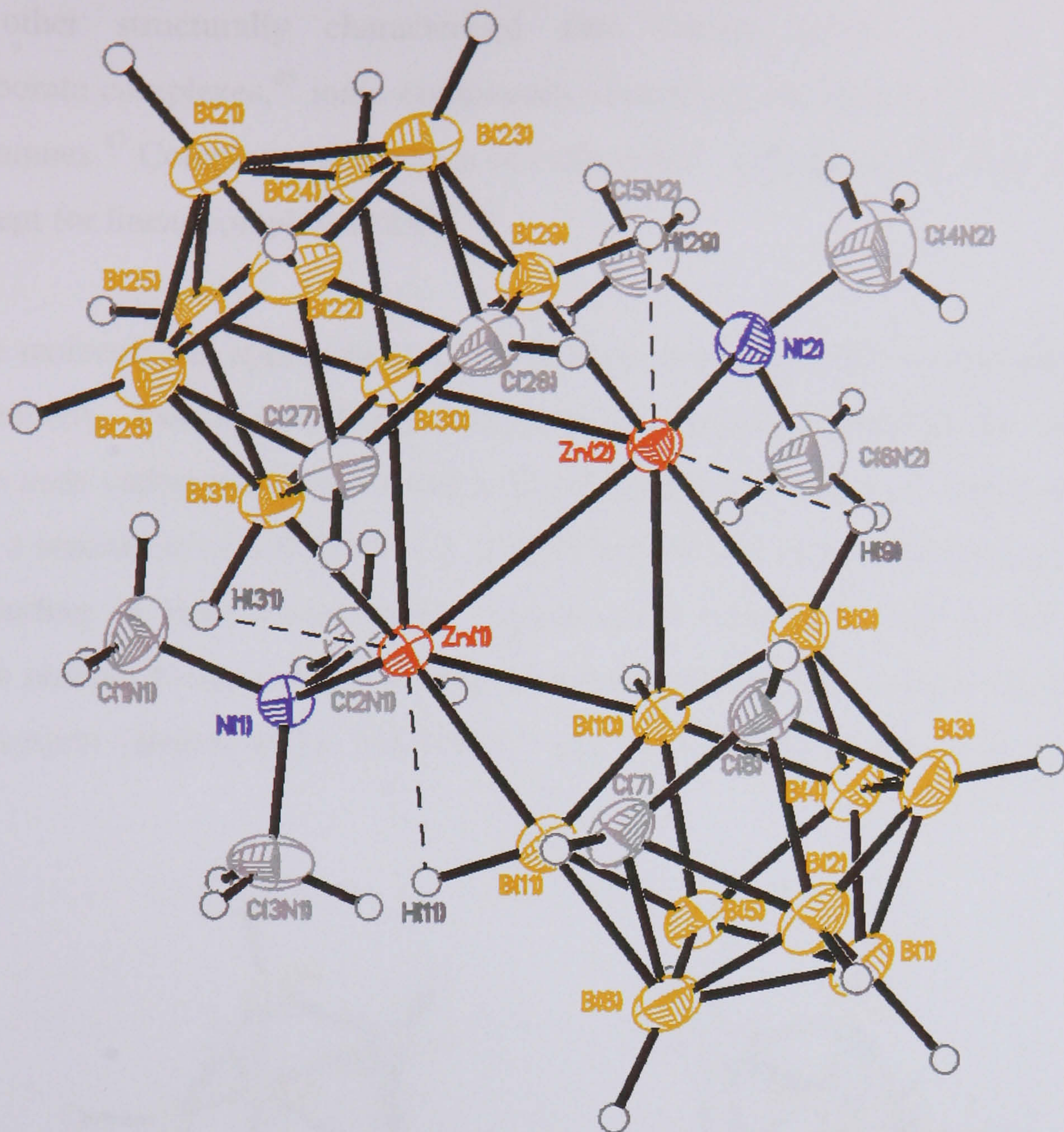


Figure 2.17 Molecular structure of the zinc complex, (13). Thermal ellipsoids of non hydrogen atoms are shown at 50% probability. Hydrogen atoms are shown as hollow circles.[†]

Table 2.4 Selected bond distances (Å), and bond angles (°) for (13).

Zn(1)-Zn(2)	2.800(1)	Zn(1)-N(1)	2.065(2)
		Zn(2)-N(2)	2.062(2)
Zn(1)-B(10)	2.315(3)		
Zn(1)-B(11)	2.177(3)	Zn(1)-Zn(2)-N(2)	127.30(8)
Zn(1)-B(30)	2.340(3)		
Zn(1)-B(31)	2.165(3)	Zn(2)-Zn(1)-N(1)	126.87(6)
Zn(2)-B(9)	2.160(3)	B(10)-Zn(1)-B(30)	108.01(11)
Zn(2)-B(10)	2.380(3)	B(10)-Zn(2)-B(30)	105.49(11)
Zn(2)-B(29)	2.163(3)		
Zn(2)-B(30)	2.352(3)	Zn(1)-B(10)-Zn(2)	73.21(9)
		Zn(1)-B(30)-Zn(2)	73.26(9)

[†] The asymmetric unit consist of one molecule of complex (13) and 1.5 molecules of toluene, with one molecule of toluene disordered over two positions. The trimethylamine group (N(2)) also exhibits disorder over two sites, the conformation shown in Figure 2.17 is that with the highest partial occupancy. The second conformer has been omitted for clarity.

The only other structurally characterised zinc borane species are a number of tetrahydridoborate complexes,⁴⁵ ionic compounds containing the [Zn(B₁₀H₁₂)₂]²⁻ anion,⁴⁶ and small zinc boranes.⁴⁷ Complexes of boranes or carboranes⁴⁸ with group 2⁴⁹ or group 12 metals are rare (except for linear complexes of Hg²⁺).

Although the molecule has approximate C_{2v} molecular symmetry it has no crystallographically imposed symmetry. Two *nido*-C₂B₉H₁₁ fragments are connected through the unique boron atoms of the *nido* carborane residues and a Me₃N-Zn-Zn-NMe₃ unit, in which the two zinc atoms are at a separation of 2.800(1) Å (cf. 2.665 Å for the shortest Zn-Zn distance in metallic Zn). The bonding of these boron atoms (coordination number 7) and of the zinc atoms (coordination number 8) are, we believe unprecedented, and involve a planar diamond-shaped Zn₂B₂ ring system [angles at Zn 108.01(11)° and 105.49(11)°; angles at B 73.21(9)° and 73.26(9)°].

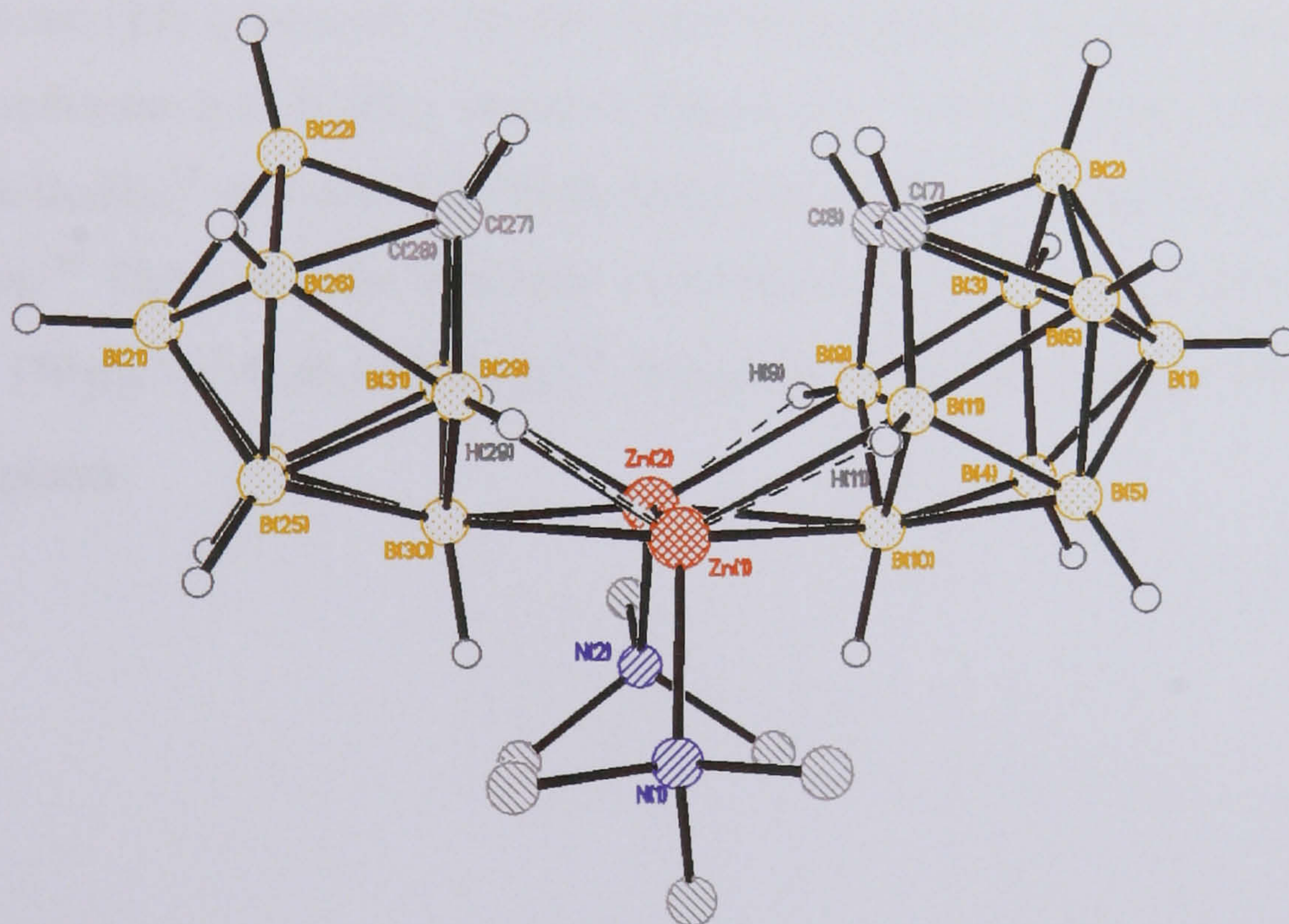


Figure 2.18 Diagram showing the cavity between the two C₂B₃ faces of the carborane cages. The hydrogen atoms on the trimethyl amine groups have been omitted for clarity.

This bonding motif results in the cluster having a large cavity between the two faces of the C₂B₉ cages (Figure 2.18) Although the distance between the two face centroids is 3.738 Å and comparable to the centroid-centroid distances in other transition metal *commo*-bis dicarbollide complexes (upper and lower limits defined by the values 3.05 Å to 4.3 Å for the complexes [Co(η⁵-1,2-C₂B₉H₁₁)(η⁵-10-(O(C₂H₄)₂O)-1,2-C₂B₉H₁₀)]⁵⁰ and [Fe(η⁵-1-(C₄H₃S)-1,2-C₂B₉H₁₀)₂]⁵¹ respectively), it is thought that the size of the two zinc atoms would preclude the formation of a tri-metallic system with the third metal sitting in between the two faces.

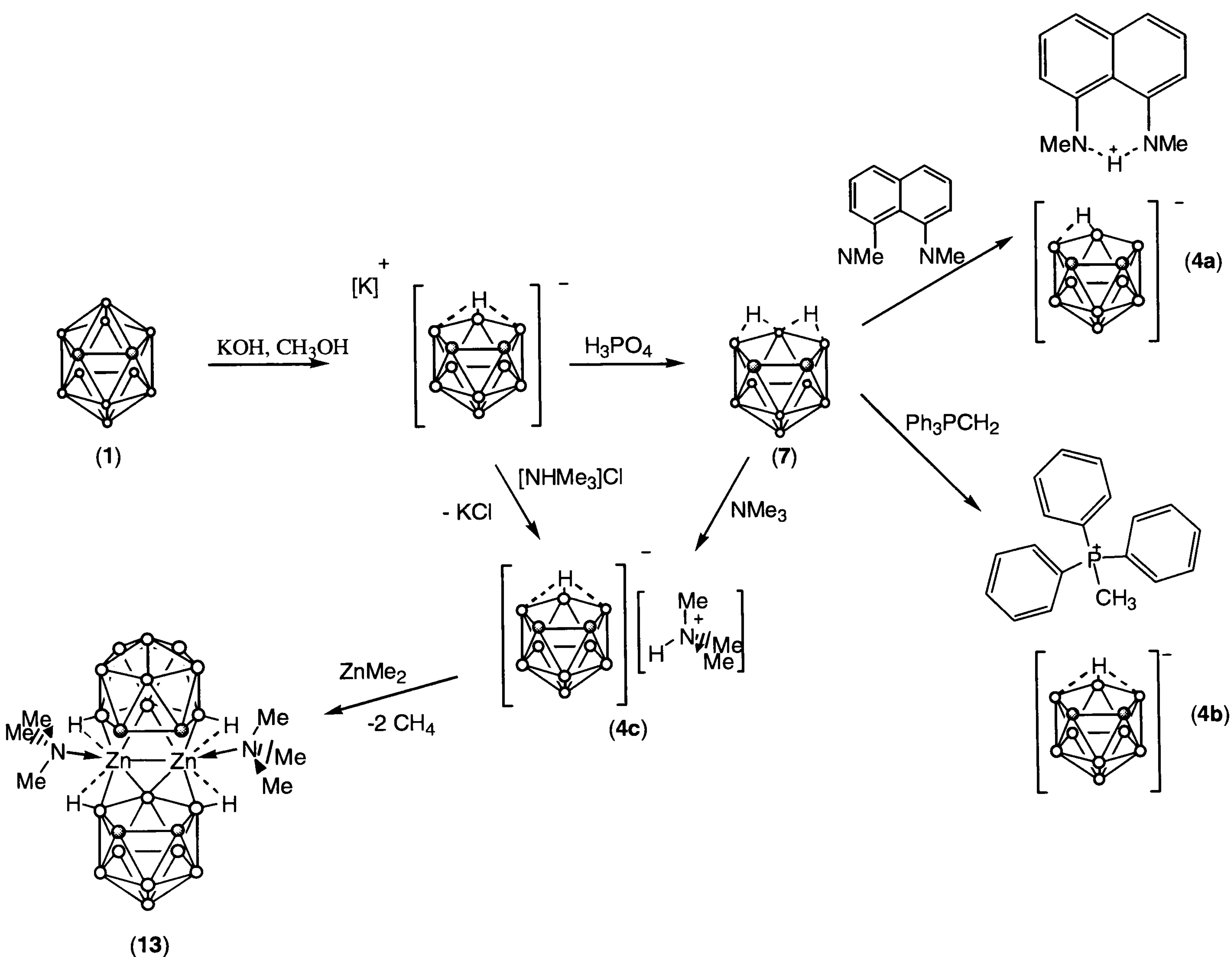
The bonding observed in the Zn₂B₂ ring is reminiscent of the 3-centre 2-electron bonds in the M₂C₂ ring systems of electropositive metal alkyls, as in Al₂Me₆,⁵² or (BeMe₂)_n,⁵³ with characteristically acute angles at the alkyl carbon and obtuse angles at the electropositive metals. In contrast, zinc alkyls, ZnR₂ (R = Me, Et, n-Pr), are monomeric by gas-phase electron diffraction,⁵⁴ although in the solid-state, diphenyl zinc is dimeric, [(C₆H₅Zn)₂(μ-C₆H₅)₂], [Zn-Zn = 2.685 Å] with unsymmetrical bridges, assigned to σ-covalent and π-dative bonds.⁵⁵ The Zn-Zn separations observed in amide-bridged [(MeZn)(μ-NPh₂)]₂ (2.913 Å),⁵⁶ chloride-bridged [Zn₂Cl₆]²⁻ (typically 3.06 to 3.3 Å)¹¹ and other electron-precise species, are longer than that in (13).

In addition to the Zn₂B₂ ring the coordination about each zinc atom is completed by one NMe₂ ligand and interaction of a pair of B-H bonds with each zinc atom. Since Me₃N-Zn is isolobal with BH, compound (13) is isolobal with the (unknown) species C₄B₂₀H₂₄ and [B₂₄H₂₄]²⁻. The closest known carborane is C₄B₁₈H₂₂, shown in Figure 2.4.¹⁶ Other clusters distantly related to (13) include *syn*-B₁₄H₂₀⁵⁷ and *anti*-{[Pt(PMe₂Ph)]₂(*nido*-B₆H₉)₂} containing square planar 16 electron platinum.⁵⁸ There is some structural resemblance to the μ-allyl ligand bridging two metal atoms in [W₂(μ²-η³-C₃H₅)₂(NMe₂)₄],⁵⁹ though in this allyl complex the central W₂C₂ ring is far from planar.

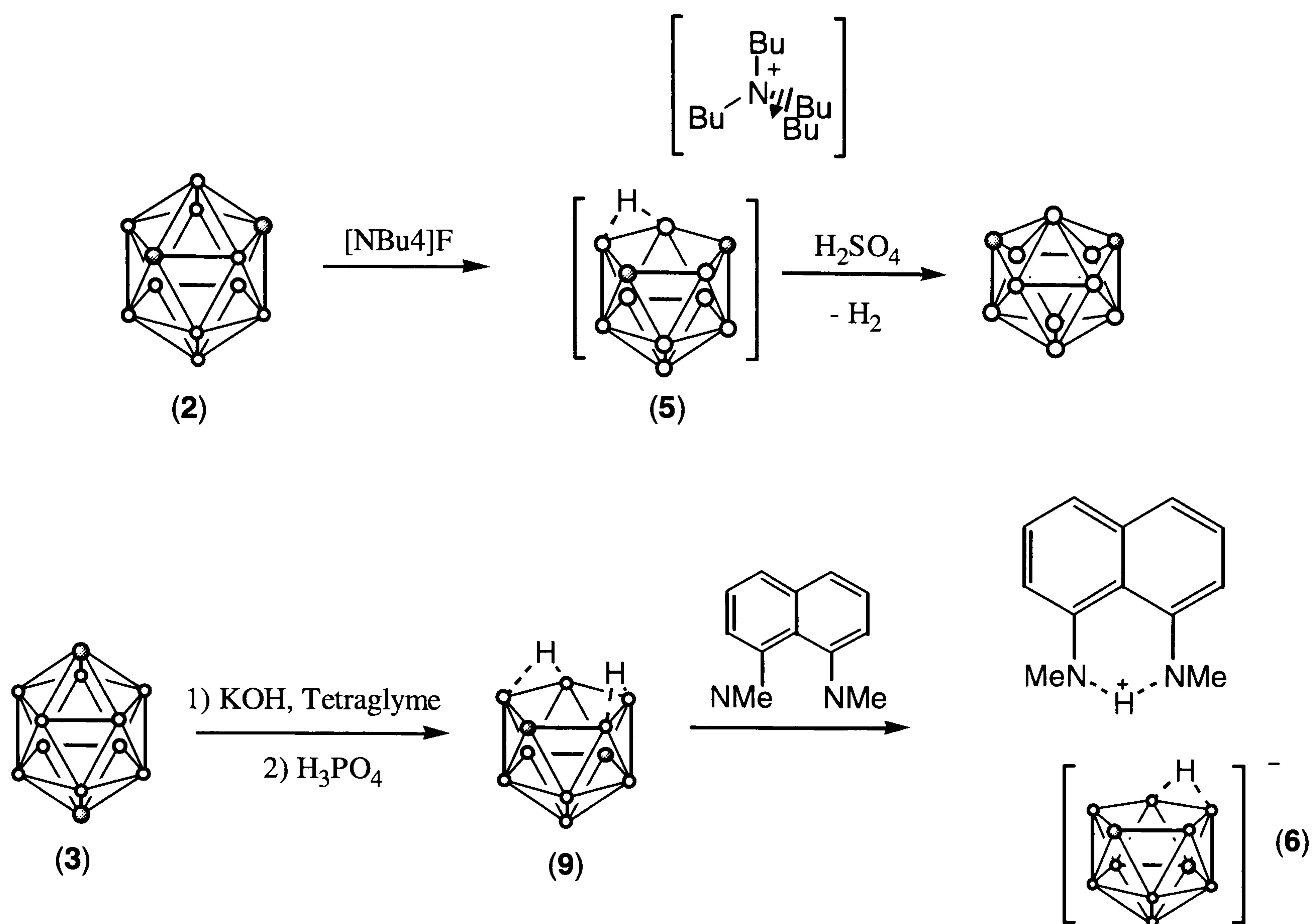
2.4 Summary

This chapter has described the synthesis and characterisation of a number of *nido*-“C₂B₉” clusters, together with selected reactions of these clusters, the orientational preferences for the “twelfth” hydrogen in the two anionic clusters [*ortho*-C₂B₉H₁₂][−] and [*para*-C₂B₉H₁₂][−].

The deprotonation reaction between the salt [NHMe₃][*ortho*-C₂B₉H₁₂] and dimethyl zinc, forms the unexpected macropolyhedral dimer [(*ortho*-C₂B₉H₁₁)ZnNMe₃]₂. This complex containing an unprecedented planar diamond-shaped Zn₂B₂ ring at its core.



Scheme 2.4 Summary of the chemistry of the *nido*-[*ortho*-C₂B₉] clusters.



Scheme 2.5 Summary of the chemistry of the *nido*-“ $[\text{meta-C}_2\text{B}_9]$ ” and “ $[\text{para-C}_2\text{B}_9]$ ” clusters.

2.5 References for Chapter Two

- 1 (a) R. N. Grimes, “*Carboranes*”, Academic Press, New York, 1970; (b) E. N. Peters, *Ind. Eng. Chem., Prod. R&D*, 1984, **23**, 28; (c) “*Gmelin Handbook of Inorganic Chemistry*”, 8th Ed., Springer-Verlag, Berlin, 3rd Supplement, Vol. 4, 1988; (d) V.I. Bregadze, *Chem. Rev.*, 1992, **92**, 209, and references therein.
- 2 M. G. Davidson, M. A. Fox, T. G. Hibbert, J. A. K. Howard, A. Mackinnon, I. S. Neretin and K. Wade, *J. Chem. Soc., Chem. Commun.*, 1999, 1649.
- 3 R. A. Wiesboeck and M. F. Hawthorne, *J. Am. Chem. Soc.*, 1964, **86**, 1634.
- 4 (a) 7,8-“C₂B₉” see: R. A. Wiesboeck and M. F. Hawthorne, *J. Am. Chem. Soc.*, 1964, **86**, 1642; (b) 7,9-“C₂B₉” see: P. M. Garrett, F. N. Tebbe and M. F. Hawthorne, *J. Am. Chem. Soc.*, 1964, **86**, 5016.
- 5 D. C. Busby and M. F. Hawthorne, *Inorg. Chem.*, 1982, **21**, 4101.
- 6 J. Plešek and S. Heřmánek, *Chem. Ind. (London)*, 1973, 381.
- 7 For general discussion see; “*Comprehensive Organometallic Chemistry*”; Eds., E. Able, F. G. A. Stone and G. Wilkinson, Pergamon Press, Oxford, 1995, Vol. 1, Chapters 6-8.
- 8 A. K. Saxena and N. S. Hosmane, *Chem. Rev.*, 1993, **93**, 1081.
- 9 G. G. Hlatky and D. J. Crowther, *Inorg. Synth.*, 1998, **32**, 229.
- 10 (a) D. V. Howe, C. J. Jones, R. J. Wiersema and M. F. Hawthorne, *Inorg. Chem.*, 1971, **10**, 2516; (b) X. L. R. Fontaine, N. N. Greenwood, J. D. Kennedy, K. Nestor and M. Thornton-Pett, *J. Chem. Soc., Dalton Trans.*, 1990, 681.
- 11 Search of Cambridge Structural Database; F. H. Allen and O. Kennard, *Chemical Design Automation News*, 1993, **8**, 1; 31.
- 12 Gaussian 94, Revision E.2, M. J. Frisch, G. W. Trucks, H. B. Schlegel, P. M. W. Gill, B. G. Johnson, M. A. Robb, J. R. Cheeseman, T. Keith, G. A. Petersson, J. A. Montgomery, K. Raghavachari, M. A. Al-Laham, V. G. Zakrzewski, J. V. Ortiz, J. B. Foresman, J.

- Cioslowski, B. B. Stefanov, A. Nanayakkara, M. Challacombe, C. Y. Peng, P. Y. Ayala, W. Chen, M. W. Wong, J. L. Andres, E. S. Replogle, R. Gomperts, R. L. Martin, D. J. Fox, J. S. Binkley, D. J. Defrees, J. Baker, J. P. Stewart, M. Head-Gordon, C. Gonzalez, and J. A. Pople, Gaussian, Inc., Pittsburgh, PA, 1995.
- 13 M. A. Fox, A. E. Goeta, J. A. K. Howard, A. K. Hughes, A. L. Johnson and K. Wade, Manuscript in preparation 1999.
- 14 F. P. Olsen and M. F. Hawthorne, *Inorg. Chem.*, 1965, **4**, 1839.
- 15 A. Herzog, A. Maderna, G. N. Harakas, C. B. Knobler and M. F. Hawthorne, *Chem. Eur. J.*, 1999, **5**, 1212.
- 16 Z. Janoušek, B. Štíbr, X. L. R. Fontaine, J. D. Kennedy and M. Thornton-Pett, *J. Chem. Soc., Dalton Trans.*, **1996**, 3813.
- 17 W. R. Pretzer and R. W. Rudolph, *Inorg. Chem.*, 1976, **15**, 1779.
- 18 F. R. Scholer, R. Brown, D. Gladkowski, W. F. Wright and L. J. Todd, *Inorg. Chem.*, 1979, **18**, 921.
- 19 V. Chowdhry, W. R. Pretzer, D. N. Rai and R. W. Rudolph, *J. Am. Chem. Soc.*, 1973, **95**, 4560.
- 20 R. E. Williams, *Prog. Boron Chem.*, 1970, **2**, 37.
- 21 M. A. Fox and K. Wade, *Polyhedron*, 1997, **16**, 2517.
- 22 R. W. Alder, P. S. Bownam, W. R. S. Steele and D. R. Winterman, *J. Chem. Soc., Chem. Commun.*, 1968, 723.
- 23 (a) D. A. Brown, W. Clegg, H. M. Colquhoun, J. A. Daniels, I. R. Stephenson and K. Wade, *J. Chem. Soc., Chem. Commun.*, 1987, 889; (b) R. Coult, M. A. Fox, W. R. Gill, K. Wade and W. Clegg, *Polyhedron*, 1992, **11**, 2717; (c) T. Jelínek, J. D. Kennedy, B. Štíbr and M. Thornton-Pett, *Inorg. Chem. Commun.*, 1998, **1**, 179; (d) J. W. Bausch, D. J. Matoka, P. J. Carroll and L. G. Sneddon, *J. Am. Chem. Soc.*, 1996, **118**, 11423; (e) T. D. McGrath, T. Jelínek, B. Štíbr, M. Thornton-Pett and J. D. Kennedy, *J. Chem. Soc., Dalton Trans.*, 1997,

- 2543; (f) A. E. Wille, K. Su, P. J. Carroll and L. G. Sneddon, *J. Am. Chem. Soc.*, 1996, **118**, 6407; (g) A. E. Wille, J. Plešek, J. Holub, B. Štíbr, P. J. Carroll and L. G. Sneddon, *Inorg. Chem.*, 1996, **35**, 5342.
- 24 E. Bartoszak, M. Jaskólski, E. Grech, T. Gustafsson and I. Olovsson, *Acta Cryst.*, 1994, **B50**, 358, and references therein.
- 25 I. Olovsson and P. G. Jönsson, “*The Hydrogen Bond*”, Vol. 2, North Amsterdam Press, Amsterdam, 1976.
- 26 (a) J. Buchanan, E. J. M. Hamilton, D. Reed and A. J. Welch, *J. Chem. Soc., Dalton Trans.*, 1990, 677; (b) J. Cowie, D. J. Donohoe, N. L. Douek and A. J. Welch, *Acta Cryst.*, 1993, **C49**, 710; (c) D. E. Smith and A. J. Welch, *Acta Cryst.*, 1986, **C42**, 1717 and refs. therein.
- 27 (a) J. Beck, W. Quintana and L. G. Sneddon, *Organometallics*, 1988, **27**, 2398; (b) T. D. Getman, J. A. Krause and S. G. Shore, *Inorg. Chem.*, 1988, **27**, 2398.
- 28 H. Lee, T. Onak, J. Jaballas, U. Tran, T. U. Truong and H. T. To, *Inorg. Chim. Acta*, 1999, **289**, 11.
- 29 For examples involving relevant chemistry or focus on the phoshonium cation see; (a) R. E. Cramer, D. M. Mo, W. Van Dorne, J. A. Ibers, T. Norton and M. Kashiwagi, *Inorg. Chem.*, 1981, **20**, 2457; (b) N. W. Alcock and J. H. Nelson, *J. Chem. Soc., Dalton Trans.*, 1982, 2415; (c) P. Jutzi, D. Wegener, H. G. Stammer, A. Karaviov and M. B. Hursthouse, *Inorg. Chim. Acta*, 1992, **198**, 369; (d) T. D. Getman, C. B. Knobler and M. F. Hawthorne, *J. Am. Chem. Soc.*, 1990, **112**, 4593; (e) H. M. Colquhoun, T. J. Greenhough and M. G. H. Wallbridge, *Acta Cryst.*, 1978, **B34**, 2373 and refs. therein.
- 30 M. G. Davidson, T. G. Hibbert, J. A. K. Howard, A. Mackinnon and K. Wade, *Chem. Commun.*, 1996, 2285.
- 31 J. March in “*Advanced Organic Chemistry*” J. Wiley and Sons, New York, 1992.
- 32 E. S. Petrov, E. Ya. Yakovleva, G. G. Kalinina, I. L. Zakharkin and A. I. Shatenshtein, *Izvest. Akad. Nauk. SSSR, Otd. Khim. Nauk.*, 1969, 1697.

- 33 (a) L. I. Kruglyak, E. S. Petrov, N. V. Kalinin, I. L. Zakharkin and A. I. Shatenshtein, *Izvest. Akad. Nauk SSSR, Ser. Khim.*, 1972, 471; (b) O. A. Reutov, I. P. Beletskaya and K. P. Butin, in “C-H Acids”, Pergamon Press, Oxford, 1978.
- 34 (a) V. C. Gibson, *J. Chem. Soc., Dalton Trans.*, 1994, 1607; (b) T. P. Hanusa, *Polyhedron*, 1982, **1**, 663; (c) D. M. P. Mingos, M. I. Forsyth and A. J. Welch, *J. Chem. Soc., Dalton Trans.*, 1978, 1363.
- 35 M. L. H. Green, *J. Organomet. Chem.*, 1995, **500**, 127.
- 36 (a) M. F. Hawthorne, *J. Organomet. Chem.*, 1975, **100**, 97; (b) H. M. Colquhoun, T. J. Greenhough and M. G. H. Wallbridge, *J. Chem. Soc., Dalton Trans.*, 1979, 619; (c) D. M. P. Mingos, M. I. Forsyth and A. J. Welch, *J. Chem. Soc., Dalton Trans.*, 1978, 1363; (d) M. J. Calhorda, D. M. P. Mingos and A. J. Welch, *J. Organomet. Chem.*, 1982, **228**, 309; (e) E. J. M. Hamilton and A. J. Welch, *Polyhedron*, 1990, **9**, 2407.
- 37 J. Kim, S. Kim and Y. Do, *J. Chem. Soc., Chem. Commun.*, 1992, 938.
- 38 M. A. Beckett, J. E. Crook, N. N. Greenwood and J. D. Kennedy, *J. Chem. Soc., Dalton Trans.*, 1986, 1879.
- 39 G. C. Bazan, W. P. Schaefer and J. E. Bercaw, *Organometallics*, 1993, **12**, 2126.
- 40 (a) C. Keruder, R. F. Jordan and H. Zhang, *Organometallics*, 1995, **14**, 2993; (b) D. J. Crowther, D. C. Swenson and R. F. Jordan, *J. Am. Chem. Soc.*, 1995, **117**, 10403.
- 41 (a) D. A. T. Young, G. R. Willey, M. F. Hawthorne, M. R. Churchill and A. H. Reis Jr., *J. Am. Chem. Soc.*, 1970, **92**, 6664; (b) D. A. T. Young, R. J. Wiersema and M. F. Hawthorne, *J. Am. Chem. Soc.*, 1971, **93**, 5698; (c) P. Jutzi and P. Galow, *J. Organomet. Chem.*, 1987, **319**, 139.
- 42 G. Popp and M. F. Hawthorne, *J. Am. Chem. Soc.*, 1968, **90**, 6553.
- 43 A. E. Goeta, J. A. K. Howard, A. K. Hughes, A. L. Johnson and K. Wade, *Chem. Commun.*, 1998, 1713.
- 44 G. Popp and M. F. Hawthorne, *Inorg. Chem.*, 1971, **10**, 391.

- 45 (a) S. Aldridge, A. J. Blake, A. J. Downs, S. Parsons and C. R. Pulham, *J. Chem. Soc., Dalton Trans.*, 1996, 853; (b) R. L. Bansamer, J. C. Huffman and K. G. Caulton, *J. Am. Chem. Soc.*, 1983, **105**, 6163; (c) A. P. Borisov, N. N. Mal'tseva and N. S. Kedrova, *Koord. Khim.*, 1991, **17**, 405; (d) M. A. Porai Koshits, A. S. Antsyshkina, A. A. Pasynskii, G. G. Sadikov, Yu. V. Skripkin and V. N. Ostrikova, *Koord. Khim.*, 1979, **5**, 1103; (e) G. A. Koutsantonis, F. C. Lee and C. L. Raston, *J. Chem. Soc., Chem. Commun.*, 1994, 1975.
- 46 (a) N. N. Greenwood, J. A. McGinnety and J. D. Owen, *J. Chem. Soc., A*, 1971, 809; (b) R. Allmann, V. Batzel, R. Pfeil and G. Schmid, *Z. Naturforsch., Teil B*, 1976, **31**, 1329.
- 47 (a) S. Aldridge, A. J. Blake, A. J. Downs and S. Parsons, *J. Chem. Soc., Chem. Commun.*, 1995, 1363; (b) S. A. Snow, M. Shimoï, C. D. Ostler, B. K. Thompson, G. Kodama and R. W. Parry, *Inorg. Chem.*, 1984, **23**, 511.
- 48 D. A. Owen and M. F. Hawthorne, *J. Am. Chem. Soc.*, 1971, **93**, 873.
- 49 N. S. Hosmane, D. Zhu, J. E. McDonald, H. Zhang, J. A. Maguire, T. G. Gray and S. C. Helfert, *Organometallics*, 1998, **17**, 1426.
- 50 J. Plešek, S. Heřmánek, A. Franken, I. Cisarova and C. Nachtigal, *Collect. Czech. Chem. Commun.*, 1997, **62**, 47.
- 51 Y. K. Yan, D. M. P. Mingos, M. Kurmoo, W. S. Li, J. J. Scowen, M. McPartlin, A. T. Coomber and R. H. Friend, *J. Chem. Soc., Dalton Trans.*, 1995, 997.
- 52 J. C. Huffman and W. E. Streib, *J. Chem. Soc., D*, 1971, 911.
- 53 A. I. Snow and R. E. Rundle, *Acta Cryst.*, 1951, **4**, 348.
- 54 A. Almenningen, T. U. Helgaker, A. Haaland and S. Samdal, *Acta Chem. Scand., Ser. A*, 1982, **36**, 159.
- 55 P. R. Markies, G. Schat, O. S. Akkerman, F. Bickelhaupt, W. J. J. Smeets and A. L. Spek, *Organometallics*, 1990, **9**, 2243.
- 56 N. A. Bell, H. M. M. Shearer and C. B. Spencer, *Acta Cryst., Sect. C*, 1983, **39**, 1182.
- 57 J. C. Huffman, D. C. Moody and R. Schaeffer, *Inorg. Chem.*, 1981, **20**, 741.

58 N. N. Greenwood, M. J. Hails, J. D. Kennedy and W. S. McDonald, *J. Chem. Soc., Dalton Trans.*, 1985, 953.

59 R. H. Cayton, M. H. Chisholm, M. J. Hampden-Smith, J. C. Huffman and K. G. Moodley, *Polyhedron*, 1992, **11**, 3197.

Chapter Three

**Dicarbollide Complexes of
Group Five Metals:
Synthesis Structure and Reactivity**

3.1 Introduction

As mentioned in Chapter 1, group 3 and 4 metallocenes provide homogenous mechanistic models for the initiation, propagation and termination steps of the polymerisation of α -olefins.¹ Catalysis requires a metal complex which formally can offer two vacant coordination sites and does not provide strong back-bonding to an incoming olefin substrate.^{1,2} These requirements were met initially by the 14 electron complexes, $d^0 \text{Cp}_2\text{MR}^+$ ($\text{M} = \text{group 4}$)³ or Cp_2MR ($\text{M} = \text{group 3}$),⁴ although it has been shown that coordinatively and electronically unsaturated complexes with d^n ($n \neq 0$) electron counts can provide very active polymerisation catalysts.^{5,6} Many research groups are exploring the synthesis of *iso*-numeral or *iso*-valence-electronic species generated by replacing the $(\eta\text{-C}_5\text{H}_5)\text{M}$ unit ($\text{M} = \text{group 4 metal}$) by other combinations of ligand and metal which provide the same overall electron count.^{7,8,9} In many of these complexes the carbon atoms of the $(\eta\text{-C}_5\text{H}_5)$ ligand have been replaced by more- or less-electronegative atoms. Ligands designed around nitrogen coordination are popular,¹⁰ a consequence of both the well-established coordination chemistry of nitrogen,¹¹ and the well-established organic chemistry of nitrogen resulting in facile ligand syntheses. Although such metallocene analogues are *iso*-numeral with metallocenes, many are not *iso*-energetic, and indeed the variation in polymerisation activity in such catalysts is undoubtedly in part a function of the frontier orbital energies.

The renewed interest in metallacarborane complexes of the early transition metals arises from the interest that metallocene chemists have in finding new $1\sigma 2\pi$ ligands. The *nido*-carborane dianion *ortho*- $\text{C}_2\text{B}_9\text{H}_{11}^{2-}$ is capable of binding to a metal atom in a η^5 -fashion, and the chemistry of this ligand with middle and late transition metals has been established by a number of research groups.¹² The use of *ortho*- Cb^{2-} in place of Cp^- ligands provides opportunities for the design of new metal/ligand charge combinations and has more recently been applied to lanthanide¹³ and early transition metal chemistry in pursuit of metallocene analogues.¹⁴

The fragment $[\text{M}(\text{C}_2\text{B}_9\text{H}_{11})]^{n+}$ is isovalence electronic to the Cp fragment $[\text{M}(\text{Cp})]^{(n+1)+}$, but carries an overall charge which is one unit lower. The coordination chemistry of the Cb^{2-} ligands to metal atoms has been discussed in chapter one. Using the neutral ligand formalism we can describe the ligand [*ortho*- $\text{C}_2\text{B}_9\text{H}_{11}$] as a 4 electron LX_2 ligand¹⁵ and thus the fragment $[\text{Ta}(\textit{ortho}\text{-C}_2\text{B}_9\text{H}_{11})]$ can be thought of as being *iso*-numeral with $[\text{Hf}(\eta\text{-C}_5\text{H}_5)]$. Many similar

ligands derived from smaller carboranes are also known and have been used as ligands to a wide range of transition metals.¹⁶

In common with many other areas of organometallic chemistry, the most extensively used method for coordinating [*ortho*-C₂B₉H₁₁] to a transition metal has been the elimination of halide salt between a metal halide and either an alkali-metal or thallium salt of [*ortho*-C₂B₉H₁₁]²⁻. This method has been used successfully by Jordan *et al.* to synthesise several tantalum(V) dicarbollide complexes,¹⁷ although the yields of such complexes are relatively low.

In recent years interest has been re-awakened in the elimination of an amine between a metal-NR₂ and acidic neutral ligands¹⁸ as a novel method for coordinating ligands,^{10h,19} occasionally providing routes to otherwise inaccessible compounds²⁰ or thermodynamic product ratios.²¹ This method has been used to synthesise the half-sandwich complexes [M(η^5 -C₂B₉H₁₁)(NR₂)(HNR₂)] (M = Ti, R = Me; M = Zr, R = Et).²² On occasions amine elimination reactions provide higher yields than the metal halide elimination reactions.

This chapter will concentrate on the synthesis of group 5 complexes containing the dicarbollide ligand in combination with π -donor NMe₂ ligands. Subsequent reaction of these complexes with 1,2-dipolar multiple bonds, e.g. 'C=O' or 'N \equiv C', protic acids such as ROH and RSH, together with the characterisation of the resulting complexes, will be discussed. The synthesis and structural characterisation of tantalum dicarbollide *tris*-dimethylamide, where the carbons in the cage are in the *ortho*-, *meta*- and *para*- positions with respect to each other will also be discussed. The structural characterisation of the complexes reveals an unusual arrangement of NMe₂ ligands which will also be discussed.

3.1.1 Metal amide complexes; Synthesis, Structure and Reactivity.

Metal amides are compounds in which an NH₂⁻, NHR⁻ or more commonly a NR₂⁻ ligand is attached to a metal, M. Such compounds are of interest in their own right, but also as reagents in the synthesis of other complexes. Their chemistry covers a wide spectrum of interests ranging from theoretical to biological. In the case of the latter, important molecules that are metal amides include chlorophyll, haemin (Figure 3.1) and vitamin B12 coenzyme.²³

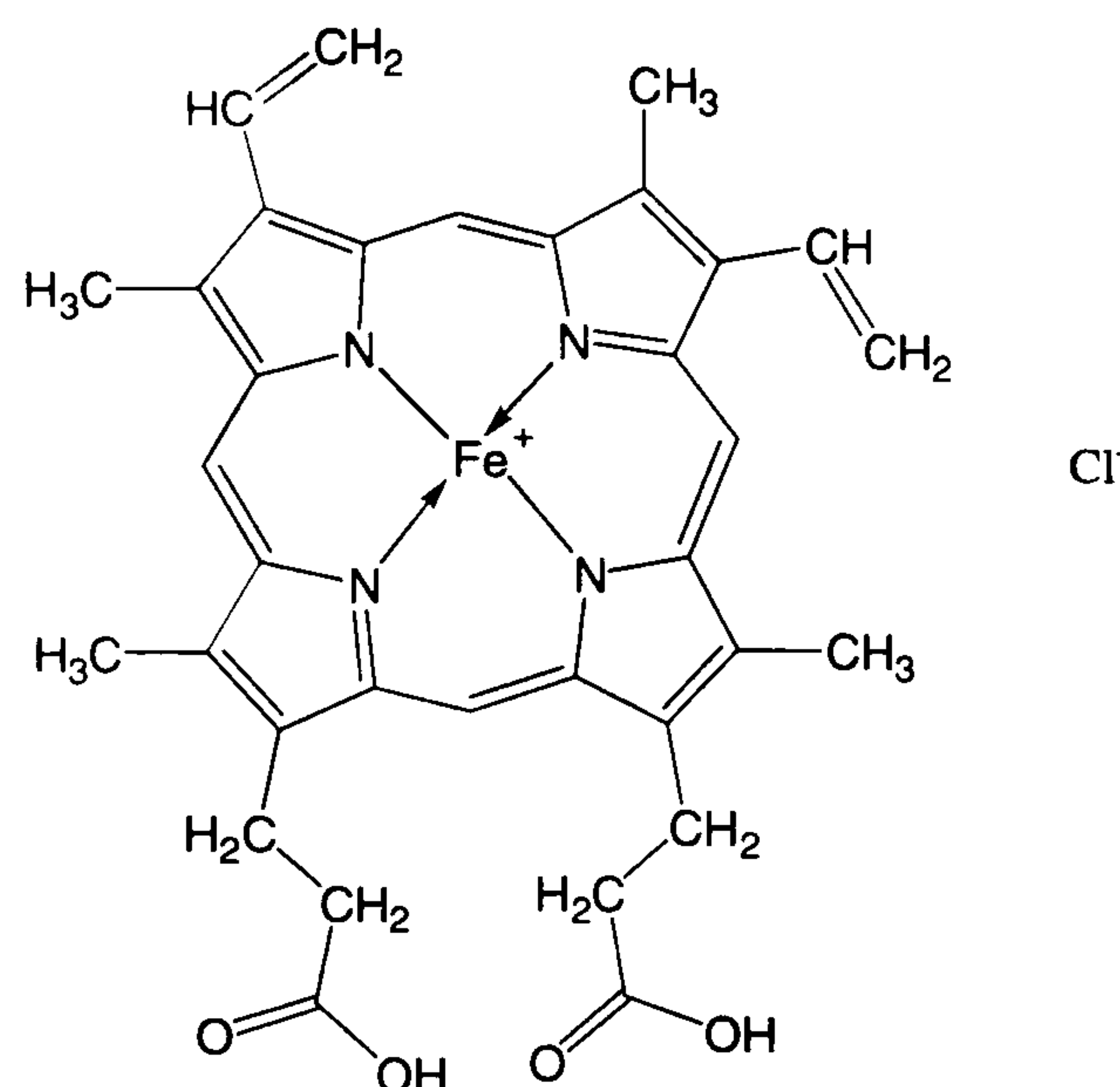


Figure 3.1 Diagram of the metalla-porpharin complex “haemin”.

Stable amide complexes are found for almost all the elements and may be *Homoleptic* i.e. $M(NRR')_n$ or *Heteroleptic*, i.e., mixed ligand complexes such as Me_3SnNMe_2 or $[Ti(\eta-C_5H_5)_2(NMe_2)_2]$. This distinction between *hetero-* and *homoleptic* complexes was first proposed for the metal alkyls and other hydrocarbyls of the elements.

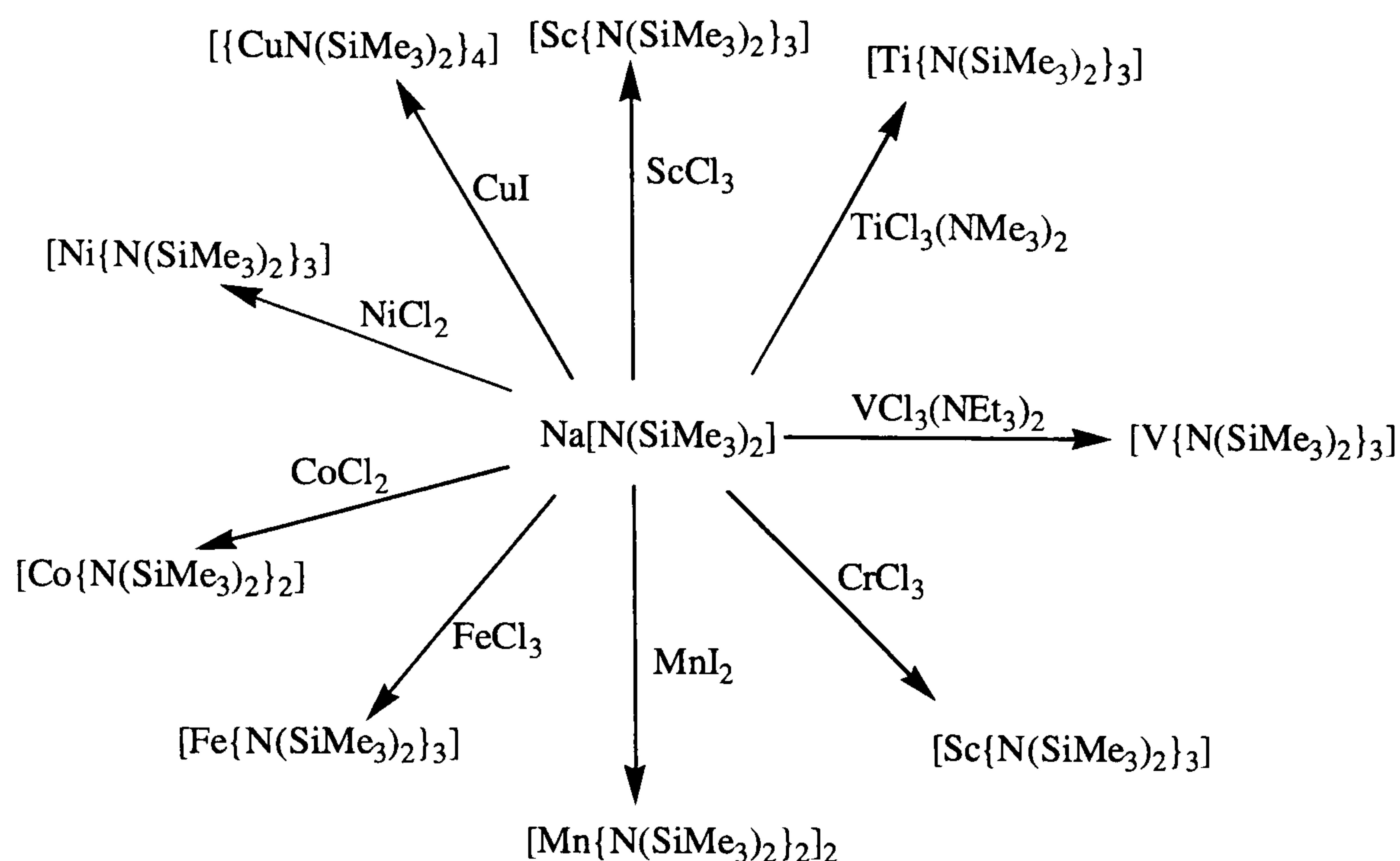
A treatise on the early contributions to the area of metal amide chemistry, including synthetic and structural aspects as well as synthesis and reactions which metal amides undergo has been given previously,^{18b} but a brief introduction to the subject is appropriate here.

The most important methods of synthesis of the transition metal amides involve transmetalation, amine hydrohalide elimination and transamination.

3.1.1.1. Transmetalation

The method shown in Scheme 3.1 is the most common preparative route for transition metal amides and is an almost exclusive process for preparing the *homoleptic* compounds. The reaction of $[TiCl_4]$ with $Na[NPh_2]$ was an early example,²⁴ but others did not emerge until the early 1960's, after Bradley and Thomas had published the first of a series of papers on complexes of the early transition metals.²⁵

The synthetic procedure has been employed to prepare a wide range of complexes, some of which are illustrated in Scheme 3.1.

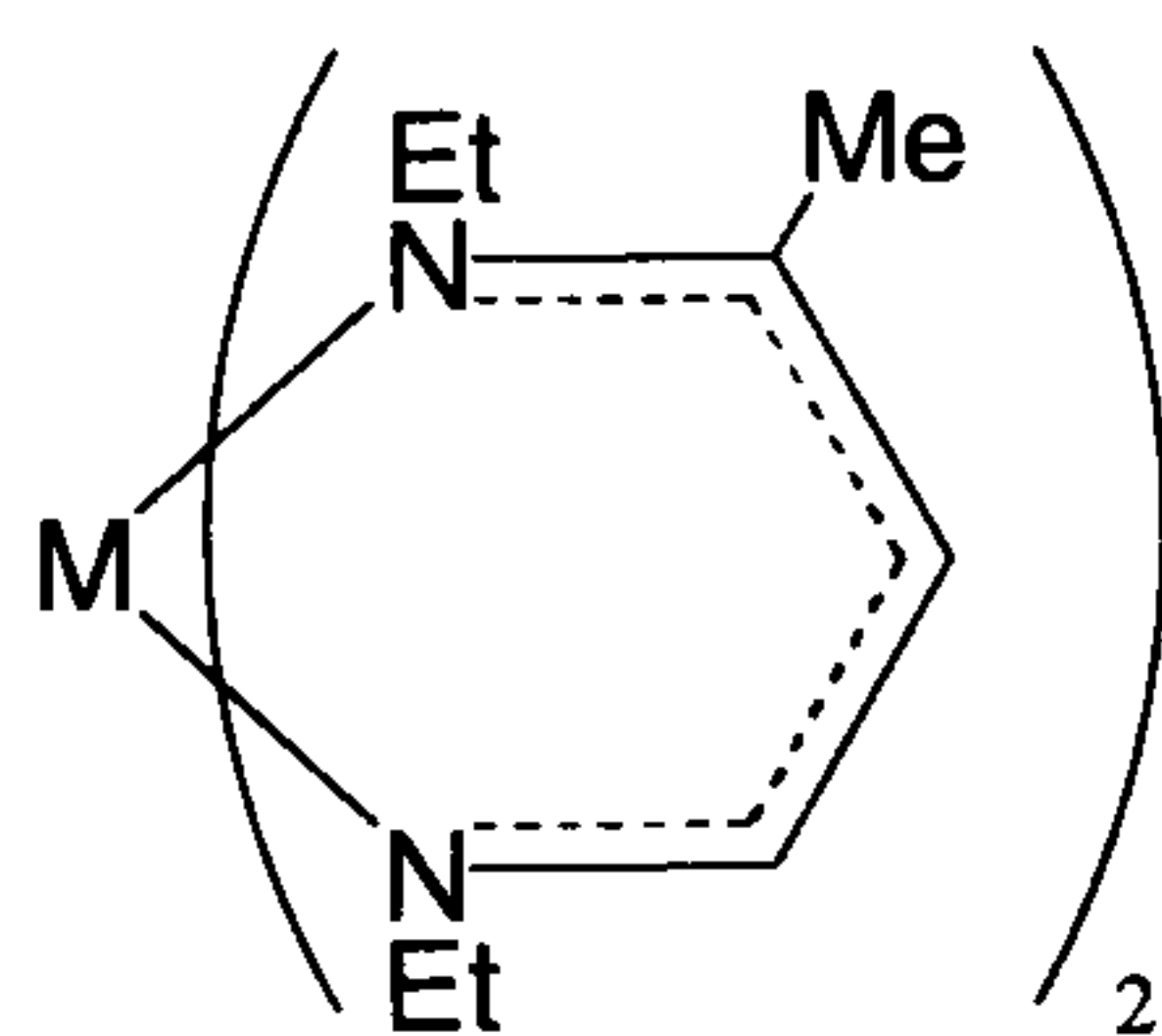


Scheme 3.1 Synthesis of first row transition metal *bis*-(trimethylsilyl)amides.

It is not inevitable that transmetallation provides (I) the amide of the same metal oxidation state as the starting chloride, or (II) a *homoleptic* metal amide. However, departures from the norm, are probably due to steric effects or disproportionation of the first formed *homoleptic* amide as in the examples below.

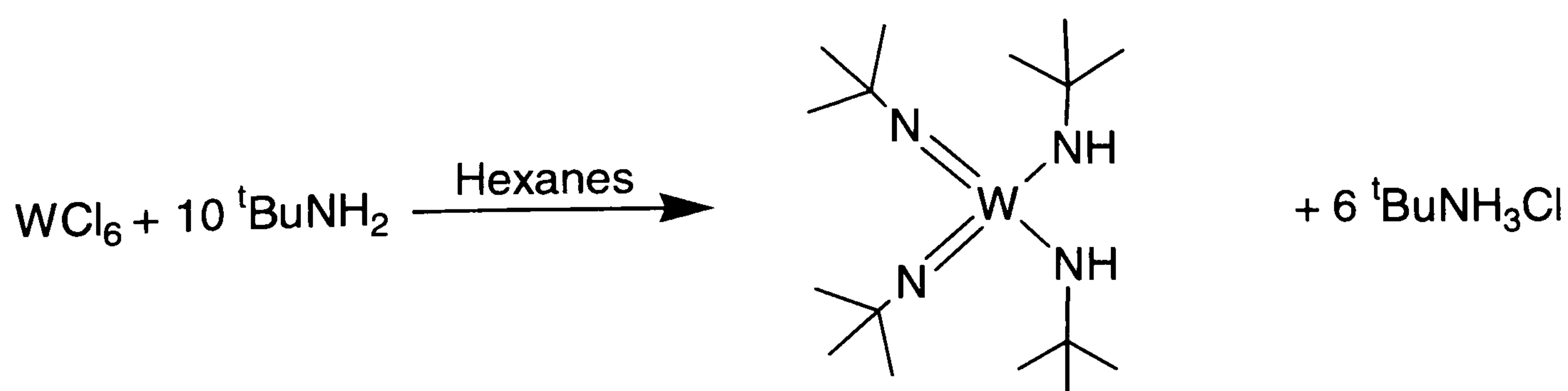


The reaction of TaCl_5 with LiNR_2 affords $[\text{Ta}(\text{NMe}_2)_5]$ or $[\text{Ta}(\text{NR})(\text{NR}_2)_3]$ ($\text{R} = \text{Et}$).²⁶ Reaction of a Co(II), Ni(II) or Cu(II) halide with LiNEt_2 leads to the unusual *di-iminato* complexes of the type shown below.²⁷



3.1.1.2. Elimination of Amine Hydrohalide

The reaction of a transition metal halide with ammonia or an amine to form a metal amine or amide complex has been known for some time. An example of such a reaction, between WCl_6 and tert-butyl amine is shown below.²⁸



Chapter Three – Dicarbollide Complexes of Group Five Metals

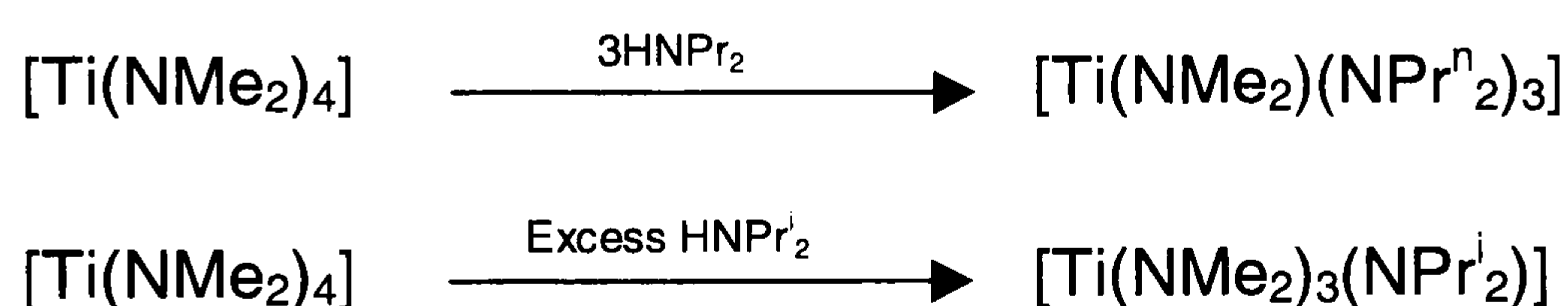
These are closely related to the amine hydrohalide elimination route to transition metal amides, which has found wide application with higher oxidation state early transition metal halides; e.g. Ti(IV),²⁹ Nb(V)³⁰ and W(VI).³¹



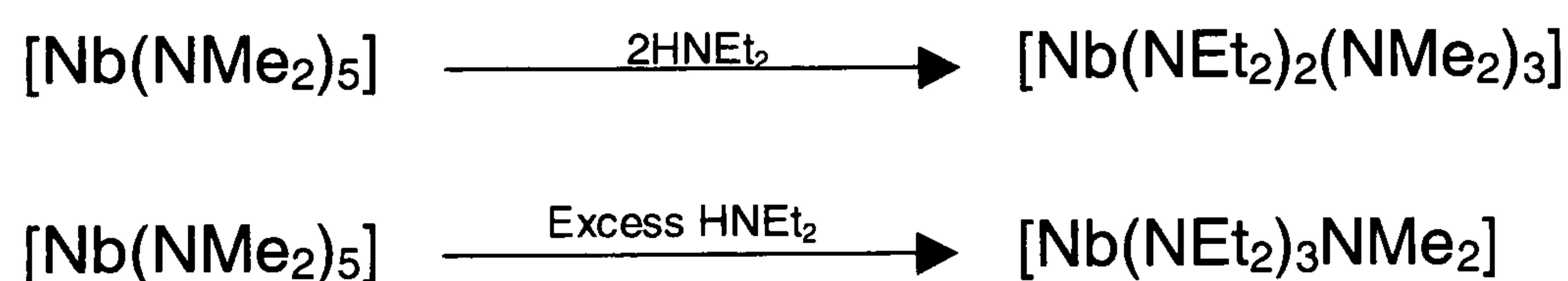
In general it has been found that the degree of solvolysis decreases in the sequence $\text{NH}_3 > \text{RNH}_2 > \text{R}_2\text{NH}$.³² Secondary amines rather than primary amines are more likely to give metal amides with the central metal in a lower oxidation state than the starting metal halide.^{32,33} The main limitation of this method of preparation is that reactions rarely go to completion, and exceptions usually involve primary amines.³⁴ Another drawback is the formation of donor complexes e.g. $\text{TaCl}_3(\text{NMe}_2)(\text{NHMe}_2)$.^{35,36}

3.1.1.3. Transamination

This reaction involves the replacement of one metal- NR_2 bond by another, the primary limitations are due to steric factors and amine volatility. The more volatile amine is usually displaced. The influence of steric factors can be seen in the example below.³⁷



In rare cases the steric bulk of ligands can induce reduction of the metal centre, as shown below.³⁸



Where applicable, transamination often proceeds smoothly and in high yield; if the eliminated amine is HNMe_2 , which is a vapour under ambient conditions, the procedure is particularly attractive because the desired product is the only non-gaseous product. A special case of transamination in which the metal chloride is Me_3SiCl is of particular interest because of its application in the synthesis of metal halide complexes from metal amides.

As mentioned above, in an ideal case the only non volatile reagent in a transamination reaction is the desired product. Reaction of a transition metal amide complex with Me_3SiX ($\text{X} = \text{F}, \text{Cl}, \text{Br}, \text{I}$) results in the formation of the corresponding transition metal halide, which can undergo

further transformation to metal alkyls etc,^{19a} and the silicon amide complex, $\text{Me}_3\text{SiNMe}_2$. The silicon amide is volatile at room temperature, so can be easily removed from the reaction mixture in much the same way HNMe_2 can be removed.

3.1.1.4 Reactions of Metal Amides; Insertion Reactions

Insertion reactions are one the most fundamental reactions in organic, inorganic and organometallic chemistry. Here we are concerned with the case where the migrating group is an amino group $[\text{NR}_2]$, such as NMe_2 . The general process, as shown in the equation below for a 1,2-dipole, $\text{A}=\text{B}$, has been known since 1962.³⁹ It was suggested that the essential characteristics of the reagent AB are that it be susceptible to attack by a nucleophile (i.e. $\text{LM-NRR}'$ acts as a nitrogen centred donor) but not an electrophile, and that the negative end of the $\text{M}^{\delta+}-\text{N}^{\delta-}$ dipole is well displaced towards to nitrogen. The tendency for the amido group to insert into unsaturated polar bonds is high, compared to ligands such as $[\text{H}]$, $[\text{R}]$, $[\text{OR}]$ and $[\text{Cl}]$, due in part to the low M-N bond strength and high bond polarity. This is represented by the transition state in Figure 3.2(I), although a concerted mechanism such as that shown in Figure 3.2(II) is also considered possible.

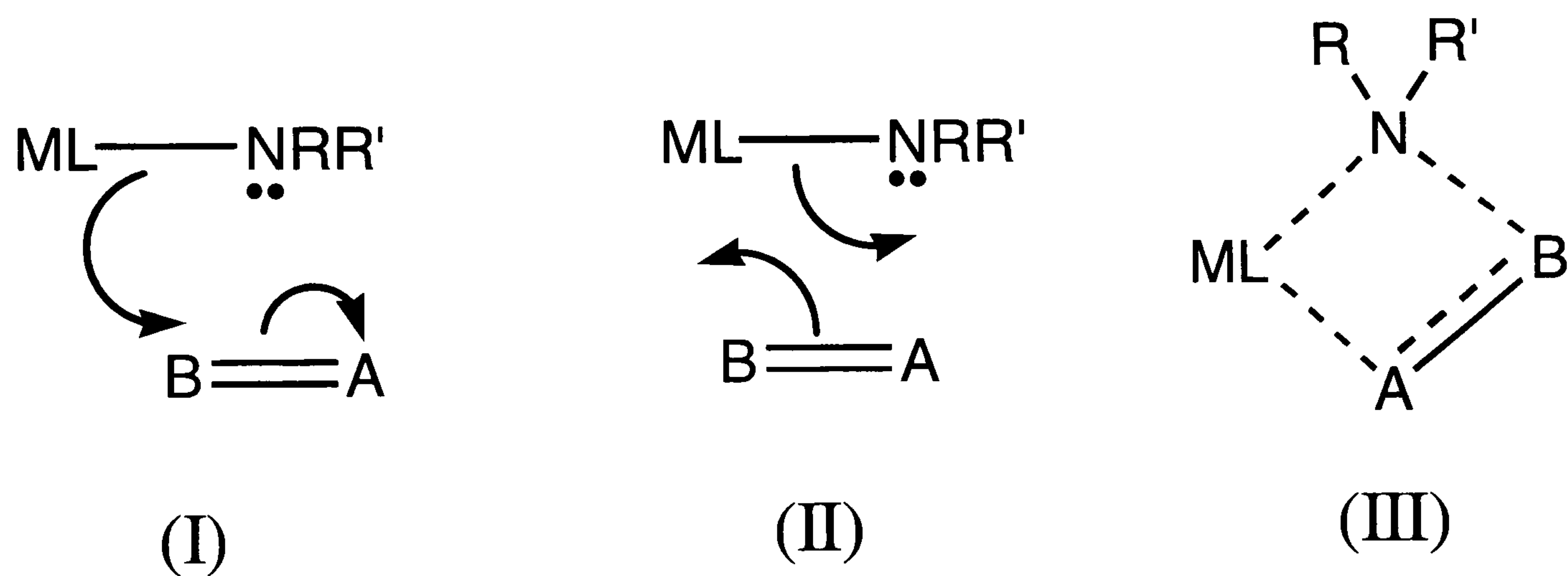


Figure 3.2 Diagram showing possible mechanisms for $\text{M-NRR}'$ insertion into a dipolar species AB .

The most prolific reactions are those in which the reagents are 1,2-dipoles such as diketene or S_4N_4 . The heterocumulenes $\text{X}=\text{Y}=\text{X}'$ have a particularly important role as reagents, especially CO_2 , CS_2 , RNCO and RNCS . Many of these reactions appear to be thermodynamically controlled and proceed under mild conditions. For heterocumulene insertion the product often enjoys additional conjugative stabilisation compared to the reagent, and this provides a favourable energy change in the reaction. A further driving force often derives from the generally greater polarity of the insertion adduct compared to the starting materials and they often precipitate from solution in non-polar solvents.

In the case of CO₂ and CS₂ the resulting ligands are referred to as N,N-dialkyl-carbamate and N,N-dialkyl-dithiocarbamate ligands respectively. Both of these ligands have the ability to bind to a metal in a *mono*- or *bi*-dentate fashion as shown in Figure 3.3.

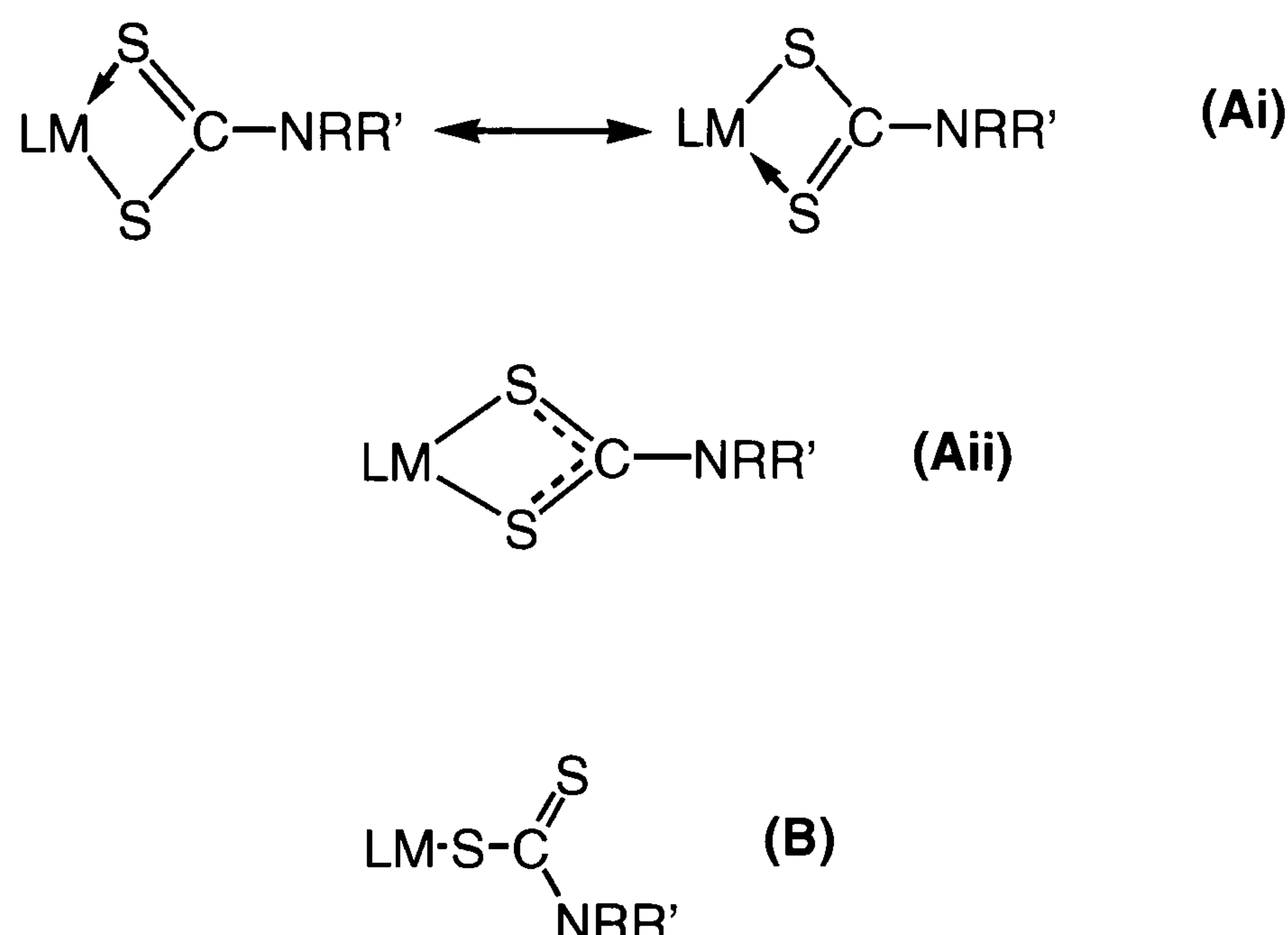


Figure 3.3 Diagram showing the principle bonding modes of a dithiocarbamate ligand to a metal centre. (Ai) shows two canonical forms of a valence bond description of the *bi*-dentate bonding mode, (Aii) shows a delocalised model for the *bi*-dentate mode of bonding and (B) shows the *mono*-dentate bonding mode.

When the carbamate or dithiocarbamate (X₂CNMe₂) ligands bond in an *bi*-dentate (κ^2 -fashion), each ligand offers the metal atom to which it is attached one frontier orbital that has M-ligand σ symmetry and one which has M-ligand π symmetry, cf. dimethylamide (NMe₂) Figure 3.4. The frontier orbitals of the (dithio)carbamate are based on the in-plane oxygen or sulfur p orbitals, the out-of-plane orbitals will be used in X₂CN π -bonding. The orientational preferences of the two ligands can be expected to be similar, taking account of the fact that the π orbital of the NMe₂ ligand is perpendicular to the NC₂ plane, whilst for the (dithio)carbamate ligand the π orbital is contained within the plane of the planar ligand.

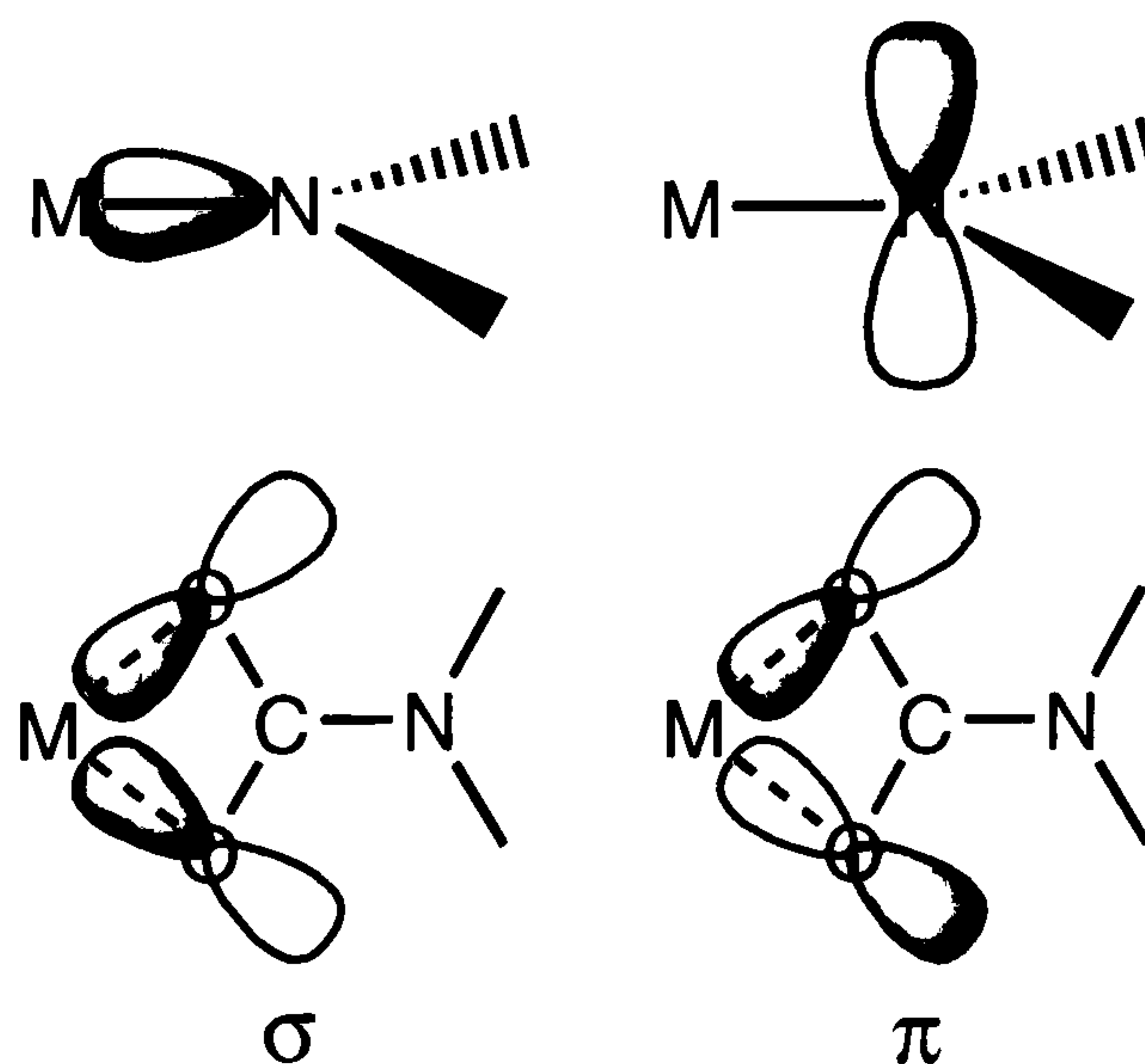


Figure 3.4 Comparison of the σ and π frontier orbitals of the amide, [NR₂], and (dithio)carbamate [X₂CNR₂] ligands.

Insertion reactions also occur with nitriles, $\text{RC}\equiv\text{N}$, and isonitriles, RNC . With a nitrile, four types of reaction have been identified with only one being an insertion reaction (Figure 3.5). Treatment of the group 4 metal amide complexes $[\text{M}(\text{NMe}_2)_4]$ with acetonitrile, benzonitrile or *p*-toluonitrile results in the formation of the metal *N,N*-dialkyl-amidinate complex (pathway (a)). $[\text{M}(\text{N}=\text{C}(\text{NMe}_2)\text{R})_4]$.⁴⁰

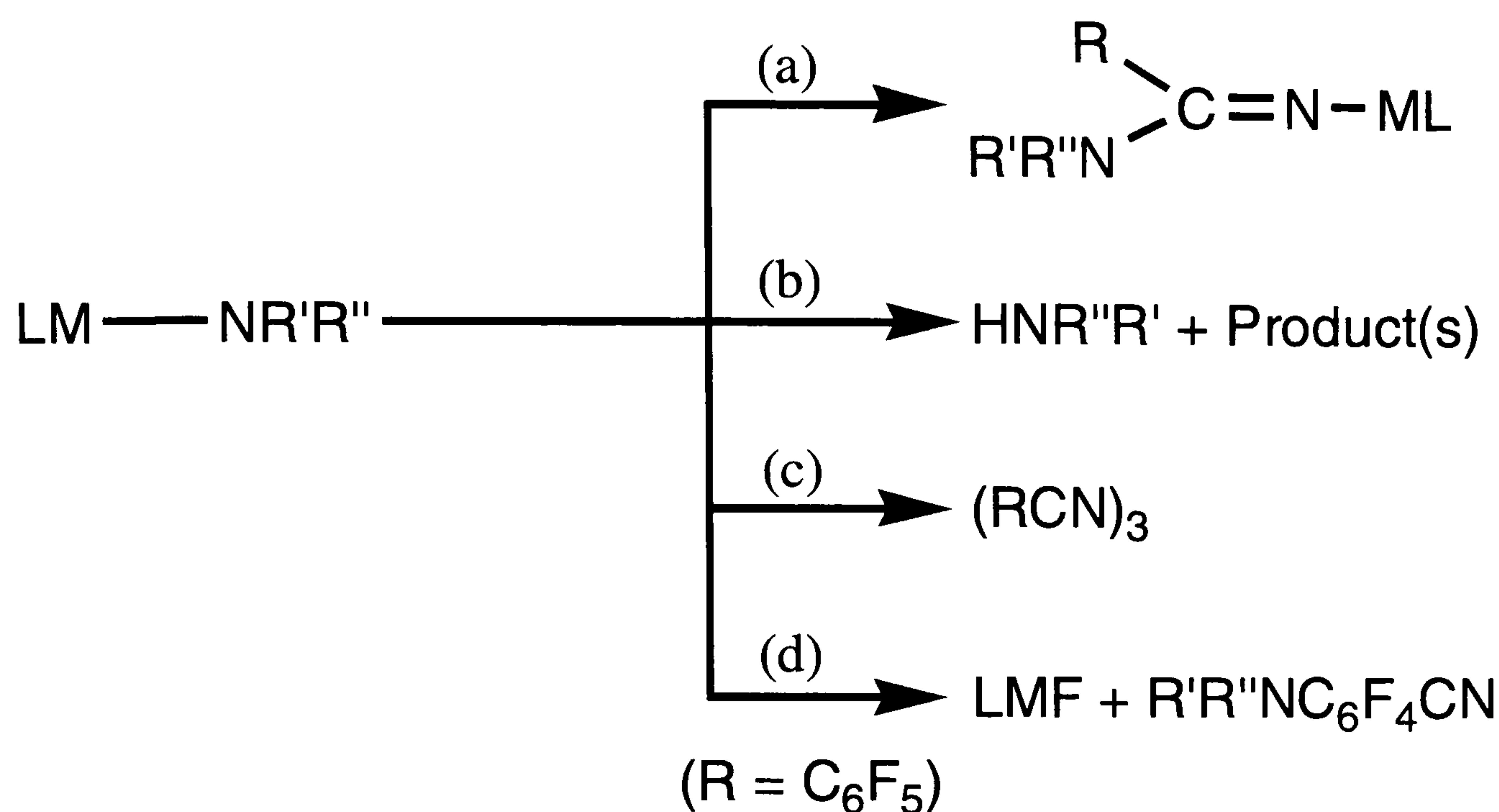
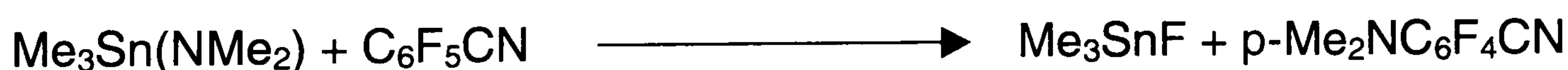


Figure 3.5 Diagram showing the possible outcomes of the insertion reaction between a metal amide and a nitrile compound: (a) insertion; (b) nitrile deprotonation; (c) nitrile trimerisation; (d) trans-metalation.

In the case of MeCN the products are thought to be highly polymeric. The insertion of acetonitrile into the metal nitrogen bond is accompanied by the formation of poly-acetonitrile.⁴¹ The reaction represented by pathway (b) is exemplified by $\text{Me}_3\text{SnNMe}_2$ and MeCN .^{18b} The reaction of lithium dimethylamide with PhCN results in the consecutive insertion of PhCN into the Li-N bond by three equivalents of nitrile followed by the elimination of LiNMe_2 and the formation of the corresponding triazene molecule, path (c).⁴² Pathway (d) is exemplified by the equation below,⁴⁰ in which a “transmetalation” reaction takes place and the *para*-F atom on the benzene ring is replaced by the NMe_2 from the metal amide.



The lack of reaction between *tert*-butyl cyanide and $[\text{Ti}(\text{NMe}_2)_4]$ is possibly due to the fact that nitriles do not have a very effective dipole unless they have a strong electron withdrawing group,⁴³ so strong electron withdrawing groups are often used e.g., CCl_3CN .⁴⁰

Chapter Three – Dicarbolide Complexes of Group Five Metals

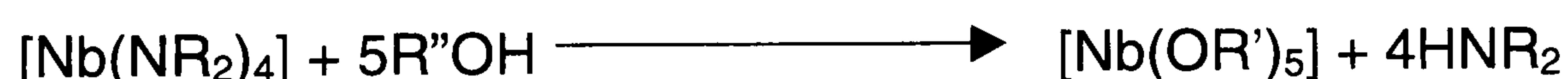
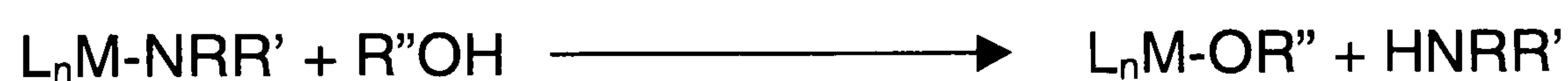
Acetonitrile has been shown to react with metal amides in two ways. In the case of main group metal amides of as tin and lead, acetonitrile acts as a protic acid with a $pK_a \approx 25$.⁴⁴ In contrast, with early transition metal complexes acetonitrile inserts readily into the metal nitrogen bond to form the corresponding amidino complex.⁴⁰

Isonitrile complexes have been shown to insert into Sn-N⁴⁵ and Pb-N⁴⁶ bonds. These examples are rare, but other examples exist of isonitriles inserting into M-X bonds (X = is not an amino group, e.g. X = H, Me₃SiH/C₆H₁₁NC,⁴⁷ X = Me, [(Et₂C₂B₄H₄)]TaMe₂Cp/^tBuNC, and X = Ph, [(Et₂C₂B₄H₄)]TaPh₂Cp/^tBuNC or C₆H₃(Me)₂NC.⁴⁸

3.1.1.5 Reactions of Metal Amides; Reactions with Protic Acids.

Reactions of metal amides with classical protic acids, such as ROH or RSH, are well established, and transamination of metal amides can also be viewed as a reaction between a basic metal amide with an acidic HNR₂ molecule.

Metal amides are extremely susceptible to hydrolysis resulting in the formation of the corresponding metal hydroxides or oxides. Control of these reactions can be gained by the reaction with what can be viewed as a “substituted water” such as an alcohol or a silanol, examples of which can be seen in the equations below



The formation of the pentavalent derivative from the reaction of niobium(IV) dialkylamide with triethylsilanol or an alcohol is surprising. Similarly treatment of the Ti(III) amide, [Ti(NMe₂)₃] with phenol gives the Ti(IV) product, although various alcohols afford the Ti(III) alkoxide.⁴⁹

Reactions of metal amide complexes with “acidic” compounds are governed by both thermodynamics and kinetics. It is true to say however that irrespective of kinetics “*a reaction between a basic metal amide complex and Brönsted acids, such as alcohols, to eliminate HNR₂ will not take place unless the acid that is to be reacted with the metal amide has a lower pK_a ,*

i.e. is more acidic than the eliminated HNR_2 , $\text{p}K_a = 35\text{-}40$ ". This relationship between an acid and a base is a general relationship and holds for both "classical" and "non-classical" acids and bases.

As with the transamination reactions mentioned earlier, the thermodynamic driving force for these reactions can also be the elimination from the system of volatile secondary amines.

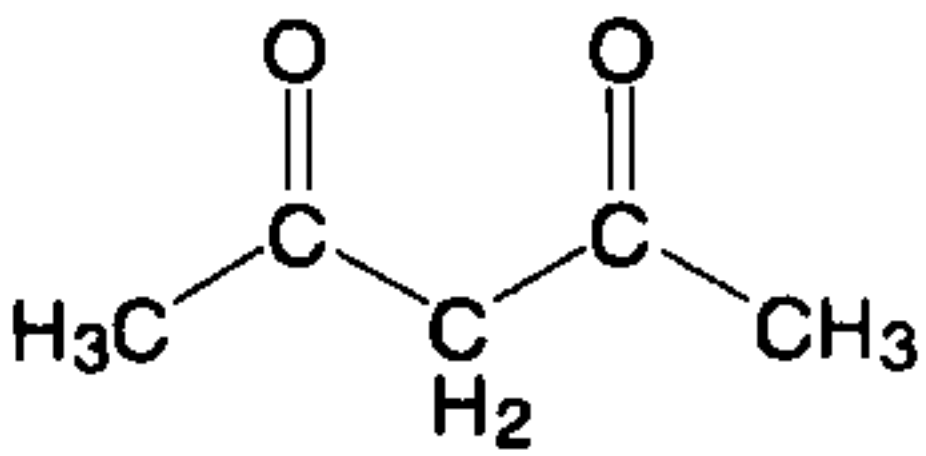
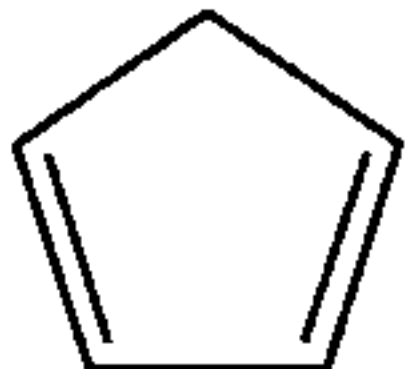
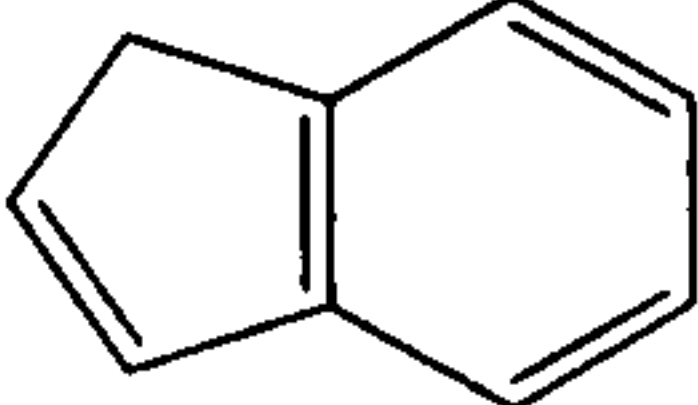
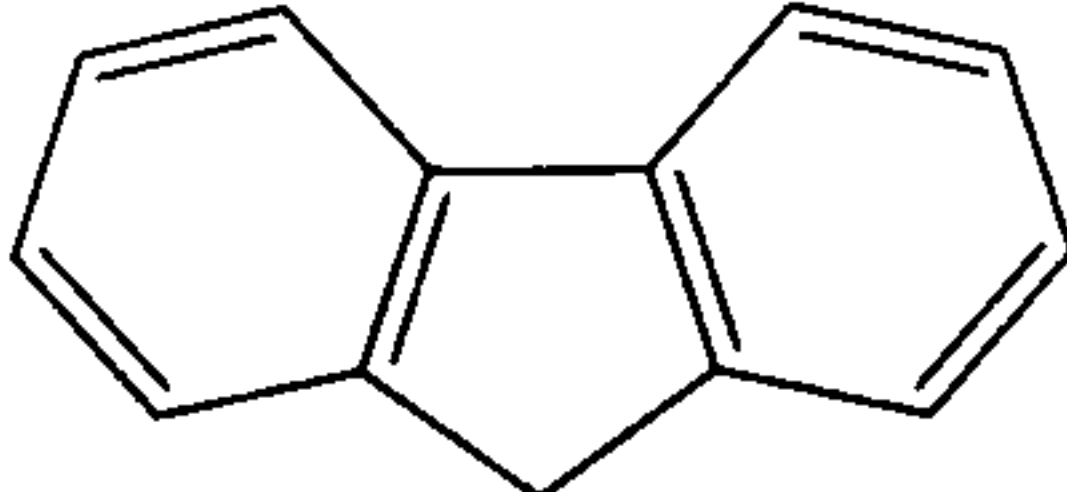
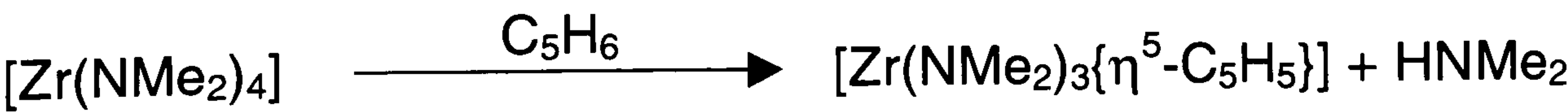
Acid "HY"	Approximate $\text{p}K_a$ (relative to water) ⁵⁰	Metal amide	Product	Ref.
HCl	-7	$\text{V}(\eta\text{-C}_5\text{H}_5)_2\text{N}(\text{SiMe}_3)_2$	$\text{V}(\eta\text{-C}_5\text{H}_5)_2\text{Cl}$	51
ArSH	6-8	$\text{Ti}(\eta\text{-C}_5\text{H}_5)_2\text{NMe}_2$	$\text{Ti}(\eta\text{-C}_5\text{H}_5)_2(\text{SAr})$	49
	9	$\text{Ti}(\text{NMe}_2)_3$	$\text{Ti}(\text{acac})_3$	52
ArOH	8-11	$\text{Ti}(\text{NMe}_2)_3$	$\text{Ti}(\text{OAr})_4$	49
$\text{R}_2\text{NH}_2^+\text{X}^-$ (X= Cl, Br or I)	10-12	$[\text{Zr}\{\eta\text{-C}_5\text{H}_4(\text{CH}_2)_3\text{-}\eta\text{-NMe}\}(\text{NMe}_2)]$	$[\text{Zr}\{\eta\text{-C}_5\text{H}_4(\text{CH}_2)_3\text{-}\eta\text{-NMe}\}(\text{X})_2(\text{HNMe}_2)]$	19a
CH_3OH	15	$\text{W}(\text{NMe}_2)_6$	$\text{W}(\text{NMe}_2)_3(\text{OMe})_3$	53
	16	$\text{Zr}(\text{NMe}_2)_4$	$\text{Zr}(\eta\text{-C}_5\text{H}_5)(\text{NMe}_2)_3$	18a
	20	$\text{Zr}(\text{NMe}_2)_4$	$\text{Zr}(\eta^5\text{-C}_9\text{H}_7)(\text{NMe}_2)_3$	18a
	23	$\text{Zr}(\text{NMe}_2)_4$	$\text{Zr}(\eta^5\text{-C}_{11}\text{H}_9)(\text{NMe}_2)_3$	18a
$\text{PhC}\equiv\text{CH}$	25	$\text{Zr}(\eta\text{-C}_5\text{H}_5)_2(\text{NMe}_2)_2$	$\text{Zr}(\eta\text{-C}_5\text{H}_5)_2(\text{CCPh})_2$	54
PhCH_3	41	No Reaction	No Reaction	

Table 3.1 The relative $\text{p}K_a$ s of protic "Acids" are given as well as examples of reactions with transition metal amides. Comparison of the $\text{p}K_a$ of dialkyl amines, $\text{R}_2\text{NH} \sim 35\text{-}40$, gives an indication as to whether a reaction will take place on the basis of thermodynamic factors.

Metal amides are being used more commonly to react with protic acids such as C_5H_6 , as in the example below.^{18a}



3.1.2 Metal Amide Complexes of the Vanadium Group

Homoleptic amides of vanadium are known for the oxidation states V(II), V(III) and V(IV), but not for V(V), for which only heteroleptic complexes are known. In comparison amide complexes are known for Nb(IV), Nb(V) and Ta(V), although only one Ta(IV) derivative is known.⁵⁵ The lack of Ta(IV) derivatives can be attributed to the relative instability of the +4 oxidation state for Ta. Thus, sterically demanding Ta(V) amides do not disproportionate to Ta(IV) complexes, whereas Nb(V) analogues will generally yield the Nb(IV) complexes.^{18b}

$\text{Nb}(\text{NMe}_2)_5$ ³⁸ and $\text{Ta}(\text{NMe}_2)_5$ ⁵⁵ are both easily prepared from the reaction of $\text{Li}(\text{NMe}_2)$ with the respective metal pentachloride. Attempts to obtain higher alkyl homologues affords the Ta(V) imido complexes $[\text{Ta}(\text{NR})(\text{NR}_2)_3]$ ($\text{R} = \text{Et}, \text{Pr}$ or Bu)²⁶ or Nb(IV) amides $[\text{Nb}(\text{NR}_2)_4]$ respectively.^{26,38,56}

X-ray crystallographic studies have been carried out on $[\text{Nb}(\text{NMe}_2)_5]$ ⁵⁷ and $[\text{Nb}(\text{NC}_5\text{H}_{10})_5]$,^{57,58,59} they have very similar structures, which are both based on a distorted square pyramid, tending towards a trigonal bipyramid. More recently, single crystal X-ray crystal structure experiments have shown the tantalum amide $[\text{Ta}(\text{NMe}_2)_5]$ ^{60,61} to have a structure based on a trigonal bipyramid, as is the case in $[\text{Ta}(\text{NEt}_2)_5]$.⁶²

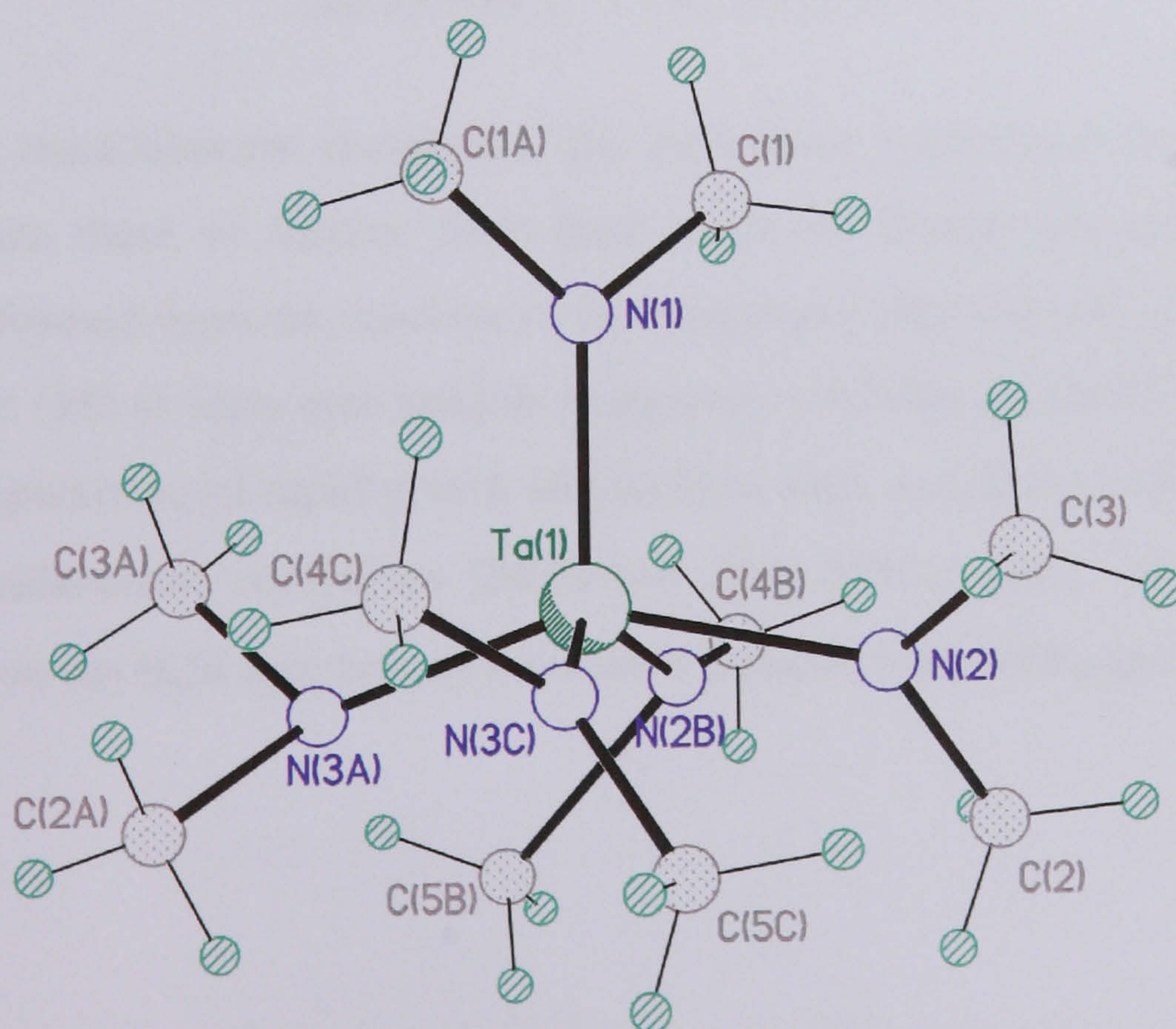
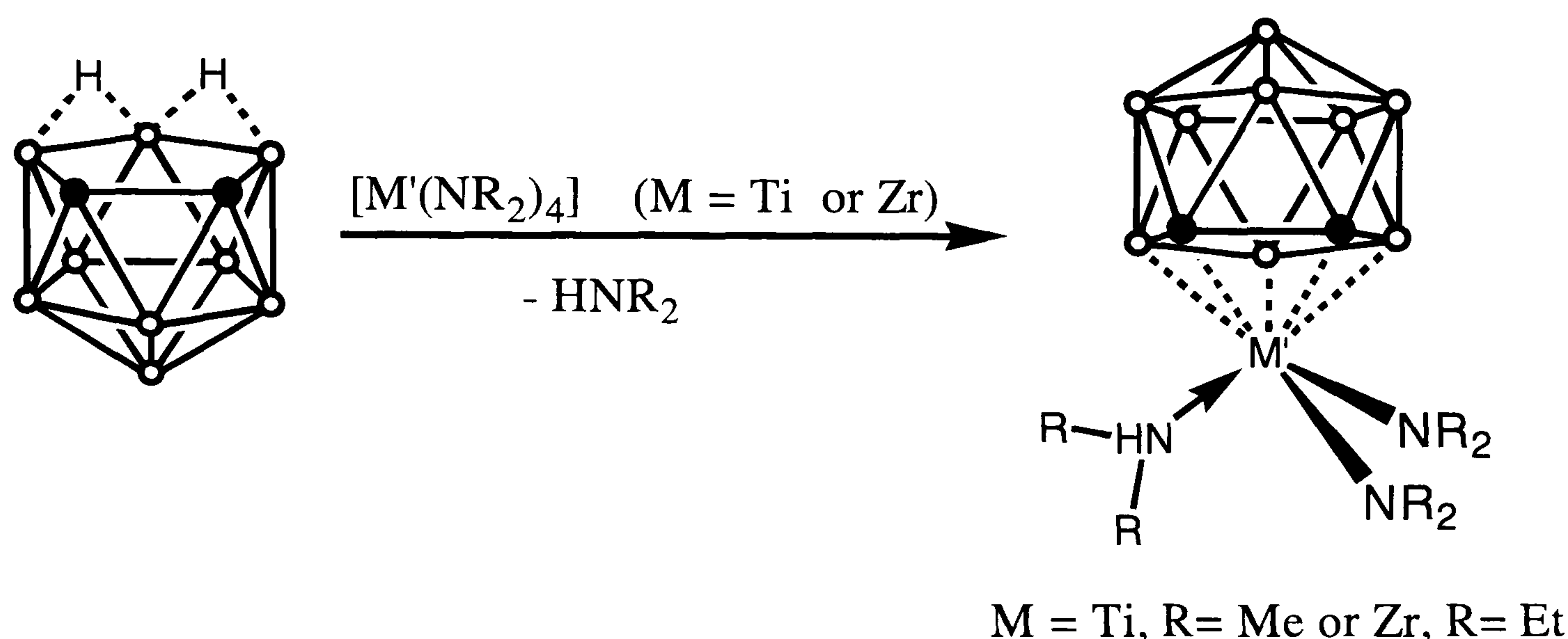


Figure 3.6 Molecular structure of the $\text{N}(2):\text{N}(3\text{C}):\text{N}(2\text{B}):\text{N}(3\text{A})$ enantiomer of $[\text{Ta}(\text{NMe}_2)_5]$. Ta1 and N1 sit on two crystallographic mirror planes one bisecting the plane defined by Ta(1)-N(1)-C(1). The second mirror plane bisects the first mirror planes at 90° through the atoms Ta(1) and N(1). For a full discussion of the crystallography see refs. 60 and 63.

3.2 Group 5 Metallacarborane *Tris*-Amide complexes.

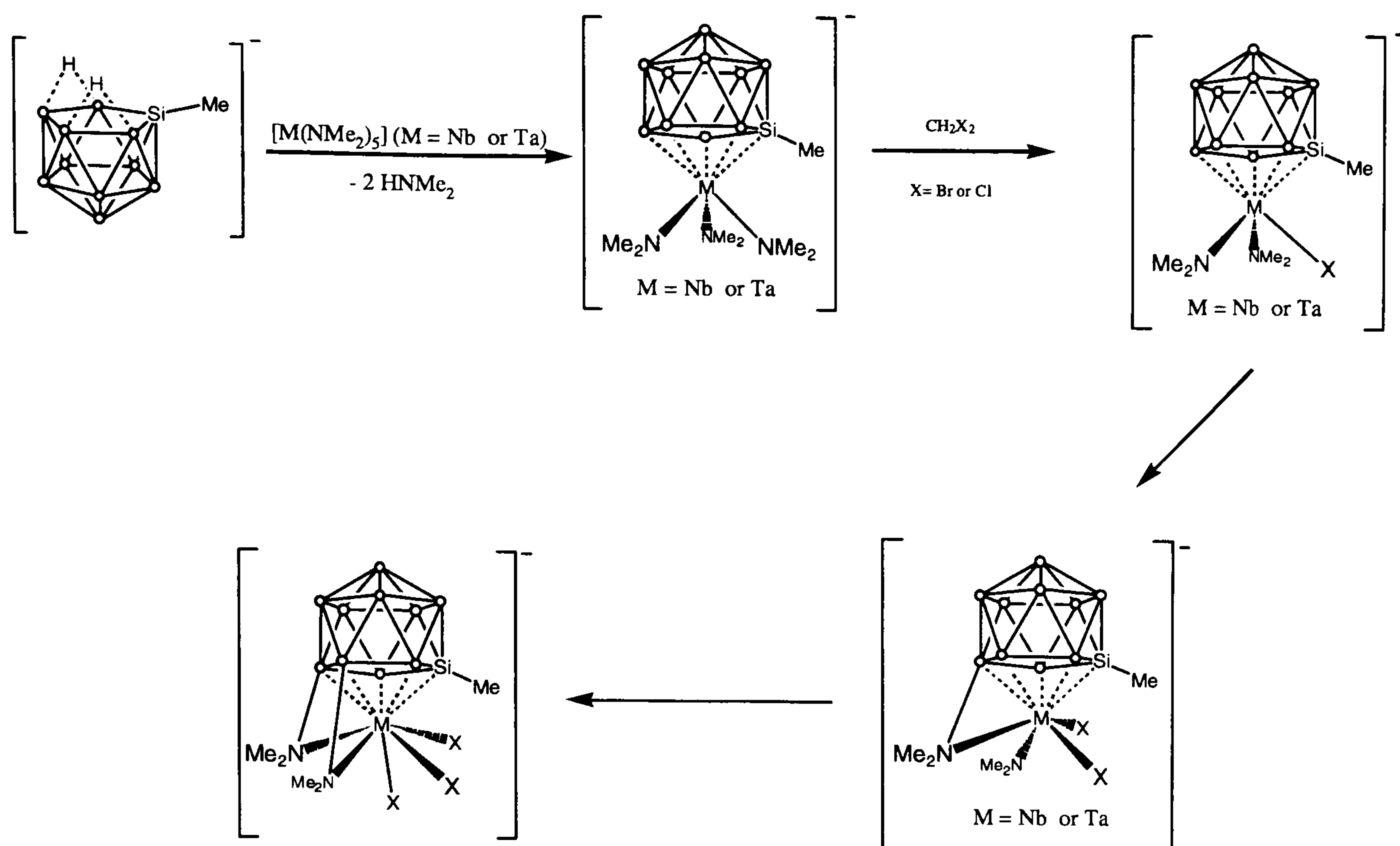
3.2.1 Synthesis and Characterisation of Group 5 Dicarbollide *Tris*-Amide Complexes

Jordan and co workers have previously shown that the neutral carborane [*ortho*-C₂B₉H₁₃], (7), is thermodynamically capable of reacting with the metal amide complexes [Zr(NEt₂)₄] and [Ti(NMe₂)₄] to form the mono dicarbollide complexes [M(η⁵-1,2-C₂B₉H₁₁)(NR₂)(NHR₂)] (Scheme 3.2).²²



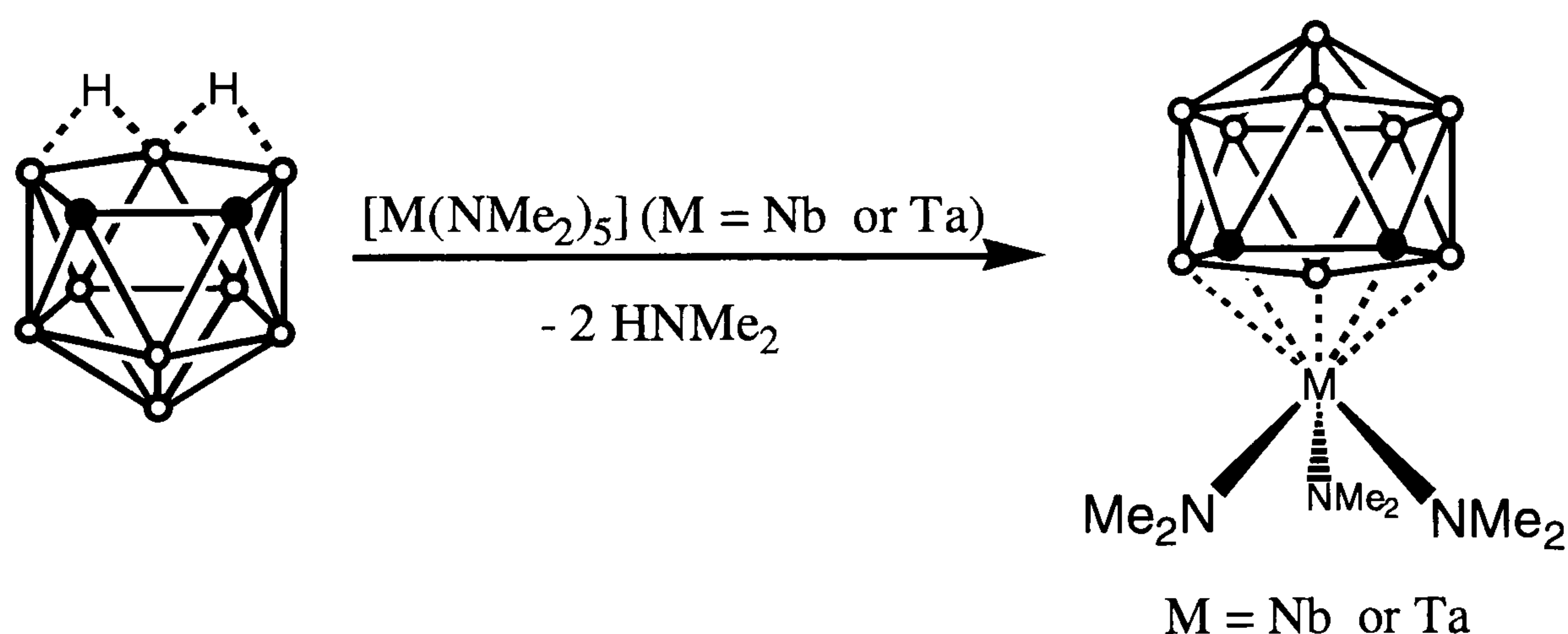
Scheme 3.2 Reaction between [*ortho*-C₂B₉H₁₃] and the group four metal amides, Ti(NMe₂)₄ and Zr(NEt₂)₄. Taken from ref. 22.

The only other metallaborane complexes that have been synthesised that contain the NMe₂ group apart from those of Jordan, have been made by Wesemann and co-workers. These complexes are formed from the reaction of the silaborane [Me-SiB₁₀H₁₂]⁻ with the homoleptic amides (14) and (15) to form non-isolable complexes [M(NMe₂)₃(MeSiB₁₀H₁₀)]⁻ (M = Nb or Ta). These complexes react rapidly with alkylhalides such as CH₂Br₂ and CH₂Cl₂ to form the tri-halo metallasilaborane complexes [M(MeSiB₁₀H₈μ-(NMe₂)₂)Br₃]⁻ (M = Nb or Ta), where two hydrogens on the B₄Si face borons have been replaced with NMe₂ groups (Scheme 3.3).⁶⁴



Scheme 3.3 Reaction of the silaborane complexes $[\text{M}(\text{NMe}_2)_3(\text{MeSiB}_{10}\text{H}_{10})]^-$ (M = Nb or Ta), with dichloromethane or dibromomethane. Taken from ref. 64.

In an analogous reaction toluene solutions of the group 5 homoleptic amides $[\text{M}(\text{NMe}_2)_5]$ (M = Nb (**14**) and Ta (**15**)) react with 1 equivalent of (**7**) to cleave two metal-amide bonds (Scheme 3.4) and give *closo*-[3-M(NMe₂)₃-1,2-C₂B₉H₁₁] (M = Nb (**16**) and Ta (**17**)) as yellow crystalline solids in high yields.* In comparison to the silaborane complexes, the dicarbollide complexes (**16**) and (**17**), are fully soluble in polar solvents such as CH₂Cl₂ and THF but only sparingly soluble in toluene. Accordingly (**16**) and (**17**) can be purified by recrystallisation from CH₂Cl₂/toluene.



Scheme 3.4 The synthesis of *ortho*-metallacarborane complexes (**16**) and (**17**).

* The compounds in this chapter have a niobium or tantalum atom in either a *closo*-1,2-dicarba-3-metalladodecaborane, *closo*-1,7-dicarba-2-metalladodecaborane or a *closo*-1,12-dicarba-2-metalladodecaborane framework. However, in order to avoid this complicated nomenclature, and to better relate them to structurally analogous imido-metal complexes and half-sandwich metallocenes, e.g., $[\text{Nb}(\text{RN})\text{X}_3]$ and $[\text{Zr}(\eta\text{-C}_5\text{H}_5)\text{X}_3]$, we treat the cages as *nido*-11-vertex ligands, (*nido*-C₂B₉H₁₁). In some cases crystallographic numbering Schemes differ from the IUPAC nomenclature for these complexes.

The ^{11}B NMR spectra of both (16) and (17) are very similar and contain five resonances in a 1:2:2:3:1 intensity ratio, which are in the range observed for other early transition metal dicarbollide complexes and are shifted to higher frequency than the resonances for $\text{C}_2\text{B}_9\text{H}_{13}$ or $\text{C}_2\text{B}_9\text{H}_{12}^-$ and $\text{C}_2\text{B}_9\text{H}_{11}^{2-}$ salts.⁶⁵ The ^1H NMR spectra contain one singlet for the dicarbollide C-H hydrogens which confirms the C_s symmetry implied by the ^{11}B NMR spectra. The ^1H NMR also show a single N-Me resonance for the three NMe_2 groups, which suggests rapid rotation around both the metal carborane axis (a) and metal nitrogen axis (b) thus giving rise to a time averaged single resonance (Figure 3.7).⁶⁶

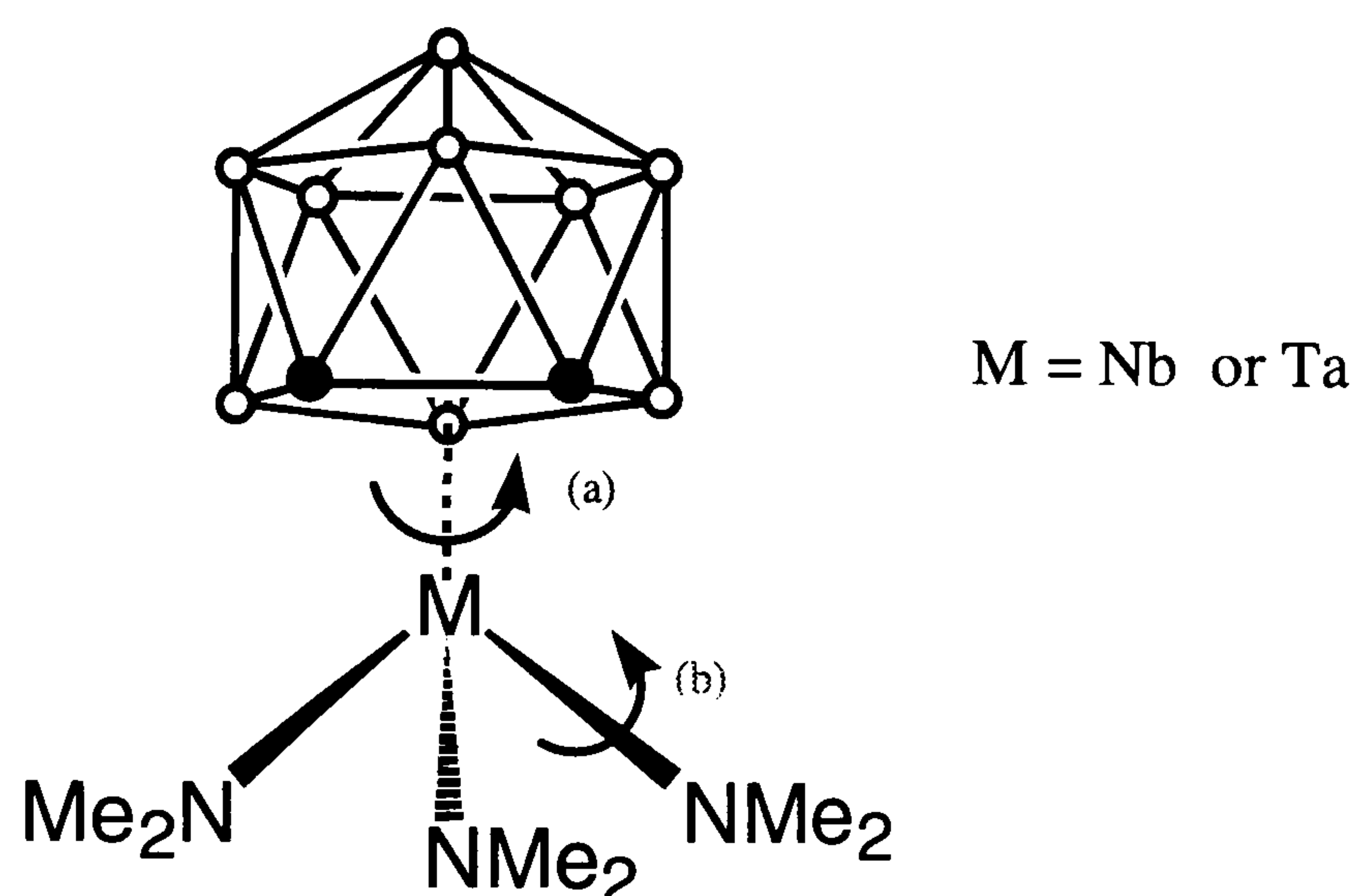


Figure 3.7 Diagram showing rotation around the M-Cb axis and M-N axis that at room temperatures show the NMe_2 groups to have a single resonance in the ^1H and ^{13}C NMR spectra.

The ^{11}B NMR spectra of (16) and (17) show signals characteristic of a $[(\text{C}_2\text{B}_9\text{H}_{11})\text{M}]$ fragment; both the ^1H and ^{13}C NMR display only a single resonance for all the NMe_2 methyl groups and the ^1H NMR spectrum of (17) in CD_2Cl_2 at -90°C is identical to the room temperature spectrum (apart from some small changes in chemical shift for the BH resonances). Given the small chemical shift range expected for such resonances, and the likelihood that rotation about the M-N bond is facile, it seems likely that the NMe_2 resonances are in fast exchange even at -90°C . Complexes that are isoelectronic with (16) and (17), containing a $\text{M}(\text{NR}_2)_3$ fragment with NR_2 ligands that are reported to be in fast exchange include $[(\text{Me}_3\text{CN})\text{M}(\text{NMe}_2)_3]$ ($\text{M} = \text{Nb}, \text{Ta}$),⁶⁷ $[(\eta\text{-C}_5\text{Me}_5)\text{Ti}(\text{NR}_2)_3]$ ($\text{R} = \text{Me}, \text{Et}$),⁶⁸ and $[\text{Nb}(\text{2,6-}^i\text{Pr}_2\text{C}_6\text{H}_3\text{N})(\text{NMe}_2)_3]$.⁶⁹ By contrast, the amide ligand rotation in $[\text{M}_2(\text{NR}_2)_6]$ ($\text{M} = \text{Mo}, \text{W}; \text{R} = \text{Me}, \text{Et}$) can be frozen out at low temperature and the barrier to rotation has been determined.⁷⁰

In comparison to the solution state, solid-state structures of (16) and (17) show two different NMe_2 ligands which would give rise to three environments for the NMe groups and would suggest three resonances of equal intensity.

Single crystals of suitable quality and dimensions were grown from concentrated toluene/CH₂Cl₂ solutions at -40°C. The dicarbollide amide complexes [M(*nido*-1,2-C₂B₉H₁₁)(NMe₂)₃] (M = Nb (**16**) and (**17**)) form isostructural crystals in the space group *P*2₁2₁2₁. The asymmetric unit comprises two molecules, A and B, with similar geometry (see Fig. 3.8, 3.9 and Table 3.2). In either case, the metal atom is co-ordinated by the open C₂B₃ face of the dicarbollide ligand (in a nearly symmetrical η^5 fashion) and by three dimethylamide ligands (Figure 3.9). All the NMe₂ ligands display planar trigonal bonding of the nitrogen atoms, compatible with them acting as 3-electron LX ligands.¹⁵ Together with the 4-electron (or LX₂) dicarbollide ligand, this completes an 18 electron ML₄X₅ configuration of the Nb or Ta atom.

A carborane cage is likely to be disordered in the solid state (with C and B positions statistically mixed), unless pinned down by substituents or by hydrogen bonds (in which C-H but not B-H groups can act as donors).⁷¹ Although the dicarbollide ligand in (**16**) or (**17**) carries no substituents and can form no hydrogen bonds, lacking any suitable acceptor (*sp*² N atom, unlike *sp*³ one, is quite inactive in this respect), it is certainly ordered. The heights of the electron density peaks, bond distances within the cage and to the hydrogen atoms, all leave no doubt as to the location of the carbon atoms C(2) and C(3).

The most notable feature of both complexes is the orientation of the NMe₂ ligands with respect to the η^5 -C₂B₃ face of the dicarbollide ligand (Figure 3.10). If the vector linking the centroid Cb of this face to the metal atom is coplanar with the NMe₂ ligand (i.e. the Cb-M-N-C torsion angle, τ is 0 or 180°), this orientation can be described as 'vertical', and the orientation perpendicular to the latter ($\tau = 90^\circ$) as 'horizontal'. In (**16**) and (**17**), the N(1)Me₂ and N(3)Me₂ ligands are 'vertical' while the N(2)Me₂ ligand is 'horizontal' (see Table 3.2). In each molecule, the 'horizontal' ligand lies opposite to the C(2)-C(3) bond and forms a M-N bond appreciably shorter than the 'vertical' ligands, by 0.035 Å (10 σ) in (**16**) and 0.032 Å (7 σ) in (**17**). However, both vertical and horizontal orientations are only approximate descriptions and the ligands are somewhat inclined, all in the same direction, thus adopting a chiral, propeller-like conformation (see Figure 3.10).



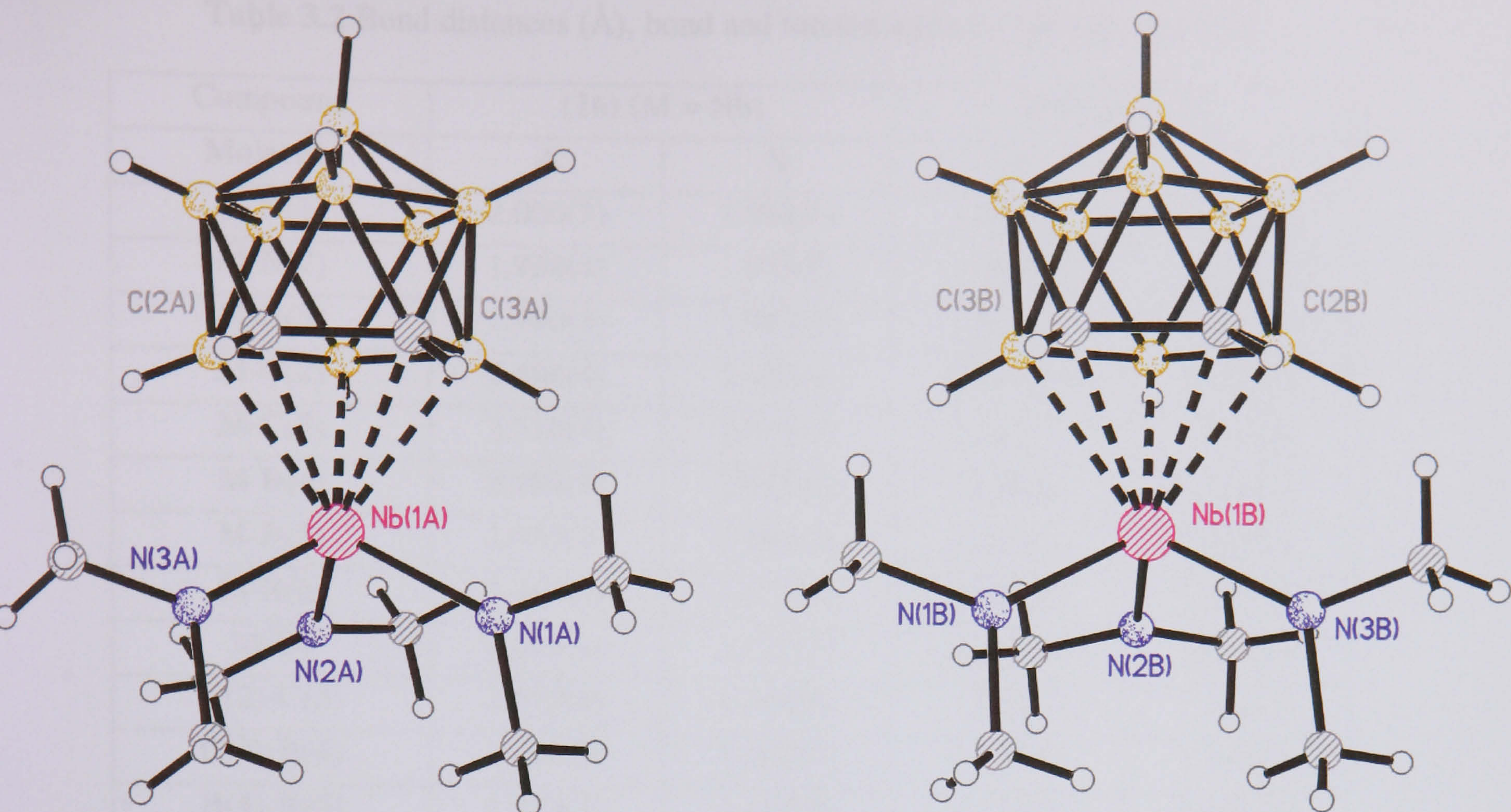


Figure 3.8 A comparison of the two independent molecules of $[\text{Nb}(\text{nido-1,2-C}_2\text{B}_9\text{H}_{11})(\text{NMe}_2)_3]$ (**16**) in the asymmetric unit.

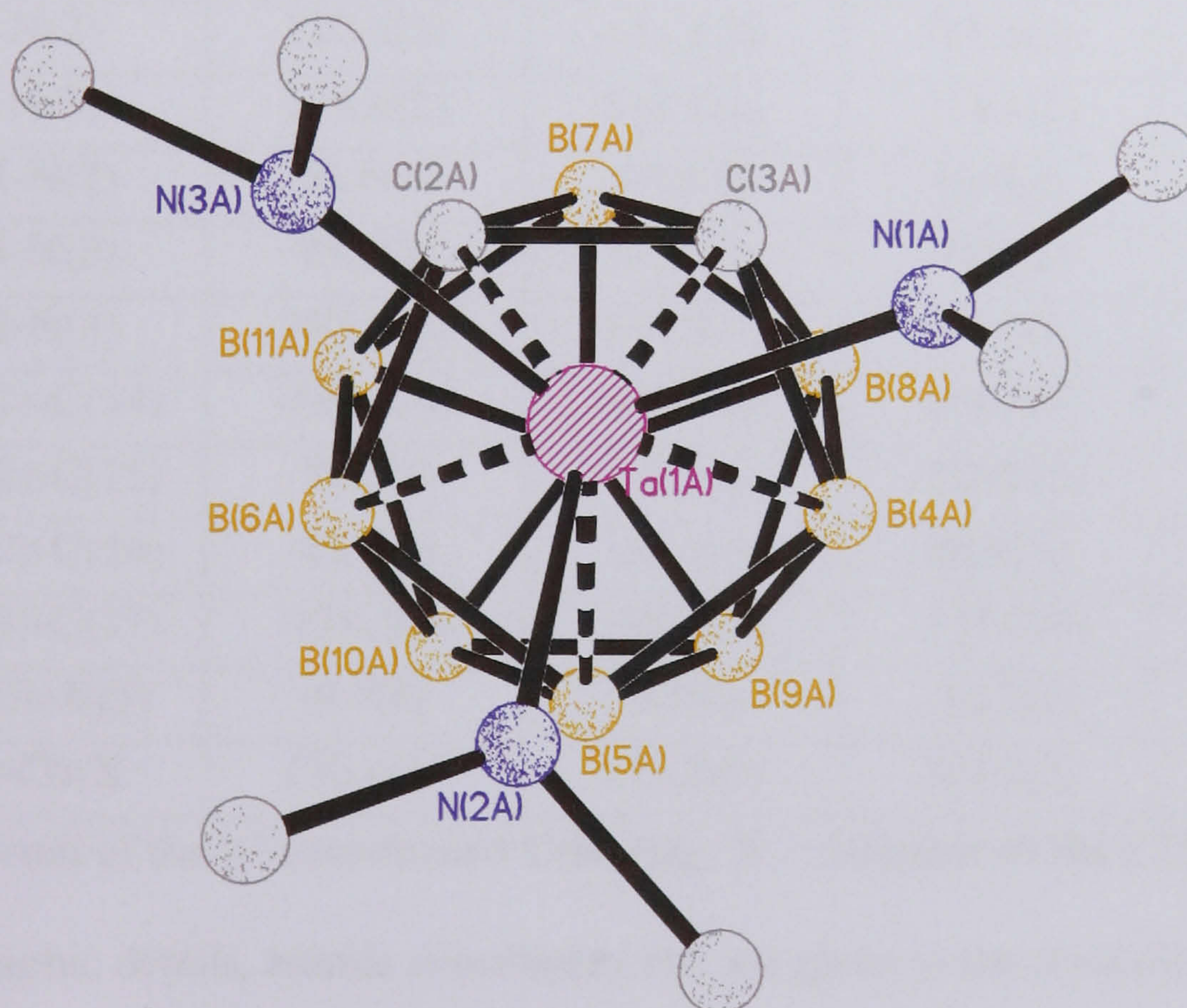


Figure 3.9 In both (**16**) and (**17**) the metal atom is co-ordinated by the open C_2B_3 face of the dicarbollide ligand (in a nearly symmetrical η^5 fashion) and by three dimethylamide ligands. An independent molecule of $[\text{Ta}(\text{NMe}_2)_3(\text{nido-1,2-C}_2\text{B}_9\text{H}_{11})]$ is shown. Hydrogen atoms have been omitted for clarity.

Table 3.2 Bond distances (Å), bond and torsion angles (°) in (16) and (17).

Compound	(16) (M = Nb)		(17) (M = Ta)	
Molecule	A	B	A	B
M-N(1)	2.000(3)	1.994(4)	1.987(5)	1.981(5)
M-N(2)	1.958(4)	1.955(3)	1.949(4)	1.955(4)
M-N(3)	1.980(3)	1.992(3)	1.980(4)	1.987(5)
M-C(2)	2.496(4)	2.482(4)	2.490(5)	2.480(5)
M-C(3)	2.510(4)	2.475(4)	2.501(5)	2.470(5)
M-B(4)	2.484(4)	2.465(4)	2.489(6)	2.444(6)
M-B(5)	2.485(5)	2.493(4)	2.470(7)	2.478(6)
M-B(6)	2.460(5)	2.471(4)	2.453(6)	2.475(5)
M-Cb	2.019(4)	2.029(5)	2.019(6)	2.003(6)
C(2)-C(3)	1.577(6)	1.558(6)	1.576(7)	1.570(7)
C(3)-B(4)	1.661(6)	1.692(7)	1.685(9)	1.699(9)
B(4)-B(5)	1.773(7)	1.764(6)	1.779(9)	1.769(9)
B(5)-B(6)	1.762(7)	1.756(7)	1.756(9)	1.771(8)
B(6)-C(2)	1.682(7)	1.671(6)	1.681(9)	1.686(8)
Cb-M-N(1)	115.8(2)	114.8(2)	116.4(2)	114.6(2)
Cb-M-N(2)	123.8(2)	121.4(2)	124.4(2)	122.0(2)
Cb-M-N(3)	114.6(2)	114.5(2)	114.4(2)	115.1(2)
N(1)-M-N(2)	96.6(1)	95.8(2)	96.0(2)	95.9(2)
N(2)-M-N(3)	95.6(1)	97.0(2)	95.9(2)	96.9(2)
N(1)-M-N(3)	107.3(2)	110.8(2)	106.4(2)	109.7(2)
Cb-M-N(1)-C(14)	-160.4(6)	-169.7(6)	-160.0(5)	-167.0(5)
Cb-M-N(2)-C(15)	-99.1(6)	76.1(6)	-100.0(5)	74.7(5)
Cb-M-N(2)-C(16)	68.1(6)	-81.3(6)	66.9(5)	-83.7(5)
Cb-M-N(3)-C(17)	-158.2(6)	-167.2(6)	-157.5(5)	-165.8(5)
N(2)-M-Cb-B(5)	-9.7(6)	-5.1(6)	-10.7(5)	-6.4(5)
N(2)-M-Cb-X	170.4(6)	175.2(6)	169.0(5)	173.5(5)

Cb – centroid of the η^5 -coordinated C_2B_3 ring; X – midpoint of the C(2)-C(3) bond

Full crystallographic details, atomic coordinates etc. are given in the crystallographic appendix.

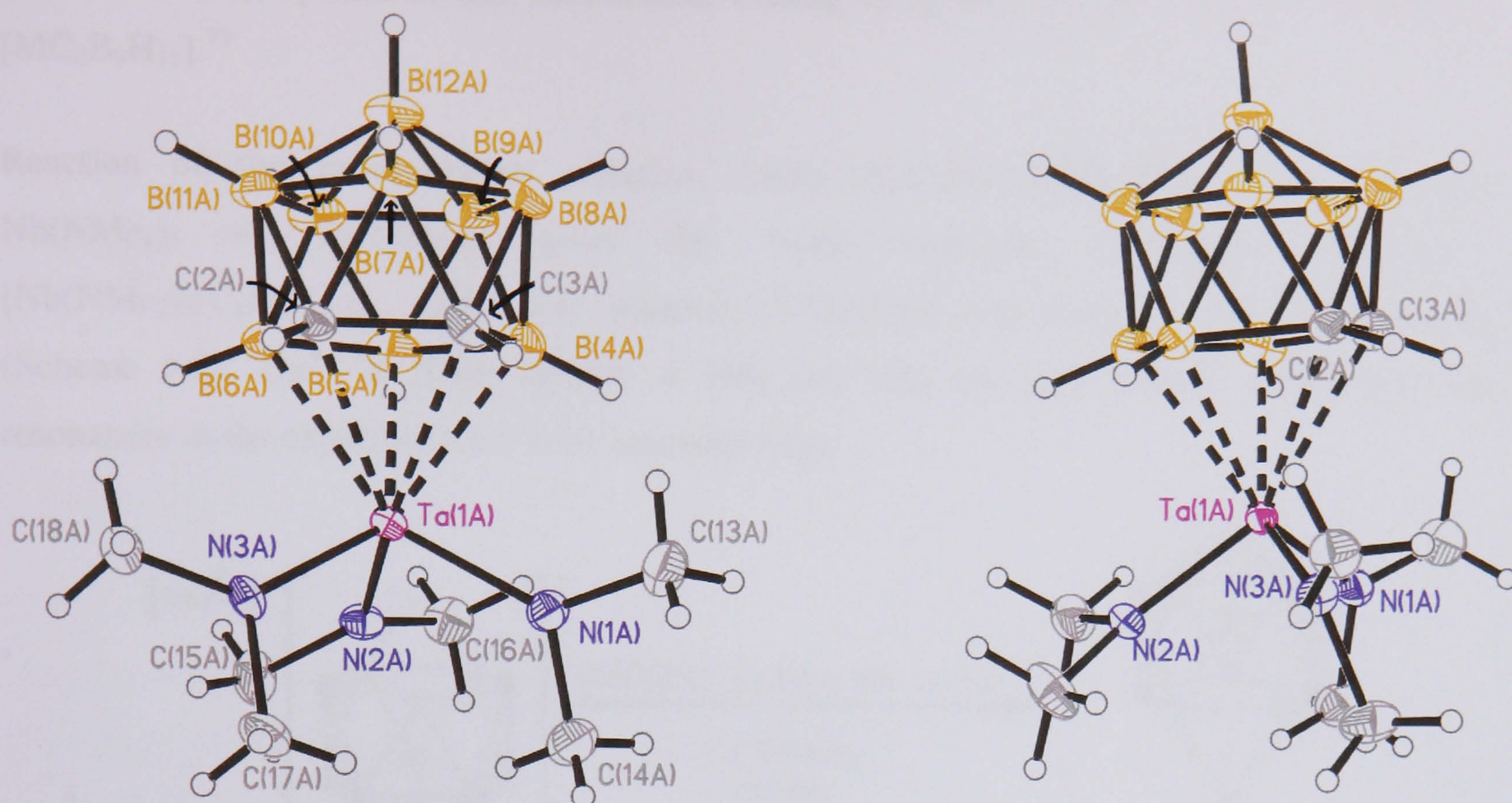


Figure 3.10 Molecular structure of $[\text{Ta}(\text{NMe}_2)_3(\text{nido-1,2-C}_2\text{B}_9\text{H}_{11})]$, (17), showing independent molecule A in 50% displacement ellipsoids. The two different NMe_2 ligand environments can be seen clearly.

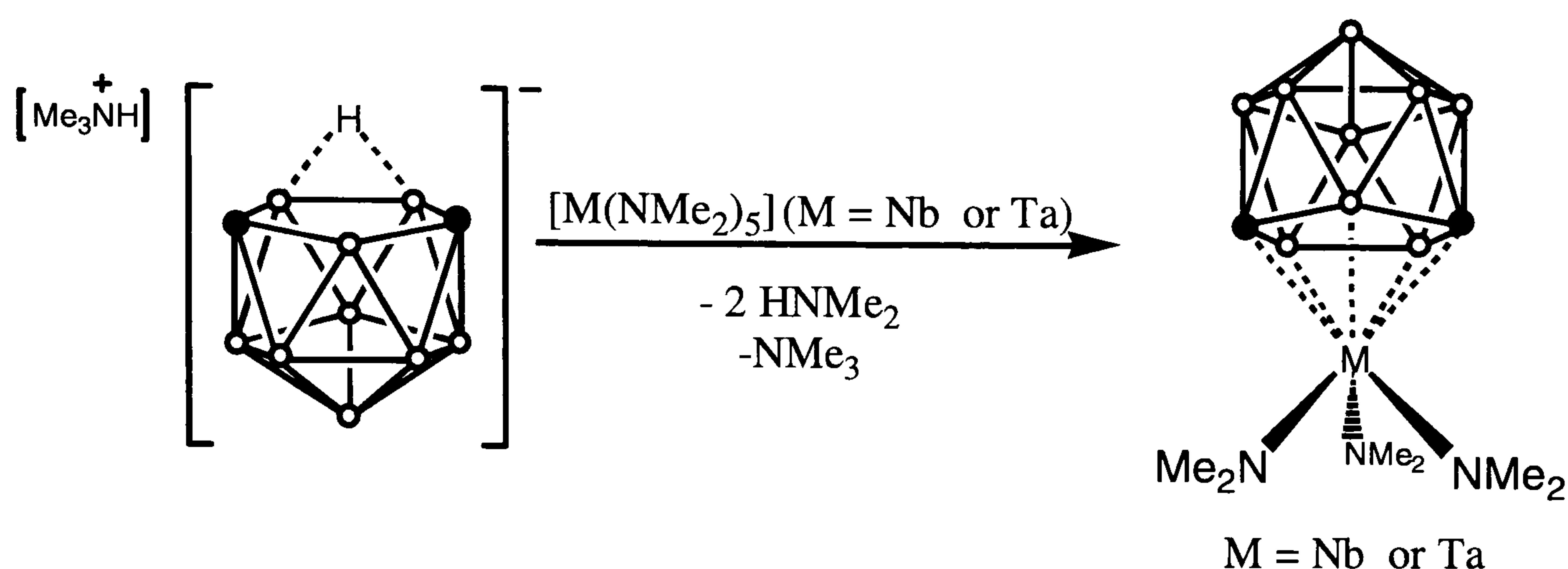
Similar ligand orientation effects have been observed for the compound $[\text{TaCl}_3(\eta^5\text{-1,2-C}_2\text{B}_9\text{H}_{11})]$ in which the Cl atom *trans* to the C-C bond in the cage has both a shorter M-Cl bond and the angle between the $\text{Cb}_{\text{centroid}}\text{-Ta-Cl}_{\text{trans}}$ is greater than the other two $\text{Cb}_{\text{centroid}}\text{-Ta-Cl}$ angles.^{14d}

In either structure, molecule A differs from B by a small rotation around the M-Cb axis (4-5°) and the M-N bonds; they can be fitted to each other with an average discrepancy of 0.14 Å for all non-hydrogen atoms, or only 0.06 Å, if methyl carbons are excluded. At the same time, molecules A and B in the crystal are related by pseudo-symmetry, corresponding approximately to the space group *Pbca*.⁶⁰

As discussed in chapter one and two the 1,2- 1,7 and 1,12 isomers of *closo*- $\text{C}_2\text{B}_{10}\text{H}_{12}$ are trivially known as “*ortho*–”, “*meta*–” and “*para*–” carborane respectively. Chapter two described the preparation of the anions $[\text{C}_2\text{B}_9\text{H}_{12}]^-$ for all three isomers. In comparison to the large number of complexes containing the “*ortho*” metallacarborane unit, $[3,1,2\text{-MC}_2\text{B}_9\text{H}_{11}]$, that have been structurally characterised there are only 33 structures containing the “*meta*” unit, $[2,1,7\text{-MC}_2\text{B}_9\text{H}_{11}]$, and to the best of our knowledge no structures containing the “*para*”

metallacarborane unit, $[2,1,12\text{-M C}_2\text{B}_9\text{H}_{11}]$.⁷² Thermal or electrochemical isomerisation of *closo*- $\text{MC}_2\text{B}_9\text{H}_{11}$ species is well established, leading to up to 7 of the 9 possible isomers of $[\text{MC}_2\text{B}_9\text{H}_{11}]$.⁷³

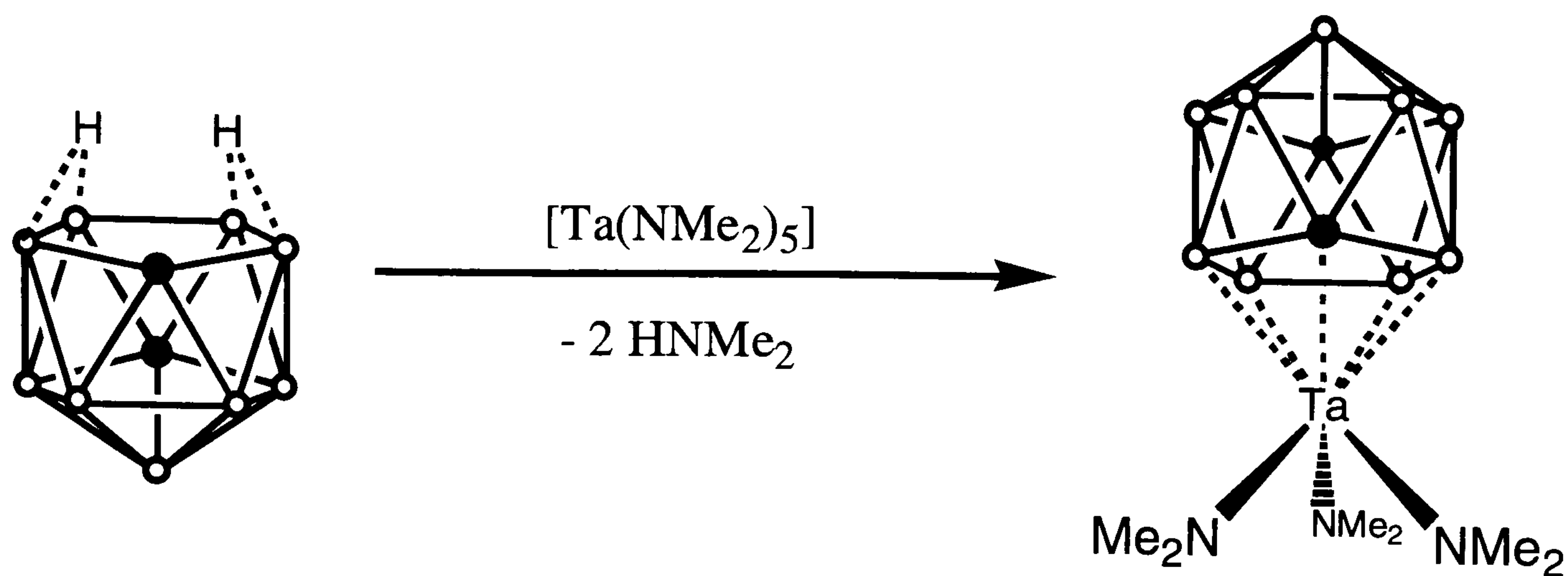
Reaction of the mono-anionic complex, $[\text{nido-7,9,-C}_2\text{B}_9\text{H}_{12}][\text{Me}_3\text{NH}]$ (**5a**) with both $\text{Nb}(\text{NMe}_2)_5$ or $\text{Ta}(\text{NMe}_2)_5$ gives the “*meta*”-carborane complexes *closo*-2,1,7- $[\text{Nb}(\text{NMe}_2)_3(\text{C}_2\text{B}_9\text{H}_{11})]$, (**18**) and *closo*-2,1,7- $[\text{Ta}(\text{NMe}_2)_3(\text{C}_2\text{B}_9\text{H}_{11})]$, (**19**) respectively (Scheme 3.5). The ^{11}B NMR spectra of (**18**) and (**19**) are very similar and contain six resonances in the expected 2:2:1:1:2:1 intensity ratio.



Scheme 3.5 Synthesis of *meta*-metallacarborane complexes (**18**) and (**19**).

The ^1H NMR contains one broad singlet for the dicarbollide C-H hydrogens which confirms the C_s symmetry implied by the ^{11}B NMR spectra. As is the case with (**16**) and (**17**) the ^1H NMR also shows a single N-Me resonance for the three NMe_2 groups.

The neutral *para*-carborane, $[2,7\text{-C}_2\text{B}_9\text{H}_{13}]$, (**9**), obtained by base-induced deboronation of *para*- $\text{C}_2\text{B}_{10}\text{H}_{12}$ and subsequent acidification, also reacts with $\text{Ta}(\text{NMe}_2)_5$ to give the third isomer, *closo*-2,1,12- $[\text{Ta}(\text{NMe}_2)_3(\text{C}_2\text{B}_9\text{H}_{11})]$, (**20**) (Scheme 3.6). Compound (**20**) has been fully characterised by NMR (^1H , ^{13}C and ^{11}B) spectroscopy, and this is consistent with the proposed structure. In the case of both the *ortho*- and *meta*- metallacarborane complexes the C-H groups on the cage are equivalent in both the ^1H and ^{13}C NMR. The *para*- complex (**20**) differs from the other isomers in this series because the cage carbons occupy non equivalent positions, one being adjacent to the metal atom in the lower ring, and the second carbon is in a *trans* position with respect to the first carbon atom, in the upper ring of the cage. This gives rise to two chemical shifts for the two C-H groups in both the ^1H and ^{13}C NMR spectra. ^{11}B NMR shows the expected five resonances in a 2:2:2:2:1 intensity ratio pattern.



Scheme 3.6 Synthesis of the *para*-metallacarborane, [*closo*-2-Ta(NMe₂)₃(1,12-C₂B₉H₁₁)].

Crystals of **(19)** and **(20)** suitable for single crystal X-ray diffraction experiments were grown from toluene/pentane solutions at -40°C and we believe that compound **(20)** is the first structurally characterised example of a *para*-2,1,12 M-C₂B₉H₁₁ carborane.

The molecular structure of **(19)** shows that the three NMe₂ ligands adopt a chiral propeller configuration, with the two enantiomers occupying the same crystallographic site, resulting in a high degree of disorder. For this reason crystallographic data on this compound will not be included as a satisfactory model for the disordered NMe₂ groups could not be found.

The molecular structure of *para*-[3-Ta(NMe₂)₃(1,12-C₂B₉H₁₁)] is shown in Figure 3.11 and selected bond lengths are given in Table 3.3. The tantalum atom is co-ordinated by the open CB₄ face of the dicarbollide ligand (in a nearly symmetrical η^5 fashion) and by three dimethylamide ligands (Figure 3.11). All the NMe₂ ligands can be considered to be acting as 3-electron LX ligands as in the case of compounds **(16)**-(**20**).

Table 3.3 Selected bond distances (Å), bond and torsion angles (°) for **(20)**.

Ta(1) N(1)	1.9724(19)	C(2) B(6)	1.674(4)
Ta(1) N(2)	1.9832(19)	C(2) B(3)	1.688(3)
Ta(1) N(3)	1.9899(19)	B(3) B(4)	1.772(4)
Ta(1) B(3)	2.446(3)	B(5) B(6)	1.782(4)
Ta(1) B(4)	2.465(2)	Ta(1) Cb	1.986(5)
Ta(1) B(5)	2.484(2)	Cb Ta(1) N(1)	122.6(2)
Ta(1) B(6)	2.494(2)	Cb Ta(1) N(2)	115.4(2)
Ta(1) C(2)	2.497(2)	Cb Ta(1) N(3)	116.7(2)

Cb = centroid of the η^5 -coordinated C₂B₃ ring.

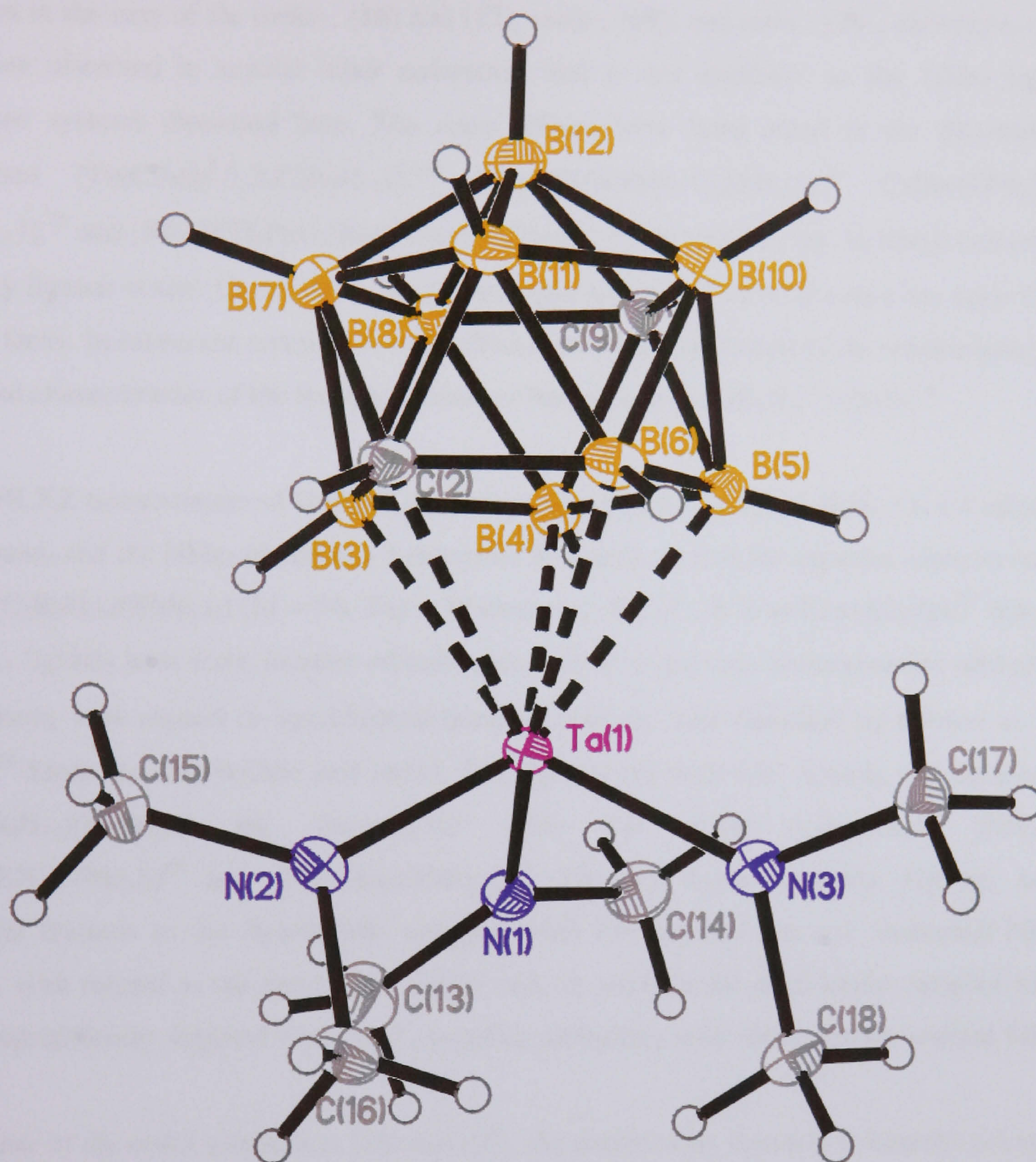


Figure 3.11 Molecular structure of the *para*-metallacarborane [2-Ta(NMe₂)₃(η⁵-1,12-C₂B₉H₁₁)], (20) in 50% displacement ellipsoids.
NB Crystallographic numbering Scheme differs from IUPAC nomenclature.

3.2.2 Π Bonding in $[M(\text{nido-C}_2\text{B}_9\text{H}_{11})(\text{NMe}_2)_3]$ Complexes

The distinctive *trans* influence exerted by the dicarbollide cage on the unique NMe_2 group observed in the case of the *ortho*-, (16) and (17), *meta*-, (19), and *para*-, (20), derivatives, has also been observed in several other complexes and is not exclusive to the NMe_2 ligand carborane systems discussed here. The same effects have been noted in the dicarbollide complexes $[\text{Ta}(\text{Cl})_3(\eta^5\text{-1,2-C}_2\text{B}_9\text{H}_{11})]$,^{14d} $[\text{Mn}(\text{CO})_3\{\text{SMe}_2\text{-C}_2\text{B}_9\text{H}_{10}\}]$,⁷⁴ $\text{Cs}[\text{Re}(\text{CO})_3\{\eta^5\text{-C}_2\text{B}_9\text{H}_{11}\}]$,⁷⁵ and $[\text{NEt}_3(\text{CH}_2\text{Ph})]_2[\text{Re}(\text{CO})_3\{\eta^5\text{-CB}_{10}\text{H}_{11}\}]$ ⁷⁶ in chapter one, in which one of the ancillary ligands (either Cl or CO) is positioned *trans* to the C-C or C in either the open C_2B_3 or CB_4 faces. In carborane complexes such effects have been attributed to the relative energies and lobar characteristics of the frontier orbitals of the respective $\text{C}_2\text{B}_9\text{H}_{11}^{2-}$ anions.⁷⁴

In the MLXZ nomenclature of Green,¹⁵ the neutral dicarbollide ligand ($\text{C}_2\text{B}_9\text{H}_{11}$) is a 4 electron LX_2 ligand, and the NMe_2 ligand is a 3 electron LX ligand, so that the apparent electron count for $[\text{M}(\text{C}_2\text{B}_9\text{H}_{11})(\text{NMe}_2)_3]$ ($\text{M} = \text{Nb, Ta}$) is 18 electrons, ML_4X_5 . It is well established⁷⁷ that the $\text{C}_2\text{B}_9\text{H}_{11}$ ligands have three frontier orbitals each, one of σ and two nondegenerate orbitals of π -symmetry with respect to ligand-metal bonding, and are thus classified by Gibson as Π'_2 ligand.⁷⁸ Since the dicarbollide and imido, RN, ligands are both LX_2 ligands, the complexes $[\text{M}(\text{C}_2\text{B}_9\text{H}_{11})(\text{NMe}_2)_3]$ are iso-numeral with the imido complexes $[\text{Nb}(\text{2,6-}^i\text{Pr}_2\text{C}_6\text{H}_3\text{N})(\text{NMe}_2)_3]$ ⁶⁹ and $[\text{Ta}(\text{N}^t\text{Bu})(\text{NMe}_2)_3]$.⁷⁹ The aryl imido complex has the same structural features as the dicarbollide complex, with two vertical and one horizontal NMe_2 ligands, with respect to the metal axial ligand axis, in contrast the alkyl imido complex has a crystallographically imposed three-fold propeller geometry, with three almost vertical NMe_2 ligands.

In the case of the *ortho* complexes, (16) and (17), the dicarbollide ligand is orientated to ensure that the more electronegative carbon atoms, and by inference the weaker donor atoms of the *nido*- $\text{C}_2\text{B}_9\text{H}_{11}$ ligand, are *trans* to the unique NMe_2 ligand. In $[\text{Nb}(\text{2,6-}^i\text{Pr}_2\text{C}_6\text{H}_3\text{N})(\text{NMe}_2)_3]$, the imido ligand is arranged with the phenyl ring coplanar with the plane defined by the $\text{N}_{\text{unique}}\text{-Ta-}\text{N}_{\text{imido}}$ atoms.

In contrast, the alkyl imido ligand has a higher symmetry than that of the aryl imido ligand, and is therefore classified as a Π_2 ligand, i.e., the two π -orbitals are degenerate. Complexes of the alkyl imido ligand show no evidence of a *trans* influence being exerted on the NMe_2 groups. Therefore it could be hypothesised that the effects observed in the Π'_2 ligands, i.e., a *trans* influence, have their origin in the non-degeneracy of the π -orbitals.

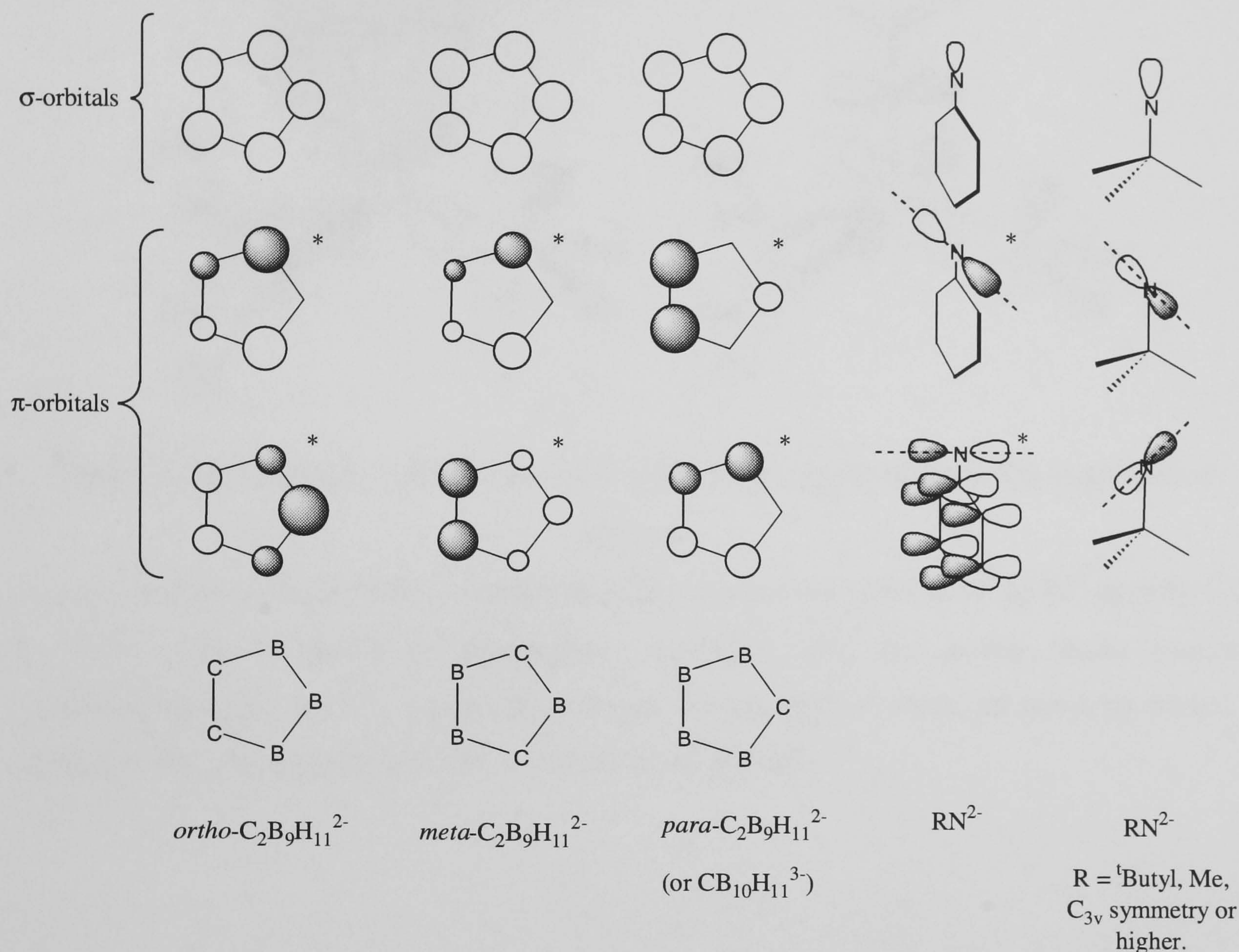


Figure 3.12 Pictographic representation of the σ and π orbitals of the *ortho*-, *meta*- and *para*- $\text{C}_2\text{B}_9\text{H}_{11}^{2-}$ anions and the imide ions $[\text{PhN}]^{2-}$ and $[\text{tBuN}]^{2-}$ that can interact with metal orbitals on an early transition metal fragment (those orbitals marked with an asterisk, *, are non degenerate i.e. if the fragment possess an overall symmetry lower than C_3 the two π -orbitals lose their degeneracy).

Preliminary MO calculations, performed by Drs. A. K. Hughes and M. A. Fox, reveal the possibility of a “through metal” interaction between a nitrogen based π orbital on the aryl imido ligand with the nitrogen lone pair on the unique NMe_2 ligand, and a “through metal interaction” of a C-C based orbital on the *ortho*- $\text{C}_2\text{B}_9\text{H}_{11}^{2-}$ cage with the nitrogen lone pair on the unique NMe_2 ligand. Although all the orbitals shown in Figure 3.12 will be involved to a greater or lesser extent in bonding to the metal atom, it can be suggested that occupied orbitals that are already involved in metal ligand bonding, lying on or over the carbon atoms of the dicarbollide ligands, and in the case of the aryl-imido, the p-orbital that has no interaction with

the π -arene system, will be more likely to form “through metal” 3 centre 4 electron bonds such as those shown in Figure 3.13.

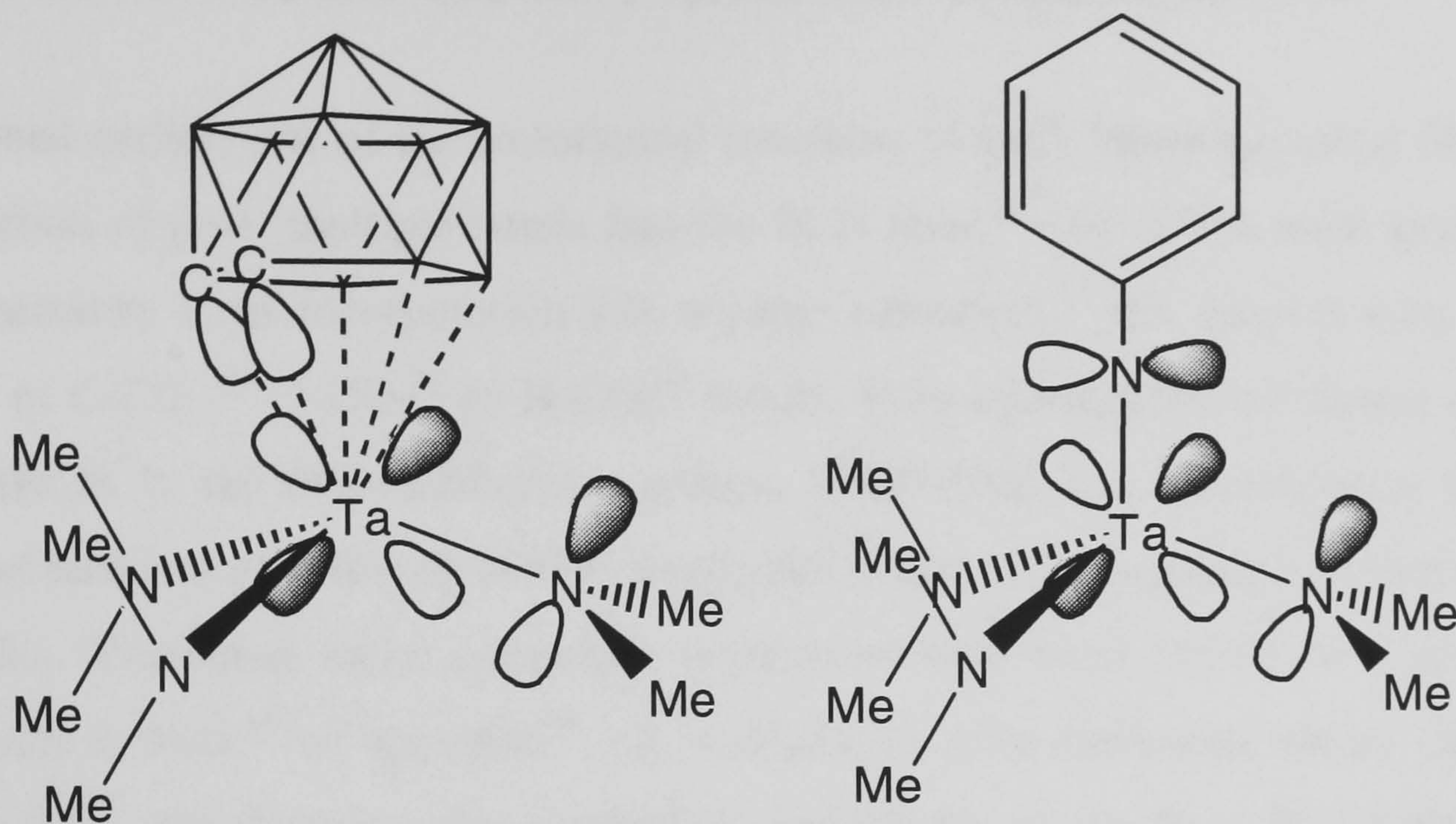


Figure 3.13 Suggested 3 centre 4 electron bonds in Π'_2 ligand systems that exert a *trans*-influence.

Such a hypothesis can be used to explain both the orientational effects of the Π'^2 ligands,⁷⁸ the so called *trans* influence in dicarbollide chemistry, and the shorter bonds observed crystallographically for the unique M-N bond. Computational work on these structures is ongoing and no firm conclusions have been reached thus far.

3.3 Reactions of Group 5 Metallocarborane *Tris*-Amide complexes

3.3.1 Insertion of CO₂ and CS₂ into [M(C₂B₉H₁₁)(NMe₂)₃] Complexes

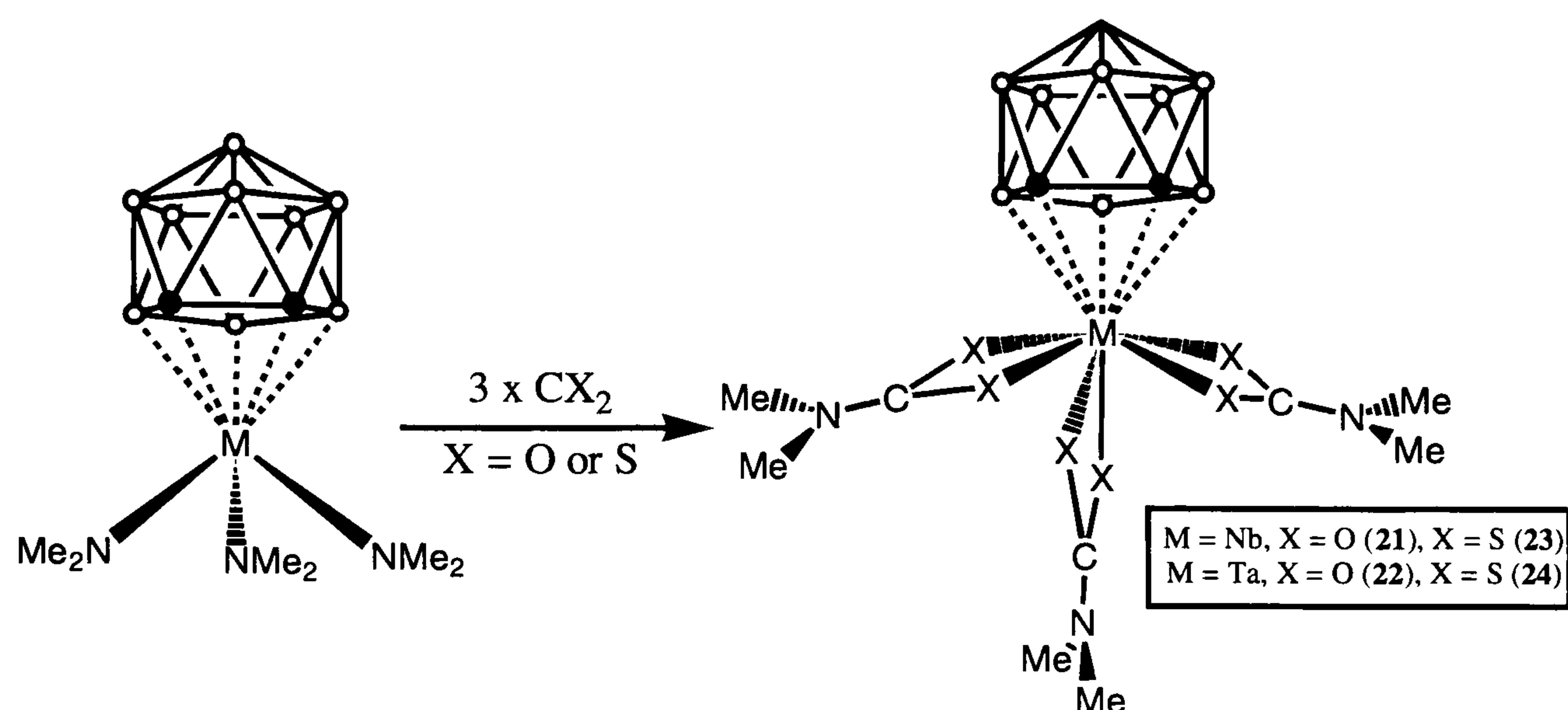
As mentioned earlier, one of the prototypical reactions of early transition metal M-NR₂ bonds is the insertion of polar multiple bonds into the M-N bond.⁸⁰ One of the main goals in carbon dioxide chemistry is its incorporation into organic substrates,⁸¹ this process may involve the formation of C-CO₂,⁸² O-CO₂⁸³ or N-CO₂⁸⁴ bonds. Prior coordination of carbon dioxide to a metal centre as in the diacylcarbamato groups, [M(O₂CNR₂)_n]_m accomplishes the two-fold objective of stabilising carbon dioxide as an oxygen donor and promoting its reactivity towards electrophiles. Transition metal carbamato complexes have been shown to react with alkyl halides, such as MeI,⁸⁵ or epoxides,⁸⁶ e.g. C₆H₁₀O, to form carbamate esters and with acyl halides to form mixed carboxylato-carbamato anhydrides of the form R''C(O)O(O)CNR'₂,⁸⁷ although a range of activity is observed depending on the metal centre and coordination number.

Complexes containing both the carbamate, [O₂CNR₂]⁻, and dithiocarbamate [S₂CNR₂]⁻ ligands can be formed by direct insertion of either CO₂ or CS₂^{84b-c} respectively into a metal amide, M-N, bond, by reacting a metal salt such as Li[O₂CNR₂] with a transition metal halide,⁸⁸ or in a *in-situ* reaction at room temperature between a metal halide and an excess of amine and carbon dioxide.⁸⁹

The *ortho*-dicarbollide amide complexes [M(1,2-C₂B₉H₁₁)(NMe₂)₃] react with CO₂ and CS₂ to give the carbamate [M(C₂B₉H₁₁)(O₂C-NMe₂)₃] (M = Nb (**21**), Ta (**22**)) and dithiocarbamate [M(C₂B₉H₁₁)(S₂C-NMe₂)₃] (M = Nb (**23**), Ta (**24**)) complexes respectively. All the complexes have been characterised by multinuclear NMR (¹H, ¹³C and ¹¹B) and IR spectroscopy. The structures of (**22**) and (**23**) have been determined by single-crystal X-ray diffraction.

The ¹¹B NMR spectra of complexes (**21**)-(**24**) display resonances characteristic of a *closo*-[C₂B₉H₁₁)M] unit. The ¹³C spectra of (**21**)-(**24**) display two resonances for the (thio)carbamate carbon atom (X₂CNMe₂) in an approximate intensity ratio of 2:1, which is consistent with a static system as shown in Scheme 3.6, in which there would be two inequivalent ligand environments. Both ¹H and ¹³C spectra of (**21**)-(**24**) each display a total of 4 closely spaced NMe resonances in a 2:2:1:1 ratio indicating four different environments for NMe₂ methyl groups, although in some of spectra the resonances are overlapped. These spectroscopic results

are consistent with the presence of "vertical" and "horizontal" X_2C-NMe_2 ligands in these complexes.



Scheme 3.6 Synthesis of the carbamate and dithiocarbamate complexes (21)-(24).

Crystals of (22) and (23) suitable for characterisation by single crystal X-ray diffraction were grown from a saturated benzene solution layered with pentane, and a saturated CD_2Cl_2 solution respectively. The molecular structures of the tantalum carbamate complex $[Ta(C_2B_9H_{11})(O_2C-NMe_2)_3]$ (22) (Figure 3.14 and Table 3.4) and the niobium dithiocarbamate complex $[Nb(nido-C_2B_9H_{11})(S_2C-NMe_2)_3]$ (23) (Figure 3.15 and Table 3.5) bear significant similarities to those of 3 and 4 and to the iso-numeral $M(\eta-C_5H_5)$ complexes $[M(\eta-C_5H_5)(S_2CNMe_2)_3]$ ($M = Ti$,⁹⁰ Zr ⁹¹) and $[M(NR)(S_2CNR'_2)_3]$ ($M = Ta$ and Nb ⁹² or V ⁹³). Each carbamate or dithiocarbamate ligand is essentially planar and co-ordinated in a bidentate fashion, with slightly asymmetric Nb-S and Ta-O distances. In both structures, the carbon atom positions in the dicarbollide cage are clearly identified, with the C_2B_3 ring and the O_5 or S_5 rings of the equatorial chalcogen atoms staggered with respect to each other. In both cases the C-C bond lies directly over the bond M-X(6), but not symmetrically.

In compound (22), the carbamate ligand containing N(1) adopts a vertical orientation, that is to say that the angle between the two planes (A) and (B), where (A) is defined by the three points C_2B_3 centroid, Ta(1) and N(1) and plane (B) is defined by the points Ta(1), O(1), C(13) and O(2) is $\tau=178.9^\circ$ and those planes containing N(2) and N(3) i.e. (C) ($Ta(1)-O(3)-C(16)-O(4)$) and (D) ($Ta(1)-O(5)-C(19)-O(6)$) are close to horizontal ($\tau=72.2^\circ$ and -70.5° , respectively). The vertical carbamate ligand lies in a position *trans* to C(3), the C(13)-Ta(1)-Cb-C(3) torsion angle being -177.8° . This means that the molecule has a local mirror symmetry, violated only by the non-equivalence of C(2) and B(4). Alternatively the molecule can be described as having a pentagonal bipyramid geometry, with five of the carbamate oxygen atoms defining the plane and the axial positions occupied by the six carbamate oxygen atom and the

dicarbollide centroid. The Ta-O bonds to the vertical carbamate ligand are on average 0.04 Å shorter than to the horizontal ones, notwithstanding the more sterically hindered position of the former (evident from the angular distortions).

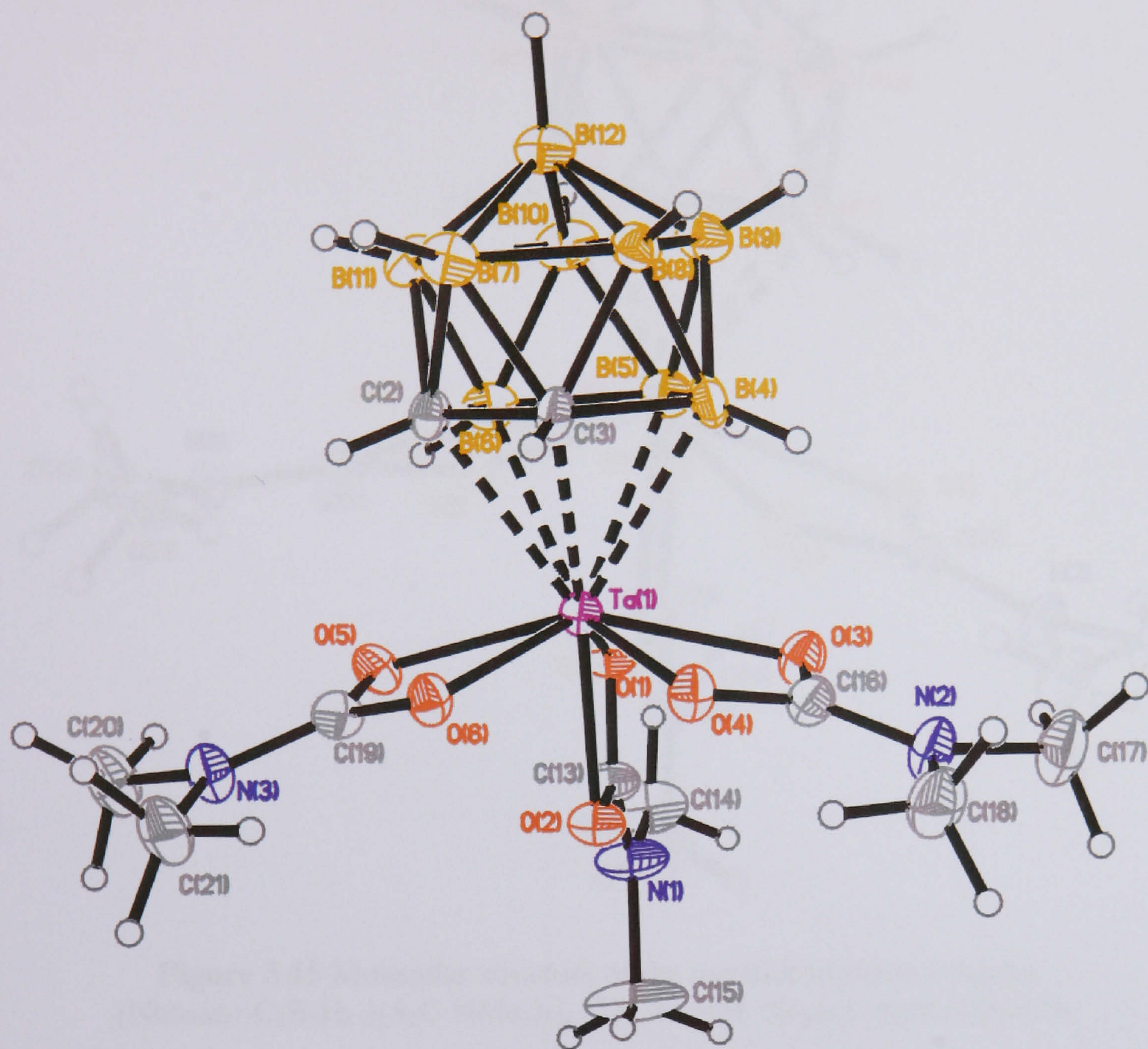


Figure 3.14 Molecular structure of the metallocarborane complex [Ta(*nido*-C₂B₉H₁₁)(O₂C-NMe₂)₃], (**22**), in 50% displacement ellipsoids.

Table 3.4 Selected bond lengths (Å) and angles (°) in (**22**).

Ta-O(1)	2.091(3)	O(1)-C(13)	1.292(6)
Ta-O(2)	2.156(4)	O(2)-C(13)	1.294(6)
Ta-O(3)	2.205(3)	O(3)-C(16)	1.280(6)
Ta-O(4)	2.106(3)	O(4)-C(16)	1.292(6)
Ta-O(5)	2.208(3)	O(5)-C(19)	1.282(6)
Ta-O(6)	2.121(3)	O(6)-C(19)	1.296(6)
Ta-C(2)	2.462(5)	C(2)-C(3)	1.590(6)
Ta-C(3)	2.486(5)	C(3)-B(4)	1.676(7)
Ta-B(4)	2.519(6)	B(4)-B(5)	1.780(9)
Ta-B(5)	2.508(6)	B(5)-B(6)	1.768(8)
Ta-B(6)	2.464(6)	B(6)-C(2)	1.657(7)
Ta-Cb	2.028(6)		
Cb-Ta···C(13)	140.2(4)	C(13)···Ta···C(16)	88.9(2)
Cb-Ta···C(16)	108.0(4)	C(13)···Ta···C(19)	89.3(2)
Cb-Ta···C(19)	107.7(4)	C(16)···Ta···C(19)	125.0(2)

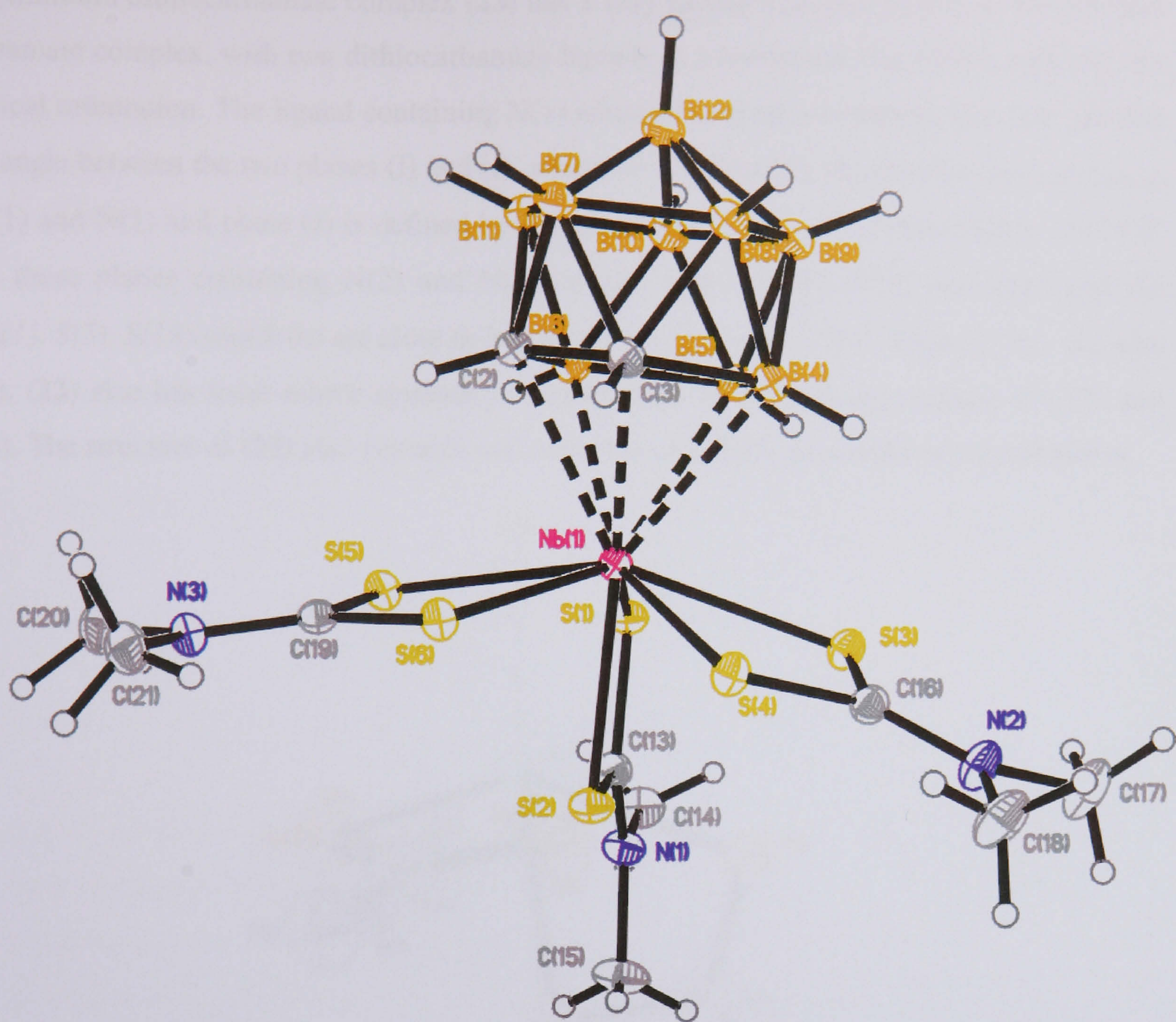


Figure 3.15 Molecular structure of the metallocarborane complex $[\text{Nb}(\text{nido-C}_2\text{B}_9\text{H}_{11})(\text{S}_2\text{C-NMe}_2)_3]$, (**23**), in 50% displacement ellipsoids.

Table 3.5 Selected bond lengths (Å) and angles (°) in (**23**).

Nb-S(1)	2.5734(8)	S(1)-C(13)	1.7126(16)
Nb-S(2)	2.6087(8)	S(2)-C(13)	1.7126(16)
Nb-S(3)	2.6287(8)	S(3)-C(16)	1.7035(16)
Nb-S(4)	2.6119(7)	S(4)-C(16)	1.7237(16)
Nb-S(5)	2.6423(9)	S(5)-C(19)	1.7087(16)
Nb-S(6)	2.6149(8)	S(6)-C(19)	1.7240(16)
Nb-C(2)	2.4841(16)	C(2)-C(3)	1.584(2)
Nb-C(3)	2.5137(16)	C(3)-B(4)	1.674(2)
Nb-B(4)	2.5438(17)	B(4)-B(5)	1.784(2)
Nb-B(5)	2.5674(17)	B(5)-B(6)	1.777(2)
Nb-B(6)	2.5058(17)	B(6)-C(2)	1.685(2)
Nb-Cb	2.067(4)		
Cb-Nb···C(13)	137.1(4)	C(13)···Nb···C(16)	86.5(2)
Cb-Nb···C(16)	108.7(4)	C(13)···Nb···C(19)	91.7(2)
Cb-Nb···C(19)	107.4(4)	C(16)···Nb···C(19)	127.9(2)

The niobium dithiocarbamate complex (**23**) has a very similar structure to that of the tantalum carbamate complex, with two dithiocarbamate ligands in a horizontal orientation, and one in a vertical orientation. The ligand containing N(1) adopts a vertical orientation, that is to say that the angle between the two planes (I) and (J), where (I) is defined by the three points C_2B_3 centroid, Nb(1) and N(1) and plane (J) is defined by the points Nb(1), S(1), C(13) and S(2) is $\tau=174.8^\circ$ and those planes containing N(2) and N(3) i.e. (K) (Nb(1), S(3), S(16) and S(4)) and (L) (Nb(1), S(5), S(19) and S(6)) are close to horizontal ($\tau=73.7^\circ$ and -75.1° , respectively). As with (**22**), (**23**) also has local mirror symmetry, violated only by the non-equivalence of C(2) and B(4). The structure of (**23**) also contains one molecule of CD_2Cl_2 as solvent of crystallisation.

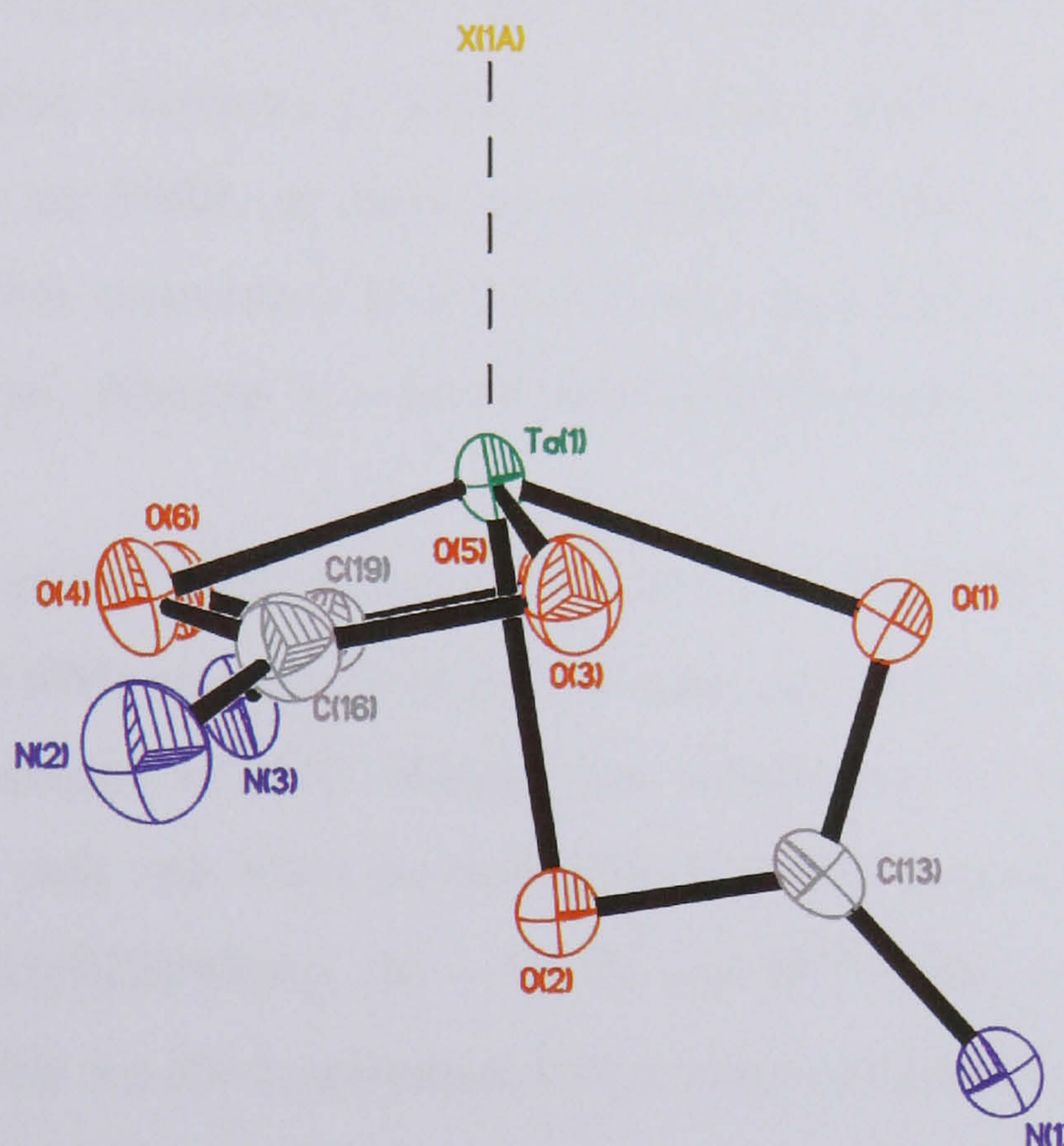


Figure 3.16 View of the X1a-Ta1-N1 plane in the molecule (**22**). X1a represents the C_2B_3 face centroid. The diagram clearly shows the obtuse angle between O2-Ta1-X1a (methyl groups and cage atoms have been removed for clarity).

The five equatorial atoms O(1), O(3), O(4), O(5) and O(6) in (**22**) and S(1), S(3), S(4), S(5) and S(6) in (**23**) are coplanar to within 0.043\AA and 0.058\AA respectively. In both cases the metal atom sits above the five membered rings by $0.592(2)\text{\AA}$ in (**22**) and $0.688(2)\text{\AA}$ in (**23**). The chief distortions from a *pseudo* pentagonal bipyramidal are due to the displacement of the axial O(2) or S(2) away from a *quasi* five fold axis resulting in a Centroid-M-X(2) angle of 171.1° and 170.4° for (**22**) and (**23**) respectively, as can be seen in Figure 3.16.

It can also be noted from Tables 3.4 and 3.5 that the M-C(2) and M-B(4) (M = Ta and Nb) bond lengths are slightly shorter than M-C(3), M-B(4) and M-B(5), i.e., there is tilting of the cage away from the carbamate and dithiocarbamate ligands containing N(2), thus making the two planes defined by the C_2B_3 face and the X_5 ring no longer parallel. This distortion is more

pronounced in the dithiocarbamate complex (**23**) with an angle between the two planes of 3.8° , compared to an angle of 1.3° in the carbamate complex (**22**). The tilting is possibly a mechanism to reduce undesirable atom-atom interactions between the B-Hs of the cage and the electron rich chalcogen atoms of the (dithio)carbamate ligands, with the differences between the two tilting angles due to the much larger size of sulfur compared to oxygen. It is noteworthy, however, that although the tilt angle between the two planes are somewhat different, the metal-cage centroid distances in the two complexes are fairly consistent i.e. 2.028\AA (**22**) and 2.067\AA (**23**).

Complexes such as $[\text{Ti}(\text{S}_2\text{CNMe}_2)_3\text{Cl}]^{94}$ and $[\text{Nb}(\text{NNMe}_2)(\text{S}_2\text{CNMe}_2)_3]^{92\text{a}}$ have previously been shown to be highly fluxional at room temperature, showing only one dithiocarbamate ligand environment in the NMR. At room temperature the complexes (**21**)-(**24**) exhibit a total of 4 closely spaced NMe resonances in a 2:2:1:1 ratio indicating four different environments for NMe₂ methyl groups, although in some of spectra the resonances are overlapped.

Variable temperature studies have shown that at 30°C the ^1H NMR spectra for complex (**22**) changes, resulting in 3 NMe resonances in a 1:1:4 ratio, and only two NMe environments when the temperature is increased to 45°C . Raising the temperature of the sample to above 60°C causes coalescence to only one NMe environment. Variable temperature NMR studies of the complexes $[\text{M}(\eta\text{-C}_5\text{H}_5)(\text{S}_2\text{CNMe}_2)_3]$ ($\text{M} = \text{Ti}, \text{Zr}$ and Hf)⁹⁵ have revealed that three kinetic processes are responsible for the coalescence into a single resonance of the ^1H MNR spectra in these pentagonal bipyramidal complexes.

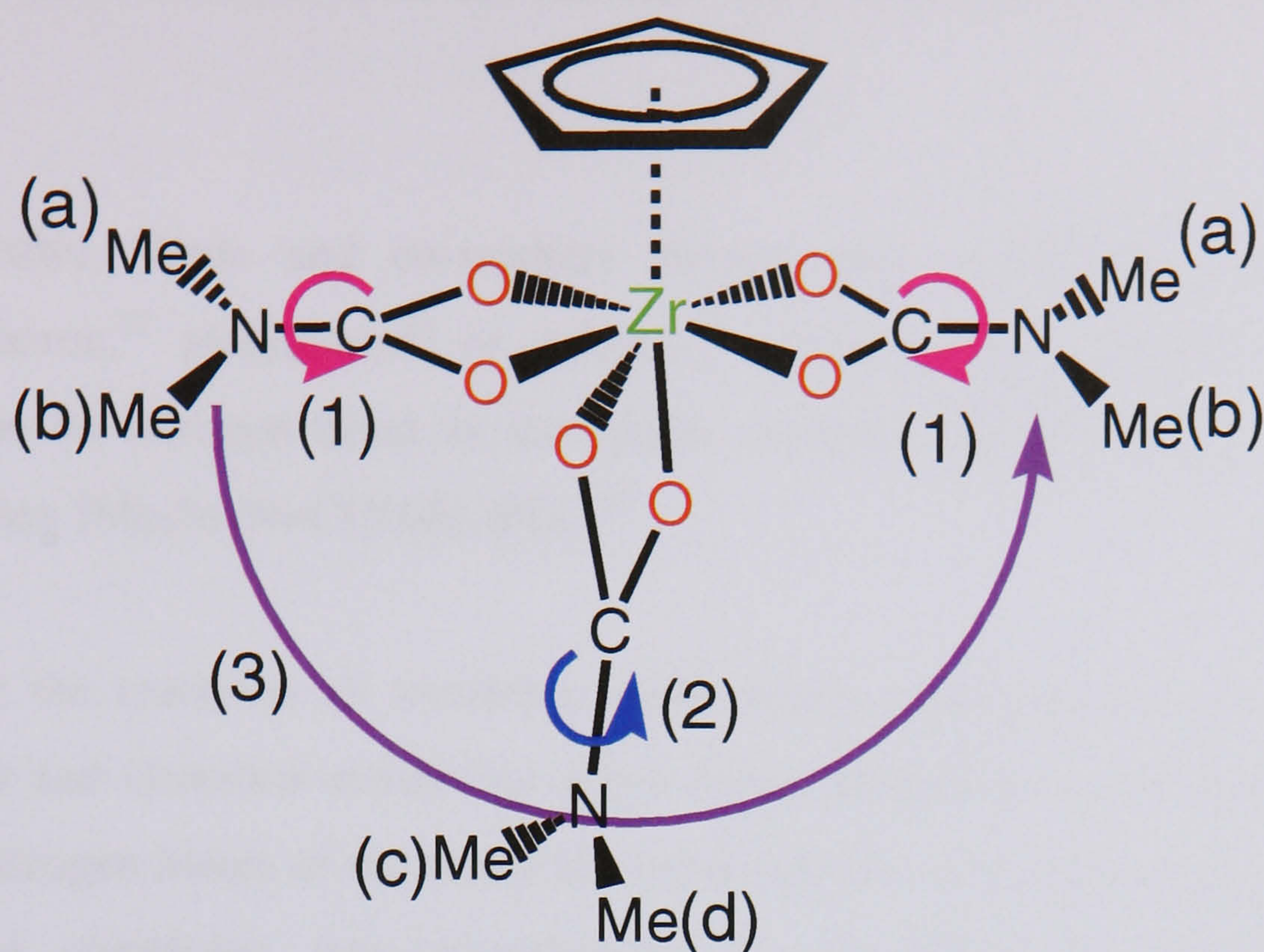


Figure 3.17 Diagram showing the four different methyl groups in the complex $[\text{Zr}(\text{C}_5\text{H}_5)(\text{O}_2\text{C-NMe}_2)_3]$. Process (1), (2) and (3) represent modes by which methyl groups can exchange. See text.

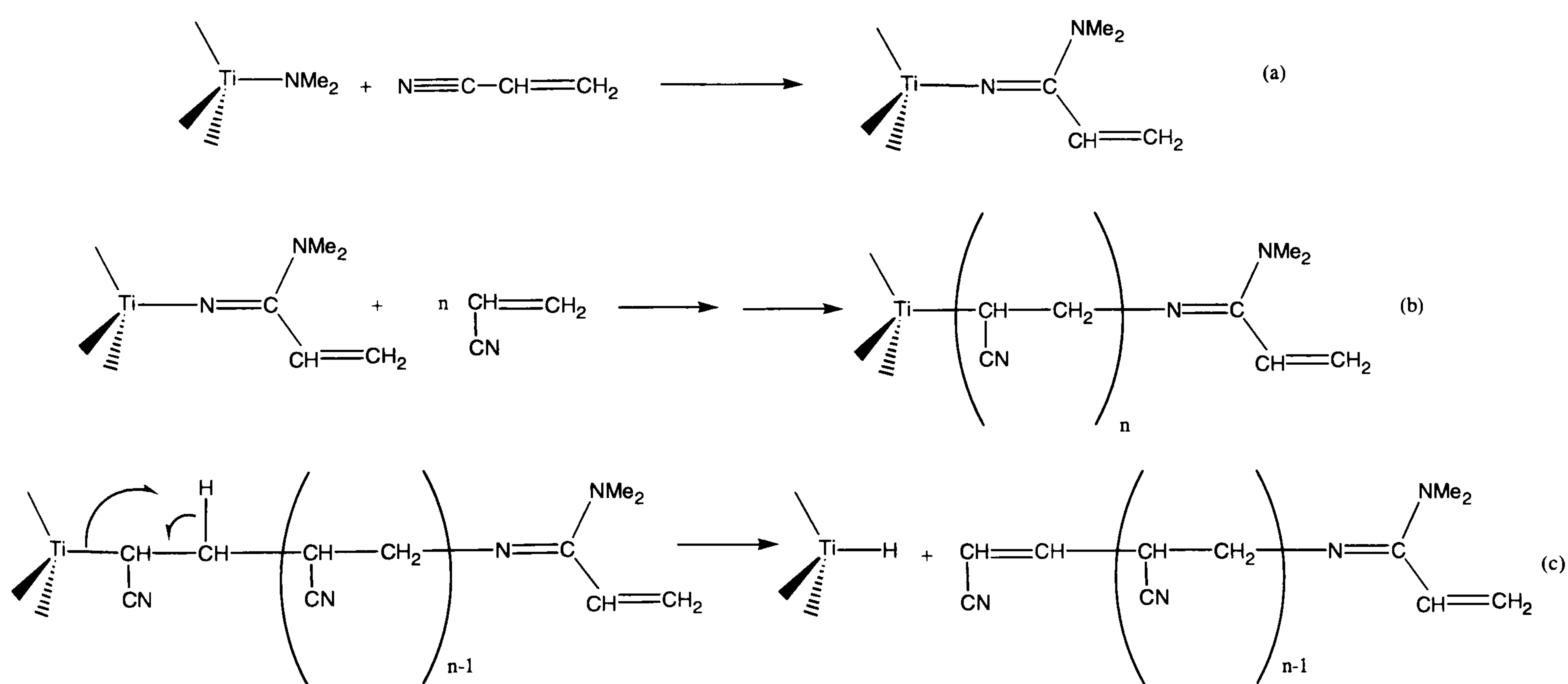
The first process (1) is a low temperature process by which the methyl groups (a) and (b) of the equatorial ligands exchange by rotation around the N-C bonds in the (dithio)carbamate ligands (see Figure 3.17). Process (2) involves rotation around the N-C bond in the unique (dithio)carbamate ligand rendering the methyl environments (c) and (d) equivalent. The third process (3) involves a metal centred rearrangement of the three (dithio)carbamate ligands and is a higher energy process, resulting in all methyl environments becoming equal. Increasing the steric bulk of the Cp, or Cb ligand, increases the energy needed for such processes.⁹⁶

We can therefore envisage similar kinetic processes occurring at the sterically crowded $\text{C}_2\text{B}_9\text{M}(\text{O})_6$ and $\text{C}_2\text{B}_9\text{M}(\text{S})_6$ ($\text{M} = \text{Nb}$ or Ta) metal centres in complexes (21)-(24).

3.3.2 Insertion of Nitriles and Isonitriles into *ortho*-[Ta(*nido*-C₂B₉H₁₁)(NMe₂)₃] Complexes

In 1964, and after, Wade and co-workers showed that acetonitrile inserted into alkyl derivatives of boron,⁹⁷ aluminium⁹⁸ or gallium.⁹⁹ Lappert later showed that benzonitrile inserted into the tin-nitrogen bond in the amide complex [Me₃SnNMe₂], to form the tin amidinate complex [Me₃Sn-N=C(NMe₂)Ph].¹⁰⁰

Whilst studying the reactions of transition metal amide complexes using acetonitrile as a solvent, Bradley and Ganorkar noted that above room temperature acetonitrile was inserting into the metal nitrogen bonds of the transition metal amides. The formation of these transition metal amidinate complexes was accompanied by the formation of *poly*-acetonitrile.⁴¹ Higginson and Wooding had already demonstrated that main group metal amides could initiate the polymerisation of vinyl monomers via an anionic mechanism.¹⁰¹ Observations by Perry suggested that transition metal amides were also possible initiators in the polymerisation of styrene, methylmethacralate and acrylonitriles.¹⁰² Studies followed that demonstrated that both acrylonitrile and methylacrylonitrile undergo rapid polymerisation in the presence of [Ti(NMe₂)₄].¹⁰³ In a series of kinetic and mechanistic studies into the metal amide promoted polymerisation of acrylonitrile,¹⁰⁴ it was hypothesised that the initial step in the polymerisation process, Scheme 3.8 (a), was the initial insertion of the N≡C unit of acrylonitrile into the metal nitrogen bond of the amide complex, thus forming a highly reactive “active site”.^{104a-d}

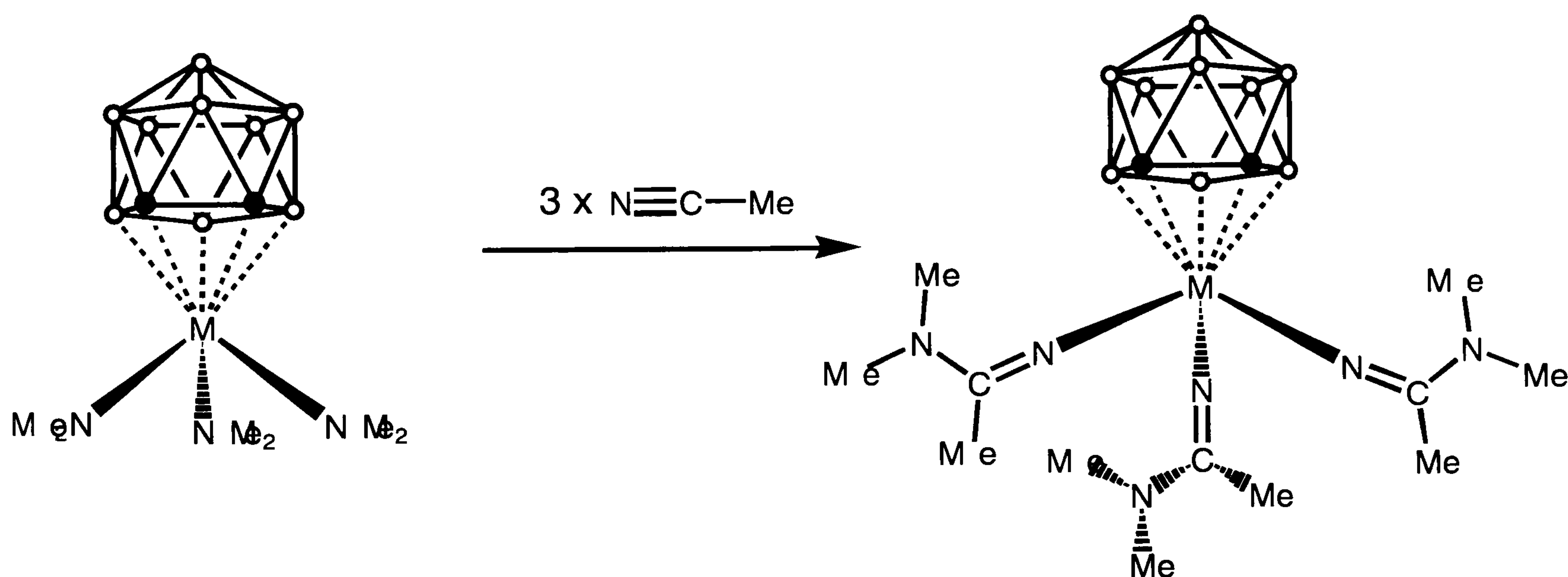


Scheme 3.8 The initiation (a), insertion of the Ti-N into C=C bond (b) and termination (c) steps in the metal amide mediated polymerisation of acrylonitrile.

Evidence for the mechanism shown in Scheme 3.8 is derived from the observation that $[M(NMe_2)_4]$ ($M = Ti, Zr$ or Hf) readily adds across the nitrile groups of benzonitrile or toluonitrile, the addition product being an effective initiator for the polymerisation of acrylonitrile.⁴⁰

Although a large amount of chemistry has centred around metal amide complexes, to the best of our knowledge there are no structurally characterised examples of the amidinide insertion product with a transition metal amide.

Acetonitrile was shown to insert into the metal amide complex *ortho*- $[Ta(NMe_2)_3(\eta^5-C_2B_9H_{11})]$, (**17**), at 130°C in toluene over a period of 2 days. The reaction mixture slowly changes from a pale yellow colour to a deep red. Re-crystallisation of the product from dichloromethane / pentane solutions allowed the isolation of the *tris*-insertion product $Ta(N=C(NMe_2)Me)_3(\eta^5-C_2B_9H_{11})$, (**25**), as a colourless micro-crystalline material in 39% yield. The red coloration is thought to be caused by the formation of *poly*-acetonitrile.

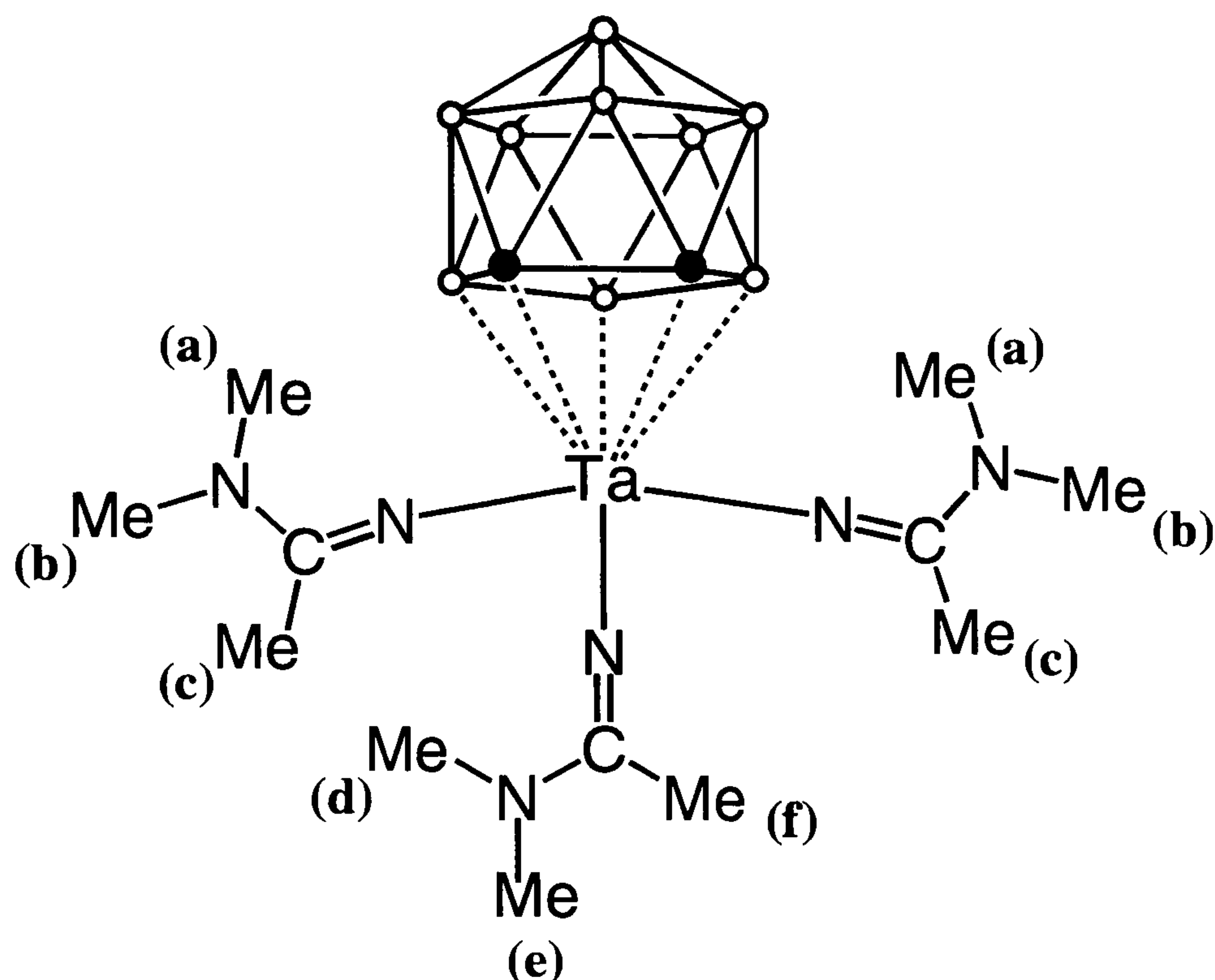


Scheme 3.9 Synthesis of *ortho*- $[Ta(N=C(NMe_2)Me)_3(\eta^5-C_2B_9H_{11})]$, (**25**).

The 1H and ^{13}C NMR spectra of (**25**) show the presence of two different environments for the NMe_2 and Me groups in the ligand, in a 2:1 ratio. The 1H NMR also shows a single broad resonance for the cage C-H hydrogen suggesting the molecule has overall C_s symmetry. The C_s symmetry is confirmed by the observation of 5 B-H resonances in the $^{11}B\{^1H\}$ NMR spectra, with a 1:2:2:3:1 intensity ratio.

Work with the uranium amidinate complexes $[U(COT)(N=C(Me)NEt_2)(THF)_2][BPh_4]$ ¹⁰⁵ and $[U(C_5H_5)_2(N=C(NMe_2)(THF))][BPh_4]$ ¹⁰⁶ have shown the NEt_2 and NMe_2 groups in the respective complexes to be non equivalent. A suggested reason for the in-equivalence is due to

restricted rotation around the C-NR₂ bond in the ligands. In the case of compound (**25**) inequivalence of methyl groups in the ligand is also observed. Both the ¹H and ¹³C NMR spectra of (**25**) show the presence of six different methyl environments in a 2:1:1:2:2:1 intensity ratio (see below). There is thought to be no evidence for the suggestion that the amidinate ligands are bidentate as the steric restrictions around the NMe₂ part of the ligand would make bonding such as this unfavourable.



An analogous reaction was conducted using *p*-flouorobenzonitrile, ($\text{N}\equiv\text{C}-\text{C}_6\text{H}_4-\text{F}$) in the hope that suitable crystals of the tris insertion product could be grown for X-ray diffraction. This was conducted using identical conditions the synthetic procedure for the insertion of acetonitrile. Following re-crystallisation from dichloromethane and pentane colourless crystals were isolated in a 41% yield.

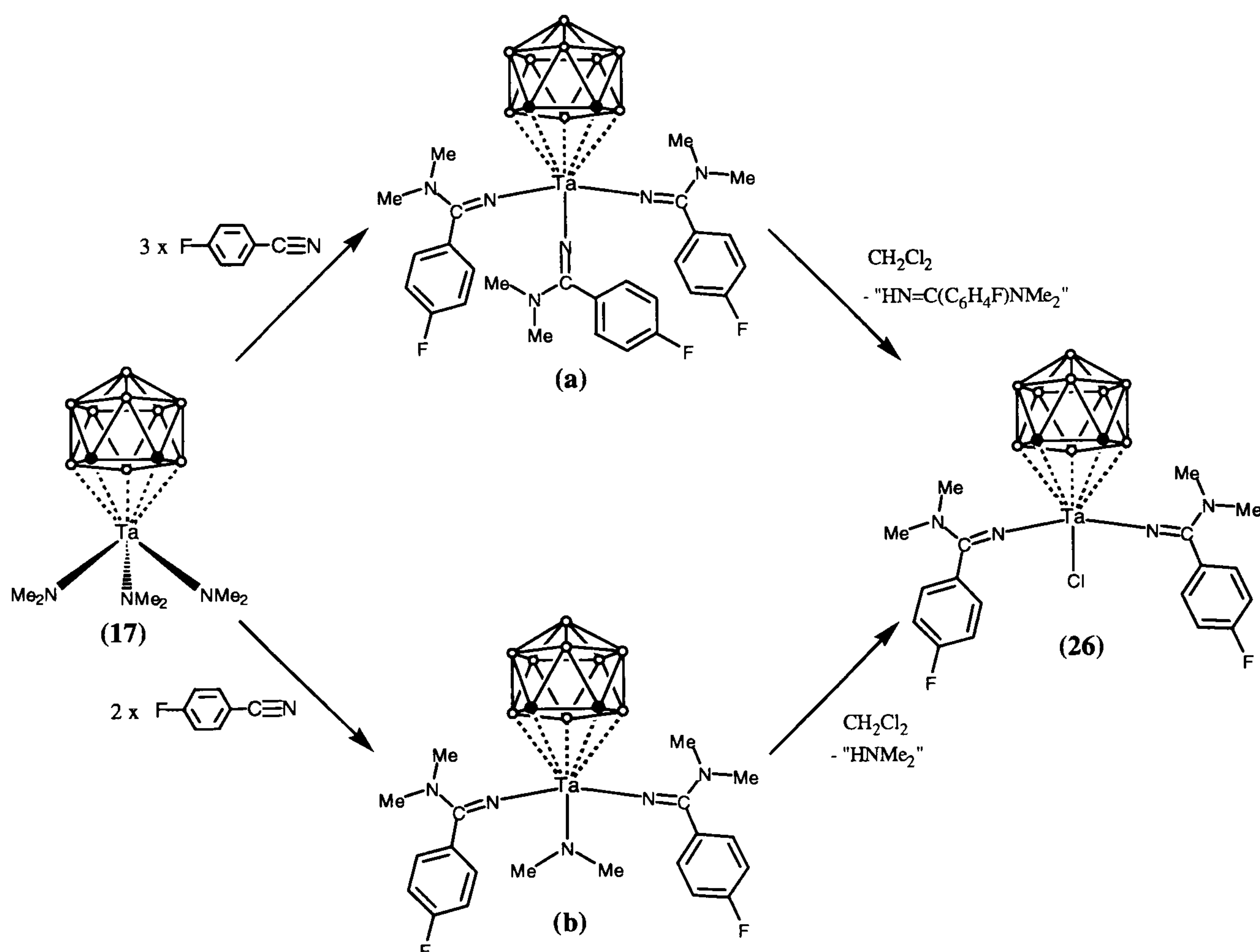
Initial analysis of this compound using ^{11}B NMR suggested an apparent C_s symmetric carborane cage showing in the ^{11}B NMR 5 resonances in a 1:2:3:2:1 intensity ratio. Initial ^1H (300MHz) and ^{13}C (50MHz) NMR spectra led to the assumption that the molecule in solution has molecular C_s symmetry with one peak in both spectra that could be assigned to the cage C-H group. In contrast ^{19}F (188MHz) NMR showed the presence of two ^{19}F environments in a 1:1 intensity ratio very close to each other, which prompted further investigation of this complex using higher field NMR instruments.

Reinvestigation of both the $^1\text{H}\{^{11}\text{B}\}$ and ^{13}C NMR revealed the presence of two cage C-H signals and a total of 8 B-H signals in a 1:1:1:1:2:1:1 ratio. The 9th B-H resonance could not be observed in the $^1\text{H}\{^{11}\text{B}\}$ NMR spectrum, intensity ratios suggest that this signal is hidden under the methyl group signals. The ^1H NMR spectrum also shows 2 broad N-Me resonance

signals, in a 2:2 intensity ratio instead of the expected 1:1:1:1 intensity ratio, which would be consistent with the restricted rotation around the C-NMe₂ bonds.^{107,108} The broadness of these resonances is thought to be due to the coincidental over lapping of two of the four NMe groups. This observation, of two similar ligand environments in a 1:1 ratio, is mirrored for the remaining signals in both the ¹H and ¹³C NMR spectra. The ¹³C NMR spectra showed the presence of 4 signals assigned to the phenyl groups, indicating free rotation about the NC-PhF bond. Assignment of specific resonances in the ¹³C spectra was made on comparison of the C-F coupling constants in the starting nitrile, *p*-fluorobenzonitrile, to those in the complex (26).

X-ray crystal structure analysis showed that unlike the acetonitrile insertion product, the isolated product from this reaction is the doubly inserted complex [Ta(N=C(C₆H₄F)(NMe₂))₂Cl(η⁵-C₂B₉H₁₁)], (26), Scheme 3.10.

It is not clear if the *tris*- insertion product, (a) is formed and then undergoes a reaction with dichloromethane to form the chloride complex, (26), or if the *bis*-amidate amide complex, (b) shown in Scheme 3.10 is formed initially then the amide ligand reacts with dichloromethane to form the product (26).



Scheme 3.10 Two possible routes to the formation of the dicarbollide complex [Ta(N=C(C₆H₄F)(NMe₂))₂Cl(η⁵-C₂B₉H₁₁)], (26).

The precise mechanism of the reaction with dichloromethane is unclear but the metal amide complex has the potential to react in several ways. Of those, the most likely reaction is dehydrochlorination.^{18b} The dehydrochlorination reaction has been observed in other areas of metal amide chemistry, an example of which is shown in Scheme 3.3,⁶⁴ and the general form of the equation is shown below.



The effectiveness of a complex to be a dehydrochlorinating reagent is attributed to the complexes high basicity and the highly polar nature of the M-N bond,¹⁰⁷ both of which we can envisage as attributes of the intermediate, (a) or (b), in Scheme 3.10. The dehydrochlorination of organic halide complexes has been well established by Lappert and co-workers in the case of tin amide complexes,¹⁰⁸ and only one report of a transition metal amide complex reacting with dichloromethane to form metal chlorides has been reported to the best of our knowledge.⁶⁴ The equation shown above may not show the exact stoichiometry or complexity of the reaction but the product (**26**) is produced in moderate yield implying the formation of a stable by-product, this implies that the leaving group B is unlikely to be the reactive carbene “C(H)Cl”, and more likely to be a chlorinated hydrocarbon such as Cl(H)C=C(H)Cl.

The solid state structure of (**26**) is comprised of one molecule of the tantalum complex [Ta(N=C(C₆H₄F)(NMe₂))₂Cl(C₂B₉H₁₁)] and two independent molecules of dichloromethane. Each amidinate ligand is coordinated to the tantalum in a mono-dentate fashion, with slightly different Ta-N bond distances i.e. Ta(1)-N(3) = 1.859(3) and Ta(1)-N(1) = 1.870(3), both of which are shorter than the Ta-N bond distances found in the *tris* amide complex (**17**). The shortening of the Ta(1)-N(3) bond is offset by the increase in the angle between the Cb_{centroid}-Ta(1)-N(3) = 123.5(2)°, the angle subtended by the second amidinide ligand being only 116.7°. The carbon atom positions in the dicarbollide cage are clearly identified, with the Ta-Cl bond lying directly beneath the cage carbon atom C(7). The Ta-Cl bond in (**26**) is 2.3975(10)Å with a Cb_{centroid}-Ta-Cl angle of 112.2°. In comparison to the Ta-Cl bond lengths in Jordan’s tri-chloro tantalum complex (average Ta-Cl bond length = 2.288(5)Å) the Ta-Cl bond length in (**26**) is ≈ 5% longer.^{17a} The much smaller angle and the longer bond length for the Ta-Cl are likely to be consequences of both the steric bulk of the two amidinate ligands, i.e., the chlorine atom is moved away to reduce the steric crowding of the Ta atom, and a reduction in the Lewis acidity of the Ta atom.

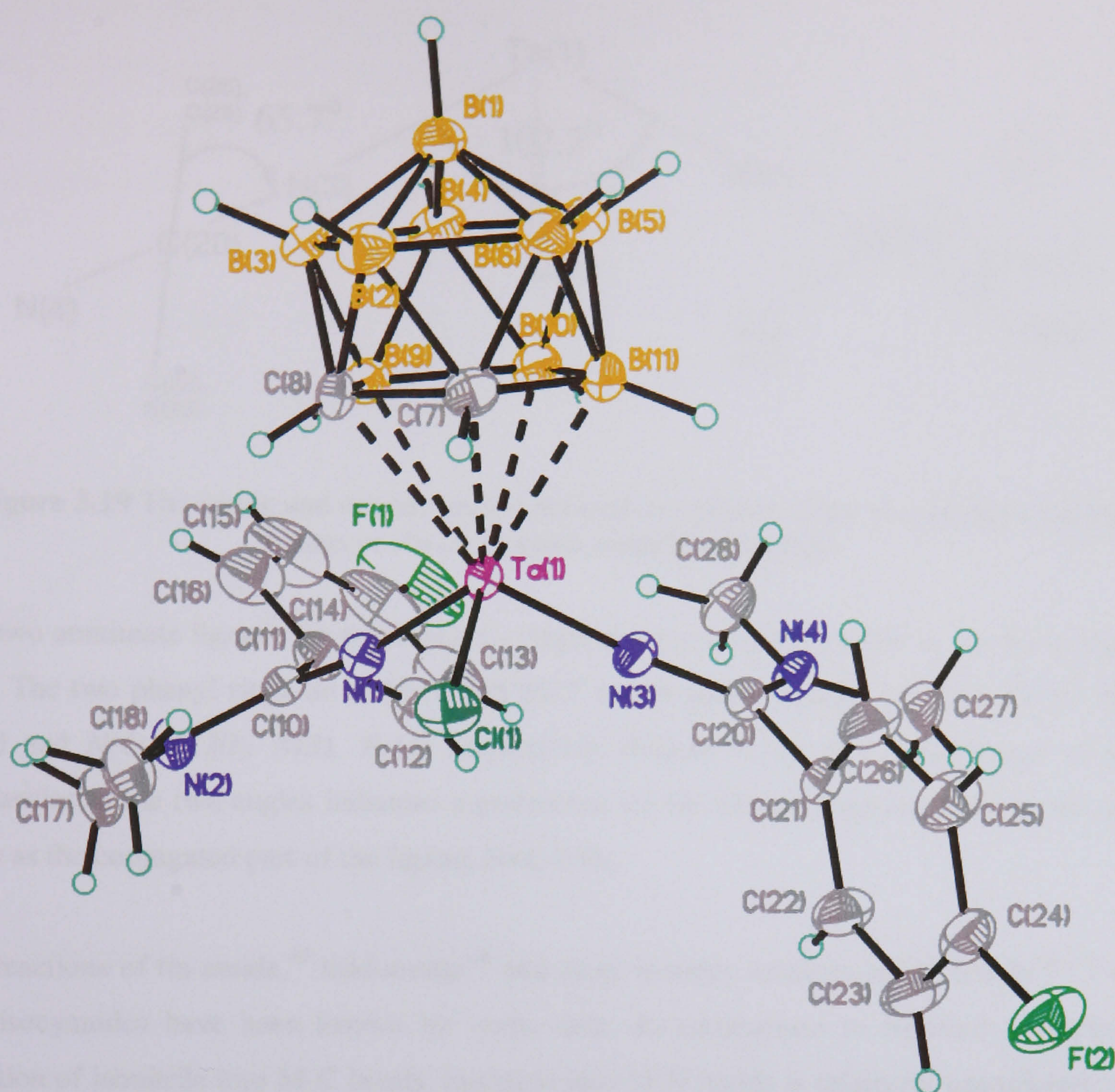


Figure 3.18 Molecular structure of the metallacarborane complex [Ta(N=C(C₆H₄F)(NMe₂))₂Cl(η⁵-C₂B₉H₁₁)], (**26**), in 50% displacement ellipsoids.

Table 3.6 Selected bond lengths (Å) and angles (°) in (**26**).

Ta(1)-N(1)	1.870(3)	Cb-Ta(1)-N(1)	116.7(3)	N(1)-C(10)	1.297(5)
Ta(1)-N(3)	1.859(3)	Cb-Ta(1)-N(3)	123.5(2)	C(10)-N(2)	1.337(5)
Ta(1)-Cl(1)	2.3975(10)	Cb-Ta(1)-Cl(1)	112.2(1)	C(10)-C(11)	1.493(5)
				C(14)-F(1)	1.352(6)
Ta(1)-C(7)	2.479(4)				
Ta(1)-C(8)	2.501(3)	N(3)-Ta(1)-N(1)	102.25(14)	N(3)-C(20)	1.304(4)
Ta(1)-B(9)	2.499(4)	N(3)-Ta(1)-Cl(1)	99.38(10)	C(20)-N(4)	1.328(5)
Ta(1)-B(10)	2.461(4)	N(1)-Ta(1)-Cl(1)	98.91(10)	C(20)-C(21)	1.498(5)
Ta(1)-B(11)	2.462(4)			C(24)-F(2)	1.360(5)
		N(1)-C(10)-N(2)	122.3(3)		
Ta(1)-Cb	2.018(5)	N(1)-C(10)-C(11)	118.5(3)	N(3)-C(20)-N(4)	123.3(3)
		N(2)-C(10)-C(11)	119.3(3)	N(3)-C(20)-C(21)	117.4(3)
				N(4)-C(20)-C(21)	119.4(3)

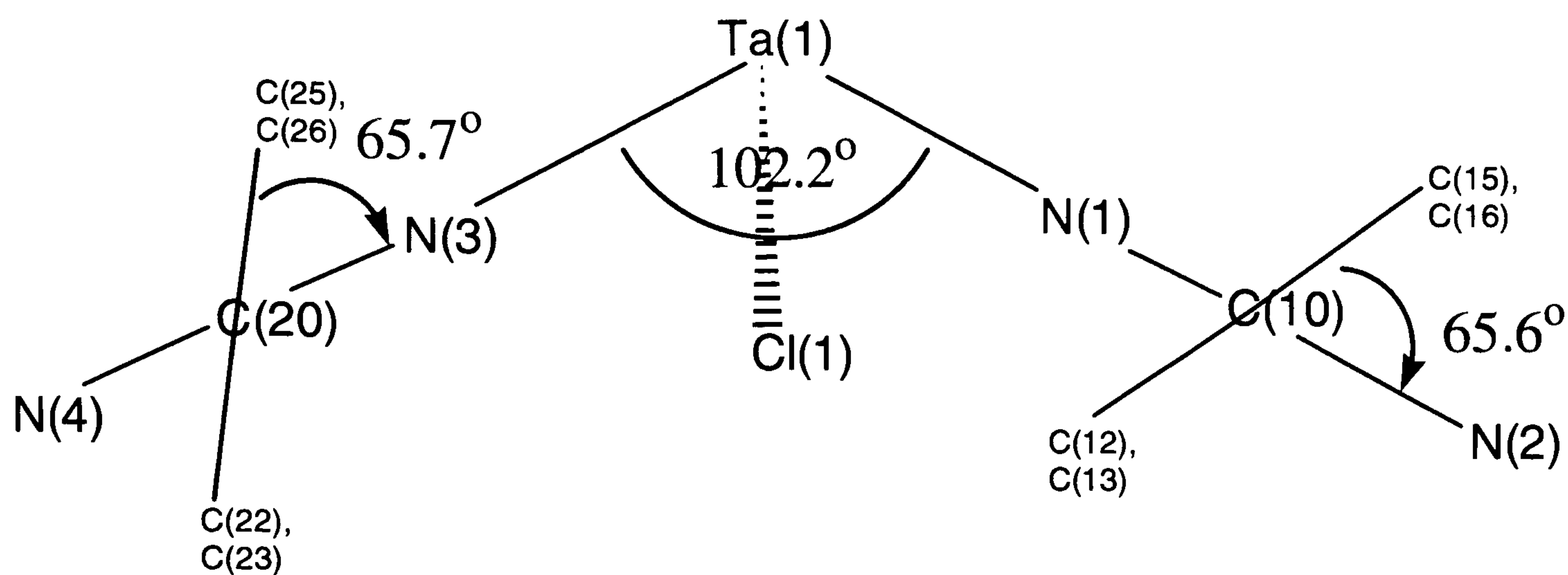


Figure 3.19 The inside and outside angles between the planes of the phenyl rings and the planes of the conjugated amidinate ligands.

The two amidinate ligands lie with their C₆ rings in a *trans* configuration as shown in Figure 3.18. The two phenyl rings lie at 65.6° and 65.7° to the planes defined by N(2), C(10), N(1), Ta(1) and N(4), C(20), N(3), Ta(1) respectively (Figure 3.19). The significance of such similarities in the two angles indicates a preference for the phenyl rings not to be in the same plane as the conjugated part of the ligand, N=C-NR₂.

The reactions of tin-amide,⁴⁵ lead-amide,⁴⁶ and more recently uranium-amide bonds^{109,110} with aryl isocyanides have been known for some time. In comparison to reported examples of insertion of isonitrile into M-C bonds, insertion into M-N bonds is relatively unexplored, with only a handful of examples of insertion into transition metal amide bonds.

Insertion into metal amide bonds results in the formation of metallaamidinides, having contributions from the resonance forms (I), (II) and (III) shown in Figure 3.20. The η²-R₂NCNAr ligand carries a formal 1⁻ charge but contributes three electrons (NLF) to the metal centre.

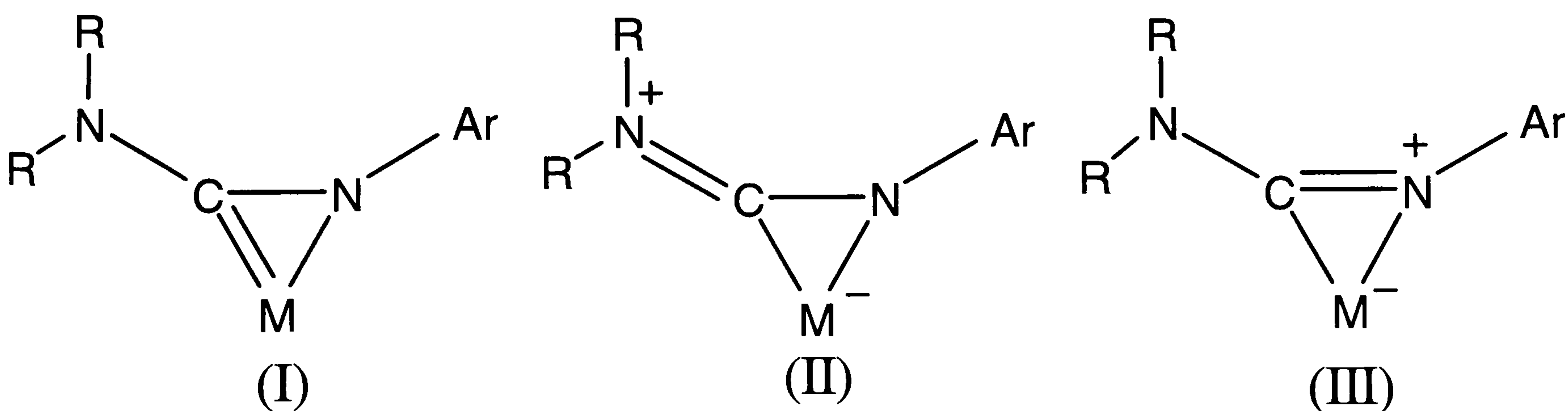
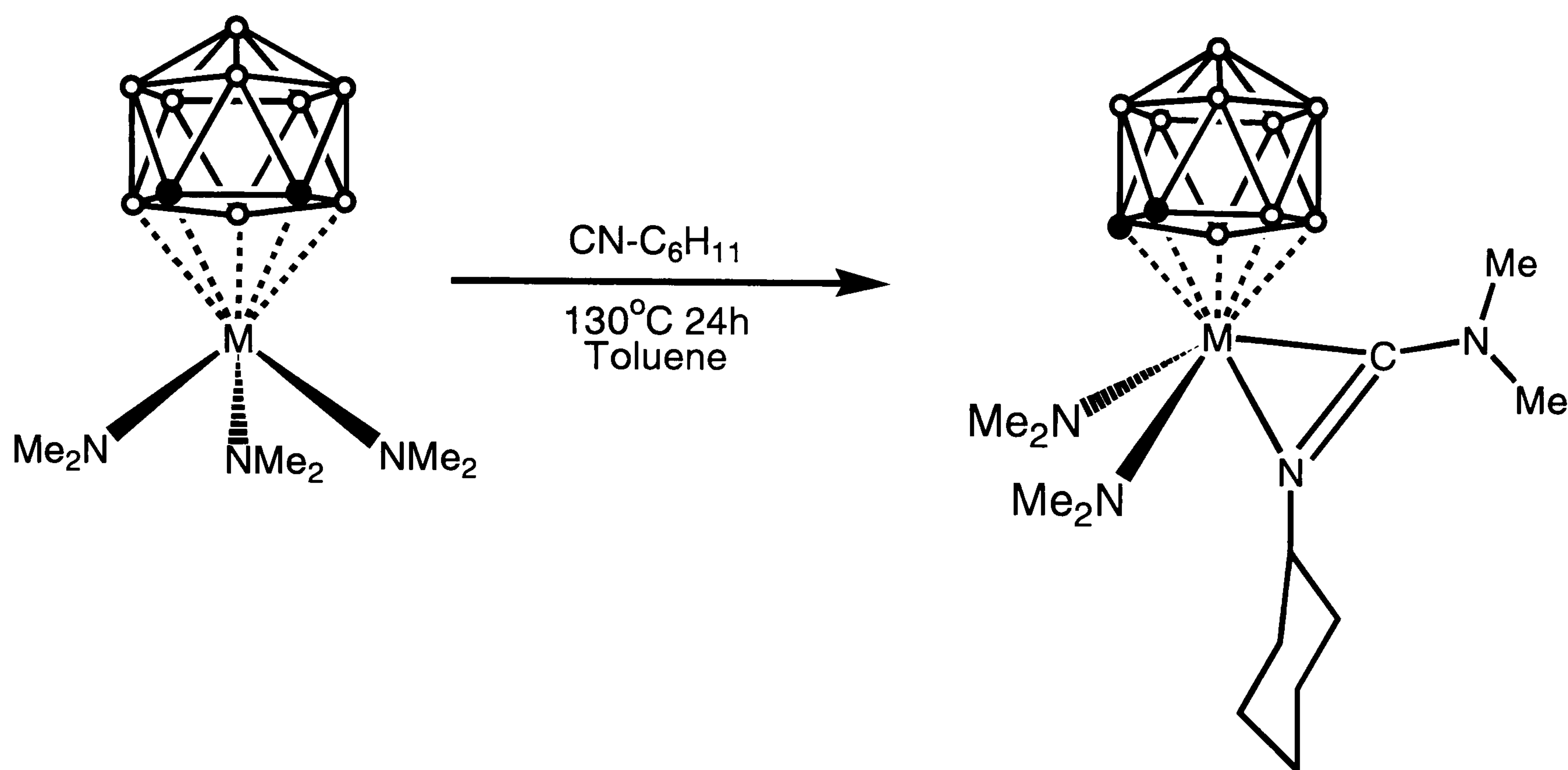


Figure 3.20 Three canonical forms of the metallaamidinide moiety.

The transition metal amide complexes $[\text{Mo}(\text{NMe}_2)_4]$,¹¹¹ $[\text{Zr}(\text{NMe}_2)_4]$ ¹¹² and $[(\eta^5:\eta^1\text{-C}_5\text{Me}_4\text{CH}_2\text{CH}_2\text{NMe})\text{TiCl}_2]$ ¹¹³ have all been shown to insert isocyanides into the metal nitrogen bond to form complexes which have been shown by X-ray crystallography to have a $\eta^2\text{-R''RNC=NR'}$ moiety bound to the metal centre.



Scheme 3.11 Synthesis of $[\text{Ta}(\text{NMe}_2)_2(\eta^2\text{-Me}_2\text{NCN}(\text{C}_6\text{H}_{11}))(\text{C}_2\text{B}_9\text{H}_{11})]$, (**27**).

The reaction between *ortho*- $[\text{Ta}(\text{NMe}_2)_3(\text{C}_2\text{B}_9\text{H}_{11})]$, (**17**), and three equivalents of cyclohexyl isocyanide at 130°C in toluene over a period of 24 hours results in the formation of the *mono*-insertion complex $[\text{Ta}(\text{NMe}_2)_2(\eta^2\text{-Me}_2\text{NCN}(\text{C}_6\text{H}_{11}))(\text{C}_2\text{B}_9\text{H}_{11})]$, (**27**), which can be recrystallised from a toluene / pentane mixture at -40°C. Unfortunately crystals of (**27**) suitable for single crystal X-ray crystallographic experiments could not be grown.

The $^{11}\text{B}\{^1\text{H}\}$ NMR spectrum shows 5 resonances in a 1:3:2:1:2 intensity ratio indicating a C_s symmetrical molecule. The ^1H and ^{13}C NMR spectra show only one resonance for the C-H unit in the cage, confirming the symmetry. The ^1H NMR spectra also shows the presence of three N-Me groups in a 4:1:1 intensity ratio, which is also seen in the ^{13}C NMR spectra, and a series of C-H multiplets with a total integral of 11H, assigned to the *cyclo*-hexyl group. This suggests a geometry consistent with that shown for (**27**) in Scheme 3.11, in which there is free rotation about the Ta-NMe₂ bonds in solution at room temperature and the (Me₂NCN(Cy)) ligand occupies a site that lies in the mirror plane of the molecule with two N-Me groups that are non-equivalent due to restricted rotation about the C-NMe₂ bond. ^{13}C DEPT experiments have been used to identify $\underline{\text{CH}}_3$, $\underline{\text{CH}}_2$ and $\underline{\text{CH}}$ units within the molecule.

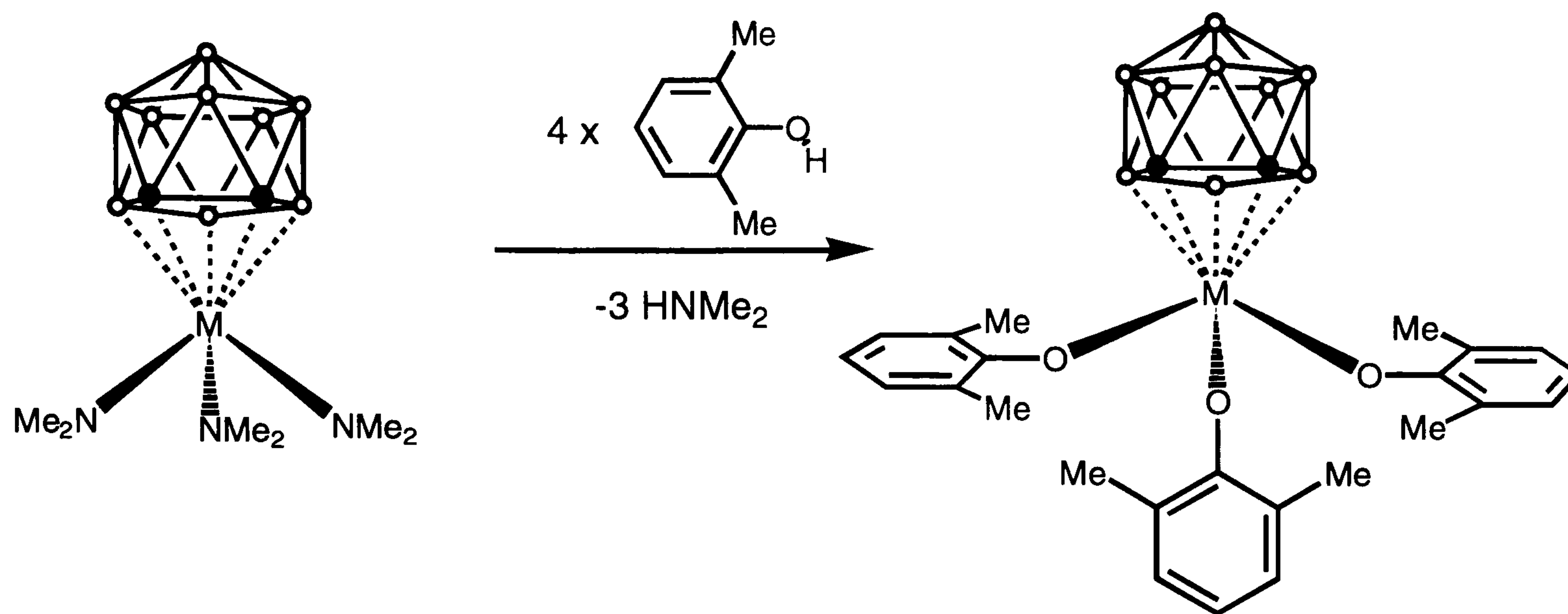
3.3.3 Reactions of *ortho*-[Ta(C₂B₉H₁₁)(NMe₂)₃] with Protic Acids.

As mentioned earlier in this chapter, the reactions of metal amide complexes with protic acids have been known for some time and have been investigated by a number of groups working in this field. Lappert and co-workers showed in 1968 that transition metal amide complexes reacted with a range of protic compounds including C₅H₆ and metal hydrides.^{18a}

Attempts were made to react [Ta(C₂B₉H₁₁)(NMe₂)₃], (**17**), with a range of C-H acids. The dicarbollide complex, (**17**), was dissolved in toluene at 60°C and one equivalent of C₅H₆, C₅H₅Me or three equivalents of H-C≡CPh was added to the toluene solutions. The mixtures were then heated to reflux for 24h, after which each reaction was cooled to room temperature and extracted into dichloromethane. It was hoped that these reactions would produce the mixed dicarbollide sandwich complexes [Ta(C₂B₉H₁₁)(η⁵-C₅H₅)(NMe₂)₂] and [Ta(C₂B₉H₁₁)(η⁵-C₅H₄Me)(NMe₂)₂], and the dicarbollide tris-alkyne complex [Ta(C₂B₉H₁₁)(C≡CPh)₃] respectively. Unfortunately these reactions were not successful and the only metal complex isolated from the dichloromethane solutions was the starting material, (**17**). A possible reason for the failure of these reactions lies in the nature of the Ta-N bonds in complex (**17**). It can be clearly seen from Figure 3.9 that the three amide ligands are planar, implying significant pπ-dπ bonding in the metal amide bonds. This secondary bonding reduces the electron density on the nitrogen atom and can explain the reduced reactivity of the amide ligands towards attack by electrophiles such as H⁺.

As a result, the reactions of more “classical”, and more acidic, protic acids such as phenols, alcohols and thiols with compound (**17**) were investigated.

The reaction of complex (**17**) with four equivalents of the bulky phenol, (2,6-Me₂C₆H₃)OH in a toluene solution at 80°C, resulted in a colour change from yellow to colourless. Recrystallisation of the crude reaction product from a dichloromethane solution layered with pentane produced colourless crystals of [3-Ta(OC₆H₃-Me₂-2,6)₃](1,2-C₂B₉H₁₁), (**28**), suitable for single crystal X-ray diffraction experiments.



Scheme 3.12 Synthesis of the *tris*-phenoxide complex of $[\text{Ta}(\text{O}-2,6\text{-Me}_2\text{C}_6\text{H}_3)_3(\text{C}_2\text{B}_9\text{H}_{11})]$, (28).

The asymmetric unit comprises two molecules, A and B, with similar geometry (see Fig. 3.21 and Table 3.7). The tantalum atom is co-ordinated by the open C_2B_3 face of the dicarbollide ligand (in a nearly symmetrical η^5 fashion) and by three dimethylphenoxide ligands. The molecular structure of one molecule in the unit cell of (28) is shown in Figure 3.21. Selected atomic distances and angles are given in Table 3.7.

The similarities between the amide ligands and the alkoxide ligand have been discussed in chapter 1, and as in solid state structure of the *tris*-amide complex (17), the *tris*-phenoxide complex exhibits evidence of the *trans*-influence caused by the dicarbollide ligand, with two phenoxide ligands having a similar geometry and one being unique. The *tris*-phenoxide complex also shares many structural features with the carbamate complex (22).

In both molecules A and B, the carbon atoms in the C_2B_3 face were clearly identified, with one of the carbon atoms lying almost directly *trans*- to the unique phenoxide ligand with the torsion angles, $\text{C}(7)\text{-Cb-Ta}(1)\text{-Ph}_{\text{cent}}$ and $\text{C}(77)\text{-Cb-Ta}(2)\text{-Ph}_{\text{cent}}$, of $\tau = -179.5^\circ$ and -174.4° respectively in the two molecules in the unit cell. This results in a *pseudo* mirror symmetry in the molecules which is violated by the non equivalence of C(8) and B(11) in molecule A and C(78) and B(81) in molecule B.

As in the carbamate system (28), the planes defined by the C_2B_3 face of the dicarbollide ligand and the three oxygen atoms of the phenoxide ligands are not parallel, with angles between the two planes of 2.6° and 1.8° in molecule A and B respectively. The dicarbollide ligand can be thought of as tilting forward, i.e., from the unique phenoxide ligand. The shorter bond between the tantalum atom and the unique phenoxide ligand results in a synergic increase in the Cb-Ta-

O angle, i.e. the oxygen moves away from the cage to reduce steric interaction, and the cage tilts forward also to relieve interaction between the phenoxide ligand and B-H bonds.^{17a}

The two horizontal phenoxide ligands in molecule A show only a very small deviation away from being parallel to the plane of the C_2B_3 face, with angle to the C_2B_3 face of 11.6° and 10.2° respectively for the phenyl groups on O(1) and O(2). Molecule B is not as symmetrical with angles of 18.4° and 6.8° on O(4) and O(5) respectively. A very similar ligand orientation is observed in the titanium complex $[Ti(tBu)(O-C_6H_3^iPr_{2-2,6})_3]$.¹¹⁴

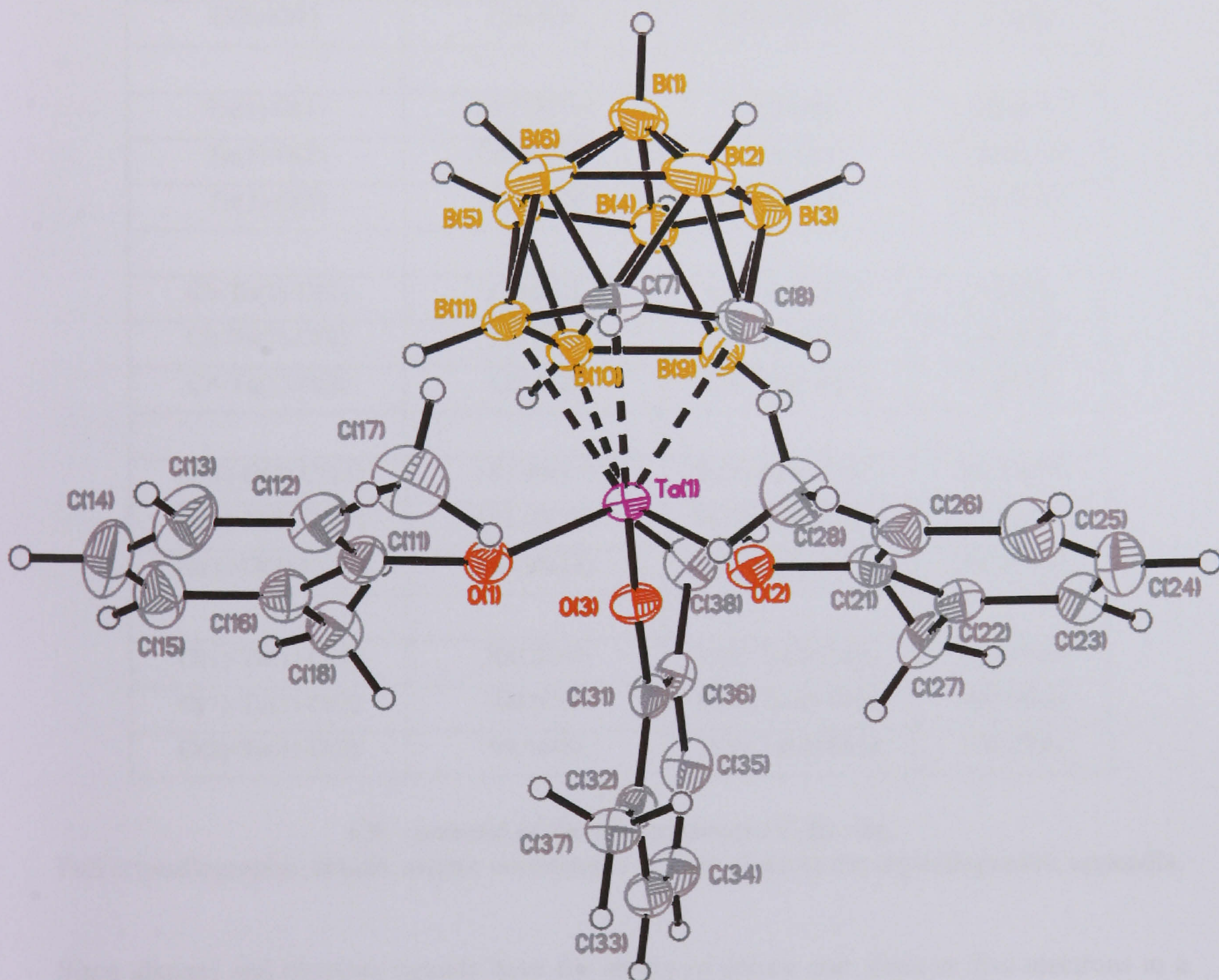


Figure 3.21 Molecular structure of the independent molecule (A) in the asymmetric unit of $[Ta(OC_6H_3-Me_{2-2,6})_3](ortho-C_2B_9H_{11})$, (**28**). Thermal ellipsoids are shown at 50% probability.

Table 3.7 Bond distances (Å), and bond angles (°) in **(28)**.

Molecule A		Molecule B	
Ta(1)-C(7)	2.462(3)	Ta(2)-C(77)	2.438(3)
Ta(1)-C(8)	2.447(3)	Ta(2)-C(78)	2.428(3)
Ta(1)-B(9)	2.400(3)	Ta(2)-B(79)	2.409(3)
Ta(1)-B(10)	2.408(3)	Ta(2)-B(80)	2.413(3)
Ta(1)-B(11)	2.443(3)	Ta(2)-B(81)	2.449(3)
Cb-Ta(1)	1.963(3)	Cb-Ta(2)	1.956(3)
C(7)-C(8)	1.612(5)	C(77)-C(78)	1.638(4)
Ta(1)-O(1)	1.8778(18)	Ta(2)-O(4)	1.8526(17)
Ta(1)-O(2)	1.8799(19)	Ta(2)-O(5)	1.8818(19)
Ta(1)-O(3)	1.8443(18)	Ta(2)-O(6)	1.8574(18)
Cb-Ta(1)-O(1)	114.6(2)	Cb-Ta(2)-O(4)	119.3(2)
Cb-Ta(1)-O(2)	114.7(2)	Cb-Ta(2)-O(5)	114.3(2)
Cb-Ta(1)-O(3)	123.8(2)	Cb-Ta(2)-O(6)	119.4(2)
Ta(1)-O(1)-C(11)	152.99(17)	Ta(2)-O(4)-C(41)	160.53(17)
Ta(1)-O(2)-C(21)	151.03(17)	Ta(2)-O(5)-C(51)	153.19(17)
Ta(1)-O(3)-C(31)	164.96(18)	Ta(2)-O(6)-C(61)	164.419(17)
O(1)-Ta(1)-O(2)	100.21(8)	O(4)-Ta(2)-O(5)	100.05(8)
O(1)-Ta(1)-O(3)	100.67(9)	O(4)-Ta(2)-O(6)	100.08(8)
O(2)-Ta(1)-O(3)	99.16(8)	O(5)-Ta(2)-O(6)	100.27(8)

Cb – centroid of the η^5 -coordinated C_2B_3 ring.

Full crystallographic details, atomic coordinates etc. are given in the crystallographic appendix.

Since alkoxyl and phenoxy ligands have the ability to donate one, three or five electrons to a metal centre, three being the most common, we can consider the complex **(28)** as an 18 electron complex with all three phenoxy ligands donating three electrons to the metal centre, i.e., they are all LX ligands.

The specific orientation of the cage carbons in a position *trans* to the vertical ligand suggests a similar through metal interaction between a filled p-orbital on the oxygen atom of the vertical

phenoxide ligand and a carbon based orbital on the cage, similar to that proposed for compounds (16)-(20) (Figure 3. 13)

As expected the $^{11}\text{B}\{^1\text{H}\}$ NMR of (28) shows 5 resonances in a typical 1:2:2:3:1 intensity ratio. The ^1H NMR spectrum confirms the molecular C_s symmetry of the molecule in solution with the presence of only one C-H resonance. The ^{13}C and ^1H NMR spectra show the presence of one Me environment. This observation suggests that at room temperature the presence of one vertical and two horizontal ligands is not observed due to the rapid rotation around the metal oxygen bonds, and exchange of the “vertical” and “horizontal” phenoxide ligands observed in the solid state structure. Attempts to freeze out the rotation of the phenoxide ligands in variable temperature NMR experiments, by cooling a sample of (28) in CD_2Cl_2 to -90°C , proved unsuccessful showing no coalescence. This indicates that the process by which the methyl groups on the respective vertical and horizontal ligands exchange is a low energy process, most probably due to rotation around the M-O bonds.¹¹⁵

Attempts to react the *tris*-amide complex (17) with stoichiometric amounts of other alcohols such as methanol and ethanol under the same conditions resulted in the formation and isolation of the *nido*-carborane salt $[\text{NH}_2\text{Me}_2][\text{C}_2\text{B}_9\text{H}_{12}]$.

The analogous reaction between thiophenol, and the *tris*-amide complex, (17), was expected to produce the analogous *tris*-thiophenoxy tantalum dicarbollide complex $[\text{3-Ta}(\text{SC}_6\text{H}_5)_3(1,2\text{-C}_2\text{B}_9\text{H}_{11})]$. The reaction was performed using analogous conditions to those used in the reaction between (17) and 2,6-dimethylphenol. Four equivalents of thiophenol were added to a toluene suspension of (17). An immediate colour change was observed from pale yellow to deep red, accompanied by complete dissolution of reactants and products. Continued stirring of the solution for 12hrs resulted in the precipitation of a red solid. Excess thiophenol and the toluene solvent were removed under vacuum. The red solid was then dissolved in 10ml of hot toluene and filtered. Recrystallisation at 5°C produced red needle like crystals suitable for single crystal X-ray diffraction experiments. The molecular structure of the resulting metal complex is shown in Figure 3.22, and reveals that a more complicated sequence of reactions has occurred.

The asymmetric unit of (29) contains one independent molecule of $[\text{3-Ta}(\text{SC}_6\text{H}_5)_4(9\text{-NHMe}_2\text{-1,2-C}_2\text{B}_9\text{H}_9)]$ and one molecule of disordered toluene.

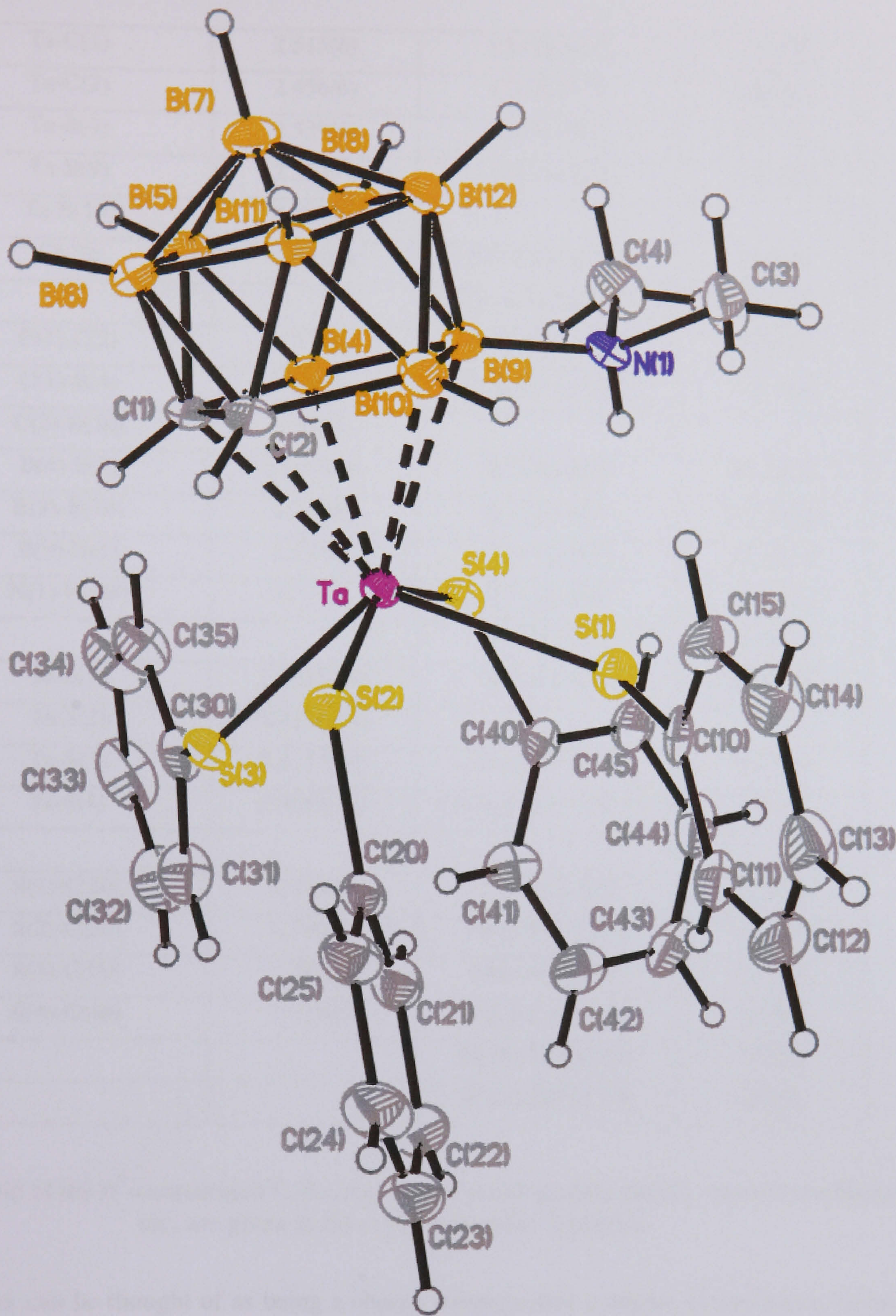


Figure 3.22 Molecular structure of [3-Ta(SC₆H₅)₄(9-NHMe₂-1,2-C₂B₉H₉)], (29). Thermal ellipsoids are shown at 50% probability.

Table 3.8 Bond distances (Å), bond and torsion angles (°) in (29).

Ta-C(1)	2.515(6)	Cb-Ta-S(1)	123.3(3)
Ta-C(2)	2.456(6)	Cb-Ta-S(2)	106.0(3)
Ta-B(4)	2.539(6)	Cb-Ta-S(3)	119.1(3)
Ta-B(9)	2.552(6)	Cb-Ta-S(4)	104.0(3)
Ta-B(10)	2.489(7)		
Cb-Ta	2.053(6)	Cb-Ta-S(1)-C(10)	90.0(3)
		Cb-Ta-S(2)-C(20)	180.0(3)
C(1)-C(2)	1.573(8)	Cb-Ta-S(3)-C(30)	83.9(4)
C(1)-B(4)	1.677(9)	Cb-Ta-S(4)-C(40)	167.9(4)
C(2)-B(10)	1.674(9)		
B(4)-B(9)	1.807(10)	S(1)-Ta-S(2)	86.76(5)
B(9)-B(10)	1.757(8)	S(1)-Ta-S(3)	117.56(5)
B(9)-N(1)	1.577(8)	S(1)-Ta-S(4)	76.36(5)
N(1)-H(1N)	0.74(5)	S(2)-Ta-S(3)	78.96(5)
		S(2)-Ta-S(4)	150.00(5)
Ta-S(1)	2.4255(14)	S(3)-Ta-S(4)	87.04(5)
Ta-S(2)	2.4224(14)		
Ta-S(3)	2.4177(14)	Cb-B(9)-N(1)	160.7(6)
Ta-S(4)	2.4580(16)	Cb-B(9)-N(1)-H(1N)	5.3(4)
S(1)-C(10)	1.775(6)	C(4)-N(1)-C(3)	112.3(3)
S(2)-C(20)	1.766(6)	B(9)-N(1)-C(3)	114.9(4)
S(3)-C(30)	1.781(6)	B(9)-N(1)-C(4)	114.4(4)
S(4)-C(40)	1.779(6)	B(9)-N(1)-H(1N)	107(4)
		H(1N)-N(1)-C(3)	107(4)
		H(1N)-N(1)-C(4)	101(4)

Cb – centroid of the η^5 -coordinated C₂B₃ ring. Full crystallographic details, atomic coordinates etc. are given in the crystallographic appendix.

The complex can be thought of as being a charge compensated complex in analogous fashion to complexes such as [Mn(CO)₃{SMe₂-C₂B₉H₁₀}],⁷⁴ in which the dicarbollide is substituted at a boron atom with a Me₂S⁺ group. This has the effect of lowering the anionic charge of the ligand from 2⁻ to 1⁻ and thus making the charge of such ligands comparable to Cp⁻. As the dicarbollide ligand [*nido*-10-NHMe₂-7,8-C₂B₉H₁₁]⁻ is mono-anionic, the tantalum is able to coordinate to itself a further [SC₆H₅] unit.

The $^{11}\text{B}\{^1\text{H}\}$ NMR spectrum for (**29**) shows 6 resonances in a 1:2:2:2:1:1 intensity ratio, with one peak shifted to low frequency at $\delta = 23.35\text{ppm}$. This peak corresponds to the unique boron on the C_2B_3 face of the dicarbollide ligand to which the NHMe_2 unit is bound and as such shows no coupling to ^1H . The ^1H NMR spectrum shows the cage to be symmetrical with a single resonance for the cage C-H at 3.19ppm. The N- CH_3 protons are clearly identified as is the resonance for the hydrogen on the NMe_2 group attached to the cage. The phenyl region of the spectrum shows a series of multiplets which integrate to 20H, this region of the spectrum along with the 4 resonances observed in the ^{13}C spectra indicates free rotation of the “ SC_6H_5 ” groups attached to the tantalum.

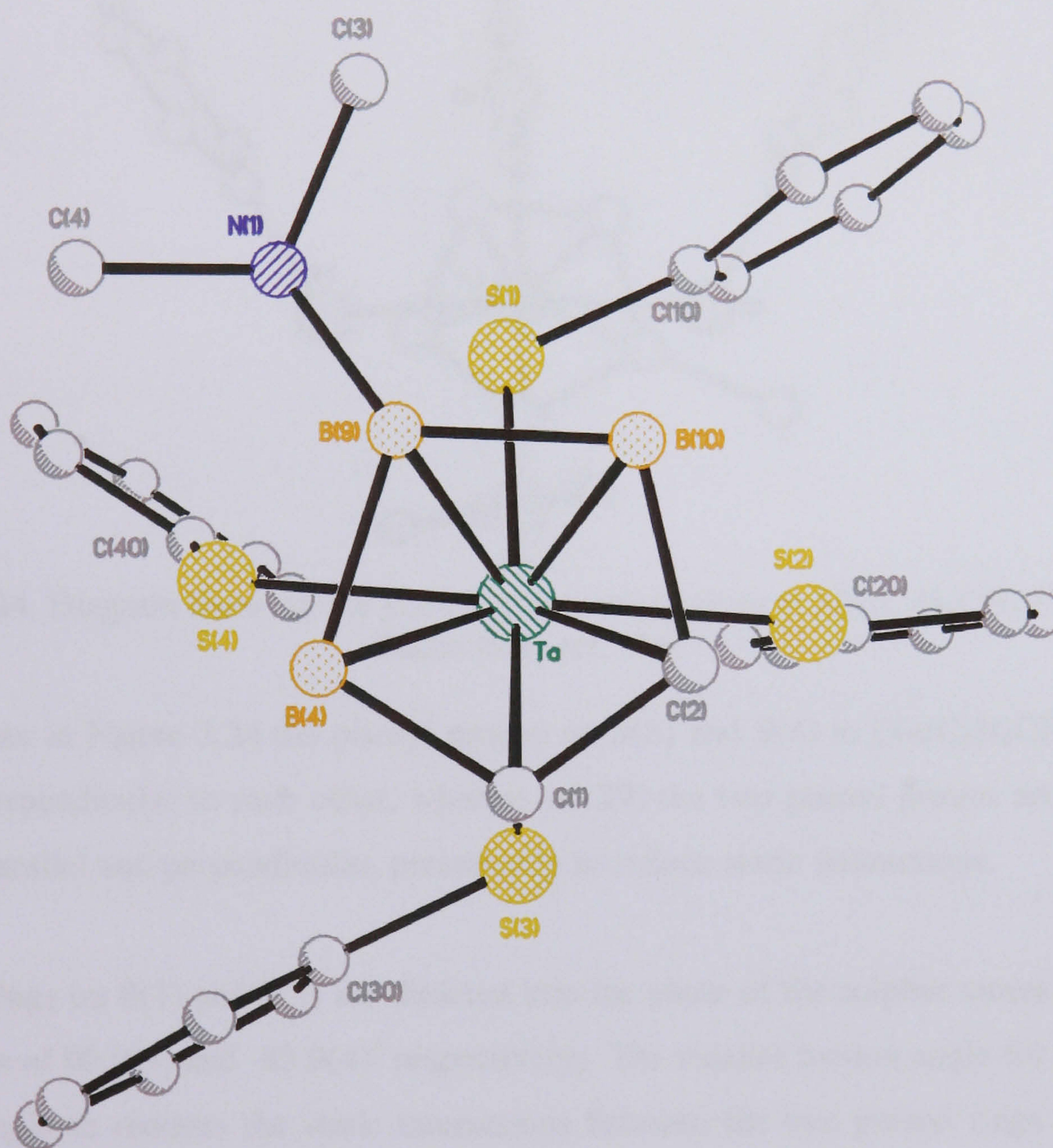


Figure 3.23 Diagram showing the orientation of the phenyl rings in (**29**).

The structure of (**29**) is that of a distorted four-legged piano-stool, whereby two of the thiolate ligands S(1) and S(3) have been bent away from the dicarbollide ligand (Cb-Ta-S angles of $123.3(3)^\circ$ and $119(3)^\circ$ respectively). The two other thiolate ligands, S(2) and S(4), do not have such pronounced angles at tantalum and can be thought of as being moved towards the dicarbollide ligand (Cb-Ta-S angles of $106.0(3)^\circ$ and $104.0(3)^\circ$, respectively). The phenyl

ligands on S(2) and S(4) are orientated away from the dicarbollide ligand (Cb-Ta-S-C torsion angles of $180.0(3)$ and $167.9(4)^\circ$ respectively) so as to avoid steric interaction with the dicarbollide ligand. The two phenyl groups on S(1) and S(3) are almost parallel, but point in opposite directions, with an angle between the two planes of the phenyl groups of 2.5° . In comparison, the two phenyl groups on S(2) and S(4) have a much greater angle (140.0°) between them as can be seen from Figure 3.23. This ligand orientation differs from that observed in the related structure of $[\text{Ta}(\text{C}_5\text{H}_4\text{CH}_3)(\text{SC}_6\text{H}_5)_4]$, a diagram of which is shown in Figure 3.24, showing the orientation of phenyl groups.¹¹⁶

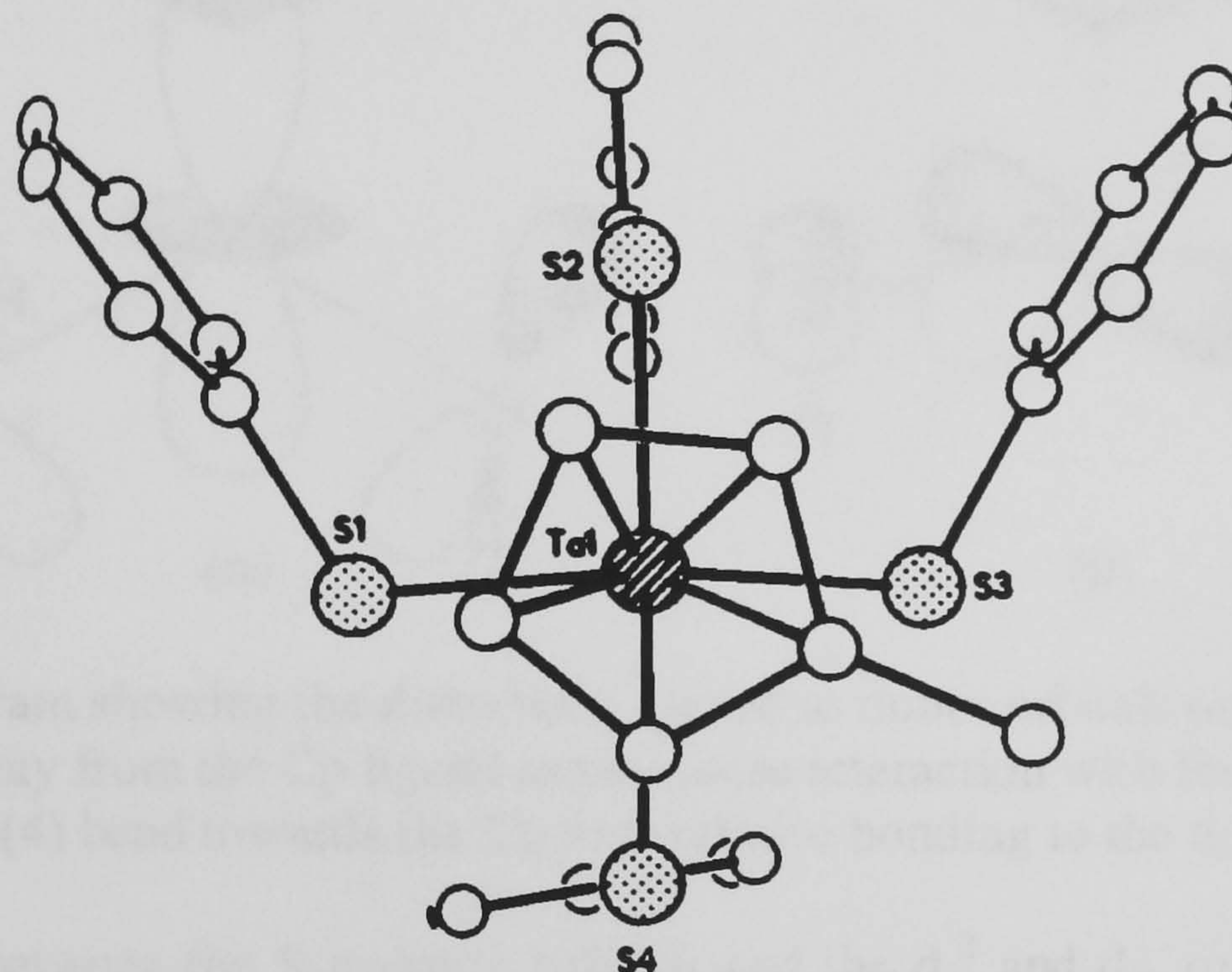


Figure 3.24. Diagram showing the phenyl group orientations in $[\text{Ta}(\text{C}_5\text{H}_4\text{CH}_3)(\text{SC}_6\text{H}_5)_4]$. Taken from ref. 116

As can be seen in Figure 3.24 the phenyl groups on S(2) and S(4) in $[\text{Ta}(\text{C}_5\text{H}_4\text{CH}_3)(\text{SC}_6\text{H}_5)_4]$ are almost perpendicular to each other, whereas in (29) the two phenyl groups are somewhere in between parallel and perpendicular, presumably to reduce steric interactions.

The phenyl rings on S(1) and S(3) are directed into the plane of the sulphur atoms (Cb-Ta-S-C torsion angles of $90.0(3)$ and $-83.9(4)^\circ$ respectively). The smaller torsion angle for Cb-Ta-S(3)-C(30) is thought to reduce the steric interactions between the two phenyl rings on S(3) and S(4) respectively.

The Ta-S(3) distance, at $2.4117(14)\text{\AA}$ is slightly shorter than the other three Ta-S distances ($2.42\text{--}2.46\text{\AA}$), although all of the Ta-S distances are in the range of typical tantalum(V)-thiolate distances, $2.35\text{--}2.47\text{\AA}$.^{117,118} The Ta-Cb distance, $2.053(6)\text{\AA}$ is slightly longer than those observed in other Ta dicarbollide species in this chapter $1.963(3)\text{--}2.028(4)\text{\AA}$. This is not unexpected as the SPh groups are very good donor groups to the metal, resulting in a weakening of the M-Cb bonding interaction.

Extended Hückel Molecular Orbital (E.H.M.O.) studies have been performed on the molecule $[\text{Ta}(\text{C}_5\text{H}_4\text{CH}_3)(\text{SC}_6\text{H}_5)_4]$ to determine the cause of the distortions.¹¹⁶ Calculations were performed on the molecule $[\text{Ta}(\text{C}_5\text{H}_5)(\text{SH})_4]$, where SH ligands were used to simplify the calculations and to remove any steric effects caused by the phenyl groups. These calculations have shown that the observed distortions in the complex $[\text{Ta}(\text{C}_5\text{H}_4\text{CH}_3)(\text{SC}_6\text{H}_5)_4]$ are not a steric effect of the phenyl groups.

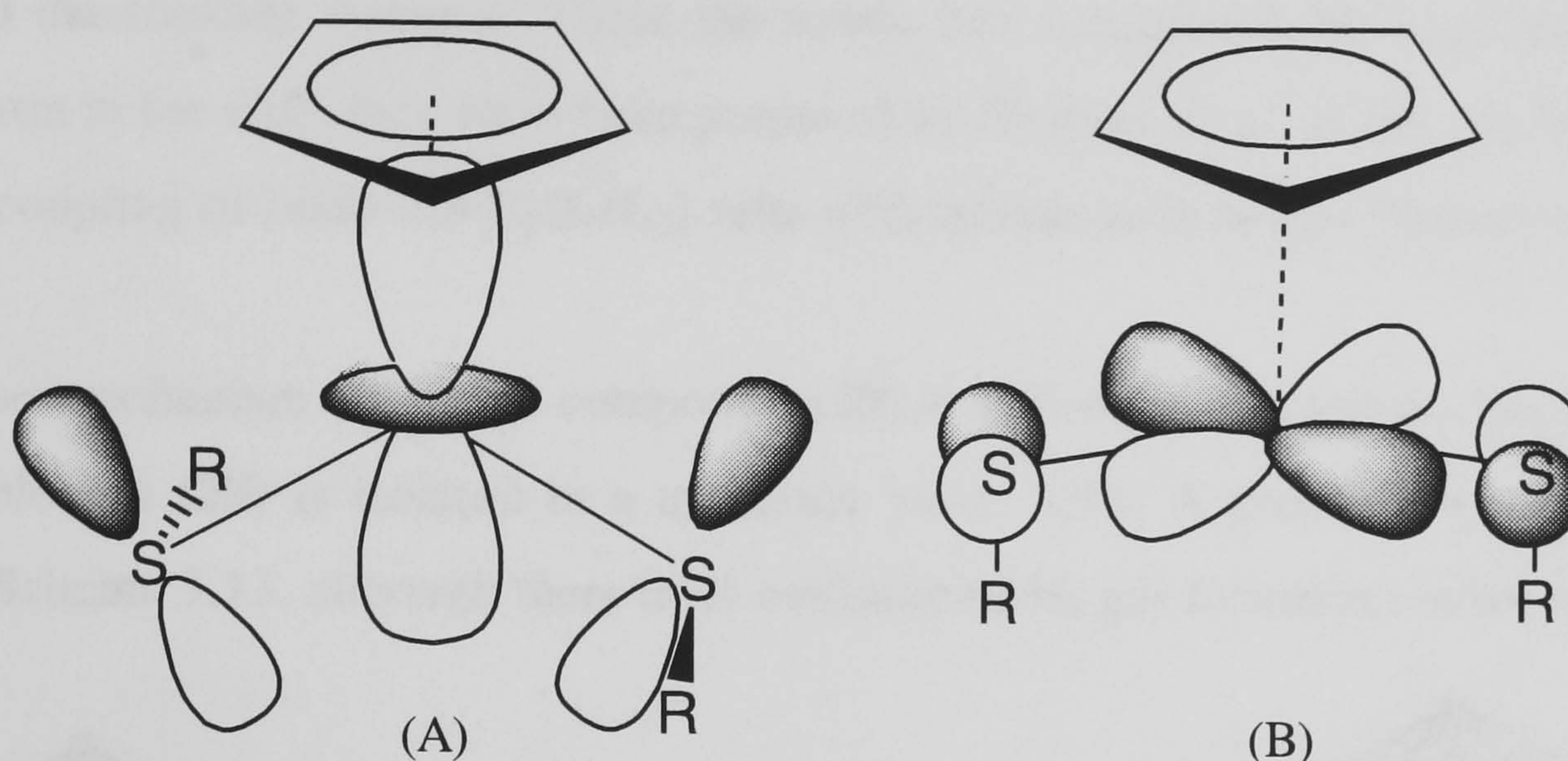


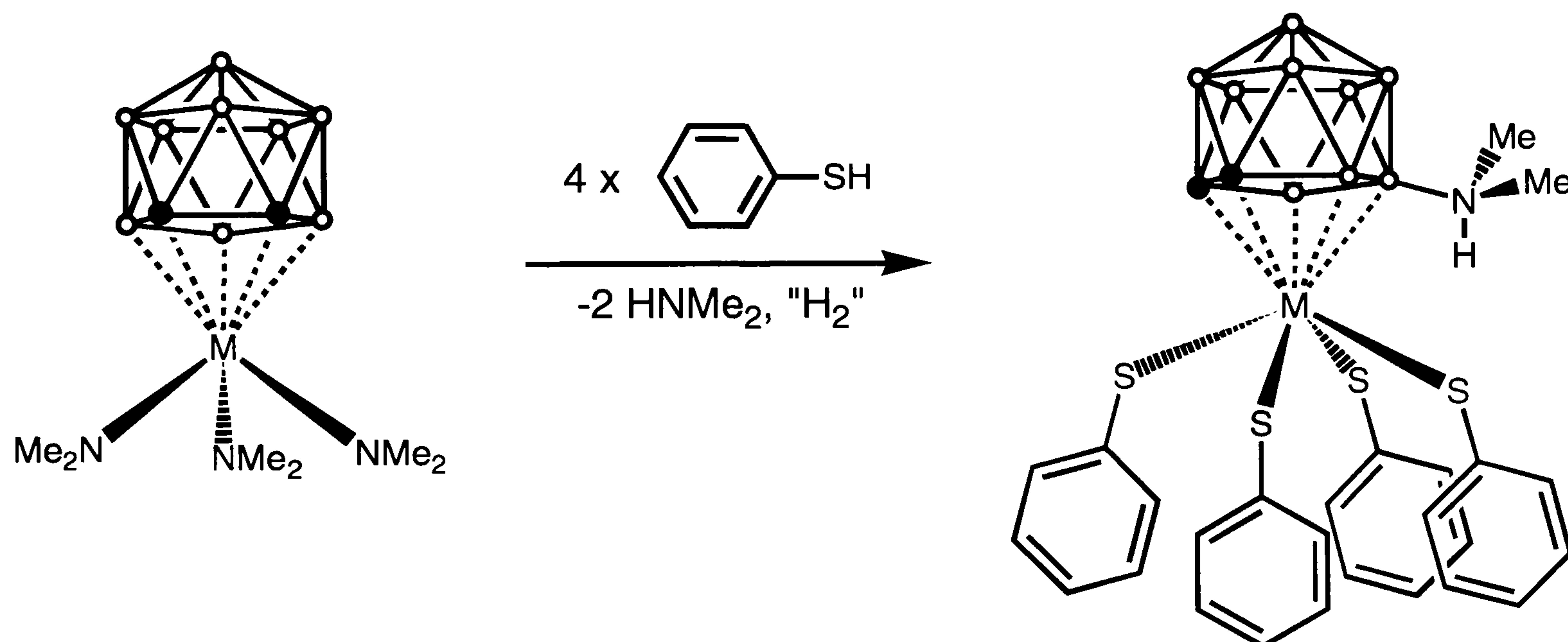
Figure 3.25 Diagram showing the distortions caused as donor orbitals on sulphur atoms S(1) and S(3) bend away from the Cp ligand to maximise interaction with the d_z^2 orbital (A) and S(2) and S(4) bend towards the Cp to maximise bonding to the d_{xy} orbital (B).

While π bonding between the S π -donor orbitals and the d_z^2 and d_{xy} orbitals can be used to explain most of the observed Cb-Ta-S angles, i.e., S(1) and S(3) are shifted down to maximise overlap with the d_z^2 orbital, while S(2) and S(4) bend towards the Cp ligand to maximise overlap with the d_{xy} orbital (Figure 3.25). The d_{xz} and d_{yz} orbitals which are Ta-Cp bonding appear to contribute significantly to the M-L σ bonding in CpML_4 compounds.¹¹⁹ In the same way that the dicarbollide ligand, $[\text{C}_2\text{B}_9\text{H}_{11}]^{2-}$, can be said to have similar frontier orbitals to $[\text{C}_5\text{H}_5]^-$, the substituted dicarbollide ligand $[\text{nido-10-NHMe}_2\text{-7,8-C}_2\text{B}_9\text{H}_{11}]^-$, has the same overall charge as the $[\text{C}_5\text{H}_5]^-$ ligand and very similar frontier orbitals to the parent dicarbollide ligand, we can assume that the same, or closely related, electronic processes that are responsible for the distorted structure in $[\text{Ta}(\text{C}_5\text{H}_4\text{CH}_3)(\text{SC}_6\text{H}_5)_4]$ are also responsible for the distortion in (29).

With regard to the polyhedral cage the structure of (29) is obviously one of a closed icosahedron with the Ta atom slightly shifted towards the C_2 facial atoms rather than the boron. A possible *trans*-influence may be discerned from the orientation of the C-C bond in the dicarbollide ligand with respect to the four thiolate ligands, with C(1) lying directly above S(1) with a C(1)-Cb-Ta-S(3) torsion angle of -179.2° . The orientation of the NHMe_2 unit is of some

interest, as Figures 3.22 and 3.23 show the NMe₂ unit lies in between S(1) and S(4), with the hydrogen atom pointing down into the plane of the sulphur atoms. Although the distances between H(1N)-S(1) and H(1N)-S(4) are 2.78 and 2.67 Å respectively and direct hydrogen bonding can be ruled out some weaker form of electrostatic interaction may be responsible for the directionality of the N(1)-H(1N) bond. The angle between N(1)-B(9)-Cb is 160.7° and not dissimilar from the angle at the unsubstituted cage boron atoms. The only other amine substituted dicarbollide systems, where the amine has substituted the hydrogen atom at the unique boron in the C₂B₃ face have been prepared by Hawthorne *et. al.* by the FeCl₃ promoted oxidative coupling of [*nido*-7,8-C₂B₉H₁₂] salts with amines such as tri-ethylamine.¹²⁰

The precise mechanism by which compound (**29**) is formed is not known but the reaction is reproducible and (**29**) is isolated in a moderate yield, 53%. A proposed reaction Scheme is shown in Scheme 3.13, although there is no evidence of H₂ gas formation in the reaction.

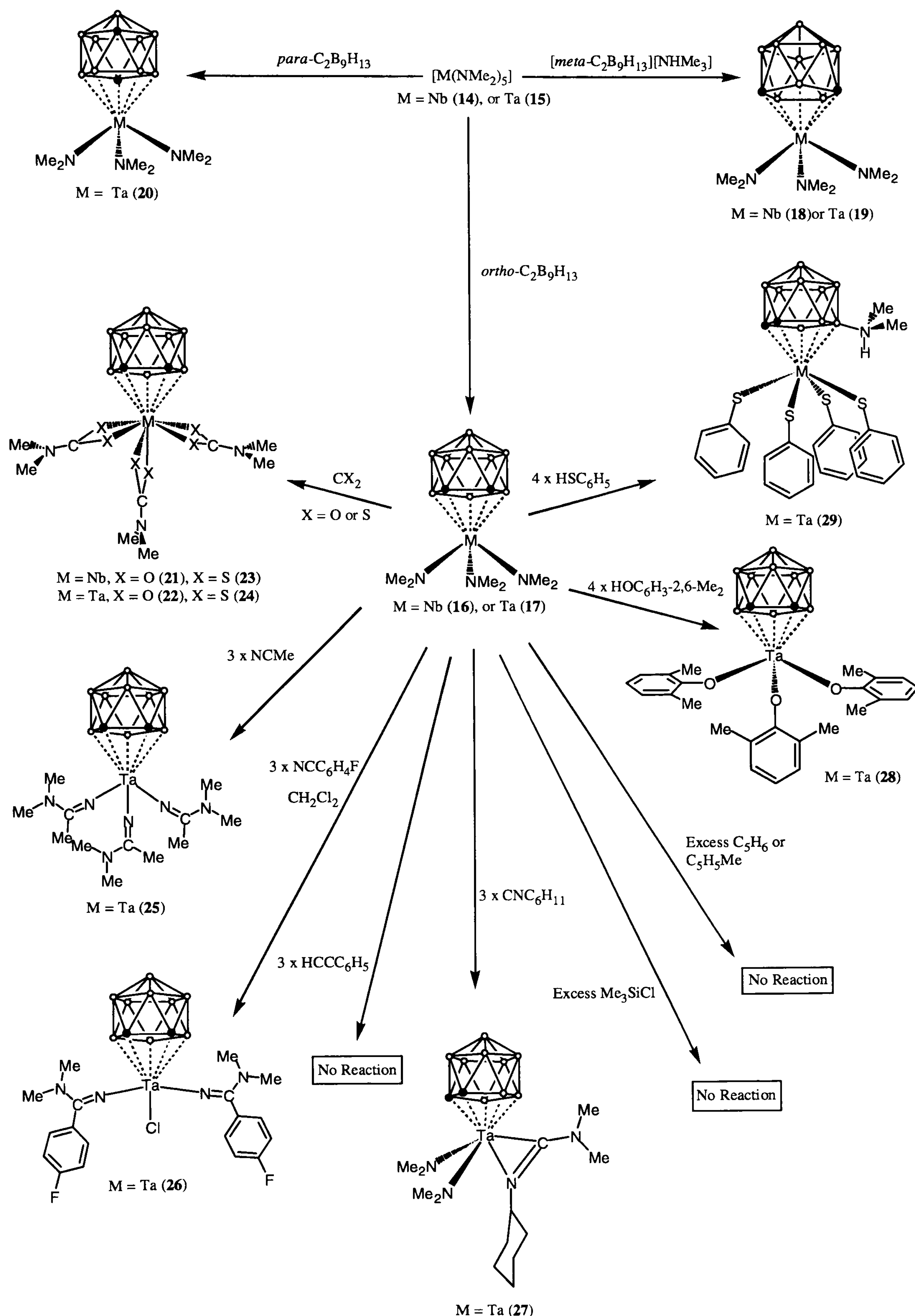


Scheme 3.13 Synthesis of *ortho*-[Ta(SC₆H₅)₄(9-NHMe₂-*nido*-C₂B₉H₉)], (**29**).

There are many reports in the literature in which charge compensated carborane ligands have been prepared, using various methods including ligand rearrangement from metal site to the carborane cage,^{120,121} reduction of a metallacarborane complex by a Lewis base,¹²² and addition of dialkyl sulphide to a protonated metallocene-type sandwich complex.¹²³ It is possible that the thiophenol also contained a quantity of diphenyl disilphide, PhSSPh, which reacted with the dicarbollide cage of the intermediate complex, [Ta(SPh)₃(C₂B₉H₁₁)] to form the cationic complex [Ta(SPh)₃(9-PhS-C₂B₉H₁₁)]⁺, which in turn is attacked by free dimethylamine in solution to form the complex (**29**). At the moment there is no substantiation for this working hypothesis.

3.4 Summary

In this chapter we have shown that the carborane acids [*ortho*-C₂B₉H₁₃], [HNMe₃][*meta*-C₂B₉H₁₂] and [*para*-C₂B₉H₁₃] react with the metal amide complexes [M(NMe₂)₅] (M = Nb (14); Ta (15)) to form the metallacarborane *tris*-dimethyl amide complexes of general formula [M(C₂B₉H₁₁)(NMe₂)₃]. Selected aspects of the chemistry of some of these complexes has been investigated and are shown in the diagram below.



Scheme 3. 14 A Scheme showing the range of reactions discussed in this chapter.

3.5 References for Chapter Three

- 1 (a) M. Bochmann, *J. Chem. Soc., Dalton Trans.*, 1996, 255; (b) H. H. Brintzinger, D. Fischer, R. Mülhaupt, B. Rieger and R. M. Waymouth, *Angew. Chem., Int. Ed. Engl.*, 1995, **34**, 1143; (c) *Ziegler Catalysis - Recent Innovations and Technological Improvements*, F. Fink, R. Mülhaupt and H. H. Brintzinger, Eds., Springer Verlag, Berlin, 1995; (d) W. E. Piers and J. E. Bercaw, *J. Am. Chem. Soc.*, 1990, **112**, 9406; (e) M. Bochmann, *Current Opinion in Solid State and Materials Science*, 1997, **2**, 639;
- 2 N. J. Long in “*Metallocenes*”, Blackwell Science Ltd, Oxford, 1998.
- 3 (a) R. F. Jordan, R. E. LaPointe, P. K. Bradley and N. Baenzinger, *J. Am. Chem. Soc.*, 1989, **111**, 2728; (b) B. J. Burger, M. E. Thomas, W. D. Cotter and J. E. Bercaw, *J. Am. Chem. Soc.*, 1990, **112**, 1566; (c) P. J. Shapiro, E. E. Bunell, W. P. Schaefer and J. E. Bercaw, *Organometallics*, 1990, **9**, 867; (d) H. H. Brintzinger, D. Fischer, R. Mülhaupt, B. Rieger and R. M. Waymouth, *Angew. Chem., Int. Ed. Engl.*, 1995, **34**, 1143.
- 4 (a) D. Stern, M. Sabat and T. J. Marks, *J. Am. Chem. Soc.*, 1990, **112**, 9558; (b) P. J. Shapiro, W. D. Cotter, W. P. Schaefer, J. A. Labinger and J. E. Bercaw, *J. Am. Chem. Soc.*, 1994, **116**, 4623; (c) P. L. Watson, *J. Am. Chem. Soc.*, 1982, **104**, 337; (d) G. Jeske, H. Lauke, H. Mauermann, P. N. Sweptson, H. Schumann and T. J. Marks, *J. Am. Chem. Soc.*, 1985, **107**, 8091.
- 5 (a) G. J. P. Britovsek, V. C. Gibson, B. S. Kimberley, P. J. Maddox, S. J. McTavish, G. A. Solan, A. J. P. White, and D. J. Williams, *Chem. Commun.*, 1998, 849; (b) D. Pappelardo, M. Mazzeo and C. Pellecchia, *Macromol. Rapid Commun.*, 1997, **18**, 1017; (c) C. Pellecchia, A. Zambelli, M. Mazzeo and D. Pappelardo, *J. Mol. Catal., A*, 1998, **128**, 229; (d) C. M. Wang, S. Friedrich, T. R. Younkin, R. T. Li, R. H. Grubbs, D. A. Bansleben and M. W. Day, *Organometallics*, 1998, **17**, 3149; (e) M. Bruce, V. C. Gibson, C. Redshaw, G. A. Solan, A. J. P. White and D. J. Williams, *Chem. Commun.*, 1998, 2523; (f) C. Pellecchia,

- M. Mazzeo and D. Pappelardo, *Macromol. Rapid Commun.*, 1998, **19**, 651; (g) X. F. Zeng and K. Zetterberg, *Macromol. Chem. and Phys.*, 1998, **199**, 2677.
- 6 L. K. Johnson, S. Mecking and M. Brookhart, *J. Am. Chem. Soc.*, 1996, **118**, 267; (b) M. J. Tanner, M. Brookhart and J. M. DeSimone, *J. Am. Chem. Soc.*, 1997, **119**, 7617; (c) B. L. Small, M. Brookhart and A. M. A. Bennett, *J. Am. Chem. Soc.*, 1998, **120**, 4049; (d) B. L. Small and M. Brookhart, *J. Am. Chem. Soc.*, 1998, **120**, 7143.
- 7 (a) D. N. Williams, J. P. Mitchell, A. D. Poole, U. Siemeling, W. Clegg, D. C. R. Hockless, P. A. O'Neil and V. C. Gibson, *J. Chem. Soc., Dalton Trans.*, 1992, 739; (b) S. Schmidt, J. Sundermeyer and F. Möller, *J. Organomet. Chem.*, 1994, **475**, 157; (c) D. M. Antonelli, A. Leins and J. M. Stryker, *Organometallics*, 1997, **16**, 2500.
- 8 M. P. Coles, C. I. Dalby, V. C. Gibson, W. Clegg and M. R. J. Elsegood, *J. Chem. Soc., Chem. Commun.*, 1995, 1709; V. C. Gibson, C. Redshaw, W. Clegg, M. R. J. Elsegood, U. Siemeling and T. Türk, *J. Chem. Soc., Dalton Trans.*, 1996, 4513;
- 9 E. B. Tjaden, D. C. Swenson, R. F. Jordan and J. L. Petersen, *Organometallics*, 1995, **14**, 371.
- 10 For examples of nitrogen containing ligands see; (a) A. L. McKnight and R. M. Waymouth, *Chem. Rev.*, 1998, **98**, 2587; (b) H. G. Alt, K. Föttinger and W. Milius, *J. Organomet. Chem.*, 1998, **564**, 115; (c) P. T. Gomes, M. L. H. Green and A. M. Martins, *J. Organomet. Chem.*, 1998, **551**, 133; (d) A. K. Hughes, S. M. B. Marsh, J. A. K. Howard and P. S. Ford, *J. Organomet. Chem.*, 1997, **528**, 195; (e) J. D. Scollard, D. H. McConville, N. C. Payne and J. J. Vittal, *Macromolecules*, 1996, **29**, 5241; (f) F. Amour and J. Okuda, *J. Organomet. Chem.*, 1996, **520**, 245; (g) C. Lensink, *Tetrahedron-Asymmetry*, 1995, **6**, 2033; (h) R. E. V. H. Spence and W. E. Piers, *Organometallics*, 1995, **14**, 6417; (i) J. C. Flores, J. C. W. Chien and M. D. Rausch, *Organometallics*, 1994, **13**, 4140; (j) A. K. Hughes, A. Meetsma and J. H. Teuben, *Organometallics*, 1993, **12**, 1936.

- 11 See “*Comprehensive Coordination Chemistry; Ligands*” Volume 2, Ed. G. Wilkinson, Pergamon Press, New York, 1987.
- 12 (a) R. N. Grimes, in *Comprehensive Organometallic Chemistry II*, Ed. E. W. Abel, F. G. A. Stone and G. Wilkinson, Pergamon Press, Oxford, 1995, vol 1, ch. 9; (b) M. F. Hawthorne, *Acc. Chem. Res.*, 1968, **1**, 281; (c) A. K. Saxena and N. S. Hosmane, *Chem. Rev.*, 1993, **93**, 1081; (d) X. L. R. Fontaine, N. N. Greenwood, J. D. Kennedy, K. Nestor, M. Thornton-Pett, S. Heřmánek, T. Jelínek and B. Štibr, *J. Chem. Soc., Dalton Trans.*, 1990, 681.
- 13 M. J. Manning, C. B. Knobler, R. Khattar and M. F. Hawthorne, *Inorg. Chem.*, 1991, **30**, 2009.
- 14 (a) Z. Xie, S. Wang, Z.-Y. Zhou, F. Xue and T. C. W. Mak, *Organometallics*, 1998, **17**, 489; (b) E. Hong, Y. Kim and Y. Do, *Organometallics*, 1998, **17**, 2933; (c) D. Rabinovich, C. M. Haswell, B. L. Scott, R. L. Miller, J. B. Nielsen and K. D. Abney, *Inorg. Chem.*, 1996, **35**, 1425; (d) R. Uhrhammer and R. F. Jordan, *Inorg. Chem.*, 1994, **33**, 4398; (e) C. Kreuder, R. F. Jordan and H. M. Zhang, *Organometallics*, 1995, **14**, 2993.
- 15 M. L. H. Green, *J. Organomet. Chem.*, 1995, **500**, 127.
- 16 (a) M. A. Curtis, E. J. Houser, M. Sabat and R. N. Grimes, *Inorg. Chem.*, 1998, **37**, 102; (b) K. E. Stockman, K. L. Houseknecht, E. A. Boring, M. Sabat, M. G. Finn and R. N. Grimes, *Organometallics*, 1995, **14**, 3014; (c) E. A. Boring, M. Sabat, M. G. Finn and R. N. Grimes, *Organometallics*, 1997, **16**, 3993; (d) S. S. H. Mao, T. D. Tilley, A. L. Rheingold and N. S. Hosmane, *J. Organomet. Chem.*, 1997, **533**, 257.
- 17 (a) R. Uhrhammer, D. J. Crowther, J. D. Olson, D. C. Swenson and R. F. Jordan, *Organometallics*, 1992, **11**, 3098; (b) D. J. Crowther, R. A. Fisher, A. M. Canich, G. G. Hlatky and H. W. Turner, US Patent 5502124 (1996); (c) D. J. Crowther, S. L. Borkowsky, D. Swenson, T. Y. Meyer and R. F. Jordan, *Organometallics*, 1993, **12**, 2897; (d) D. J. Crowther, D. C. Swenson and R. F. Jordan, *J. Am. Chem. Soc.*, 1995, **117**, 10403.

- 18 (a) G. Chandra and M. F. Lappert, *J. Chem. Soc., A*, 1968, 1940; (b) M. F. Lappert, P. P. Power, A. R. Sanger and R. C. Srivastava, “*Metal and Metalloid Amides*”, Ellis Horwood Publishers, Chichester, 1980; (c) M. H. Chisholm and I. P. Rothwell in *Comprehensive Coordination Chemistry*, eds. G. Wilkinson, R. D. Gillard and J. A. McCleverty, Volume 2, Chapter 13.4, Pergamon Press, Oxford, 1987.
- 19 (a) W. A. Hermann and W. Baratta, *J. Organomet. Chem.*, 1996, **506**, 357; (b) Y. Mu, W. E. Piers, M. A. MacDonald and M. J. Zaworotko, *Can. J. Chem.*, 1995, **73**, 2233; (c) Y. Mu, W. E. Piers, D. C. MacQuarrie, M. J. Zaworotko and V. G. Young, *Organometallics*, 1996, **15**, 2720; (d) Z. Ziniuk, I. Goldberg and M. Kol, *J. Organomet. Chem.*, 1997, **546**, 441.
- 20 (a) I. A. Guzei, A. G. Baboul, G. P. A. Yap, A. L. Rheingold, H. B. Schlegel and C. H. Winter, *J. Am. Chem. Soc.*, 1997, **119**, 3387; (b) I. A. Guzei, G. P. A. Yap and C. H. Winter, *Inorg. Chem.*, 1997, **36**, 1738; (c) Y. Mu, W. E. Piers, L. R. Macgillivray and M. J. Zaworotko, *Polyhedron*, 1995, **14**, 1.
- 21 (a) G. M. Diamond, R. F. Jordan and J. L. Petersen, *Organometallics*, 1996, **15**, 4045; (b) J. N. Christopher, G. M. Diamond, R. F. Jordan and J. L. Petersen, *Organometallics*, 1996, **15**, 4038; (c) G. M. Diamond, R. F. Jordan and J. L. Petersen, *J. Am. Chem. Soc.*, 1996, **118**, 8024.
- 22 D. E. Bowen, R. F. Jordan and R. D. Rogers, *Organometallics*, 1995, **14**, 3630.
- 23 N.N. Greenwood and A. Earnshaw, “*Chemistry of the Elements*”, Pergamon Press, Oxford, 1994.
- 24 O. C. Dermer and W. C. Fernelius., *Z. Anorg. Chem.*, 1935, **221**, 83.
- 25 D. C. Bradley and I. M. Thomas, *Proc. Chem. Soc.*, 1959, 225.
- 26 D. C. Bradley, M. H. Gitlitz, *J. Chem. Soc., (A)*, 1969, 980.
- 27 R. Bonnett, D. C. Bradley, K. J. Fisher and I. F. Rendall, *J. Chem. Soc., (A)*, 1971, 1622.
- 28 W. A. Nugent, *Inorg. Chem.*, 1983, **22**, 965.
- 29 R. T. Cowdell and G. W. A. Fowles, *J. Chem. Soc.*, 1960, 2522.

Chapter Three – Dicarbollide Complexes of Group Five Metals

- 30 G. W. A. Fowles and C. M. Pleass, *J. Chem. Soc.*, 1957, 2078.
- 31 B. J. Brisdon, G. W. A. Fowles and B. P. Osborne, *J. Chem. Soc.*, 1962, 1330.
- 32 D. A. Edwards and G. W. A. Fowles, *J. Chem. Soc.*, 1961, 24.
- 33 B. J. Brisdon, G. W. A. Fowles and B. P. Osborne, *J. Chem. Soc.*, 1962, 1330.
- 34 K. Issleib and H. Haeckert, *Z. Naturforsch.*, 1966, **21b**, 519.
- 35 P. J. H. Carnell and G. W. A. Fowles, *J. Chem. Soc.*, 1959, 4113.
- 36 M. H. Chisholm, J. C. Huffman and L. S. Tan, *Inorg. Chem.*, 1981, **20**, 1859.
- 37 D. C. Bradley and I. M. Thomas, *J. Chem. Soc.*, 1960, 3857.
- 38 D. C. Bradley and I. M. Thomas, *Can. J. Chem.*, 1962, **40**, 449.
- 39 K. Jones and M. F. Lappert, *Proc. Chem. Soc.*, 1962, 358.
- 40 C. Chandra, A. D. Jenkins, M. F. Lappert and R. C. Srivastava, *J. Chem. Soc.*, (A), 1970, 2550.
- 41 D.C. Bradley and M.C. Ganorkar, *Chem. Ind.*, 1968, 1521.
- 42 A. R. Sanger, *Inorg. Nucl. Chem. Letters*, 1973, **9**, 351.
- 43 A. G. Davies and P. G. Harrison, *J. Chem. Soc.*, (C), 1967, 1313.
- 44 K. Jones and M. F. Lappert, *J. Organomet. Chem.*, 1965, **3**, 295.
- 45 T. A. George and M. F. Lappert, *J. Organomet. Chem.*, 1968, **14**, 327.
- 46 W. P. Neumann and K. Kühlein, *Tetrahedron Letters*, 1966, 3423.
- 47 T. Sagusa, Y. Ito, S. Kobayashi and K. Hirota, *J. Am. Chem. Soc.*, 1967, **89**, 2240.
- 48 E. A. Boring, M. Sabat, M.G. Finn and R.N. Grimes, *Organometallics*, 1997, **16**, 3993.
- 49 M. F. Lappert and A. R. Sanger, *J. Chem. Soc. (A)*, 1971, 1314
- 50 J. March, “*Advanced Organic Chemistry*” 3rd Edition, Wiley-Interscience, New York, 1984.
- 51 J. E. Rie and J. P. Oliver, *J. Organomet. Chem.* 1977, **133**, 147
- 52 E. C. Alyae, D. C. Bradley, M. F. Lappert and A. R. Sanger, *Chem. Commun.*, 1969, 495

- 53 D. C. Bradley, M. H. Chisholm, M. W. Extine and M. E. Stager, *Inorg. Chem.*, 1977, **16**, 1794
- 54 A. D. Jenkins, M. F. Lappert and R. C. Srivastava, *J. Organomet. Chem.*, 1970, **23**, 165.
- 55 D. C. Bradley and I. M. Thomas, *Can. J. Chem.*, 1962, **40**, 1355
- 56 D. C. Bradley and M. H. Chisholm, *J. Chem. Soc., (A)*, 1971, 1511.
- 57 C. E. Heath and M. B. Hursthouse, *Chem. Commun.*, 1971, 143.
- 58 D. C. Bradley, M. H. Chisholm, C. E. Heath, and M. B. Hursthouse, *Chem. Commun.*, 1969, 1261.
- 59 R. J. Gillespie, *J. Chem. Soc.*, 1963, 4672.
- 60 A. S. Batsanov, A. V. Churakov, J. A. K. Howard, A. K. Hughes, A. L. Johnson, A. J. Kingsley, I. S. Neretin and K Wade, *J. Chem. Soc. Dalton Trans.*, 1999 3867.
- 61 K. Hagen, C. J. Holwill, D. A. Rice and J. D. Runnacles, *Inorg. Chem.*, 1992, **31**, 4733.
- 62 D. C. Bradley and M. H. Chisholm, *Acc. Chem. Res.*, 1976, **9**, 273.
- 63 A. J. Kingsley, PhD Thesis, University of Durham, 1998.
- 64 L. Wesemann, M. Trinkaus and M. Ruck, *Angew. Chem., Int. Ed. Engl.*, 1999, **38**, 2375.
- 65 (a) A. R. Siedle, G. M. Bodner and L. J. Todd, *J. Organomet. Chem*, 1971, **33**, 137. (b) P. Jutzi, P. Galow, S. Abu-Orabi, A. M. Arif A. H. Cowley and N. C. Norman, *Organometallics* 1987, **6**, 1024. (c) J. Buchanan, E. J. M. Hamilton, D. Reed and A. J. Welch, *J. Chem. Soc., Dalton Trans.*, 1990, 677.
- 66 T. B. Marder, R. T. Baker, J. A. Long, J. A. Doi and M. F. Hawthorne, *J. Am. Chem. Soc.*, 1981, **103**, 2988.
- 67 W. A. Nugent and R. L. Harlow, *J. Chem. Soc., Chem. Commun.*, 1978, 579.
- 68 A. Martín, M. Mena, C. Yélamos, R. Serrano and P. R. Raithby, *J. Organomet. Chem.*, 1994, **467**, 79.

- 69 (a) W. A. Herrmann, W. A. Baratta and E. Herdtweck, *Angew. Chem., Int. Ed. Engl.*, 1996, **35**, 1951; (b) W. A. Herrmann, W. A. Baratta and E. Herdtweck, *J. Organomet. Chem.*, 1997, **541**, 445.
- 70 (a) M. H. Chisholm, F. A. Cotton, B. A. Frenz, W. W. Reichert, L. W. Shive and B. R. Stults, *J. Am. Chem. Soc.*, 1976, **89**, 4469; (b) M. H. Chisholm, F. A. Cotton, M. Extine and B. R. Stults, *J. Am. Chem. Soc.*, 1976, **89**, 4477.
- 71 M. G. Davidson, T. G. Hibbert, J. A. K. Howard, A. Mackinnon and K. Wade, *J. Chem. Soc., Chem. Commun.*, 1996, 2285.
- 72 A search of the April 1999 release of the Cambridge Structural Database revealed 33 examples of structurally characterised 2,1,7-MC₂B₉H₁₁ clusters. F. H. Allen and O. Kennard, *Chemical Design Automation News*, 1993, **8**, 1; 31.
- 73 (a) M. K. Kaloustian, R. J. Wiersema and M. F. Hawthorne, *J. Am. Chem. Soc.*, 1972, **94**, 6679; (b) T. P. Hanusa and L. J. Todd, *Polyhedron*, 1985, **4**, 2063.
- 74 J. Crowe, E. J. M. Hamilton, J. C. V. Laurie and A. J. Welch, *J. Organomet. Chem.*, 1990, **394**, 1
- 75 A. Zalkin, T. E. Hopkins and D. H. Templeton, *Inorg. Chem.*, 1966, **5**, 1189.
- 76 I. Blandford, J. C. Jeffery, P. A. Jelliss and F. G. A. Stone, *Organometallics*, 1998, **17**, 1402.
- 77 M. F. Hawthorne, *J. Organomet. Chem.*, 1975, **100**, 97.
- 78 V. C. Gibson, *J. Chem. Soc., Dalton Trans.*, 1994, 1607.
- 79 W. A. Nugent and R. L. Harlow, *J. Chem. Soc., Chem. Commun.*, 1978, 579.
- 80 M. H. Chisholm and M. W. Extine, *J. Am. Chem. Soc.*, 1977, **99**, 782; (b) M. H. Chisholm and M. W. Extine, *J. Am. Chem. Soc.*, 1975, **97**, 1623.
- 81 (a) A. Behr, in “*Catalysis in C₁ Chemistry*”, Ed. W. Keim, Reidel Publishing, Dordrecht, 1983; (b) D. J. Darensbourg and R. A. Kudarowski, *Adv. Organomet. Chem.*, 1983, **22**, 129.

- 82 H. Hoberg, K. Jennii, K. Angermund and C. Kruger, *Angew. Chem., Int. Ed. Engl.*, 1987, **26**, 153.
- 83 I. K. Bezougli, A. Bashall, M. McPartlin and D. M. P. Mingos *J. Chem. Soc., Dalton Trans.*, 1998, 2671.
- 84 (a) Y. Sasaki and P. H. Dixneuf, *J. Org. Chem.*, 1987, **52**, 314; (b) M. H. Chisholm and M. Extine, *J. Am. Chem. Soc.*, 1974, **96**, 6214; (c) M. H. Chisholm and M. Extine, *J. Am. Chem. Soc.*, 1975, **97**, 1623.
- 85 (a) T. Tetsuda, K. Watanabe, K. Miyata, H. Yamamoto and T. Saegusa, *Inorg. Chem.*, 1981, **20**, 2728; (b) A. Belforte and F. Calderazzo, *J. Chem. Soc., Dalton Trans.*, 1989, 1007.
- 86 (a) Y. Yoshida and S. Inoue, *Bull. Chem. Soc. Jpn.*, 1978, **51**, 559; (b) Y. Yoshida, S. Ishii, A. Kwato, T. Yamashita, M. Yano and S. Inoue, *Bull. Chem. Soc. Jpn.*, 1988, **61**, 2913; (c) Y. Yoshida and S. Inoue, *Polym. J.*, 1980, **12**, 763.
- 87 (a) D. B. D. Amico, F. Calderazzo and U. Giurlani, *J. Chem. Soc., Chem. Commun.*, 1986, 1000; (b) A. Belfore, D. B. Dellamico, F. Calderazzo, U. Giurlani and L. Labella, *Gazz. Chimica. Ital.*, 1993, **123**, 119.
- 88 D. A. Femec, T. L. Groy and R. C. Fay, *Acta Cryst.*, 1991, **C47**, 1811.
- 89 (a) F. Calderazzo, S. Lanelli, G. Pampaloni, G. Pelizza and M. Sperrle, *J. Chem. Soc., Dalton Trans.*, 1991, 693; (b) P. B. Arimondo, F. Calderazzo, U. Englert, C. M. Mossmer, G. Pampaloni and J. Strahle, *J. Chem. Soc., Dalton Trans.*, 1996, 311.
- 90 W. L. Steffen, H. K. Chun and R. C. Fay, *Inorg. Chem.*, 1978, **17**, 3498.
- 91 A. H. Bruder, R. C. Fay, D. F. Lewis and A. A. Sayler, *J. Am. Chem. Soc.*, 1976, **98**, 6932.
- 92 (a) L. S. Tan, G. V. Goeden and B. L. Haymore, *Inorg. Chem.*, 1983, **22**, 1744; (b) E. O. Bishop, G. Butler, J. Chatt, J. R. Dilworth, G. J. Leigh, D. Orchard and M. W. Bishop, *J. Chem. Soc., Dalton Trans.*, 1978, 1655.
- 93 F. Montilla, A. Pastor, A. Monge, E. G. Puebla and A. Galindo, *J. Chem. Soc., Dalton Trans.*, 1999, 2893.

Chapter Three – Dicarbollide Complexes of Group Five Metals

- 94 D. F. Lewis and R. C. Fay, *J. Am. Chem. Soc.*, 1974, **96**, 3843.
- 95 R. C. Fay, J. R. Weir and A. H. Bruder, *Inorg. Chem.*, 1984, **23**, 1079.
- 96 H. M. Gau and R. C. Fay, *Inorg. Chem.*, 1987, **26**, 3701.
- 97 J. E. Lloyd and K. Wade, *J. Chem. Soc.*, 1964, 1649.
- 98 J. R. Jennings, J. E. Lloyd and K. Wade, *J. Chem. Soc.*, 1965, 5083
- 99 J. R. Jennings and K. Wade, *J. Chem. Soc.*, 1967, 1222.
- 100 (a) K. Jones and M. F. Lappert, *Proc. Chem. Soc.*, 1964, 22; (b) T. A. George, K. Jones and M. F. Lappert, *J. Chem. Soc.*, 1965, 2157.
- 101 W. C. E. Higginson and N. S. Wooding, *J. Chem. Soc.*, 1952, 1178.
- 102 (a) E. Perry, *Makromol. Chem.*, 1963, **65**, 145; (b) L. J. Hughes and E. Perry, *J. Polym. Sci.*, 1965, **A3**, 1527.
- 103 A. D. Jenkins, M. F. Lappert and R. C. Srivastava, *Polymer Letters*, 1968, **6**, 865.
- 104 (a) A. D. Jenkins, M. F. Lappert and R. C. Srivastava, *Euro. Polymer Jnl.*, 1971, **7**, 289; (b) N. C. Billingham, *Euro. Poymer Jnl.*, 1972, **8**, 1045; (c) N. C. Billingham, L. M. Boxall, A. D. Jenkins and P. D. Lees, *Euro. Poymer Jnl.*, 1974, **10**, 981; (d) N. C. Billingham, L. M. Boxall, A. D. Jenkins and P. D. Lees, *Euro. Poymer Jnl.*, 1974, **10**, 991; (e) N. C. Billingham and A. D. Jenkins, *App. Polymer Symp.*, 1975, **26**, 13.
- 105 C. Boisson, J. C. Berthet, M. Ephritikine, M. Lance and M. Nierlich, *J. Organomet. Chem.*, 1996, **522**, 249.
- 106 C. Boisson, J. C. Berthet, M. Lance, M. Nierlich and M. Ephritikine, *J. Organomet. Chem.*, 1997, **548**, 9.
- 107 (a) T. A. George, K. Jones and M. F. Lappert, *Chem. Commun.*, 1966, 463; (b) T. A. George, K. Jones and M. F. Lappert, *J. Chem. Soc. (A)*, 1969, 992.
- 108 D. J. Cardin and M. F. Lappert, *Chem. Commun.*, 1967, 1034.
- 109 A. Dormond, A. Aaliti and C. Moïse, *J. Chem. Soc., Chem. Commun.*, 1985, 1231.

- 110 P. Zanella, N. Brianese, U. Casellato, F. Ossola, M. Porchia, G. Rossetto and R. Graziani, *J. Chem. Soc., Dalton Trans.*, 1987, 2039.
- 111 M. H. Chisholm, C. E. Hammond, D. Ho and J. C. Huffman, *J. Am. Chem. Soc.*, 1986, **108**, 7860.
- 112 Z. Z. Wu, J. B. Diminno and Z. L. Xue, *Organometallics*, 1999, **18**, 1002.
- 113 M. Galakhov, P. Gómez-Sal, A. Martín, M. Mena and C. Yélamos, *Eur. J. Inorg. Chem.*, 1998, 1319.
- 114 H. Nöth and M. Schmidt, *Organometallics*, 1995, **14**, 6601.
- 115 R. A. Kresinski, L. Isam, T. A. Hamor, C. J. Jones and J. A. McCleverty, *J. Chem. Soc., Dalton Trans.*, 1991, 1835.
- 116 O. J. Curnow, M. D. Curtis, A. Rheingold and B. S. Haggerty, *Inorg. Chem.* 1991, **30**, 4043.
- 117 K. Tatsumi, I. Matsubara, Y. Inoue, A. Nakamura, K. Miki and N. Kasai, *J. Am. Chem. Soc.*, 1989, **111**, 7766.
- 118 S. M. Koo, R. Bergero, A. Salifoglou and D. Coucouvains, *Inorg. Chem.*, 1990, **29**, 4844.
- 119 P. Kubáček, R. Hoffmann and Z. Havalas, *Organometallics*, 1982, **1**, 180.
- 120 R. E. King III, S. B. Miller, C. B. Knobler and M. F. Hawthorne, *Inorg. Chem.*, 1983, **22**, 3548.
- 121 S. B. Miller and M. F. Hawthorne, *J. Chem. Soc., Chem. Commun.*, 1976, 787.
- 122 (a) C. J. Jones, J. N. Francis and M. F. Hawthorne, *J. Am. Chem. Soc.*, 1973, **95**, 7633; (b) M. R. Churchill and K. Gold, *Inorg. Chem.*, 1973, **12**, 1157; (c) J. Plešek, B. Štíbr and S. Heřmánek, *Collect. Czech. Chem. Commun.*, 1984, **49**, 1492.
- 123 M. F. Hawthorne, L. F. Warren Jr., K. P. Calahan and N. F. Travers, *J. Am. Chem. Soc.*, 1973, **95**, 7633.

**PAGE
NUMBERING
AS ORIGINAL**

Chapter Four

Dicarbollide Complexes of

Tungsten (VI):

Synthesis, Structure and Reactivity

4.1 Introduction

The similarities between metal imido, metal cyclopentadienyl and metal dicarbollide complexes have been discussed in chapter one. It was our intention to explore this analogy by synthesising a series of complexes in which an imido ligand is formally replaced by a dicarbollide ligand, the final aim being the synthesis and characterisation of group 6 metal complexes isostructural with systems such as the Schrock alkylidene catalyst shown below.¹

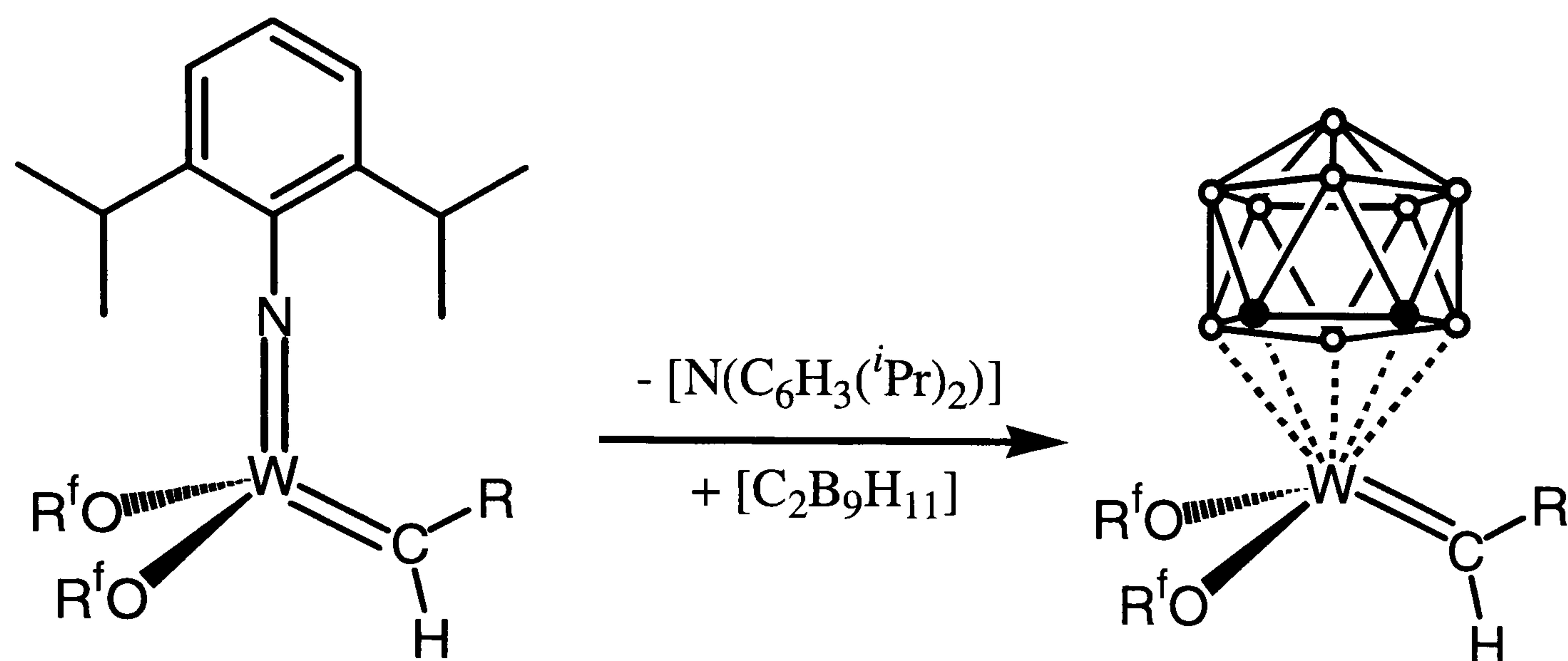


Figure 4.1 Hypothetical replacement of the 2,6-*di*-isopropylphenyl imido, [NAr], ligand in Schrock's catalyst by a dicarbollide ligand, [Cb].

Organoimido complexes^{2,3} have come under considerable scrutiny in recent years, in part due to their presumed involvement in industrial processes such as propylene ammoxidation,⁴ nitrile reduction⁵ and hydrodenitrogenation catalysis.⁶ Although traditionally considered to be inert spectator ligands capable of stabilising high oxidation state metals,⁷ highly reactive $L_nM=NR$ species have been generated that can engage in cycloaddition chemistry,⁸ function as [NR] transfer reagents,⁹ and even activate methane.¹⁰ Carbodiimide metathesis¹¹ and imine metathesis¹² have also been catalysed by imido complexes. A common feature of such reactive complexes is a coordination sphere containing multiple π donor ligands, a feature which has aroused a great deal of interest in so-called “ π -loaded” multiple ligand complexes.

This research group has, for a some time, had an interest in using the relatively under-utilised complex, $[W(N^tBu)_2(NH^tBu)_2]$ (**30**), as a starting material to synthesise complexes which have several π -donor ligands, as in the complexes $[M(\eta^5:\sigma^1-C_5H_5(CH_2)_3NMe)(N^tBu)_2]$ ($M = Mo$ or W).¹³

4.2 Imido Complexes; General Introduction

Transition metal imido complexes, ($M=NR$), constitute one of the richest classes of compounds, both in variety of structural possibilities and the diversity of the chemistry associated with them.¹⁴ The bonding of the $[NR]$ ligands to transition metal centres has been discussed in detail in chapter one. The $[NR]$ ligand can be thought to coordinate to the metal via a metal-nitrogen multiple bond consisting of one σ and either one or two π interactions. A unique set of properties are imparted to the imido ligand as discussed in chapter one.

Many reactions of imido ligands are known, but the reactivity is a sensitive function of the chemical environment and is found to depend on the following:

- i) the d electron count of the transition metal to which it is bound;
- ii) the oxidation state of the metal;
- iii) the nature of other ligands that are present;

These three factors are important because they control the nature of the ligand- p to metal- $d\pi$ interaction, which can sometimes even encompass both the HOMO and LUMO of the complex (see chapter one). For example a more electronegative metal in a higher oxidation state with less competitive π -bonding ligands will increase the π -bonding capability of the nitrogen in the imido. These chemical effects of increasing π donation are summarised in Figure 4.2.

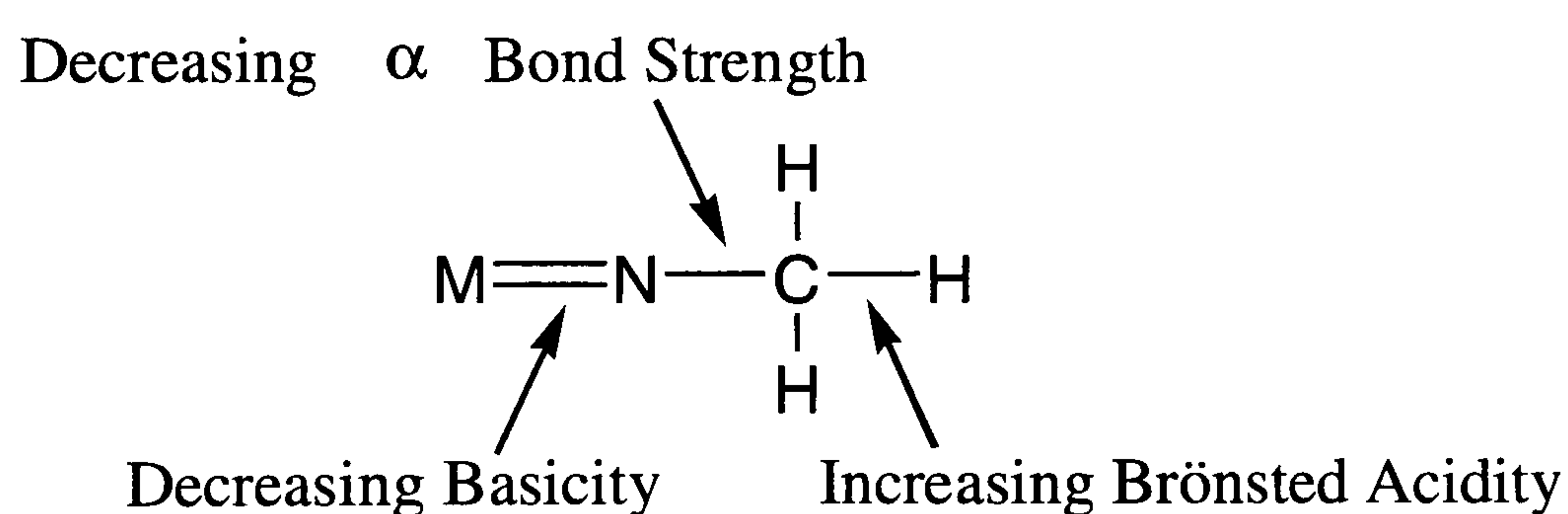


Figure 4.2

A good illustration of the effect of increasing the electronegativity of the metal was provided by Henderson. In the complex $trans-[M(NH)X(dppe)_2]^+X^-$, on changing M from tungsten to molybdenum, the acidity of the imido proton is increased 1000-fold.¹⁵

Numerous reactions of imido complexes with electrophiles have been reported, and reactions with excess electrophile often result in complete removal of the imido ligand from the metal.

The capacity of the imido ligand to act as a $1e^-$, $3e^-$ or $5e^-$ ligand has been discussed in detail in chapter one, with the majority of terminally bound imido ligands being either $3e^-$ or $5e^-$ donor ligands.¹⁶ An indication of whether an imido ligand is acting as a $3e^-$ or a $5e^-$ donor comes from the M-N-R angle of the organoimido system. Angles of 180° imply sp -hybridisation while, bending suggests a component of sp^2 -hybridisation and a lone pair at the nitrogen. Compared to other multiply bound ligands in compounds such as alkylidyne or vinylidene complexes, imido ligands are found to have M-N-R angles over a larger range than that found in M-C-R angles, usually from 150° to 180° . This suggests that almost all terminal imido ligands have essentially sp -hybridised nitrogen and close to a M-N triple bond.

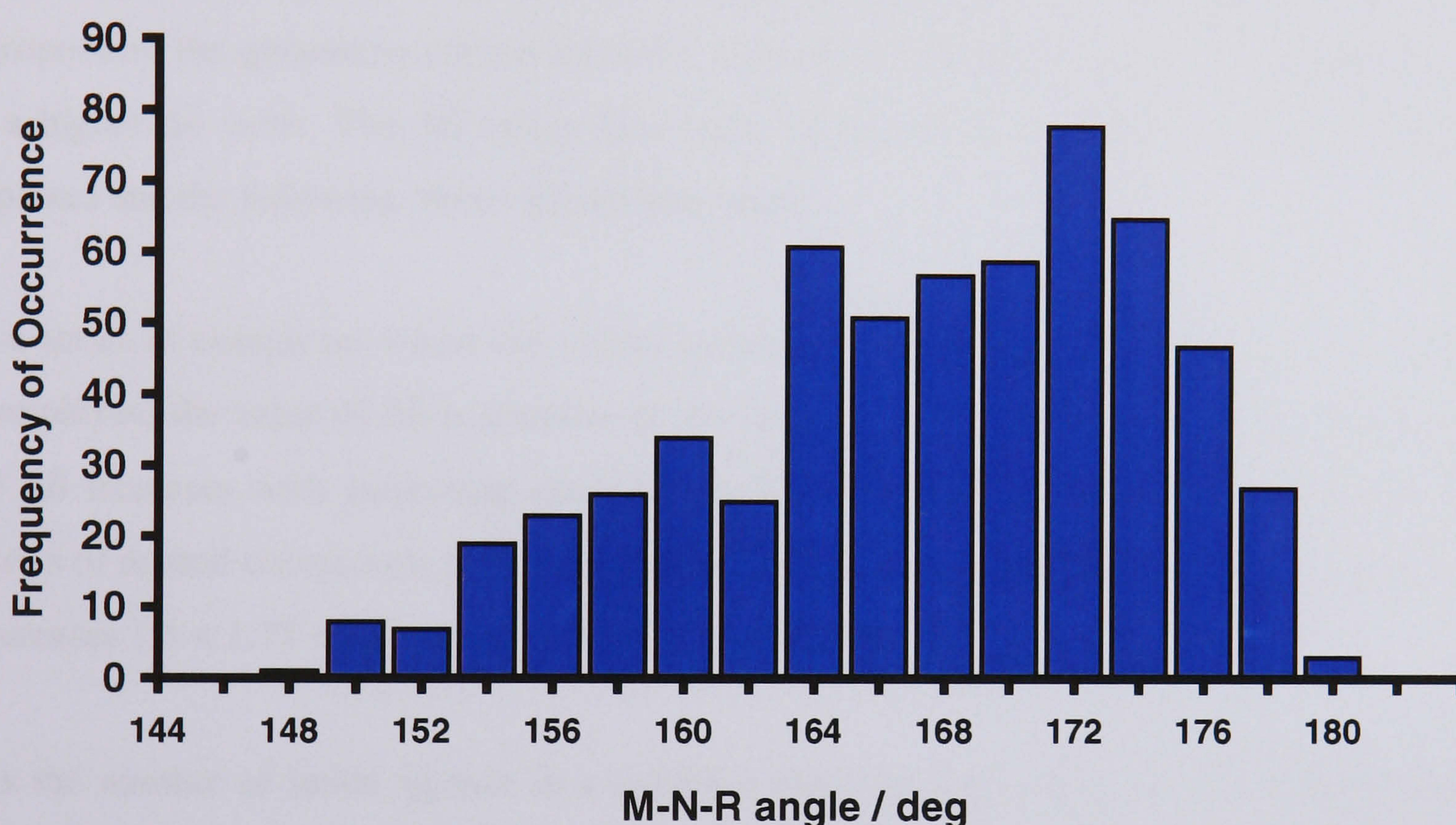


Figure 4.3 Histogram showing angles of M-N-R for terminal imido ligands in metal organoimido complexes. Data taken from the Cambridge Structural Database.¹⁷

Imido ligands are predicted to be bent if the metal centre to which they are bound does not have two π -symmetry orbitals to bind to the nitrogen. This case most often occurs in octahedral complexes with multiply bonded ligands sharing the three d_π symmetry orbitals. Examples of strongly bent imido ligands with R-N-M angles of ~ 128 - 129° are found in several complexes, all of which contain more than one π -donor ligand.¹⁸ Such investigations into the bonding of the imido ligand can only be conducted if crystals suitable for single crystal X-ray diffraction experiments are able to be grown and the experiments performed. In many cases crystals cannot be grown and the bonding interaction of the imido ligand with the metal can only be approximated.

4.2.1 ^{13}C NMR Spectroscopy

It has been reported that the difference between the ^{13}C NMR chemical shifts for α and β carbon atoms of d^0 transition metal *tert*-butylimido complexes can be used as an appropriate probe into the electronic structure of the ligand.¹⁹ The difference in the ^{13}C NMR chemical shift ($\Delta\delta$) between the quaternary carbon and the methyls of the *tert*-butylimido group [$\delta(\text{CMe}_3) - \delta(\text{CMe}_3)$] has been proposed to afford a qualitative indication of the degree of electron donation from the imido group to the metal centre. The contribution from the lone pair of the nitrogen in a metal-imido bond has an effect on the electronic nature of the adjacent quaternary carbon and therefore the chemical shift. The greater the contribution of the lone pair, the more electropositive the quaternary carbon becomes, causing a ^{13}C shift to higher frequencies and in turn a higher $\Delta\delta$ value. The $\Delta\delta$ values have been measured for a number of *tert*-butylimido complexes and the following observations were made:

- i) In a series of complexes where the imido ligand has a similar bond order (e.g., monoimido complexes) the value of $\Delta\delta$ is sensitive to the identity of the metal atom and the magnitude of $\Delta\delta$ increases with increasing electronegativity of the metal atom. For example in the series of related compounds $\text{M}(\text{N}^t\text{Bu})_2(\text{OSiR}_3)_2$ where $\text{M} = \text{W}, \text{Mo}, \text{Cr}$, the electronegativity increases $1.5 < 1.75 < 2.3$ and $\Delta\delta$ increases $33 < 37 < 46$.²⁰
- ii) As the number of imido ligands in a complex increases (and hence as their π -bond order decreases) the value of $\Delta\delta$ falls. This is seen most clearly in the series $\text{Os}(\text{N}^t\text{Bu})_n\text{O}_{(4-n)}$; the magnitude of $\Delta\delta$ decreases $55 > 46 > 41$ for $n = 1, 2$ and 3 respectively.¹²
- iii) There is some dependence on the ancillary ligands present but their effect is much smaller than is the nature of the metal atom.

In general, the lower the electronegativity of the metal atom and the more *tert*-butylimido groups and ancillary groups present, the smaller the contribution from the imido lone pair and consequently a smaller $\Delta\delta$ value will be observed.

A qualitative indication of electron donation from the imido group to the metal centre, and the effects of ancillary ligands on the donation ability, has been explored, and the results from several complexes are tabulated against each other, so that comparisons can be drawn (Table 4.1).

Included in the Table is the *bis*-imido *bis*-amide complex, $W(N^tBu)_2(NH^tBu)_2$ and also a mono *tert*-butyl imido complex, $W(N^tBu)Cl_3(C_5H_5)$.

$W(N^tBu)_2$ complexes ⁽ⁱ⁾	$\Delta\delta/ppm$	Ref.
$W(N^tBu)_2(NH^tBu)_2^{(ii)} (20e^-)$	32.2	21
$W(N^tBu)Cl_3(C_5H_5) (18e^-)$	49.1	22
$W(N^tBu)_2Cl_2py (18e^-)$	37.9	23
$W(N^tBu)_2(C_5H_5)Cl (20e^-)$	35.8	23
$W(N^tBu)_2(C_5H_5)Me (20e^-)$	33.9	22
$[W(N^tBu)(\mu-N^tBu)Me_2]_2 (16e^-)^{(ii)}$	33.8	24
$[W(N^tBu)(\mu-N^tBu)_3(\mu-Li)_2]_2^{(ii)}$	24.0	25

- i) formal electron count in brackets.
- ii) $\Delta\delta$ for terminal imido groups only.

Table 4.1

Further studies on *iso*-propyl complexes have shown a similar relationship to that observed in the *tert*-butyl complexes.²⁶ ¹³C NMR data for arylimido complexes have also been examined and have shown that the *ipso*- and *para*- positions in the ring are the most sensitive to demand for electron density in the metal with the *ipso*- carbon the most deshielded, and the shielding on the *para*- carbon being the greatest.²⁷

4.3 Tungsten (VI) Imido Dicarbollide Complexes.

As discussed in chapter one, the dicarbollide chemistry of group 6 has been dominated for some time by the work of Stone and co-workers,²⁸ but to the best of our knowledge very few complexes containing W(VI) or Mo(VI) have been presented in the general chemical literature.

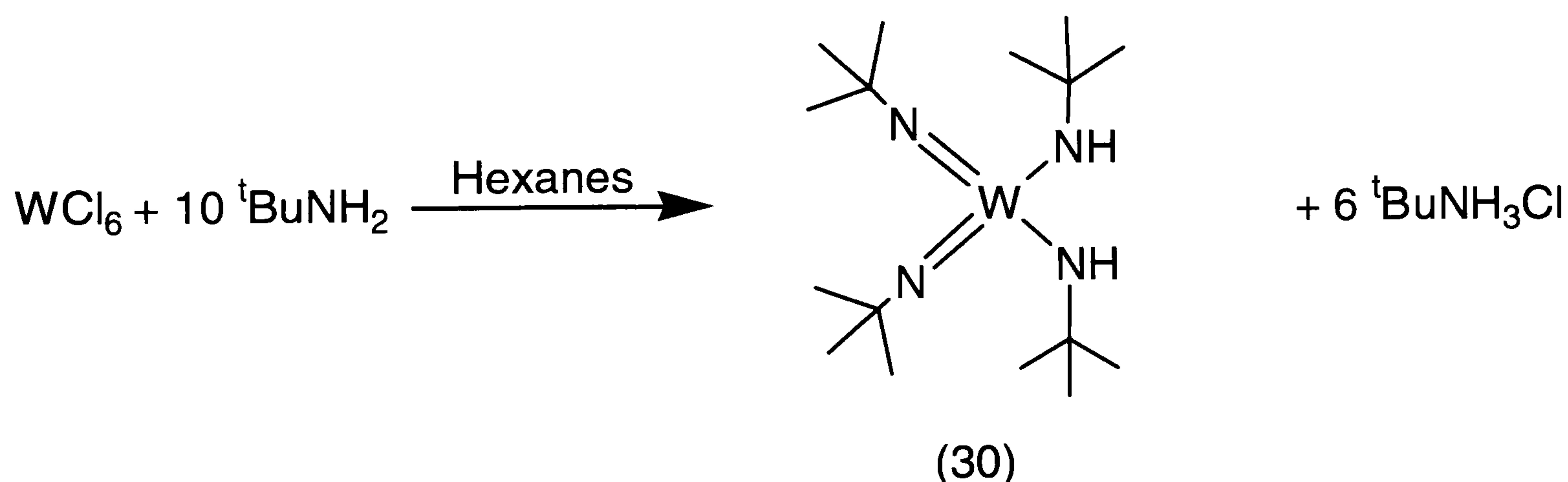
Y. Do and co-workers synthesised both $[Ph_3P-p\text{-xylyl-PPh}_3]_2[(\eta^5-C_2B_9H_{11})MoO_2-(\mu-O)-MoO_2(\eta^5-C_2B_9H_{11})]$ and $[NMe_4]_2[(\eta^1-C_2B_9H_{11})MoO_3]$ from the oxidation of the dithiolate complex $[NMe_4]_2[(\eta^5-C_2B_9H_{11})Mo(CO)_2(SPh)_2]$ with a 4-fold molar amount of iodosylbenzene in the presence of different cations.²⁹ The chemistry and oxidative properties of these and other compounds have been discussed elsewhere.³⁰

Chapter Four – Dicarbollide Complexes of Tungsten (VI)

The only other example of relevance to this work is presented in a U.S. patent by Exxon Chemicals.³¹ The complex $[\text{W}(\eta^5\text{-C}_2\text{B}_9\text{H}_{11})(\text{NAr})(\text{Me})(\text{Cl})]$, ($\text{Ar} = 2,6\text{-dimethylbenzene}$) is prepared from the reaction of [*ortho*- $\text{C}_2\text{B}_9\text{H}_{13}$], (**7**), with the tungsten alkyl complex $[\text{W}(\text{NAr})(\text{Me})_3\text{Cl}]$ with the evolution of two equivalents of methane. As the source of this information by its nature does not reveal clear and precise results, no data for this compound exists in the chemical literature. The patent goes on to report the effectiveness of the tungsten complex in the polymerisation of ethylene in the presence of MAO. The starting material, $[\text{W}(\text{NAr})(\text{Me})_3\text{Cl}]$, is not an attractive complex with which to begin an investigation into such species; the complex itself is not a trivial material to synthesise.³²

In chapter three, group 5 metal amide complexes were shown to react with the acidic carborane, *ortho*- $\text{C}_2\text{B}_9\text{H}_{13}$ in high yields. The analogous group 6 homoleptic amide complexes are difficult to prepare, i.e., it is relatively easy to synthesise $[\text{M}(\text{NMe}_2)_5]$ from MCl_5 ($\text{M} = \text{Nb}$ or Ta) and $\text{Li}(\text{NMe}_2)$, whereas the analogous MCl_6 ($\text{M} = \text{W}$, Mo) yields mixtures of $\text{M}(\text{NMe}_2)_6$ and $\text{M}_2(\text{NMe}_2)_6$. Therefore $\text{M}(\text{NMe}_2)_6$ ($\text{M} = \text{W}$, Mo) is prepared from MCl_4L_2 ($\text{L} = \text{THF}$, Et_2O) and LiNMe_2 giving very low yields (16% for W).³³ Furthermore, $\text{M}(\text{IV})$ complexes such as the homoleptic amides $\text{M}(\text{NMe}_2)_4$ ($\text{M} = \text{W}$, Mo) are paramagnetic.

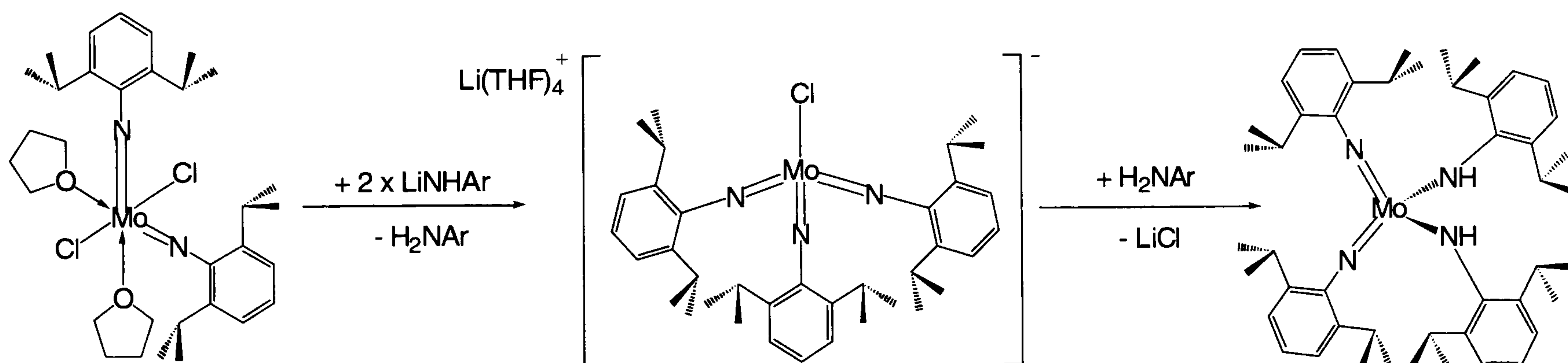
Difficulties synthesising $\text{M}(\text{NMe}_2)_6$ ($\text{M} = \text{Mo}$, W) led us to seek alternative molybdenum and tungsten(VI) amide reagents as starting materials to react with the neutral ligand. The *bis*-(*tert*-butyl imido)(*bis-tert*-butyl amide)tungsten(VI) complex (**30**) can be readily synthesised from the reaction of tungsten hexachloride and ten equivalents of *t*-butylamine.^{21a}



Although the unit cell of (**30**) has been published, the molecular structure has not been determined due to large amounts of disorder.^{21b} In contrast X-ray crystallography has shown the *iso*-propyl analogue $[\text{W}(\mu\text{-NPr}^i)(\text{NPr}^i)(\text{NHPr}^i)_2]_2$ to form a dimeric complex in the solid state.³⁴

Complex (30) has been shown to undergo reactions with weak protic acids, such as 2-hydroxypyridine and 8-hydroxyquinoline to form the alkoxy imido complexes $[W(N^tBu)_2(ONC_4H_4)_2]$ and $[W(N^tBu)(OC_9H_6N)_2]$ respectively.³⁵ Deprotonation of the amide groups is achieved by metal alkyls such as MeLi to form $[Li_2W(N^tBu)_4]$,²⁵ and AlMe₃ to form $[W\{(\mu-N^tBu)_2AlMe_2\}_2]$.³⁶ The insertion chemistry of isocyanates with the series of complexes $[M(N^tBu)_2(NH^tBu)_2]$ (M = Cr, Mo and W) has also been investigated,^{18b} but it was only very recently that the first substitution of one of the amide ligands for a cyclopentadienyl group was achieved.¹³

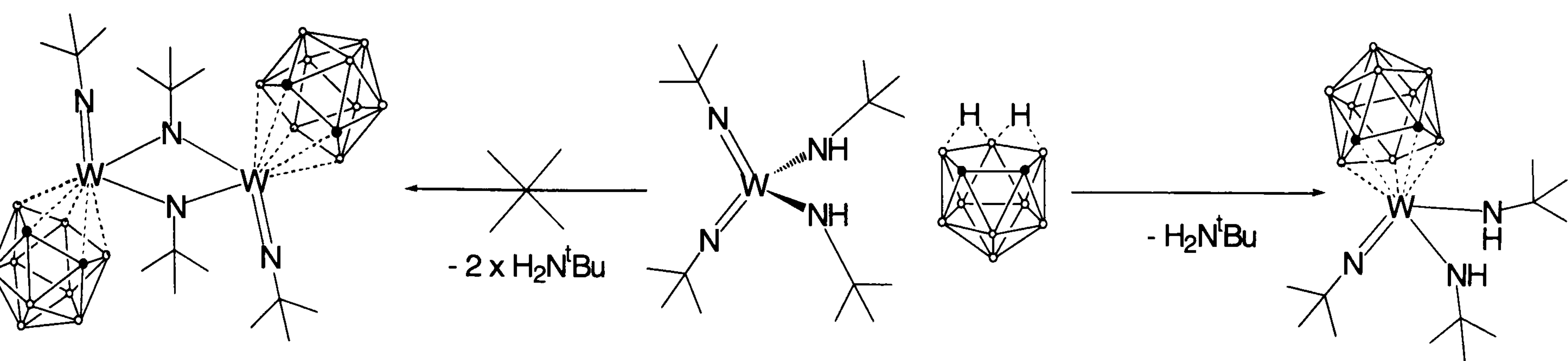
It was envisaged that reaction of the tungsten complex *bis(tert-butylimido)bis(tert-butylamide)tungsten* (VI), (30), with the acid *nido*-7,8- $C_2B_9H_{13}$ would result in the formation of the *bis*-imido dicarbollide complex $[W(\eta^5-C_2B_9H_{11})(N^tBu)_2]$ which would be analogous to some of the *tris*-imido complexes synthesised by Wigley and co-workers.³⁷ The reasoning behind this assumption was that Wigley showed that the *tris*-imido product was the kinetic product in the reaction of $[Mo(NAr)_2Cl_2(THF)_2]$ with 2 equivalents of LiNHAr in THF Scheme 4.1.³⁸



Scheme 4.1 Reaction of $[Mo(NAr)_2Cl_2(THF)_2]$ with 2 equiv. of LiNHAr in THF results in the isolation of the kinetic product $[Li(THF)_4][W(NAr)_3Cl]$. The chloro adduct reacts further with free aniline over time to form the *bis*-imido *bis*-amide complex $[W(NAr)_2(NHAr)_2]$.

4.3.1 Synthesis of $[W(N^tBu)(NH^tBu)_2(ortho-C_2B_9H_{11})]$

It was thought that reaction of the tungsten complex, (30), with the carborane *ortho*- $C_2B_9H_{13}$ would result in the evolution of two equivalents of *tert*-butyl amine and the formation of the *bis*-imido dicarbollide complex, shown below, as a bridged dimer. This was found not to be the case.



Scheme 4.2 Proposed reaction between [W(N^tBu)₂(NH^tBu)₂] and C₂B₉H₁₃.

The neutral carborane, (7), indeed reacts with [W(N^tBu)₂(NH^tBu)₂] in toluene to evolve only one equivalent of amine and form the monomeric imido carborane complex [W(N^tBu)(η⁵-C₂B₉H₁₁)(NH^tBu)₂], (31). This compound is highly air- and moisture- sensitive changing colour from a golden yellow to blue on contact with either.

Table 4.2 Selected bond lengths (Å) and angles (°) in (31).

W-N(1)	1.721(3)	Cb-W-N(1)	124.5(3)	N(1)-C(11)	1.472(5)
W-N(2)	1.955(3)	Cb-W-N(2)	113.0(3)	N(2)-C(21)	1.472(6)
W-N(3)	1.949(4)	Cb-W-N(3)	109.7(3)	N(3)-C(31)	1.496(5)
W-C(1)	2.531(4)				
W-C(2)	2.572(4)	N(1)-W-N(2)	101.7(2)	W-N(1)-C(11)	165.3(3)
W-B(3)	2.507(4)	N(1)-W-N(3)	105.6(2)	W-N(2)-C(21)	1.41.6(3)
W-B(4)	2.437(4)	N(2)-W-N(3)	99.2(2)	W-N(3)-C(31)	1.34.8(3)
W-B(5)	2.392(4)	C(1)-C(2)	1.567(5)		
		C(1)-B(5)	1.693(6)	N(2)-H(2N)	0.88()
W-Cb	2.026(4)	C(2)-B(3)	1.690(6)	N(3)-H(3N)	0.94(6)
		B(3)-B(4)	1.764(6)		
		B(4)-B(5)	1.787(6)		

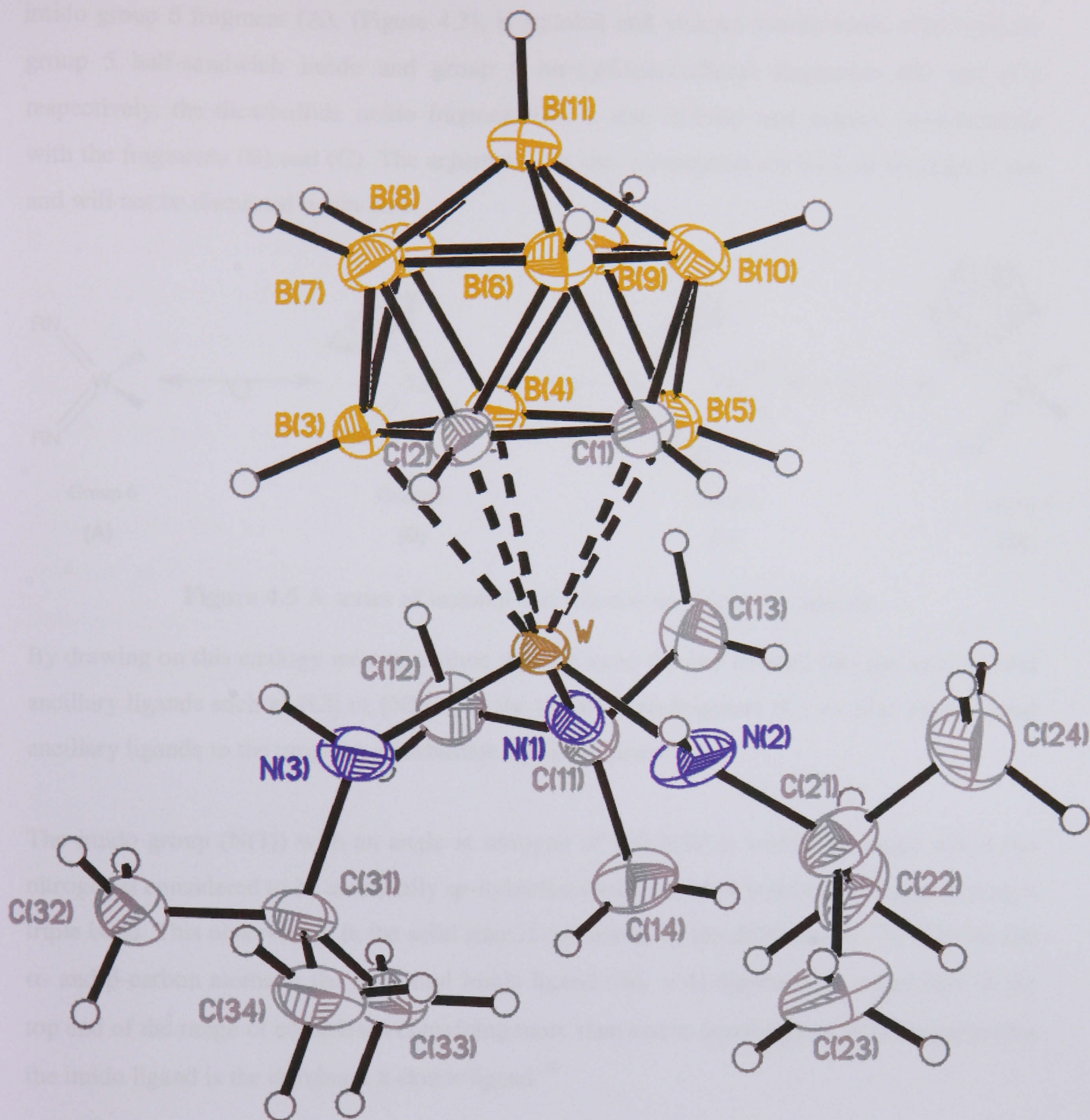


Figure 4.4 Molecular structure of the complex $[W(N^tBu)(NH^tBu)_2(ortho-C_2B_9H_{11})]$, (31). Thermal ellipsoids are shown at 50% probability, and hydrogen atoms as hollow spheres.

The molecular structure of the complex $[W(N^tBu)(NH^tBu)_2(ortho-C_2B_9H_{11})]$, (31), is shown in Figure 4.4 and selected bond lengths are given in Table 4.2. The asymmetric unit also contains one molecule of toluene which has a methyl group disordered over two adjacent sites on the ring. Tables containing complete crystallographic data can be found in the appendix.

Complex (31) can be viewed as a metallocene analogue by virtue of the fact that, since the bis-imido group 6 fragment (A), (Figure 4.5), is isolobal and valence isoelectronic with both the group 5 half-sandwich imido and group 4 bis-cyclopentadienyl fragments (B) and (C), respectively, the dicarbollide imido fragment (D) is also isolobal and valence *iso*-electronic with the fragments (B) and (C). The arguments for this assumption are laid out in chapter one and will not be discussed again here.

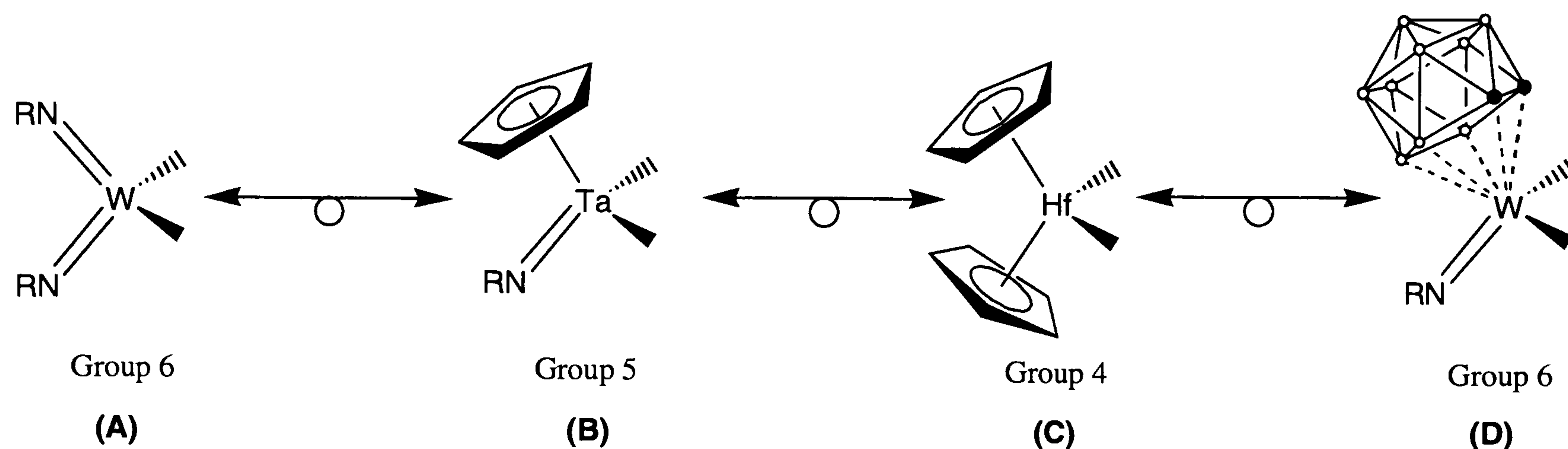


Figure 4.5 A series of isolobal and valence iso-electronic species.

By drawing on this analogy we can assume that the same frontier orbitals that are used to bind ancillary ligands such as [Cl] or [NMe₂] to the metallocene fragment (C) are also used to bind ancillary ligands to the tungsten dicarbollide imido fragment (D).

The imido group (N(1)) with an angle at nitrogen of 165.3(3)^o is within the range where the nitrogen is considered to be essentially *sp*-hybridised with the M-N bond closely approaching a triple bond. This observation in the solid state is confirmed by the difference in ¹³C shift for the α - and β -carbon atoms in the *tert*-butyl imido ligand ($\Delta\delta_c = 41.5\text{ppm}$). This value falls at the top end of the range of complexes containing more than one π -donor ligand. This suggests that the imido ligand is the dominant π -donor ligand.³⁹

The two amide ligands (NH^tBu) in (31) are both planar (sum of angles around N(2) is 358.6^o, and N(3) is 359.9^o), indicating *sp*²-hybridisation of the nitrogen atoms. Both amide ligands orientate themselves so that the *tert*-butyl groups are pointing away from the carborane ligand (Cb-W-N(2)-C(21) torsion angle is ~115^o, and Cb-W-N(3)-C(31) torsion angle is ~180^o). Similar ligand orientations are observed in the analogous bis-cyclopentadienyl amide complexes of group 4 metals.⁴⁰ For d⁰ Cp₂M(NR₂)₂ complexes, which are related to complex (31), M-N π -donation is maximised when the NR₂ ligand lies perpendicular to the N-M-N plane, i.e., the dihedral angle is 90^o, and minimised when the amide is in a parallel orientation (i.e. 0^o N-M-N/R-N-R).⁴¹

In complex (**31**) the W-N distances, averaging 1.95\AA , are in the range of other W-N amide complexes (1.87\AA - 2.03\AA).⁴² The dihedral angles between the N-W-N plane and the amide H-N-C planes of (**31**) are 60.7° for N(3) and 24.8° for N(2), i.e., the two amide ligands are twisted away from the maximum bonding orientation of 90° by $\sim 29^\circ$ and $\sim 65^\circ$ respectively. This suggests that one amide ligand N(3) is much more strongly bound to the tungsten, as it is able to bind to the $1a_1$ orbital (Figure 4.6). This observation is in contrast to (**31**)'s metallocene cousins in which a dihedral angle of $\sim 55^\circ$ is observed for both ligands, implying M-N bonding which lies between single and double bonds.⁴⁰ The deviation of the larger dihedral angle of the N(2) amide away from 90° is possibly a result of steric interaction between the *tert*-butyl group and the carborane cage. By moving away from the cage these interactions are relieved.

Bercaw previously reported that the H-Hf-N/Me-N-H dihedral angle in $[\text{Cp}^*_2\text{Hf}(\text{H})(\text{NHMe})]$ deviates from the orientation for optimum π -bonding by 27° ,⁴³ this angle is similar to that observed in the tungsten complex (**31**), suggesting exclusive π -donation from the amide into the $1a_1$ orbital, as observed in the Bercaw complex where only one π -ligand is present.

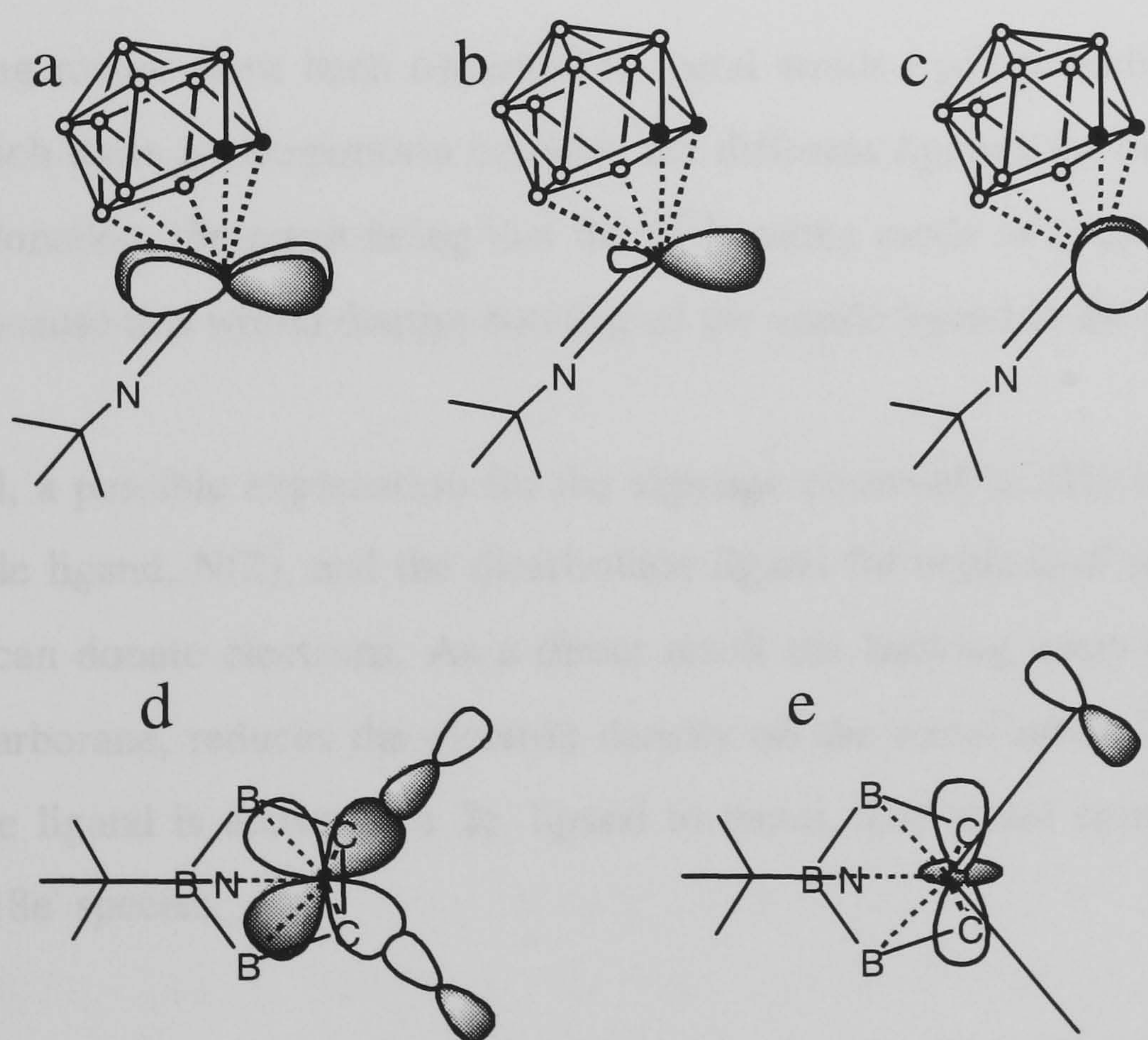


Figure 4.6 Schematic depiction of the (a) $2a_1$, (b), b_2 , and (c) $1a_1$ orbitals of the metallocene fragment analogue $\text{CbM}(\text{NR})$, (d) σ -interaction of the b_2 orbitals of the $\text{CbM}(\text{NR})$ fragment with the ligand σ -orbitals, and (e) π -interaction of one of the ligand π -orbitals with the $1a_1$ orbital.

However, complexes where there is dominance of one of the two π -donor ligands over the other, as in $[\text{Cp}_2\text{Hf}(\text{PR}_2)_2]$ ($\text{R} = \text{Et}, \text{SiMe}_3$), $[\text{Cp}_2\text{Zr}(\text{As}(\text{TMS})_2)_2]$ and $[\text{Cp}_2\text{Zr}(\text{NHPH})(\text{PHMes})]$ adopt structures with one short (double) M-E bond to a planar, sp^2 -hybridized ER_2 group, and one long (single) M-E bond to a pyramidal, sp^3 -hybridised ER_2 group.^{44,45,46} This is not the case in complex (31).

As a direct result of the dominance of the nitrogen ligands in bonding to the tungsten the carborane ligand moves away from the metal centre. The W-Cb distance in (31), 2.026(4) Å, is fractionally longer than that observed in the electronically-loaded 18 electron complex, $[\text{W}(\text{10-CH}_2\text{C}_6\text{H}_4\text{CH}_3\text{-1,2-C}_2\text{B}_9\text{H}_{10})(\text{PPh}_3)_2(\text{CO})_2]$ at 1.95 Å.⁴⁷ The carborane ligand in (31) tilts, with an increase of ~5-7% in the length of the W-C bonds compared to the W-B bonds. This “slippage” of a dicarbollide ligand on an electron rich metal centre has been known for some time in late transition metal dicarbollide complexes such as the d^8 - gold complex $[\text{Au}(\text{S}_2\text{CNEt}_2)(\text{C}_2\text{B}_9\text{H}_{11})]$,⁴⁸ in which the much more pronounced slippage (M-C is 25% longer than M-B) results in a η^3 -bonded dicarbollide cage with only weak ionic interactions between the gold atom and the carbons of the cage.⁴⁹

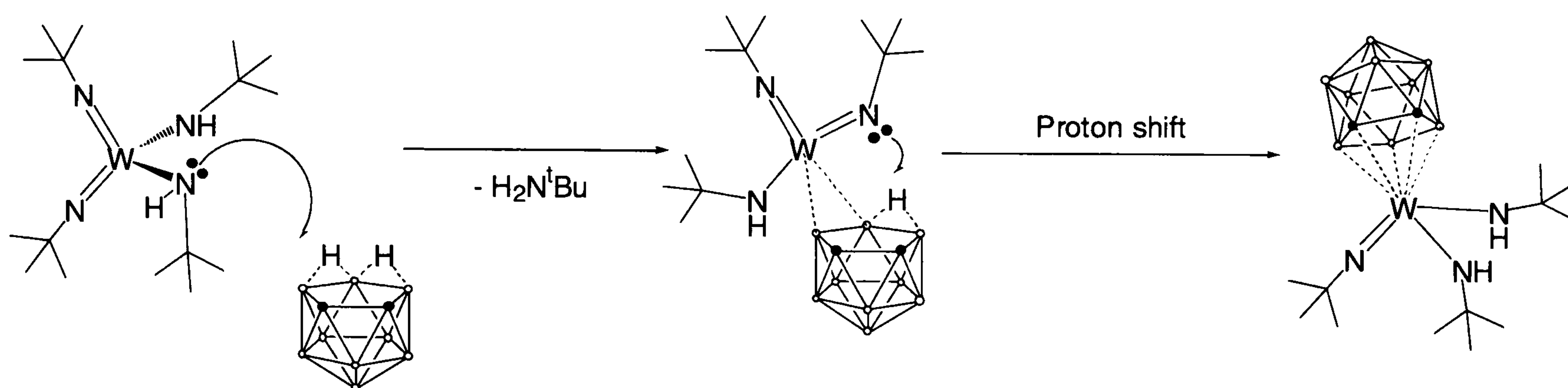
Similar η^3 -bonding modes have been observed in metal amide cyclopentadienyl and indenyl complexes in which there is competition between the different ligands for orbitals of suitable symmetry for π -donation, the result being that the η^5 -bonding mode of [Cp] and [Ind] ligands is not favoured because this would disrupt bonding of the amide ligand to the metal.⁵⁰

With this in mind, a possible explanation for the slippage observed in (31) is the competition between the amide ligand, N(2), and the dicarbollide ligand for orbitals of suitable symmetry into which they can donate electrons. As a direct result the backing away of the weaker π -donor, i.e., the carborane, reduces the electron density on the metal atom. This would mean that the carborane ligand is acting as a $2e^-$ ligand to metal. The metal complex can now be thought of as an $18e^-$ species.

Although there is a significant increase in the W-Cb bond length, the cage orientates itself with the two carbon atoms *trans* to a unique π -ligand, in this instance the imido ligand, with the C-C centroid (C_2) transoid to the imido ligand ($\text{C}_2\text{-Cb-W-N(1)}$ $\tau = -157.9^\circ$). The carbon atom C(1) in the C_2B_3 face lies directly beneath the nitrogen atom of the amide ligand N(2) (C(1)-Cb-W-N(2) $\tau = -180^\circ$).

In solution the solid state inequivalence of the two amide ligands does not persist, with the ^1H and ^{13}C NMR spectra showing the presence of two different ^tBu groups in a 2:1 intensity ratio. This, along with the presence of 5 resonances in the $^{11}\text{B}\{^1\text{H}\}$ NMR spectrum in a 2:2:3:1:1:1 intensity ratio, suggests a C_s symmetric solution state structure for **(31)**.

It is still unclear why this product is preferred over the *bis*-imido complex but a mechanism for the reaction is suggested (Scheme 4.3) in which the tungsten *bis*-imido *bis*-amide complex, **(31)**, is protonated by the acidic carborane (**7**) and loses one equivalent of amine. The carborane is then loosely coordinated to the metal atom and undergoes an intermolecular proton transfer to form the complex **(31)**.

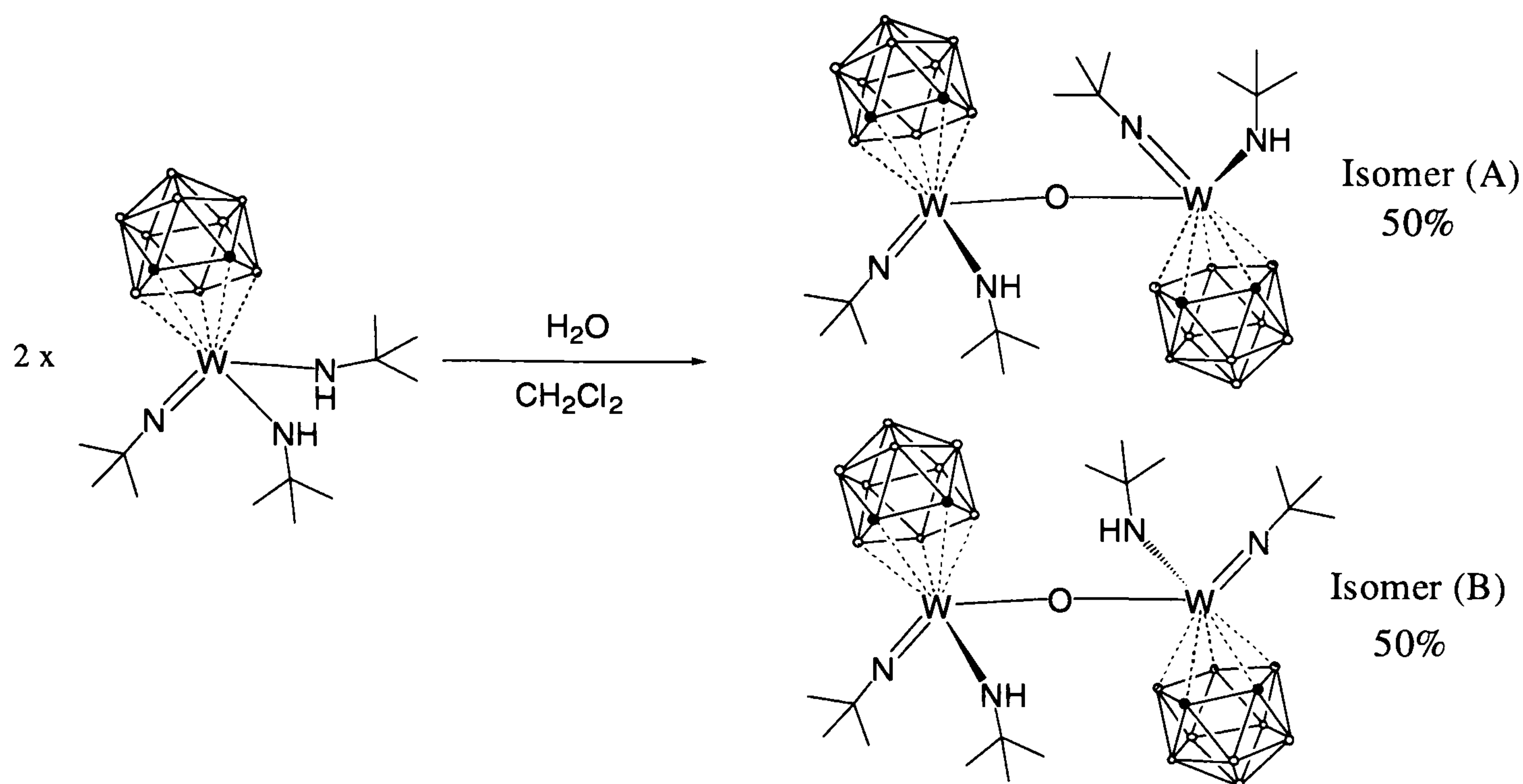


Scheme 4.3 Proposed mechanism for the formation of **(31)**.

4.3.2 Reactions of $[\text{W}(\text{N}^t\text{Bu})(\text{NH}^t\text{Bu})_2(\text{ortho-}\text{C}_2\text{B}_9\text{H}_{11})]$ with Protic Acids.

In one of our many attempts to isolate crystals of **(31)**, crystals of the hydrolysis product $[\{\text{W}(\text{C}_2\text{B}_9\text{H}_{11})(\text{N}^t\text{Bu})(\text{NH}^t\text{Bu})\}_2(\mu\text{-O})]$, **(32)**, were isolated from a solution of dichloromethane layered with pentane in almost 90% yield. This reaction was repeated quantitatively using a saturated solution of water dissolved in dry and degassed dichloromethane.

Attempts to react **(31)** with more than half an equivalent of water resulted in more extensive hydrolysis, turning the solution blue/green. The only isolable product was characterised by $^{11}\text{B}\{^1\text{H}\}$ NMR spectroscopy as a $[\text{ortho-}\text{C}_2\text{B}_9\text{H}_{12}]^-$ containing species, most probably $[\text{tBuNH}_3][\text{ortho-}\text{C}_2\text{B}_9\text{H}_{12}]$.



Scheme 4.4 Synthesis of the bridged oxo complex $[\{W(C_2B_9H_{11})(N^tBu)(NH^tBu)\}_2(\mu-O)]$, (32).

As can be seen from Scheme 4.4, the bridged oxo complex (32) possesses two chiral centres, at the tungsten atoms, this results in the existence of both *rac*- (isomer A) and *meso*-isomers (isomer B).⁵¹ The two isomers possess a C_2 rotational axis and a centre of inversion respectively, which results in the presence of only two CMe_3 resonances in NMR spectra for each of the two isomers. The 1H and ^{13}C NMR spectra of (32) show the presence of 4 independent CMe_3 group resonances in a 1:1:1:1 intensity ratio. This observation is consistent with the solid state observation that the complex (32) exists as racemic, 50:50, mixture of *rac*- and *meso*-isomers.

Both the 1H and ^{13}C NMR spectra show only 2 broad resonances for the cage C-H groups, instead of the expected 8 resonances. This is thought to be caused by a combination of poor resolution of the NMR spectra and close similarity of the resonance shifts.

The poor resolution also results in the $^{11}B\{^1H\}$ and $^1H\{^{11}B\}$ NMR spectra showing only 6 and 9 broad resonances in a 1:1:1:3:2:1 and 2:2:2:2:2:2:2:2:2 intensity ratio respectively. The 1H NMR spectra also shows the presence of two N-H resonances at δ_H 8.07 and 8.1ppm respectively

Crystals of (32), which were suitable for single crystal X-ray diffraction, have been grown in two different solvents, $CDCl_3$ and CH_2Cl_2 . A suitable solution to the data has not been found even after several attempts to solve the structure and model the large amounts of disorder. Although the data is of poor quality and of an unpublishable standard, after collecting the X-

ray diffraction data on this compound 4 times, we are confident that the molecular structure is that shown in Figure 4.7. The disorder observed in the solid state is thought to arise from the co-crystallisation of the *meso*- and *rac*-isomers.

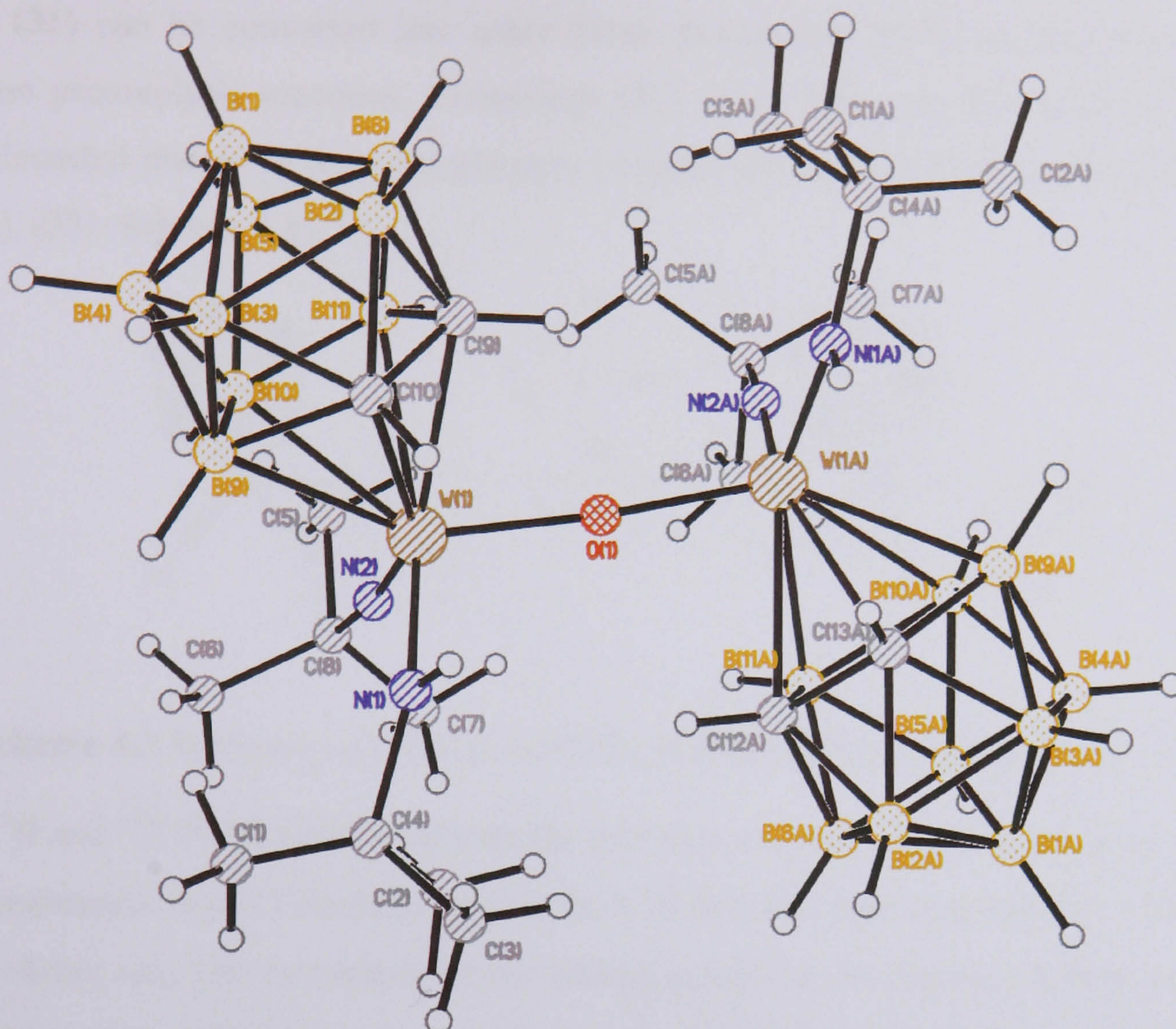


Figure 4.7 Molecular structure of the bridged-oxo complex (32).

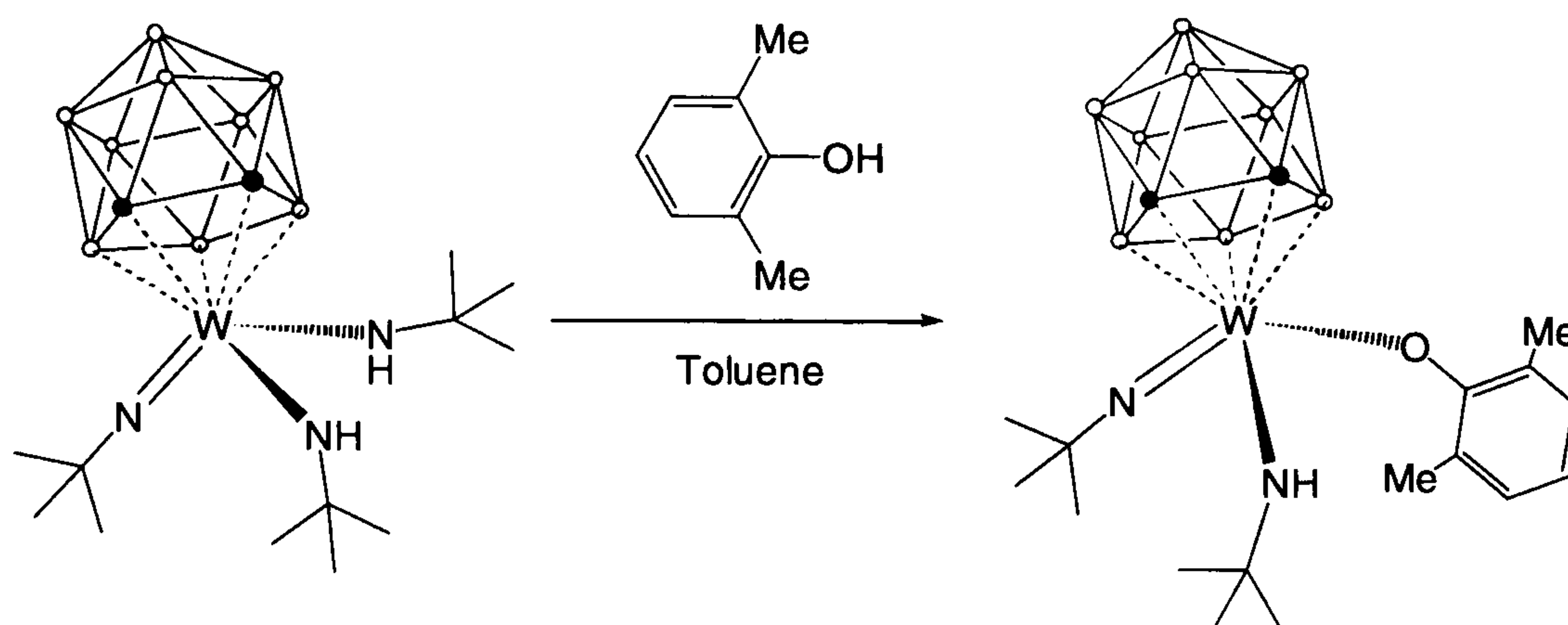
Although no confidence can be placed on the bond lengths and angles, it is clear that the molecule adopts a *transoid* configuration with the two cages as far away from each other as possible.

The structure of CH_2Cl_2 solvate (Figure 4.7) shows large amounts of disorder in a solvent channel with up to approximately two molecules of dichloromethane disordered over multiple sites within that channel. There is also apparent disorder in two of the *tert*-butyl groups attached to the same metal atom. The same metal atom is attached to a carborane cage which also appears to be disordered over two sites which are close to each other.

Although crystallography is unable to help with the question of the number of electrons the imido ligands donate to the metal centre, as bond lengths and bond angles in such a poor quality refinement can not be laboured upon, the ^{13}C NMR spectrum, which shows a single

broad resonance for the α -carbon atoms in the imido group, suggests that $\Delta\delta \sim 41$ ppm, indicating donation of 4 electrons, as expected, to the metal centre from the imido ligands.

Complex (**31**) can be converted into other mono-dicarbollide W(VI) complexes via ligand substitution protonolysis reactions. Compound (**31**) reacts with one equivalent of the protic acid 2,6-dimethyl phenol to form the phenoxy complex $[3\text{-W}(\text{N}^t\text{Bu})(\text{NH}^t\text{Bu})(\text{OC}_6\text{Me}_2\text{H}_3)(1,2\text{-C}_2\text{B}_9\text{H}_{11})]$, (**33**) (Scheme 4.5).⁵²



Scheme 4.5 Synthesis of $[\text{W}(\text{N}^t\text{Bu})(\text{NH}^t\text{Bu})(\text{OC}_6\text{Me}_2\text{H}_3)(\text{ortho-C}_2\text{B}_9\text{H}_{11})]$, (**33**).

Both the ^1H and ^{13}C NMR spectra indicate the presence of a unsymmetric carborane cage with two CH resonances in a 1:1 intensity ratio at δ_{H} 3.18 and 2.81 ppm respectively. The ^1H NMR spectrum shows only one resonance for the methyl groups on the phenoxy ligand, as well as a simple pattern in the aromatic region indicating free rotation of the phenoxide ligand around the O-C bond.^{52c} Free rotation is also observed for both *tert*-butyl groups with two resonances in methyl region of the spectrum in a 1:1 intensity ratio. The ^{13}C NMR spectrum shows the difference between the chemical shifts of the α - and β - carbon atoms in the *tert*-butyl imido group to be $\Delta\delta \sim 46$ ppm, implying significant nitrogen π -donation to the tungsten.

The bond order of the nitrogen atom in the imido ligand is confirmed in the solid state with a W(1)-N(1)-C(11) angle of $168.8(2)^\circ$ (Figure 4.9, Table 4.3).

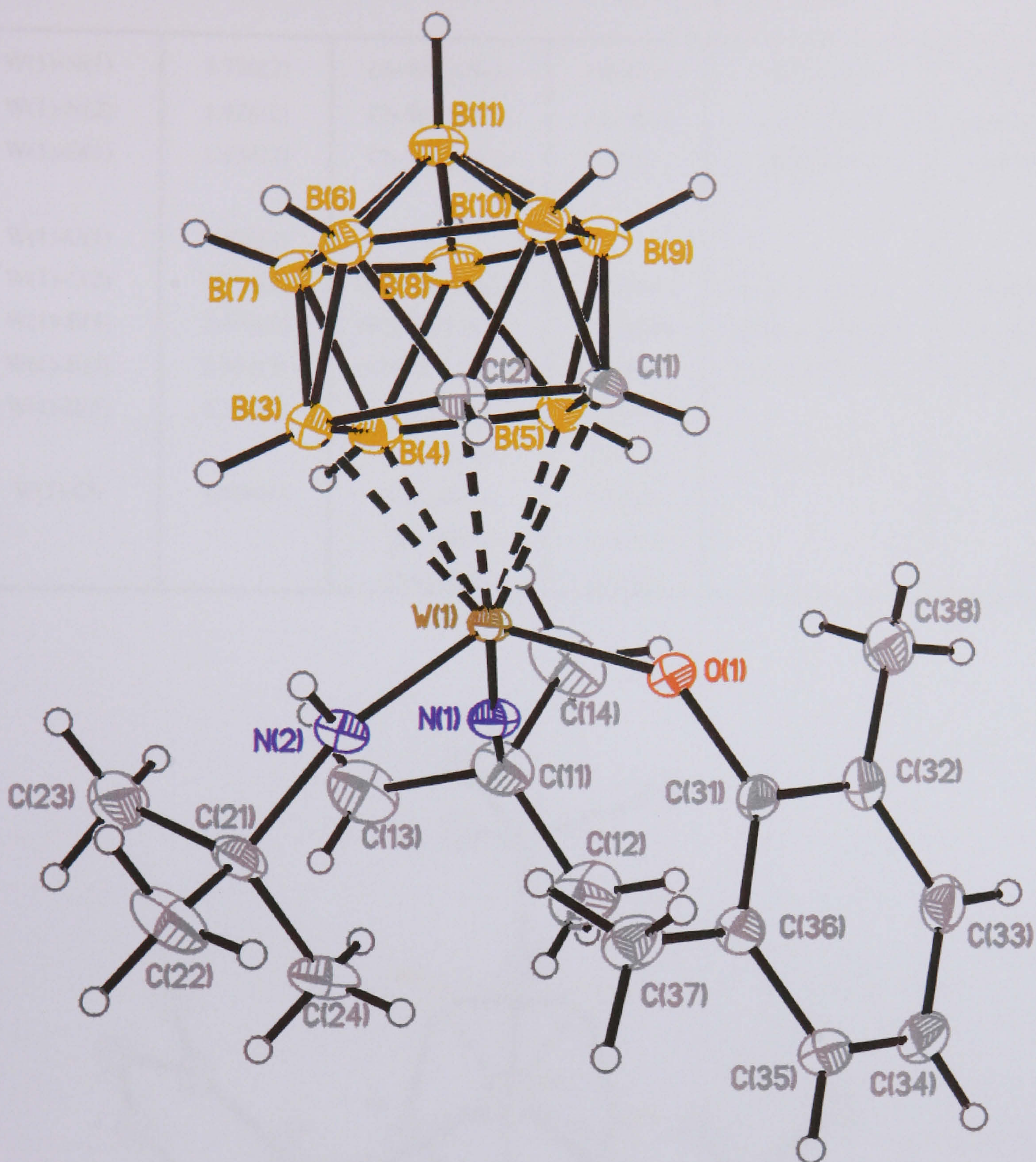


Figure 4.8 Molecular structure of the tungsten complex $[W(N^tBu)(NH^tBu)(OC_6Me_2H_3)(C_2B_9H_{11})]$, (33). Thermal ellipsoids of non-hydrogen are shown at 50% probability, hydrogen atoms are shown as hollow circles.

As in the case of the starting material the dicarbollide ligand experiences an orientation effect with a torsion angle, C(2)-Cb-W(1)-N(1) of 177.3° . The linearity of this torsion angle can be clearly seen in Figure 4.9.

Table 4.3 Selected bond lengths (Å) and angles (°) in (33).

W(1)-N(1)	1.720(2)	Cb-W(1)-N(1)	124.7(3)	N(1)-C(11)	1.481(3)
W(1)-N(2)	1.926(2)	Cb-W(1)-N(2)	112.9(3)	N(2)-C(21)	1.497(3)
W(1)-O(1)	1.934(2)	Cb-W(1)-O(1)	108.5(3)	O(1)-C(31)	1.387(3)
W(1)-C(1)	2.471(3)				
W(1)-C(2)	2.516(2)	N(1)-W(1)-N(2)	101.25(9)	W(1)-N(1)-C(11)	168.8(2)
W(1)-B(3)	2.491(3)	N(1)-W(1)-O(1)	104.30(9)	W(1)-N(2)-C(21)	137.3(2)
W(1)-B(4)	2.401(3)	N(2)-W(1)-O(1)	102.99(8)	W(1)-O(1)-C(31)	128.03(14)
W(1)-B(5)	2.392(3)	C(1)-C(2)	1.580(3)		
		C(1)-B(5)	1.672(4)	N(2)-H(2N)	0.86(3)
W(1)-Cb	1.984(3)	C(2)-B(3)	1.672(4)		
		B(3)-B(4)	1.786(4)		
		B(4)-B(5)	1.792(4)		

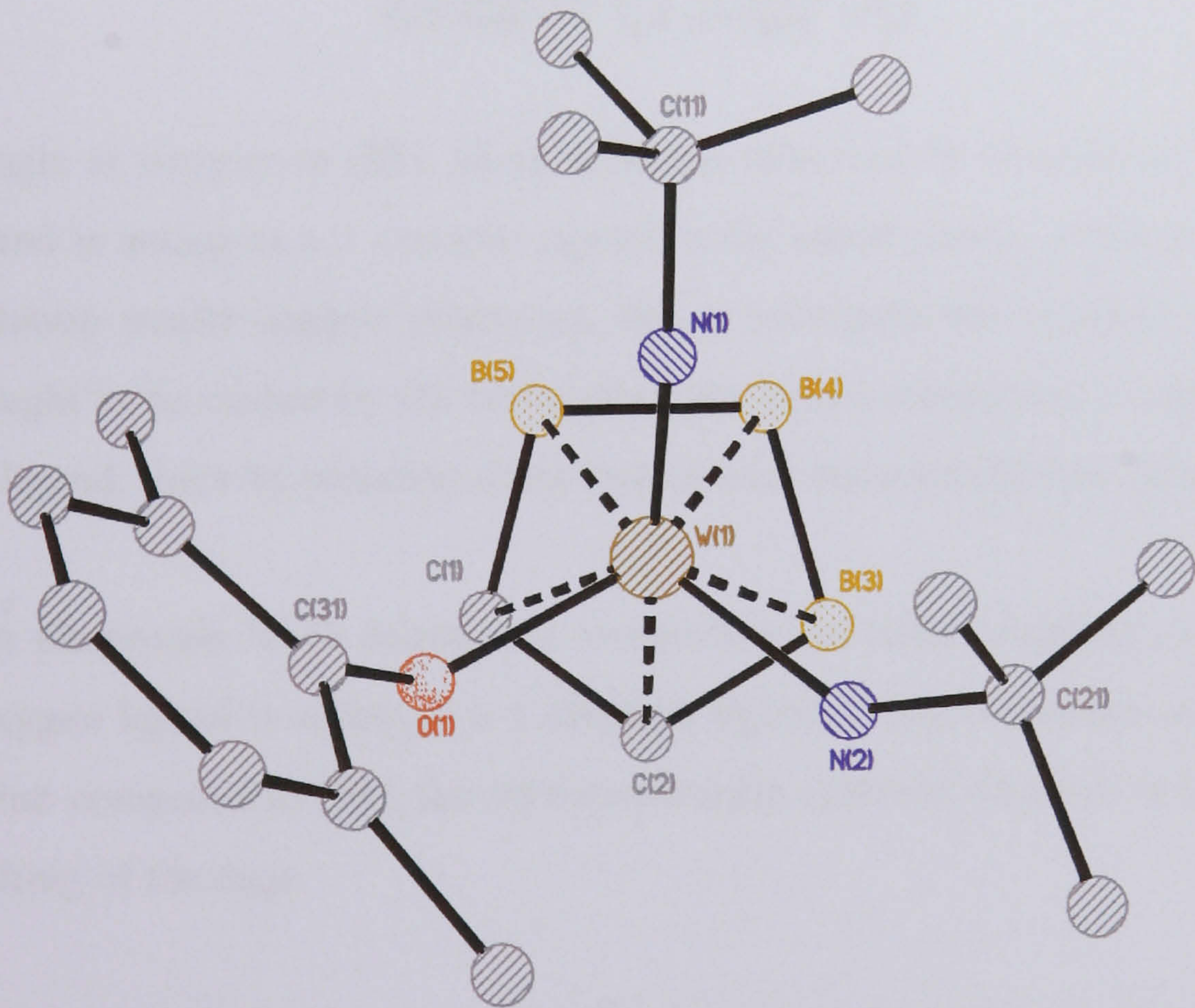
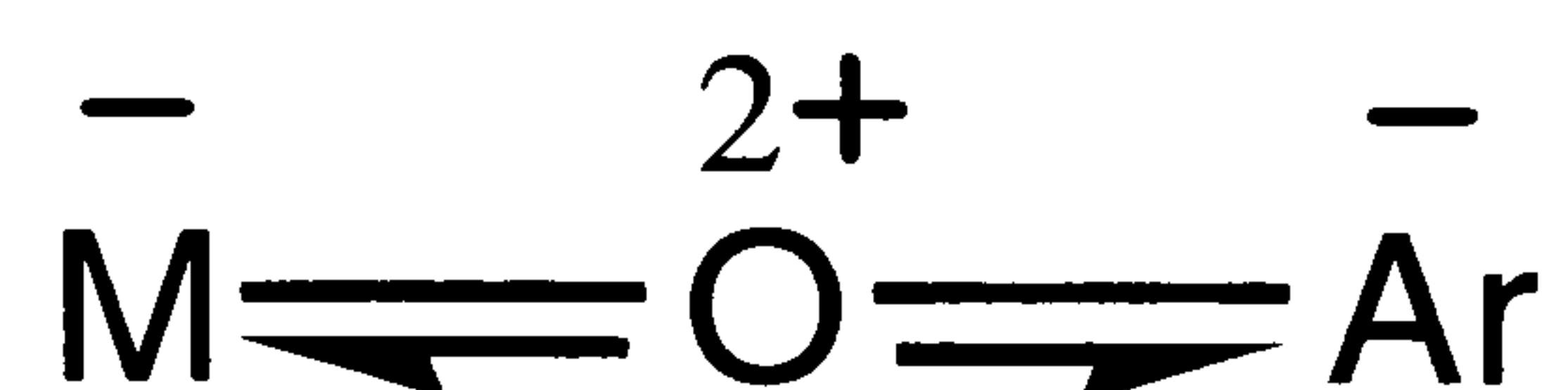


Figure 4.9 An alternative view of (32) from under the metal atom along the metal-centroid axis. All hydrogen atoms and all boron atoms except those in the C₂B₃ face have been omitted for clarity.

The ligands adopt a very symmetrical arrangement with respect to the C₂B₃ face, with the imido ligand *trans* to one carbon atom, (C(2)-Cb-W(1)-N(1) $\tau = 177.3^\circ$). The phenoxide and amide ligand lie under the two atoms either side of C(2), i.e., C(1) and B(3), with torsion

angles to those atoms of $\tau = 9.8^\circ$ and 17.2° respectively. The amide ligand in (33), N(2) has a dihedral angle (N-M-O/R-N-H) of 82° , i.e., 8° from the maximum bonding orientation of 90° . The second π -donor ligand, the phenoxy ligand, also has a dihedral angle that is close to the optimum, in fact the phenoxy ligand is only 3.7° away from the maximum bonding orientation.

Large M-O-C angles, which may be close to 180° , are characteristically associated with short M-O distances. However, although aryloxy ligands are expected to be poorer donors than their aliphatic counterparts, structural studies show that M-O-Ar angles are characteristically larger than M-O-alkyl angles, even in the absence of steric effects. Angles (M-O-C) of 160° - 180° are common, although M-O-Ar distances are slightly longer than M-O-alkyl distances in related complexes.⁵³ This ability of aryloxy ligands to increase the angle at oxygen is attributed to the fact that p-orbitals on the oxygen interact with the π -orbitals on the aromatic ring, and in order to do so the angle at oxygen is increased. This is best represented by the resonance structure shown below.⁵⁴



The small angle at oxygen in (33), along with the observed W-O distance, suggests that the phenoxy ligand is acting as a 1 electron ligand to the metal centre, although at first sight the ligand orientation would suggest otherwise, but in retrospect the orientation of the phenoxy ligand is thought to be caused by the bulky phenoxy ligand attempting to move away from the dicarbollide ligand, thereby reducing steric interactions between the two ligands.

The tungsten phenoxide W-O distance is comparable to other tungsten oxygen distances in which the oxygen ligand is acting as a 1 electron ligand.⁵⁵ This statement is further supported by the fact that compared to (31), the metal carborane centroid distance in (33) is shorter and there is no tilting of the cage.

A direct structural comparison of the phenoxy complex, (33), and the starting material, (31), reveals several similarities and several differences between the two structures. We can consider the phenoxy ligand in (33), as formally replacing the amide ligand N(2) in the starting material (Figure 4.10).

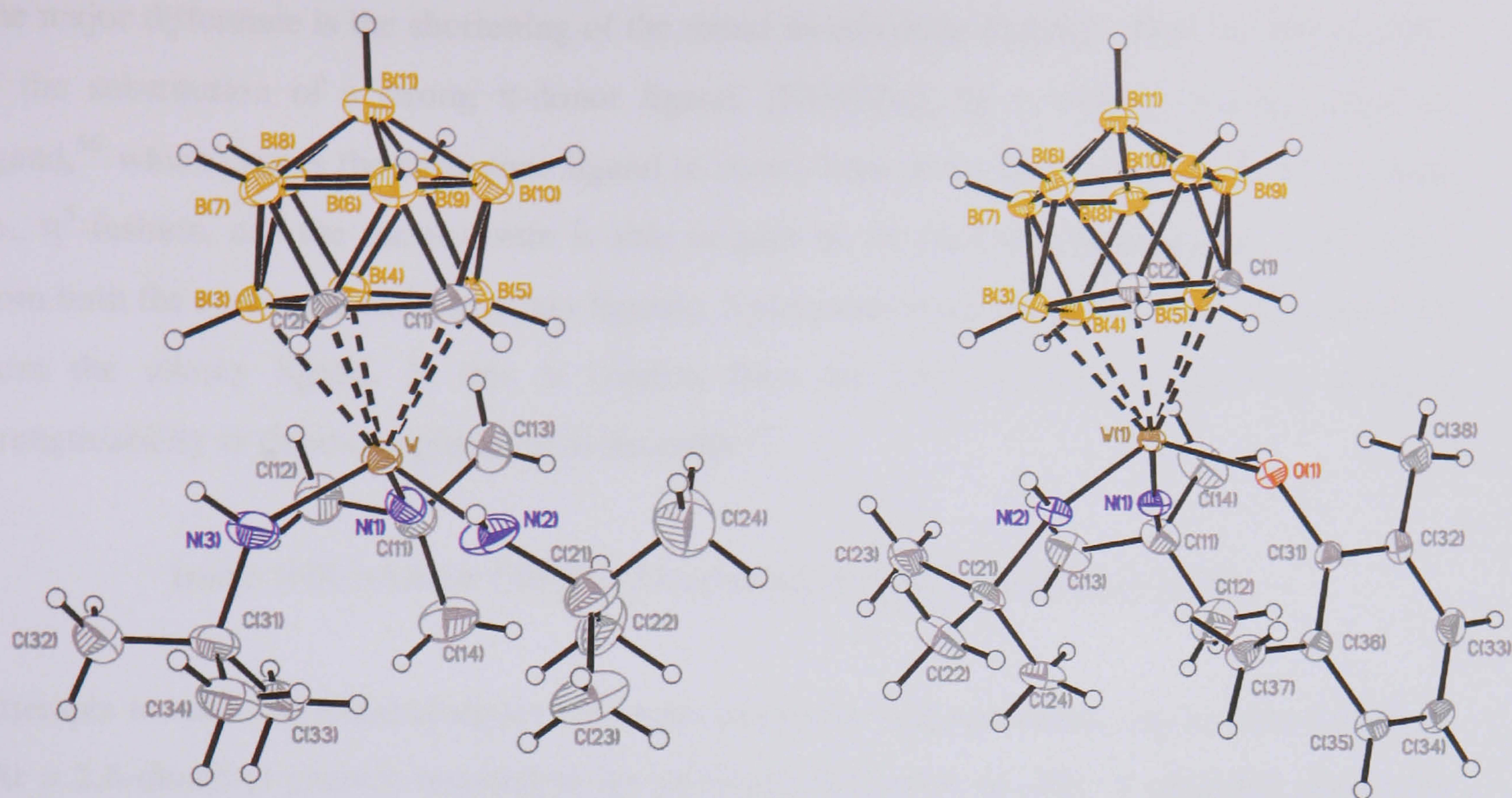


Figure 4.10 Diagram showing the structural similarities between (31) and (33).

Table 4.4 selected bond lengths (Å) and angles(°) in (31) and (33).

(31)		(33)	
W(1)-N(1)	1.721(3)	W(1)-N(1)	1.720(2)
W(1)-N(3)	1.949(4)	W(1)-N(2)	1.926(2)
W(1)-N(1)-C(11)	165.3(3)	W(1)-N(1)-C(11)	168.8(2)
W(1)-Cb	2.026(4)	W(1)-Cb	1.984(3)
Cb-W(1)-N(1)	124.5(3)	Cb-W(1)-N(1)	124.7(3)
Cb-W(1)-N(3)	109.7(3)	Cb-W(1)-N(2)	112.9(3)
Cb-W(1)-N(1)-C(11)	158.4	Cb-W(1)-N(1)-C(11)	162.4
Cb-W(1)-N(3)-C(31)	180.5	Cb-W(1)-N(2)-C(21)	130.8

It can be clearly seen from both Figure 4.9 and Table 4.4 that similarities between (31) and (33) exist, e.g. in both complexes the bond distances between the metal and the imido or amide nitrogen are comparable, as are the angles at nitrogen in the imido ligand and Cb-W-N(1).

The major difference is the shortening of the metal dicarbollide distance. This is a direct result of the substitution of a strong π -donor ligand, $[\text{N}(\text{H})^t\text{Bu}]$, by a weaker π -donor alkoxide ligand,⁵⁶ which causes the carborane ligand to revert back to its more usual mode of bonding, i.e., η^5 -fashion, and the metal centre is able to gain its 18 electron configuration, 4 electrons from both the carborane and the imido ligands, 3 electrons from the amide and only 1 electron from the alkoxy ligand. If this is correct, then we can see that a trend in π -donor strength/ability in these complexes is in the order:⁵⁶

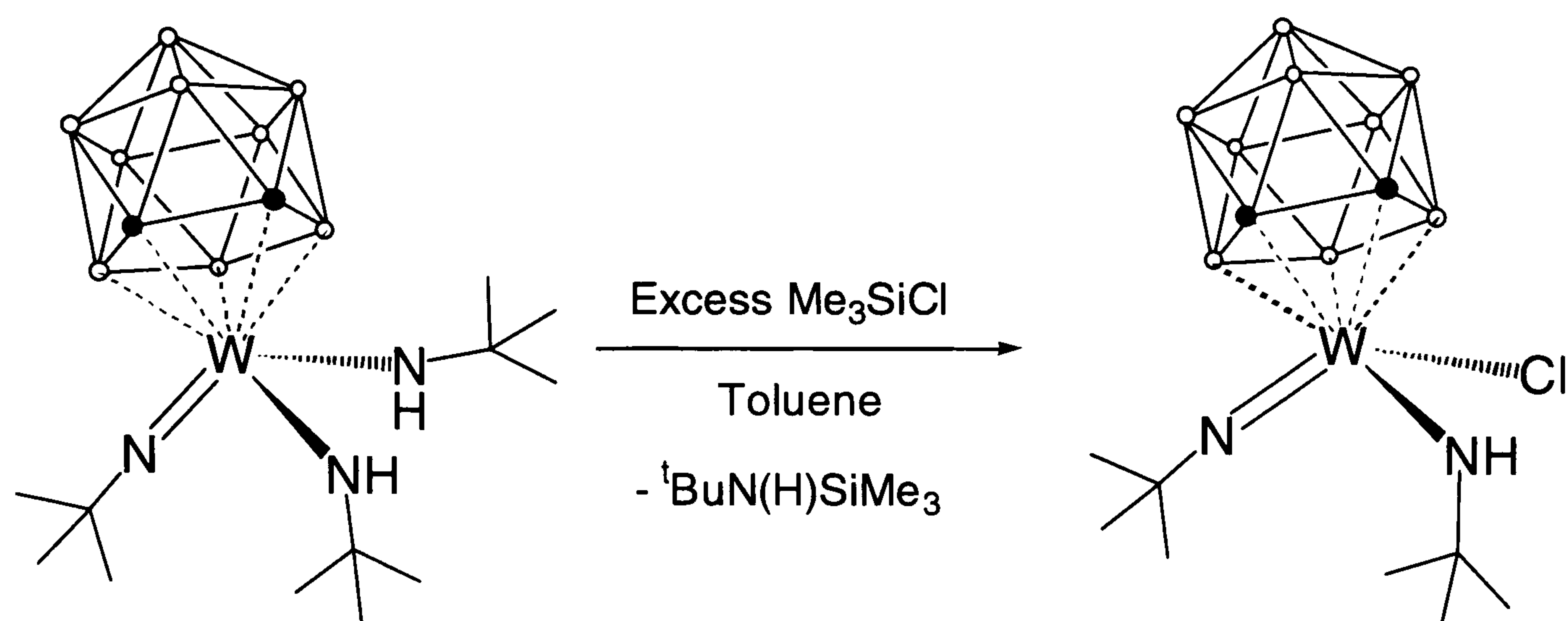


Attempts to react the metal complex (**31**) with more than one equivalent (up to four) of HOAr ($\text{Ar} = 2,6\text{-dimethyl phenol}$) resulted in the exclusive formation of (**33**). A plausible reason for this is that substitution of one of the amide ligands is possible because a substantial amount of electron density resides on the amide ligand, thereby making it susceptible to attack by electrophiles, i.e. protic acids. When one of the amides is substituted the metal centre accepts the electrons from the p orbital on the nitrogen atom of the amide ligand and the imido ligand and this reduces the susceptibility of the complex to further attack by electrophilic species.³ If this is true then the alkoxide ligand has the potential to undergo reactions itself such as protonolysis, insertion and reactions with alkyl halide complexes to form metal halides and ethers, while the rest of the metal complex remains unaffected.⁵⁴

The mono-chloro complex $[\text{W}(\text{N}^t\text{Bu})(\text{NH}^t\text{Bu})\text{Cl}(\textit{ortho}\text{-C}_2\text{B}_9\text{H}_{11})]$, (**34**), is formed as the exclusive tungsten-containing product in the reaction between the parent amide complex (**31**) and an excess of Me_3SiCl . The principle behind the transamination reaction has been discussed previously in chapter 3, and will not be discussed here. Even though the reactions were carried out in a high excess of trimethylsilylchloride, TMSCl (on one occasion neat TMSCl was used), only one amide ligand is substituted. We believe this to be explained by the same reasoning discussed above for (**33**), as halide atoms have previously been found to be much weaker π -donor ligands than amides and aryloxides.⁵⁶

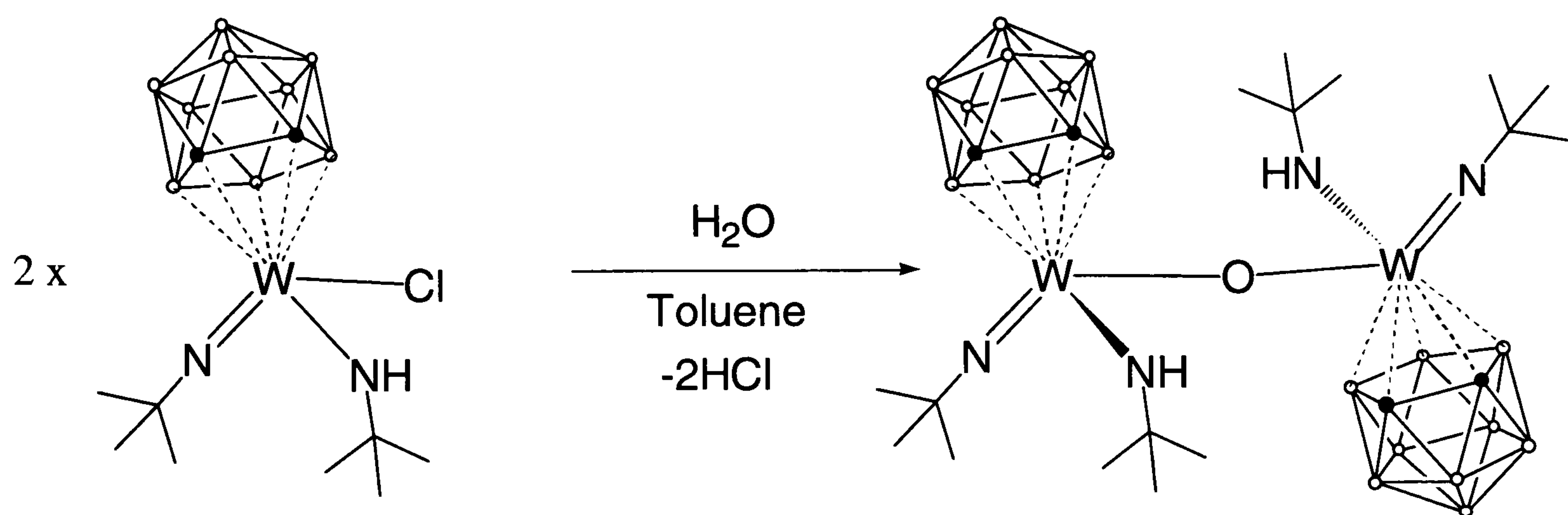
As with (**33**) the ^1H and ^{13}C NMR spectra of complex (**34**) show an unsymmetrical molecule with 2 *tert*-butyl groups in a 1:1 intensity ratio and two carborane CH resonances, also in a 1:1 intensity ratio. The $^1\text{H}\{^{11}\text{B}\}$ NMR spectrum shows the presence of 8 {BH} resonances in 1:1:2:1:1:1:1:1 intensity ratio, however this inequivalence is not mirrored in the $^{11}\text{B}\{^1\text{H}\}$

NMR spectrum with what can only be explained as coincidental overlapping of the boron peaks to show 6 broad resonances in a 2:1:2:2:1:1 intensity ratio.



Scheme 4.6 Synthesis of $[\text{W}(\text{N}^t\text{Bu})(\text{NH}^t\text{Bu})\text{Cl}(\text{ortho-C}_2\text{B}_9\text{H}_{11})]$, (34).

Both the starting material (31), the mono chloro complex are air- and moisture-sensitive, reacting with both atmospheric moisture, on more than one occasion, and stoichiometric amounts of water in toluene, to form the bridged oxo species (32). It is assumed that this reaction is accompanied by the *in situ* production of HCl, which apparently does not react with the oxo amide complex (32) (Scheme 4.7).



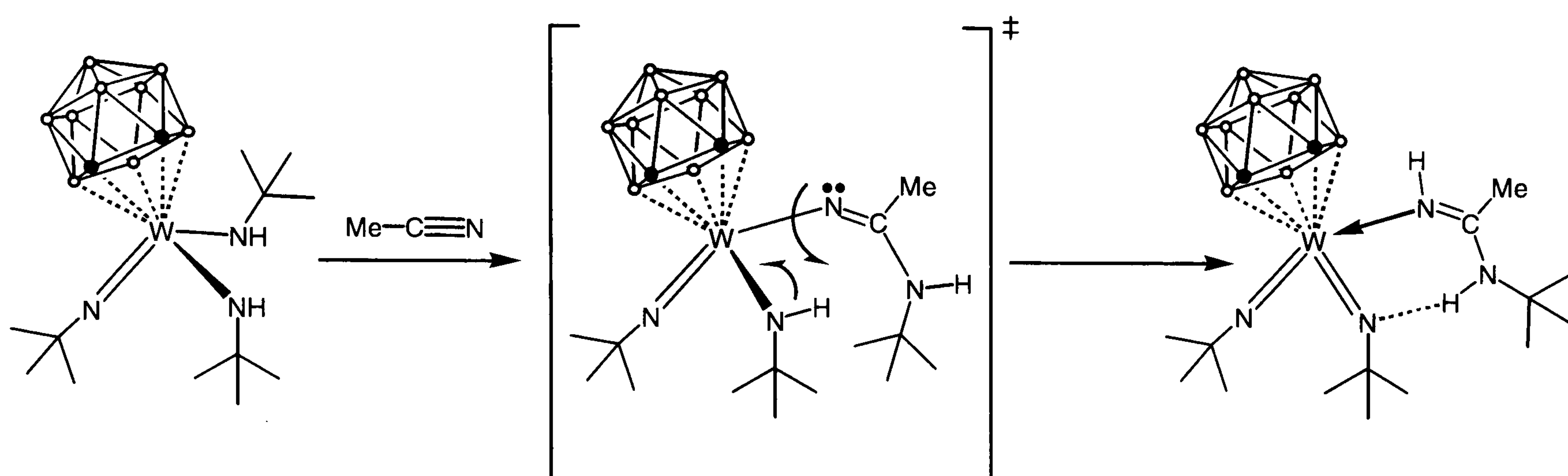
Scheme 4.7 Synthesis of $[\{\text{W}(\text{N}^t\text{Bu})(\text{NH}^t\text{Bu})(\text{ortho-C}_2\text{B}_9\text{H}_{11})\}_2(\mu\text{-O})]$, (32), from the reaction of $[\text{W}(\text{N}^t\text{Bu})(\text{NH}^t\text{Bu})\text{Cl}(\text{ortho-C}_2\text{B}_9\text{H}_{11})]$ with both atmospheric or stoichiometric amounts of H_2O .

4.3.3 Insertion reactions with $[\text{W}(\text{N}^t\text{Bu})(\text{NH}^t\text{Bu})_2(\text{ortho-C}_2\text{B}_9\text{H}_{11})]$.

The *bis*-amide complex (31) has also been shown to undergo insertion reactions. Stirring (31) in dry and deoxygenated acetonitrile results in the 100% conversion of (31) into the amidine complex, $[3\text{-W}(\text{N}^t\text{Bu})_2(\text{N}(\text{H})\text{C}(\text{CH}_3)\text{NH}^t\text{Bu})(1,2\text{-C}_2\text{B}_9\text{H}_{11})]$, (35) (Figure 4.12).

Both ^1H and ^{13}C NMR spectroscopy show the presence of 3 different *tert*-butyl environments in a 1:1:1 intensity ratio and two carborane CH peaks. Both the $^1\text{H}\{^{11}\text{B}\}$ and ^{11}B NMR spectra show the presence of an unsymmetrical carborane cage with 9 resonances in both spectra.

It is thought that the first stage in the formation of (35) is the insertion of one molecule of acetonitrile into one of the metal amide bonds of (31), to form an amidinate complex similar to those discussed in chapter 3. The amidinate intermediate then undergoes an intramolecular proton transfer to form the *bis*-imido complex (35), Scheme 4.8.



Scheme 4.8 Proposed mechanism for the synthesis of $[3\text{-W}(\text{N}^t\text{Bu})_2(\text{N}(\text{H})\text{C}(\text{CH}_3)\text{NH}(^t\text{Bu})(1,2\text{-C}_2\text{B}_9\text{H}_{11}))]$, (35).

It is presumed that this rearrangement is caused by the presence of the N-H group on the second amide ligand, and would not occur if the same reaction was conducted using a secondary amide complex. The *bis*-imido dicarbollide complex, (35), can still be regarded as a metallocene analogue and is iso-valence electronic and iso-structural with other “ $\text{M}(1\sigma 2\pi)_3$ ” complexes such as the group 4 *bis*-cyclopentadienyl imido complexes⁵⁷ and the group 6 *tris*-imido complexes^{37, 38, 58} shown in Figure 4.11.

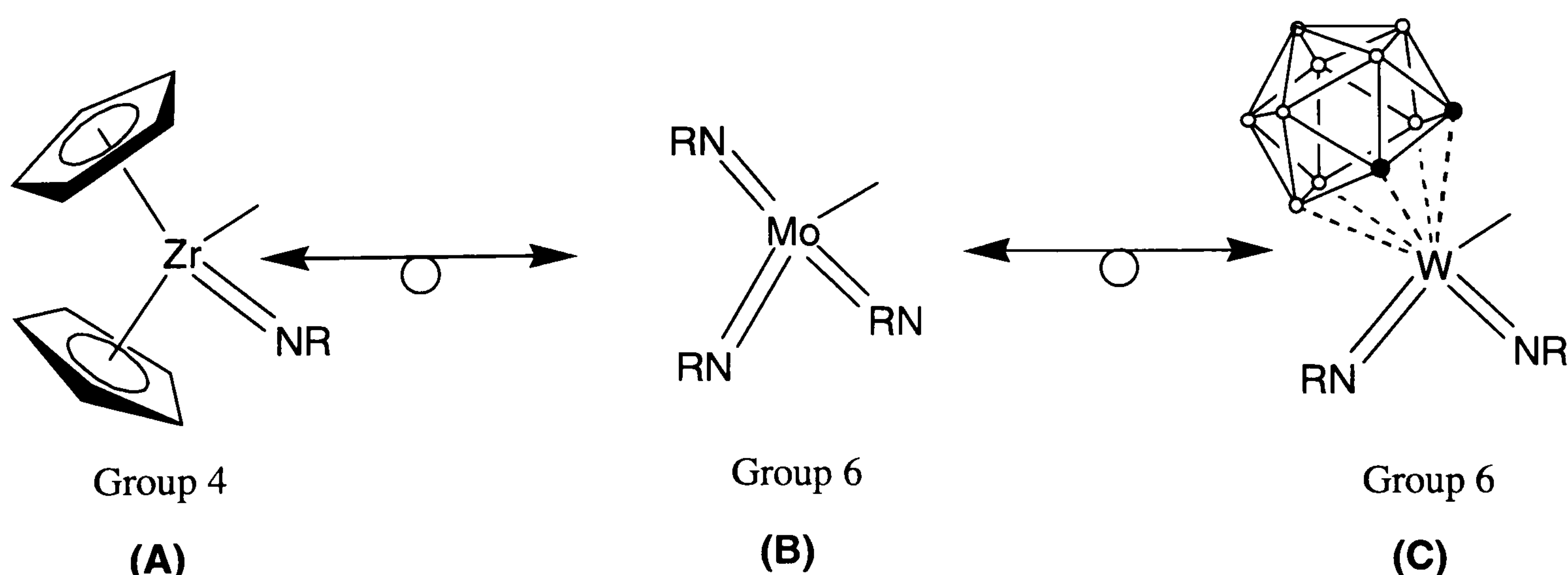


Figure 4.11 Isolobal relationships in imido “ $\text{M}(1\sigma 2\pi)_3$ ” fragments.

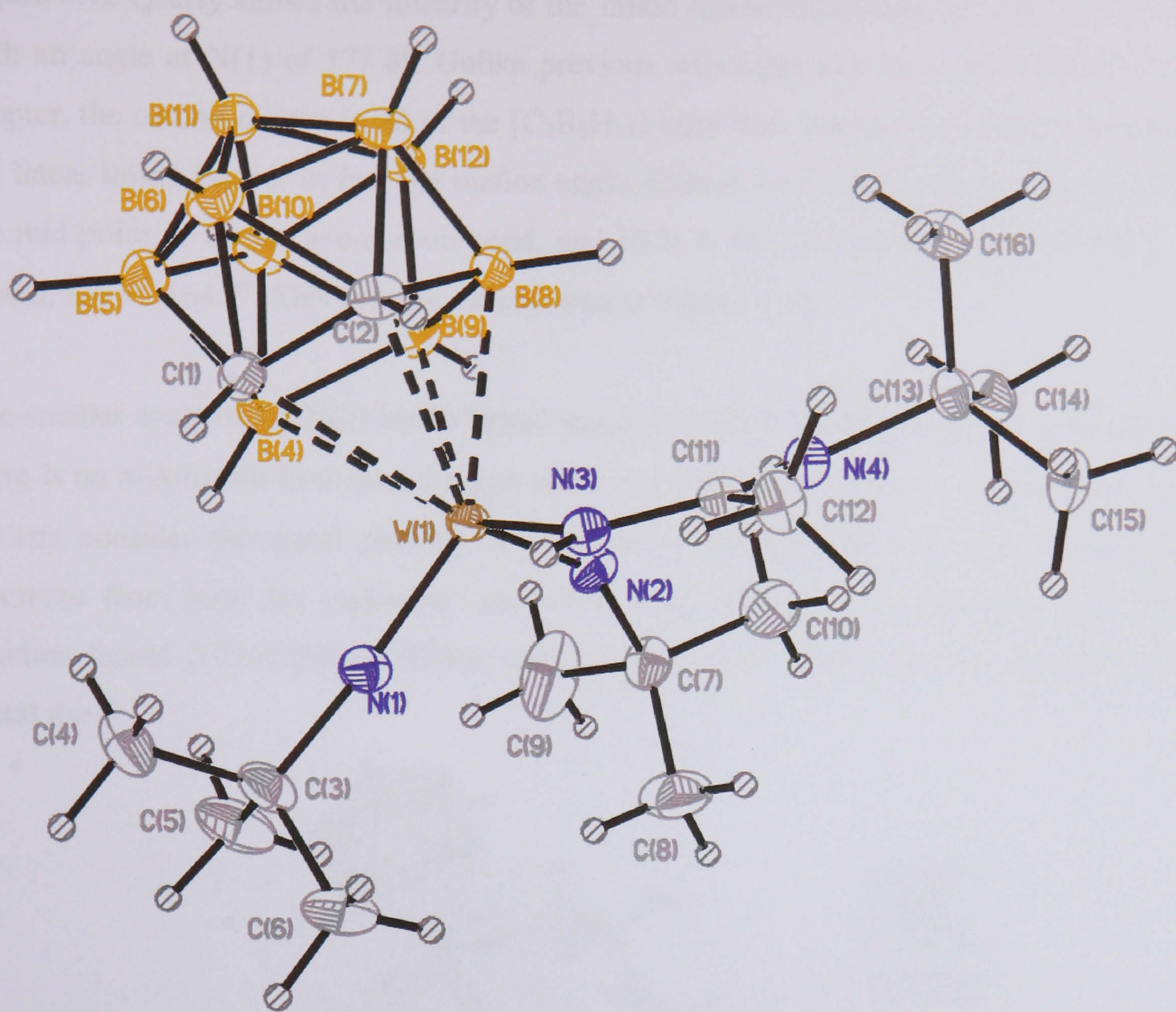


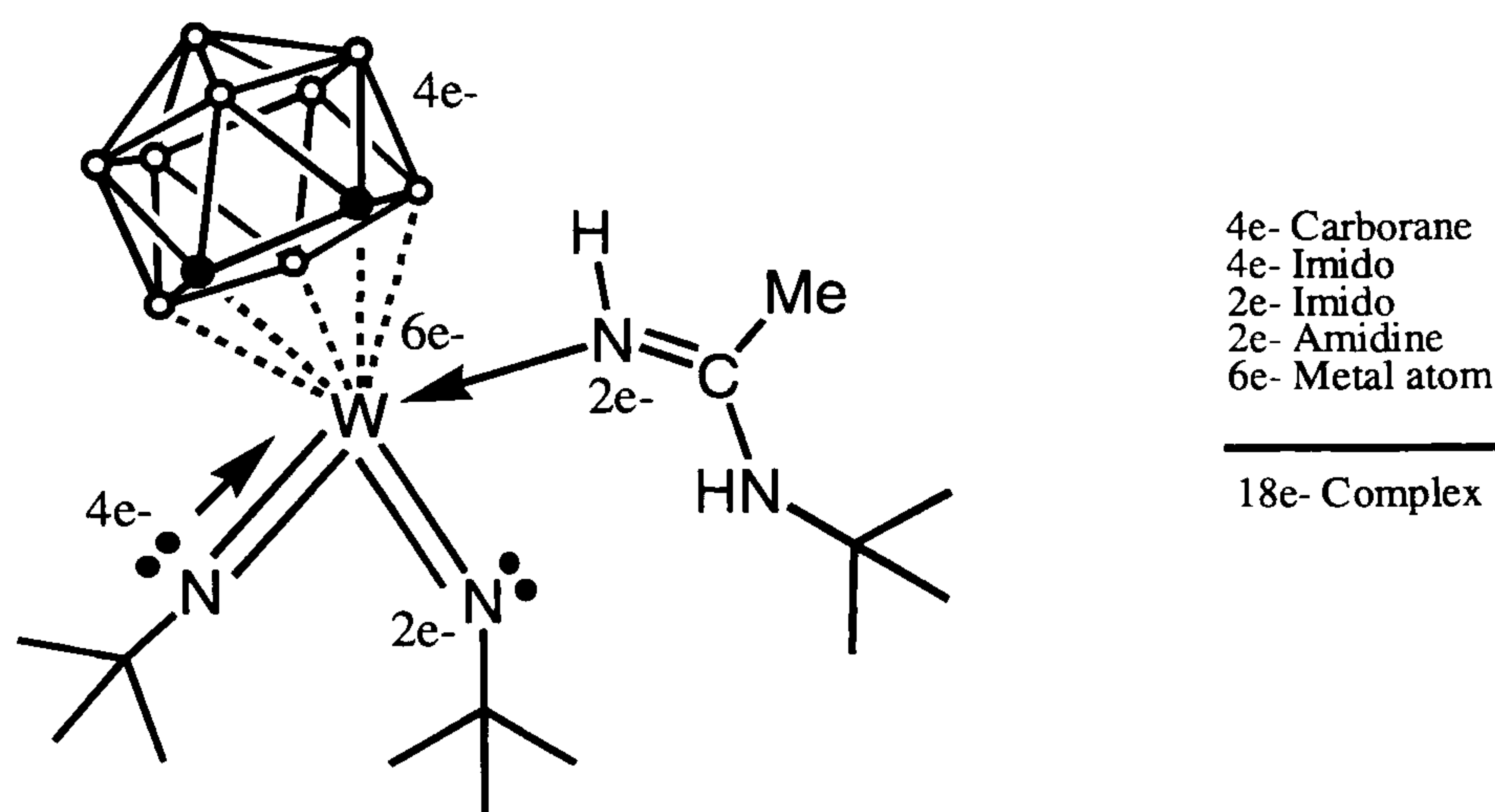
Figure 4.12 Molecular structure of the tungsten complex $[W(N^tBu)_2(C_2B_9H_{11})(N(H)C(CH_3)NH^tBu)]$, (**35**). Thermal ellipsoids of non-hydrogen atoms are shown at 50% probability, hydrogen atoms are shown as circles.

Table 4.3 Selected bond lengths (Å) and angles (°) in (**35**).

W(1)-N(1)	1.750(3)	Cb-W(1)-N(1)	114.5(4)	N(1)-C(3)	1.461(4)
W(1)-N(2)	1.795(3)	Cb-W(1)-N(2)	124.9(4)	N(2)-C(21)	1.469(4)
W(1)-N(3)	2.094(3)	Cb-W(1)-N(3)	109.3(4)	N(3)-C(11)	1.318(4)
W(1)-C(1)	2.620(4)	N(1)-W(1)-N(2)	107.21(14)	C(11)-N(4)	1.320(4)
W(1)-C(2)	2.573(3)	N(1)-W(1)-3(3)	95.89(12)	C(11)-C(12)	1.496(4)
W(1)-B(4)	2.461(4)	N(2)-W(1)-O(1)	99.90(13)	N(4)-C(13)	1.504(4)
W(1)-B(8)	2.469(4)	C(1)-C(2)	1.556(5)	W(1)-N(1)-C(3)	173.8(3)
W(1)-B(9)	2.455(4)	C(1)-B(4)	1.668(6)	W(1)-N(2)-C(7)	151.4(3)
W(1)-Cb	2.065(4)	C(2)-B(8)	1.669(5)	N(3)-H(3N)	0.71(4)
N(2)-H(4N)	2.43(4)	B(4)-B(9)	1.801(6)	N(4)-H(4N)	0.91(4)
		B(8)-B(9)	1.770(5)		

Figure 4.12 clearly shows the linearity of the imido ligand containing the nitrogen atom N(1), with an angle at N(1) of 173.8° . Unlike previous structures that have been discussed in this chapter, the carbon-carbon bond of the $[C_2B_9H_{11}]$ cage does not lie in a transoid orientation to the linear imido ligand. In fact the torsion angle defined by $C_2-W(1)-N(2)-C(7)$, where (C_2) is the mid point of the carbon-carbon bond, and N(2) is the nitrogen atom of the “bent” imido ligand, is $\tau = -164.7^\circ$. This is more clearly seen in Figure 4.14.

The smaller angle of the N(2) imido ligand suggests that the M-N bond order is less than 3, i.e. there is no π -donation from the nitrogen atom into the metal d-orbitals. If this is the case then we can consider the metal gaining its 18 electron configuration from the donation of four electrons from both the carborane and linear imido ligands, two electrons each from the amidine ligand $[HN=C(Me)N(H)^tBu]$ and the bent imido ligand and six electrons from the metal itself.



In both the group 4 “ $M(1\sigma 2\pi)_3$ ” complex, $[(C_5H_5)_2Ti(N^tBu)py]$, and group 6 “ $M(1\sigma 2\pi)_3$ ” complexes $[W(NAr)_3L]$ ($L = Cl^-$ or PMe_3), one of the $1\sigma 2\pi$ ligands is found to have a greater “bend” than the others (in the case of $[(C_5H_5)_2Ti(N^tBu)py]$ the imido ligand bends), thereby reducing the electron donation of that ligand.^{37,38,57,58} This is caused by the fact that the metal atom does not have enough orbitals of appropriate symmetry to accommodate donation from all three $1\sigma 2\pi$ ligands at the same time (see chapter one), and results in the need for a σ -donor such as Cl , PMe_3 , pyridine or, in the case of (35), an amidine ligand to supply two more electrons to the metal centre. Attempts to remove the σ -donor ligands from both the titanium complex and the tungsten *tris*-amide complexes have not yielded the desired unligated “ $M(1\sigma 2\pi)_3$ ” complex, but substitution of the σ -donor for another ligand is possible.

With this in mind it is surprising to find the dicarbollide ligand in (35) showing similar behaviour to the cage in complex (31), in that the dicarbollide ligand has backed away from the metal centre, $W-Cb = 2.065\text{\AA}$. As with the dicarbollide ligand in (31) the carbon atoms in the

C₂B₃ face of the ligand are moved further away from the metal atom, with W-C_{av} being 5% bigger than the average W-B bond length.

A search of the Cambridge Crystallographic Database reveals that the tungsten nitrogen bond distance between the metal centre and the amidine ligand is shorter than other W(VI)-N dative bonds at 2.094 Å.⁵⁹ The shortness of this bond compared to similar complexes may be due, in some part, to possible π -donation from the conjugated N(H)=C bond of amidine ligand, which lies in the same plane as the d_{z^2} orbital.

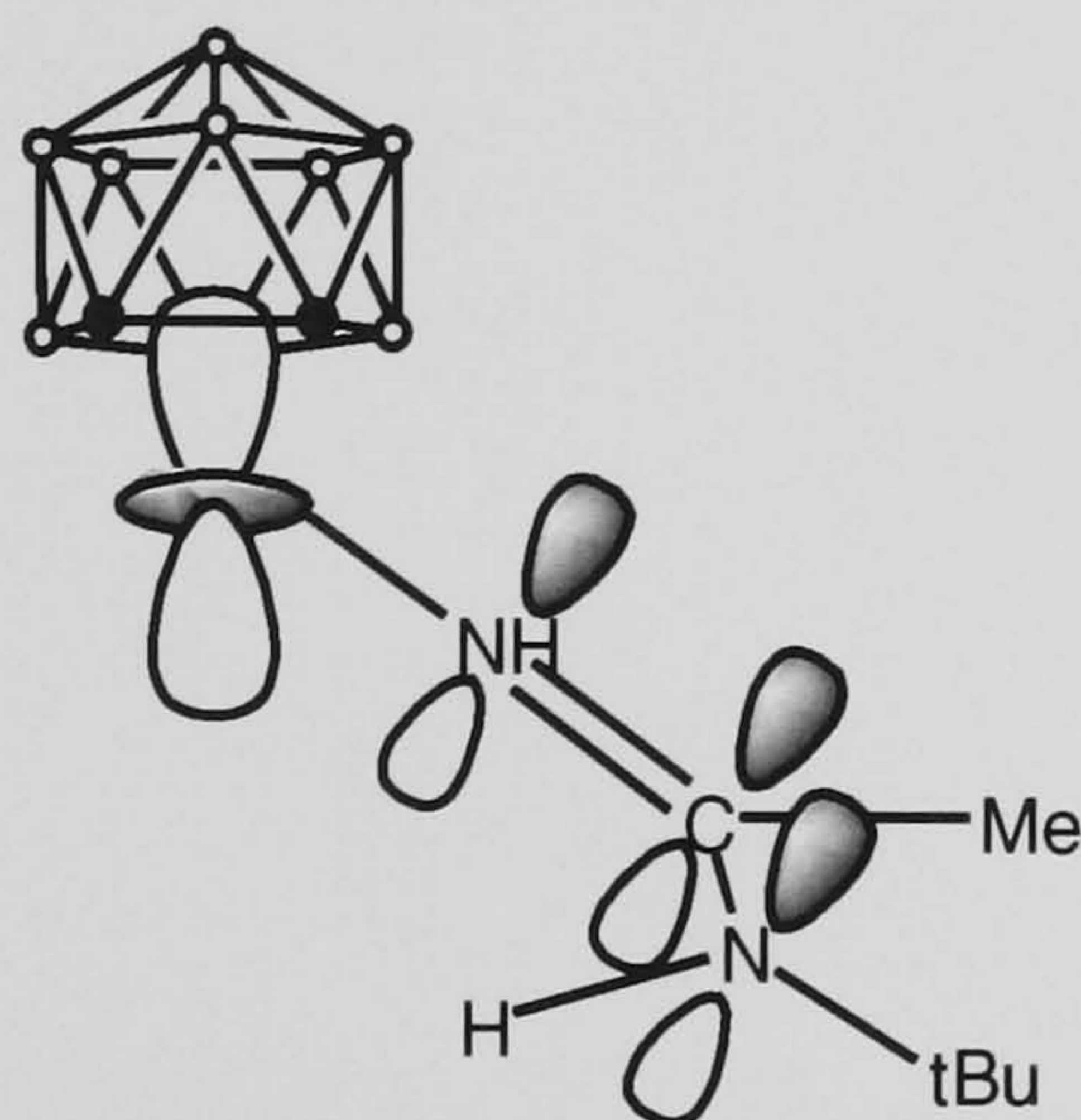


Figure 4.13 Possible π -bonding interaction between the conjugated N=C-N group of the amidine ligand and the d_{z^2} orbital on tungsten.

Such interactions can go some way to explain the lengthening of the tungsten dicarbollide bond, in that π -donation from the planar amidine ligand not only forces competition between the dicarbollide ligand and the amidine for suitable orbitals with which to bond but donation of electrons into a low lying dicarbollide–tungsten anti-bonding orbital would cause lengthening of the W-Cb bond.

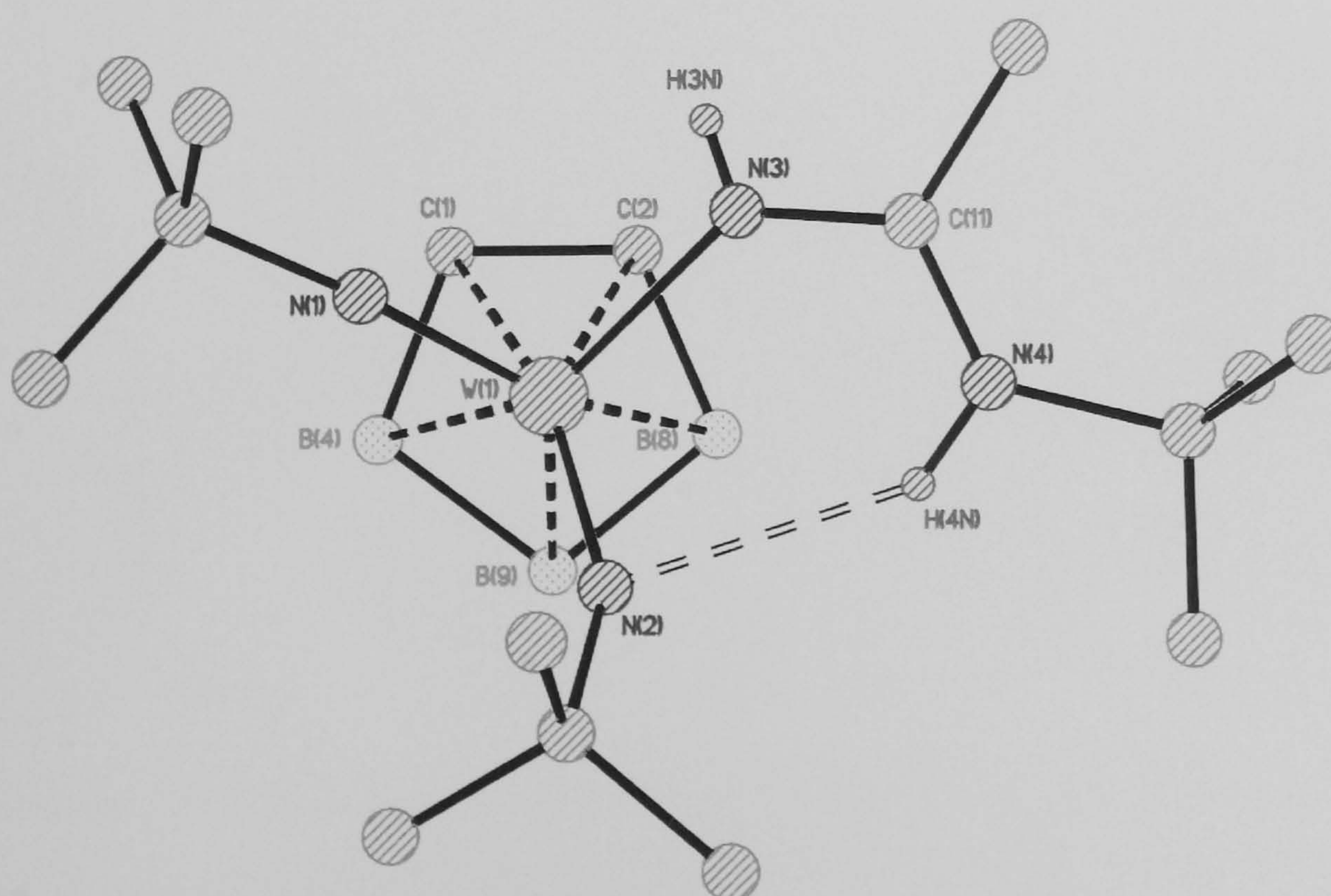


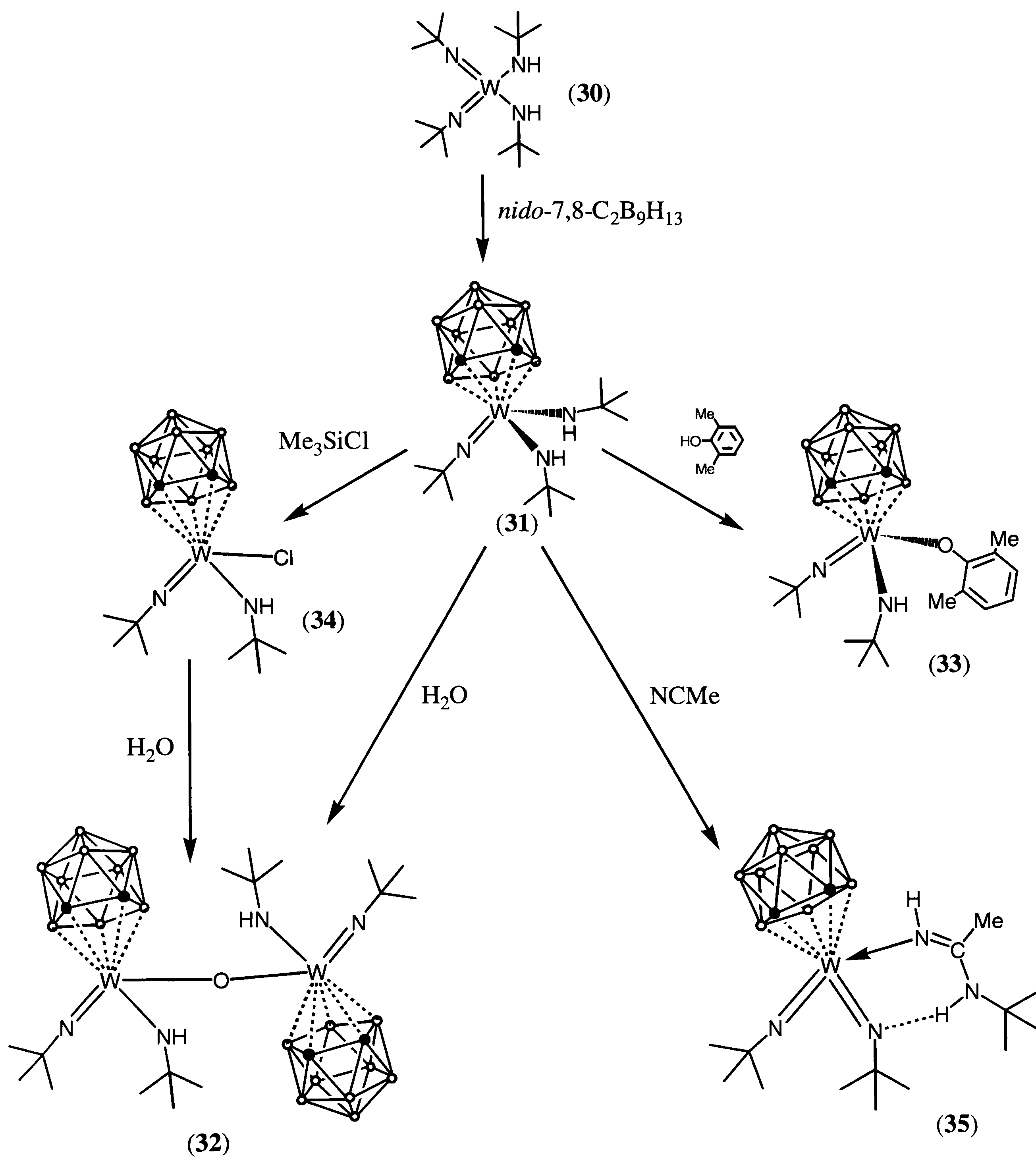
Figure 4.14 Diagram showing the hydrogen bond between the bent imido group and the second hydrogen atom on the amidine ligand.

Chapter Four – Dicarbollide Complexes of Tungsten (VI)

We can see from Figure 4.14 that the amidine is also involved in what is thought to be the first example of a $\text{N}\cdots\text{H}-\text{N}$ hydrogen bond, where the hydrogen bond acceptor is a metal organoimide complex. The $\text{N}_{\text{imido}}\cdots\text{H}$ bond lies well within the accepted parameters for $\text{N}\cdots\text{H}$ hydrogen bonds.⁶⁰ The hydrogen bond exerts an ordering effect upon the amidine ligand such that the atoms N(2), W(1), N(3), C(11), N(4) and H(4N) form a very distorted 6 membered ring.

4.4 Summary

The chemistry described in this chapter demonstrates the ability of $[\text{C}_2\text{B}_9\text{H}_{11}]$ to coordinate as a spectator ligand to W(VI), and allow the remaining imido and amide ligands to display their typical reactivity. The chemistry reported is summarised in scheme 4.9.



Scheme 4.9 A scheme showing the range of reactions discussed in this chapter.

4.5 References for Chapter Four

- 1 (a) R. R. Schrock, J. S. Murdzek, G. C. Bazan, J. Robbins, M. DiMare and M. B. O'Regan, *J. Am. Chem. Soc.*, 1980, **102**, 73; (b) G. C. Bazan, E. Khosravi, R. R. Schrock, W. J. Feast, V. C. Gibson, M. B. O'Regan, J. K. Thomas and W. M. Davis, *J. Am. Chem. Soc.*, 1990, **112**, 8378; (c) G. C. Bazan, J. H. Oskam, H. N. Cho, L. Y. Park and R. R. Schrock, *J. Am. Chem. Soc.*, 1991, **113**, 6899.
- 2 D. E. Wigley, *Prog. Inorg. Chem.*, 1994, **42**, 239.
- 3 W. A. Nugent and J. M. Mayer, *Metal-Ligand Multiple Bonds*; John Wiley and Sons, New York, 1988.
- 4 (a) E. A. Maatta, Y. Du and A. L. Rheingold, *J. Chem. Soc., Chem. Commun.*, 1990, 756; (b) E. A. Maatta and Y. Du, *J. Am. Chem. Soc.*, 1988, **110**, 8249. (c) D. M. T. Chan, W. C. Fultz, W. A. Nugent, D. C. Roe and T. H. Tulip, *J. Am. Chem. Soc.*, 1985, **107**, 251.
- 5 (a) M. Bakir, P. E. Fanwick and R. A. Walton, *Inorg. Chem.*, 1988, **27**, 2016; (b) S. H. Han, G. L. Geoffroy, *Polyhedron*, 1988, **7**, 2331.
- 6 D. S. Gary, D. P. Smith, M. A. Bruck and D. E. Wigley, *J. Am. Chem. Soc.*, 1992, **114**, 5459; (b) G. Perot, *Catal. Today*, 1991, **10**, 447.
- 7 (a) J. S. Murdzek and R. R. Schrock, *Organometallics*, 1987, **6**, 1373; (b) R. R. Schrock, S. A. Krouse, K. Knoll, J. Feldman, J. S. Murdzek and D. C. Yang, *J. Mol. Catal.*, 1988, **46**, 243; (c) W. A. Nugent and B. L. Haymore, *Coord. Chem. Rev.*, 1980, **31**, 123; (d) C. C. Cummins, S. M. Baxter and P. T. Wolczanski, *J. Am. Chem. Soc.* 1988, **110**, 8731; (e) V. C. Gibson, C. Redshaw, W. Clegg and M. R. J. Elsegood, *J. Chem. Soc., Chem. Commun.*, 1995, 2371.
- 8 (a) P. L. McGrane, M. Jensen and T. Livinghouse, *J. Am. Chem. Soc.*, 1992, **114**, 5459; (b) P. J. Walsh, F. J. Hollander and R. G. Bergman, *Organometallics*, 1993, **12**, 3705; (c) J. L. Bennett and P. T. Wolczanski, *J. Am. Chem. Soc.*, 1994, **116**, 2179.

Chapter Four – Dicarbollide Complexes of Tungsten (VI)

- 9 (a) E. W. Harlan and R. H. Holm, *J. Am. Chem. Soc.*, 1990, **112**, 186; (b) P. J. Walsh, A. M. Baranger and R. G. Bergman, *J. Am. Chem. Soc.*, 1992, **114**, 1708.
- 10 (a) T. R. Cundari, C. P. Schaller, J. B. Bonanno and P. T. Wolczanski, *J. Am. Chem. Soc.*, 1994, **116**, 4133; (b) C. C. Cummins, G. D. VanDuyne, C. P. Schaller and P. T. Wolczanski, *Organometallics*, 1991, **10**, 164.
- 11 (a) I. Meisel, G. Hertel and K. Weiss, *J. Mol. Catal.* 1986, **36**, 159; (b) K. R. Birdwhistell, T. Boucher, M. Ensminger, S. Harris M. Johnson and S. Toporek, *Organometallics*, 1993, **12**, 1023.
- 12 (a) K. E. Mayer, P. J. Walsh and R. G. Bergman, *J. Am. Chem. Soc.*, 1994, **116**, 2669; (b) G. K. Cantrell and T. Y. Mayer, *Organometallics*, 1997, **16**, 5381; (c) S. H. Kim, N. Bowden and R. H. Grubbs, *J. Am. Chem. Soc.*, 1994, **116**, 10801.
- 13 A. K. Hughes and A. J. Kingsley, *J. Chem. Soc., Dalton Trans.*, 1997, 4139.
- 14 (a) W. A. Nugent and B. L. Haymore, *Coord. Chem. Rev.*, 1980, **31**, 123; (b) R. R. Schrock, J. S. Murdzek, G. C. Bazan, J. Robbins, M. DiMare and M. O'Regan, *J. Am. Chem. Soc.*, 1990, **112**, 3875; (c) G. R. Clark, A. J. Nielson, C. E. F. Richards and D. C. Ware, *J. Chem. Soc., Chem. Commun.*, 1989, 343; (d) D. N. Williams, J. P. Mitchell, A. D. Poole, U. Siemeling, W. Clegg, D. C. R. Hockless, P. A. O'Neill and V. C. Gibson, *J. Chem. Soc., Dalton Trans.*, 1992, 739.
- 15 R. A. Henderson, *J. Chem. Soc., Dalton Trans.*, 1983, 51.
- 16 T. R. Cundari, *J. Am. Chem. Soc.*, 1992, **114**, 7879.
- 17 F. H. Allen and O. Kennard, *Chemical Design Automation News*, 1993, **8**, 1; 31.
- 18 (a) [$\{\text{Ta}(\text{N}^t\text{Bu})(\text{NH}_2^t\text{Bu})\text{Cl}_2\}_2(\mu^2\text{-OEt})_2$] R-N-M = 129.15° M-N = 2.27 Å see B. H. Bates, A. J. Nelson, and J. M. Waters, *Polyhedron*, 1985, **4**, 1391; (b) [$[\text{W}(\text{N}^t\text{Bu})_2(\text{NH}_2^t\text{Bu})(\text{N}_3)_2]_2$] R-N-M = 128.09°, M-N = 2.20 Å see H. W. Lam, G. Wilkinson, B. H. Bates and M. B. Hursthouse, *J. Chem. Soc., Dalton Trans.*, 1993, 781; (c) $[\text{Li}(\text{OEt}_2)][\text{Mn}(\text{N}^t\text{Bu})_3(\text{N})][\text{LiCl}]$

Chapter Four – Dicarbollide Complexes of Tungsten (VI)

- R-N-M = 128.8°, M-N = 1.76 Å see M. A. Danopoulos, G. Wilkinson, T. K. N. Sweet and M. B. Hursthouse, *J. Chem. Soc., Dalton Trans.*, 1995, 205.
- 19 P. Klingelhofer and U. Müller, *Z. Anorg. Allg. Chem.*, 1984, **516**, 85.
- 20 L. Banci, A. Bencini, A. Dei and D. Gatteschi, *Inorg. Chim. Acta*, 1984, **84**, L11.
- 21 (a) W. A. Nugent, *Inorg. Chem.*, 1983, **22**, 965; (b) W. A. Nugent and R. L. Harlow, *Inorg. Chem.*, 1980, **19**, 777.
- 22 U. Radius and J. Sundermayer, *Chem. Ber.*, 1992, **125**, 2183.
- 23 J. Sundermayer, *Chem. Ber.*, 1991, **124**, 1977.
- 24 W. A. Nugent and R. L. Harlow, *J. Am. Chem. Soc.*, 1980, **102**, 1759.
- 25 A. A. Danopolous, G. Wilkinson, B. Hussain and M. B. Hursthouse, *J. Chem. Soc., Chem. Commun.*, 1989, 896.
- 26 B. R. Ashcroft, G. R. Clark, A. J. Nelson and C. E. F. Rickard, *Polyhedron*, 1986, **12**, 2081.
- 27 A. J. Nielson, *Inorg. Chim. Acta*, 1987, **133**, 305.
- 28 (a) F. G. A. Stone, *Adv. Organomet. Chem.*, 1990, **31**, 53; (b) S. A. Brew and F. G. A. Stone, *Adv. Organomet. Chem.*, 1993, **35**, 135; (c) F. G. A. Stone, *Pure and Appl. Chem.*, 1986, **58**, 529.
- 29 J. H. Kim, E. Hong, J. Kim and Y. Do, *Inorg. Chem.*, 1996, **35**, 5112.
- 30 J. H. Kim and Y. Do, in “*Advances in Boron Chemistry*”, Ed. W. Siebert, Royal Society of Chemistry, Cambridge, UK, 1997.
- 31 D. J. Crowther, R. A. Fisher, J. A. M. Canich, G. G. Malky and H. W. Turner, U.S. Patent No. 5,502,124. Exxon Chemical Patents Inc., 1996.
- 32 S. F. Pendersen and R. R. Schrock, *J. Am. Chem. Soc.*, 1982, **104**, 7483.
- 33 M. H. Chisholm, F. A. Cotton, M. Extine and B. R. Stults, *J. Am. Chem. Soc.*, 1976, **98**, 4477.
- 34 H. T. Chiu, S. H. Chuang, G. H. Lee and S. M. Peng, *Polyhedron*, 1994, **13**, 2443.
- 35 J. Takacs and R. G. Cavell, *Inorg. Chem.*, 1994, **33**, 2635.

- 36 A. Danopoulos, G. Wilkinson, B. H. Bates and M. B. Hursthouse, *J. Chem. Soc., Dalton Trans.*, 1990, 2753.
- 37 Y. W. Chao, P. M. Rodgers, D. E. Wigley, S. J. Alexander and A. L. Rheingold, *J. Am. Chem. Soc.*, 1991, **113**, 6326.
- 38 D. L. Morrison and D. E. Wigley, *J. Chem. Soc., Chem. Commun.*, 1995, 79.
- 39 R. A. Andersen, D. B. Beach and W. L. Jolly, *Inorg. Chem.*, 1985, **24**, 4741.
- 40 (a) R. V. Bynum, W. E. Hunter, R. D. Rogers and J. L. Atwood, *Inorg. Chem.*, 1980, **19**, 2368; (b) G. M. Diamond, R. F. Jordan and J. L. Petersen, *Organometallics*, 1996, **15**, 4030; (c) J. N. Christopher, G. M. Diamond, R. F. Jordan and J. L. Petersen, *Organometallics*, 1996, **15**, 4038; (d) G. M. Diamond, R. F. Jordan and J. L. Petersen, *Organometallics*, 1996, **15**, 4045; (e) G. M. Diamond, R. F. Jordan and J. L. Petersen, *J. Am. Chem. Soc.*, 1996, **118**, 8024; (f) W. A. Herrmann, M. J. A. Morawietz and T. Priermeier, *J. Organomet. Chem.*, 1996, **506**, 351; (g) A. Vogel, T. T. Priermeier and W. A. Herrmann, *J. Organomet. Chem.*, 1997, **527**, 297; (h) J. N. Christopher, R. F. Jordan, J. L. Petersen and V. G. Young, Jr., *Organometallics*, 1997, **16**, 3044.
- 41 J. W. Lauher and R. Hoffmann, *J. Am. Chem. Soc.*, 1976, **98**, 1729.
- 42 (a) H. Schultz, K. Folting, J. C. Huffman, W. E. Streib and M. H. Chisholm, *Inorg. Chem.*, 1993, **32**, 6056; (b) M. H. Chisholm, F. A. Cotton, M. W. Extine, M. Millar and B. R. Stults, *Inorg. Chem.*, 1977, **14**, 320; (c) F. A. Cotton, E. V. Dikarev and W. Y. Wong, *Inorg. Chem.*, 1997, **99**, 593; (d) Z. Gebeyehu, F. Weller, B. Neumuller and K. Dehnick, *Z. Anorg. Allg. Chem.*, 1991, **36**, 593; (e) K. W. Chiu, R. A. Jones, G. Wilkinson, A. M. R. Galas and M. B. Hursthouse, *J. Chem. Soc., Dalton Trans.*, 1981, 2088; (f) R. H. Cayton, M. H. Chisholm, M. J. Hampden-Smith, J. C. Huffman and K. G. Moodley, *Polyhedron*, 1992, **11**, 3192; (g) M. H. Chisholm, M. J. Hampden-Smith, J. C. Huffman, J. D. Martin, K. A. Stahl and K. G. Moodley, *Polyhedron*, 1988, **7**, 1991; (h) R. L. Huff, S. Y. S. Wang, K. A. Abboud and J. M. Boncella, *Organometallics*, 1997, **16**, 1779; (i) P. Legzdins, K. J.

- Ross, S. F. Sayer and S. J. Rettig, *Organometallics*, 1997, **16**, 190; (j) M. H. Chisholm, J. C. Huffmann and R. L. Kelly, *Inorg. Chem.*, 1979, **18**, 3554; (k) R. H. Cayton, S. T. Chacon, M. H. Chisholm, K. Folting and K. G. Moodley, *Organometallics*, 1996, **15**, 992; (l) D. M. Berg and P. R. Sharp, *Inorg. Chem.*, 1987, **26**, 2959; (m) M. H. Chisholm, I. P. Parkin, W. E. Streib and K. S. Folting, *Polyhedron*, 1991, **10**, 2309; (n) S. W. Seidel, R. R. Schrock and W. M. Davis, *Organometallics*, 1998, **17**, 1058.
- 43 L. G. Hillhouse, A. R. Bulls, D. B. Santarsiero and J. E. Bercaw, *Organometallics*, 1988, **7**, 1309.
- 44 (a) R. T. Baker, J. F. Whitney and S. S. Wreford, *Organometallics*, 1983, **2**, 1049; (b) L. Weber, G. Meeine, R. Boese and N. Augart, *Organometallics*, 1987, **6**, 2484.
- 45 E. Hey-Hawkins and F. Lindenberg, *Organometallics*, 1994, **13**, 4643.
- 46 T. L. Breen and D. W. Stephan, *Organometallics*, 1996, **15**, 4223.
- 47 See ref. 17, (a) S. A. Brew, D. D. Devore, P. D. Jenkins, M. U. Pilotti and F. G. A. Stone, *J. Chem. Soc., Dalton Trans.*, 1992, 393.
- 48 H. M. Colquhoun, T. J. Greenhough and M. G. H. Wallbridge, *J. Chem. Soc., Chem. Commun.*, 1976, 1019.
- 49 H. M. Colquhoun, T. J. Greenhough and M. G. H. Wallbridge, *J. Chem. Soc., Chem. Commun.*, 1977, 737; (b) H. M. Colquhoun, T. J. Greenhough and M. G. H. Wallbridge, *J. Chem. Soc., Dalton Trans.*, 1979, 619.
- 50 R. H. Cayton, M. H. Chisholm, K. Folting, J. L. Wesemann and K. G. Moodley, *J. Chem. Soc., Dalton Trans.*, 1997, 3161.
- 51 (a) F. R. W. P. Wild, L. Zsolnai, G. Hutter and H. H. Brintzinger, *J. Organomet. Chem.*, 1982, **232**, 233; (b) F. P. W. P. Wild, M. Wasiucionek, G. Hutter and H. H. Brintzinger, *J. Organomet. Chem.*, 1985, **288**, 63.
- 52 For reviews on metal alkoxide and metal phenoxide chemistry see (a) R. C. Mehrotra, *Adv. Inorg. Chem. Radiochem.*, 1973, **15**, 259 (b) D. C. Bradley, R. C. Mehrotra and D. P. Gaur,

- “*Metal Alkoxides*”, Academic Press, London, 1978; (c) K. C. Malhotra and R. L. Martin, *J. Organomet. Chem.*, 1982, **239**, 159.
- 53 (a) T. W. Coffindaffer, I. P. Rothwell and J. C. Huffman, *Inorg. Chem.*, 1983, **22**, 2906; (b) S. Latesky, A. K. McMullen, I. P. Rothwell and J. C. Huffman, *Organometallics*, 1985, **4**, 902.
- 54 M. H. Chisholm and I. P. Rothwell, Chapter 15.3, in “*Comprehensive Coordination Chemistry; Ligands*”, Vol. 2, Ed. G. Wilkinson, Pergamon Press, Oxford, 1983.
- 55 (a) J. I. Davies, J. F. Gibson, A. C. Skapski, G. Wilkinson and W. K. Wong, *Polyhedron*, 1982, **1**, 641; (b) A. Lehtonen and R. Sillanpää, *Polyhedron*, 1999, **18**, 175; (c) V. M. Visciglio, P. E. Fanwick and I. P. Rothwell, *Inorg. Chim. Acta*, 1993, **211**, 203.
- 56 M. H. Chisholm, I. P. Parkin, J. C. Huffman, E. M. Lobkovsky and K. Folting, *Polyhedron*, 1991, **10**, 2839.
- 57 (a) P. Mountford, *Chem. Commun.*, 1997, 2127; (b) S. C. Dunn, P. Mountford and D. A. Robson, *J. Chem. Soc., Dalton Trans.*, 1997, 293.
- 58 (a) D. L. Morrison and D. Wigley, *Inorg. Chem.*, 1995, **34**, 2610; (b) D. L. Morrison, P. M. Rodgers, Y. W. Chao, M. A. Bruck, C. Grittini, T. L. Tajima, S. J. Alexander, A. L. Rheingold and D. E. Wigley, *Organometallics*, 1995, **14**, 2435.
- 59 The shortest W(VI)-N bond in the cationic *oxo*-complex $[\text{W}(\text{O})_2\text{Br}((\text{HN})_3(\text{C}_2\text{H}_6)_3)]^+$ is 2.12 Å, see P. Schreiber, K. Wieghardt, B. Müber and J. Weiss, *Z. Anorg. Allg. Chem.*, 1990, **587**, 174.
- 60 (a) C. B. Aakeröy and K. R. Seddon, *Chem. Soc. Rev.*, 1993, 397; (b) G. Desiraju, “*Crystal Engineering*”, Elsevier Publishing, Amsterdam, 1989.

Chapter Five

Experimental

Details

5.1 General Experimental Techniques

All manipulations of air- and moisture-sensitive compounds were performed on a conventional vacuum / nitrogen line using standard Schlenk and cannula techniques or in a nitrogen filled glove box. When required, solvents were dried by prolonged reflux over an appropriate drying agent prior to distillation and deoxygenation by freeze-thaw processes. Drying agents used were sodium metal (toluene), potassium metal (benzene, hexanes, THF), calcium hydride (dichloromethane), sodium hydride (pentane) and sodium potassium alloy, NaK, (diethyl ether). NMR solvents, when required dry, were vacuum distilled from suitable drying agents and stored in ampoules under a dry nitrogen atmosphere. These drying agents were phosphorous pentoxide (d_3 -chloroform, d_8 -toluene, d_6 -benzene) and calcium hydride (d_2 -dichloromethane, d_5 -pyridine and d_3 -acetonitrile).

Elemental analysis was performed by the microanalytical service within the Department of Chemistry at the University of Durham.

Infrared spectra were run as liquid films on a Perkin-Elmer 1615 FTIR spectrometer or as solid samples on a Graseby Specac 10500 Golden Gate coupled to a Perkin Elmer 1000 series “Paragon” spectrometer.

Mass spectra were recorded on a Micromass Autospec instrument operating in EI mode. [M] is used to denote the molecular ion.

NMR spectra were recorded on the following machines at frequencies listed unless stated otherwise; Varian XL-200 (^1H), Varian Gemini-200 (^1H , ^{13}C , ^{31}P and ^{19}F), Brüker AC-250 (^1H and ^{13}C), Varian Unity-300 (^1H , ^{11}B , $^{11}\text{B}\{^1\text{H}\}$ and $^{13}\text{C}\{^1\text{H}\}$) or Varian VXR-400 (^1H , ^{13}C , ^1H - ^1H COSY and ^1H - ^{13}C HETCOR). All chemical shifts are reported in δ (ppm) and coupling constants in Hz. ^1H NMR spectra were referenced to residual protio impurity in the solvent ($\text{C}_6\text{D}_5\text{H}$, 7.15 ppm; CHCl_3 , 7.26 ppm; CD_2HCN , 2.34 ppm, CDHCl_2 , 5.25 ppm and $\text{C}_5\text{D}_4\text{HN}$, 8.71 ppm). ^{13}C NMR spectra were referenced to the solvent resonance (C_6D_6 , 128.0ppm; CDCl_3 , 77.0 ppm; CD_2Cl_2 , 53.5 ppm). ^{19}F and ^{11}B NMR were referenced externally to CFCl_3 , and $\text{BF}_3\text{:Et}_2\text{O}$ respectively, $\delta = 0$ ppm. Unless stated otherwise all spectra were recorded at ambient temperature.

The abbreviations have been used for multiplicities: s (singlet), d (doublet), t (triplet), q (quartet), sept (septet), br (broad), M (unresolved multiplet).

Unless otherwise stated chemicals used and not described here, were purchased commercially and used without further purification.

For each compound structurally analysed using single crystal X-ray diffraction a suitable crystal was selected by ensuring that all dimensions were in the order of 0.05 mm - 0.5 mm (if not the crystal was cut with a sharp scalpel blade so as to leave as many natural faces as possible) and testing that the crystals extinguished sharply and completely when rotated under polarised light.

The crystal was then mounted onto the end of a glass fibre using an oil-drop method in which the crystal is encapsulated in a viscous perfluoroether oil which acts as a protective film and which solidifies when placed onto the diffractometer under a 150 K nitrogen gas flow;¹ the diffractometer is equipped with an Oxford Cryosystems Cryostream unit which allows experiments to be carried out at any temperature in the range 85-300 K.² By means of a brass-pip and goniometer head the crystal was placed in the diffractometer; the goniometer head allows crystal translation in three perpendicular directions, so that, once the goniometer head is secured in the diffractometer, the position of the crystal can be adjusted such that it lies in the centre of the oncoming beam.

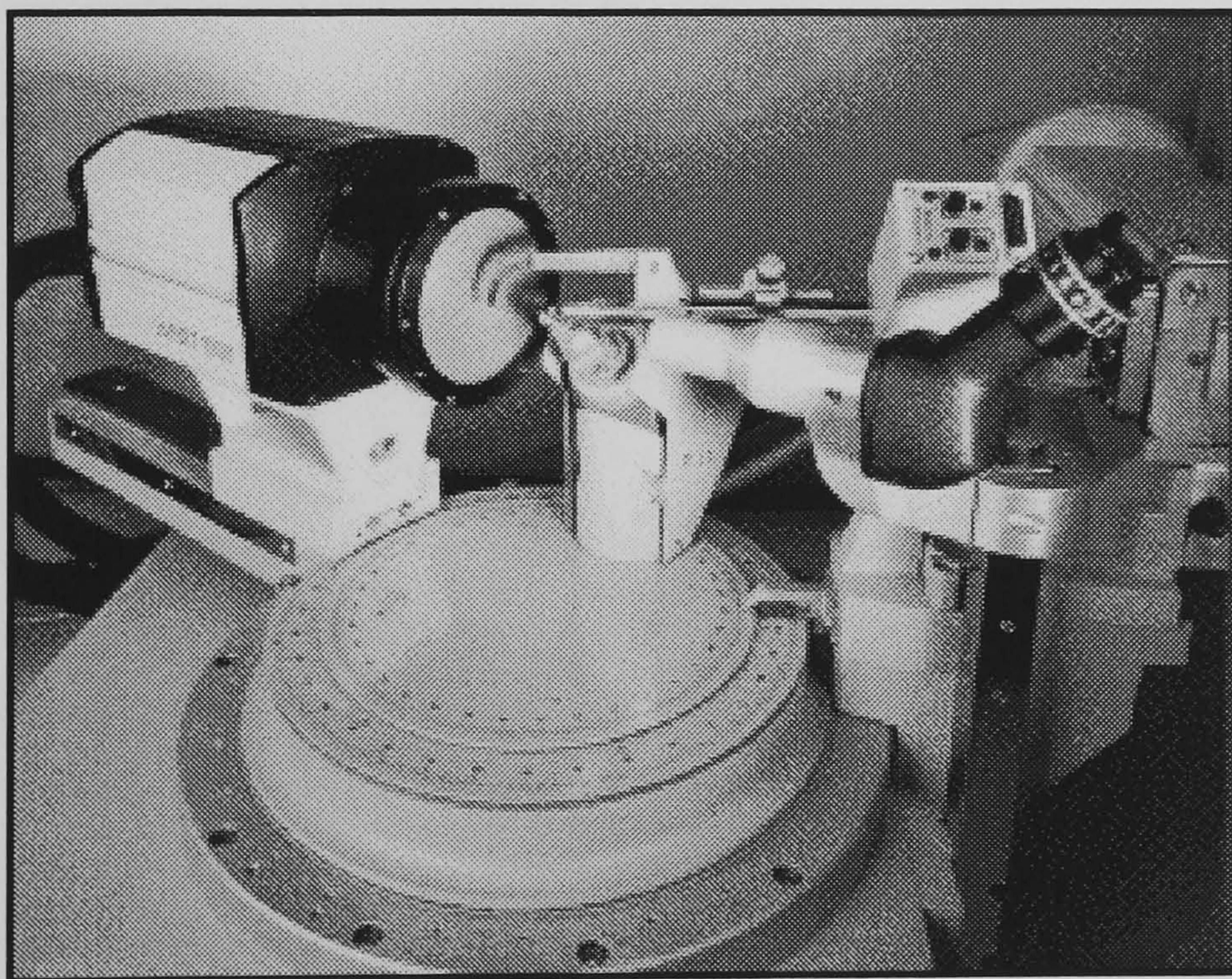


Figure. 5.1 A Siemens SMART-CCD diffractometer.

The diffractometer used was a Siemens SMART-CCD diffractometer, pictured in Fig. 5.1. Once the crystal is centred using the built-in microscope, diffraction is measured using a 512 x 512 pixel scintillation area detector that uses a charged-couple-device (CCD) to amplify the output. A lead beam-stop is fixed in the direct line of the incident X-ray beam and a 'glass-panelled' interlock prevents user intervention when the X-ray shutter is open.

Chapter Five – Experimental Details

Lattice parameters were obtained by least squares fitting of positional parameters of 999 reflections in the range of 0.5-4Å.³

Data were collected using graphite monochromated Mo K $\bar{\alpha}$ radiation, $\lambda = 0.71073\text{\AA}$. Other data for each structure are presented in appendix A. All computations used SHELXTL, data reduction, corrections and analysis were by SAINT and XPREP.⁴ Structures were solved by direct methods using XS and subsequently refined by Fourier and least squares using XL.⁵ Hydrogen atoms were freely refined in all cases.

Molecular structure diagrams were rendered using XP in SHELXTL .

5.2 Experimental Details to Chapter Two

Ortho-, *meta*- and *para*- carborane ($C_2B_{10}H_{12}$) were obtained commercially (KatChem) and sublimed prior to use. The carborane salts $[NBu_4][meta-C_2B_9H_{12}]^6$ and $[NHMe_3][ortho-C_2B_9H_{12}]^7$ were prepared by literature methods. The ylide, triphenyl phosphonium methyllide was also prepared by a literature method.⁸

5.2.1 Synthesis of [7,8- $C_2B_9H_{13}$], (7).

A mixture of *ortho*-carborane [$1,2-C_2B_{10}H_{12}$] (12 g, 83.3 mmol), KOH (10.1 g, 180 mmol) and MeOH (200ml, handled in air) was refluxed under nitrogen for 2 d. The MeOH was removed under reduced pressure, leaving a white semisolid material. Benzene (200 ml) was added, and an azeotropic distillation was performed to remove H_2O and MeOH. The remaining white solid was dried under vacuum over night at 40 °C. The white solid was slurried in benzene (150 ml) under N_2 , H_3PO_4 (60 ml, 85 %) was added, and the two-phase mixture was stirred for 15 h. The benzene layer was quickly decanted from the lower layer to minimise exposure to air. The H_3PO_4 layer was then extracted with benzene (2 x 50 ml); the benzene extracts were combined and dried over $MgSO_4$, and distilled to dryness under reduced pressure. Sublimation of the solid residue (40-50 °C, <0.001 mmHg) yielded pure [7,8- $C_2B_9H_{13}$] (9.4 g, 84 %).

1H NMR (300 MHz, C_6D_6):

δ_H 2.62 (br s, 2 C-H), -2.29 (br s, 2 H_μ)

Additional peaks in $^1H\{^{11}B\}$ NMR (300 MHz, C_6D_6):

δ_H 2.90 (s, 2H), 2.53 (s, 2H), 1.93 (s, 1H), 1.76 (s, 2H), 1.43 (s, 2H)

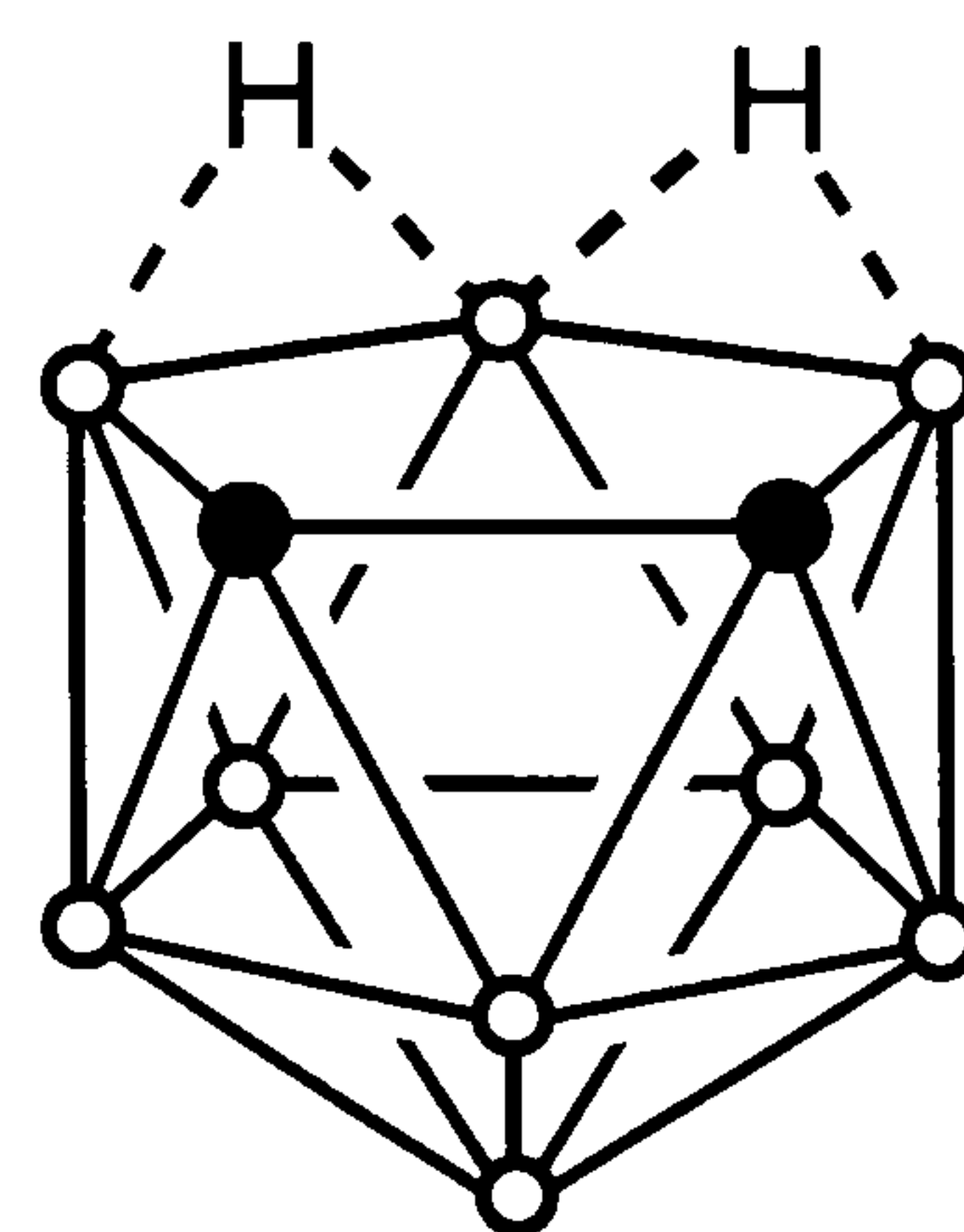
$^{13}C\{^1H\}$ NMR (75 MHz, C_6D_6):

δ_C 65.3 (br s, 2C)

^{11}B NMR (96.2 MHz, C_6D_6):

δ_B 4.6 (d, 2B, J_{B-H} 164), -3.9 (d, 2B, J_{B-H} 155), -15.8 (d, 1B, J_{B-H} 178), -16.4 (d, 1B, J_{B-H} 164)

-26.8 (dd, 3B, J_{B-H} 147, 56)



Analysis $\text{C}_2\text{H}_{13}\text{B}_9$:

Calc. C%, 17.8; H%, 9.7 and found: C%, 17.9; H%, 9.8

5.2.2 Acidification of 7,9- $\text{C}_2\text{B}_9\text{H}_{12}^-$.

With vigorous stirring under nitrogen, a slurry of $[\text{NBu}_4^+][7,9\text{-C}_2\text{B}_9\text{H}_{12}^-]$ (3.75 g, 10 mmol) in benzene (100 ml) was cooled to 0 °C (ice bath) and treated dropwise with concentrated H_2SO_4 (100 ml). Gas evolution was immediately observed and after one hour the benzene layer was decanted, dried and the solvent was removed under reduced pressure. Sublimation of the residue at 50 °C/0.1 mmHg gave a white air-sensitive solid identified⁹ by NMR as *closo*-2,3- $\text{C}_2\text{B}_9\text{H}_{11}$ **14** (1.12 g, 85 %).

^1H NMR (300 MHz, C_6D_6):

δ_{H} 5.19 (br s, 2 C-H)

Additional peaks in $^1\text{H}\{^{11}\text{B}\}$ NMR (300 MHz, C_6D_6):

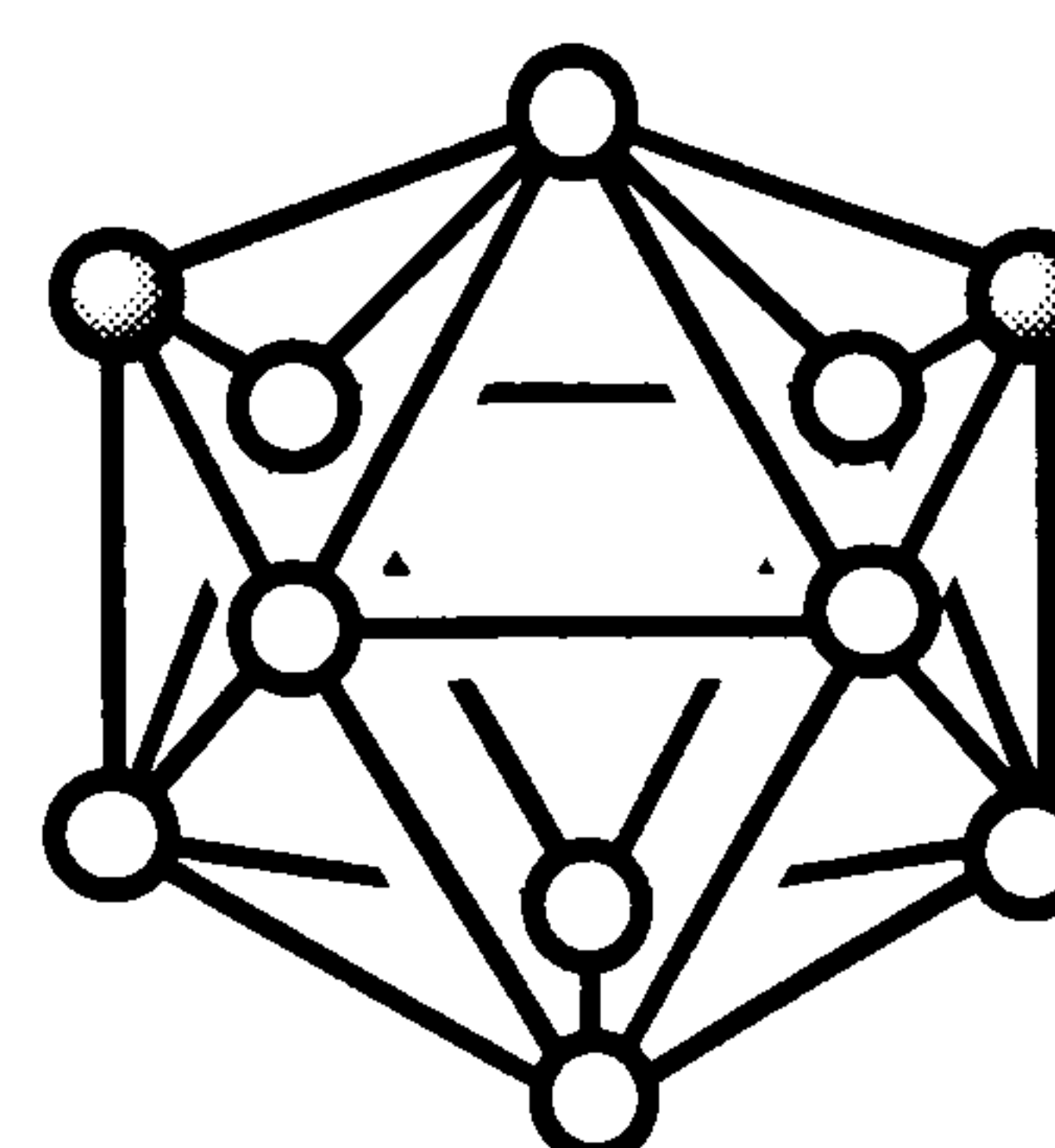
δ_{H} 2.76 (br s, 6H), 2.25 (br s, 2H), 0.62 (s, 1B)

$^{13}\text{C}\{^1\text{H}\}$ NMR (75 MHz, C_6D_6):

δ_{C} 87.3 (br s, 2C)

^{11}B NMR (96.2 MHz, C_6D_6):

δ_{B} -4.2 (d, 4B, $J_{\text{B-H}}$ 164), -8.5 (M, 2B), -10.2 (M, 2B), -15.8 (d, 1B, $J_{\text{B-H}}$ 169)



5.2.3 Synthesis of [2,9- $\text{C}_2\text{B}_9\text{H}_{13}$], (**9**).

Under nitrogen, a solution of the *closo* carborane 1,12- $\text{C}_2\text{B}_{10}\text{H}_{12}$ (5.76 g, 0.04 mol) in dry toluene (100 ml) was treated with powdered KOH (20 g, 0.36 mol) and dry tetraglyme (100 ml). The mixture was refluxed under nitrogen for 18 h. The mixture was filtered and the solid was slurried in 100 ml of dry benzene. With vigorous stirring the slurry was slowly treated with 85% H_3PO_4 acid (70 ml). The benzene layer was then washed with distilled water (2 x 20 ml), dried and the solvent was carefully removed. Sublimation of the residue at 80 °C/0.1

Chapter Five – Experimental Details

mmHg gave a white crystalline solid identified by NMR spectroscopy as a 9:1 mixture of 2,9- $\text{C}_2\text{B}_9\text{H}_{13}$ (**9**) and 1,12- $\text{C}_2\text{B}_{10}\text{H}_{12}$. Careful resublimation at 30 °C/0.1 mmHg gave a white crystalline solid identified (see table for NMR data) as pure $\text{C}_2\text{B}_9\text{H}_{13}$ (**9**) (2.42 g 45 %).

^1H NMR (300 MHz, C_6D_6):

δ_{H} 2.52 (br s, 1C-H), 1.74 (br s, 1C-H), -3.96 (br s, 2H)

Additional peaks in $^1\text{H}\{^{11}\text{B}\}$ NMR (300 MHz, C_6D_6):

δ_{H} 2.40 (s, 2H), 2.16 (s, 2H), 1.82 (s, 1H), 1.67 (s, 2H), 0.97 (s, 2H)

$^{13}\text{C}\{^1\text{H}\}$ NMR (75 MHz, C_6D_6):

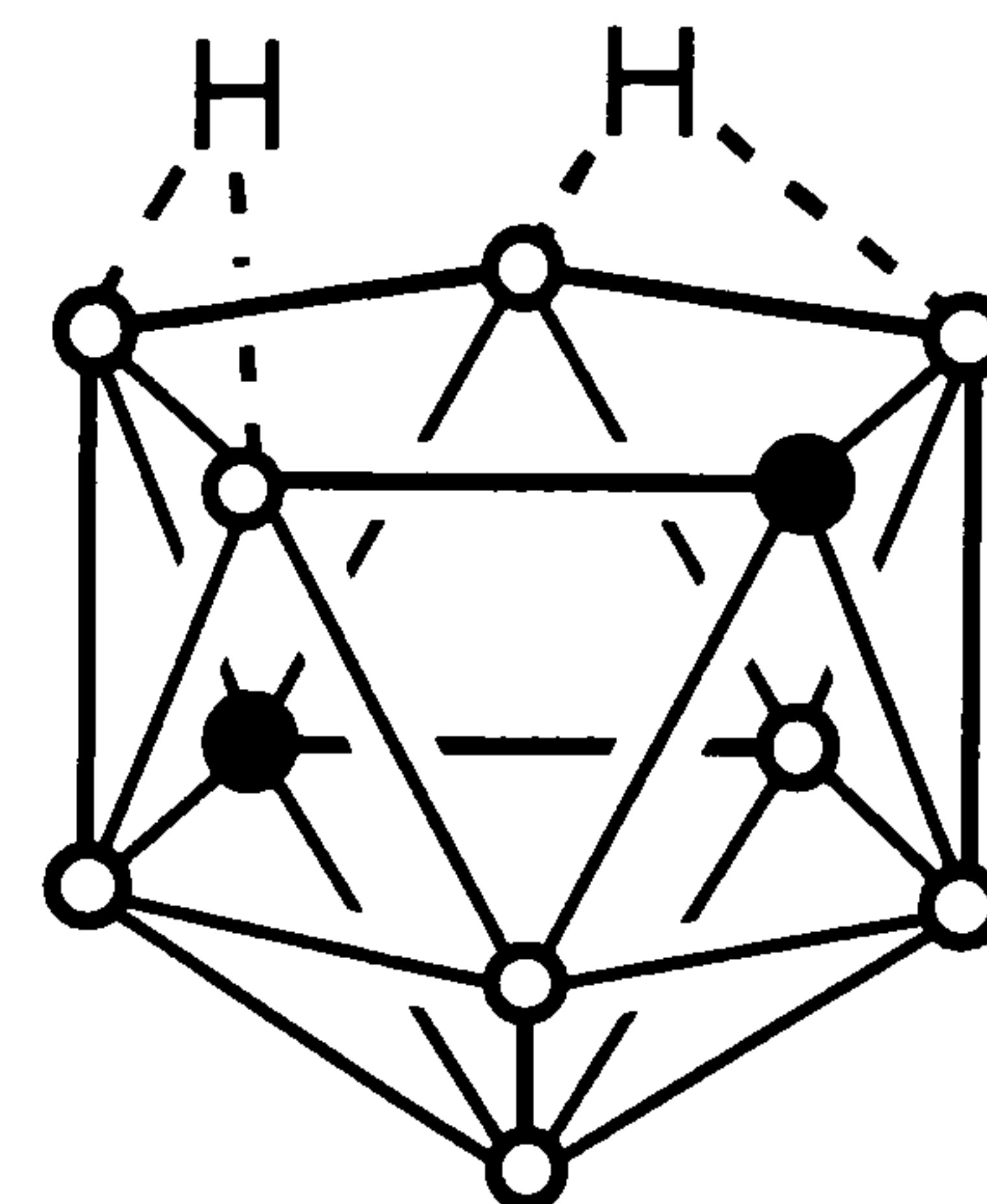
δ_{C} 71.1 (s, 1C), 45.7 (br s, 1C)

^{11}B NMR (96.2 MHz, C_6D_6):

δ_{B} -8.0 (d, 2B, $J_{\text{B-H}}$ 149), -10.7 (d, 2B, $J_{\text{B-H}}$ 164), -25.5 (dd, 2B, $J_{\text{B-H}}$ 169, 71), -26.0 (d, 1B, $J_{\text{B-H}}$ 170), -35.3 (d, 2B, $J_{\text{B-H}}$ 167)

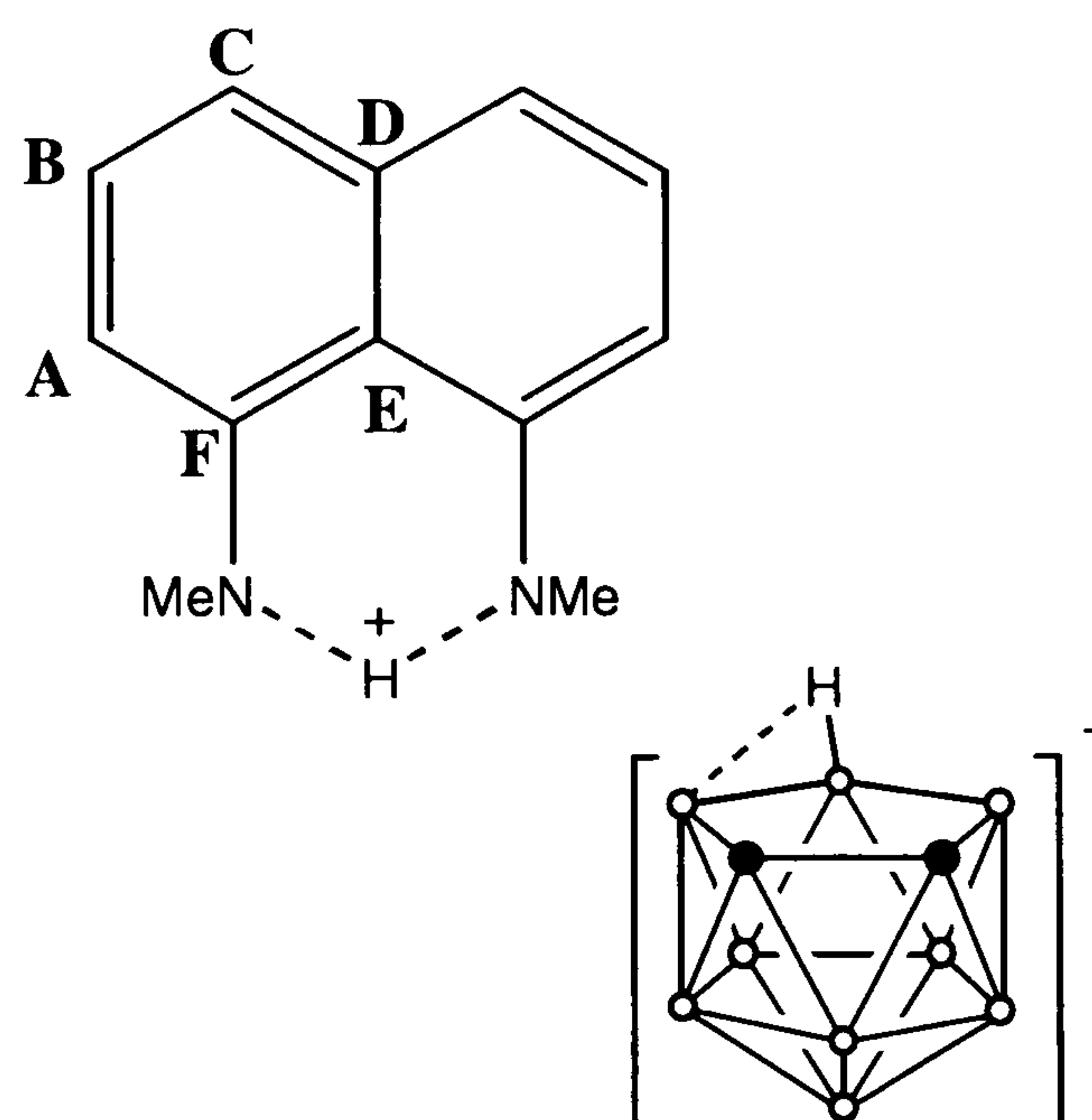
Analysis $\text{C}_2\text{H}_{13}\text{B}_9$:

Calc.: C%, 17.8; H%, 9.7 and found: C%, 17.3; H%, 9.7



5.2.4 Synthesis of the protonated proton sponge salt of 7,8- $\text{C}_2\text{B}_9\text{H}_{12}^-$ (**4a**).

Addition of a hexane solution (40 ml) of proton sponge (0.214 g, 1 mmol) to the neutral carborane 7,8- $\text{C}_2\text{B}_9\text{H}_{13}$ (**7**) (0.134 g, 1 mmol) in hexane afforded a precipitate. This solid was filtered and recrystallised from dichloromethane with slow diffusion of hexane at -30 °C to yield crystals structurally characterised as the proton sponge salt of 7,8- $\text{C}_2\text{B}_9\text{H}_{12}^-$ (0.268 g, 77 %)



^1H NMR (300 MHz, $(\text{CD}_3)_2\text{CO}$):

δ_{H} 18.79 (s, 1H, $\text{NH}^+\cdots\text{N}$), 7.97 (d, C, $^2J_{\text{H-H}}$ 8), 7.91 (d, A $^2J_{\text{H-H}}$ 8), 7.63 (dd, 2H, B), 3.17 (s, 12H, NMe_2), 1.81 (br s, 2H, $\text{C}_2\text{B}_9\text{H}_{12}$), -2.95 (br s, 1H, H_μ)

Chapter Five – Experimental Details

Additional peaks in $^1\text{H}\{^{11}\text{B}\}$ NMR (300 MHz, $(\text{CD}_3)_2\text{CO}$):

δ_{H} 1.86 (s, 2H), 1.68 (s, 1H), 1.14 (s, 4H), 0.46 (s, 1H), 0.01 (s, 1H)

$^{13}\text{C}\{^1\text{H}\}$ NMR (75 MHz, $(\text{CD}_3)_2\text{CO}$):

δ_{C} 144.8 (s, 2C, F), 135 (s, 1C, D), 129.7 (s, 2C, C), 127.5 (s, 2C B), 122.0 (s, 2C, A), 119.9 (s, 1C, E), 46.1 (s, 4C, NMe_2), 42.2 (br s, 2C, $\text{C}_2\text{B}_9\text{H}_{12}$)

^{11}B NMR (96.2 MHz, $(\text{CD}_3)_2\text{CO}$):

δ_{B} -10.4 (d, 2B, $J_{\text{B-H}}$ 136), -15.9 (d, 2B, $J_{\text{B-H}}$ 127), -16.4, (d, 1B, $J_{\text{B-H}}$ 169), -21.4 (d, 2B, $J_{\text{B-H}}$ 150), -32.5 (dd, 1B, $J_{\text{B-H}}$ 129, 48), -37.2 (d, 1B, $J_{\text{B-H}}$ 135)

Analysis $\text{C}_{16}\text{H}_{31}\text{B}_9\text{N}_2$:

Calc.: C%, 55.11; H%, 8.96; N% 8.03, and found: C%, 54.70; H%, 8.87; N% 7.92

5.2.5 Synthesis of the Triphenyl methyl Phosphonium salt of 7,8- $\text{C}_2\text{B}_9\text{H}_{12}^-$ (4b).

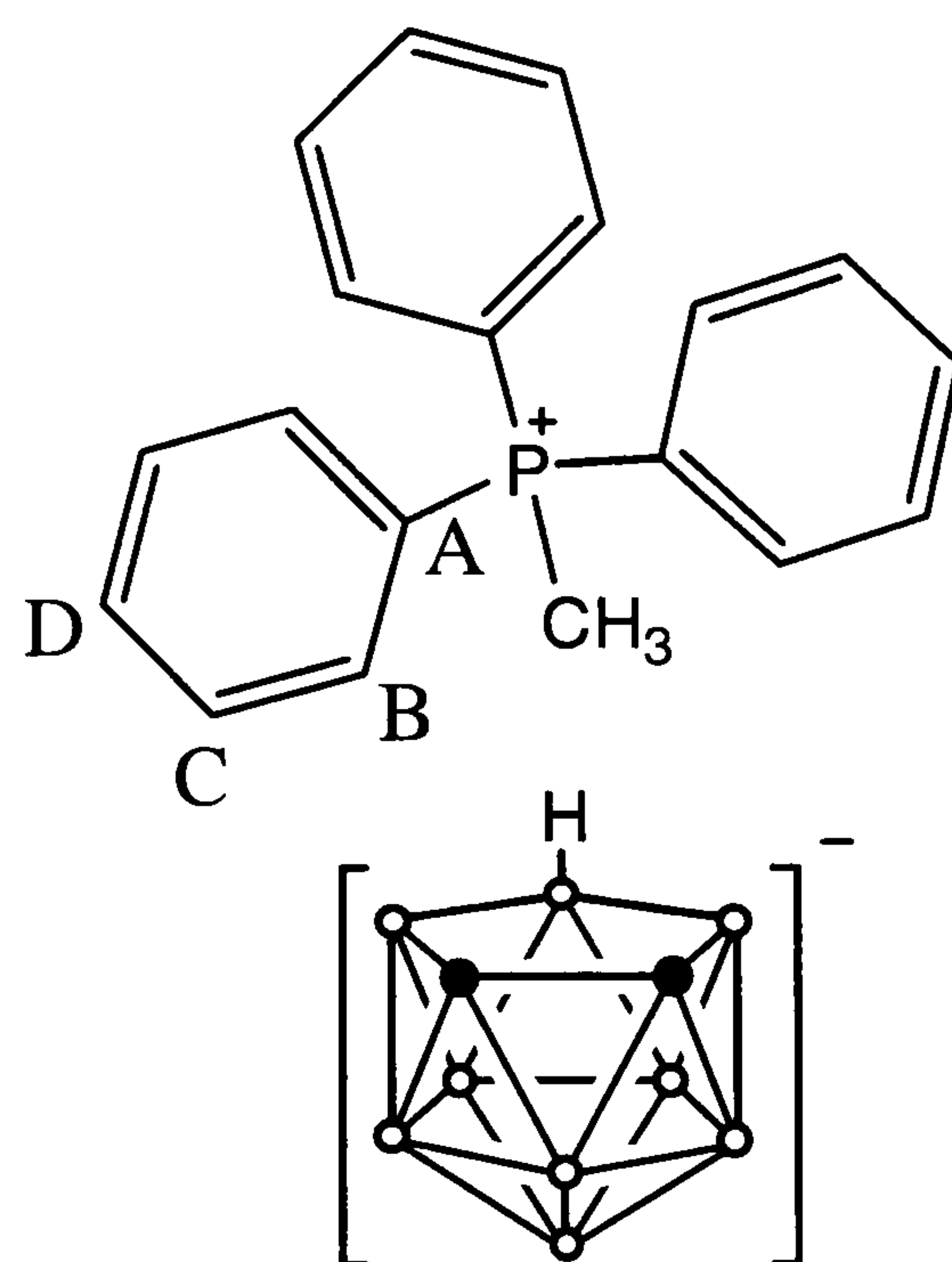
Addition of a hexane solution (40 ml) of triphenyl phosphonium methyide, $[\text{Ph}_3\text{PCH}_2]$, (0.28 g, 1 mmol) to the neutral carborane 7,8- $\text{C}_2\text{B}_9\text{H}_{13}$ **7** (0.134 g, 1 mmol) in hexane afforded a precipitate. This solid was filtered and recrystallised from dichloromethane with slow diffusion of hexane at $-30\text{ }^\circ\text{C}$ to yield crystals structurally characterised as the phosphonium salt of 7,8- $\text{C}_2\text{B}_9\text{H}_{12}^-$ (0.268 g, 77 %)

^1H NMR (300 MHz, CDCl_3):

δ_{H} 7.86-7.55 (m, 15H, Ph), 2.81 (d, 3H, P-Me, $^2J_{\text{H-P}}$ 12), 1.80 (br s, 2H, $\text{C}_2\text{B}_9\text{H}_{12}$), -2.90 (br s, 1H, H_μ)

Additional peaks in $^1\text{H}\{^{11}\text{B}\}$ NMR (300 MHz, CDCl_3):

δ_{H} .1.86 (s, 2H), 1.67 (s, 1H), 1.20 (s, 4H), 0.52 (s, 1H), 0.07 (s, 1H)



$^{13}\text{C}\{^1\text{H}\}$ NMR (75 MHz, CDCl_3):

δ_{C} 135.3 (d, 1C, D, $^4J_{\text{C-P}}$ 4), 133.1 (d, 2C, C, $^3J_{\text{C-P}}$ 11), 130.7 (d, 2C, B, $^2J_{\text{C-P}}$ 13), 118.5 (d, 1C, A, $^1J_{\text{C-P}}$ 85), 43.8, (br s, 2C, $\text{C}_2\text{B}_9\text{H}_{12}$), 10.3 (d, 1C, P-Me, $^1J_{\text{C-P}}$ 59)

^{11}B NMR (96.2 MHz, CDCl_3):

δ_{B} -11.16 (d, 2B, $J_{\text{B-H}}$ 136), -17 (d, 3B, $J_{\text{B-H}}$ 127), -21.9 (d, 2B, $J_{\text{B-H}}$ 150), -33.1 (dd, 1B, $J_{\text{B-H}}$ 129, 46), -37.8 (d, 1B, $J_{\text{B-H}}$ 134)

$^{31}\text{P}\{^1\text{H}\}$ NMR (80.9 MHz, CDCl_3):

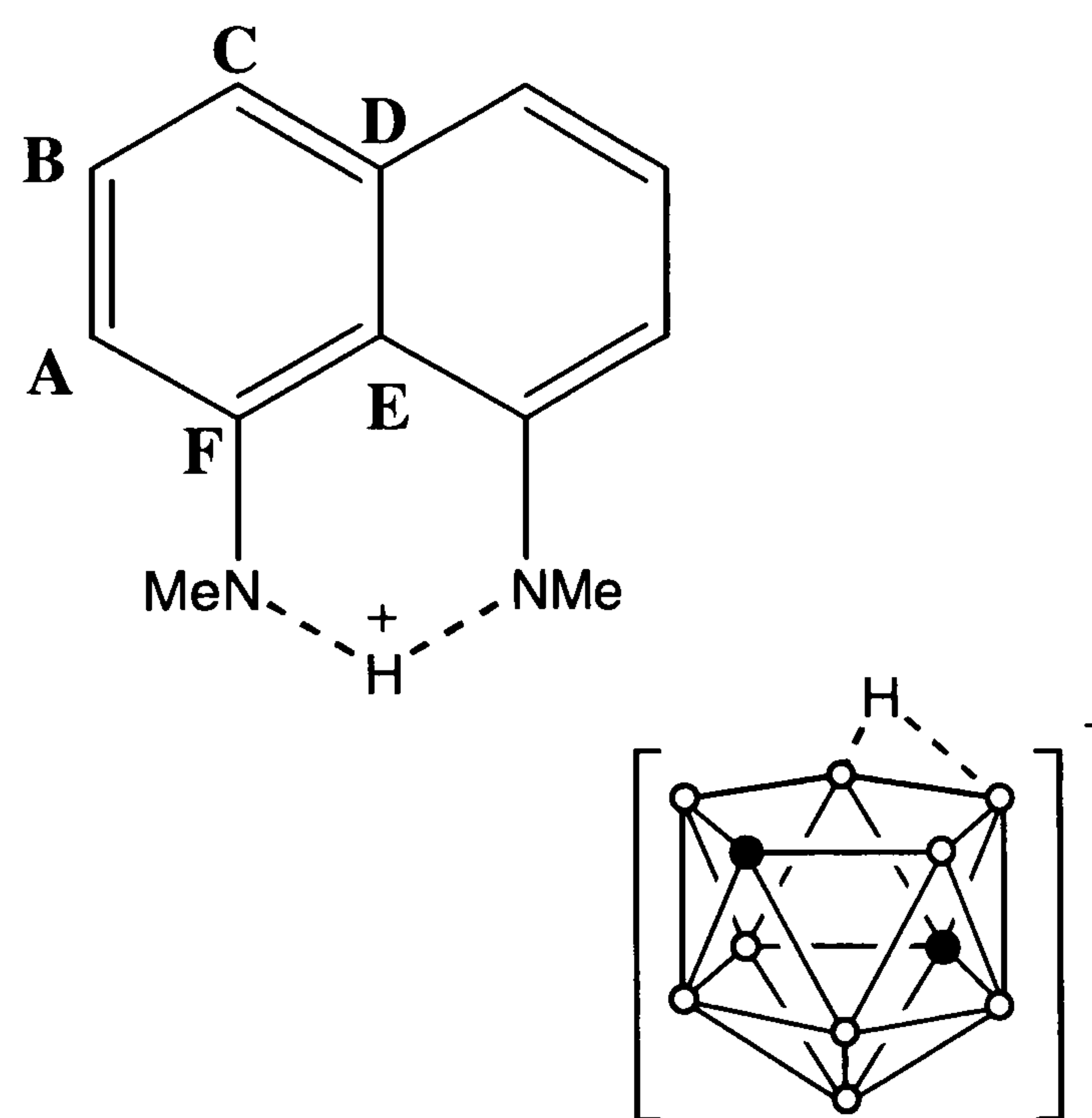
δ_{P} 21.98 (s, 1P, $\text{Ph}_3\text{P}^+\text{Me}$)

Analysis $\text{C}_{21}\text{H}_{29}\text{B}_9\text{P}$:

Calc.: C%, 61.41; H%, 7.36 and found: C%, 61.64; H%, 7.39

5.2.6 Synthesis of the protonated proton sponge salt of 2,9- $\text{C}_2\text{B}_9\text{H}_{12}^-$ (9a).

A hexane solution (40 ml) of 2,9- $\text{C}_2\text{B}_9\text{H}_{13}$ (0.134 g, 1 mmol) was treated with a hexane solution (40 ml) of proton sponge (0.214 g, 1 mmol) to produce a white precipitate. The precipitate was filtered and vacuum sublimed at 150 °C/0.1 mmHg to give a pure sample of the protonated proton sponge salt of 2,9- $\text{C}_2\text{B}_9\text{H}_{12}^-$ **6** (85 %). Crystals of the salt suitable for X-ray structural determination were obtained by recrystallization from a hexane/dichloromethane mixture at -30 °C.



^1H NMR (300 MHz, $(\text{CD}_3)_2\text{CO}$):

δ_{H} 18.83 (s, 1H, $\text{NH}^+\cdots\text{N}$), 7.95 (d, C, $^2J_{\text{H-H}}$ 8), 7.89 (d, A, $^2J_{\text{H-H}}$ 8), 7.72 (dd, 2H, B), 3.28 (s, 12H, NMe_2), 1.53 (s, 1H, $\text{C}_2\text{B}_9\text{H}_{12}$), 1.14 (br s, 1H, $\text{C}_2\text{B}_9\text{H}_{12}$), -1.01 (br s, 1H, H_μ).

Additional peaks in $^1\text{H}\{^{11}\text{B}\}$ NMR (300 MHz, $(\text{CD}_3)_2\text{CO}$):

δ_{H} 1.78 (s, 2H), 1.60 (s, 2H), 1.36 (s, 2H), 0.88 (s, 1H), 0.42 (s, 2H)

$^{13}\text{C}\{^1\text{H}\}$ NMR (75 MHz, $(\text{CD}_3)_2\text{CO}$):

δ_{C} 145.8 (s, 2C, F), 134.8 (s, 1C, D), 129.7 (s, 2C, C), 126.9 (s, 2C B), 121.8 (s, 2C, A), 120.0 (s, 1C, E), 50.6 (br s, 1C, $\text{C}_2\text{B}_9\text{H}_{12}$) 44.9 (s, 4C, NMe_2), 27.7 (s, 1C, $\text{C}_2\text{B}_9\text{H}_{12}$)

^{11}B NMR (96.2 MHz, $(\text{CD}_3)_2\text{CO}$):

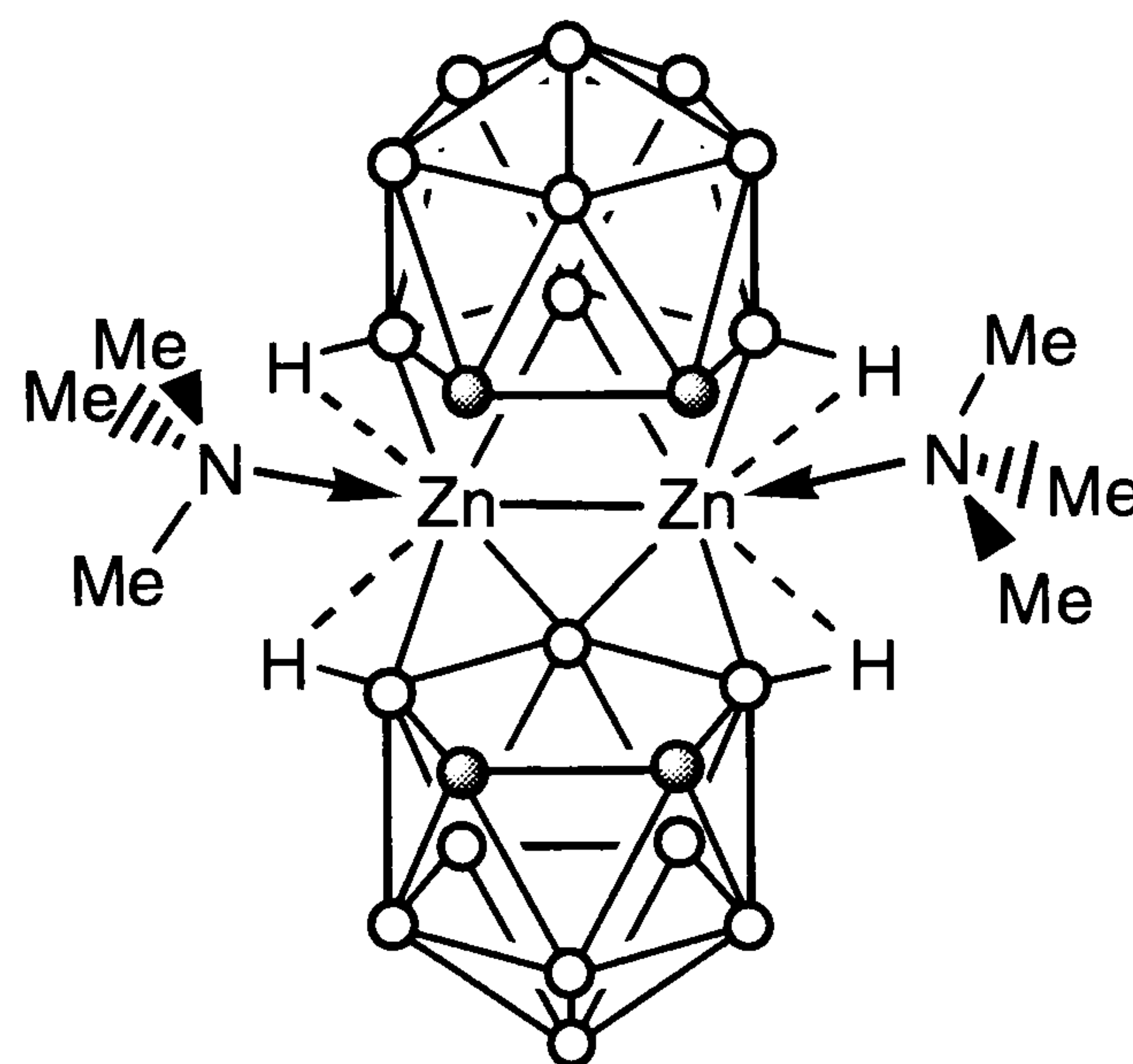
δ_{B} -13.7 (d, 2B, $J_{\text{B-H}}$ 121), -19.6 (d, 2B, $J_{\text{B-H}}$ 155), -22.0 (d, 2B, $J_{\text{B-H}}$ 152), -28.9 (t, 2B, $J_{\text{B-H}}$ 95, 65), -43.2 (d, 1B, $J_{\text{B-H}}$ 150)

Analysis $\text{C}_{16}\text{H}_{31}\text{B}_9\text{N}_2$:

Calc.: C%, 55.11; H%, 8.96; N% 8.03, and found: C%, 54.69; H%, 8.86; N% 7.71

5.276 Synthesis of $[\{(nido-7,8-\text{C}_2\text{B}_9\text{H}_{11})\text{ZnNMe}_3\}_2]$ (13).

A stirred suspension of $[\text{ortho}-\text{C}_2\text{B}_9\text{H}_{11}][\text{NMe}_3\text{H}]^7$ (0.288 g, 1.5 mmol) in toluene (20 ml) was treated dropwise with Me_2Zn (0.75 ml of 2M soln. in toluene, 1.5 mmol). After stirring for 18 h the solution was briefly refluxed and filtered whilst hot. Slow cooling to room temperature gave 3 crops of colourless crystals of $[\{(nido-7,8-\text{C}_2\text{B}_9\text{H}_{11})\text{ZnNMe}_3\}_2]$. Total yield 1.00g, 96%.



^1H NMR (300 MHz, $\text{C}_5\text{D}_5\text{N}$):

δ_{H} 2.07 (s, 9H, NMe_3), 1.24 (2H, CH).

Additional peaks in $^1\text{H}\{^{11}\text{B}\}$ NMR (300 MHz, $\text{C}_5\text{D}_5\text{N}$):

δ_{H} 2.57 (s, 2H), 2.44 (s, 1H), 2.37 (s, 2H), 2.27 (s, 2H), 1.88 (s, 1H), 1.37 (s, 1H)

$^{13}\text{C}\{^1\text{H}\}$ NMR (75 MHz, $\text{C}_5\text{D}_5\text{N}$):

δ_{C} 48.7 (br s, 4C, $\text{C}_2\text{B}_9\text{H}_{11}$), 28.3 (s, 6C, NMe_3)

^{11}B NMR (96.2 MHz, $\text{C}_5\text{D}_5\text{N}$):

δ_{B} -16.3 (d, 5B, $J_{\text{B-H}}$ 172), -21.5 (d, 2B, $J_{\text{B-H}}$ 133), -32.3 (d, 1B, $J_{\text{B-H}}$ 128), -38.5 (d, 1B, $J_{\text{B-H}}$ 109)

Analysis; $C_{10}H_{40}B_{18}N_2Zn_2(C_7H_8)_{1.35}$:

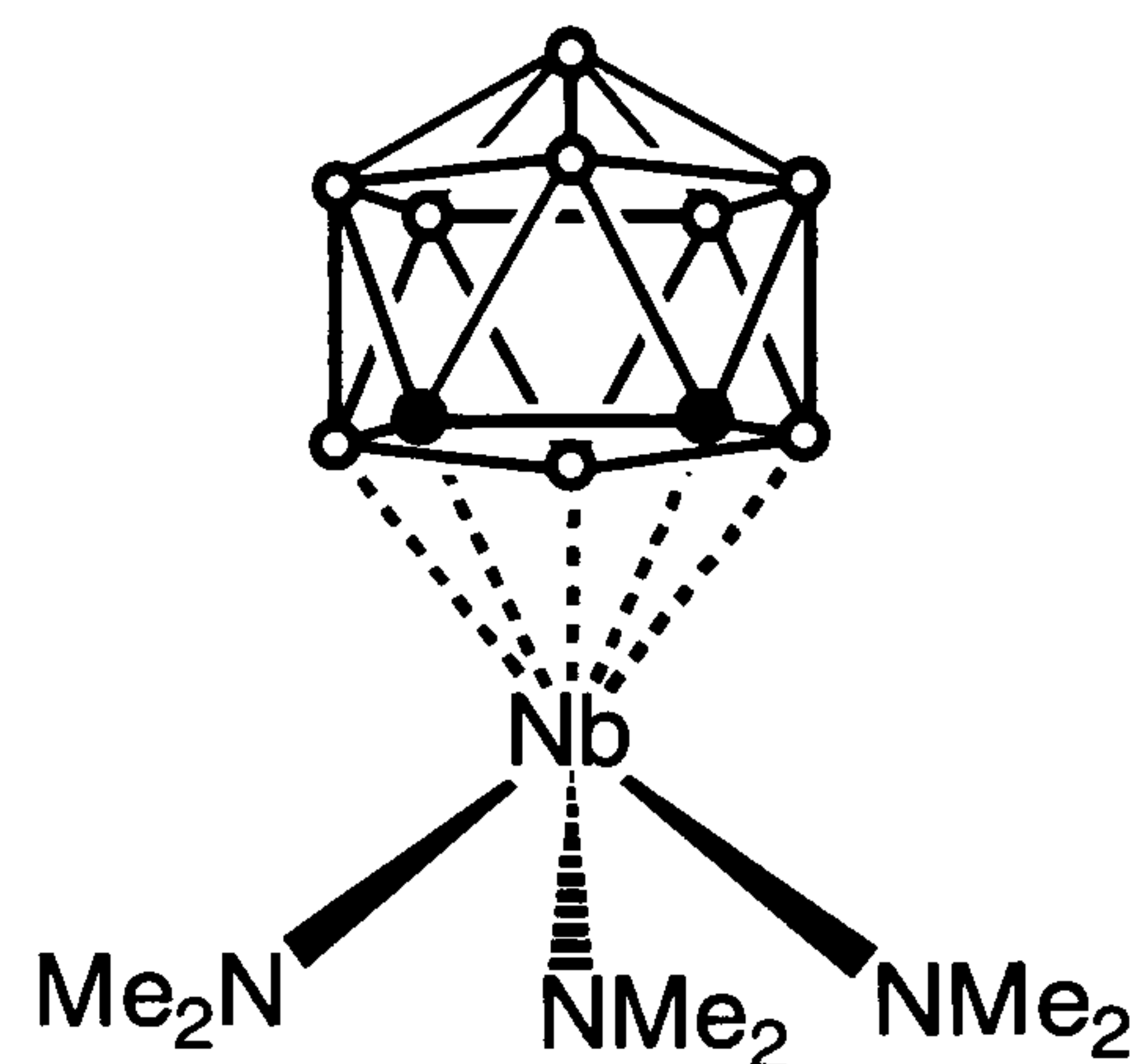
Calc.: C%, 36.6; H%, 8.0; N% 4.4, and found: C%, 36.3; H%, 7.9; N% 4.9

5.3 Experimental Details to Chapter Three

Literature methods were used for the preparation of both $[Ta(NMe_2)_5]$,¹⁰ and $[Nb(NMe_2)_5]$.¹¹

5.3.1 Synthesis of $[3-Nb(NMe_2)_3(1,2-C_2B_9H_{11})]$, (16).

A stirred toluene (50 cm^3) solution of $Nb(NMe_2)_5$ (**14**) (0.94 g, 3 mmol) was treated dropwise at room temperature with a toluene (10 cm^3) solution of *ortho*- $C_2B_9H_{13}$ (0.43 g, 3 mmol). The solution was stirred at room temperature for 12 h and slowly lightened from brown to orange. The solution was concentrated to 10 cm^3 under reduced pressure, leaving a yellow solid, which was isolated by filtration and washed with 10 cm^3 of pentane before drying *in vacuo*. Yield 0.93 g, 87 %. Crystals suitable for X-ray structure determination were grown at $-30\text{ }^\circ\text{C}$, from a concentrated dichloromethane solution of (**16**), layered with toluene.



^1H NMR (300 MHz, CDCl_3):

δ_{H} 3.54 (s, 18H, 3 x NMe_2), 2.73 (br s, 2H, carborane C-H)

Additional peaks in $^1\text{H}\{^{11}\text{B}\}$ NMR (300 MHz, CDCl_3):

δ_{H} 2.37 (s, 1H), 2.25 (s, 3H), 2.11 (s, 2H), 2.06 (s, 1H), 1.90 (s, 2H)

$^{13}\text{C}\{^1\text{H}\}$ NMR (75 MHz, CDCl_3):

δ_{C} 53.0 (carborane C), 51.2 (NMe_2)

^{11}B NMR (96.2 MHz, CDCl_3):

δ_{B} 3.3 (d, 1B, $J_{\text{B-H}}$ 121), -2.9 (d, 2B, $J_{\text{B-H}}$ 149), -5.1 (d, 2B, $J_{\text{B-H}}$ 146), -13.2 (d, 3B, $J_{\text{B-H}}$ 147), -14.4 (d, 1B, $J_{\text{B-H}}$ 112)

Chapter Five – Experimental Details

Analysis $C_8H_{29}B_9N_3Nb$:

Calc.; C%, 26.88; H%, 8.18; N%, 11.75 and found: C%, 27.4; H%, 8.16; N%, 10.90

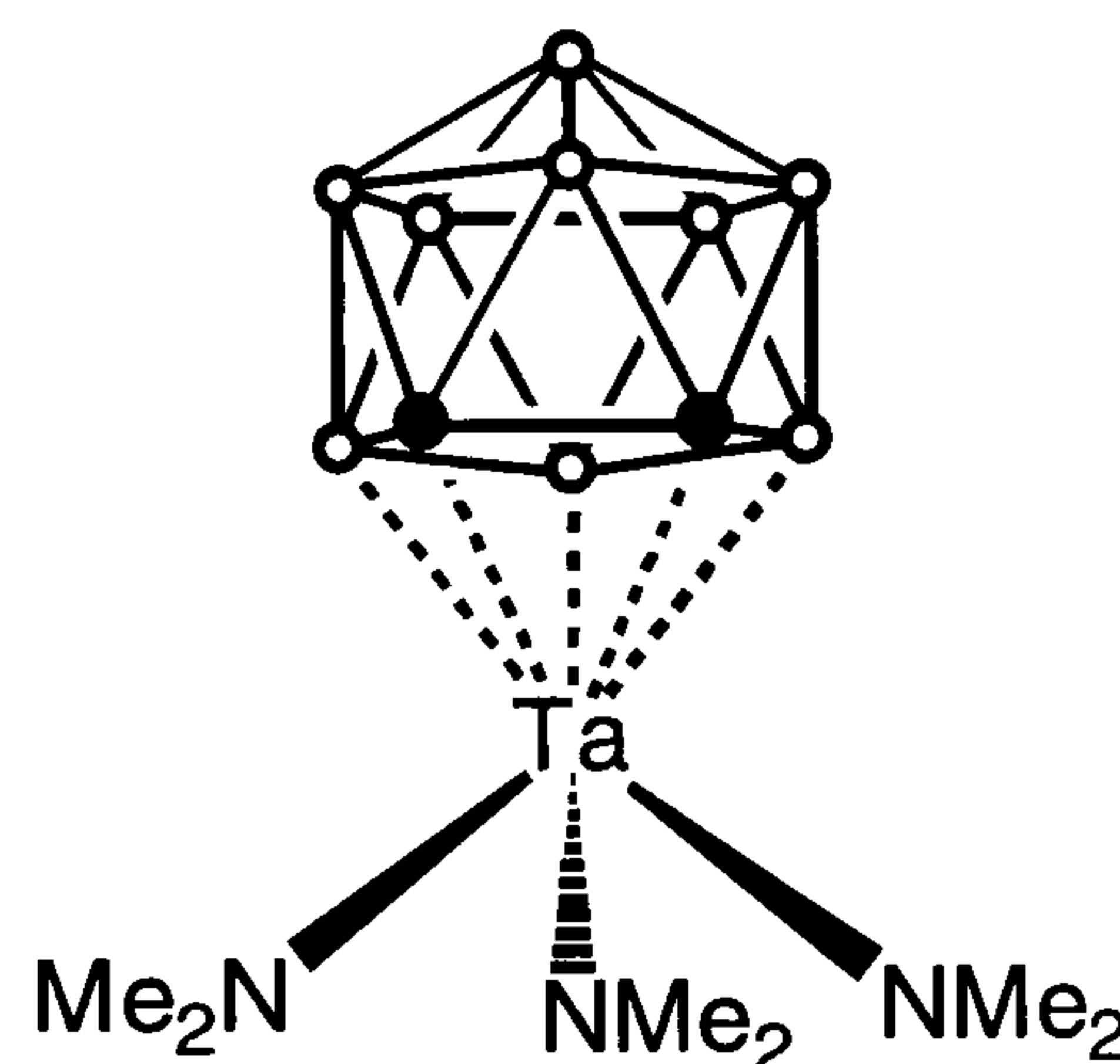
Mass Spec:

m/e (assignment) 358 [M^+], 343 [$M - CH_3^+$] and 225 [$M - C_2B_9H_{11}^+$]

IR: 2516s, 1444w, 1414w, 1230s, 1135w 1032s cm^{-1}

5.3.2 Synthesis of $[3-Ta(NMe_2)_3(1,2-C_2B_9H_{11})]$, (17).

A stirred toluene (100 cm^3) solution of $Ta(NMe_2)_5$ (15) (8.026 g, 20 mmol) was treated dropwise at room temperature with a toluene (50 cm^3) solution of *ortho*- $C_2B_9H_{13}$ (2.68 g, 20 mmol). The solution was stirred at room temperature for 15 h and slowly changed from yellow to orange. The solution was concentrated to 20 cm^3 under reduced pressure, leaving a pale yellow solid, which was isolated by filtration and washed with 10 cm^3 of pentane before drying *in vacuo*. Yield 7.9 g, 89%. Crystals suitable for X-ray structure determination were grown at $-30\text{ }^\circ C$, from a concentrated dichloromethane solution of (17), layered with toluene.



1H NMR (300 MHz, $CDCl_3$):

δ_H 3.62 (s, 18H, 3 x NMe_2), 2.73 (br s, 2H, carborane C-H)

Additional peaks in $^1H\{^{11}B\}$ NMR (300 MHz, $CDCl_3$):

δ_H 3.02 (s, 1H), 2.37 (s, 1H), 2.29 (s, 2H), 2.18 (s, 2H), 1.62 (br s, 3H)

$^{13}C\{^1H\}$ NMR (75 MHz, $CDCl_3$):

δ_C 52.1 (carborane C), 49.1 (NMe_2)

^{11}B NMR (96.2 MHz, $CDCl_3$):

δ_B 1.7 (d, 1B, J_{B-H} 124), -3.4 (d, 2B, J_{B-H} 144), -5.7 (d, 2B, J_{B-H} 138), -13.8 (d, 3B, J_{B-H} 158), -16.2 (d, 1B, J_{B-H} 158)

Analysis $C_8H_{29}B_9N_3Ta$:

Calc.: C%, 21.56; H%, 6.6; N%, 9.43 and found: C%, 21.14; H%, 6.55; N%, 8.71

Mass Spec:

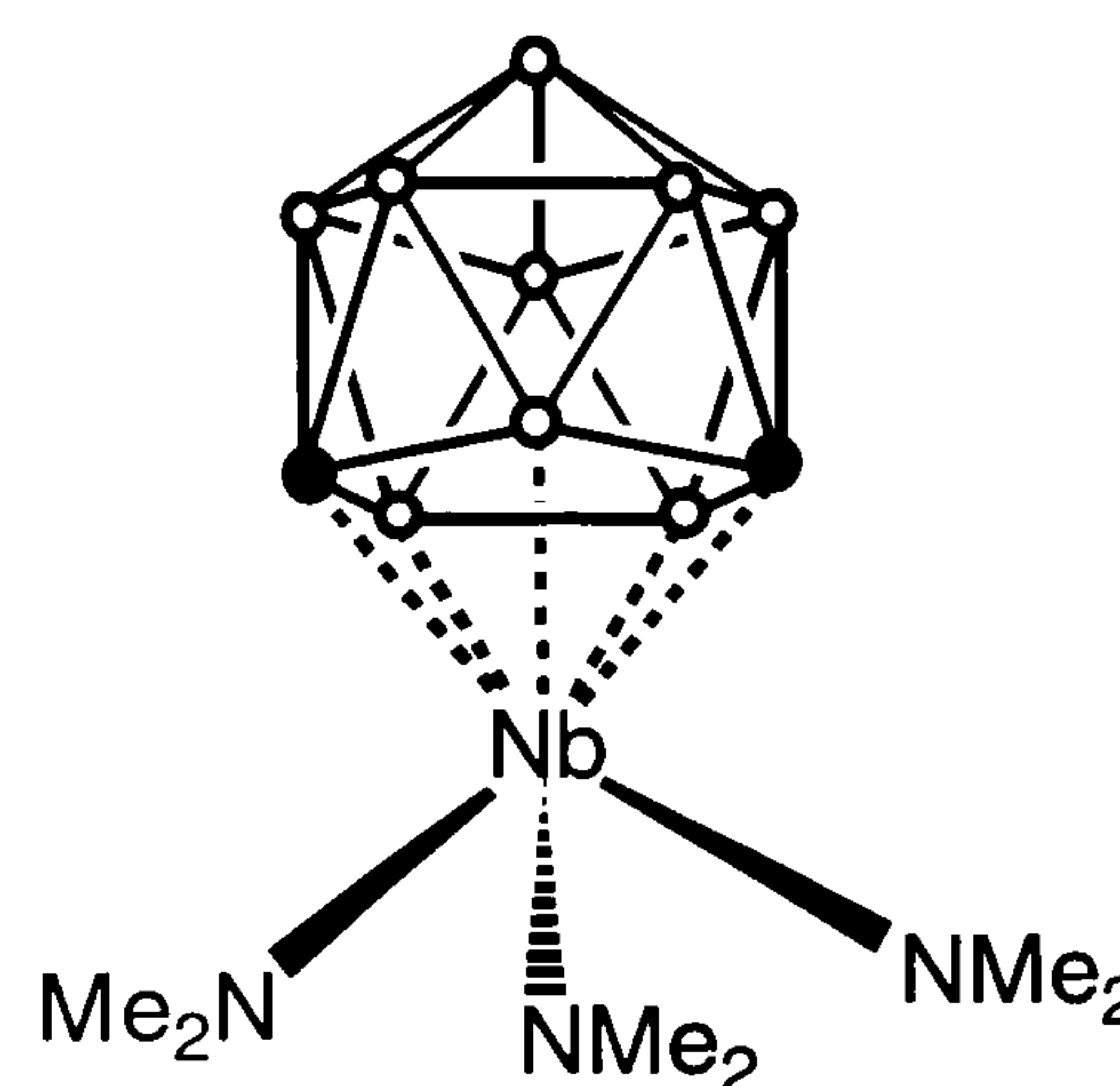
m/e (assignment) 446 [M^+], 431 [$M - CH_3^+$] and 313 [$M - C_2B_9H_{11}^+$]

IR:

2552vs, 1446s, 1420w, 1238s, 1124w, 1035s cm^{-1}

5.3.3 Synthesis of $[2-Nb(NMe_2)_3(1,7-C_2B_9H_{11})]$, (18).

A stirred suspension of [*meta*- $C_2B_9H_{12}$][Me_3NH] (0.92 g, 5 mmol) in toluene (20 cm^3) was treated dropwise with a toluene solution of $Nb(NMe_2)_5$ (14) (1.6 g, 5 mmol). After refluxing for 15 h, the solution was cooled to 20 °C and concentrated to 5 cm^3 under reduced pressure. The solution was layered with pentane and cooled to -40 °C giving crystalline product. Yield 1.29 g, 72 %.



1H NMR (300 MHz, $CDCl_3$):

δ_H 3.46 (18H, NMe), 2.35 (2H, CH),

Additional peaks in $^1H\{^{11}B\}$ NMR (300 MHz, $CDCl_3$):

δ_H 3.68 (s, 1H), 2.39 (s, 2H), 2.08 (s, 2H), 2.04 (s, 1H), 1.94 (s, 2H). 1.87 (s, 2H)

$^{13}C\{^1H\}$ NMR (75 MHz, $CDCl_3$):

δ_C 59.3 ($C_2B_9H_{11}$), 50.7 (NMe)

^{11}B NMR (96.2 MHz, $CDCl_3$):

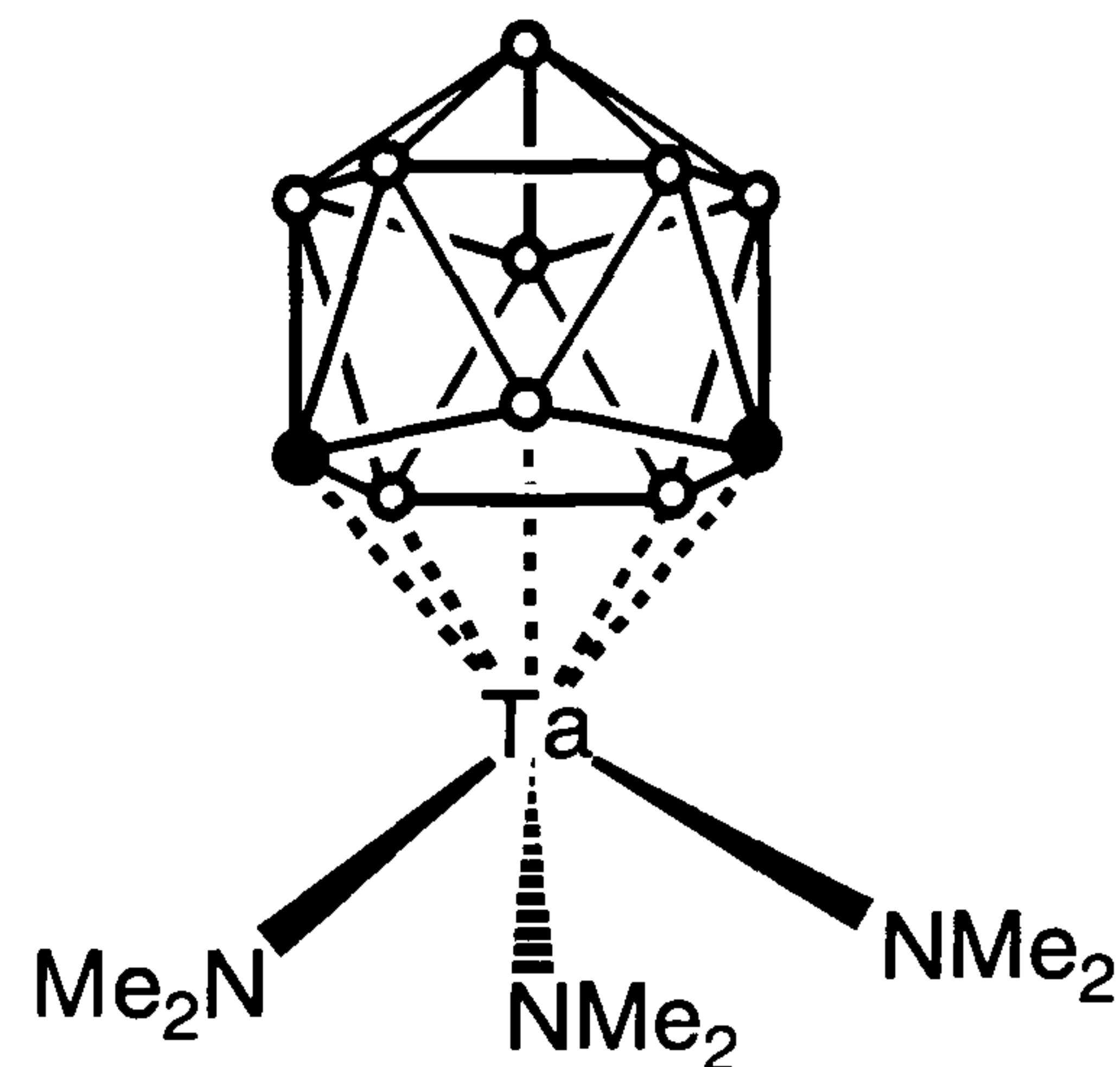
δ_B -4.7 (d, 2B), -5.8 (d, 2B), -8.0 (d, 1B), -11.4 (d, 1B), -12.9 (d, 2B); -15.6 (d, 1B)

Analysis $C_8H_{29}B_9N_3Nb$:

Calc.: C%, 26.88; H%, 8.18; N%, 11.75 and found: C%, 26.5; H%, 8.7; N%, 9.86

5.3.4 Synthesis of [2-Ta(NMe₂)₃(1,7-C₂B₉H₁₁)], (19).

A stirred suspension of [*meta*-C₂B₉H₁₂][Me₃NH] (0.92 g, 5 mmol) in toluene (20 cm³) was treated dropwise with a toluene solution of Ta(NMe₂)₅ (2.0 g, 5 mmol). After refluxing for 15 h, the solution was cooled to 20 °C and concentrated to 5 cm³ under reduced pressure. The solution was layered with pentane and cooled to -40 °C giving crystalline product. Yield 1.7 g, 76 %. Crystals suitable for X-ray structure determination were grown at -30 °C, from a concentrated dichloromethane solution of (17), layered with toluene.



¹H NMR (300 MHz, CDCl₃):

δ_H 3.64 (18H, NMe), 3.03 (1H, BH), 2.22 (2H, CH)

Additional peaks in ¹H{¹¹B} NMR (300 MHz, CDCl₃):

δ_H 3.03 (s, 1H), 2.46 (s, 2H), 2.35 (s, 2H), 2.22 (s, 1H), 1.99 (s, 1H), 1.71 (s, 2H)

¹³C{¹H} NMR (75 MHz, CDCl₃):

δ_C 57.7 (C₂B₉H₁₁), 49.4 (NMe)

¹¹B NMR (96.2 MHz, CDCl₃)

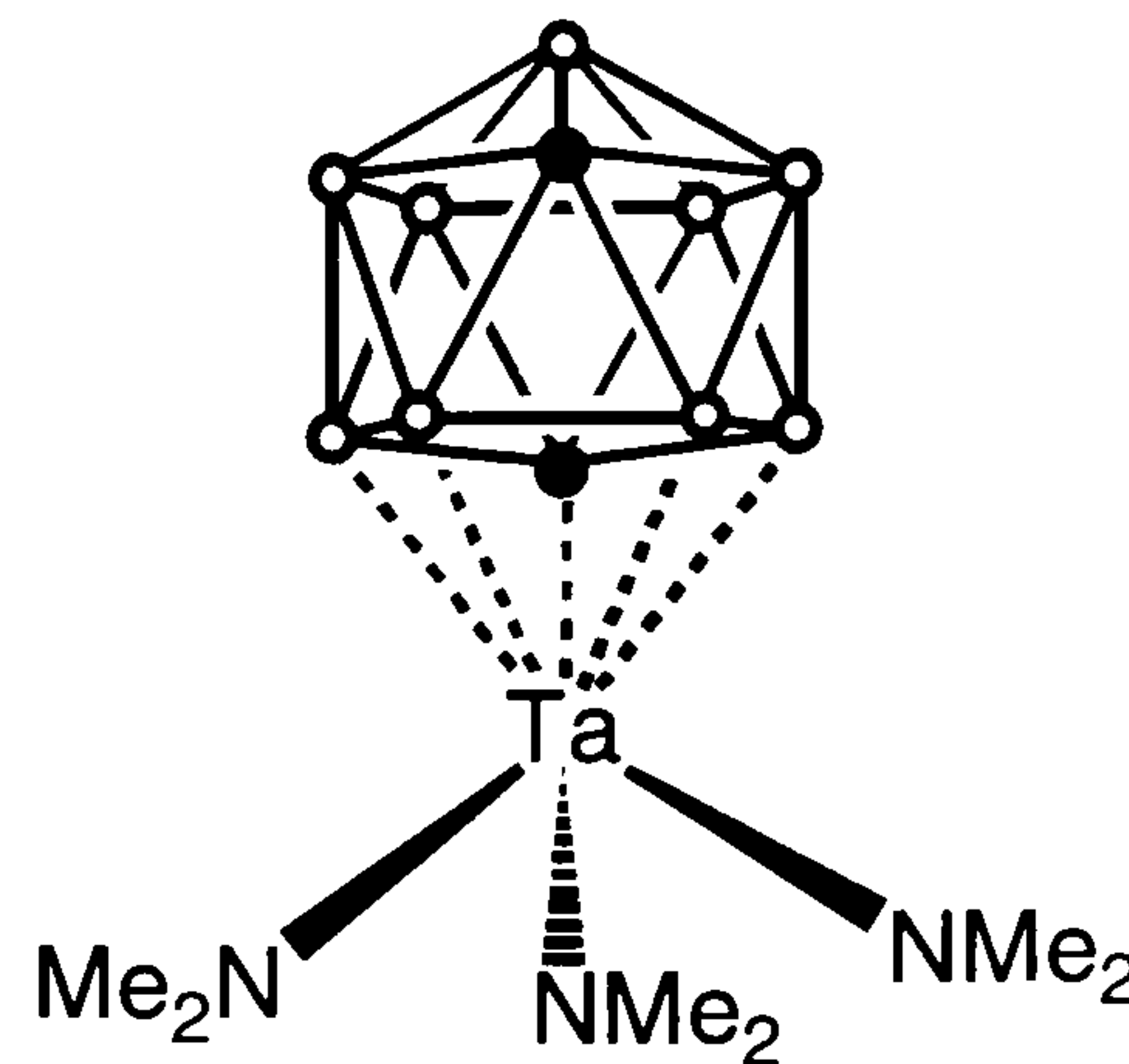
δ_B -16.9 (d, 1B J_{B-H} 144), -13.1 (M, 2B), -11.8 (M, 1B), -11.1 (M, 1B), -5.9 (M, 2B), -5.2 (M, 2B)

Analysis C₈H₂₉B₉N₃Ta₁:

Calc.: C%, 21.5; H%, 6.6; N%, 9.43 and found: C%, 21.0; H%, 6.6; N%, 7.36

5.3.5 Synthesis of [2-Ta(NMe₂)₃(1,12-C₂B₉H₁₁)], (20).

A solution of [*para*-C₂B₉H₁₃] (0.67 g, 5 mmol) in toluene (20 cm³) was treated dropwise with a toluene solution of Ta(NMe₂)₅ (2 g, 5 mmol). After stirring at 20 °C for 15 h the solution was refluxed for 2 h. The solution was filtered and the filtrate was concentrated to about 5 cm³. The solution was layered with pentane and cooled to -40 °C giving crystalline product. Yield 2.02 g, 91%. Crystals suitable for X-ray structure determination were grown at -30 °C, from a concentrated toluene solution of (17), layered with pentane.



¹H NMR (300 MHz, CDCl₃):

δ_H 3.52 (18H, NMe₂), 2.79 (1H, CH), 2.23 (1H, CH)

Additional peaks in ¹H{¹¹B} NMR (300 MHz, CDCl₃):

δ_H 3.04 (s, 1H), 2.32 (s, 2H), 2.24 (s, 2H), 1.64 (s, 2H), 1.52 (s, 2H)

¹³C{¹H} NMR (75 MHz, CDCl₃):

δ_C 64.1 and 62.3 (C₂B₉H₁₁), 49.6 (NMe)

¹¹B NMR (96.2 MHz, CDCl₃):

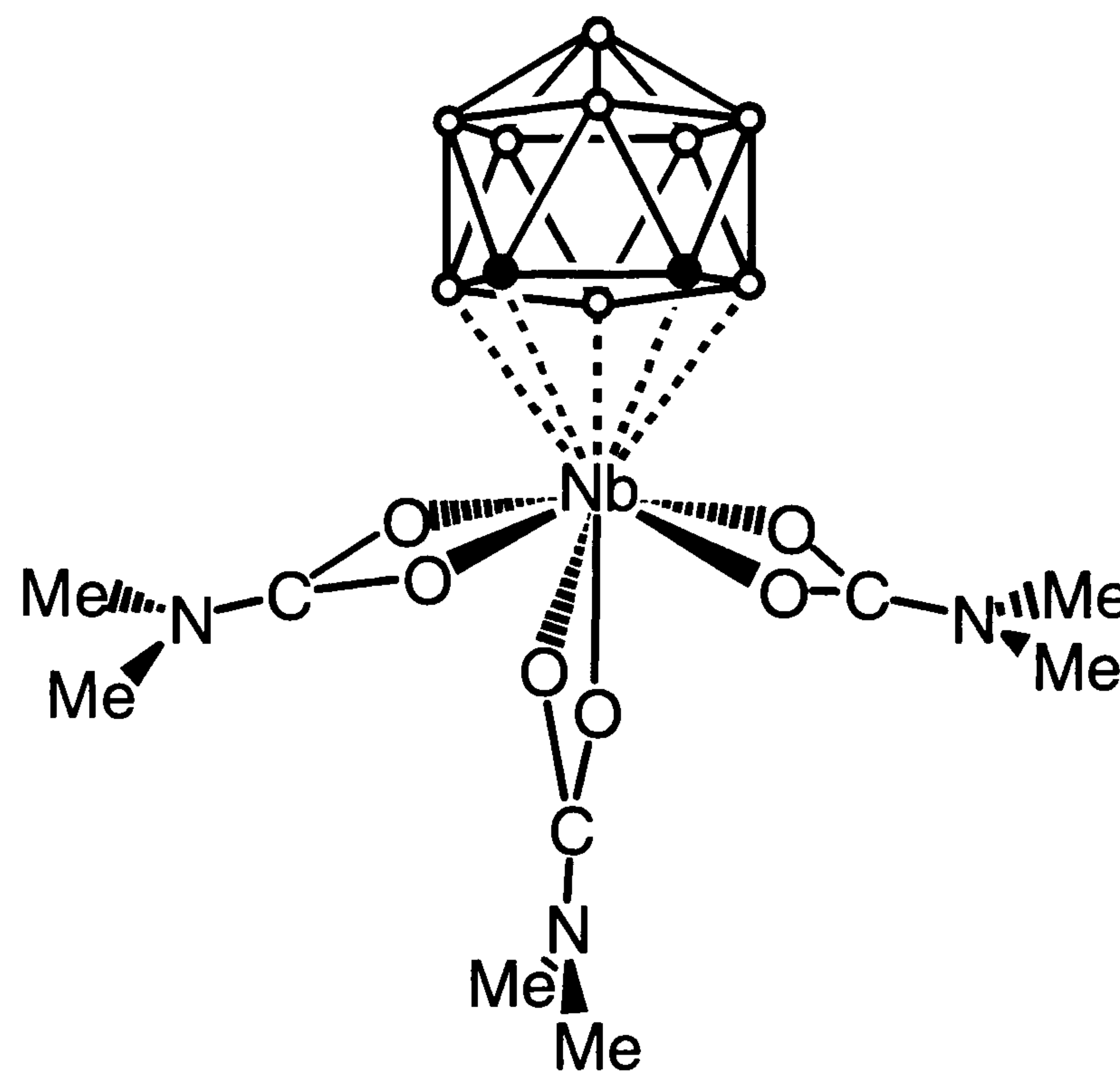
δ_B -19.3 (d, 1B, J_{B-H} 161), -14.2 (M, 2B), -13.7 (M, 2B), -6.2 (d, 2B, J_{B-H} 158), -4.1 (d, 2B, J_{B-H} 189)

Analysis C₈H₂₉B₉N₃Ta₁:

Calc.: C%, 21.5; H%, 6.6; N%, 943 and found: C%, 21.1; H%, 6.5; N%, 7.93.

5.3.6 Synthesis of $[3\text{-Nb}(\text{O}_2\text{C-NMe}_2)_3(1,2\text{-C}_2\text{B}_9\text{H}_{11})]$, (21).

A stream of CO_2 in N_2 , was generated by passing nitrogen through a Schlenk containing dry ice, was passed through a toluene (20 cm^3) solution of $[\text{Nb}(\text{NMe}_2)_3(\text{ortho-C}_2\text{B}_9\text{H}_{11})]$, (16) (0.357 g, 1 mmol) at room temperature. The yellow solution rapidly changed to a pale green solution over a small amount of flocculent white precipitate. The gas flow was stopped when no further colour change was apparent. After stirring at room temperature for 2 h, the solution was filtered and the filtrate was layered with pentane (10 cm^3) and allowed to stand at room temperature. After 2 d, pale green micro crystals of $[\text{Nb}(\text{O}_2\text{C-NMe}_2)_3(\text{ortho-C}_2\text{B}_9\text{H}_{11})]$ were isolated by filtration and washed with a small volume of pentane. Yield 0.19 g, 49 %.



^1H NMR (300 MHz, C_6D_6):

δ_{H} 3.7 (s, 2H, carborane C-H), 2.01 (s, 3H, NMe), 1.98 (s, 3H, NMe), 1.94 (s, 12H, NMe_2)

Additional peaks in $^1\text{H}\{^{11}\text{B}\}$ NMR (300 MHz, C_6D_6):

δ_{H} 4.12 (s, 1H), 3.40 (s, 2H), 3.21 (s, 2H), 3.11 (s, 1H), 2.87 (s, 2H), 2.80 (s, 1H)

$^{13}\text{C}\{^1\text{H}\}$ NMR (75 MHz, C_6D_6):

δ_{C} 171.2 (1 x O_2CN), 167.7 (2 x O_2CN), 73.1 (carborane C), 34.6, 34.2, 34.1, 34.0 (NMe)

^{11}B NMR (96.2 MHz, C_6D_6):

δ_{B} 23.0 (d, 1B, $J_{\text{B-H}}$ 114), 6.9 (M, 2B), 3.1 (d, 3B, $J_{\text{B-H}}$ 144), -4.0 (M, 1B), -7.4 (M, 2B)

Analysis $\text{C}_{11}\text{H}_{29}\text{B}_9\text{N}_3\text{O}_6\text{Nb}(\text{C}_7\text{H}_8)_{0.45}$:

Calc.: C%, 32.00; H%, 6.19 and found: C%, 31.95; H%, 6.50

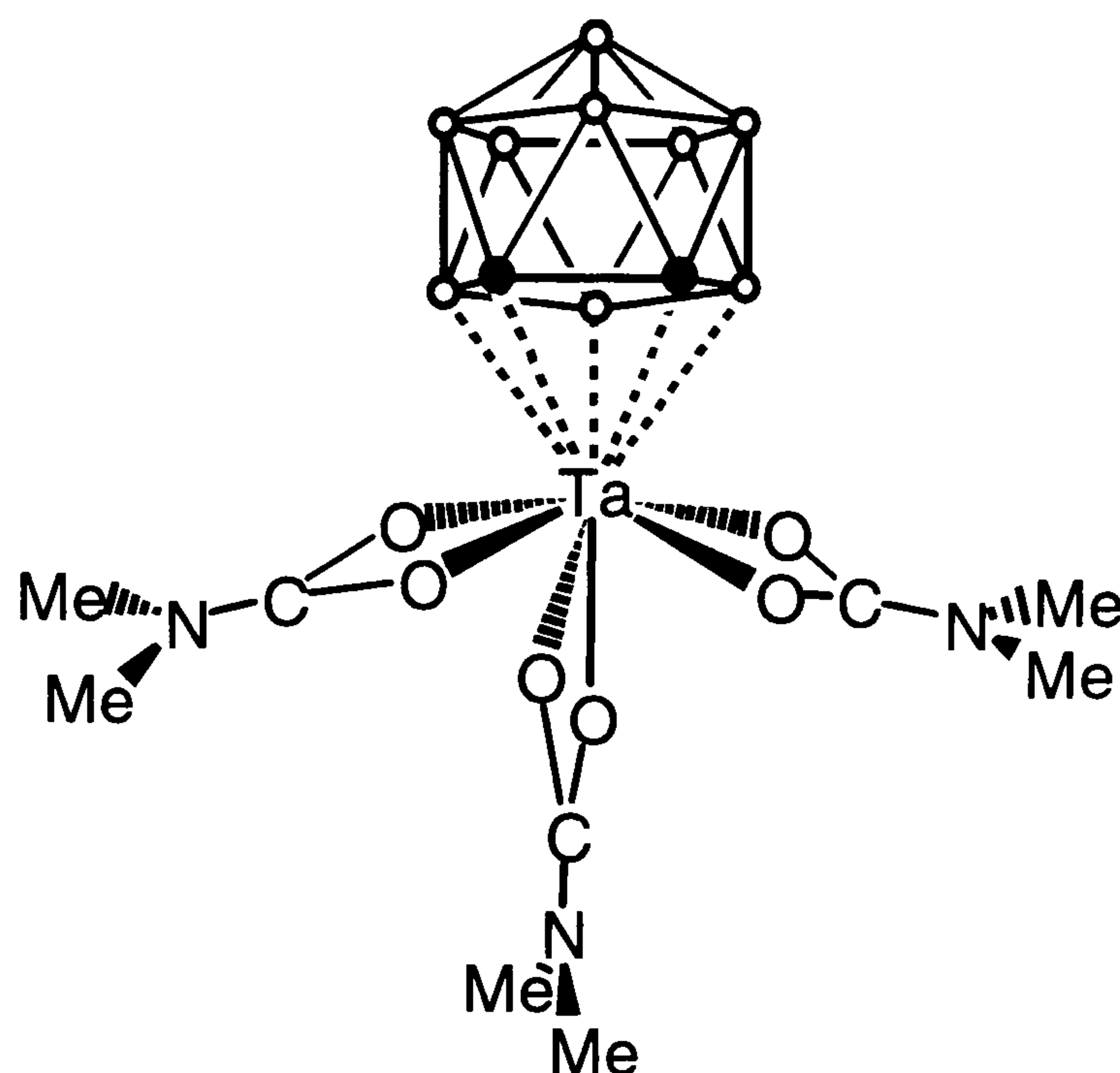
Mass Spec:

m/e (assignment) 446 [$\text{M}^+ - \text{NMe}_2$], 402 [$\text{M} - \text{O}_2\text{CNMe}_2^+$], 357 [$\text{M} - \text{C}_2\text{B}_9\text{H}_{11}^+$]

IR: 2566s, 1632s, 1459s, 1416s, 1260w, 1093vw cm^{-1}

5.3.7 Synthesis of [3-Ta(O₂C-NMe₂)₃(1,2-C₂B₉H₁₁)], (22).

A stream of CO₂ in N₂, was generated by passing nitrogen through a Schlenk containing dry ice, was passed through a toluene (20 cm³) solution of [Ta(NMe₂)₃(*ortho*-C₂B₉H₁₁)], (17) (0.445 g, 1 mmol) at room temperature. The yellow solution rapidly changed to a pale yellow solution over a small amount of flocculent white precipitate. The gas flow was stopped when no further colour change was apparent. After stirring at room temperature for 2 h, the solution was filtered and the filtrate was layered with pentane (10 cm³) and allowed to stand at room temperature. After 3 d, colourless crystals of [Ta(O₂C-NMe₂)₃(*ortho*-C₂B₉H₁₁)] were isolated by filtration and washed with a small volume of pentane. Yield 0.3 g, 52 %.



¹H (300 MHz, C₆D₆):

δ_H 3.73 (s, 2H, carborane C-H), 2.28 (s, 3H, NMe), 2.23 (s, 3H, NMe), 2.19 (s, 6H, NMe₂), 2.17 (s, 6H, NMe₂)

Additional peaks in ¹H{¹¹B} NMR (300 MHz, C₆D₆):

δ_H 4.18 (1H), 3.92 (2H), 3.72 (s, 1H), 3.30 (s, 2H), 3.17 (s, 3H)

¹³C{¹H} NMR (75 MHz, C₆D₆):

δ_C 170.0 (1 x NCO₂), 166.9 (2 x NCO₂), 68.3 (carborane C), 34.3, 34.1, 33.9, 33.8 (NMe)

¹¹B NMR (96.2 MHz, C₆D₆):

δ_B 16.4 (d, 1B, J_{B-H} 122), 3.41 (M, 2B), 1.2 (M, 3B), -8.6 (M, 1B), -9.6 (M, 2B)

Analysis C₁₁H₂₉B₉N₃O₆Ta(C₇H₈)_{0.25}:

Calc.: C%, 25.50; H%, 5.20 and found: C%, 25.44; H% 5.15

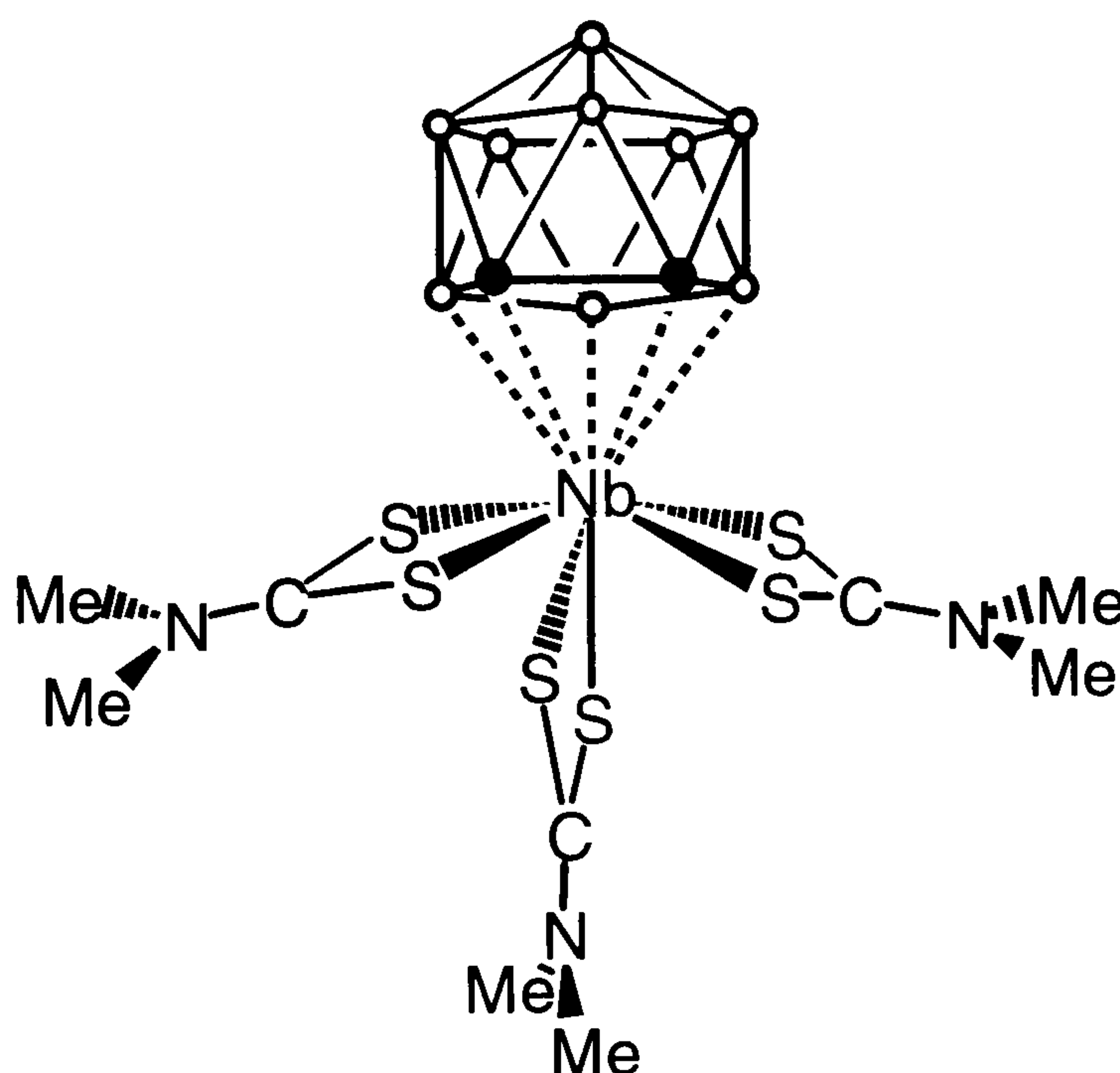
Mass Spec:

m/e (assignment) 475 [M - CH₃⁺], 490 [M - O₂CNMe₂⁺]

IR:2559s, 1641s, 1471m, 1451m, 1269s, 1022vw cm⁻¹.

5.3.8 Synthesis of [3-Nb(S₂C-NMe₂)₃(1,2-C₂B₉H₁₁)], (23).

A stirred toluene (20 cm³) solution of [Nb(NMe₂)₃(*ortho*-C₂B₉H₁₁)], (16) (0.357 g, 1 mmol) was cooled to -78 °C and treated dropwise with CS₂ (0.228 g, 3 mmol). The yellow solution was allowed to warm to room temperature, giving an orange solution over a small amount of yellow precipitate. After stirring at room temperature for 16 h, the solution was filtered and the volatiles were removed from the filtrate under reduced pressure. The residue was extracted with dichloromethane (15 cm³) and the extract was layered with toluene (10 cm³) and cooled to -20 °C giving yellow crystals of [Nb(S₂C-NMe₂)₃(*ortho*-C₂B₉H₁₁)], which were isolated by filtration and washed with a small volume of toluene. Yield 0.307 g, 71 %.



¹H NMR (300 MHz, CD₂Cl₂):

δ_H 3.61 (s, 2H, carborane C-H), 3.34 (s, 3H, NMe), 3.25 (s, 3H, NMe), 3.20 (s, 6H, NMe₂), 3.12 (s, 6H, NMe₂)

Additional peaks in ¹H{¹¹B} NMR (300 MHz, CD₂Cl₂):

δ_H 2.83 (s, 1H), 2.35 (s, 1H), 2.21 (s, 2H), 2.10 (s, 3H), 1.88 (s, 2H)

¹³C{¹H} NMR (75 MHz, CD₂Cl₂):

δ_C 207.5 (1 x NCS₂), 204.5 (2 x NCS₂), 66.6 (carborane C), 39.7, 39.0, 38.6, 36.9 (NMe)

¹¹B NMR (96.2 MHz, CD₂Cl₂):

δ_B 16.2 (d, 1B, J_{B-H} 131), 0.9 (M, 2B), -3.1 (M, 3B), -12.5 (M, 2B), -16.4 (d, 1B, J_{B-H} 130)

Analysis C₁₁H₂₉B₉N₃S₆Nb(C₇H₈)_{0.85}:

Calc.: C%, 30.65 ; H%, 5.43 and found: C%, 30.65; H%, 5.51

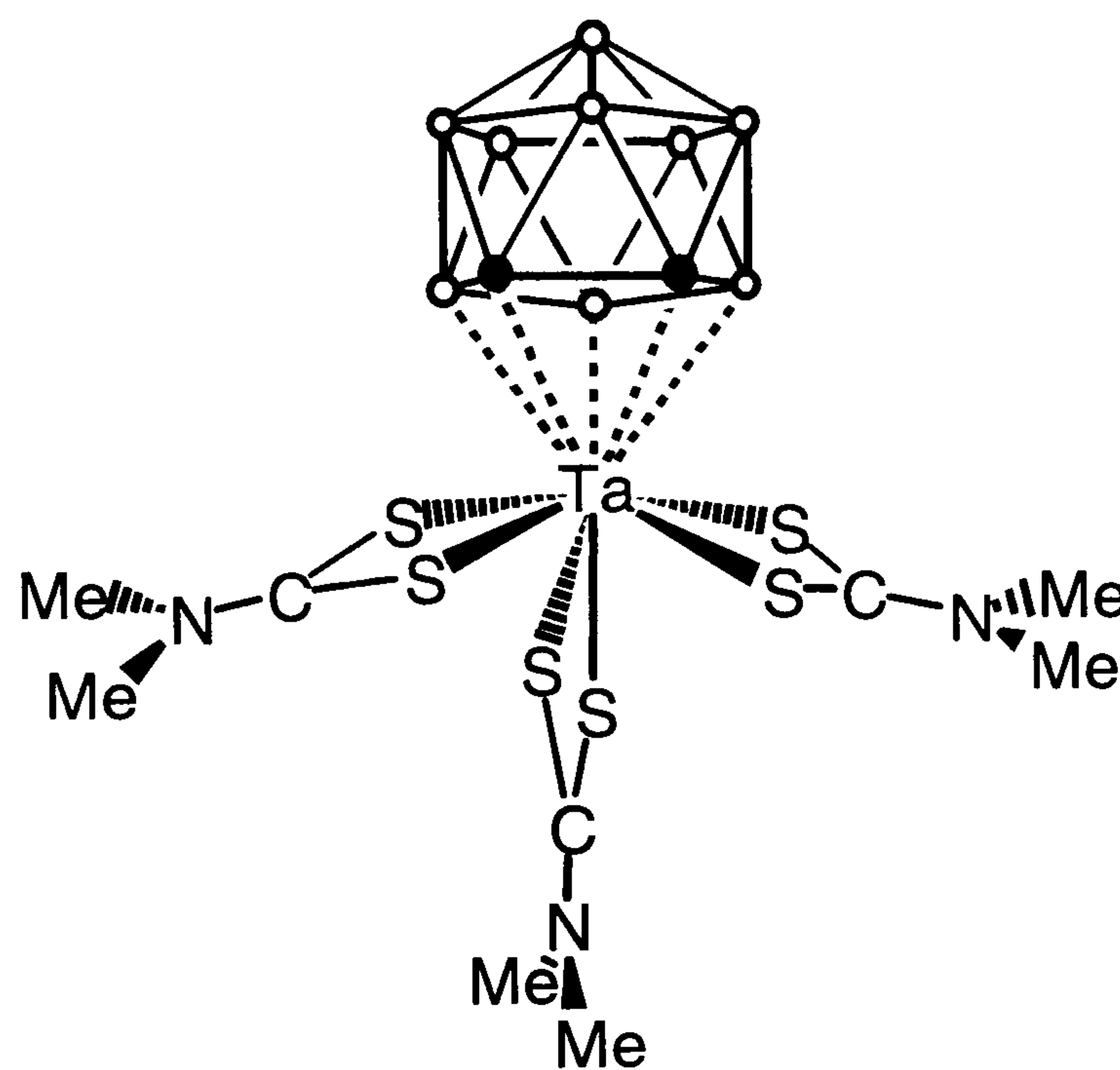
Mass Spec:

m/e (assignment) 586 [M^+], 466 [$M - S_2CMe_2^+$], 453 [$M - C_2B_9H_{11}^+$]

IR: 2533s, 1510vs, 1450s, 1392vs, 1257s, 1166s, 1096w, 1016vw cm^{-1}

5.3.9 Synthesis of $[3-Ta(S_2C-NMe_2)_3(1,2-C_2B_9H_{11})]$, (24).

A stirred toluene (20 cm^3) solution of $[Ta(NMe_2)_3(ortho-C_2B_9H_{11})]$, (17) (0.445 g, 1 mmol) was cooled to $-78\text{ }^\circ C$ and treated dropwise with CS_2 (0.228 g, 3 mmol). The yellow solution was allowed to warm to room temperature, giving an orange solution over a yellow precipitate. After stirring at room temperature for 12 h, the solution was filtered and the volatiles were removed from the filtrate under reduced pressure. The residue was extracted with dichloromethane (10 cm^3) and the extract was layered with toluene (10 cm^3) and cooled to $-20\text{ }^\circ C$ giving yellow crystals of $[Ta(S_2C-NMe_2)_3(ortho-C_2B_9H_{11})]$, which were isolated by filtration and washed with a small volume of toluene. Yield 0.411 g, 61 %.



1H NMR (300 MHz, $CDCl_3$):

δ_H 3.59 (s, 2H, carborane C-H), 3.30 (s, 3H, NMe), 3.25 (s, 6H, NMe₂), 3.21 (s, 6H, NMe₂), 3.19 (s, 3H, NMe)

Additional peaks in $^1H\{^{11}B\}$ NMR (300 MHz, $CDCl_3$):

δ_H 3.36 (s, 1H), 2.75 (s, 3H), 2.54 (s, 1H), 2.42 (s, 2H), 2.20 (s, 2H)

$^{13}C\{^1H\}$ NMR (75 MHz, $CDCl_3$):

δ_C 207.9 (1 x NCO₂), 204.6 (2 x NCO₂), 66.9 (carborane CH), 40.3, 39.8, 39.6 38.9 (NMe)

^{11}B NMR (96.2 MHz, $CDCl_3$):

δ_B 13 (d, 1B, J_{B-H} 121 Hz), -0.5 (M, 2B), -3.6 (M, 2B), -5.8 (M, 1B), -13.6 (d, 2B, J_{B-H} 113), -17.2 (d, 1B, J_{B-H} 131)

Analysis $C_{11}H_{29}B_9N_3S_6Nb(C_7H_8)$:

Calc.: C%, 28.22; H%, 4.87 and found: C%, 28.15; H%, 4.87

Mass Spec:

m/e (assignment) 674 [M^+], 629 [$M - 2CH_3^+$], 541 [$M - C_2B_9H_{11}^+$], 554 [$M - S_2CNMe_2^+$]

IR:

2535s, 1528s, 1442m, 1393vs, 1258s, 1166s, 1098w, 1019w cm^{-1}

5.3.10 Synthesis of $[3-Ta(NC(Me)NMe_2)_3(1,2-C_2B_9H_{11})]$, (25).

In a Young's ampoule, a stirred toluene (20 cm^3) solution of $[Ta(NMe_2)_3(ortho-C_2B_9H_{11})]$, (17) (0.445 g, 1 mmol) was treated dropwise with $NCMe_3$ (0.143 g, 3.5 mmol). The ampoule was evacuated and the solution was heated to 130 °C and was maintained at this temperature for 48 h. The reaction mixture slowly changed from a pale yellow colour to a deep red. The solution was allowed to cool to room temperature and the solvent was evaporated under reduced pressure.

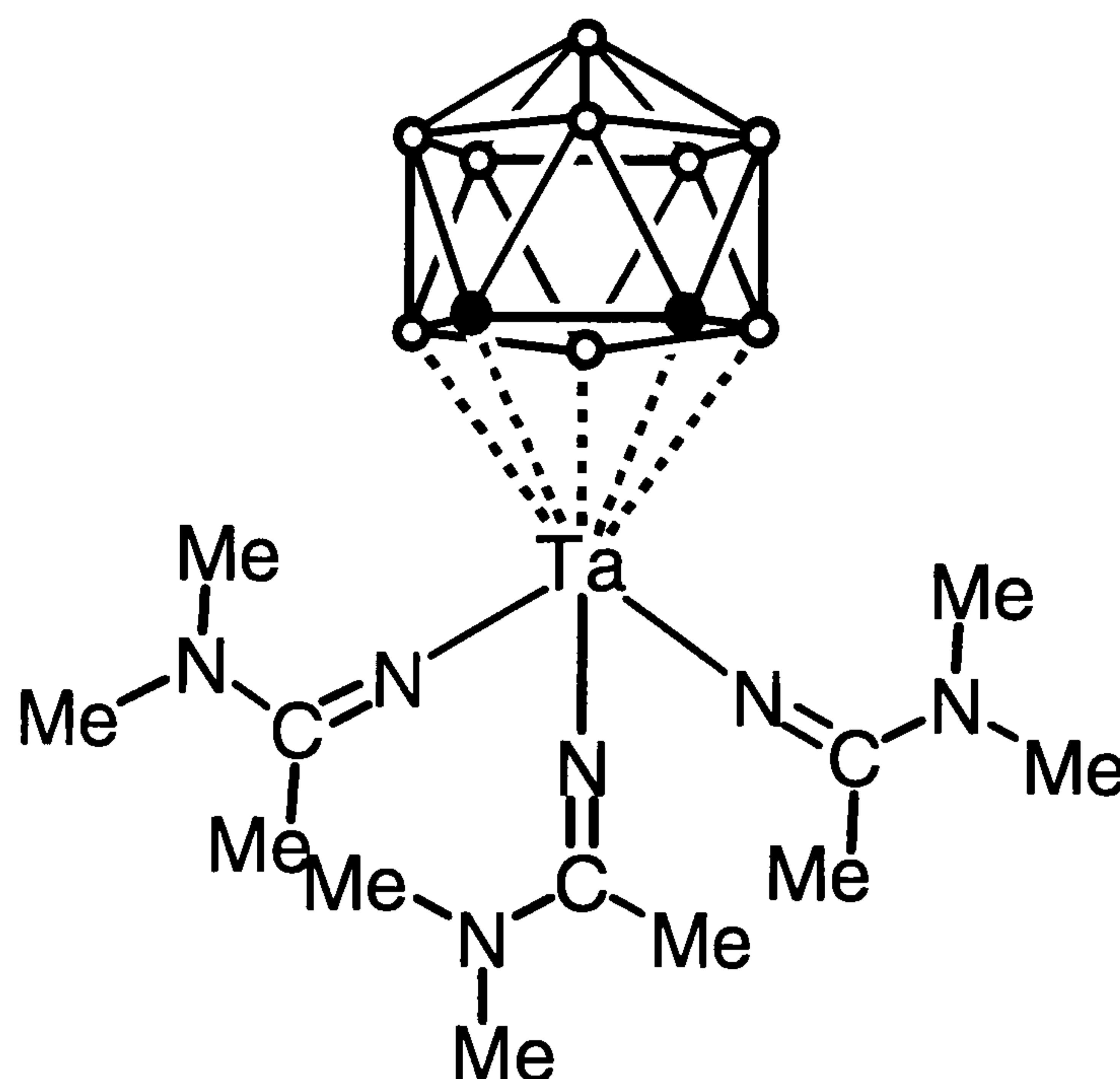
The orange residue was extracted with dichloromethane (10 cm^3) and layered with pentane (10 cm^3), which produced a pale yellow powder which was isolated by careful filtration. This process was repeated a further two times and resulted in the isolation of colourless microcrystalline precipitate of $[Ta(NC(Me)NMe_2)_3(ortho-C_2B_9H_{11})]$. Yield 0.22 g, 39 %.

1H NMR (300 MHz, CD_2Cl_2):

δ_H 3.22 (s, 3H, NMe) 3.13 (s, 6H, NMe), 3.06 (s, 6H, NMe), 3.04 (s, 3H, NMe), 2.90 (s, 2H, carborane C-H), 2.31 (s, 3H, C-Me), 2.21 (s, 6H, C-Me)

Additional peaks in $^1H\{^{11}B\}$ NMR (300 MHz, CD_2Cl_2):

δ_H 2.77 (s, 1H), 2.14 (s, 2H), 2.02 (s, 2H), 1.85 (s, 1H), 1.69 (s, 3H)



$^{13}\text{C}\{^1\text{H}\}$ NMR (75 MHz, CD_2Cl_2):

δ_{C} 169.9 (s, 1 x $\text{N}=\underline{\text{C}}(\text{Me})\text{NMe}_2$), 163.8 (s, 2 x $\text{N}=\underline{\text{C}}(\text{Me})\text{NMe}_2$), 52.3 (M, carborane CH), 39.4 (s, C-NMe) 39.3 (s, C-NMe), 38.9 (s, 2 x C-NMe), 38.5 (2 x C-NMe), 21.8 (2 x $\text{N}=\text{C}-\underline{\text{Me}}$), 17.7 (1 x $\text{N}=\text{C}-\underline{\text{Me}}$)

^{11}B NMR (96.2 MHz, CDCl_3):

δ_{B} -0.5 (d, 1B, $J_{\text{B-H}}$ 108), -4.9 (d, 2B, $J_{\text{B-H}}$ 138), -8.1 (d, 2B, $J_{\text{B-H}}$ 99), -13.4 (d, 3B, $J_{\text{B-H}}$ 153), -17.4 (d, 1B, $J_{\text{B-H}}$ 144)

Analysis $\text{C}_{14}\text{H}_{38}\text{B}_9\text{N}_6\text{Ta}$:

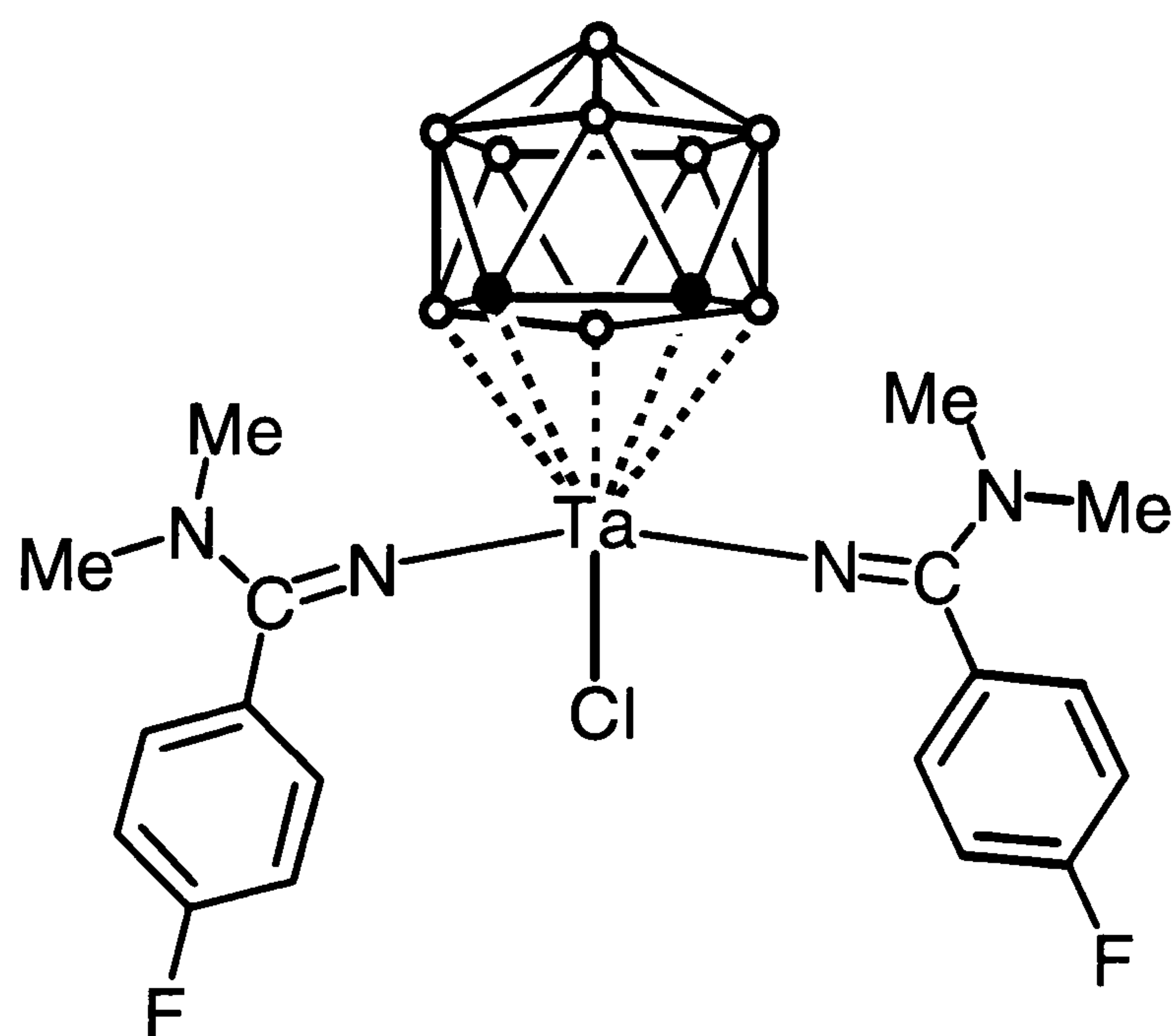
Calc.: C%, 29.57; H%, 6.73; N% 14.78 and found: C%, 29.55; H, 6.91; N% 14.06

Mass Spec:

m/e (assignment) 569 [M^+], 484 [$\text{M}^+ - (\text{NC}(\text{Me})\text{NMe}_2)$], 436, [$\text{M}^+ - \text{C}_2\text{B}_9\text{H}_{11}$]

5.3.11 Synthesis of $[\text{3-Ta}(\text{NC}(\text{C}_6\text{H}_4\text{F})\text{NMe}_2)_2\text{Cl}(1,2\text{-C}_2\text{B}_9\text{H}_{11})]$, (26).

In a Young's ampoule, a stirred toluene (10 cm^3) solution of $[\text{Ta}(\text{NMe}_2)_3(\text{ortho-C}_2\text{B}_9\text{H}_{11})]$, (17) (0.445 g, 1 mmol) was treated dropwise with a toluene solution (10 cm^3) of $\text{NCC}_6\text{H}_4\text{F}$ (0.42 g, 3.5 mmol). The ampoule was evacuated and the solution was heated to 130 $^\circ\text{C}$ and was maintained at this temperature for 48 h. The reaction mixture slowly changed from a pale yellow colour to a deep red. The solution was then allowed to cool to room



temperature and the solvent was evaporated under reduced pressure. The red/orange residue was extracted with dichloromethane (10 cm^3) and layered with pentane (10 cm^3), which produced a pale yellow powder which was isolated by careful filtration. This process was repeated a further two times and resulted in the isolation of yellow microcrystalline precipitate of $[\text{Ta}(\text{NC}(\text{C}_6\text{H}_4\text{F})\text{NMe}_2)_2\text{Cl}(\text{ortho-C}_2\text{B}_9\text{H}_{11})]$. Slow recrystallisation from a concentrated dichloromethane solution layered with pentane at -20 $^\circ\text{C}$ formed crystals suitable for single crystal X-ray diffraction experiments. Yield 0.33 g, 49 %.

^1H NMR (400 MHz, CD_2Cl_2):

δ_{H} 3.10 (s, 1H, carborane C-H), 3.32 (s, 1H, carborane C-H), 3.00 (br s, 6H, NMe_2), 3.20 (br s, 6H, NMe_2), 6.98-7.5 (M, 8H, 2 x $\text{C}_6\text{H}_4\text{F}$)

Additional peaks in $^1\text{H}\{^{11}\text{B}\}$ NMR (300 MHz, CD_2Cl_2):

δ_{H} 1.50 (s, 1H), 1.58 (s, 1H), 1.798 (s, 1H), 1.99 (s, 1H), 2.06 (s, 2H), 2.32 (s, 1H), 2.749 (s, 1H); 9th B-H hidden under C-H and NMe region

^{19}F NMR (188 MHz, CD_2Cl_2):

δ_{F} -107.15 (s, 1F), -110.06 (s, 1F)

$^{13}\text{C}\{^1\text{H}\}$ NMR (100.57 MHz, CD_2Cl_2):

δ_{C} 39.5 (s, 2C, NMe_2), 40.7 (br s, 1C, $\text{C}_2\text{B}_9\text{H}_{11}$), 41.7 (s, 2C, NMe_2), 42.5 (br s, 1C, $\text{C}_2\text{B}_9\text{H}_{11}$), 115.7 (d, 2C, *ortho*- $\text{C}_6\text{H}_4\text{F}$, $J_{\text{C-F}}$ 22), 116.8 (d, 2C, *ortho*- $\text{C}_6\text{H}_4\text{F}$, $J_{\text{C-F}}$ 23), 128.4 (s, 1C, $\text{N}=\underline{\text{C}}$), 129.2 (s, 1C, $\text{N}=\underline{\text{C}}$), 130.0 (d, 1C, *para*- $\text{C}_6\text{H}_4\text{F}$, $J_{\text{C-F}}$ 3), 130.2 (d, 2C, *meta*- $\text{C}_6\text{H}_4\text{F}$, $J_{\text{C-F}}$ 9), 130.9 (d, 1C, *para*- $\text{C}_6\text{H}_4\text{F}$, $J_{\text{C-F}}$ 3), 131.2 (d, 2C, *meta*- $\text{C}_6\text{H}_4\text{F}$, $J_{\text{C-F}}$ 9), 163.6 (d, 1C, $\underline{\text{C}}\text{-F}$, $J_{\text{C-F}}$ 251), 165.1 (d, 1C, C-F, $J_{\text{C-F}}$ 254)

^{11}B NMR (96.2 MHz, CDCl_3):

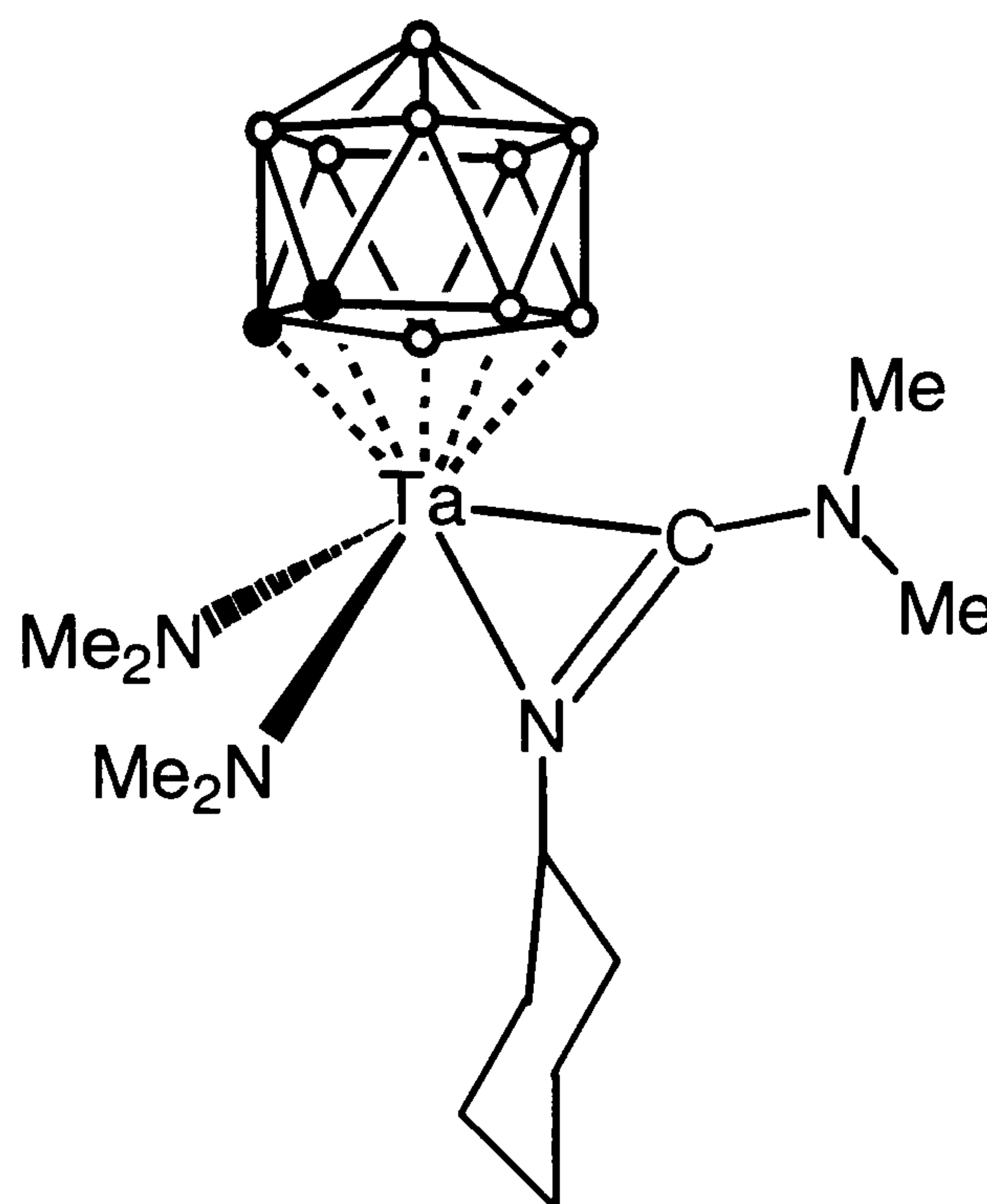
δ_{B} 0.7 (d, 1B, $J_{\text{B-H}}$ 118), -4.3 (d, 2B, $J_{\text{B-H}}$ 141), -7.5 [d, 3B $J_{\text{B-H}}$ 130), -13.9, (d, 2B $J_{\text{B-H}}$ 144), -16.9 (d, 1B, $J_{\text{B-H}}$ 139)

Analysis $\text{C}_{20}\text{H}_{31}\text{Cl}_1\text{B}_9\text{F}_2\text{N}_4\text{Ta}(\text{CH}_2\text{Cl}_2)_{1.3}$:

Calc.: C%, 32.4; H%, 4.29; N% 7.1 and found: C%, 32.6; H% 4.28; N% 7.16

5.3.12 Synthesis of [3-Ta(NMe₂)₂(η^2 -(Me₂N)C=N(C₆H₁₁))(1,2-C₂B₉H₁₁)], (27).

A stirred toluene (10 cm³) solution of [Ta(NMe₂)₃(*ortho*-C₂B₉H₁₁)], (17) (0.445 g, 1 mmol) was treated dropwise with a toluene solution (10 cm³) of CNC₆H₁₁ (0.35 g, 3.2 mmol). The yellow solution was warmed to 110 °C and was maintained at this temperature for 12 h. The reaction mixture was allowed to cool to room temperature and the solvent was evaporated under reduced pressure. The orange residue was extracted with fresh toluene (10 cm³) filtered and carefully layered with pentane (10 cm³). Slow recrystallisation at -20 °C produced yellow crystalline material characterised as [Ta(NMe₂)₂(Me₂N)C=N(C₆H₁₁)(*ortho*-C₂B₉H₁₁)]. Yield 0.37 g 67 %.



¹H NMR (300 MHz, C₆D₆):

δ_{H} 3.31 (s, 2H, carborane C-H), 3.35 (s, 12H, 2 x NMe₂), 2.85 (s, 3H, NMe), 2.54 (s, 3H, NMe), 0.7-1.38 (m, 11H, C₆H₁₁).

Additional peaks in ¹H{¹¹B}NMR (300 MHz, C₆D₆):

δ_{H} 1.90 (s, 2H), 2.20 (s, 1H), 2.50 (s, 1H), 2.76 (s, 1H), 2.84 (s, 2H), 3.93 (s, 2H).

¹³C{¹H} NMR (75 MHz, C₆D₆):

δ_{C} 211.4 (s, 1C, N-C=N), 58.5 (s, 1C, CH in C₆H₁₁), 50.9 (s, 4C, NMe₂), 50.1 (br s, 2C, C₂B₉H₁₁), 45.8 (s, 1C NMe), 40 (s, 1C, NMe), 34.9 (s, 1C, CH₂ in C₆H₁₁), 25.5 (s, 2C, CH₂ in C₆H₁₁), 25.5 (s, 2C, CH₂ in C₆H₁₁).

¹¹B NMR (96.2 MHz, C₆D₆):

δ_{B} 3.2 (d, 1B, J_{B-H} 116), -3.4 (d, 3B, J_{B-H} 124), -8.1 (d, 2B, J_{B-H} 87), -13.9 (d, 1 B), -15.6 (d, 2B).

Analysis C₁₅H₄₀B₉N₄Ta:

Calc.: C%, 32.28; H%, 7.27; N% 10.10 and found: C%, 32.51; H% 7.47; N% 8.30

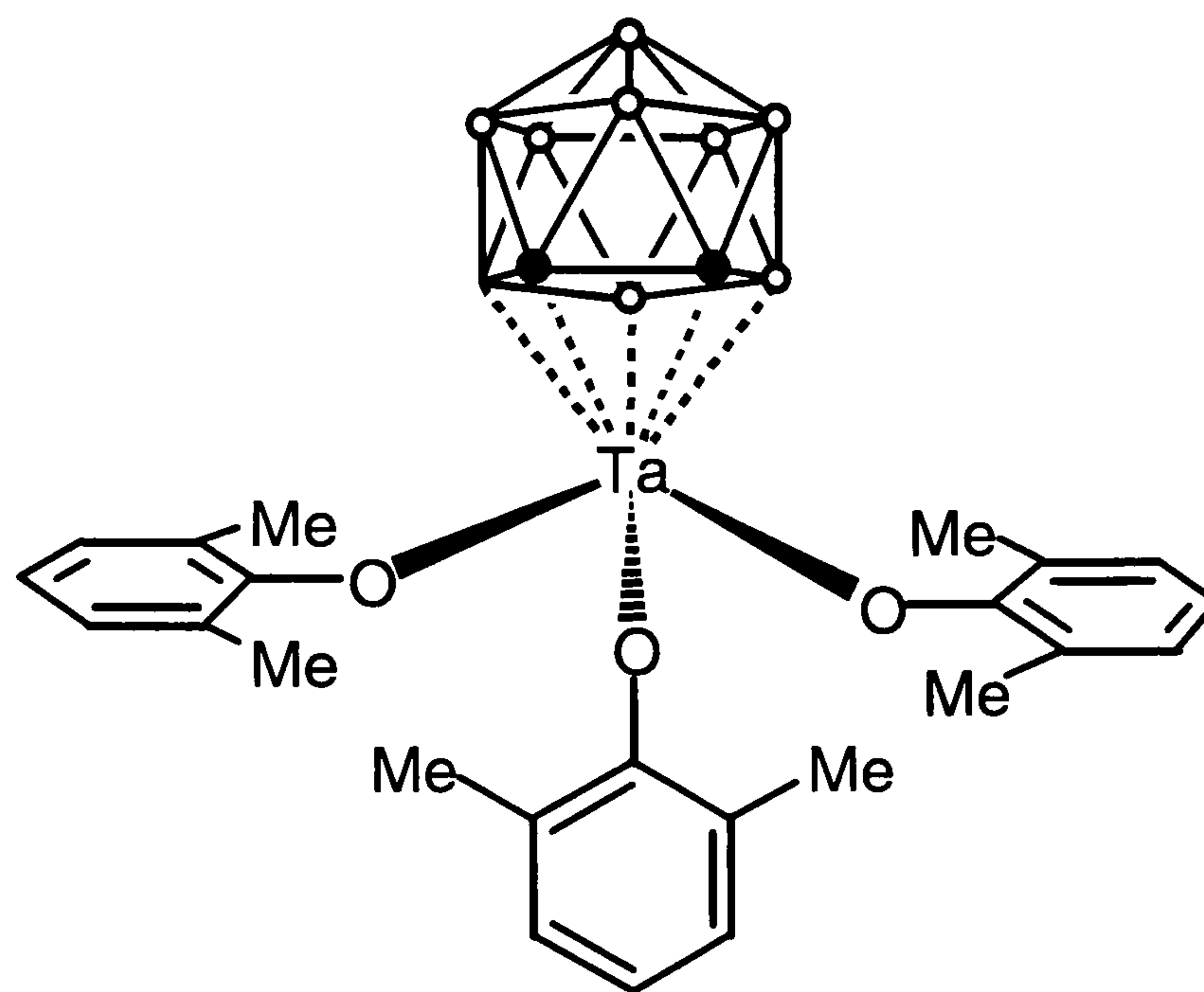
Mass Spec:

m/e (assignment) 555 [M^+], 510 [$M - NMe_2^+$], 402 [$M - (Me_2NC=N-C_6H_{11})^+$]

5.3.13 Synthesis of $[3-Ta(OC_6H_3-2,6-Me_2)_3(1,2-C_2B_9H_{11})]$, (28).

A stirred toluene (10 cm³) solution of $[Ta(NMe_2)_3(ortho-C_2B_9H_{11})]$, (17) (0.89 g, 2 mmol) was treated dropwise with a toluene solution (10 cm³) of HO-2,6-Me₂C₆H₃ (0.9g, 7.4 mmol).

The yellow solution was refluxed for 12 h. The reaction mixture was then allowed to cool to room temperature and the solvent was evaporated under reduced pressure. The pale yellow residue was extracted with fresh toluene (10 cm³) filtered and carefully layered with pentane (10 cm³). Slow recrystallisation at -20°C produced colourless crystals, which analysed to be $[Ta(OC_6H_3Me_2)_3(ortho-C_2B_9H_{11})]$. Yield 1.1 g 82 %.



¹H NMR (300 MHz, CD₂Cl₂):

δ_H 2.38 (s, 18H, OC₆H₃-Me₂), 3.37 (br s, 2H, C₂B₉H₁₁) 6.92 (t, 6H, 3 x *meta*-C₆H₃-Me₂), 7.11 (d, 3H, 3 x *para*-C₆H₃-Me₂)

Additional peaks in ¹H{¹¹B} MNR (300 MHz, CD₂Cl₂):

δ_H 1.21 (s, 1H), 2.31 (s, 2H), 2.36 (s, 2H), 2.66 (s, 2H), 2.89 (s, 1H), 3.07 (s, 1H)

¹³C{¹H} NMR (75 MHz, CD₂Cl₂):

δ_C 17.4 (s, 6C, 6 x Me-Ph), 60.3 (br s, 2C, C₂B₉H₁₁), 125.4 (s, 2C, *para*-OC₆H₃Me₂), 124.7 (s, 1C, *para*-OC₆H₃Me₂), 124.7 (s, *para*-OC₆H₃Me₂), 128.7 (s, *ortho*-OC₆H₃Me₂), 129.4 (s, *meta*-OC₆H₃Me₂), 158.6 (s, 2C, *ipso*-OC₆H₃Me₂)

¹¹B NMR (96.2 MHz, CD₂Cl₂):

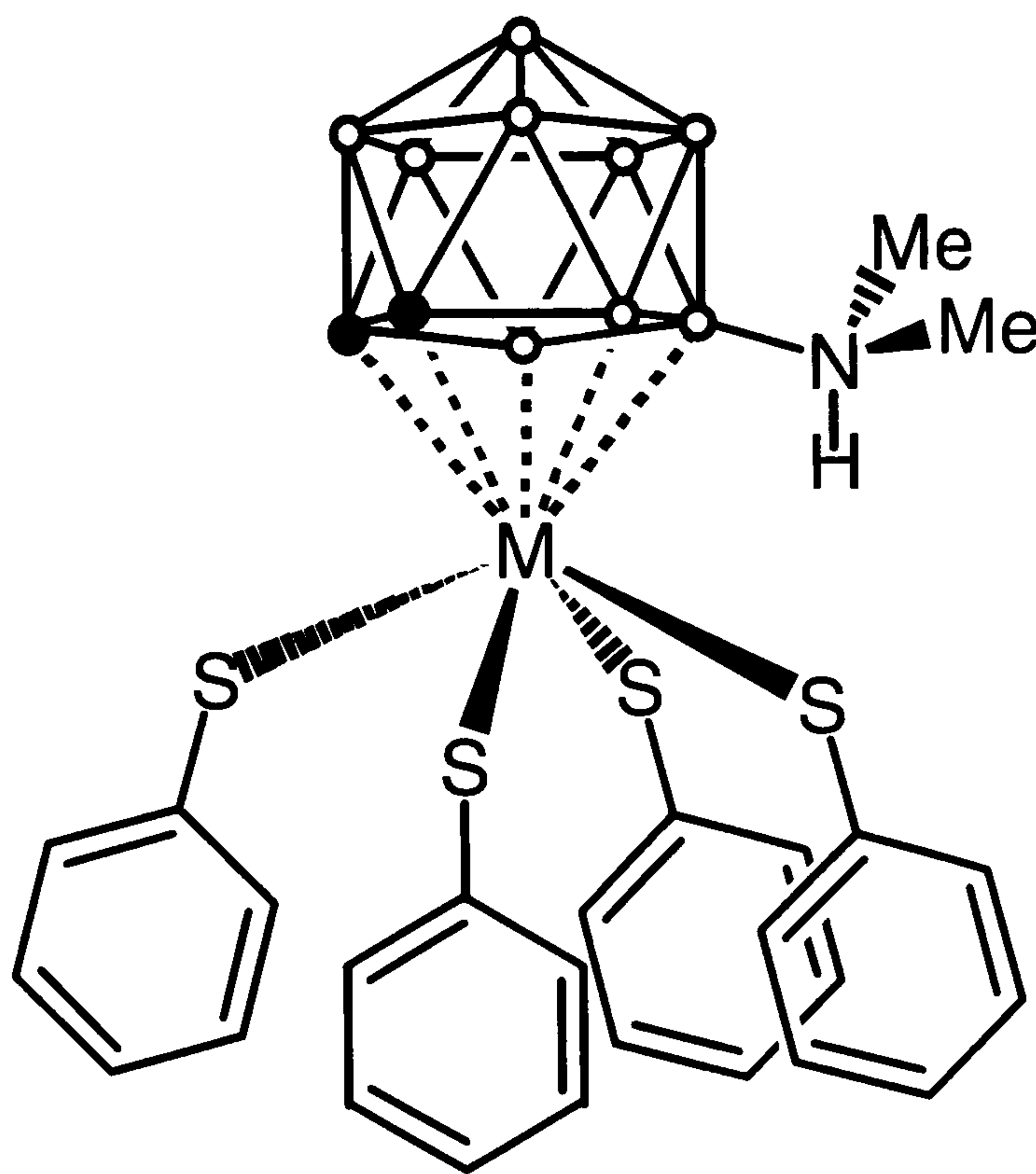
δ_B 7.3 (d, 1B, J_{B-H} 138), 0.7 (d, 2B, J_{B-H} 138), -3.4 (d, 2B, J_{B-H} 138), -9.2 (d, 3 B), -15.3 (d, 1B, J_{B-H} 172)

Analysis $C_{24}H_{38}B_9O_3Ta$:

Calc.: C%, 46.14; H%, 5.66 and found: C%, 45.9; H% 5.63

5.3.14 Synthesis of $[3-Ta(SC_6H_5)_4(9-NHMe_2-1,2-C_2B_9H_{10})]$, (29).

A stirred toluene (10 cm^3) solution of $[Ta(NMe_2)_3(ortho-C_2B_9H_{11})]$, (17) (0.89 g, 2 mmol) was cooled to $-60\text{ }^\circ\text{C}$ and treated dropwise with a toluene solution (10 cm^3) of $HS-C_6H_5$ (0.88 g, 8 mmol). On warming the solution to ambient temperatures, the yellow solution rapidly turned blood red. The reaction mixture was then stirred at room temperature for 12 h, after which the solvent was evaporated under reduced pressure. The red residue was extracted with toluene (10 cm^3) filtered and carefully layered with pentane (10 cm^3). Slow recrystallisation at $-20\text{ }^\circ\text{C}$ produced deep red crystals of $[Ta(SC_6H_5)_4(9-NHMe_2-ortho-C_2B_9H_9)]$. Yield 0.84 g 53 %.



1H NMR (300 MHz, CD_2Cl_2):

δ_H 3.19 (s, 2H, $\underline{H}_2C_2B_9H_8NHMe_2$), 3.27 (s, 6H, $N\underline{Me}_2$), 3.49 (br s, $N\underline{H}$) 7.11-7.30 (M, 4 x $SC_6\underline{H}_5$)

Additional peaks in $^1H\{^{11}B\}$ NMR (300 MHz, CD_2Cl_2):

δ_H 3.11 (s, 1H), 2.86 (s, 2H), 2.394 (s, 2H), 1.99 (s, 1H), 1.58 (s, 2H)

$^{13}C\{^1H\}$ NMR (75 MHz, CD_2Cl_2):

δ_C 50.3 (s, $N\underline{Me}_2$), 56.3 (br s, $\underline{C}_2B_9H_{10}NHMe_2$), 127.7 (s, *para*- SC_6H_5), 128.8 (s, *meta*- SC_6H_5), 132.5 (s, *ortho*- SC_6H_5), 143.1 (s, *para*- SC_6H_5)

^{11}B NMR (96.2 MHz, CD_2Cl_2):

δ_B 23.3 (s, 1B), -3.4 (d, 2B, J_{B-H} 124), -4.4 (d, 2B, J_{B-H} 113), -8.7 (d, 2B, J_{B-H} 172), -10.5 (d, 1B, J_{B-H} 157), -16.3 (d, 1B, J_{B-H} 117)

Analysis $C_{28}H_{37}B_9N_1S_4Ta;(C_7H_8)_{0.2}$:

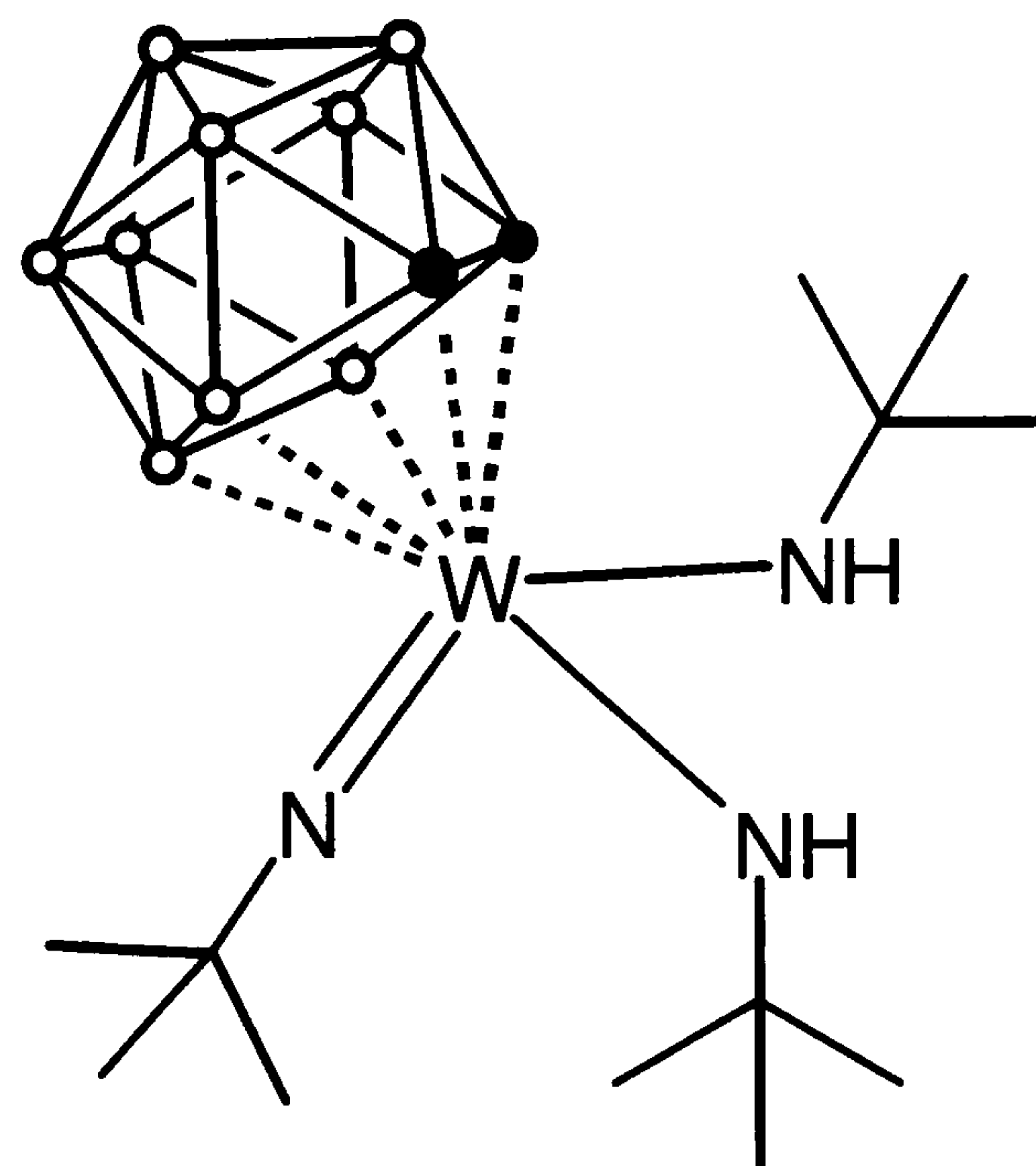
Calc.: C%, 43.46; H%, 4.79; N% 1.72 and found: C%, 43.49; H% 4.98; N% 1.64.

5.4 Experimental Details to Chapter Four

A literature method was used for the synthesis of $W(N^tBu)_2(NH^tBu)_2$.¹²

5.4.1 Synthesis of $[3-W(N^tBu)(NH^tBu)_2(1,2-C_2B_9H_{11})]$, (31).

A stirred toluene (50 cm^3) solution of $W(N^tBu)_2(NH^tBu)_2$ (30) (4.7 g, 10 mmol) was treated dropwise at room temperature with a toluene (20 cm^3) solution of *ortho*- $C_2B_9H_{13}$ (1.34 g, 10 mmol). The solution was stirred at room temperature for 12 h, during which time the solution gradually darkened. The solution then refluxed for 12 h, after which it was cooled to room temperature and the solvent removed under reduced pressure, leaving a golden honeycomb solid, which was washed with pentane ($2 \times 10\text{ cm}^3$) and isolated by filtration and before drying *in vacuo* overnight. Yield 4.8 g, 91 %.



1H NMR (300 MHz, C_6D_6):

δ_H 1.12 (s, 9H, $C(Me)_3$), 1.46 (s, 6H, $C(Me)_3$), 2.79 (br s, 2H, $C_2B_9H_{11}$), 7.96 (br s, 2H, NH)

Additional peaks in $^1H\{^{11}B\}$ NMR (300 MHz, C_6D_6):

δ_H 1.62 (s, 2H), 2.72, (s, 2H), 2.87 (s, 1H), 3.06(s, 1H), 3.31 (s, 2H), 4.28(s, 1H)

$^{13}C\{^1H\}$ NMR (75 MHz, C_6D_6):

δ_C 31.0 (s, 3C, $C(\underline{Me})_3$), 32.8, (s, 6C, 2 x $C(\underline{Me})_3$), 55.7, (br s, 2C, $\underline{C}_2B_9H_{11}$), 58.5 (s, 2C, $\underline{C}(\underline{Me})_3$), 72.5 (s, 1C, $\underline{C}(\underline{Me})_3$)

^{11}B NMR (96.2 MHz, C_6D_6):

δ_B 2.2 (d, 2B, J_{B-H} 124), -1.9 (d, 2B, J_{B-H} 141), -9.4 (d, 3B, J_{B-H} 138), -11.7(M, 1B,), -13.0 (M, 1B)

Chapter Five – Experimental Details

Analysis $C_{14}H_{40}B_9N_3W (C_7H_8)_{0.9}$:

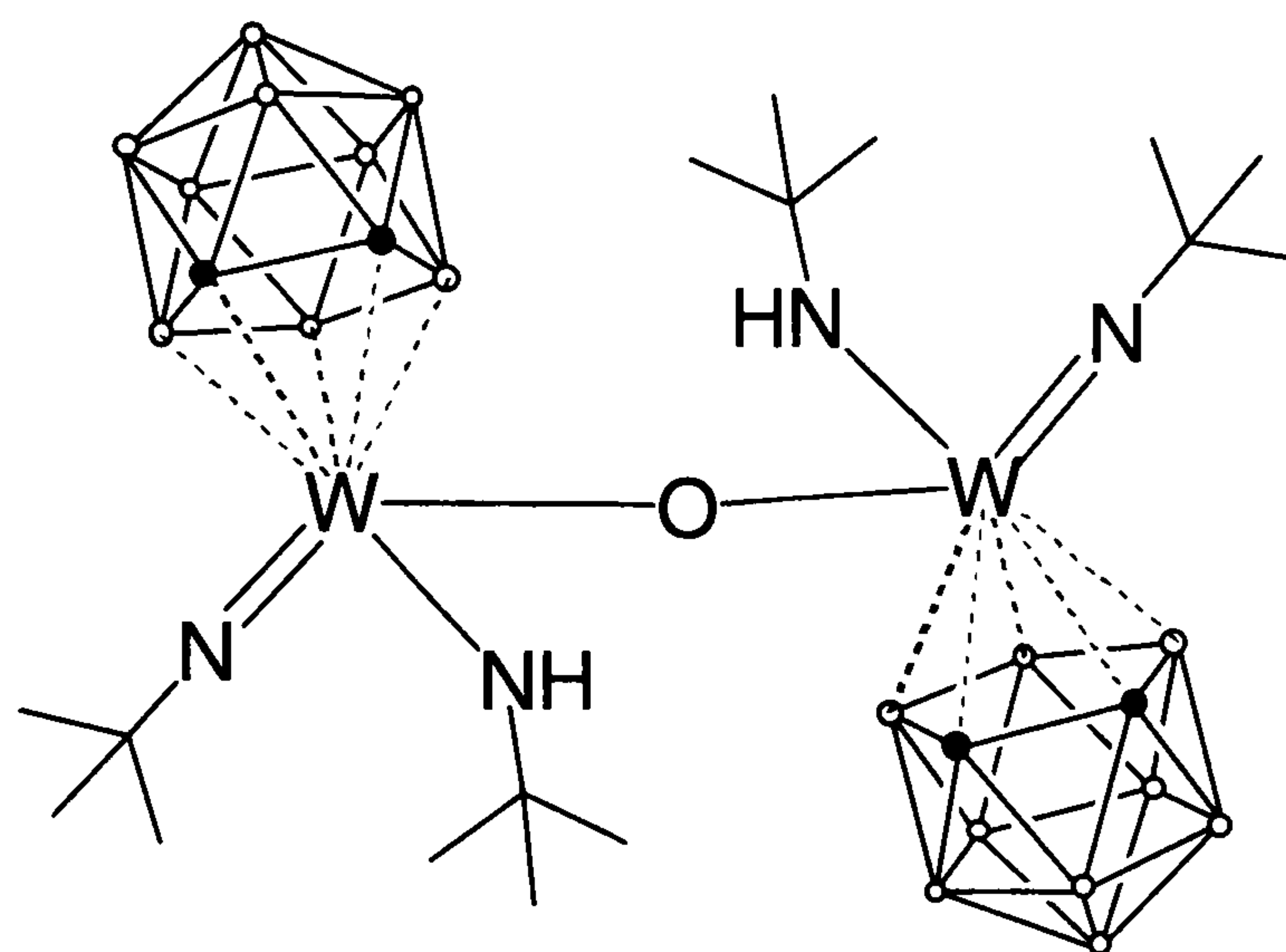
Calc.: C%, 39.67; H%, 7.74; N%, 6.84 and found: C%, 39.83; H%, 7.67; N%, 6.27

Mass Spec:

m/e (assignment) 532 [M^+], and 424 [$M - C_2B_9H_{11}^+$]

5.4.2 Synthesis of 3,1,2- $[\{3-W(N^tBu)(NH^tBu)(1,2-C_2B_9H_{11})\}_2 (\mu-O)]$, (32).

A stirred dichloromethane (10 cm^3) solution of $[W(N^tBu)(NH^tBu)_2(ortho-C_2B_9H_{11})]$, (31) (1 g, 2 mmol) was treated dropwise with 20 cm^3 of a $\approx 0.05\text{ M}$ solution of water in dichloromethane. The yellow solution was stirred for 12 h. The solvent was then evaporated under reduced pressure. The pale yellow residue was extracted with fresh dichloromethane (10 cm^3) filtered and carefully layered with pentane (10 cm^3). Slow recrystallisation at $-20\text{ }^\circ\text{C}$ produced yellow crystals, which analysed to be $[\{W(N^tBu)(NH^tBu)(ortho-C_2B_9H_{11})\}_2 (\mu-O)]$. Yield 0.79 g 84 %.



The same procedure was followed using of $[W(N^tBu)(NH^tBu)Cl(ortho-C_2B_9H_{11})]$, (34) (1 g, 2 mmol), in dichloromethane to yield 0.6 g, 64 % of the bridged oxo complex (32).

The data presented here is for the both the *rac*- and *meso*-isomers, of (32). Assignment of resonances to specific isomers was not possible.

1H (300 MHz, CD_2Cl_2):

δ_H 1.37 (s, 18H, $C(Me)_3$), 1.40 (s, 18H, $C(Me)_3$), 1.55 (s, 18H, $C(Me)_3$), 1.58 (s, 18H, $C(Me)_3$), 3.124 (br s, 4H, $C_2B_9H_{11}$), 3.20 (br s, 4H, $C_2B_9H_{11}$), 8.07 (br s, 2H, NH), 8.1 (br s, 2H, NH)

Additional peaks in $^1H\{^{11}B\}$ NMR (300 MHz, CD_2Cl_2):

δ_H 1.59 (br s 4H), 1.69 (br s, 4H), 2.18 (br s, 4H), 2.33 (br s, 4H), 2.39 (br s, 4H), 2.56 (br s, 4H), 2.78 (br s, 4H), 2.96 (br s, 4H), 3.495 (br s, 4H)

$^{13}\text{C}\{^1\text{H}\}$ NMR (75 MHz, CD_2Cl_2):

δ_{C} 30.4 (s, 6C, $\text{C}(\underline{\text{Me}})_3$), 30.5 (s, 6C, $\text{C}(\underline{\text{Me}})_3$), 32.3 (s, 6C, $\text{C}(\underline{\text{Me}})_3$), 32.4 (s, 6C, $\text{C}(\underline{\text{Me}})_3$), 61.1 (s, 2C, $\text{N}(\text{H})\underline{\text{C}}(\text{Me})_3$), 61.2 (s, 2C, $\text{N}(\text{H})\underline{\text{C}}(\text{Me})_3$), 63.3 (br s, 4C, $\text{C}_2\text{B}_9\text{H}_{11}$), 64.1 (br s, 4C, $\text{C}_2\text{B}_9\text{H}_{11}$), 72.3 (br s, 8C, $\text{NC}(\underline{\text{Me}})_3$)

^{11}B NMR (96.2 MHz, CD_2Cl_2):

δ_{B} 3.0 (M, 2B), 1.3 (M, 2B), -6.1 (M, 2B), -8.6 (M, 6B), -12.3 (M, 4B), -2.4 (M, 2B)

Analysis $\text{C}_{20}\text{H}_{60}\text{B}_{18}\text{N}_4\text{O}_1\text{W}_2$ (CH_2Cl_2)_{0.8}:

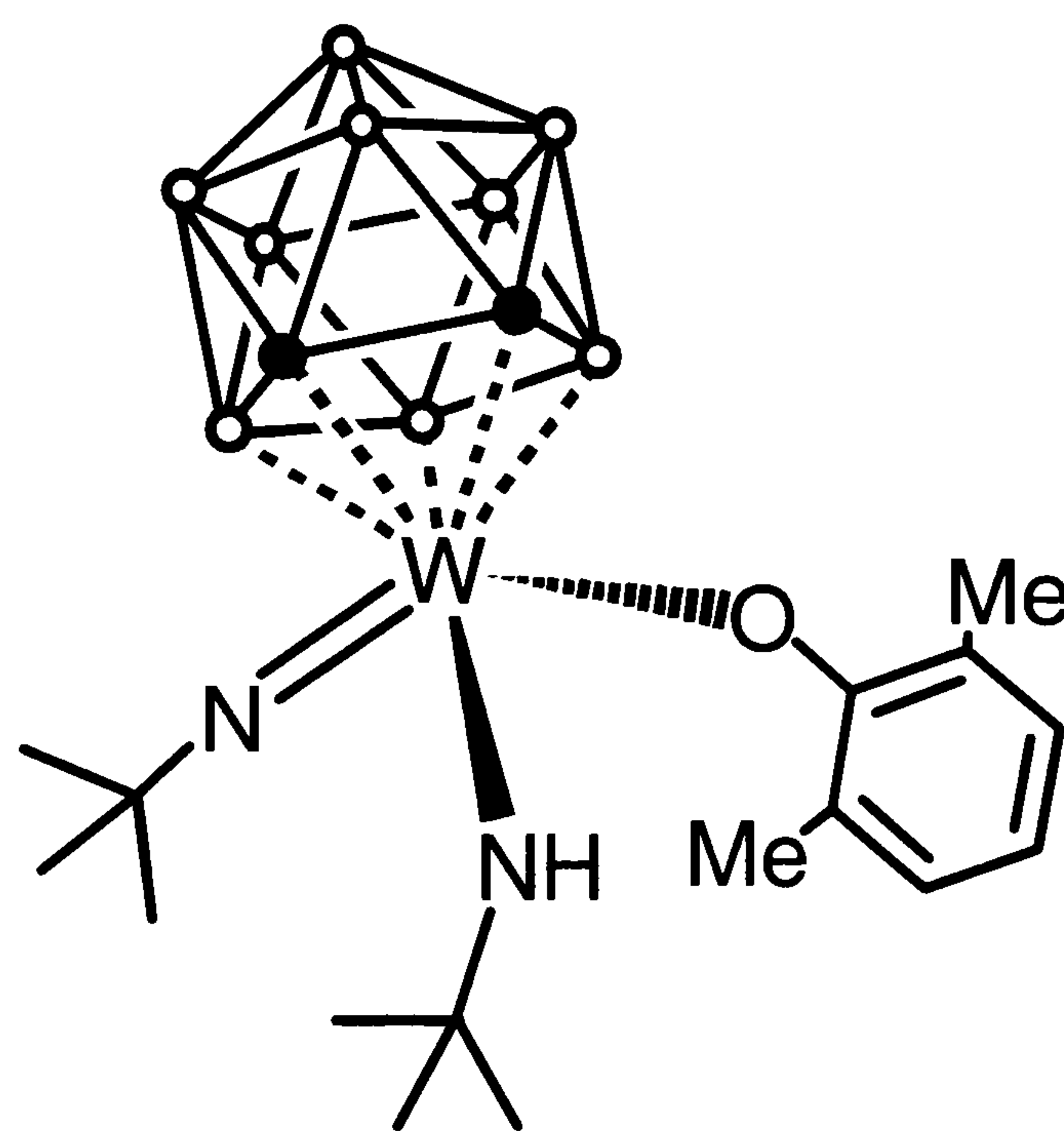
Calc.: C%, 24.91; H%, 6.19; N% 5.59 and found: C%, 25.15; H% 6.17; N% 5.07

Mass Spec:

m/e (assignment) 934 [M^+], 800 [$\text{M}-\text{C}_2\text{B}_9\text{H}_{11}^+$], 403 [$\text{M}-(\text{C}_2\text{B}_9\text{H}_{11}\text{WNC}_4\text{H}_9(\text{NHC}_4\text{H}_9)_2)^+$]

5.4.3 Synthesis of $[3\text{-W}(\text{N}^t\text{Bu})(\text{NH}^t\text{Bu})(\text{OC}_6\text{H}_3\text{Me}_2)(1,2\text{-C}_2\text{B}_9\text{H}_{11})]$, (33).

A stirred toluene (10 cm^3) solution of $[\text{W}(\text{N}^t\text{Bu})(\text{NH}^t\text{Bu})_2(\text{ortho-C}_2\text{B}_9\text{H}_{11})]$, (31) (0.53 g, 1 mmol) was treated dropwise with a toluene solution (10 cm^3) of $\text{HOC}_6\text{H}_3\text{Me}_2$ (0.12 g, 1 mmol). The yellow solution was refluxed for 12 h. The reaction mixture was then allowed to cool to room temperature and the solvent was evaporated under reduced pressure. The yellow residue was extracted with fresh toluene (10 cm^3) filtered and carefully layered with pentane (10 cm^3). Slow recrystallisation at $-20\text{ }^\circ\text{C}$ produced yellow crystalline material which analysed to be $[\text{W}(\text{N}^t\text{Bu})(\text{NH}^t\text{Bu})(\text{OC}_6\text{H}_3\text{Me}_2)(\text{ortho-C}_2\text{B}_9\text{H}_{11})]$. Yield 0.45 g 78 %.



^1H NMR (300 MHz, C_6D_6):

δ_{H} 1.08 (s, 9H, $\text{C}(\underline{\text{CH}}_3)_3$), 1.27 (s, 9H, $\text{C}(\underline{\text{CH}}_3)_3$), 2.02 (s, 6H, $\text{OC}_6\text{H}_3\underline{\text{Me}}_2$), 2.81 (br s, 1H, $\text{C}_2\text{B}_9\text{H}_{11}$), 3.19 (br s, 1H, $\text{C}_2\text{B}_9\text{H}_{11}$), 6.73 (t, 1H, *para*-CH, $^3J_{\text{H-H}}$ 15), 6.85 (d, 2H, *meta*-CH, $^3J_{\text{H-H}}$ 7) 8.09 (br s, 1H, NH)

Chapter Five – Experimental Details

Additional peaks in $^1\text{H}\{^{11}\text{B}\}$ NMR (300 MHz, C_6D_6):

δ_{H} 2.34 (s, 1H), 2.47 (s, 1H), 2.78 (s, 1H), 2.92 (s, 1H), 3.10 (s, 1H), 3.22 (s, 1H), 3.36 (s, 1H), 4.19 (s, 1H), 4.61 (s, 1H)

$^{13}\text{C}\{^1\text{H}\}$ NMR (75 MHz, C_6D_6):

δ_{C} 17.3 (s, 2C, $\text{OC}_6\text{H}_3\text{Me}_2$) 31.0 (s, 3C, $\text{C}(\underline{\text{CH}}_3)_3$), 33.1 (s, 3C, $\text{C}(\underline{\text{CH}}_3)_3$), 53.4 (br s, 1C, $\text{C}_2\text{B}_9\text{H}_{11}$), 62.3 (s, 1C, $\underline{\text{C}}(\text{CH}_3)_3$), 65.3 (br, s, 1C, $\text{C}_2\text{B}_9\text{H}_{11}$), 77.3 (s, 1C, $\underline{\text{C}}(\text{CH}_3)_3$), 122.6 (s, 1C, *para*- $\underline{\text{CH}}$), 127.08 (s, 2C, *ortho*- $\underline{\text{CMe}}$), 129.2 (s, 2C, *meta*- $\underline{\text{CH}}$), 160.1 (s, 1C, *ipso*- $\text{OC}_6\text{H}_3\text{Me}_2$)

^{11}B NMR (96.2 MHz, C_6D_6):

δ_{B} 3.4 (br M, 3B), -4.7 (br M, 1B), -6.7 (br M, 1B), -8.9 (br M, 2B), -10.9 (br M, 1B), -12.2 (br M, 1B)

Analysis $\text{C}_{18}\text{H}_{39}\text{B}_9\text{N}_2\text{O}_1\text{W}_1$:

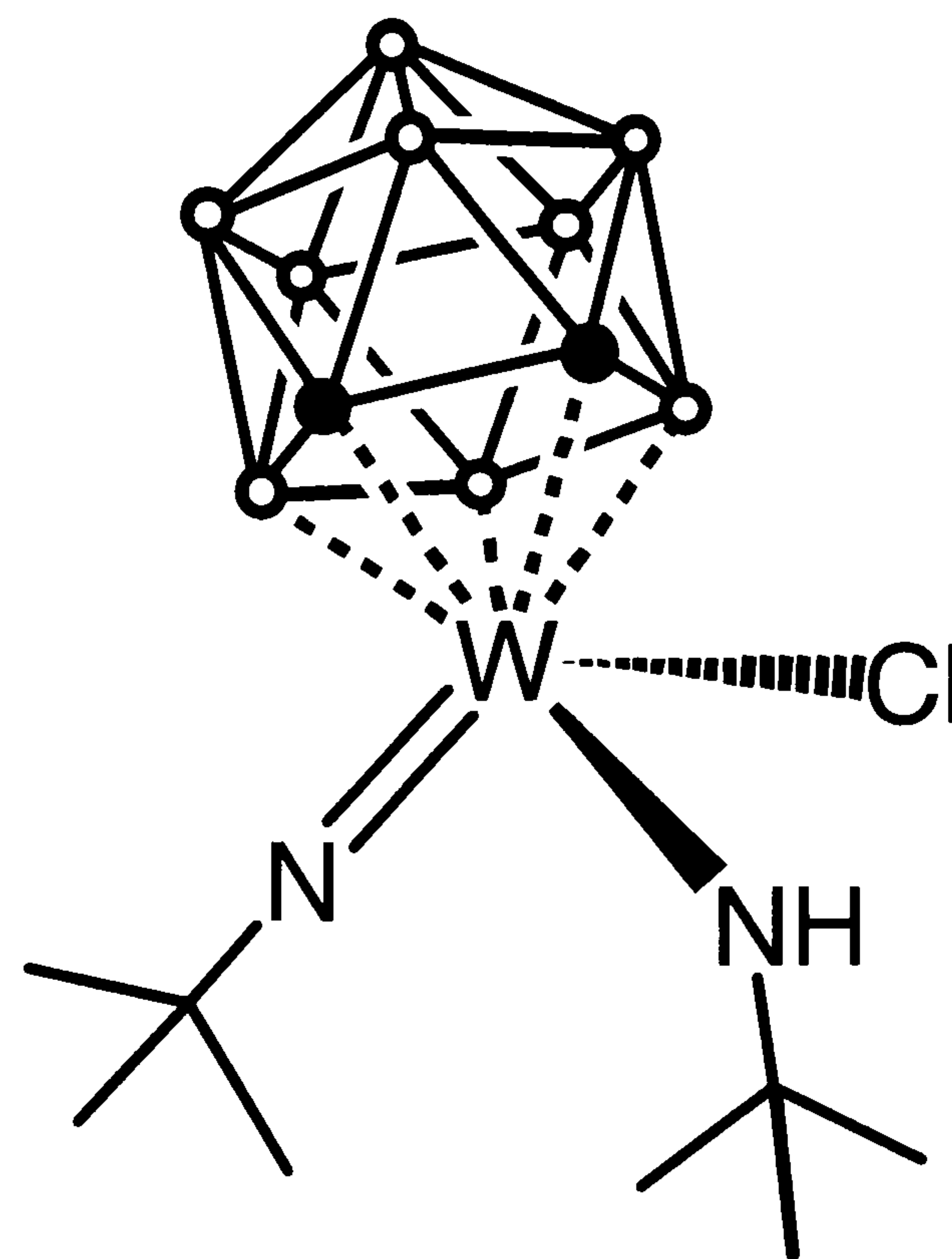
Calc.: C% 37.23; H% 6.77; N% 4.82 and found: C% 37.25, H% 6.42; N% 4.79

Mass Spec:

m/e (assignment) 580 [M^+], 448, [$\text{M}-\text{C}_2\text{B}_9\text{H}_{11}^+$]

5.4.4 Synthesis of [3-*W*(*N*^tBu)(*NH*^tBu)Cl(1,2-*C*₂B₉H₁₁)], (34).

A stirred toluene (20 cm³) solution of [*W*(*N*^tBu)(*NH*^tBu)₂(*ortho*-C₂B₉H₁₁)], (31) (0.53 g, 1 mmol) was treated dropwise with neat Me₃SiCl (0.54 g, 5 mmol) at room temperature. After stirring at room temperature for 12 h, the solution was refluxed for 1 h, and then allowed to cool down to room temperature. Solvent and residual Me₃SiCl were removed under reduced pressure. The residue was washed with hexanes (2 x 10 cm³) and then extracted with dichloromethane and filtered. The dichloromethane solution was layer with pentane (10 cm³) and cooled to -20 °C giving yellow microcrystals of [*W*(*N*^tBu)(*NH*^tBu)Cl(*ortho*-C₂B₉H₁₁)], (34), which were isolated by filtration and washed with a small volume of pentane. Yield 0.3 g, 61 %.



¹H NMR (300 MHz, CDCl₃):

δ_H 1.58 (s, 9H, C(Me)₃), 1.72 (s, 9H, C(Me)₃), 3.37 (br s, 1H, C₂B₉H₁₁), 3.85 (br s, 1H, C₂B₉H₁₁), 9.78 (br s, 1H, NH)

Additional peaks in ¹H{¹¹B} NMR (300 MHz, CDCl₃):

δ_H 2.03 (s, 1H), 2.48 (s, 2H), 2.63 (s, 1H), 2.71 (s, 1H), 2.83 (s, 1H), 3.24 (s, 1H), 3.36 (s, 1H), 3.89 (s, 1H).

¹³C{¹H} NMR (75 MHz, CDCl₃):

δ_C 30.3 (s, 3C, NC(Me)₃), 32.7 (s, 3C, N(H)C(Me)₃), 54.3 (br s, 1C, C₂B₉H₁₁), 62.3 (br s, 1C, C₂B₉H₁₁), 64.1 (s, 1C, N(H)C(Me)₃) 74.0 (s, 1C, NC(Me)₃)

¹¹B NMR (96.2 MHz, CDCl₃):

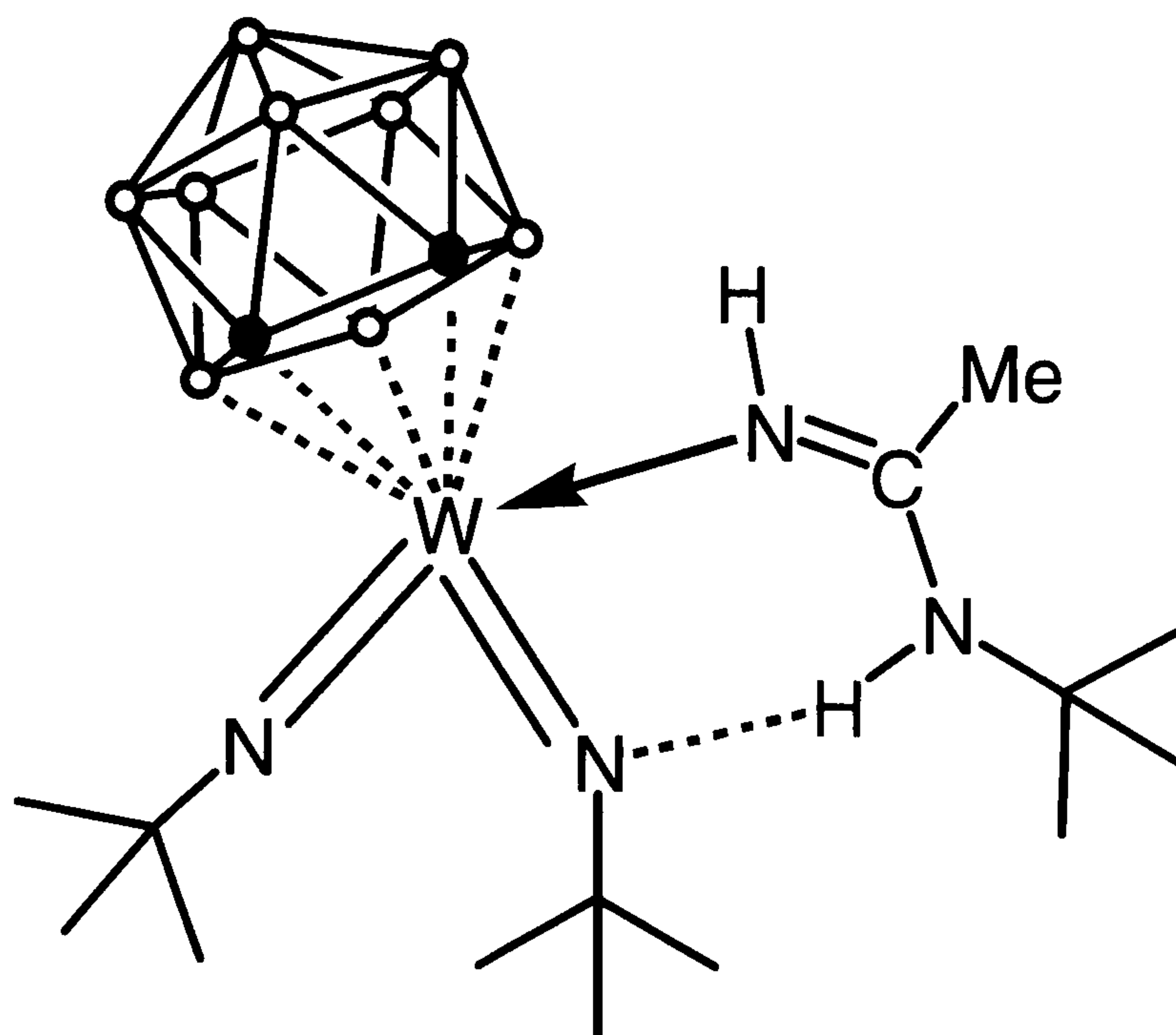
δ_B 3.1 (d, 2B, J_{B-H} 141 Hz), -5.0 (M, 1B), -7.5 (M, 2B), -8.9 (M, 2B), -11.5 (M, 1B), -13.6 (M, 1B).

Analysis C₁₀H₃₀B₉Cl₁N₂W:

Calc.: C% 24.81; H% 6.25; N% 5.79 and found: C% 25.19; H% 6.22; N% 5.72

5.4.5 Synthesis of $[W(N^tBu)_2(N(H)C(CH_3)NH^tBu)(1,2-C_2B_9H_9)]$, (35).

$[W(N^tBu)(NH^tBu)_2(ortho-C_2B_9H_{11})]$, (31) (1 g, 2 mmol) was dissolved in 20 cm³ of dry degassed acetonitrile and stirred until all the solid had dissolved. The solution was then filtered and the volume of solvent reduced to 10 cm³. Slow recrystallisation over 48 h at -20 °C gave yellow crystals of $[W(N^tBu)_2(N(H)C(CH_3)NH^tBu)(ortho-C_2B_9H_{11})]$, (35), which were isolated by filtration and washed with a small volume of pentane. Yield 0.95 g, 83 %.



¹H NMR (300 MHz, C₆D₆):

δ_H 1.32 (s, 9H, C(Me)₃), 1.35 (s, 9H, C(Me)₃), 1.46 (s, 9H, C(Me)₃), 1.53 (s, 3H, CH₃), 2.81 (br s, 1H, C₂B₉H₁₁), 3.42 (br s, 1H, C₂B₉H₁₁), 5.27 (br s, 1H, NH), 6.44 (br s, 1H, NH)

Additional peaks in ¹H{¹¹B} NMR (300 MHz, C₆D₆):

δ_H 1.38 (s, 1H), 2.38 (s, 1H), 2.93 (s, 1H), 3.19 (s, 1H), 3.40 (s, 1H), 3.64 (s, 1H), 3.82 (s, 1H), 4.06 (s, 1H), 4.54 (s, 1H)

¹³C{¹H} NMR (75 MHz, CDCl₃):

δ_C 30.9 (s, 1C, CH₃), 31.5 (s, 3C, C(Me)₃), 32.5 (s, 3C, C(Me)₃), 34.0 (s, 3C, C(Me)₃), 49.6 (m, 1C, C₂B₉H₁₁), 56.5 (m, 1C, C₂B₉H₁₁), 58.2 (s, 1C, C(Me)₃), 69.1 (s, 1C, C(Me)₃), 71.6 (s, 1C, C(Me)₃), 168.9 (s, 1C, N=C(Me)-N)

¹¹B NMR (96.2 MHz, C₆D₆):

δ_B 2.2 (M, 1B), 0.8 (M, 1B), -0.1 (M, 1B), -4.8 (d, 1B, J_{B-H} 129.9Hz), -8.9 (M, 1B), -10.6 (M, 1B), -12.9 (M, 1B), -14.2 (M, 1B), -18.4 (M, 1B)

Analysis C₁₆H₃₄B₉N₄W₁:

Calc.: C% 33.56; H% 7.57; N% 9.78 and found: C% 33.76; H% 7.58; N% 9.67

5.5 References for Chapter 5

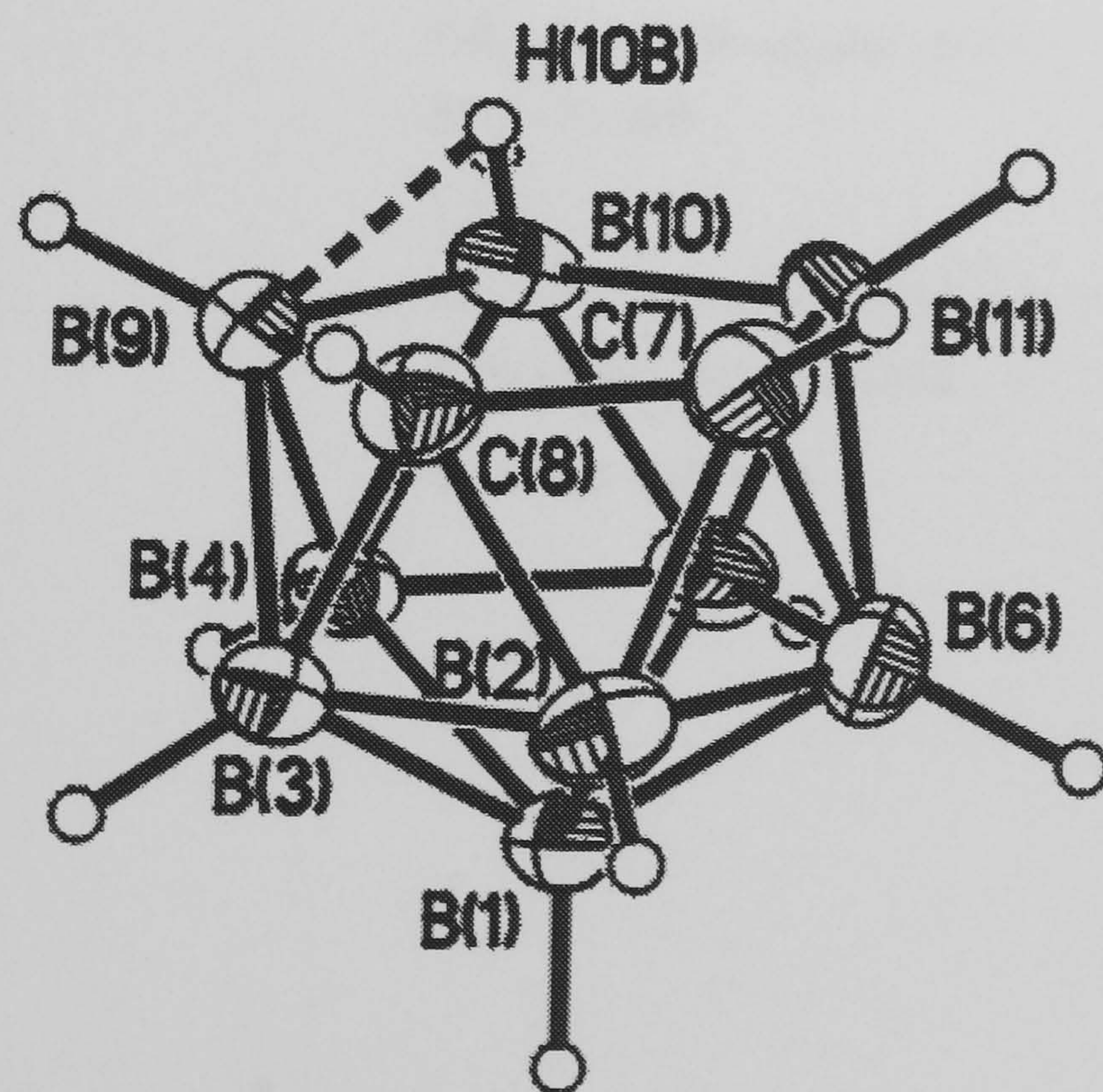
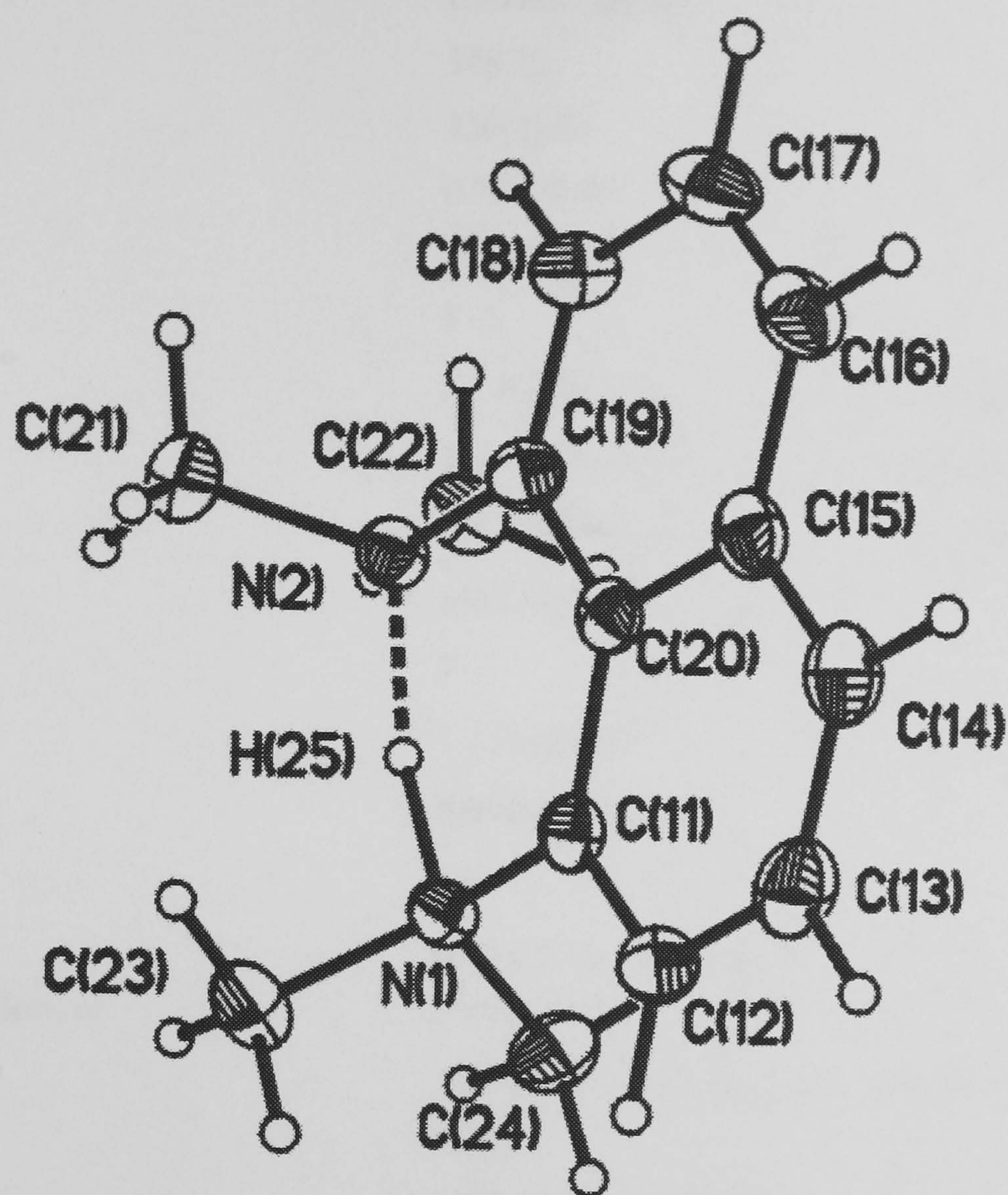
- 1 D. S. Stalke and T. Kottke, *J. Appl. Cryst.*, 1993, **26**, 615.
- 2 J. Cosier and A. M. Glazer, *J. Appl. Cryst.*, 1986, **19**, 105.
- 3 (a) Siemens Analytical X-ray Instruments, *SMART*, Version 4.050, Siemens Analytical X-ray Instruments, Inc., Madison, Wisconsin, U.S.A., 1995; (b) W. Kabsch, *J. Appl. Cryst.*, 1993, **26**, 795.
- 4 (a) Siemens Analytical X-ray Instruments, *SAINT*, Version 4.050, Siemens Analytical X-ray Instruments, Inc., Madison, Wisconsin, U.S.A., 1995; (b) W. Kabsch, *J. Appl. Cryst.*, 1988, **21**, 916; (c) G. M. Sheldrick, *XPREF in SHELXTL*, Version 5.03/VMS, Siemens Analytical X-ray Instruments, Inc., Madison, Wisconsin, U.S.A., 1995.
- 5 (a) G. M. Sheldrick, *Acta Cryst.*, 1990, **A46**, 467; (b) G. M. Sheldrick, *SHELXL-93, Program for the Refinement of Crystal Structures using Single Crystal Diffraction Data*, University of Göttingen, Germany, 1993.
- 6 (a) H. Lee, T. Onak, J. Jaballas and U. Tran, *Heteroatom. Chem.*, 1997, **9**, 95; (b) M. A. Fox and K. Wade, *Polyhedron*, 1997, **16**, 2517.
7. (a) J. Li, C. F. Logan and M. Jones Jr., *Inorg. Chem.*, 1991, **30**, 4866; (b) M. F. Hawthorne, D. C. Young, P. M. Garret, D. A. Owens, S. G. Schwerin, F. N. Tebbe and P. A. Wegner, *J. Am. Chem. Soc.*, 1968, **90**, 862.
- 8 H. Schmidbaur, J. Jeong, A. Scier, W. Graf, D. L. Wilkinson and G. Müller, *New J. Chem.*, 1989, **13**, 341.
- 9 F. R. Scholer, R. Brown, D. Gladkowski, W. F. Wright and L. J. Todd, *Inorg. Chem.*, 1979, **18**, 921.
- 10 D. C. Bradley and I. M. Thomas, *Can. J. Chem.*, 1962, **40**, 1355.
- 11 D. C. Bradley and I. M. Thomas, *Can. J. Chem.*, 1962, **40**, 449.

12 (a) W. A. Nugent, *Inorg. Chem.*, 1983, **22**, 965; (b) W. A. Nugent and R. L. Harlow, *Inorg. Chem.*, 1980, **19**, 777.

Appendix A

Crystal Data

A1 Crystal data for $[1,8-(N(CH_3)_2)(NH(CH_3)_2C_{10}H_8)][7,8-C_2B_9H_{12}]$; (4a).



Appendix A – Crystal Data

Table 1. Crystal data and structure refinement for 4a.

Identification code	98srv012	
Empirical formula	C16 H31 B9 N2	
Formula weight	348.72	
Temperature	150(2) K	
Wavelength	0.71073 Å	
Crystal system	Triclinic	
Space group	P -1	
Unit cell dimensions	a = 8.129(1) Å	α= 68.524(5)°.
	b = 11.251(2) Å	β= 86.359(7)°.
	c = 12.392(2) Å	γ = 79.712(8)°.
Volume	1037.7(3) Å ³	
Z	2	
Density (calculated)	1.116 Mg/m ³	
Absorption coefficient	0.058 mm ⁻¹	
F(000)	372	
Crystal size	0.36 x 0.32 x 0.28 mm ³	
Theta range for data collection	1.77 to 23.53°.	
Index ranges	-11<=h<=11, -15<=k<=14, -17<=l<=13	
Reflections collected	5550	
Independent reflections	3073 [R(int) = 0.0443]	
Absorption correction	None	
Refinement method	Full-matrix least-squares on F ²	
Data / restraints / parameters	3073 / 0 / 368	
Goodness-of-fit on F ²	1.280	
Final R indices [I>2sigma(I)]	R1 = 0.0504, wR2 = 0.1080	
R indices (all data)	R1 = 0.0699, wR2 = 0.1384	
Largest diff. peak and hole	0.170 and -0.227 e.Å ⁻³	

Table 2. Atomic coordinates (x 10⁴) and equivalent isotropic displacement parameters (Å²x 10³)

Appendix A – Crystal Data

for 4a. U(eq) is defined as one third of the trace of the orthogonalized U^{ij} tensor.

	x	y	z	U(eq)
N(2)	3178(2)	7070(2)	2938(2)	24(1)
C(19)	4077(3)	7297(2)	1832(2)	24(1)
B(9)	6834(4)	13501(3)	2583(3)	31(1)
N(1)	5036(2)	8442(2)	3454(2)	23(1)
C(18)	3717(3)	6748(3)	1071(2)	31(1)
B(10)	7964(4)	11836(3)	3268(3)	33(1)
C(17)	4589(4)	6955(3)	15(2)	35(1)
B(11)	9856(4)	11887(3)	2408(3)	36(1)
C(16)	5799(3)	7717(3)	-273(2)	32(1)
B(6)	11037(4)	12954(3)	2676(3)	37(1)
C(15)	6212(3)	8313(2)	482(2)	27(1)
B(2)	9862(4)	14529(3)	2084(3)	35(1)
C(14)	7462(3)	9111(3)	181(2)	31(1)
B(3)	7993(4)	14580(3)	2868(3)	32(1)
C(13)	7866(3)	9685(3)	903(2)	33(1)
B(4)	7916(4)	13028(3)	3907(3)	30(1)
C(12)	7063(3)	9462(2)	1986(2)	27(1)
B(5)	9871(4)	12001(3)	3789(3)	35(1)
C(11)	5846(3)	8694(2)	2310(2)	22(1)
B(1)	9843(4)	13663(3)	3604(3)	28(1)
C(20)	5345(3)	8097(2)	1570(2)	22(1)
C(22)	3334(4)	5665(3)	3664(2)	30(1)
C(21)	1388(3)	7688(3)	2770(3)	34(1)
C(23)	4053(4)	9647(3)	3567(3)	32(1)
C(24)	6262(4)	7758(3)	4426(2)	33(1)
C(7)	9714(3)	13368(3)	1501(2)	37(1)
C(8)	8071(3)	14277(3)	1604(2)	33(1)

Table 3. Bond lengths [Å] and angles [°] for 4a.

N(2)-C(19)	1.469(3)	B(11)-C(7)	1.622(5)	C(13)-H(13)	1.01(3)
N(2)-C(21)	1.489(3)	B(11)-B(5)	1.763(4)	B(4)-B(1)	1.798(4)
N(2)-C(22)	1.492(3)	B(11)-B(6)	1.793(5)	B(4)-B(5)	1.822(5)
N(2)-H(25)	1.40(4)	B(11)-H(11)	1.14(3)	B(4)-H(4)	1.10(3)
C(19)-C(18)	1.372(3)	C(16)-C(15)	1.421(4)	C(12)-C(11)	1.374(3)
C(19)-C(20)	1.433(3)	C(16)-H(16)	0.97(3)	C(12)-H(12)	0.98(3)
B(9)-C(8)	1.621(4)	B(6)-C(7)	1.737(4)	B(5)-B(1)	1.795(4)
B(9)-B(4)	1.767(4)	B(6)-B(5)	1.751(5)	B(5)-H(5)	1.09(3)
B(9)-B(3)	1.803(4)	B(6)-B(2)	1.768(5)	C(11)-C(20)	1.432(3)
B(9)-B(10)	1.842(5)	B(6)-B(1)	1.776(4)	B(1)-H(1)	1.12(2)
B(9)-H(9)	1.07(3)	B(6)-H(6)	1.12(3)	C(22)-H(22B)	1.02(3)
B(9)-H(10B)	1.54(4)	C(15)-C(14)	1.418(4)	C(22)-H(22C)	0.97(3)
N(1)-C(11)	1.476(3)	C(15)-C(20)	1.440(3)	C(22)-H(22A)	1.03(3)
N(1)-C(23)	1.494(3)	B(2)-C(8)	1.713(4)	C(21)-H(21C)	1.01(3)
N(1)-C(24)	1.496(3)	B(2)-C(7)	1.732(4)	C(21)-H(21B)	1.00(3)
N(1)-H(25)	1.25(4)	B(2)-B(3)	1.754(5)	C(21)-H(21B)	0.99(3)
C(18)-C(17)	1.410(4)	B(2)-B(1)	1.776(4)	C(23)-H(23B)	0.96(3)
C(18)-H(18)	1.03(3)	B(2)-H(2)	1.11(3)	C(23)-H(23B)	1.03(3)
B(10)-B(5)	1.780(4)	C(14)-C(13)	1.365(4)	C(23)-H(23A)	1.03(3)
B(10)-B(4)	1.783(4)	C(14)-H(14)	0.97(3)	C(24)-H(24C)	1.00(3)
B(10)-B(11)	1.812(4)	B(3)-C(8)	1.716(4)	C(24)-H(24B)	1.02(3)
B(10)-H(10)	1.15(3)	B(3)-B(1)	1.758(4)	C(24)-H(24A)	1.00(3)
B(10)-H(10B)	1.16(4)	B(3)-B(4)	1.759(4)	C(7)-C(8)	1.560(4)
C(17)-C(16)	1.364(4)	B(3)-H(3)	1.11(3)	C(7)-H(7)	1.05(3)
C(17)-H(17)	0.95(3)	C(13)-C(12)	1.411(4)	C(8)-H(8)	1.00(3)
C(19)-N(2)-C(21)	112.2(2)	B(11)-B(10)-B(9)	101.5(2)	B(2)-B(6)-H(6)	118.1(16)
C(19)-N(2)-C(22)	112.5(2)	B(5)-B(10)-H(10)	117.1(14)	B(1)-B(6)-H(6)	123.9(16)
C(21)-N(2)-C(22)	110.5(2)	B(4)-B(10)-H(10)	119.1(14)	B(11)-B(6)-H(6)	123.1(16)
C(19)-N(2)-H(25)	99.4(15)	B(11)-B(10)-H(10)	124.6(14)	C(14)-C(15)-C(16)	121.0(2)
C(21)-N(2)-H(25)	110.3(15)	B(9)-B(10)-H(10)	128.4(14)	C(14)-C(15)-C(20)	119.8(2)
C(22)-N(2)-H(25)	111.6(15)	B(5)-B(10)-H(10B)	124.8(17)	C(16)-C(15)-C(20)	119.2(2)
C(18)-C(19)-C(20)	120.8(2)	B(4)-B(10)-H(10B)	112.7(18)	C(8)-B(2)-C(7)	53.8(2)
C(18)-C(19)-N(2)	120.7(2)	B(11)-B(10)-H(10B)	73.7(17)	C(8)-B(2)-B(3)	59.3(2)
C(20)-C(19)-N(2)	118.6(2)	B(9)-B(10)-H(10B)	56.3(18)	C(7)-B(2)-B(3)	102.5(2)
C(8)-B(9)-B(4)	104.8(2)	H(10)-B(10)-H(10B)	112.2(22)	C(8)-B(2)-B(6)	103.5(2)
C(8)-B(9)-B(3)	59.9(2)	C(16)-C(17)-C(18)	120.4(3)	C(7)-B(2)-B(6)	59.5(2)
B(4)-B(9)-B(3)	59.0(2)	C(16)-C(17)-H(17)	121.3(17)	B(3)-B(2)-B(6)	108.4(2)
C(8)-B(9)-B(10)	106.5(2)	C(18)-C(17)-H(17)	118.2(17)	C(8)-B(2)-B(1)	103.8(2)
B(4)-B(9)-B(10)	59.2(2)	C(7)-B(11)-B(5)	104.9(2)	C(7)-B(2)-B(1)	103.5(2)
B(3)-B(9)-B(10)	107.9(2)	C(7)-B(11)-B(6)	60.9(2)	B(3)-B(2)-B(1)	59.7(2)
C(8)-B(9)-H(9)	123.2(16)	B(5)-B(11)-B(6)	59.0(2)	B(6)-B(2)-B(1)	60.2(2)
B(4)-B(9)-H(9)	122.6(16)	C(7)-B(11)-B(10)	105.8(2)	C(8)-B(2)-H(2)	120.3(15)
B(3)-B(9)-H(9)	119.4(16)	B(5)-B(11)-B(10)	59.7(2)	C(7)-B(2)-H(2)	121.2(15)
B(10)-B(9)-H(9)	123.2(16)	B(6)-B(11)-B(10)	108.6(2)	B(3)-B(2)-H(2)	123.4(15)
C(8)-B(9)-H(10B)	88.3(13)	C(7)-B(11)-H(11)	121.8(16)	B(6)-B(2)-H(2)	123.7(15)
B(4)-B(9)-H(10B)	96.7(14)	B(5)-B(11)-H(11)	124.5(16)	B(1)-B(2)-H(2)	129.7(15)
B(3)-B(9)-H(10B)	127.6(13)	B(6)-B(11)-H(11)	119.1(16)	C(13)-C(14)-C(15)	121.3(2)
B(10)-B(9)-H(10B)	38.9(14)	B(10)-B(11)-H(11)	123.9(16)	C(13)-C(14)-H(14)	119.9(17)
H(9)-B(9)-H(10B)	112.8(21)	C(17)-C(16)-C(15)	121.0(3)	C(15)-C(14)-H(14)	118.8(17)
C(11)-N(1)-C(23)	112.2(2)	C(17)-C(16)-H(16)	121.2(16)	C(8)-B(3)-B(2)	59.2(2)
C(11)-N(1)-C(24)	112.0(2)	C(15)-C(16)-H(16)	117.8(16)	C(8)-B(3)-B(1)	104.4(2)
C(23)-N(1)-C(24)	111.3(2)	C(7)-B(6)-B(5)	100.6(2)	B(2)-B(3)-B(1)	60.7(2)
C(11)-N(1)-H(25)	100.9(16)	C(7)-B(6)-B(2)	59.2(2)	C(8)-B(3)-B(4)	101.2(2)
C(23)-N(1)-H(25)	109.2(17)	B(5)-B(6)-B(2)	108.5(2)	B(2)-B(3)-B(4)	108.8(2)
C(24)-N(1)-H(25)	110.8(17)	C(7)-B(6)-B(1)	103.3(2)	B(1)-B(3)-B(4)	61.5(2)
C(19)-C(18)-C(17)	120.8(3)	B(5)-B(6)-B(1)	61.2(2)	C(8)-B(3)-B(9)	54.8(2)
C(19)-C(18)-H(18)	118.3(16)	B(2)-B(6)-B(1)	60.1(2)	B(2)-B(3)-B(9)	106.1(2)
C(17)-C(18)-H(18)	120.9(17)	C(7)-B(6)-B(11)	54.7(2)	B(1)-B(3)-B(9)	108.3(2)
B(5)-B(10)-B(4)	61.5(2)	B(5)-B(6)-B(11)	59.6(2)	B(4)-B(3)-B(9)	59.5(2)
B(5)-B(10)-B(11)	58.8(2)	B(2)-B(6)-B(11)	106.4(2)	C(8)-B(3)-H(3)	121.9(15)
B(4)-B(10)-B(11)	105.9(2)	B(1)-B(6)-B(11)	108.1(2)	B(2)-B(3)-H(3)	119.6(14)
B(5)-B(10)-B(9)	105.4(2)	C(7)-B(6)-H(6)	123.7(16)	B(1)-B(3)-H(3)	125.4(14)
B(4)-B(10)-B(9)	58.3(2)	B(5)-B(6)-H(6)	127.1(16)	B(4)-B(3)-H(3)	126.4(15)

Appendix A – Crystal Data

B(9)-B(3)-H(3)	121.0(14)	B(10)-B(5)-H(5)	117.7(14)	H(21C)-C(21)-H(21B)	108.5(23)
C(14)-C(13)-C(12)	120.0(3)	B(1)-B(5)-H(5)	121.3(14)	H(21B)-C(21)-H(21B)	108.0(24)
C(14)-C(13)-H(13)	121.9(15)	B(4)-B(5)-H(5)	121.1(14)	N(1)-C(23)-H(23B)	107.3(17)
C(12)-C(13)-H(13)	118.1(15)	C(12)-C(11)-C(20)	121.8(2)	N(1)-C(23)-H(23B)	107.7(16)
B(3)-B(4)-B(9)	61.5(2)	C(12)-C(11)-N(1)	120.2(2)	H(23B)-C(23)-H(23B)	112.3(23)
B(3)-B(4)-B(10)	112.6(2)	C(20)-C(11)-N(1)	118.1(2)	N(1)-C(23)-H(23A)	111.1(15)
B(9)-B(4)-B(10)	62.5(2)	B(3)-B(1)-B(2)	59.5(2)	H(23B)-C(23)-H(23A)	112.0(22)
B(3)-B(4)-B(1)	59.2(2)	B(3)-B(1)-B(6)	107.8(2)	H(23B)-C(23)-H(23A)	106.5(21)
B(9)-B(4)-B(1)	108.1(2)	B(2)-B(1)-B(6)	59.7(2)	N(1)-C(24)-H(24C)	111.1(16)
B(10)-B(4)-B(1)	109.6(2)	B(3)-B(1)-B(5)	108.1(2)	N(1)-C(24)-H(24B)	107.2(15)
B(3)-B(4)-B(5)	106.8(2)	B(2)-B(1)-B(5)	106.1(2)	H(24C)-C(24)-H(24B)	108.2(21)
B(9)-B(4)-B(5)	106.8(2)	B(6)-B(1)-B(5)	58.7(2)	N(1)-C(24)-H(24A)	107.6(16)
B(10)-B(4)-B(5)	59.2(2)	B(3)-B(1)-B(4)	59.3(2)	H(24C)-C(24)-H(24A)	111.6(22)
B(1)-B(4)-B(5)	59.5(2)	B(2)-B(1)-B(4)	106.1(2)	H(24B)-C(24)-H(24A)	111.0(22)
B(3)-B(4)-H(4)	122.6(15)	B(6)-B(1)-B(4)	107.4(2)	C(8)-C(7)-B(11)	114.4(2)
B(9)-B(4)-H(4)	124.0(15)	B(5)-B(1)-B(4)	60.9(2)	C(8)-C(7)-B(2)	62.5(2)
B(10)-B(4)-H(4)	118.5(15)	B(3)-B(1)-H(1)	120.6(12)	B(11)-C(7)-B(2)	116.4(2)
B(1)-B(4)-H(4)	120.3(14)	B(2)-B(1)-H(1)	123.1(12)	C(8)-C(7)-B(6)	111.9(2)
B(5)-B(4)-H(4)	120.6(15)	B(6)-B(1)-H(1)	123.3(12)	B(11)-C(7)-B(6)	64.4(2)
C(11)-C(12)-C(13)	120.4(2)	B(5)-B(1)-H(1)	122.8(13)	B(2)-C(7)-B(6)	61.3(2)
C(11)-C(12)-H(12)	120.1(15)	B(4)-B(1)-H(1)	121.4(12)	C(8)-C(7)-H(7)	116.3(17)
C(13)-C(12)-H(12)	119.4(15)	C(11)-C(20)-C(19)	125.4(2)	B(11)-C(7)-H(7)	121.1(16)
B(6)-B(5)-B(11)	61.4(2)	C(11)-C(20)-C(15)	116.7(2)	B(2)-C(7)-H(7)	112.4(16)
B(6)-B(5)-B(10)	112.1(2)	C(19)-C(20)-C(15)	117.9(2)	B(6)-C(7)-H(7)	118.4(16)
B(11)-B(5)-B(10)	61.5(2)	N(2)-C(22)-H(22B)	106.3(14)	C(7)-C(8)-B(9)	111.6(2)
B(6)-B(5)-B(1)	60.1(2)	N(2)-C(22)-H(22C)	110.2(16)	C(7)-C(8)-B(2)	63.7(2)
B(11)-B(5)-B(1)	108.6(2)	H(22B)-C(22)-H(22C)	108.7(21)	B(9)-C(8)-B(2)	116.9(2)
B(10)-B(5)-B(1)	109.8(2)	N(2)-C(22)-H(22A)	108.1(16)	C(7)-C(8)-B(3)	112.2(2)
B(6)-B(5)-B(4)	107.4(2)	H(22B)-C(22)-H(22A)	111.0(21)	B(9)-C(8)-B(3)	65.3(2)
B(11)-B(5)-B(4)	106.3(2)	H(22C)-C(22)-H(22A)	112.3(22)	B(2)-C(8)-B(3)	61.5(2)
B(10)-B(5)-B(4)	59.3(2)	N(2)-C(21)-H(21C)	108.9(15)	C(7)-C(8)-H(8)	117.6(16)
B(1)-B(5)-B(4)	59.6(2)	N(2)-C(21)-H(21B)	109.0(16)	B(9)-C(8)-H(8)	121.2(16)
B(6)-B(5)-H(5)	122.7(14)	H(21C)-C(21)-H(21B)	110.4(22)	B(2)-C(8)-H(8)	112.6(16)
B(11)-B(5)-H(5)	123.1(14)	N(2)-C(21)-H(21B)	112.0(18)	B(3)-C(8)-H(8)	118.2(16)

Symmetry transformations used to generate equivalent atoms:

Table 4. Anisotropic displacement parameters ($\text{\AA}^2 \times 10^3$) for 4a. The anisotropic

Appendix A – Crystal Data

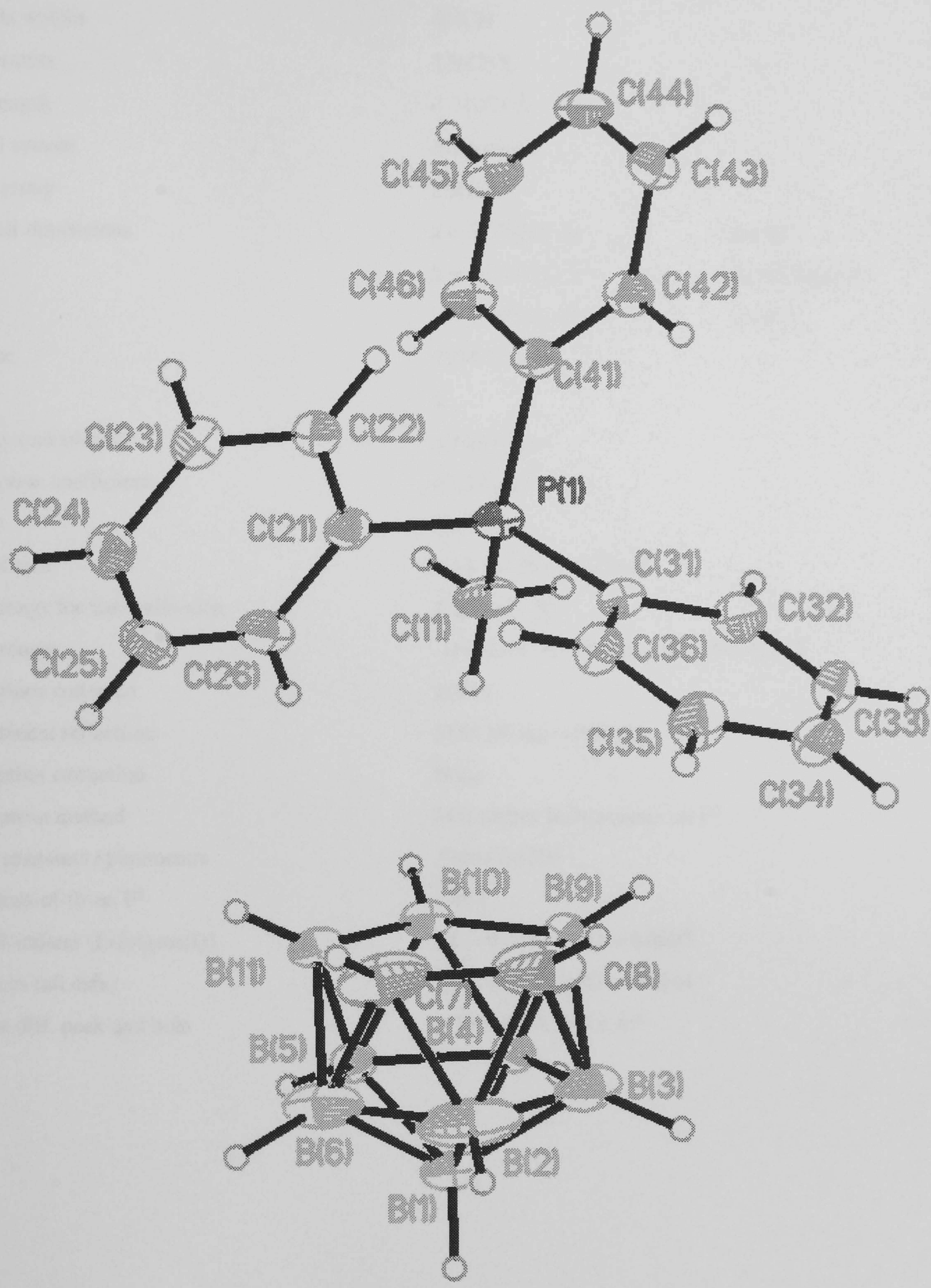
displacement factor exponent takes the form: $-2\pi^2[h^2 a^{*2}U^{11} + \dots + 2 h k a^* b^* U^{12}]$

	U ¹¹	U ²²	U ³³	U ²³	U ¹³	U ¹²
N(2)	24(1)	25(1)	24(1)	-10(1)	3(1)	-6(1)
C(19)	25(1)	24(1)	21(1)	-7(1)	-2(1)	-4(1)
B(9)	24(2)	37(2)	40(2)	-22(2)	1(1)	-6(1)
N(1)	24(1)	23(1)	22(1)	-10(1)	1(1)	-5(1)
C(18)	33(2)	33(2)	27(2)	-12(1)	-2(1)	-9(1)
B(10)	45(2)	35(2)	27(2)	-16(2)	6(2)	-19(2)
C(17)	46(2)	38(2)	26(2)	-17(1)	-5(1)	-6(1)
B(11)	36(2)	40(2)	36(2)	-23(2)	0(1)	1(2)
C(16)	38(2)	34(2)	21(1)	-10(1)	1(1)	0(1)
B(6)	26(2)	50(2)	36(2)	-18(2)	0(1)	-4(2)
C(15)	27(1)	25(1)	24(1)	-7(1)	0(1)	3(1)
B(2)	37(2)	37(2)	33(2)	-9(2)	-1(1)	-17(2)
C(14)	27(1)	31(2)	29(2)	-7(1)	7(1)	-4(1)
B(3)	31(2)	29(2)	42(2)	-19(2)	-4(1)	-5(1)
C(13)	25(1)	33(2)	38(2)	-9(1)	7(1)	-10(1)
B(4)	32(2)	38(2)	29(2)	-19(1)	9(1)	-16(1)
C(12)	26(1)	27(1)	32(2)	-13(1)	1(1)	-7(1)
B(5)	43(2)	29(2)	31(2)	-10(2)	-7(2)	-5(2)
C(11)	20(1)	20(1)	25(1)	-7(1)	-1(1)	0(1)
B(1)	28(2)	32(2)	30(2)	-15(1)	0(1)	-8(1)
C(20)	22(1)	20(1)	22(1)	-6(1)	-4(1)	3(1)
C(22)	37(2)	26(2)	28(2)	-9(1)	4(1)	-10(1)
C(21)	25(2)	39(2)	39(2)	-16(2)	1(1)	-3(1)
C(23)	36(2)	27(2)	35(2)	-15(1)	8(1)	-5(1)
C(24)	32(2)	36(2)	28(2)	-7(1)	-4(1)	-8(1)
C(7)	34(2)	53(2)	27(2)	-17(1)	5(1)	-12(1)
C(8)	35(2)	32(2)	30(2)	-8(1)	-8(1)	-4(1)

Table 5. Hydrogen coordinates (x 10⁴) and isotropic displacement parameters (Å²x 10⁻³) for 4a.

	x	y	z	U(eq)
H(18)	2789(38)	6192(29)	1286(25)	49(8)
H(10)	7426(34)	10911(28)	3774(24)	43(8)
H(16)	6381(34)	7889(27)	-1008(26)	39(8)
H(6)	12430(40)	12843(30)	2605(27)	58(9)
H(2)	10418(35)	15400(29)	1586(25)	47(8)
H(14)	8054(36)	9233(28)	-550(26)	44(8)
H(3)	7351(34)	15516(28)	2919(24)	44(8)
H(13)	8731(33)	10270(26)	690(23)	35(7)
H(4)	7299(35)	12875(27)	4752(25)	44(8)
H(12)	7393(32)	9848(25)	2512(23)	32(7)
H(5)	10447(33)	11213(27)	4546(25)	40(8)
H(1)	10416(29)	13957(23)	4247(21)	25(6)
H(22B)	2733(32)	5614(24)	4426(24)	31(7)
H(22C)	2777(32)	5223(25)	3287(23)	32(7)
H(21C)	868(32)	7597(24)	3550(24)	31(7)
H(21B)	1315(34)	8624(30)	2270(25)	39(8)
H(23B)	3471(36)	9393(28)	4295(27)	42(8)
H(24C)	7061(35)	8334(28)	4452(23)	38(8)
H(24B)	5597(33)	7536(25)	5179(24)	34(7)
H(7)	10243(36)	13580(29)	670(27)	50(9)
H(8)	7617(35)	15002(29)	878(26)	44(8)
H(21B)	749(38)	7280(30)	2382(27)	51(9)
H(17)	4289(35)	6570(28)	-495(26)	43(8)
H(11)	10547(38)	11035(31)	2181(27)	59(9)
H(23B)	3246(36)	10080(28)	2870(26)	42(8)
H(23A)	4822(33)	10306(27)	3513(22)	33(7)
H(9)	5496(39)	13736(29)	2520(26)	53(9)
H(22A)	4591(39)	5286(28)	3804(25)	45(8)
H(24A)	6860(35)	6958(29)	4312(24)	40(8)
H(25)	4053(45)	7718(35)	3424(31)	83(12)
H(10B)	7539(43)	12281(35)	2304(32)	78(11)

A2 Crystal data for $[(C_6H_5)_3PCH_3][7,8-C_2B_9H_{12}]$; (4b).



Appendix A – Crystal Data

Table 1. Crystal data and structure refinement for 4b.

Identification code	98srv002	
Empirical formula	C21 H30 B9 P	
Formula weight	410.71	
Temperature	120(2) K	
Wavelength	0.71073 Å	
Crystal system	Monoclinic	
Space group	P2(1)/n	
Unit cell dimensions	a = 12.348(1) Å	α= 90°.
	b = 14.135(1) Å	β= 96.816(4)°.
	c = 13.472(1) Å	γ= 90°.
Volume	2334.8(3) Å ³	
Z	4	
Density (calculated)	1.168 Mg/m ³	
Absorption coefficient	0.125 mm ⁻¹	
F(000)	864	
Crystal size	0.48 x 0.26 x 0.22 mm ³	
Theta range for data collection	2.10 to 27.50°.	
Index ranges	-16<=h<=16, -16<=k<=18, -17<=l<=17	
Reflections collected	20980	
Independent reflections	5355 [R(int) = 0.0410]	
Absorption correction	None	
Refinement method	Full-matrix least-squares on F ²	
Data / restraints / parameters	5346 / 0 / 396	
Goodness-of-fit on F ²	1.065	
Final R indices [I>2sigma(I)]	R1 = 0.0417, wR2 = 0.0995	
R indices (all data)	R1 = 0.0725, wR2 = 0.1244	
Largest diff. peak and hole	0.299 and -0.397 e.Å ⁻³	

Table 2. Atomic coordinates (x 10⁴) and equivalent isotropic displacement parameters (Å²x 10³) for 4b. U(eq) is defined as one third of the trace of the orthogonalized U^{ij} tensor.

	x	y	z	U(eq)
P(1)	5654(1)	1187(1)	7857(1)	20(1)
C(11)	4266(2)	1530(2)	7909(2)	30(1)
B(11)	3910(2)	4144(2)	6278(2)	25(1)
B(10)	3201(2)	3911(2)	7307(2)	26(1)
B(9)	4156(2)	4186(2)	8346(2)	27(1)
B(3)	4485(2)	5405(2)	8339(2)	45(1)
B(2)	5111(2)	5628(2)	7258(3)	57(1)
B(6)	4201(2)	5364(2)	6206(2)	43(1)
B(5)	2959(2)	4972(2)	6612(2)	23(1)
B(4)	3129(2)	5001(2)	7944(2)	24(1)
B(1)	3729(2)	5907(2)	7260(2)	29(1)
C(8)	5282(2)	4539(2)	7895(3)	66(1)
C(7)	5111(2)	4530(2)	6676(2)	54(1)
C(21)	6001(1)	1284(1)	6606(1)	21(1)
C(22)	6862(2)	741(1)	6323(1)	26(1)
C(23)	7200(2)	863(1)	5386(1)	30(1)
C(24)	6679(2)	1518(1)	4719(1)	31(1)
C(25)	5824(2)	2054(1)	4995(2)	33(1)
C(26)	5484(2)	1944(1)	5937(2)	29(1)
C(31)	6520(1)	1963(1)	8651(1)	21(1)
C(32)	6310(2)	2105(1)	9639(1)	29(1)
C(33)	6919(2)	2758(2)	10236(2)	32(1)
C(34)	7740(2)	3261(1)	9855(2)	31(1)
C(35)	7966(2)	3112(2)	8887(2)	32(1)
C(36)	7355(2)	2464(1)	8275(1)	26(1)
C(41)	5825(1)	-22(1)	8263(1)	21(1)
C(42)	6726(2)	-301(1)	8918(1)	27(1)
C(43)	6844(2)	-1249(2)	9197(2)	32(1)
C(44)	6078(2)	-1908(1)	8817(2)	31(1)
C(45)	5176(2)	-1635(1)	8161(2)	30(1)
C(46)	5044(2)	-690(1)	7885(2)	26(1)

Appendix A – Crystal Data

Table 3. Bond lengths [Å] and angles [°] for 4b.

P(1)-C(11)	1.790(2)	B(2)-B(6)	1.741(5)	C(25)-H(25)	0.98(2)
P(1)-C(31)	1.794(2)	B(2)-B(1)	1.753(3)	C(26)-H(26)	0.95(2)
P(1)-C(21)	1.794(2)	B(2)-C(8)	1.762(4)	C(31)-C(36)	1.395(2)
P(1)-C(41)	1.799(2)	B(2)-H(2)	1.09(3)	C(31)-C(32)	1.401(2)
C(11)-H(11C)	0.97(3)	B(6)-C(7)	1.699(4)	C(32)-C(33)	1.386(3)
C(11)-H(11B)	0.97(2)	B(6)-B(1)	1.772(3)	C(32)-H(32)	0.96(2)
C(11)-H(11A)	0.97(2)	B(6)-B(5)	1.778(3)	C(33)-C(34)	1.386(3)
B(11)-C(7)	1.612(3)	B(6)-H(6)	1.09(2)	C(33)-H(33)	0.99(2)
B(11)-B(5)	1.754(3)	B(5)-B(4)	1.782(3)	C(34)-C(35)	1.382(3)
B(11)-B(10)	1.756(3)	B(5)-B(1)	1.792(3)	C(34)-H(34)	0.96(2)
B(11)-B(6)	1.767(3)	B(5)-H(5)	1.11(2)	C(35)-C(36)	1.393(3)
B(11)-H(11)	0.94(2)	B(4)-B(1)	1.789(3)	C(35)-H(35)	1.01(2)
B(10)-B(9)	1.764(3)	B(4)-H(4)	1.14(2)	C(36)-H(36)	0.96(2)
B(10)-B(4)	1.771(3)	B(1)-H(1)	1.10(2)	C(41)-C(42)	1.393(3)
B(10)-B(5)	1.775(3)	C(8)-C(7)	1.630(4)	C(41)-C(46)	1.402(3)
B(10)-H(10A)	1.10(2)	C(8)-H(8)	1.09(4)	C(42)-C(43)	1.395(3)
B(9)-C(8)	1.658(4)	C(7)-H(7)	1.04(3)	C(42)-H(42)	0.98(2)
B(9)-B(4)	1.751(3)	C(21)-C(26)	1.397(3)	C(43)-C(44)	1.383(3)
B(9)-B(3)	1.770(3)	C(21)-C(22)	1.399(3)	C(43)-H(43)	0.95(2)
B(9)-H(9)	0.98(2)	C(22)-C(23)	1.388(3)	C(44)-C(45)	1.391(3)
B(3)-C(8)	1.721(4)	C(22)-H(22)	0.97(2)	C(44)-H(44)	0.93(3)
B(3)-B(2)	1.756(5)	C(23)-C(24)	1.394(3)	C(45)-C(46)	1.390(3)
B(3)-B(1)	1.780(4)	C(23)-H(23)	0.97(2)	C(45)-H(45)	0.99(2)
B(3)-B(4)	1.789(3)	C(24)-C(25)	1.387(3)	C(46)-H(46)	0.97(2)
B(3)-H(3)	1.09(3)	C(24)-H(24)	0.98(2)		
B(2)-C(7)	1.738(4)	C(25)-C(26)	1.392(3)		
C(11)-P(1)-C(31)	108.47(9)	B(3)-B(9)-H(9)	117.0(14)	C(7)-B(6)-H(6)	122.0(13)
C(11)-P(1)-C(21)	110.67(10)	C(8)-B(3)-B(2)	60.9(2)	B(2)-B(6)-H(6)	122.4(13)
C(31)-P(1)-C(21)	108.75(8)	C(8)-B(3)-B(9)	56.70(15)	B(11)-B(6)-H(6)	120.3(13)
C(11)-P(1)-C(41)	108.88(9)	B(2)-B(3)-B(9)	107.7(2)	B(1)-B(6)-H(6)	125.9(13)
C(31)-P(1)-C(41)	111.06(8)	C(8)-B(3)-B(1)	105.4(2)	B(5)-B(6)-H(6)	123.4(13)
C(21)-P(1)-C(41)	109.01(8)	B(2)-B(3)-B(1)	59.4(2)	B(11)-B(5)-B(10)	59.67(12)
P(1)-C(11)-H(11C)	108.0(14)	B(9)-B(3)-B(1)	107.1(2)	B(11)-B(5)-B(6)	60.03(12)
P(1)-C(11)-H(11B)	108.2(14)	C(8)-B(3)-B(4)	102.9(2)	B(10)-B(5)-B(6)	109.2(2)
H(11C)-C(11)-H(11B)	110.2(19)	B(2)-B(3)-B(4)	107.4(2)	B(11)-B(5)-B(4)	105.7(2)
P(1)-C(11)-H(11A)	109.3(14)	B(9)-B(3)-B(4)	58.94(13)	B(10)-B(5)-B(4)	59.74(12)
H(11C)-C(11)-H(11A)	113.0(20)	B(1)-B(3)-B(4)	60.17(13)	B(6)-B(5)-B(4)	107.4(2)
H(11B)-C(11)-H(11A)	108.0(19)	C(8)-B(3)-H(3)	122.8(14)	B(11)-B(5)-B(1)	106.50(15)
C(7)-B(11)-B(5)	107.9(2)	B(2)-B(3)-H(3)	122.3(14)	B(10)-B(5)-B(1)	108.7(2)
C(7)-B(11)-B(10)	109.0(2)	B(9)-B(3)-H(3)	120.2(14)	B(6)-B(5)-B(1)	59.52(14)
B(5)-B(11)-B(10)	60.73(12)	B(1)-B(3)-H(3)	125.0(14)	B(4)-B(5)-B(1)	60.05(12)
C(7)-B(11)-B(6)	60.2(2)	B(4)-B(3)-H(3)	123.6(14)	B(11)-B(5)-H(5)	119.7(11)
B(5)-B(11)-B(6)	60.65(12)	C(7)-B(2)-B(6)	58.5(2)	B(10)-B(5)-H(5)	119.9(11)
B(10)-B(11)-B(6)	110.5(2)	C(7)-B(2)-B(1)	104.7(2)	B(6)-B(5)-H(5)	120.0(11)
C(7)-B(11)-H(11)	121.4(14)	B(6)-B(2)-B(1)	60.96(15)	B(4)-B(5)-H(5)	125.6(11)
B(5)-B(11)-H(11)	119.6(14)	C(7)-B(2)-B(3)	103.7(2)	B(1)-B(5)-H(5)	124.6(11)
B(10)-B(11)-H(11)	122.9(14)	B(6)-B(2)-B(3)	109.4(2)	B(9)-B(4)-B(10)	60.08(12)
B(6)-B(11)-H(11)	116.6(14)	B(1)-B(2)-B(3)	61.0(2)	B(9)-B(4)-B(5)	106.92(15)
B(11)-B(10)-B(9)	103.7(2)	C(7)-B(2)-C(8)	55.5(2)	B(10)-B(4)-B(5)	59.91(12)
B(11)-B(10)-B(4)	106.13(15)	B(6)-B(2)-C(8)	103.8(2)	B(9)-B(4)-B(3)	60.01(13)
B(9)-B(10)-B(4)	59.38(12)	B(1)-B(2)-C(8)	104.8(2)	B(10)-B(4)-B(3)	108.8(2)
B(11)-B(10)-B(5)	59.60(12)	B(3)-B(2)-C(8)	58.6(2)	B(5)-B(4)-B(3)	107.5(2)
B(9)-B(10)-B(5)	106.71(15)	C(7)-B(2)-H(2)	118.8(15)	B(9)-B(4)-B(1)	107.6(2)
B(4)-B(10)-B(5)	60.34(12)	B(6)-B(2)-H(2)	121.9(15)	B(10)-B(4)-B(1)	109.0(2)
B(11)-B(10)-H(10A)	123.8(11)	B(1)-B(2)-H(2)	129.4(15)	B(5)-B(4)-B(1)	60.26(12)
B(9)-B(10)-H(10A)	126.3(11)	B(3)-B(2)-H(2)	124.9(15)	B(3)-B(4)-B(1)	59.67(14)
B(4)-B(10)-H(10A)	119.7(12)	C(8)-B(2)-H(2)	120.3(15)	B(9)-B(4)-H(4)	120.5(11)
B(5)-B(10)-H(10A)	117.6(12)	C(7)-B(6)-B(2)	60.7(2)	B(10)-B(4)-H(4)	120.7(11)
C(8)-B(9)-B(4)	107.2(2)	C(7)-B(6)-B(11)	55.38(13)	B(5)-B(4)-H(4)	123.9(11)
C(8)-B(9)-B(10)	106.6(2)	B(2)-B(6)-B(11)	106.2(2)	B(3)-B(4)-H(4)	120.8(11)
B(4)-B(9)-B(10)	60.53(12)	C(7)-B(6)-B(1)	105.5(2)	B(1)-B(4)-H(4)	122.8(11)
C(8)-B(9)-B(3)	60.1(2)	B(2)-B(6)-B(1)	59.8(2)	B(2)-B(1)-B(6)	59.2(2)
B(4)-B(9)-B(3)	61.05(13)	B(11)-B(6)-B(1)	106.8(2)	B(2)-B(1)-B(3)	59.6(2)
B(10)-B(9)-B(3)	110.0(2)	C(7)-B(6)-B(5)	103.0(2)	B(6)-B(1)-B(3)	106.9(2)
C(8)-B(9)-H(9)	118.7(14)	B(2)-B(6)-B(5)	108.2(2)	B(2)-B(1)-B(4)	107.6(2)
B(4)-B(9)-H(9)	124.0(14)	B(11)-B(6)-B(5)	59.32(12)	B(6)-B(1)-B(4)	107.4(2)
B(10)-B(9)-H(9)	126.0(14)	B(1)-B(6)-B(5)	60.64(13)	B(3)-B(1)-B(4)	60.16(14)

Appendix A – Crystal Data

B(2)-B(1)-B(5)	107.1(2)	B(2)-C(7)-H(7)	116.3(17)	C(35)-C(34)-C(33)	120.6(2)
B(6)-B(1)-B(5)	59.85(13)	C(26)-C(21)-C(22)	119.6(2)	C(35)-C(34)-H(34)	118.9(13)
B(3)-B(1)-B(5)	107.5(2)	C(26)-C(21)-P(1)	120.98(14)	C(33)-C(34)-H(34)	120.4(13)
B(4)-B(1)-B(5)	59.69(12)	C(22)-C(21)-P(1)	119.19(14)	C(34)-C(35)-C(36)	120.2(2)
B(2)-B(1)-H(1)	122.6(11)	C(23)-C(22)-C(21)	120.0(2)	C(34)-C(35)-H(35)	118.7(13)
B(6)-B(1)-H(1)	122.7(11)	C(23)-C(22)-H(22)	119.8(12)	C(36)-C(35)-H(35)	121.1(13)
B(3)-B(1)-H(1)	122.0(11)	C(21)-C(22)-H(22)	120.2(12)	C(35)-C(36)-C(31)	119.4(2)
B(4)-B(1)-H(1)	121.4(11)	C(22)-C(23)-C(24)	120.2(2)	C(35)-C(36)-H(36)	121.7(12)
B(5)-B(1)-H(1)	121.9(11)	C(22)-C(23)-H(23)	119.8(13)	C(31)-C(36)-H(36)	118.9(12)
C(7)-C(8)-B(9)	110.7(2)	C(24)-C(23)-H(23)	120.0(13)	C(42)-C(41)-C(46)	120.2(2)
C(7)-C(8)-B(3)	110.1(2)	C(25)-C(24)-C(23)	119.9(2)	C(42)-C(41)-P(1)	121.15(14)
B(9)-C(8)-B(3)	63.2(2)	C(25)-C(24)-H(24)	119.4(13)	C(46)-C(41)-P(1)	118.61(14)
C(7)-C(8)-B(2)	61.5(2)	C(23)-C(24)-H(24)	120.8(13)	C(41)-C(42)-C(43)	119.5(2)
B(9)-C(8)-B(2)	112.6(2)	C(24)-C(25)-C(26)	120.4(2)	C(41)-C(42)-H(42)	122.5(13)
B(3)-C(8)-B(2)	60.5(2)	C(24)-C(25)-H(25)	118.7(13)	C(43)-C(42)-H(42)	118.0(13)
C(7)-C(8)-H(8)	116.9(18)	C(26)-C(25)-H(25)	120.9(13)	C(44)-C(43)-C(42)	120.2(2)
B(9)-C(8)-H(8)	124.4(18)	C(25)-C(26)-C(21)	119.9(2)	C(44)-C(43)-H(43)	119.6(15)
B(3)-C(8)-H(8)	120.1(18)	C(25)-C(26)-H(26)	120.4(13)	C(42)-C(43)-H(43)	120.2(15)
B(2)-C(8)-H(8)	114.3(18)	C(21)-C(26)-H(26)	119.7(13)	C(43)-C(44)-C(45)	120.6(2)
B(11)-C(7)-C(8)	110.0(2)	C(36)-C(31)-C(32)	120.0(2)	C(43)-C(44)-H(44)	119.9(15)
B(11)-C(7)-B(6)	64.5(2)	C(36)-C(31)-P(1)	120.53(13)	C(45)-C(44)-H(44)	119.4(15)
C(8)-C(7)-B(6)	111.8(2)	C(32)-C(31)-P(1)	119.33(14)	C(46)-C(45)-C(44)	119.7(2)
B(11)-C(7)-B(2)	113.8(2)	C(33)-C(32)-C(31)	119.9(2)	C(46)-C(45)-H(45)	121.5(13)
C(8)-C(7)-B(2)	63.0(2)	C(33)-C(32)-H(32)	119.8(13)	C(44)-C(45)-H(45)	118.8(13)
B(6)-C(7)-B(2)	60.9(2)	C(31)-C(32)-H(32)	120.3(13)	C(45)-C(46)-C(41)	119.8(2)
B(11)-C(7)-H(7)	118.9(17)	C(34)-C(33)-C(32)	119.8(2)	C(45)-C(46)-H(46)	120.7(13)
C(8)-C(7)-H(7)	122.7(17)	C(34)-C(33)-H(33)	120.8(13)	C(41)-C(46)-H(46)	119.6(13)
B(6)-C(7)-H(7)	115.0(17)	C(32)-C(33)-H(33)	119.3(14)		

Symmetry transformations used to generate equivalent atoms:

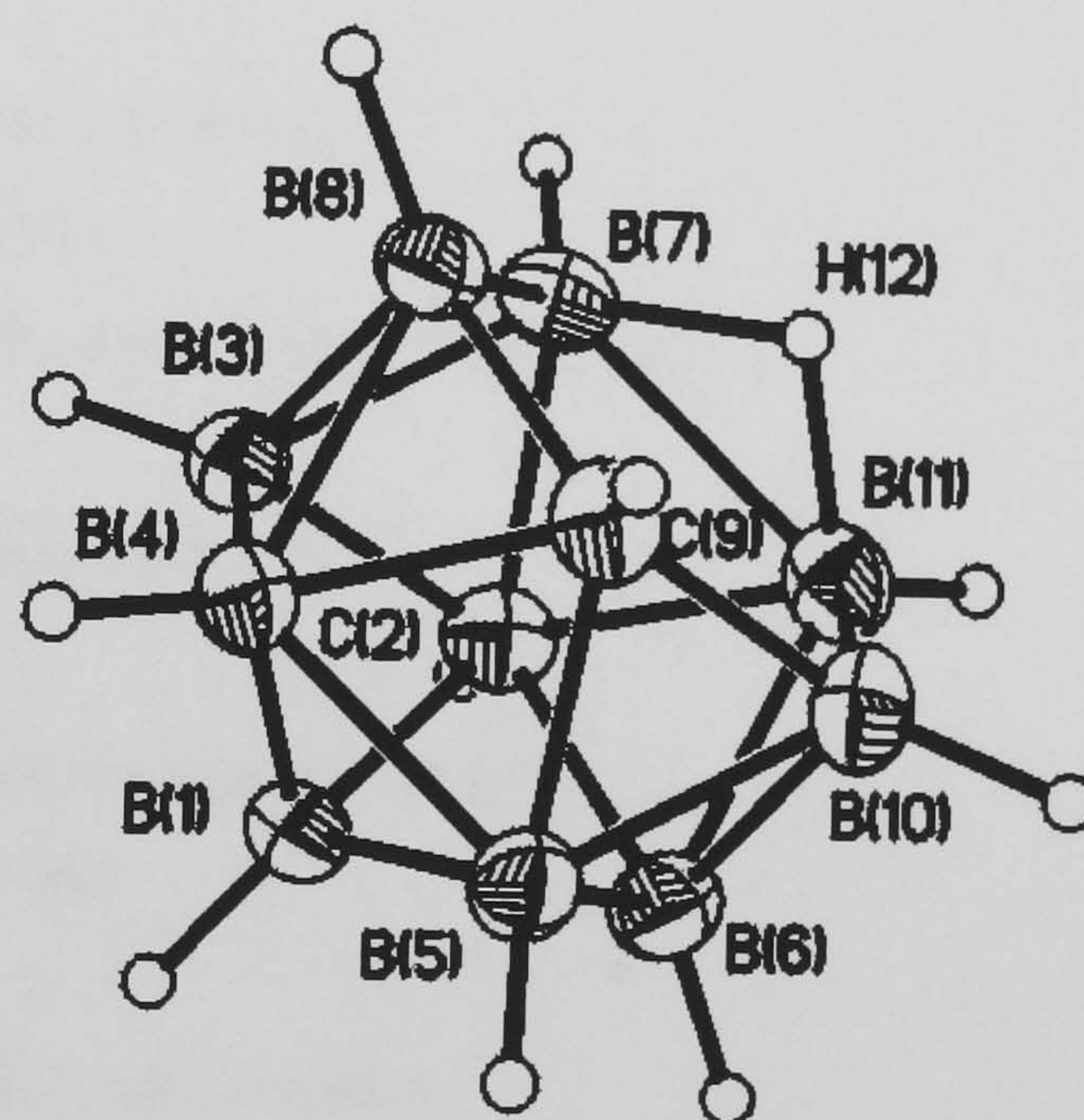
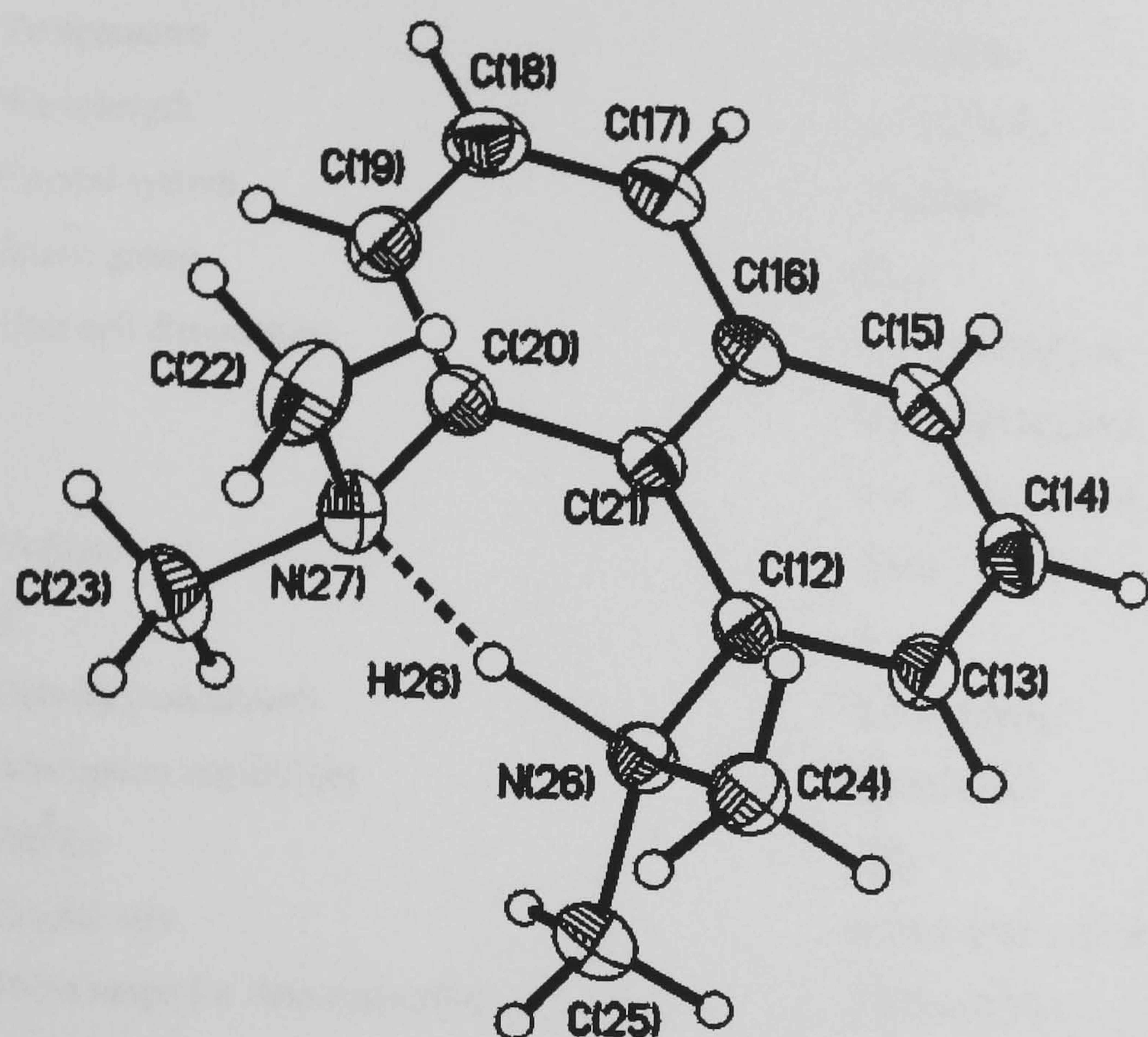
Table 4. Anisotropic displacement parameters ($\text{\AA}^2 \times 10^3$) for 4b. The anisotropic displacement factor exponent takes the form: $-2\pi^2[h^2 a^{*2}U^{11} + \dots + 2 h k a^* b^* U^{12}]$

	U ¹¹	U ²²	U ³³	U ²³	U ¹³	U ¹²
P(1)	17(1)	16(1)	28(1)	-1(1)	4(1)	0(1)
C(11)	19(1)	20(1)	52(1)	-1(1)	7(1)	1(1)
B(11)	25(1)	17(1)	34(1)	-5(1)	6(1)	2(1)
B(10)	26(1)	17(1)	34(1)	1(1)	3(1)	0(1)
B(9)	33(1)	20(1)	25(1)	4(1)	-4(1)	4(1)
B(3)	39(1)	23(1)	66(2)	-8(1)	-28(1)	2(1)
B(2)	24(1)	23(1)	127(3)	-4(2)	13(2)	-6(1)
B(6)	47(2)	23(1)	66(2)	3(1)	37(1)	3(1)
B(5)	25(1)	20(1)	26(1)	-1(1)	6(1)	2(1)
B(4)	26(1)	20(1)	25(1)	1(1)	-3(1)	2(1)
B(1)	26(1)	17(1)	45(1)	-1(1)	6(1)	1(1)
C(8)	41(1)	32(1)	115(3)	-2(2)	-29(2)	7(1)
C(7)	46(1)	29(1)	94(2)	-10(1)	41(1)	0(1)
C(21)	20(1)	17(1)	26(1)	-3(1)	-1(1)	-3(1)
C(22)	30(1)	22(1)	24(1)	-1(1)	0(1)	5(1)
C(23)	36(1)	28(1)	26(1)	-4(1)	5(1)	3(1)
C(24)	43(1)	27(1)	22(1)	-2(1)	0(1)	-7(1)
C(25)	39(1)	24(1)	32(1)	8(1)	-6(1)	-2(1)
C(26)	28(1)	21(1)	36(1)	3(1)	0(1)	2(1)
C(31)	21(1)	16(1)	26(1)	-2(1)	4(1)	0(1)
C(32)	33(1)	28(1)	29(1)	1(1)	11(1)	-1(1)
C(33)	41(1)	31(1)	24(1)	-4(1)	3(1)	4(1)
C(34)	35(1)	24(1)	32(1)	-5(1)	-7(1)	-1(1)
C(35)	29(1)	30(1)	36(1)	-2(1)	2(1)	-9(1)
C(36)	26(1)	27(1)	25(1)	-2(1)	6(1)	-4(1)
C(41)	22(1)	17(1)	25(1)	1(1)	8(1)	2(1)
C(42)	27(1)	24(1)	29(1)	-1(1)	2(1)	4(1)
C(43)	38(1)	29(1)	29(1)	4(1)	2(1)	12(1)
C(44)	42(1)	18(1)	35(1)	5(1)	16(1)	8(1)
C(45)	33(1)	19(1)	40(1)	-1(1)	11(1)	-1(1)
C(46)	23(1)	20(1)	36(1)	1(1)	3(1)	0(1)

Table 5. Hydrogen coordinates (x 10⁴) and isotropic displacement parameters (Å²x 10³) for 4b.

	x	y	z	U(eq)
H(11C)	4196(19)	2190(19)	7725(17)	47(7)
H(11B)	4099(19)	1441(17)	8592(18)	44(7)
H(11A)	3786(19)	1119(17)	7474(17)	40(6)
H(11)	3772(18)	3819(16)	5670(17)	41(6)
H(10A)	2527(18)	3404(16)	7292(16)	39(6)
H(9)	4223(18)	3870(16)	8996(17)	42(6)
H(3)	4719(21)	5779(19)	9043(19)	59(8)
H(2)	5808(24)	6099(21)	7222(20)	74(9)
H(6)	4250(20)	5700(18)	5481(18)	53(7)
H(5)	2176(17)	5072(15)	6126(15)	33(6)
H(4)	2439(18)	5146(15)	8416(15)	35(6)
H(1)	3429(17)	6638(15)	7249(15)	32(6)
H(8)	6108(29)	4413(24)	8260(25)	101(11)
H(7)	5745(25)	4404(22)	6252(22)	79(9)
H(22)	7238(16)	290(14)	6790(15)	25(5)
H(23)	7797(18)	483(16)	5191(16)	37(6)
H(24)	6912(17)	1608(16)	4056(16)	34(6)
H(25)	5479(19)	2519(17)	4525(17)	42(6)
H(26)	4913(19)	2323(16)	6134(16)	38(6)
H(32)	5749(18)	1746(16)	9908(15)	36(6)
H(33)	6763(19)	2855(16)	10935(17)	42(6)
H(34)	8147(18)	3734(17)	10255(16)	39(6)
H(35)	8574(19)	3485(17)	8635(16)	43(6)
H(36)	7492(16)	2353(14)	7594(15)	27(5)
H(42)	7285(18)	146(16)	9200(15)	32(6)
H(43)	7456(20)	-1447(17)	9640(17)	47(7)
H(44)	6166(19)	-2539(19)	8993(17)	47(7)
H(45)	4641(19)	-2121(16)	7903(16)	38(6)
H(46)	4411(18)	-487(15)	7443(15)	31(6)

A3 Crystal data for $[1,8-(N(CH_3)_2)(NH(CH_3)_2C_{10}H_8)][2,9-C_2B_9H_{12}]$; (6a).



Appendix A – Crystal Data

Table 1. Crystal data and structure refinement for 6a.

Identification code	99srv093	
Empirical formula	C16 H31 B9 N2	
Formula weight	348.72	
Temperature	293(2) K	
Wavelength	0.71073 Å	
Crystal system	Triclinic	
Space group	P –1	
Unit cell dimensions	a = 8.4571(2) Å	α= 68.4460(10)°.
	b = 10.3180(3) Å	β= 84.6840(10)°.
	c = 12.9440(3) Å	γ = 76.9740(10)°.
Volume	1023.42(5) Å ³	
Z	2	
Density (calculated)	1.132 Mg/m ³	
Absorption coefficient	0.059 mm ⁻¹	
F(000)	372	
Crystal size	0.10 x 0.44 x 0.78 mm ³	
Theta range for data collection	1.69 to 23.25°.	
Index ranges	-9<=h<=9, -11<=k<=11, -14<=l<=14	
Reflections collected	8405	
Independent reflections	2946 [R(int) = 0.0317]	
Completeness to theta = 23.25°	99.9 %	
Refinement method	Full-matrix least-squares on F ²	
Data / restraints / parameters	2946 / 0 / 368	
Goodness-of-fit on F ²	1.027	
Final R indices [I>2sigma(I)]	R1 = 0.0341, wR2 = 0.0874	
R indices (all data)	R1 = 0.0416, wR2 = 0.0925	
Largest diff. peak and hole	0.149 and -0.180 e.Å ⁻³	

Appendix A – Crystal Data

Table 2. Atomic coordinates (x 10⁴) and equivalent isotropic displacement parameters (Å²x 10³) for 6a. U(eq) is defined as one third of the trace of the orthogonalized U^{ij} tensor.

	x	y	z	U(eq)
B(1)	-2063(2)	-734(2)	3073(1)	28(1)
C(2)	-1427(2)	-838(2)	1800(1)	28(1)
B(3)	-161(2)	-343(2)	2514(1)	27(1)
B(4)	-274(2)	-1441(2)	3890(1)	28(1)
B(5)	-1705(2)	-2531(2)	3993(1)	28(1)
B(6)	-2471(2)	-2104(2)	2686(1)	28(1)
B(7)	619(2)	-1357(2)	1648(1)	30(1)
B(8)	1334(2)	-1896(2)	3017(1)	27(1)
C(9)	337(2)	-3109(2)	3811(1)	27(1)
B(10)	-895(2)	-3601(2)	3186(1)	30(1)
B(11)	-877(2)	-2520(2)	1764(1)	31(1)
C(12)	4003(2)	2272(1)	1936(1)	22(1)
C(13)	3532(2)	1599(2)	1320(1)	28(1)
C(14)	4312(2)	1651(2)	300(1)	30(1)
C(15)	5536(2)	2378(2)	-79(1)	29(1)
C(16)	6058(2)	3085(1)	539(1)	25(1)
C(17)	7327(2)	3847(2)	141(1)	31(1)
C(18)	7808(2)	4551(2)	726(1)	34(1)
C(19)	7079(2)	4491(2)	1761(1)	30(1)
C(20)	5873(2)	3749(1)	2188(1)	23(1)
C(21)	5287(2)	3038(1)	1583(1)	22(1)
C(22)	6363(2)	2831(2)	4186(1)	38(1)
C(23)	4382(2)	5045(2)	3356(1)	37(1)
C(24)	3231(2)	759(2)	3810(1)	28(1)
C(25)	1462(2)	3076(2)	2826(1)	32(1)
N(26)	3167(1)	2235(1)	2997(1)	24(1)
N(27)	5161(1)	3636(1)	3290(1)	26(1)

Table 3. Bond lengths [Å] and angles [°] for 6a.

B(1)-C(2)	1.719(2)	B(6)-H(6)	1.118(15)	C(17)-H(17)	0.972(16)
B(1)-B(3)	1.771(2)	B(7)-B(8)	1.772(2)	C(18)-C(19)	1.408(2)
B(1)-B(5)	1.772(2)	B(7)-B(11)	1.891(2)	C(18)-H(18)	0.979(17)
B(1)-B(6)	1.773(2)	B(7)-H(7)	1.084(15)	C(19)-C(20)	1.367(2)
B(1)-B(4)	1.780(2)	B(7)-H(12)	1.293(17)	C(19)-H(19)	0.943(16)
B(1)-H(1)	1.092(15)	B(8)-C(9)	1.644(2)	C(20)-C(21)	1.4330(18)
C(2)-B(7)	1.707(2)	B(8)-H(8)	1.113(14)	C(20)-N(27)	1.4695(17)
C(2)-B(11)	1.709(2)	C(9)-B(10)	1.642(2)	C(22)-N(27)	1.4830(19)
C(2)-B(6)	1.742(2)	C(9)-H(9)	0.984(16)	C(22)-H(22A)	1.001(18)
C(2)-B(3)	1.743(2)	B(10)-B(11)	1.768(2)	C(22)-H(22B)	1.006(17)
C(2)-H(2)	0.992(17)	B(10)-H(10)	1.127(16)	C(22)-H(22C)	1.009(18)
B(3)-B(4)	1.732(2)	B(11)-H(11)	1.094(15)	C(23)-N(27)	1.4848(19)
B(3)-B(8)	1.750(2)	B(11)-H(12)	1.261(16)	C(23)-H(23A)	1.009(17)
B(3)-B(7)	1.790(2)	C(12)-C(13)	1.3663(19)	C(23)-H(23B)	0.985(17)
B(3)-H(3)	1.080(16)	C(12)-C(21)	1.4295(19)	C(23)-H(23C)	0.987(18)
B(4)-C(9)	1.720(2)	C(12)-N(26)	1.4772(16)	C(24)-N(26)	1.4919(18)
B(4)-B(8)	1.780(2)	C(13)-C(14)	1.409(2)	C(24)-H(24A)	0.990(17)
B(4)-B(5)	1.794(2)	C(13)-H(13)	0.958(16)	C(24)-H(24B)	0.988(17)
B(4)-H(4)	1.114(15)	C(14)-C(15)	1.364(2)	C(24)-H(24C)	0.975(17)
B(5)-C(9)	1.719(2)	C(14)-H(14)	0.978(16)	C(25)-N(26)	1.4950(18)
B(5)-B(6)	1.733(2)	C(15)-C(16)	1.417(2)	C(25)-H(25A)	0.998(17)
B(5)-B(10)	1.776(2)	C(15)-H(15)	0.947(16)	C(25)-H(25B)	0.992(16)
B(5)-H(5)	1.100(15)	C(16)-C(17)	1.420(2)	C(25)-H(25C)	0.998(17)
B(6)-B(10)	1.755(2)	C(16)-C(21)	1.4344(18)	N(26)-H(26)	1.212(18)
B(6)-B(11)	1.801(2)	C(17)-C(18)	1.364(2)	N(27)-H(26)	1.415(18)
C(2)-B(1)-B(3)	59.91(9)	C(9)-B(4)-B(3)	102.14(11)	C(2)-B(7)-B(8)	102.77(11)
C(2)-B(1)-B(5)	104.11(11)	C(9)-B(4)-B(8)	56.02(9)	C(2)-B(7)-B(3)	59.74(9)
B(3)-B(1)-B(5)	107.45(11)	B(3)-B(4)-B(8)	59.78(9)	B(8)-B(7)-B(3)	58.87(9)
C(2)-B(1)-B(6)	59.81(9)	C(9)-B(4)-B(1)	102.31(11)	C(2)-B(7)-B(11)	56.41(8)
B(3)-B(1)-B(6)	109.69(11)	B(3)-B(4)-B(1)	60.53(9)	B(8)-B(7)-B(11)	104.63(11)
B(5)-B(1)-B(6)	58.54(9)	B(8)-B(4)-B(1)	106.81(11)	B(3)-B(7)-B(11)	106.27(10)
C(2)-B(1)-B(4)	104.26(10)	C(9)-B(4)-B(5)	58.53(9)	C(2)-B(7)-H(7)	115.0(8)
B(3)-B(1)-B(4)	58.38(9)	B(3)-B(4)-B(5)	108.18(11)	B(8)-B(7)-H(7)	131.7(8)
B(5)-B(1)-B(4)	60.67(9)	B(8)-B(4)-B(5)	106.31(11)	B(3)-B(7)-H(7)	116.6(8)
B(6)-B(1)-B(4)	107.80(11)	B(1)-B(4)-B(5)	59.44(9)	B(11)-B(7)-H(7)	120.8(8)
C(2)-B(1)-H(1)	118.6(8)	C(9)-B(4)-H(4)	124.1(8)	C(2)-B(7)-H(12)	96.5(7)
B(3)-B(1)-H(1)	119.4(8)	B(3)-B(4)-H(4)	126.1(8)	B(8)-B(7)-H(12)	86.1(7)
B(5)-B(1)-H(1)	127.5(8)	B(8)-B(4)-H(4)	123.9(7)	B(3)-B(7)-H(12)	126.8(7)
B(6)-B(1)-H(1)	118.9(7)	B(1)-B(4)-H(4)	124.0(8)	B(11)-B(7)-H(12)	41.6(7)
B(4)-B(1)-H(1)	127.6(7)	B(5)-B(4)-H(4)	118.5(8)	H(7)-B(7)-H(12)	116.6(11)
B(7)-C(2)-B(11)	67.23(10)	C(9)-B(5)-B(6)	102.57(11)	C(9)-B(8)-B(3)	104.50(11)
B(7)-C(2)-B(1)	115.53(11)	C(9)-B(5)-B(1)	102.67(11)	C(9)-B(8)-B(7)	106.72(11)
B(11)-C(2)-B(1)	115.64(11)	B(6)-B(5)-B(1)	60.74(9)	B(3)-B(8)-B(7)	61.09(9)
B(7)-C(2)-B(6)	117.85(11)	C(9)-B(5)-B(10)	56.01(8)	C(9)-B(8)-B(4)	60.15(9)
B(11)-C(2)-B(6)	62.93(9)	B(6)-B(5)-B(10)	59.98(9)	B(3)-B(8)-B(4)	58.75(9)
B(1)-C(2)-B(6)	61.61(9)	B(1)-B(5)-B(10)	107.06(11)	B(7)-B(8)-B(4)	109.82(11)
B(7)-C(2)-B(3)	62.49(9)	C(9)-B(5)-B(4)	58.57(8)	C(9)-B(8)-H(8)	121.5(8)
B(11)-C(2)-B(3)	117.16(11)	B(6)-B(5)-B(4)	108.93(11)	B(3)-B(8)-H(8)	123.5(8)
B(1)-C(2)-B(3)	61.50(9)	B(1)-B(5)-B(4)	59.88(9)	B(7)-B(8)-H(8)	124.1(7)
B(6)-C(2)-B(3)	112.47(11)	B(10)-B(5)-B(4)	106.50(11)	B(4)-B(8)-H(8)	117.5(7)
B(7)-C(2)-H(2)	117.3(9)	C(9)-B(5)-H(5)	125.6(8)	B(10)-C(9)-B(8)	116.78(12)
B(11)-C(2)-H(2)	118.6(9)	B(6)-B(5)-H(5)	123.2(8)	B(10)-C(9)-B(5)	63.74(9)
B(1)-C(2)-H(2)	114.5(9)	B(1)-B(5)-H(5)	123.6(8)	B(8)-C(9)-B(5)	116.49(11)
B(6)-C(2)-H(2)	118.0(9)	B(10)-B(5)-H(5)	122.7(8)	B(10)-C(9)-B(4)	116.62(11)
B(3)-C(2)-H(2)	116.6(9)	B(4)-B(5)-H(5)	120.4(8)	B(8)-C(9)-B(4)	63.83(9)
B(4)-B(3)-C(2)	105.32(11)	B(5)-B(6)-C(2)	104.84(11)	B(5)-C(9)-B(4)	62.90(9)
B(4)-B(3)-B(8)	61.47(9)	B(5)-B(6)-B(10)	61.22(9)	B(10)-C(9)-H(9)	117.6(9)
C(2)-B(3)-B(8)	102.19(11)	C(2)-B(6)-B(10)	101.79(11)	B(8)-C(9)-H(9)	117.4(9)
B(4)-B(3)-B(1)	61.09(9)	B(5)-B(6)-B(1)	60.72(9)	B(5)-C(9)-H(9)	113.7(9)
C(2)-B(3)-B(1)	58.59(8)	C(2)-B(6)-B(1)	58.58(8)	B(4)-C(9)-H(9)	113.4(9)
B(8)-B(3)-B(1)	108.53(12)	B(10)-B(6)-B(1)	107.99(11)	C(9)-B(10)-B(6)	104.91(11)
B(4)-B(3)-B(7)	111.19(12)	B(5)-B(6)-B(11)	110.36(11)	C(9)-B(10)-B(11)	106.62(12)
C(2)-B(3)-B(7)	57.77(8)	C(2)-B(6)-B(11)	57.64(9)	B(6)-B(10)-B(11)	61.50(9)
B(8)-B(3)-B(7)	60.04(9)	B(10)-B(6)-B(11)	59.61(9)	C(9)-B(10)-B(5)	60.24(9)
B(1)-B(3)-B(7)	108.99(11)	B(1)-B(6)-B(11)	108.56(11)	B(6)-B(10)-B(5)	58.80(9)
B(4)-B(3)-H(3)	128.5(8)	B(5)-B(6)-H(6)	128.5(7)	B(11)-B(10)-B(5)	109.93(12)
C(2)-B(3)-H(3)	116.8(8)	C(2)-B(6)-H(6)	116.8(8)	C(9)-B(10)-H(10)	121.2(8)
B(8)-B(3)-H(3)	129.6(8)	B(10)-B(6)-H(6)	130.5(8)	B(6)-B(10)-H(10)	121.9(8)
B(1)-B(3)-H(3)	118.4(8)	B(11)-B(6)-H(6)	118.0(8)	B(11)-B(10)-H(10)	125.5(8)
B(7)-B(3)-H(3)	115.7(8)	B(11)-B(6)-H(6)	116.8(7)	B(5)-B(10)-H(10)	115.5(8)

Appendix A – Crystal Data

C(2)-B(11)-B(10)	102.57(11)	C(15)-C(16)-C(17)	121.20(13)	N(27)-C(23)-H(23C)	110.6(10)
C(2)-B(11)-B(6)	59.43(9)	C(15)-C(16)-C(21)	119.55(12)	H(23A)-C(23)-H(23C)	111.7(14)
B(10)-B(11)-B(6)	58.89(9)	C(17)-C(16)-C(21)	119.24(12)	H(23B)-C(23)-H(23C)	108.8(13)
C(2)-B(11)-B(7)	56.35(8)	C(18)-C(17)-C(16)	121.19(13)	N(26)-C(24)-H(24A)	107.3(9)
B(10)-B(11)-B(7)	105.08(11)	C(18)-C(17)-H(17)	121.0(9)	N(26)-C(24)-H(24B)	110.1(9)
B(6)-B(11)-B(7)	106.25(11)	C(16)-C(17)-H(17)	117.8(9)	H(24A)-C(24)-H(24B)	110.7(12)
C(2)-B(11)-H(11)	114.8(8)	C(17)-C(18)-C(19)	120.01(14)	N(26)-C(24)-H(24C)	109.0(9)
B(10)-B(11)-H(11)	133.3(8)	C(17)-C(18)-H(18)	122.2(9)	H(24A)-C(24)-H(24C)	109.6(13)
B(6)-B(11)-H(11)	118.5(8)	C(19)-C(18)-H(18)	117.7(9)	H(24B)-C(24)-H(24C)	110.2(12)
B(7)-B(11)-H(11)	118.3(8)	C(20)-C(19)-C(18)	120.89(14)	N(26)-C(25)-H(25A)	108.4(9)
C(2)-B(11)-H(12)	97.7(8)	C(20)-C(19)-H(19)	120.1(9)	N(26)-C(25)-H(25B)	107.0(9)
B(10)-B(11)-H(12)	86.2(7)	C(18)-C(19)-H(19)	119.0(9)	H(25A)-C(25)-H(25B)	112.1(13)
B(6)-B(11)-H(12)	127.6(7)	C(19)-C(20)-C(21)	121.01(12)	N(26)-C(25)-H(25C)	109.6(9)
B(7)-B(11)-H(12)	42.9(8)	C(19)-C(20)-N(27)	120.88(12)	H(25A)-C(25)-H(25C)	109.9(13)
H(11)-B(11)-H(12)	113.8(11)	C(21)-C(20)-N(27)	118.10(11)	H(25B)-C(25)-H(25C)	109.8(13)
C(13)-C(12)-C(21)	122.07(12)	C(12)-C(21)-C(20)	125.55(12)	C(12)-N(26)-C(24)	113.00(10)
C(13)-C(12)-N(26)	120.09(12)	C(12)-C(21)-C(16)	116.86(12)	C(12)-N(26)-C(25)	112.00(10)
C(21)-C(12)-N(26)	117.84(11)	C(20)-C(21)-C(16)	117.58(12)	C(24)-N(26)-C(25)	111.29(11)
C(12)-C(13)-C(14)	120.13(14)	N(27)-C(22)-H(22A)	110.7(10)	C(12)-N(26)-H(26)	99.8(8)
C(12)-C(13)-H(13)	120.4(9)	N(27)-C(22)-H(22B)	108.8(9)	C(24)-N(26)-H(26)	110.4(9)
C(14)-C(13)-H(13)	119.4(9)	H(22A)-C(22)-H(22B)	110.7(13)	C(25)-N(26)-H(26)	109.8(9)
C(15)-C(14)-C(13)	120.16(13)	N(27)-C(22)-H(22C)	108.6(9)	C(20)-N(27)-C(22)	111.82(11)
C(15)-C(14)-H(14)	120.0(9)	H(22A)-C(22)-H(22C)	108.8(13)	C(20)-N(27)-C(23)	112.54(11)
C(13)-C(14)-H(14)	119.8(9)	H(22B)-C(22)-H(22C)	109.2(13)	C(22)-N(27)-C(23)	111.03(12)
C(14)-C(15)-C(16)	121.22(13)	N(27)-C(23)-H(23A)	107.6(9)	C(20)-N(27)-H(26)	98.4(7)
C(14)-C(15)-H(15)	120.2(9)	N(27)-C(23)-H(23B)	107.2(9)	C(22)-N(27)-H(26)	111.1(7)
C(16)-C(15)-H(15)	118.5(9)	H(23A)-C(23)-H(23B)	110.8(13)	C(23)-N(27)-H(26)	111.4(7)

Symmetry transformations used to generate equivalent atoms:

Appendix A – Crystal Data

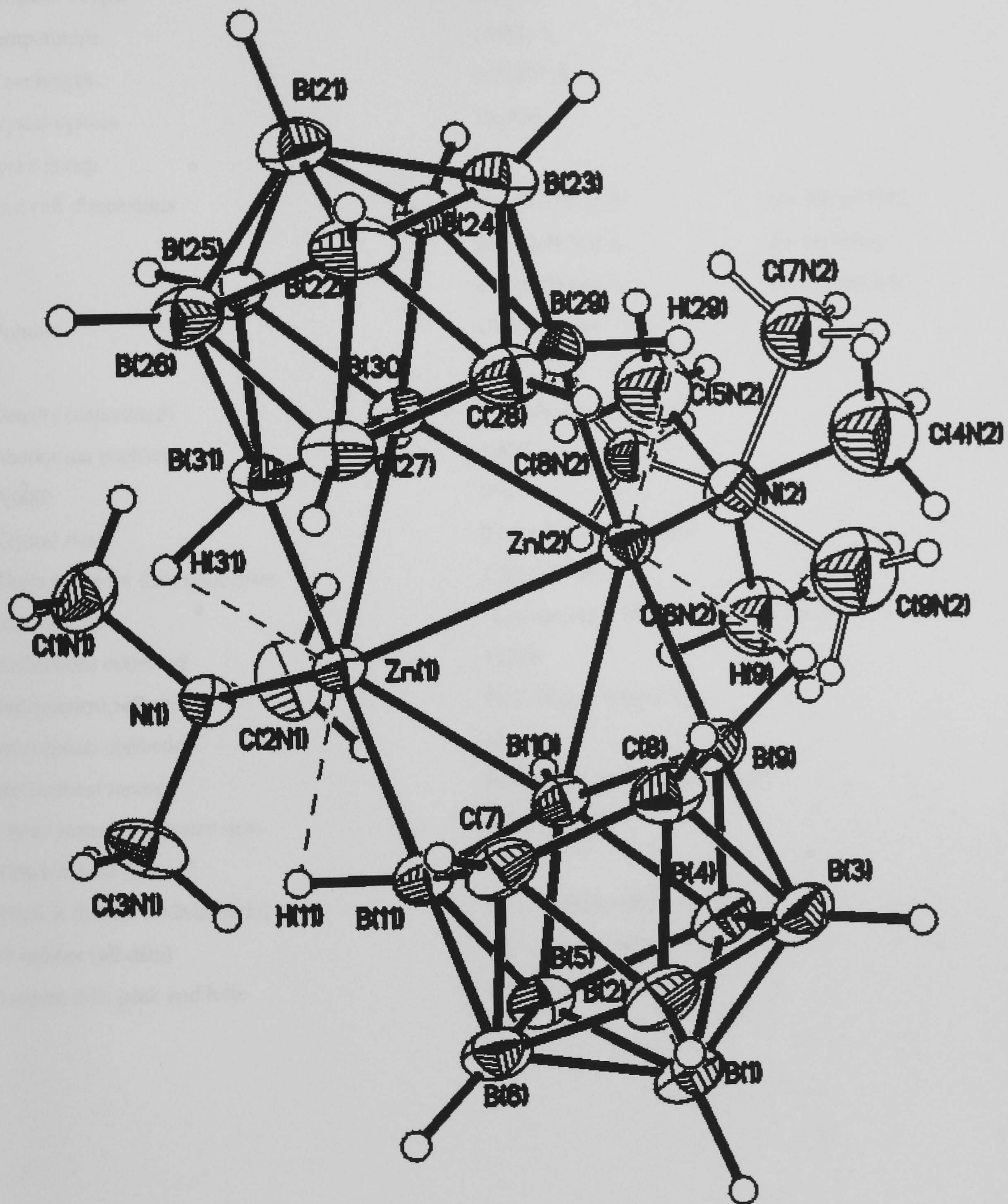
Table 4. Anisotropic displacement parameters ($\text{\AA}^2 \times 10^3$) for 6a. The anisotropic displacement factor exponent takes the form: $-2\pi^2[h^2 a^{*2}U^{11} + \dots + 2 h k a^* b^* U^{12}]$

	U ¹¹	U ²²	U ³³	U ²³	U ¹³	U ¹²
B(1)	24(1)	27(1)	35(1)	-14(1)	4(1)	-4(1)
C(2)	26(1)	28(1)	25(1)	-5(1)	-3(1)	-3(1)
B(3)	25(1)	23(1)	33(1)	-10(1)	3(1)	-6(1)
B(4)	29(1)	30(1)	29(1)	-15(1)	3(1)	-8(1)
B(5)	30(1)	29(1)	26(1)	-10(1)	4(1)	-10(1)
B(6)	26(1)	29(1)	31(1)	-10(1)	-1(1)	-7(1)
B(7)	27(1)	35(1)	26(1)	-11(1)	4(1)	-5(1)
B(8)	22(1)	30(1)	30(1)	-14(1)	0(1)	-3(1)
C(9)	30(1)	25(1)	24(1)	-6(1)	-5(1)	-2(1)
B(10)	34(1)	24(1)	32(1)	-11(1)	-4(1)	-6(1)
B(11)	32(1)	35(1)	29(1)	-16(1)	-4(1)	-4(1)
C(12)	23(1)	21(1)	22(1)	-7(1)	-2(1)	-1(1)
C(13)	28(1)	28(1)	32(1)	-12(1)	-3(1)	-5(1)
C(14)	33(1)	31(1)	30(1)	-16(1)	-7(1)	0(1)
C(15)	31(1)	30(1)	22(1)	-11(1)	-2(1)	5(1)
C(16)	23(1)	21(1)	25(1)	-6(1)	-1(1)	3(1)
C(17)	28(1)	30(1)	29(1)	-8(1)	6(1)	-2(1)
C(18)	26(1)	33(1)	41(1)	-11(1)	6(1)	-9(1)
C(19)	27(1)	28(1)	36(1)	-12(1)	-2(1)	-7(1)
C(20)	23(1)	19(1)	24(1)	-6(1)	-2(1)	0(1)
C(21)	21(1)	19(1)	23(1)	-5(1)	-4(1)	2(1)
C(22)	45(1)	38(1)	29(1)	-7(1)	-10(1)	-12(1)
C(23)	48(1)	28(1)	38(1)	-17(1)	10(1)	-9(1)
C(24)	30(1)	24(1)	29(1)	-7(1)	3(1)	-7(1)
C(25)	29(1)	32(1)	34(1)	-13(1)	2(1)	0(1)
N(26)	24(1)	23(1)	24(1)	-9(1)	2(1)	-4(1)
N(27)	32(1)	23(1)	23(1)	-9(1)	-1(1)	-6(1)

Table 5. Hydrogen coordinates (x 10⁴) and isotropic displacement parameters (Å²x 10⁻³) for 6a.

	x	y	z	U(eq)
H(1)	-3063(18)	132(16)	3104(12)	35(4)
H(2)	-2019(19)	-68(18)	1159(13)	38(4)
H(3)	-44(18)	757(17)	2185(12)	36(4)
H(4)	-95(17)	-1184(16)	4630(12)	36(4)
H(5)	-2400(18)	-2919(16)	4766(12)	35(4)
H(6)	-3742(18)	-2017(16)	2454(12)	36(4)
H(7)	1115(17)	-793(16)	847(13)	36(4)
H(8)	2587(18)	-1903(16)	3218(12)	34(4)
H(9)	878(18)	-3827(17)	4486(13)	35(4)
H(10)	-1124(18)	-4717(17)	3525(13)	41(4)
H(11)	-1211(17)	-2623(16)	1006(13)	36(4)
H(12)	630(20)	-2688(18)	1869(13)	49(5)
H(13)	2668(19)	1091(17)	1575(12)	34(4)
H(14)	3946(18)	1195(16)	-150(12)	34(4)
H(15)	6055(18)	2421(16)	-768(14)	36(4)
H(17)	7841(18)	3855(16)	-565(13)	34(4)
H(18)	8650(20)	5114(18)	450(13)	42(4)
H(19)	7446(18)	4962(16)	2165(12)	33(4)
H(22A)	7230(20)	3373(18)	4134(13)	45(5)
H(22B)	5783(19)	2644(17)	4925(14)	42(4)
H(22C)	6880(20)	1890(20)	4101(14)	48(5)
H(23A)	3540(20)	5523(18)	2755(14)	45(5)
H(23B)	3870(19)	4867(17)	4097(14)	40(4)
H(23C)	5200(20)	5624(19)	3275(13)	48(5)
H(24A)	2824(19)	838(17)	4531(14)	42(4)
H(24B)	2553(19)	275(17)	3553(12)	37(4)
H(24C)	4360(20)	237(17)	3886(12)	37(4)
H(25A)	1486(18)	4066(19)	2309(14)	41(4)
H(25B)	1014(18)	3051(17)	3567(14)	40(4)
H(25C)	810(20)	2629(18)	2499(13)	44(4)
H(26)	3990(20)	2840(20)	3311(15)	62(5)

A4 *Crystal data for $[\{(7,8\text{-C}_2\text{B}_9\text{H}_{12})\text{ZnN}(\text{CH}_3)_3\}_2]:(\text{C}_7\text{H}_8)_{1.5}$; (13).*



Appendix A – Crystal Data

Table 1. Crystal data and structure refinement for (13).

Identification code	98srv020	
Empirical formula	C20.50 H52 B18 N2 Zn2	
Formula weight	651.96	
Temperature	150(2) K	
Wavelength	0.71073 Å	
Crystal system	Triclinic	
Space group	P -1	
Unit cell dimensions	a = 10.528(3) Å	α= 102.677(4)°.
	b = 10.915(3) Å	β= 96.566(4)°.
	c = 16.612(4) Å	γ = 107.892(4)°.
Volume	1738.0(7) Å ³	
Z	2	
Density (calculated)	1.246 Mg/m ³	
Absorption coefficient	1.398 mm ⁻¹	
F(000)	678	
Crystal size	0.26 x 0.24 x 0.16 mm ³	
Theta range for data collection	1.28 to 27.48°.	
Index ranges	-13<=h<=13, -14<=k<=13, -9<=l<=21	
Reflections collected	11976	
Independent reflections	7907 [R(int) = 0.0174]	
Absorption correction	None	
Refinement method	Full-matrix least-squares on F ²	
Data / restraints / parameters	7873 / 0 / 556	
Goodness-of-fit on F ²	1.111	
Final R indices [I>2sigma(I)]	R1 = 0.0324, wR2 = 0.0704	
R indices (all data)	R1 = 0.0459, wR2 = 0.0838	
Largest diff. peak and hole	0.385 and -0.315 e.Å ⁻³	

Appendix A – Crystal Data

Table 2. Atomic coordinates (x 10⁴) and equivalent isotropic displacement parameters (Å²x 10³) for (13). U(eq) is defined as one third of the trace of the orthogonalized U^{ij} tensor.

	x	y	z	U(eq)
Zn(1)	4837(1)	1180(1)	3701(1)	20(1)
Zn(2)	3722(1)	1463(1)	2168(1)	22(1)
N(1)	6647(2)	2423(2)	4495(1)	23(1)
N(2)	4593(2)	2866(2)	1556(1)	31(1)
B(1)	4906(3)	-2522(3)	1549(2)	32(1)
B(2)	3259(3)	-3121(3)	1782(2)	33(1)
B(3)	3544(3)	-2162(3)	1048(2)	32(1)
B(4)	5160(3)	-894(3)	1409(2)	30(1)
B(5)	5897(3)	-1081(3)	2384(2)	29(1)
B(6)	4712(3)	-2462(3)	2602(2)	31(1)
C(7)	2711(2)	-1773(2)	1848(2)	30(1)
C(8)	3330(2)	-1942(2)	2678(2)	29(1)
B(9)	4808(3)	-816(3)	3100(2)	27(1)
B(10)	5165(2)	216(2)	2390(2)	24(1)
B(11)	3664(3)	-529(3)	1579(2)	28(1)
B(21)	1031(3)	2601(3)	4163(2)	33(1)
B(22)	247(3)	838(3)	3749(2)	36(1)
B(23)	1628(3)	1499(3)	4608(2)	32(1)
B(24)	2811(3)	2945(3)	4454(2)	27(1)
B(25)	2129(3)	3173(3)	3476(2)	27(1)
B(26)	536(3)	1873(3)	3063(2)	32(1)
C(27)	1596(2)	279(2)	3745(2)	29(1)
C(28)	1008(2)	480(2)	2913(2)	30(1)
B(29)	1999(3)	1742(3)	2679(2)	27(1)
B(30)	3467(2)	2465(2)	3517(2)	22(1)
B(31)	3069(2)	1376(2)	4191(2)	24(1)
C(1N)	6387(3)	3214(3)	5264(2)	40(1)
C(2N)	7482(2)	3373(3)	4088(2)	40(1)
C(3N)	7441(2)	1614(3)	4747(2)	40(1)
C(4N)	5868(5)	2724(4)	1291(3)	69(2)
C(5N)	3645(5)	2657(6)	786(3)	83(2)
C(6N)	4951(6)	4232(3)	2085(3)	65(2)
C(7N)	4717(21)	2247(20)	750(12)	57(5)
C(8N)	3469(16)	3526(16)	1357(11)	42(4)
C(9N)	5698(18)	3951(18)	2093(11)	46(4)
C(1T)	306(6)	-586(5)	-168(4)	61(2)
C(2T)	218(6)	533(6)	-406(3)	58(2)
C(3T)	-492(6)	1282(5)	1(4)	68(2)
C(4T)	-1113(6)	912(6)	647(4)	78(5)
C(5T)	-1025(6)	-207(6)	886(3)	70(2)
C(6T)	-316(6)	-956(5)	479(4)	64(3)
C(7T)	1022(14)	-1383(17)	-623(7)	92(4)
C(11T)	9145(7)	-4295(7)	1700(2)	53(2)
C(12T)	8551(5)	-3372(7)	2032(4)	50(2)
C(13T)	8531(4)	-3054(4)	2887(5)	48(2)
C(14T)	9105(6)	-3659(6)	3410(2)	42(1)
C(15T)	9699(8)	-4582(7)	3078(4)	46(2)
C(16T)	9719(8)	-4900(6)	2223(4)	51(2)
C(17T)	9220(7)	-4655(7)	783(4)	101(3)
C(21T)	8669(8)	-3946(13)	1635(8)	38(3)
C(22T)	8432(10)	-3271(10)	2383(12)	57(5)
C(23T)	8918(15)	-3467(17)	3142(8)	69(6)
C(24T)	9643(20)	-4336(21)	3152(7)	68(7)
C(25T)	9881(17)	-5011(16)	2404(11)	59(5)
C(26T)	9394(10)	-4815(12)	1645(7)	44(3)
C(27T)	8051(13)	-3835(15)	806(9)	91(6)

Table 3. Bond lengths [Å] and angles [°] for (13).

Zn(1)-N(1)	2.065(2)	B(9)-H(9)	1.10(3)	C(6N)-H(6N2)	0.98
Zn(1)-B(31)	2.166(2)	B(10)-B(11)	1.792(4)	C(6N)-H(6N3)	0.98
Zn(1)-B(9)	2.177(3)	B(10)-H(10)	1.10(2)	C(7N)-H(7N1)	0.98
Zn(1)-B(10)	2.314(2)	B(11)-H(11)	1.11(2)	C(7N)-H(7N2)	0.98
Zn(1)-B(30)	2.339(2)	B(21)-B(26)	1.771(4)	C(7N)-H(7N3)	0.98
Zn(1)-Zn(2)	2.7996(6)	B(21)-B(23)	1.771(4)	C(8N)-H(8N1)	0.98
Zn(1)-H(9)	2.07(2)	B(21)-B(24)	1.779(4)	C(8N)-H(8N2)	0.98
Zn(1)-H(31)	2.03(3)	B(21)-B(22)	1.781(4)	C(8N)-H(8N3)	0.98
Zn(2)-N(2)	2.062(2)	B(21)-B(25)	1.788(4)	C(9N)-H(9N1)	0.98
Zn(2)-B(11)	2.158(3)	B(21)-H(21)	1.08(3)	C(9N)-H(9N2)	0.98
Zn(2)-B(29)	2.163(3)	B(22)-C(27)	1.709(3)	C(9N)-H(9N3)	0.98
Zn(2)-B(30)	2.352(2)	B(22)-C(28)	1.711(4)	C(1T)-C(2T)	1.39
Zn(2)-B(10)	2.379(2)	B(22)-B(26)	1.760(4)	C(1T)-C(6T)	1.39
Zn(2)-H(11)	2.00(2)	B(22)-B(23)	1.761(4)	C(1T)-C(7T)	1.464(13)
Zn(2)-H(29)	2.03(3)	B(22)-H(22)	1.06(3)	C(2T)-C(3T)	1.39
N(1)-C(2N)	1.479(3)	B(23)-C(27)	1.719(4)	C(2T)-H(2T)	0.95
N(1)-C(3N)	1.479(3)	B(23)-B(31)	1.768(3)	C(3T)-C(4T)	1.39
N(1)-C(1N)	1.481(3)	B(23)-B(24)	1.775(4)	C(3T)-H(3T)	0.95
N(2)-C(7N)	1.40(2)	B(23)-H(23)	1.08(3)	C(4T)-C(5T)	1.39
N(2)-C(9N)	1.42(2)	B(24)-B(31)	1.784(3)	C(4T)-H(4T)	0.95
N(2)-C(5N)	1.458(4)	B(24)-B(25)	1.799(4)	C(5T)-C(6T)	1.39
N(2)-C(6N)	1.464(4)	B(24)-B(30)	1.812(3)	C(5T)-H(5T)	0.95
N(2)-C(4N)	1.501(4)	B(24)-H(24)	1.10(3)	C(6T)-H(6T)	0.95
N(2)-C(8N)	1.60(2)	B(25)-B(29)	1.770(4)	C(7T)-H(7T1)	0.98
B(1)-B(3)	1.766(4)	B(25)-B(26)	1.773(4)	C(7T)-H(7T2)	0.98
B(1)-B(6)	1.774(4)	B(25)-B(30)	1.805(3)	C(7T)-H(7T3)	0.98
B(1)-B(2)	1.775(4)	B(25)-H(25)	1.11(2)	C(11T)-C(12T)	1.39
B(1)-B(4)	1.785(4)	B(26)-C(28)	1.717(4)	C(11T)-C(16T)	1.39
B(1)-B(5)	1.786(4)	B(26)-B(29)	1.767(4)	C(11T)-C(17T)	1.506(7)
B(1)-H(1)	1.11(3)	B(26)-H(26)	1.08(2)	C(12T)-C(13T)	1.39
B(2)-C(8)	1.718(4)	C(27)-C(28)	1.536(4)	C(12T)-H(12T)	0.95
B(2)-C(7)	1.724(4)	C(27)-B(31)	1.610(3)	C(13T)-C(14T)	1.39
B(2)-B(3)	1.767(4)	C(27)-H(27)	0.93(2)	C(13T)-H(13T)	0.95
B(2)-B(6)	1.769(4)	C(28)-B(29)	1.607(3)	C(14T)-C(15T)	1.39
B(2)-H(2)	1.06(2)	C(28)-H(28)	0.89(3)	C(14T)-H(14T)	0.95
B(3)-C(7)	1.720(4)	B(29)-B(30)	1.796(4)	C(15T)-C(16T)	1.39
B(3)-B(11)	1.766(4)	B(29)-H(29)	1.13(3)	C(15T)-H(15T)	0.95
B(3)-B(4)	1.768(4)	B(30)-B(31)	1.796(3)	C(16T)-H(16T)	0.95
B(3)-H(3)	1.06(3)	B(30)-H(30)	1.13(2)	C(17T)-H(17A)	0.98
B(4)-B(11)	1.776(4)	B(31)-H(31)	1.14(3)	C(17T)-H(17B)	0.98
B(4)-B(5)	1.795(4)	C(1N)-H(1N1)	0.98	C(17T)-H(17C)	0.98
B(4)-B(10)	1.802(4)	C(1N)-H(1N2)	0.98	C(21T)-C(22T)	1.39
B(4)-H(4)	1.11(3)	C(1N)-H(1N3)	0.98	C(21T)-C(26T)	1.39
B(5)-B(6)	1.774(4)	C(2N)-H(2N1)	0.98	C(21T)-C(27T)	1.501(14)
B(5)-B(9)	1.782(4)	C(2N)-H(2N2)	0.98	C(22T)-C(23T)	1.39
B(5)-B(10)	1.806(4)	C(2N)-H(2N3)	0.98	C(22T)-H(22T)	0.95
B(5)-H(5)	1.08(3)	C(3N)-H(3N1)	0.98	C(23T)-C(24T)	1.39
B(6)-C(8)	1.724(4)	C(3N)-H(3N2)	0.98	C(23T)-H(23T)	0.95
B(6)-B(9)	1.771(4)	C(3N)-H(3N3)	0.98	C(24T)-C(25T)	1.39
B(6)-H(6)	1.07(3)	C(4N)-H(4N1)	0.98	C(24T)-H(24T)	0.95
C(7)-C(8)	1.531(4)	C(4N)-H(4N2)	0.98	C(25T)-C(26T)	1.39
C(7)-B(11)	1.607(3)	C(4N)-H(4N3)	0.98	C(25T)-H(25T)	0.95
C(7)-H(7)	0.91(3)	C(5N)-H(5N1)	0.98	C(26T)-H(26T)	0.95
C(8)-B(9)	1.619(3)	C(5N)-H(5N2)	0.98	C(27T)-H(27A)	0.98
C(8)-H(8)	0.94(3)	C(5N)-H(5N3)	0.98	C(27T)-H(27B)	0.98
B(9)-B(10)	1.796(4)	C(6N)-H(6N1)	0.98	C(27T)-H(27C)	0.98
N(1)-Zn(1)-B(31)	112.78(9)	B(30)-Zn(1)-Zn(2)	53.57(6)	N(2)-Zn(2)-B(11)	114.00(9)
N(1)-Zn(1)-B(9)	114.92(9)	N(1)-Zn(1)-H(9)	93.8(7)	N(2)-Zn(2)-B(29)	113.91(9)
B(31)-Zn(1)-B(9)	118.36(10)	B(31)-Zn(1)-H(9)	113.6(7)	B(11)-Zn(2)-B(29)	119.71(10)
N(1)-Zn(1)-B(10)	112.10(8)	B(9)-Zn(1)-H(9)	30.0(7)	N(2)-Zn(2)-B(30)	111.88(8)
B(31)-Zn(1)-B(10)	133.81(9)	B(10)-Zn(1)-H(9)	73.4(7)	B(11)-Zn(2)-B(30)	132.38(9)
B(9)-Zn(1)-B(10)	47.01(9)	B(30)-Zn(1)-H(9)	154.9(7)	B(29)-Zn(2)-B(30)	46.66(9)
N(1)-Zn(1)-B(30)	108.06(8)	Zn(2)-Zn(1)-H(9)	121.6(7)	N(2)-Zn(2)-B(10)	110.11(8)
B(31)-Zn(1)-B(30)	46.79(9)	N(1)-Zn(1)-H(31)	92.6(7)	B(11)-Zn(2)-B(10)	46.23(9)
B(9)-Zn(1)-B(30)	136.01(9)	B(31)-Zn(1)-H(31)	31.2(7)	B(29)-Zn(2)-B(10)	134.41(9)
B(10)-Zn(1)-B(30)	107.99(9)	B(9)-Zn(1)-H(31)	111.5(7)	B(30)-Zn(2)-B(10)	105.45(8)
N(1)-Zn(1)-Zn(2)	126.86(5)	B(10)-Zn(1)-H(31)	152.1(7)	N(2)-Zn(2)-Zn(1)	127.38(6)
B(31)-Zn(1)-Zn(2)	89.38(7)	B(30)-Zn(1)-H(31)	74.4(7)	B(11)-Zn(2)-Zn(1)	88.23(7)
B(9)-Zn(1)-Zn(2)	91.61(7)	Zn(2)-Zn(1)-H(31)	120.5(7)	B(29)-Zn(2)-Zn(1)	90.43(7)
B(10)-Zn(1)-Zn(2)	54.44(6)	H(9)-Zn(1)-H(31)	92.9(10)	B(30)-Zn(2)-Zn(1)	53.14(6)

Appendix A – Crystal Data

B(10)-Zn(2)-Zn(1)	52.33(6)	B(3)-B(4)-B(1)	59.6(2)	Zn(1)-B(9)-H(9)	69.4(13)
N(2)-Zn(2)-H(11)	94.4(7)	B(11)-B(4)-B(1)	106.6(2)	B(11)-B(10)-B(9)	102.3(2)
B(11)-Zn(2)-H(11)	30.7(7)	B(3)-B(4)-B(5)	107.5(2)	B(11)-B(10)-B(4)	59.22(14)
B(29)-Zn(2)-H(11)	113.1(7)	B(11)-B(4)-B(5)	106.4(2)	B(9)-B(10)-B(4)	105.3(2)
B(30)-Zn(2)-H(11)	151.4(7)	B(1)-B(4)-B(5)	59.9(2)	B(11)-B(10)-B(5)	105.2(2)
B(10)-Zn(2)-H(11)	74.0(7)	B(3)-B(4)-B(10)	109.4(2)	B(9)-B(10)-B(5)	59.29(14)
Zn(1)-Zn(2)-H(11)	118.8(7)	B(11)-B(4)-B(10)	60.12(14)	B(4)-B(10)-B(5)	59.65(15)
N(2)-Zn(2)-H(29)	91.8(8)	B(1)-B(4)-B(10)	109.1(2)	B(11)-B(10)-Zn(1)	115.36(15)
B(11)-Zn(2)-H(29)	116.1(8)	B(5)-B(4)-B(10)	60.29(15)	B(9)-B(10)-Zn(1)	62.47(11)
B(29)-Zn(2)-H(29)	31.0(8)	B(3)-B(4)-H(4)	122.4(13)	B(4)-B(10)-Zn(1)	166.4(2)
B(30)-Zn(2)-H(29)	73.9(8)	B(11)-B(4)-H(4)	124.5(13)	B(5)-B(10)-Zn(1)	113.82(15)
B(10)-Zn(2)-H(29)	155.8(8)	B(1)-B(4)-H(4)	120.9(13)	B(11)-B(10)-Zn(2)	60.39(11)
Zn(1)-Zn(2)-H(29)	121.4(8)	B(5)-B(4)-H(4)	120.9(13)	B(9)-B(10)-Zn(2)	118.21(14)
H(11)-Zn(2)-H(29)	95.0(11)	B(10)-B(4)-H(4)	120.4(13)	B(4)-B(10)-Zn(2)	110.45(15)
C(2N)-N(1)-C(3N)	108.5(2)	B(6)-B(5)-B(9)	59.76(15)	B(5)-B(10)-Zn(2)	165.3(2)
C(2N)-N(1)-C(1N)	107.8(2)	B(6)-B(5)-B(1)	59.8(2)	Zn(1)-B(10)-Zn(2)	73.23(7)
C(3N)-N(1)-C(1N)	108.4(2)	B(9)-B(5)-B(1)	106.7(2)	B(11)-B(10)-H(10)	126.3(13)
C(2N)-N(1)-Zn(1)	111.76(14)	B(6)-B(5)-B(4)	107.5(2)	B(9)-B(10)-H(10)	129.9(13)
C(3N)-N(1)-Zn(1)	109.67(14)	B(9)-B(5)-B(4)	106.2(2)	B(4)-B(10)-H(10)	109.1(13)
C(1N)-N(1)-Zn(1)	110.64(14)	B(1)-B(5)-B(4)	59.8(2)	B(5)-B(10)-H(10)	111.0(13)
C(7N)-N(2)-C(9N)	120.4(11)	B(6)-B(5)-B(10)	109.3(2)	Zn(1)-B(10)-H(10)	84.3(13)
C(5N)-N(2)-C(6N)	110.3(3)	B(9)-B(5)-B(10)	60.06(14)	Zn(2)-B(10)-H(10)	81.9(13)
C(5N)-N(2)-C(4N)	106.3(3)	B(1)-B(5)-B(10)	108.8(2)	C(7)-B(11)-B(3)	61.1(2)
C(6N)-N(2)-C(4N)	107.2(3)	B(4)-B(5)-B(10)	60.06(14)	C(7)-B(11)-B(4)	106.0(2)
C(7N)-N(2)-C(8N)	102.5(10)	B(6)-B(5)-H(5)	123.1(14)	B(3)-B(11)-B(4)	59.9(2)
C(9N)-N(2)-C(8N)	103.6(10)	B(9)-B(5)-H(5)	123.6(14)	C(7)-B(11)-B(10)	105.8(2)
C(7N)-N(2)-Zn(2)	110.9(8)	B(1)-B(5)-H(5)	122.3(14)	B(3)-B(11)-B(10)	109.9(2)
C(9N)-N(2)-Zn(2)	112.1(7)	B(4)-B(5)-H(5)	121.1(14)	B(4)-B(11)-B(10)	60.66(15)
C(5N)-N(2)-Zn(2)	108.8(2)	B(10)-B(5)-H(5)	119.3(14)	C(7)-B(11)-Zn(2)	119.3(2)
C(6N)-N(2)-Zn(2)	111.9(2)	C(8)-B(6)-B(2)	58.92(15)	B(3)-B(11)-Zn(2)	176.6(2)
C(4N)-N(2)-Zn(2)	112.2(2)	C(8)-B(6)-B(9)	55.19(14)	B(4)-B(11)-Zn(2)	122.2(2)
C(8N)-N(2)-Zn(2)	105.4(6)	B(2)-B(6)-B(9)	106.3(2)	B(10)-B(11)-Zn(2)	73.38(12)
B(3)-B(1)-B(6)	107.7(2)	C(8)-B(6)-B(5)	101.8(2)	C(7)-B(11)-H(11)	118.9(13)
B(3)-B(1)-B(2)	59.9(2)	B(2)-B(6)-B(5)	108.4(2)	B(3)-B(11)-H(11)	110.1(13)
B(6)-B(1)-B(2)	59.8(2)	B(9)-B(6)-B(5)	60.33(15)	B(4)-B(11)-H(11)	120.3(13)
B(3)-B(1)-B(4)	59.7(2)	C(8)-B(6)-B(1)	103.1(2)	B(10)-B(11)-H(11)	130.2(13)
B(6)-B(1)-B(4)	107.9(2)	B(2)-B(6)-B(1)	60.1(2)	Zn(2)-B(11)-H(11)	66.6(13)
B(2)-B(1)-B(4)	107.6(2)	B(9)-B(6)-B(1)	107.6(2)	B(26)-B(21)-B(23)	107.4(2)
B(3)-B(1)-B(5)	107.9(2)	B(5)-B(6)-B(1)	60.5(2)	B(26)-B(21)-B(24)	108.2(2)
B(6)-B(1)-B(5)	59.8(2)	C(8)-B(6)-H(6)	120.0(15)	B(23)-B(21)-B(24)	60.00(15)
B(2)-B(1)-B(5)	107.6(2)	B(2)-B(6)-H(6)	119.7(15)	B(26)-B(21)-B(22)	59.4(2)
B(4)-B(1)-B(5)	60.3(2)	B(9)-B(6)-H(6)	119.0(15)	B(23)-B(21)-B(22)	59.4(2)
B(3)-B(1)-H(1)	121.3(14)	B(5)-B(6)-H(6)	127.4(15)	B(24)-B(21)-B(22)	107.3(2)
B(6)-B(1)-H(1)	122.9(14)	B(1)-B(6)-H(6)	128.7(15)	B(26)-B(21)-B(25)	59.8(2)
B(2)-B(1)-H(1)	122.6(13)	C(8)-C(7)-B(11)	113.5(2)	B(23)-B(21)-B(25)	108.0(2)
B(4)-B(1)-H(1)	120.8(13)	C(8)-C(7)-B(3)	112.6(2)	B(24)-B(21)-B(25)	60.56(15)
B(5)-B(1)-H(1)	121.8(14)	B(11)-C(7)-B(3)	64.0(2)	B(22)-B(21)-B(25)	107.0(2)
C(8)-B(2)-C(7)	52.79(14)	C(8)-C(7)-B(2)	63.4(2)	B(26)-B(21)-H(21)	120.8(15)
C(8)-B(2)-B(3)	101.9(2)	B(11)-C(7)-B(2)	116.3(2)	B(23)-B(21)-H(21)	122.7(15)
C(7)-B(2)-B(3)	59.0(2)	B(3)-C(7)-B(2)	61.7(2)	B(24)-B(21)-H(21)	122.5(16)
C(8)-B(2)-B(6)	59.21(15)	C(8)-C(7)-H(7)	117.7(16)	B(22)-B(21)-H(21)	122.0(15)
C(7)-B(2)-B(6)	101.8(2)	B(11)-C(7)-H(7)	120.8(16)	B(25)-B(21)-H(21)	121.7(15)
B(3)-B(2)-B(6)	107.9(2)	B(3)-C(7)-H(7)	116.6(17)	C(27)-B(22)-C(28)	53.38(14)
C(8)-B(2)-B(1)	103.3(2)	B(2)-C(7)-H(7)	111.7(17)	C(27)-B(22)-B(26)	102.5(2)
C(7)-B(2)-B(1)	102.9(2)	C(7)-C(8)-B(9)	112.6(2)	C(28)-B(22)-B(26)	59.2(2)
B(3)-B(2)-B(1)	59.8(2)	C(7)-C(8)-B(2)	63.8(2)	C(27)-B(22)-B(23)	59.4(2)
B(6)-B(2)-B(1)	60.1(2)	B(9)-C(8)-B(2)	116.2(2)	C(28)-B(22)-B(23)	102.7(2)
C(8)-B(2)-H(2)	120.4(13)	C(7)-C(8)-B(6)	112.7(2)	B(26)-B(22)-B(23)	108.4(2)
C(7)-B(2)-H(2)	122.8(13)	B(9)-C(8)-B(6)	63.9(2)	C(27)-B(22)-B(21)	103.4(2)
B(3)-B(2)-H(2)	125.9(13)	B(2)-C(8)-B(6)	61.9(2)	C(28)-B(22)-B(21)	103.4(2)
B(6)-B(2)-H(2)	121.8(13)	C(7)-C(8)-H(8)	118.0(17)	B(26)-B(22)-B(21)	60.0(2)
B(1)-B(2)-H(2)	129.5(13)	B(9)-C(8)-H(8)	122.1(17)	B(23)-B(22)-B(21)	60.0(2)
C(7)-B(3)-B(11)	54.87(14)	B(2)-C(8)-H(8)	110.1(17)	C(27)-B(22)-H(22)	121.1(15)
C(7)-B(3)-B(1)	103.5(2)	B(6)-C(8)-H(8)	115.7(17)	C(28)-B(22)-H(22)	120.1(16)
B(11)-B(3)-B(1)	107.9(2)	C(8)-B(9)-B(6)	60.91(15)	B(26)-B(22)-H(22)	122.8(15)
C(7)-B(3)-B(2)	59.3(2)	C(8)-B(9)-B(5)	105.8(2)	B(23)-B(22)-H(22)	124.6(16)
B(11)-B(3)-B(2)	106.5(2)	B(6)-B(9)-B(5)	59.91(15)	B(21)-B(22)-H(22)	130.2(15)
B(1)-B(3)-B(2)	60.3(2)	C(8)-B(9)-B(10)	105.7(2)	C(27)-B(23)-B(22)	58.8(2)
C(7)-B(3)-B(4)	101.6(2)	B(6)-B(9)-B(10)	109.9(2)	C(27)-B(23)-B(31)	54.98(14)
B(11)-B(3)-B(4)	60.35(15)	B(5)-B(9)-B(10)	60.65(14)	B(22)-B(23)-B(31)	106.0(2)
B(1)-B(3)-B(4)	60.7(2)	C(8)-B(9)-Zn(1)	116.8(2)	C(27)-B(23)-B(21)	103.4(2)
B(2)-B(3)-B(4)	108.7(2)	B(6)-B(9)-Zn(1)	177.7(2)	B(22)-B(23)-B(21)	60.6(2)
C(7)-B(3)-H(3)	122.8(15)	B(5)-B(9)-Zn(1)	121.7(2)	B(31)-B(23)-B(21)	107.6(2)
B(11)-B(3)-H(3)	121.4(15)	B(10)-B(9)-Zn(1)	70.52(12)	C(27)-B(23)-B(24)	101.8(2)
B(1)-B(3)-H(3)	125.4(15)	C(8)-B(9)-H(9)	120.9(13)	B(22)-B(23)-B(24)	108.4(2)
B(2)-B(3)-H(3)	119.2(14)	B(6)-B(9)-H(9)	111.4(13)	B(31)-B(23)-B(24)	60.47(14)
B(4)-B(3)-H(3)	126.1(14)	B(5)-B(9)-H(9)	119.5(13)	B(21)-B(23)-B(24)	60.2(2)
B(3)-B(4)-B(11)	59.8(2)	B(10)-B(9)-H(9)	128.3(13)	C(27)-B(23)-H(23)	121.4(14)

Appendix A – Crystal Data

B(22)-B(23)-H(23)	120.2(14)	B(30)-B(29)-Zn(2)	72.22(11)	N(2)-C(7N)-H(7N1)	109.5(9)
B(31)-B(23)-H(23)	119.8(14)	C(28)-B(29)-H(29)	120.6(14)	N(2)-C(7N)-H(7N2)	109.5(9)
B(21)-B(23)-H(23)	127.4(14)	B(26)-B(29)-H(29)	111.3(14)	H(7N1)-C(7N)-H(7N2)	109.5
B(24)-B(23)-H(23)	126.4(14)	B(25)-B(29)-H(29)	119.2(14)	N(2)-C(7N)-H(7N3)	109.5(8)
B(23)-B(24)-B(21)	59.8(2)	B(30)-B(29)-H(29)	128.2(14)	H(7N1)-C(7N)-H(7N3)	109.5
B(23)-B(24)-B(31)	59.56(14)	Zn(2)-B(29)-H(29)	68.0(14)	H(7N2)-C(7N)-H(7N3)	109.5
B(21)-B(24)-B(31)	106.6(2)	B(31)-B(30)-B(29)	102.1(2)	N(2)-C(8N)-H(8N1)	109.5(6)
B(23)-B(24)-B(25)	107.4(2)	B(31)-B(30)-B(25)	105.2(2)	N(2)-C(8N)-H(8N2)	109.5(6)
B(21)-B(24)-B(25)	59.98(15)	B(29)-B(30)-B(25)	58.88(14)	H(8N1)-C(8N)-H(8N2)	109.5
B(31)-B(24)-B(25)	105.9(2)	B(31)-B(30)-B(24)	59.28(13)	N(2)-C(8N)-H(8N3)	109.5(6)
B(23)-B(24)-B(30)	109.0(2)	B(29)-B(30)-B(24)	104.9(2)	H(8N1)-C(8N)-H(8N3)	109.5
B(21)-B(24)-B(30)	109.0(2)	B(25)-B(30)-B(24)	59.65(14)	H(8N2)-C(8N)-H(8N3)	109.5
B(31)-B(24)-B(30)	59.90(13)	B(31)-B(30)-Zn(1)	61.52(10)	N(2)-C(9N)-H(9N1)	109.5(8)
B(25)-B(24)-B(30)	59.97(14)	B(29)-B(30)-Zn(1)	117.73(14)	N(2)-C(9N)-H(9N2)	109.5(7)
B(23)-B(24)-H(24)	122.5(14)	B(25)-B(30)-Zn(1)	166.2(2)	H(9N1)-C(9N)-H(9N2)	109.5
B(21)-B(24)-H(24)	123.5(14)	B(24)-B(30)-Zn(1)	111.85(14)	N(2)-C(9N)-H(9N3)	109.5(8)
B(31)-B(24)-H(24)	122.1(14)	B(31)-B(30)-Zn(2)	115.54(14)	H(9N1)-C(9N)-H(9N3)	109.5
B(25)-B(24)-H(24)	122.7(14)	B(29)-B(30)-Zn(2)	61.13(11)	H(9N2)-C(9N)-H(9N3)	109.5
B(30)-B(24)-H(24)	119.0(14)	B(25)-B(30)-Zn(2)	112.18(14)	C(2T)-C(1T)-C(6T)	120.0
B(29)-B(25)-B(26)	59.83(15)	B(24)-B(30)-Zn(2)	164.9(2)	C(2T)-C(1T)-C(7T)	119.0(7)
B(29)-B(25)-B(21)	106.7(2)	Zn(1)-B(30)-Zn(2)	73.28(7)	C(6T)-C(1T)-C(7T)	120.9(7)
B(26)-B(25)-B(21)	59.6(2)	B(31)-B(30)-H(30)	127.4(13)	C(3T)-C(2T)-C(1T)	120.0
B(29)-B(25)-B(24)	106.6(2)	B(29)-B(30)-H(30)	128.8(13)	C(3T)-C(2T)-H(2T)	120.0
B(26)-B(25)-B(24)	107.2(2)	B(25)-B(30)-H(30)	111.3(13)	C(1T)-C(2T)-H(2T)	120.0
B(21)-B(25)-B(24)	59.46(15)	B(24)-B(30)-H(30)	110.6(13)	C(2T)-C(3T)-C(4T)	120.0
B(29)-B(25)-B(30)	60.33(14)	Zn(1)-B(30)-H(30)	81.5(12)	C(2T)-C(3T)-H(3T)	120.0
B(26)-B(25)-B(30)	109.5(2)	Zn(2)-B(30)-H(30)	84.0(13)	C(4T)-C(3T)-H(3T)	120.0
B(21)-B(25)-B(30)	108.9(2)	C(27)-B(31)-B(23)	61.0(2)	C(3T)-C(4T)-C(5T)	120.0
B(24)-B(25)-B(30)	60.38(14)	C(27)-B(31)-B(24)	105.9(2)	C(3T)-C(4T)-H(4T)	120.0
B(29)-B(25)-H(25)	123.4(13)	B(23)-B(31)-B(24)	59.97(15)	C(5T)-C(4T)-H(4T)	120.0
B(26)-B(25)-H(25)	121.9(13)	C(27)-B(31)-B(30)	105.8(2)	C(6T)-C(5T)-C(4T)	120.0
B(21)-B(25)-H(25)	121.7(13)	B(23)-B(31)-B(30)	110.1(2)	C(6T)-C(5T)-H(5T)	120.0
B(24)-B(25)-H(25)	121.9(13)	B(24)-B(31)-B(30)	60.82(14)	C(4T)-C(5T)-H(5T)	120.0
B(30)-B(25)-H(25)	120.4(13)	C(27)-B(31)-Zn(1)	118.8(2)	C(5T)-C(6T)-C(1T)	120.0
C(28)-B(26)-B(22)	59.0(2)	B(23)-B(31)-Zn(1)	178.2(2)	C(5T)-C(6T)-H(6T)	120.0
C(28)-B(26)-B(29)	54.93(14)	B(24)-B(31)-Zn(1)	121.48(15)	C(1T)-C(6T)-H(6T)	120.0
B(22)-B(26)-B(29)	106.0(2)	B(30)-B(31)-Zn(1)	71.69(11)	C(1T)-C(7T)-H(7T1)	109.5(7)
C(28)-B(26)-B(21)	103.7(2)	C(27)-B(31)-H(31)	121.3(13)	C(1T)-C(7T)-H(7T2)	109.5(5)
B(22)-B(26)-B(21)	60.6(2)	B(23)-B(31)-H(31)	110.5(13)	H(7T1)-C(7T)-H(7T2)	109.5
B(29)-B(26)-B(21)	107.6(2)	B(24)-B(31)-H(31)	118.3(13)	C(1T)-C(7T)-H(7T3)	109.5(7)
C(28)-B(26)-B(25)	101.6(2)	B(30)-B(31)-H(31)	128.4(13)	H(7T1)-C(7T)-H(7T3)	109.5
B(22)-B(26)-B(25)	108.6(2)	Zn(1)-B(31)-H(31)	68.0(13)	H(7T2)-C(7T)-H(7T3)	109.5
B(29)-B(26)-B(25)	59.98(15)	N(1)-C(1N)-H(1N1)	109.47(13)	C(12T)-C(11T)-C(16T)	120.0
B(21)-B(26)-B(25)	60.6(2)	N(1)-C(1N)-H(1N2)	109.47(13)	C(12T)-C(11T)-C(17T)	122.2(7)
C(28)-B(26)-H(26)	123.1(13)	H(1N1)-C(1N)-H(1N2)	109.5	C(16T)-C(11T)-C(17T)	117.8(7)
B(22)-B(26)-H(26)	119.1(13)	N(1)-C(1N)-H(1N3)	109.47(12)	C(13T)-C(12T)-C(11T)	120.0
B(29)-B(26)-H(26)	122.2(13)	H(1N1)-C(1N)-H(1N3)	109.5	C(13T)-C(12T)-H(12T)	120.0
B(21)-B(26)-H(26)	124.8(13)	H(1N2)-C(1N)-H(1N3)	109.5	C(11T)-C(12T)-H(12T)	120.0
B(25)-B(26)-H(26)	126.2(13)	N(1)-C(2N)-H(2N1)	109.47(13)	C(12T)-C(13T)-C(14T)	120.0
C(28)-C(27)-B(31)	113.2(2)	N(1)-C(2N)-H(2N2)	109.47(12)	C(12T)-C(13T)-H(13T)	120.0
C(28)-C(27)-B(22)	63.4(2)	H(2N1)-C(2N)-H(2N2)	109.5	C(14T)-C(13T)-H(13T)	120.0
B(31)-C(27)-B(22)	116.2(2)	N(1)-C(2N)-H(2N3)	109.47(13)	C(15T)-C(14T)-C(13T)	120.0
C(28)-C(27)-B(23)	112.7(2)	H(2N1)-C(2N)-H(2N3)	109.5	C(15T)-C(14T)-H(14T)	120.0
B(31)-C(27)-B(23)	64.0(2)	H(2N2)-C(2N)-H(2N3)	109.5	C(13T)-C(14T)-H(14T)	120.0
B(22)-C(27)-B(23)	61.8(2)	N(1)-C(3N)-H(3N1)	109.47(13)	C(14T)-C(15T)-C(16T)	120.0
C(28)-C(27)-H(27)	118.4(15)	N(1)-C(3N)-H(3N2)	109.47(12)	C(14T)-C(15T)-H(15T)	120.0
B(31)-C(27)-H(27)	120.6(15)	H(3N1)-C(3N)-H(3N2)	109.5	C(16T)-C(15T)-H(15T)	120.0
B(22)-C(27)-H(27)	111.8(15)	N(1)-C(3N)-H(3N3)	109.47(14)	C(15T)-C(16T)-C(11T)	120.0
B(23)-C(27)-H(27)	116.1(15)	H(3N1)-C(3N)-H(3N3)	109.5	C(15T)-C(16T)-H(16T)	120.0
C(27)-C(28)-B(29)	112.9(2)	H(3N2)-C(3N)-H(3N3)	109.5	C(11T)-C(16T)-H(16T)	120.0
C(27)-C(28)-B(22)	63.2(2)	N(2)-C(4N)-H(4N1)	109.5(2)	C(11T)-C(17T)-H(17A)	109.5(4)
B(29)-C(28)-B(22)	116.1(2)	N(2)-C(4N)-H(4N2)	109.5(2)	C(11T)-C(17T)-H(17B)	109.5(3)
C(27)-C(28)-B(26)	112.5(2)	H(4N1)-C(4N)-H(4N2)	109.5	H(17A)-C(17T)-H(17B)	109.5
B(29)-C(28)-B(26)	64.1(2)	N(2)-C(4N)-H(4N3)	109.5(2)	C(11T)-C(17T)-H(17C)	109.5(5)
B(22)-C(28)-B(26)	61.8(2)	H(4N1)-C(4N)-H(4N3)	109.5	H(17A)-C(17T)-H(17C)	109.5
C(27)-C(28)-H(28)	118.4(16)	H(4N2)-C(4N)-H(4N3)	109.5	H(17B)-C(17T)-H(17C)	109.5
B(29)-C(28)-H(28)	120.1(16)	N(2)-C(5N)-H(5N1)	109.5(2)	C(22T)-C(21T)-C(26T)	120.0
B(22)-C(28)-H(28)	113.3(17)	N(2)-C(5N)-H(5N2)	109.5(3)	C(22T)-C(21T)-C(27T)	120.6(13)
B(26)-C(28)-H(28)	117.3(16)	H(5N1)-C(5N)-H(5N2)	109.5	C(26T)-C(21T)-C(27T)	119.2(14)
C(28)-B(29)-B(26)	60.9(2)	N(2)-C(5N)-H(5N3)	109.5(3)	C(21T)-C(22T)-C(23T)	120.0
C(28)-B(29)-B(25)	106.3(2)	H(5N1)-C(5N)-H(5N3)	109.5	C(21T)-C(22T)-H(22T)	120.0
B(26)-B(29)-B(25)	60.2(2)	H(5N2)-C(5N)-H(5N3)	109.5	C(23T)-C(22T)-H(22T)	120.0
C(28)-B(29)-B(30)	106.1(2)	N(2)-C(6N)-H(6N1)	109.5(2)	C(24T)-C(23T)-C(22T)	120.0
B(26)-B(29)-B(30)	110.2(2)	N(2)-C(6N)-H(6N2)	109.5(2)	C(24T)-C(23T)-H(23T)	120.0
B(25)-B(29)-B(30)	60.80(14)	H(6N1)-C(6N)-H(6N2)	109.5	C(22T)-C(23T)-H(23T)	120.0
C(28)-B(29)-Zn(2)	116.4(2)	N(2)-C(6N)-H(6N3)	109.5(2)	C(25T)-C(24T)-C(23T)	120.0
B(26)-B(29)-Zn(2)	176.7(2)	H(6N1)-C(6N)-H(6N3)	109.5	C(25T)-C(24T)-H(24T)	120.0
B(25)-B(29)-Zn(2)	123.1(2)	H(6N2)-C(6N)-H(6N3)	109.5	C(23T)-C(24T)-H(24T)	120.0

Appendix A – Crystal Data

C(24T)-C(25T)-C(26T)	120.0	C(25T)-C(26T)-H(26T)	120.0	H(27A)-C(27T)-H(27B)	109.5
C(24T)-C(25T)-H(25T)	120.0	C(21T)-C(26T)-H(26T)	120.0	C(21T)-C(27T)-H(27C)	109.5(8)
C(26T)-C(25T)-H(25T)	120.0	C(21T)-C(27T)-H(27A)	109.5(6)	H(27A)-C(27T)-H(27C)	109.5
C(25T)-C(26T)-C(21T)	120.0	C(21T)-C(27T)-H(27B)	109.5(8)	H(27B)-C(27T)-H(27C)	109.5

Symmetry transformations used to generate equivalent atoms:

Table 4. Anisotropic displacement parameters ($\text{\AA}^2 \times 10^3$) for (13). The anisotropic displacement factor exponent takes the form: $-2\pi^2[h^2 a^{*2}U^{11} + \dots + 2 h k a^* b^* U^{12}]$

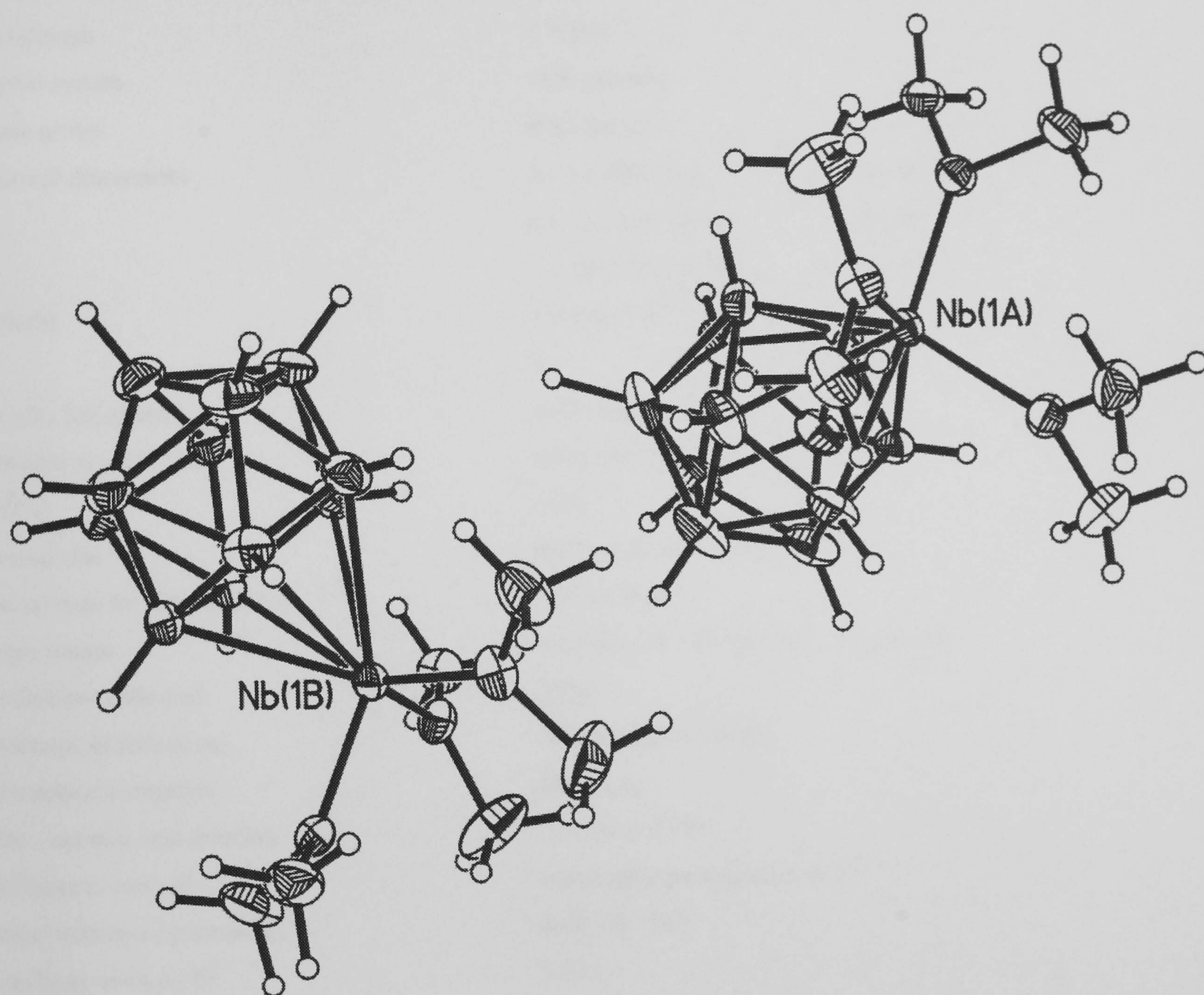
	U ¹¹	U ²²	U ³³	U ²³	U ¹³	U ¹²
Zn(1)	19(1)	19(1)	22(1)	3(1)	4(1)	6(1)
Zn(2)	26(1)	19(1)	22(1)	5(1)	7(1)	9(1)
N(1)	20(1)	22(1)	24(1)	6(1)	4(1)	6(1)
N(2)	40(1)	27(1)	26(1)	10(1)	10(1)	11(1)
B(1)	41(2)	22(1)	33(1)	1(1)	12(1)	14(1)
B(2)	39(2)	20(1)	36(2)	0(1)	10(1)	8(1)
B(3)	39(2)	24(1)	29(1)	-3(1)	5(1)	11(1)
B(4)	35(1)	24(1)	30(1)	3(1)	12(1)	10(1)
B(5)	29(1)	28(1)	33(1)	4(1)	8(1)	13(1)
B(6)	39(2)	22(1)	35(1)	5(1)	9(1)	15(1)
C(7)	25(1)	24(1)	36(1)	1(1)	5(1)	7(1)
C(8)	32(1)	20(1)	34(1)	3(1)	13(1)	7(1)
B(9)	33(1)	22(1)	27(1)	4(1)	7(1)	11(1)
B(10)	25(1)	20(1)	25(1)	3(1)	5(1)	7(1)
B(11)	31(1)	22(1)	27(1)	1(1)	1(1)	9(1)
B(21)	30(1)	38(2)	39(2)	11(1)	16(1)	18(1)
B(22)	22(1)	36(2)	51(2)	11(1)	13(1)	11(1)
B(23)	28(1)	36(2)	37(2)	14(1)	18(1)	14(1)
B(24)	30(1)	26(1)	28(1)	5(1)	11(1)	14(1)
B(25)	28(1)	26(1)	29(1)	5(1)	7(1)	15(1)
B(26)	26(1)	35(1)	40(2)	9(1)	6(1)	17(1)
C(27)	24(1)	25(1)	41(1)	12(1)	11(1)	9(1)
C(28)	22(1)	28(1)	38(1)	3(1)	4(1)	8(1)
B(29)	24(1)	28(1)	28(1)	5(1)	5(1)	12(1)
B(30)	22(1)	22(1)	24(1)	5(1)	7(1)	8(1)
B(31)	21(1)	25(1)	28(1)	10(1)	8(1)	10(1)
C(1N)	36(1)	40(1)	32(1)	-8(1)	1(1)	9(1)
C(2N)	27(1)	40(1)	42(1)	15(1)	2(1)	-5(1)
C(3N)	27(1)	32(1)	57(2)	12(1)	-5(1)	10(1)
C(4N)	73(3)	66(3)	111(4)	60(3)	71(3)	39(2)
C(5N)	74(3)	100(4)	56(3)	54(3)	-15(2)	-12(3)
C(6N)	125(4)	23(2)	52(2)	16(2)	44(3)	20(2)
C(1T)	51(4)	62(5)	48(4)	-7(3)	-24(3)	18(3)
C(2T)	57(5)	59(5)	48(5)	19(4)	-9(4)	10(4)
C(3T)	52(4)	66(5)	75(6)	15(4)	-19(4)	18(4)
C(4T)	43(5)	106(10)	67(8)	6(7)	-14(5)	20(5)
C(5T)	47(4)	93(6)	54(4)	12(4)	-8(3)	15(4)
C(6T)	61(5)	61(5)	59(5)	20(4)	-11(4)	10(4)
C(7T)	97(9)	114(9)	50(7)	-12(5)	-18(6)	53(7)
C(11T)	43(4)	45(4)	50(3)	9(3)	10(3)	-12(3)
C(12T)	37(3)	45(4)	65(5)	23(4)	5(3)	4(3)
C(13T)	42(3)	36(3)	62(4)	16(3)	2(3)	10(2)
C(14T)	33(3)	42(3)	49(3)	14(3)	4(3)	11(2)
C(15T)	34(4)	43(3)	66(6)	23(3)	15(4)	11(3)
C(16T)	39(4)	43(3)	70(5)	15(3)	24(4)	7(3)
C(17T)	104(6)	86(5)	53(3)	3(3)	6(3)	-37(4)
C(21T)	26(5)	33(6)	75(9)	30(6)	25(5)	19(4)
C(22T)	46(7)	38(6)	76(13)	-3(8)	25(8)	8(5)
C(23T)	57(10)	77(14)	46(8)	-5(8)	-2(8)	5(8)
C(24T)	46(12)	80(13)	56(11)	22(9)	-3(9)	-8(9)
C(25T)	44(7)	65(10)	60(10)	32(8)	-13(6)	7(6)
C(26T)	36(5)	55(8)	55(7)	19(6)	14(5)	29(6)
C(27T)	61(8)	111(12)	118(12)	88(10)	10(7)	17(7)

Appendix A – Crystal Data

Table 5. Hydrogen coordinates (x 10⁴) and isotropic displacement parameters (Å²x 10³) for (13).

	x	y	z	U(eq)
H(1)	5376(26)	-3193(26)	1191(16)	35(7)
H(2)	2580(25)	-4118(25)	1655(15)	28(6)
H(3)	3039(27)	-2603(26)	415(17)	37(7)
H(4)	5809(26)	-517(25)	974(16)	34(7)
H(5)	6986(27)	-806(26)	2571(17)	36(7)
H(6)	4923(28)	-3077(28)	2982(18)	44(8)
H(7)	1786(28)	-2036(26)	1708(16)	33(7)
H(8)	2735(28)	-2332(27)	3003(18)	40(7)
H(9)	5203(25)	-548(25)	3782(16)	33(7)
H(10)	5962(25)	1191(25)	2480(15)	29(6)
H(11)	3189(25)	-80(24)	1145(16)	31(7)
H(21)	513(29)	3211(28)	4489(18)	46(8)
H(22)	-734(29)	200(28)	3759(18)	43(8)
H(23)	1499(27)	1286(26)	5205(17)	39(7)
H(24)	3477(28)	3782(28)	4979(18)	42(8)
H(25)	2327(25)	4176(25)	3373(16)	30(7)
H(26)	-322(25)	1925(24)	2670(16)	30(6)
H(27)	1365(24)	-584(25)	3805(15)	24(6)
H(28)	481(26)	-239(26)	2507(16)	29(7)
H(29)	1928(27)	1795(26)	2005(17)	40(7)
H(30)	4485(25)	3229(24)	3539(16)	30(7)
H(31)	3796(26)	1169(25)	4660(16)	33(7)
H(1N1)	5862(17)	2608(3)	5558(7)	60
H(1N2)	5870(17)	3764(15)	5109(2)	60
H(1N3)	7256(3)	3793(14)	5635(6)	60
H(2N1)	7720(17)	2875(3)	3597(7)	60
H(2N2)	8316(10)	3965(13)	4489(4)	60
H(2N3)	6964(8)	3907(13)	3910(11)	60
H(3N1)	6916(9)	1007(14)	5040(11)	60
H(3N2)	8300(9)	2208(3)	5123(10)	60
H(3N3)	7632(17)	1093(15)	4245(2)	60
H(4N1)	6570(12)	2937(33)	1792(3)	103
H(4N2)	6191(20)	3340(25)	950(18)	103
H(4N3)	5677(9)	1804(10)	960(18)	103
H(5N1)	4038(19)	3335(26)	498(14)	125
H(5N2)	2786(16)	2729(41)	925(3)	125
H(5N3)	3474(33)	1765(17)	416(11)	125
H(6N1)	5659(24)	4390(11)	2571(11)	97
H(6N2)	4143(9)	4355(10)	2280(17)	97
H(6N3)	5290(33)	4867(3)	1758(7)	97
H(7N1)	3814(27)	1670(113)	421(32)	86
H(7N2)	5300(121)	1708(117)	795(13)	86
H(7N3)	5122(137)	2931(20)	469(36)	86
H(8N1)	3267(89)	3957(102)	1885(11)	62
H(8N2)	2636(43)	2831(24)	1010(62)	62
H(8N3)	3816(49)	4195(85)	1053(65)	62
H(9N1)	5394(35)	4349(82)	2590(40)	69
H(9N2)	6035(87)	4625(61)	1791(28)	69
H(9N3)	6430(53)	3631(29)	2269(65)	69
H(2T)	642(7)	786(8)	-848(4)	69
H(3T)	-552(8)	2047(6)	-162(6)	82
H(4T)	-1598(8)	1424(8)	926(6)	94
H(5T)	-1450(7)	-460(9)	1328(4)	84
H(6T)	-256(8)	-1721(6)	642(5)	77
H(7T1)	378(20)	-2280(28)	-913(36)	138
H(7T2)	1743(49)	-1451(61)	-224(9)	138
H(7T3)	1426(61)	-952(40)	-1036(31)	138
H(12T)	8159(8)	-2958(10)	1675(7)	60
H(13T)	8126(7)	-2423(5)	3114(8)	57
H(14T)	9091(10)	-3442(8)	3994(3)	50
H(15T)	10091(12)	-4996(11)	3435(6)	55
H(16T)	10125(11)	-5531(8)	1996(7)	61
H(17A)	9055(58)	-5615(13)	587(10)	151
H(17B)	10125(20)	-4152(43)	707(6)	151
H(17C)	8528(39)	-4432(52)	456(6)	151
H(22T)	7936(16)	-2677(15)	2376(18)	68
H(23T)	8756(21)	-3006(24)	3653(10)	83
H(24T)	9976(28)	-4470(32)	3670(9)	82
H(25T)	10376(25)	-5605(22)	2410(17)	70
H(26T)	9557(15)	-5276(18)	1134(9)	53
H(27A)	7101(35)	-4434(82)	640(35)	136
H(27B)	8560(69)	-4088(104)	377(17)	136
H(27C)	8089(99)	-2912(29)	858(20)	136

A5 Crystal data for $[3\text{-Nb}(\text{NMe}_2)_3(1,2\text{-C}_2\text{B}_9\text{H}_{11})]$; (16).



Appendix A – Crystal Data

Table 1.Crystal data and structure refinement for (16).

Identification code	99srv027	
Empirical formula	C8 H29 B9 N3 Nb	
Formula weight	357.54	
Temperature	150(2) K	
Wavelength	0.71073 Å	
Crystal system	Orthorhombic	
Space group	P2(1)2(1)2(1)	
Unit cell dimensions	a = 13.4562(7) Å	α= 90°.
	b = 15.6233(12) Å	β= 90°.
	c = 16.9319(10) Å	γ = 90°.
Volume	3559.6(4) Å ³	
Z	8	
Density (calculated)	1.334 Mg/m ³	
Absorption coefficient	0.665 mm ⁻¹	
F(000)	1472	
Crystal size	0.40 x 0.30 x 0.12 mm ³	
Theta range for data collection	1.77 to 30.46°.	
Index ranges	-18<=h<=18, -21<=k<=21, -15<=l<=23	
Reflections collected	28901	
Independent reflections	9724 [R(int) = 0.0352]	
Absorption correction	Multiscan	
Max. and min. transmission	0.875 and 0.732	
Refinement method	Full-matrix least-squares on F ²	
Data / restraints / parameters	9689 / 0 / 502	
Goodness-of-fit on F ²	1.172	
Final R indices [I>2sigma(I)]	R1 = 0.0362, wR2 = 0.0625	
R indices (all data)	R1 = 0.0581, wR2 = 0.0757	
Absolute structure parameter	0.48(5)	
Largest diff. peak and hole	0.466 and -0.489 e.Å ⁻³	

Appendix A – Crystal Data

Table 2. Atomic coordinates (x 10⁴) and equivalent isotropic displacement parameters (Å²x 10³) for (16). U(eq) is defined as one third of the trace of the orthogonalized U^{ij} tensor.

	x	y	z	U(eq)
Nb(1A)	1508(1)	3913(1)	3994(1)	18(1)
N(1A)	675(3)	4310(2)	4901(2)	26(1)
N(2A)	2322(3)	3105(2)	4596(2)	27(1)
N(3A)	735(3)	3029(2)	3423(2)	25(1)
C(2A)	1403(3)	4667(2)	2697(2)	25(1)
C(3A)	1226(3)	5349(2)	3369(3)	27(1)
B(4A)	2180(4)	5394(3)	3990(3)	34(1)
B(5A)	3072(4)	4658(3)	3626(3)	35(1)
B(6A)	2506(4)	4173(3)	2801(3)	27(1)
B(7A)	1474(5)	5731(3)	2425(3)	34(1)
B(8A)	1991(4)	6211(3)	3269(3)	42(1)
B(9A)	3175(4)	5773(3)	3408(3)	41(1)
B(10A)	3391(4)	5006(3)	2664(3)	38(1)
B(11A)	2323(4)	4965(3)	2052(3)	32(1)
B(12A)	2737(4)	5969(3)	2435(3)	37(1)
C(13A)	167(4)	5116(3)	5085(3)	42(1)
C(14A)	485(3)	3740(3)	5587(2)	40(1)
C(15A)	2580(4)	2227(3)	4385(3)	49(1)
C(16A)	2911(3)	3420(3)	5259(3)	36(1)
C(17A)	20(3)	2540(2)	3900(3)	38(1)
C(18A)	599(3)	2774(3)	2599(2)	30(1)
Nb(1B)	6531(1)	6155(1)	3938(1)	20(1)
N(1B)	5733(3)	5651(2)	4814(2)	32(1)
N(2B)	7321(3)	6915(2)	4607(2)	26(1)
N(3B)	5766(3)	7065(2)	3382(2)	27(1)
C(2B)	6395(3)	5335(2)	2686(2)	23(1)
C(3B)	6451(4)	4689(3)	3386(3)	32(1)
B(4B)	7504(3)	4818(3)	3919(3)	30(1)
B(5B)	8165(3)	5639(3)	3433(3)	27(1)
B(6B)	7390(3)	5974(3)	2658(3)	25(1)
B(7B)	6609(5)	4275(3)	2452(3)	34(1)
B(8B)	7365(4)	3938(3)	3264(3)	37(1)
B(9B)	8470(4)	4550(3)	3260(3)	34(1)
B(10B)	8404(4)	5269(3)	2457(3)	32(1)
B(11B)	7256(4)	5114(3)	1969(3)	30(1)
B(12B)	7915(4)	4216(3)	2350(3)	36(1)
C(13B)	5120(4)	6242(4)	5258(3)	63(2)
C(14B)	5585(4)	4784(3)	5138(3)	45(1)
C(15B)	7849(4)	7662(3)	4308(3)	49(1)
C(16B)	7743(4)	6664(3)	5364(3)	42(1)
C(17B)	5450(4)	7821(3)	3848(3)	58(2)
C(18B)	5421(4)	7205(3)	2574(3)	32(1)

Table 3. Bond lengths [Å] and angles [°] for (16).

Nb(1A)-N(2A)	1.958(3)	B(5A)-B(9A)	1.786(7)	N(3B)-C(17B)	1.483(5)
Nb(1A)-N(3A)	1.980(3)	B(6A)-B(10A)	1.778(7)	C(2B)-C(3B)	1.558(6)
Nb(1A)-N(1A)	2.000(3)	B(6A)-B(11A)	1.788(7)	C(2B)-B(6B)	1.671(6)
Nb(1A)-B(6A)	2.460(5)	B(7A)-B(12A)	1.740(8)	C(2B)-B(11B)	1.714(7)
Nb(1A)-B(4A)	2.484(4)	B(7A)-B(8A)	1.757(7)	C(2B)-B(7B)	1.727(6)
Nb(1A)-B(5A)	2.485(5)	B(7A)-B(11A)	1.771(8)	C(3B)-B(4B)	1.692(7)
Nb(1A)-C(2A)	2.496(4)	B(8A)-B(9A)	1.750(8)	C(3B)-B(8B)	1.712(7)
Nb(1A)-C(3A)	2.510(4)	B(8A)-B(12A)	1.773(8)	C(3B)-B(7B)	1.722(6)
N(1A)-C(13A)	1.466(5)	B(9A)-B(10A)	1.762(8)	B(4B)-B(5B)	1.764(6)
N(1A)-C(14A)	1.487(5)	B(9A)-B(12A)	1.777(7)	B(4B)-B(9B)	1.763(7)
N(2A)-C(15A)	1.459(5)	B(10A)-B(11A)	1.773(8)	B(4B)-B(8B)	1.777(6)
N(2A)-C(16A)	1.460(5)	B(10A)-B(12A)	1.786(7)	B(5B)-B(6B)	1.756(6)
N(3A)-C(18A)	1.463(5)	B(11A)-B(12A)	1.786(8)	B(5B)-B(9B)	1.774(6)
N(3A)-C(17A)	1.470(5)	Nb(1B)-N(2B)	1.955(3)	B(5B)-B(10B)	1.780(6)
C(2A)-C(3A)	1.577(6)	Nb(1B)-N(3B)	1.992(3)	B(6B)-B(10B)	1.786(7)
C(2A)-B(6A)	1.682(7)	Nb(1B)-N(1B)	1.994(4)	B(6B)-B(11B)	1.790(7)
C(2A)-B(11A)	1.715(7)	Nb(1B)-B(4B)	2.465(4)	B(7B)-B(12B)	1.768(9)
C(2A)-B(7A)	1.727(6)	Nb(1B)-B(6B)	2.471(4)	B(7B)-B(11B)	1.773(7)
C(3A)-B(4A)	1.661(6)	Nb(1B)-C(3B)	2.475(4)	B(7B)-B(8B)	1.790(7)
C(3A)-B(8A)	1.703(6)	Nb(1B)-C(2B)	2.482(4)	B(8B)-B(9B)	1.769(7)
C(3A)-B(7A)	1.738(6)	Nb(1B)-B(5B)	2.493(4)	B(8B)-B(12B)	1.771(8)
B(4A)-B(9A)	1.764(7)	N(1B)-C(13B)	1.448(6)	B(9B)-B(10B)	1.765(7)
B(4A)-B(5A)	1.773(7)	N(1B)-C(14B)	1.474(6)	B(9B)-B(12B)	1.791(7)
B(4A)-B(8A)	1.784(7)	N(2B)-C(16B)	1.455(6)	B(10B)-B(11B)	1.770(7)
B(5A)-B(6A)	1.762(7)	N(2B)-C(15B)	1.457(6)	B(10B)-B(12B)	1.780(7)
B(5A)-B(10A)	1.770(7)	N(3B)-C(18B)	1.461(5)	B(11B)-B(12B)	1.780(7)
N(2A)-Nb(1A)-N(3A)	95.61(14)	C(3A)-C(2A)-Nb(1A)	72.1(2)	B(11A)-B(6A)-Nb(1A)	128.4(3)
N(2A)-Nb(1A)-N(1A)	96.55(14)	B(6A)-C(2A)-Nb(1A)	69.0(2)	C(2A)-B(7A)-C(3A)	54.1(2)
N(3A)-Nb(1A)-N(1A)	107.29(15)	B(11A)-C(2A)-Nb(1A)	130.4(3)	C(2A)-B(7A)-B(12A)	104.9(4)
N(2A)-Nb(1A)-B(6A)	103.2(2)	B(7A)-C(2A)-Nb(1A)	133.3(3)	C(3A)-B(7A)-B(12A)	104.6(4)
N(3A)-Nb(1A)-B(6A)	90.1(2)	C(2A)-C(3A)-B(4A)	111.6(3)	C(2A)-B(7A)-B(8A)	102.4(3)
N(1A)-Nb(1A)-B(6A)	152.32(15)	C(2A)-C(3A)-B(8A)	111.8(4)	C(3A)-B(7A)-B(8A)	58.3(3)
N(2A)-Nb(1A)-B(4A)	113.5(2)	B(4A)-C(3A)-B(8A)	64.0(3)	B(12A)-B(7A)-B(8A)	60.9(3)
N(3A)-Nb(1A)-B(4A)	147.1(2)	C(2A)-C(3A)-B(7A)	62.6(3)	C(2A)-B(7A)-B(11A)	58.7(3)
N(1A)-Nb(1A)-B(4A)	85.3(2)	B(4A)-C(3A)-B(7A)	114.8(4)	C(3A)-B(7A)-B(11A)	102.7(3)
B(6A)-Nb(1A)-B(4A)	69.2(2)	B(8A)-C(3A)-B(7A)	61.4(3)	B(12A)-B(7A)-B(11A)	61.1(3)
N(2A)-Nb(1A)-B(5A)	87.6(2)	C(2A)-C(3A)-Nb(1A)	71.2(2)	B(8A)-B(7A)-B(11A)	108.8(4)
N(3A)-Nb(1A)-B(5A)	130.5(2)	B(4A)-C(3A)-Nb(1A)	69.8(2)	C(3A)-B(8A)-B(9A)	103.2(3)
N(1A)-Nb(1A)-B(5A)	121.5(2)	B(8A)-C(3A)-Nb(1A)	131.1(3)	C(3A)-B(8A)-B(7A)	60.3(3)
B(6A)-Nb(1A)-B(5A)	41.8(2)	B(7A)-C(3A)-Nb(1A)	131.7(3)	B(9A)-B(8A)-B(7A)	107.7(4)
B(4A)-Nb(1A)-B(5A)	41.8(2)	C(3A)-B(4A)-B(9A)	104.3(3)	C(3A)-B(8A)-B(12A)	104.7(4)
N(2A)-Nb(1A)-C(2A)	142.53(15)	C(3A)-B(4A)-B(5A)	106.1(3)	B(9A)-B(8A)-B(12A)	60.6(3)
N(3A)-Nb(1A)-C(2A)	82.54(13)	B(9A)-B(4A)-B(5A)	60.7(3)	B(7A)-B(8A)-B(12A)	59.1(3)
N(1A)-Nb(1A)-C(2A)	119.86(14)	C(3A)-B(4A)-B(8A)	59.1(3)	C(3A)-B(8A)-B(4A)	56.8(3)
B(6A)-Nb(1A)-C(2A)	39.7(2)	B(9A)-B(4A)-B(8A)	59.1(3)	B(9A)-B(8A)-B(4A)	59.9(3)
B(4A)-Nb(1A)-C(2A)	65.1(2)	B(5A)-B(4A)-B(8A)	108.9(4)	B(7A)-B(8A)-B(4A)	107.9(3)
B(5A)-Nb(1A)-C(2A)	66.8(2)	C(3A)-B(4A)-Nb(1A)	71.4(2)	B(12A)-B(8A)-B(4A)	108.2(4)
N(2A)-Nb(1A)-C(3A)	151.73(14)	B(9A)-B(4A)-Nb(1A)	126.2(3)	B(8A)-B(9A)-B(10A)	108.6(4)
N(3A)-Nb(1A)-C(3A)	109.77(14)	B(5A)-B(4A)-Nb(1A)	69.1(2)	B(8A)-B(9A)-B(4A)	61.0(3)
N(1A)-Nb(1A)-C(3A)	87.82(14)	B(8A)-B(4A)-Nb(1A)	128.0(3)	B(10A)-B(9A)-B(4A)	107.2(3)
B(6A)-Nb(1A)-C(3A)	65.70(15)	B(6A)-B(5A)-B(10A)	60.4(3)	B(8A)-B(9A)-B(12A)	60.3(3)
B(4A)-Nb(1A)-C(3A)	38.85(15)	B(6A)-B(5A)-B(4A)	105.1(3)	B(10A)-B(9A)-B(12A)	60.6(3)
B(5A)-Nb(1A)-C(3A)	66.7(2)	B(10A)-B(5A)-B(4A)	106.5(4)	B(4A)-B(9A)-B(12A)	108.9(3)
C(2A)-Nb(1A)-C(3A)	36.72(13)	B(6A)-B(5A)-B(9A)	106.7(3)	B(8A)-B(9A)-B(5A)	109.8(3)
C(13A)-N(1A)-C(14A)	105.6(3)	B(10A)-B(5A)-B(9A)	59.4(3)	B(10A)-B(9A)-B(5A)	59.8(3)
C(13A)-N(1A)-Nb(1A)	133.7(3)	B(4A)-B(5A)-B(9A)	59.4(3)	B(4A)-B(9A)-B(5A)	59.9(3)
C(14A)-N(1A)-Nb(1A)	120.7(3)	B(6A)-B(5A)-Nb(1A)	68.4(2)	B(12A)-B(9A)-B(5A)	109.5(4)
C(15A)-N(2A)-C(16A)	112.1(4)	B(10A)-B(5A)-Nb(1A)	125.4(3)	B(9A)-B(10A)-B(5A)	60.8(3)
C(15A)-N(2A)-Nb(1A)	127.8(3)	B(4A)-B(5A)-Nb(1A)	69.1(2)	B(9A)-B(10A)-B(11A)	108.0(4)
C(16A)-N(2A)-Nb(1A)	119.1(3)	B(9A)-B(5A)-Nb(1A)	125.0(3)	B(5A)-B(10A)-B(11A)	109.3(3)
C(18A)-N(3A)-C(17A)	107.5(3)	C(2A)-B(6A)-B(5A)	105.5(3)	B(9A)-B(10A)-B(6A)	107.1(3)
C(18A)-N(3A)-Nb(1A)	136.2(3)	C(2A)-B(6A)-B(10A)	104.0(3)	B(5A)-B(10A)-B(6A)	59.6(3)
C(17A)-N(3A)-Nb(1A)	115.9(3)	B(5A)-B(6A)-B(10A)	60.0(3)	B(11A)-B(10A)-B(6A)	60.5(3)
C(3A)-C(2A)-B(6A)	111.6(3)	C(2A)-B(6A)-B(11A)	59.1(3)	B(9A)-B(10A)-B(12A)	60.1(3)
C(3A)-C(2A)-B(11A)	112.6(3)	B(5A)-B(6A)-B(11A)	108.9(3)	B(5A)-B(10A)-B(12A)	109.9(4)
B(6A)-C(2A)-B(11A)	63.5(3)	B(10A)-B(6A)-B(11A)	59.6(3)	B(11A)-B(10A)-B(12A)	60.2(3)
C(3A)-C(2A)-B(7A)	63.3(3)	C(2A)-B(6A)-Nb(1A)	71.3(2)	B(6A)-B(10A)-B(12A)	108.4(4)
B(6A)-C(2A)-B(7A)	114.9(4)	B(5A)-B(6A)-Nb(1A)	69.9(2)	C(2A)-B(11A)-B(7A)	59.4(3)
B(11A)-C(2A)-B(7A)	61.9(3)	B(10A)-B(6A)-Nb(1A)	126.4(3)	C(2A)-B(11A)-B(10A)	102.8(3)

Appendix A – Crystal Data

B(7A)-B(11A)-B(10A)	106.9(4)	C(3B)-C(2B)-B(6B)	111.7(3)	B(12B)-B(7B)-B(11B)	60.4(3)
C(2A)-B(11A)-B(12A)	103.4(4)	C(3B)-C(2B)-B(11B)	112.1(3)	C(3B)-B(7B)-B(8B)	58.3(3)
B(7A)-B(11A)-B(12A)	58.6(3)	B(6B)-C(2B)-B(11B)	63.8(3)	C(2B)-B(7B)-B(8B)	101.6(3)
B(10A)-B(11A)-B(12A)	60.2(3)	C(3B)-C(2B)-B(7B)	63.0(3)	B(12B)-B(7B)-B(8B)	59.7(3)
C(2A)-B(11A)-B(6A)	57.3(3)	B(6B)-C(2B)-B(7B)	115.6(4)	B(11B)-B(7B)-B(8B)	107.1(4)
B(7A)-B(11A)-B(6A)	107.7(4)	B(11B)-C(2B)-B(7B)	62.0(3)	C(3B)-B(8B)-B(9B)	103.5(3)
B(10A)-B(11A)-B(6A)	59.9(3)	C(3B)-C(2B)-Nb(1B)	71.4(2)	C(3B)-B(8B)-B(12B)	103.7(3)
B(12A)-B(11A)-B(6A)	107.9(4)	B(6B)-C(2B)-Nb(1B)	69.9(2)	B(9B)-B(8B)-B(12B)	60.8(3)
B(7A)-B(12A)-B(8A)	60.0(3)	B(11B)-C(2B)-Nb(1B)	131.2(3)	C(3B)-B(8B)-B(4B)	58.0(3)
B(7A)-B(12A)-B(9A)	107.2(4)	B(7B)-C(2B)-Nb(1B)	132.7(3)	B(9B)-B(8B)-B(4B)	59.6(3)
B(8A)-B(12A)-B(9A)	59.1(3)	C(2B)-C(3B)-B(4B)	111.6(3)	B(12B)-B(8B)-B(4B)	108.1(3)
B(7A)-B(12A)-B(11A)	60.3(3)	C(2B)-C(3B)-B(8B)	112.8(4)	C(3B)-B(8B)-B(7B)	58.9(3)
B(8A)-B(12A)-B(11A)	107.4(4)	B(4B)-C(3B)-B(8B)	62.9(3)	B(9B)-B(8B)-B(7B)	108.4(4)
B(9A)-B(12A)-B(11A)	106.8(3)	C(2B)-C(3B)-B(7B)	63.3(3)	B(12B)-B(8B)-B(7B)	59.5(3)
B(7A)-B(12A)-B(10A)	107.7(3)	B(4B)-C(3B)-B(7B)	115.5(4)	B(4B)-B(8B)-B(7B)	108.1(3)
B(8A)-B(12A)-B(10A)	106.6(4)	B(8B)-C(3B)-B(7B)	62.8(3)	B(4B)-B(9B)-B(10B)	107.4(3)
B(9A)-B(12A)-B(10A)	59.3(3)	C(2B)-C(3B)-Nb(1B)	71.9(2)	B(4B)-B(9B)-B(8B)	60.4(3)
B(11A)-B(12A)-B(10A)	59.5(3)	B(4B)-C(3B)-Nb(1B)	69.6(2)	B(10B)-B(9B)-B(8B)	107.7(3)
N(2B)-Nb(1B)-N(3B)	96.98(15)	B(8B)-C(3B)-Nb(1B)	130.4(3)	B(4B)-B(9B)-B(5B)	59.8(2)
N(2B)-Nb(1B)-N(1B)	95.80(15)	B(7B)-C(3B)-Nb(1B)	133.5(3)	B(10B)-B(9B)-B(5B)	60.4(2)
N(3B)-Nb(1B)-N(1B)	110.8(2)	C(3B)-B(4B)-B(5B)	105.1(3)	B(8B)-B(9B)-B(5B)	108.9(3)
N(2B)-Nb(1B)-B(4B)	103.47(15)	C(3B)-B(4B)-B(9B)	104.6(3)	B(4B)-B(9B)-B(12B)	107.8(4)
N(3B)-Nb(1B)-B(4B)	150.8(2)	B(5B)-B(4B)-B(9B)	60.4(3)	B(10B)-B(9B)-B(12B)	60.1(3)
N(1B)-Nb(1B)-B(4B)	87.8(2)	C(3B)-B(4B)-B(8B)	59.1(3)	B(8B)-B(9B)-B(12B)	59.7(3)
N(2B)-Nb(1B)-B(6B)	108.84(14)	B(5B)-B(4B)-B(8B)	109.0(3)	B(5B)-B(9B)-B(12B)	109.0(3)
N(3B)-Nb(1B)-B(6B)	84.78(15)	B(9B)-B(4B)-B(8B)	60.0(3)	B(9B)-B(10B)-B(11B)	108.5(4)
N(1B)-Nb(1B)-B(6B)	149.2(2)	C(3B)-B(4B)-Nb(1B)	70.3(2)	B(9B)-B(10B)-B(5B)	60.1(2)
B(4B)-Nb(1B)-B(6B)	69.1(2)	B(5B)-B(4B)-Nb(1B)	70.0(2)	B(11B)-B(10B)-B(5B)	108.7(4)
N(2B)-Nb(1B)-C(3B)	143.5(2)	B(9B)-B(4B)-Nb(1B)	127.0(3)	B(9B)-B(10B)-B(12B)	60.7(3)
N(3B)-Nb(1B)-C(3B)	117.4(2)	B(8B)-B(4B)-Nb(1B)	127.4(3)	B(11B)-B(10B)-B(12B)	60.2(3)
N(1B)-Nb(1B)-C(3B)	83.81(15)	B(6B)-B(5B)-B(4B)	105.4(3)	B(5B)-B(10B)-B(12B)	109.2(3)
B(4B)-Nb(1B)-C(3B)	40.1(2)	B(6B)-B(5B)-B(9B)	107.4(3)	B(9B)-B(10B)-B(6B)	106.5(3)
B(6B)-Nb(1B)-C(3B)	65.42(15)	B(4B)-B(5B)-B(9B)	59.8(3)	B(11B)-B(10B)-B(6B)	60.5(3)
N(2B)-Nb(1B)-C(2B)	147.99(14)	B(6B)-B(5B)-B(10B)	60.7(3)	B(5B)-B(10B)-B(6B)	59.0(2)
N(3B)-Nb(1B)-C(2B)	85.79(13)	B(4B)-B(5B)-B(10B)	106.7(3)	B(12B)-B(10B)-B(6B)	107.9(4)
N(1B)-Nb(1B)-C(2B)	113.07(14)	B(9B)-B(5B)-B(10B)	59.6(3)	C(2B)-B(11B)-B(10B)	103.3(3)
B(4B)-Nb(1B)-C(2B)	65.88(14)	B(6B)-B(5B)-Nb(1B)	68.6(2)	C(2B)-B(11B)-B(7B)	59.4(3)
B(6B)-Nb(1B)-C(2B)	39.44(14)	B(4B)-B(5B)-Nb(1B)	68.3(2)	B(10B)-B(11B)-B(7B)	108.3(4)
C(3B)-Nb(1B)-C(2B)	36.64(13)	B(9B)-B(5B)-Nb(1B)	124.8(3)	C(2B)-B(11B)-B(12B)	103.8(4)
N(2B)-Nb(1B)-B(5B)	85.13(14)	B(10B)-B(5B)-Nb(1B)	125.6(3)	B(10B)-B(11B)-B(12B)	60.2(3)
N(3B)-Nb(1B)-B(5B)	121.65(15)	C(2B)-B(6B)-B(5B)	106.1(3)	B(7B)-B(11B)-B(12B)	59.7(3)
N(1B)-Nb(1B)-B(5B)	127.1(2)	C(2B)-B(6B)-B(10B)	104.4(3)	C(2B)-B(11B)-B(6B)	56.9(2)
B(4B)-Nb(1B)-B(5B)	41.7(2)	B(5B)-B(6B)-B(10B)	60.3(3)	B(10B)-B(11B)-B(6B)	60.2(3)
B(6B)-Nb(1B)-B(5B)	41.42(15)	C(2B)-B(6B)-B(11B)	59.3(3)	B(7B)-B(11B)-B(6B)	107.7(4)
C(3B)-Nb(1B)-B(5B)	67.1(2)	B(5B)-B(6B)-B(11B)	108.9(3)	B(12B)-B(11B)-B(6B)	107.7(3)
C(2B)-Nb(1B)-B(5B)	66.80(14)	B(10B)-B(6B)-B(11B)	59.3(3)	B(7B)-B(12B)-B(8B)	60.8(3)
C(13B)-N(1B)-C(14B)	108.4(4)	C(2B)-B(6B)-Nb(1B)	70.6(2)	B(7B)-B(12B)-B(10B)	108.0(3)
C(13B)-N(1B)-Nb(1B)	116.2(3)	B(5B)-B(6B)-Nb(1B)	69.9(2)	B(8B)-B(12B)-B(10B)	107.0(3)
C(14B)-N(1B)-Nb(1B)	135.4(3)	B(10B)-B(6B)-Nb(1B)	126.5(3)	B(7B)-B(12B)-B(11B)	59.9(3)
C(16B)-N(2B)-C(15B)	109.4(4)	B(11B)-B(6B)-Nb(1B)	127.6(3)	B(8B)-B(12B)-B(11B)	107.6(4)
C(16B)-N(2B)-Nb(1B)	124.0(3)	C(3B)-B(7B)-C(2B)	53.7(2)	B(10B)-B(12B)-B(11B)	59.6(3)
C(15B)-N(2B)-Nb(1B)	123.4(3)	C(3B)-B(7B)-B(12B)	103.4(4)	B(7B)-B(12B)-B(9B)	108.4(4)
C(18B)-N(3B)-C(17B)	106.7(3)	C(2B)-B(7B)-B(12B)	103.8(4)	B(8B)-B(12B)-B(9B)	59.6(3)
C(18B)-N(3B)-Nb(1B)	135.5(3)	C(3B)-B(7B)-B(11B)	101.9(3)	B(10B)-B(12B)-B(9B)	59.2(3)
C(17B)-N(3B)-Nb(1B)	117.7(3)	C(2B)-B(7B)-B(11B)	58.6(3)	B(11B)-B(12B)-B(9B)	106.9(3)

Table 4. Anisotropic displacement parameters ($\text{\AA}^2 \times 10^3$) for (16). The anisotropic displacement factor exponent takes the form: $-2\pi^2 [h^2 a^{*2} U^{11} + \dots + 2 h k a^* b^* U^{12}]$

	U ¹¹	U ²²	U ³³	U ²³	U ¹³	U ¹²
Nb(1A)	16(1)	19(1)	20(1)	1(1)	-1(1)	-1(1)
N(1A)	24(2)	30(2)	25(2)	-3(1)	2(1)	1(1)
N(2A)	26(2)	27(2)	29(2)	8(1)	-3(2)	2(2)
N(3A)	25(2)	24(2)	24(2)	0(1)	1(1)	-4(1)
C(2A)	22(2)	23(2)	29(2)	2(1)	-5(2)	-5(2)
C(3A)	26(2)	18(2)	37(2)	0(2)	1(2)	-1(1)
B(4A)	38(3)	33(2)	30(2)	0(2)	-7(2)	-17(2)
B(5A)	24(2)	47(3)	34(3)	11(2)	-9(2)	-7(2)
B(6A)	21(2)	27(2)	34(2)	5(2)	4(2)	2(2)
B(7A)	36(3)	27(2)	40(3)	10(2)	-7(3)	-5(2)
B(8A)	52(3)	26(2)	47(3)	4(2)	-3(2)	-14(2)
B(9A)	38(3)	47(3)	37(3)	11(2)	-14(2)	-22(2)
B(10A)	20(2)	53(3)	41(3)	17(2)	2(2)	-8(2)
B(11A)	30(3)	40(3)	26(2)	8(2)	-4(2)	-8(2)
B(12A)	36(3)	39(3)	36(3)	12(2)	-4(2)	-14(2)
C(13A)	48(3)	43(2)	35(2)	-6(2)	5(2)	13(2)
C(14A)	39(2)	51(3)	31(2)	0(2)	7(2)	-6(2)
C(15A)	61(3)	39(2)	45(3)	3(2)	-7(3)	20(2)
C(16A)	28(2)	43(2)	36(2)	9(2)	-12(2)	-2(2)
C(17A)	41(2)	35(2)	39(2)	-1(2)	4(2)	-18(2)
C(18A)	30(2)	25(2)	34(2)	-6(2)	-3(2)	-1(2)
Nb(1B)	17(1)	20(1)	23(1)	-1(1)	-1(1)	1(1)
N(1B)	22(2)	38(2)	36(2)	4(2)	-1(2)	-2(2)
N(2B)	24(2)	32(2)	23(2)	-7(1)	5(2)	-1(2)
N(3B)	23(2)	28(2)	31(2)	1(1)	1(2)	7(1)
C(2B)	18(2)	27(2)	25(2)	0(1)	-7(2)	-2(2)
C(3B)	36(2)	26(2)	34(2)	1(1)	4(2)	-9(2)
B(4B)	34(2)	26(2)	29(2)	0(2)	-7(2)	5(2)
B(5B)	19(2)	30(2)	31(2)	-4(2)	-4(2)	2(2)
B(6B)	21(2)	27(2)	27(2)	-4(2)	1(2)	-1(2)
B(7B)	41(3)	26(2)	35(2)	-9(2)	-7(2)	-3(2)
B(8B)	51(3)	21(2)	38(2)	-1(2)	-9(2)	5(2)
B(9B)	27(2)	34(2)	40(2)	-10(2)	-10(2)	10(2)
B(10B)	24(2)	41(2)	31(2)	-11(2)	2(2)	3(2)
B(11B)	29(2)	30(2)	31(3)	-6(2)	-3(2)	3(2)
B(12B)	36(3)	30(2)	42(3)	-9(2)	-5(2)	10(2)
C(13B)	58(3)	63(3)	67(3)	6(3)	37(3)	10(3)
C(14B)	44(3)	50(3)	40(3)	11(2)	3(2)	-16(2)
C(15B)	58(3)	49(3)	40(3)	-11(2)	3(2)	-30(2)
C(16B)	38(3)	43(2)	44(3)	-13(2)	-15(2)	4(2)
C(17B)	80(4)	55(3)	39(3)	0(2)	6(3)	39(3)
C(18B)	34(2)	30(2)	33(2)	3(2)	-6(2)	3(2)

Appendix A – Crystal Data

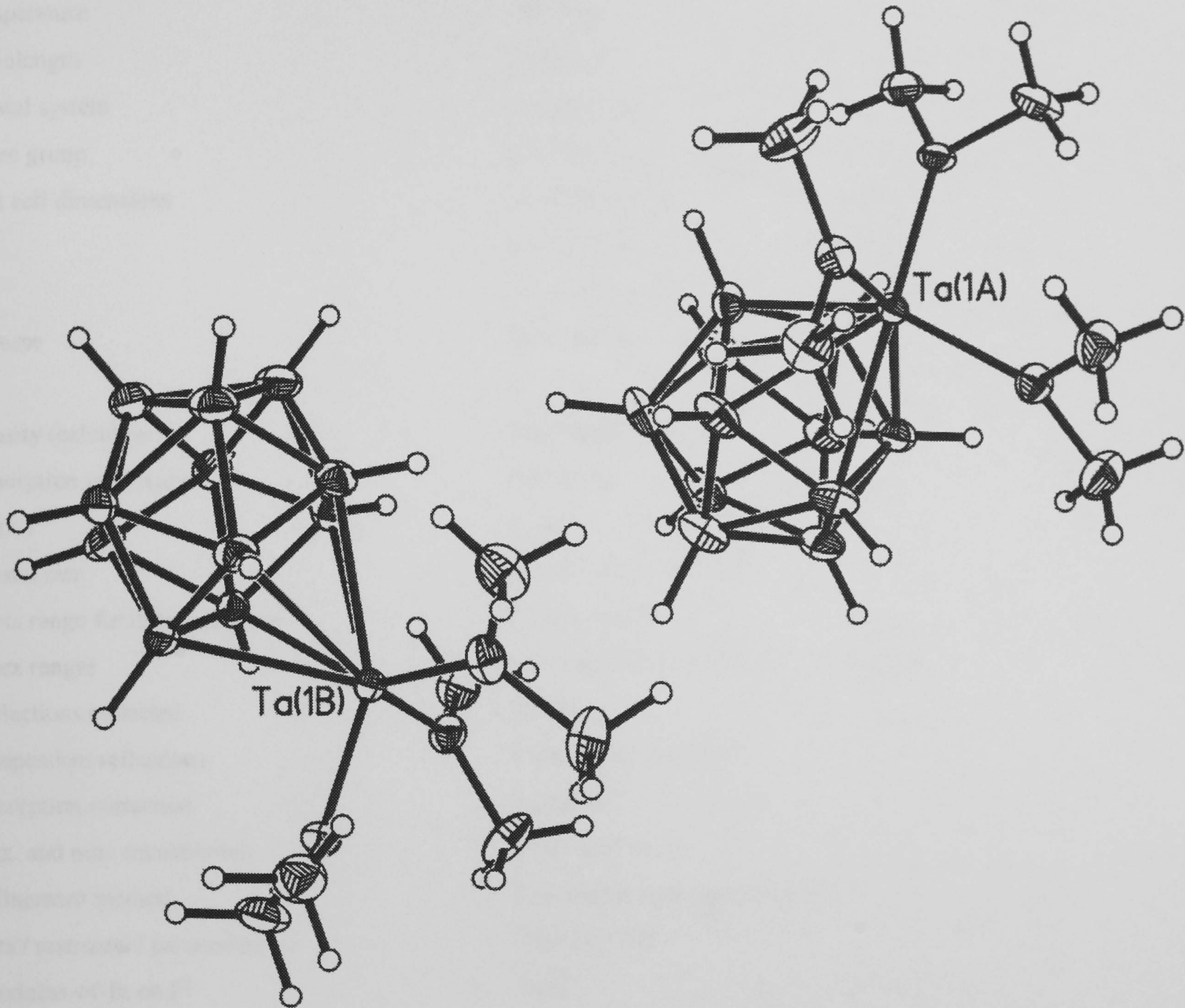
Table 5. Hydrogen coordinates (x 10⁴) and isotropic displacement parameters (Å²x 10³) for (16).

	x	y	z	U(eq)
H(2A)	966(31)	4486(27)	2517(26)	23(12)
H(3A)	570(26)	5441(21)	3545(20)	14(9)
H(4A)	2117(26)	5530(22)	4593(22)	20(9)
H(5A)	3643(30)	4370(24)	3986(24)	38(11)
H(6A)	2569(29)	3624(25)	2558(21)	23(10)
H(7A)	875(32)	5969(28)	2078(25)	40(12)
H(8A)	1747(29)	6875(24)	3444(22)	33(11)
H(9A)	3700(40)	6121(34)	3649(30)	74(16)
H(10A)	4143(28)	4824(23)	2362(23)	25(10)
H(11A)	2203(32)	4812(26)	1489(27)	33(12)
H(12A)	3091(26)	6498(23)	2114(21)	22(10)
H(31A)	315(19)	5526(14)	4690(14)	67(9)
H(32A)	385(18)	5321(12)	5582(17)	67(9)
H(33A)	-528(20)	5023(6)	5101(18)	67(9)
H(41A)	851(18)	3198(15)	5516(8)	55(8)
H(42A)	-234(17)	3619(14)	5621(10)	55(8)
H(43A)	707(19)	4021(10)	6078(12)	55(8)
H(51A)	2118(18)	2015(9)	3994(17)	64(9)
H(52A)	2549(23)	1871(11)	4851(13)	64(9)
H(53A)	3246(19)	2214(4)	4172(18)	64(9)
H(61A)	2714(13)	4022(14)	5382(10)	32(6)
H(62A)	3633(16)	3402(14)	5119(6)	32(6)
H(63A)	2789(13)	3050(12)	5732(11)	32(6)
H(71A)	79(13)	2709(12)	4445(13)	41(7)
H(72A)	159(12)	1938(14)	3851(12)	41(7)
H(73A)	-644(16)	2654(13)	3717(11)	41(7)
H(81A)	1078(17)	3045(15)	2283(8)	37(7)
H(82A)	-37(17)	2938(15)	2432(7)	37(7)
H(83A)	666(19)	2179(14)	2553(4)	37(7)
H(2B)	5673(28)	5519(23)	2480(23)	19(10)
H(3B)	6007(35)	4544(31)	3537(29)	38
H(4B)	7477(26)	4679(21)	4510(21)	14(8)
H(5B)	8761(27)	6027(24)	3707(21)	30(10)
H(6B)	7372(26)	6670(22)	2402(20)	20(9)
H(7B)	6022(27)	3887(25)	2197(21)	23(10)
H(8B)	7234(33)	3402(29)	3502(25)	45(13)
H(9B)	9139(27)	4257(23)	3472(21)	25(10)
H(10B)	9069(31)	5482(27)	2134(25)	40(12)
H(11B)	7082(32)	5251(26)	1323(26)	37(13)
H(12B)	8226(30)	3790(27)	1998(23)	38(11)
H(31B)	5106(21)	6776(18)	4998(13)	80(11)
H(32B)	5386(16)	6312(17)	5770(17)	80(11)
H(33B)	4468(21)	6023(13)	5295(17)	80(11)
H(41B)	5958(20)	4379(12)	4836(13)	60(9)
H(42B)	4893(19)	4643(9)	5111(16)	60(9)
H(43B)	5800(21)	4768(6)	5677(16)	60(9)
H(51B)	7534(14)	7854(12)	3809(15)	49(8)
H(52B)	8553(18)	7514(6)	4208(15)	49(8)
H(53B)	7814(17)	8129(13)	4703(12)	49(8)
H(61B)	7331(15)	6237(18)	5601(10)	55(8)
H(62B)	7781(20)	7151(13)	5704(11)	55(8)
H(63B)	8394(19)	6436(17)	5282(4)	55(8)
H(71B)	5766(19)	7813(10)	4344(15)	58(8)
H(72B)	4755(18)	7808(10)	3919(14)	58(8)
H(73B)	5628(20)	8323(13)	3574(11)	58(8)
H(81B)	4696(19)	7185(19)	2557(4)	53(8)
H(82B)	5692(19)	6763(16)	2228(10)	53(8)
H(83B)	5648(19)	7767(16)	2395(8)	53(8)

A6 Crystal data for $[3\text{-Ta}(\text{NMe}_2)_3(1,2\text{-C}_2\text{B}_9\text{H}_{11})]$; (17).

Identification code
Empirical formula
Formula weight
Temperature
Wavelength
Crystal system
Space group
Unit cell dimensions

Volume
Z
Density
Absorption
F(000)
Crystal size
Theta range
Index range
Reflections
Independent reflections
R-intensity
Max. and min. ρ
Extinction
Data/restraints
Goodness of fit
Final R indices
Weighted R indices
Absolute structure
Large data sets: go to page 100



Appendix A – Crystal Data

Table 1. Crystal data and structure refinement for (17).

Identification code	97srv163	
Empirical formula	C8 H29 B9 N3 Ta	
Formula weight	445.58	
Temperature	150(2) K	
Wavelength	0.71073 Å	
Crystal system	Orthorhombic	
Space group	P2(1)2(1)2(1)	
Unit cell dimensions	a = 13.484(1) Å	α= 90°.
	b = 15.472(1) Å	β= 90°.
	c = 17.042(1) Å	γ = 90°.
Volume	3555.4(4) Å ³	
Z	8	
Density (calculated)	1.665 Mg/m ³	
Absorption coefficient	6.172 mm ⁻¹	
F(000)	1728	
Crystal size	0.50 x 0.45 x 0.40 mm ³	
Theta range for data collection	1.78 to 30.34°.	
Index ranges	-18<=h<=19, -19<=k<=21, -23<=l<=23	
Reflections collected	29543	
Independent reflections	9760 [R(int) = 0.0427]	
Absorption correction	Multiscan	
Max. and min. transmission	0.207 and 0.127	
Refinement method	Full-matrix least-squares on F ²	
Data / restraints / parameters	9744 / 0 / 502	
Goodness-of-fit on F ²	1.083	
Final R indices [I>2sigma(I)]	R1 = 0.0284, wR2 = 0.0621	
R indices (all data)	R1 = 0.0375, wR2 = 0.0687	
Absolute structure parameter	0.485(12)	
Largest diff. peak and hole	1.446 and -1.715 e.Å ⁻³	

Appendix A – Crystal Data

Table 2. Atomic coordinates (x 10⁴) and equivalent isotropic displacement parameters (Å²x 10³) for (17). U(eq) is defined as one third of the trace of the orthogonalized U^{ij} tensor.

	x	y	z	U(eq)
Ta(1A)	1522(1)	3937(1)	4002(1)	14(1)
N(1A)	690(4)	4329(3)	4896(3)	21(1)
N(2A)	2325(3)	3128(3)	4606(3)	20(1)
N(3A)	741(3)	3045(3)	3442(3)	19(1)
C(2A)	1420(4)	4665(3)	2702(3)	19(1)
C(3A)	1214(4)	5363(3)	3355(3)	23(1)
B(4A)	2171(5)	5443(4)	3988(4)	28(1)
B(5A)	3070(5)	4693(4)	3642(4)	27(1)
B(6A)	2529(5)	4188(4)	2825(4)	22(1)
B(7A)	1470(6)	5733(4)	2413(4)	26(1)
B(8A)	1967(5)	6242(4)	3250(4)	31(1)
B(9A)	3189(5)	5804(4)	3398(4)	32(2)
B(10A)	3403(5)	5032(4)	2684(4)	27(1)
B(11A)	2338(5)	4968(4)	2063(4)	25(1)
B(12A)	2736(5)	5990(4)	2434(4)	28(1)
C(13A)	152(5)	5139(4)	5045(4)	33(1)
C(14A)	506(5)	3772(4)	5584(3)	31(1)
C(15A)	2576(5)	2229(4)	4417(4)	35(2)
C(16A)	2931(5)	3444(4)	5255(4)	31(1)
C(17A)	24(5)	2561(4)	3921(4)	31(1)
C(18A)	617(5)	2781(4)	2628(3)	25(1)
Ta(1B)	6571(1)	6157(1)	3902(1)	15(1)
N(1B)	5773(4)	5640(3)	4758(3)	26(1)
N(2B)	7351(4)	6920(3)	4577(3)	22(1)
N(3B)	5792(4)	7077(3)	3372(3)	23(1)
C(2B)	6415(5)	5327(3)	2663(3)	22(1)
C(3B)	6483(5)	4675(3)	3367(3)	22(1)
B(4B)	7549(5)	4827(4)	3880(4)	23(1)
B(5B)	8195(4)	5662(4)	3389(4)	20(1)
B(6B)	7403(4)	5993(4)	2616(3)	19(1)
B(7B)	6653(6)	4258(4)	2438(4)	27(1)
B(8B)	7409(5)	3934(4)	3237(4)	28(1)
B(9B)	8503(5)	4555(3)	3212(3)	22(1)
B(10B)	8404(6)	5293(4)	2412(3)	25(1)
B(11B)	7256(5)	5118(4)	1941(4)	24(1)
B(12B)	7934(6)	4220(4)	2310(4)	29(1)
C(13B)	5118(5)	6224(5)	5194(4)	43(2)
C(14B)	5649(5)	4766(4)	5087(4)	35(2)
C(15B)	7885(5)	7666(4)	4268(4)	34(2)
C(16B)	7741(5)	6677(4)	5347(4)	35(1)
C(17B)	5494(5)	7851(4)	3830(4)	38(2)
C(18B)	5411(5)	7195(4)	2575(3)	30(1)

Appendix A – Crystal Data

Table 3. Bond lengths [Å] and angles [°] for 97srv163.

Ta(1A)-N(2A)	1.949(4)	B(5A)-B(9A)	1.776(10)	N(3B)-C(17B)	1.485(7)
Ta(1A)-N(3A)	1.980(4)	B(6A)-B(10A)	1.775(9)	C(2B)-C(3B)	1.570(7)
Ta(1A)-N(1A)	1.987(5)	B(6A)-B(11A)	1.791(9)	C(2B)-B(6B)	1.686(8)
Ta(1A)-B(6A)	2.453(6)	B(7A)-B(12A)	1.753(10)	C(2B)-B(11B)	1.704(9)
Ta(1A)-B(5A)	2.470(7)	B(7A)-B(8A)	1.762(9)	C(2B)-B(7B)	1.728(8)
Ta(1A)-B(4A)	2.489(6)	B(7A)-B(11A)	1.768(10)	C(3B)-B(4B)	1.699(9)
Ta(1A)-C(2A)	2.490(5)	B(8A)-B(12A)	1.779(10)	C(3B)-B(8B)	1.710(9)
Ta(1A)-C(3A)	2.501(5)	B(8A)-B(9A)	1.799(10)	C(3B)-B(7B)	1.726(8)
N(1A)-C(13A)	1.470(7)	B(9A)-B(10A)	1.730(10)	B(4B)-B(9B)	1.768(9)
N(1A)-C(14A)	1.477(7)	B(9A)-B(12A)	1.776(9)	B(4B)-B(5B)	1.769(9)
N(2A)-C(16A)	1.460(7)	B(10A)-B(12A)	1.785(10)	B(4B)-B(8B)	1.775(9)
N(2A)-C(15A)	1.466(7)	B(10A)-B(11A)	1.787(10)	B(5B)-B(6B)	1.771(8)
N(3A)-C(18A)	1.456(7)	B(11A)-B(12A)	1.785(10)	B(5B)-B(10B)	1.782(8)
N(3A)-C(17A)	1.469(7)	Ta(1B)-N(2B)	1.955(4)	B(5B)-B(9B)	1.789(8)
C(2A)-C(3A)	1.576(7)	Ta(1B)-N(1B)	1.981(5)	B(6B)-B(10B)	1.765(9)
C(2A)-B(6A)	1.681(9)	Ta(1B)-N(3B)	1.987(5)	B(6B)-B(11B)	1.788(9)
C(2A)-B(11A)	1.713(9)	Ta(1B)-B(4B)	2.444(6)	B(7B)-B(12B)	1.741(11)
C(2A)-B(7A)	1.726(7)	Ta(1B)-C(3B)	2.470(5)	B(7B)-B(8B)	1.773(9)
C(3A)-B(4A)	1.685(9)	Ta(1B)-B(6B)	2.475(5)	B(7B)-B(11B)	1.774(10)
C(3A)-B(8A)	1.706(8)	Ta(1B)-B(5B)	2.478(6)	B(8B)-B(9B)	1.761(9)
C(3A)-B(7A)	1.739(8)	Ta(1B)-C(2B)	2.480(5)	B(8B)-B(12B)	1.787(10)
B(4A)-B(5A)	1.779(10)	N(1B)-C(13B)	1.467(8)	B(9B)-B(10B)	1.783(8)
B(4A)-B(8A)	1.784(10)	N(1B)-C(14B)	1.474(8)	B(9B)-B(12B)	1.795(9)
B(4A)-B(9A)	1.791(10)	N(2B)-C(15B)	1.459(7)	B(10B)-B(11B)	1.765(10)
B(5A)-B(6A)	1.756(9)	N(2B)-C(16B)	1.464(8)	B(10B)-B(12B)	1.786(9)
B(5A)-B(10A)	1.772(9)	N(3B)-C(18B)	1.463(7)	B(11B)-B(12B)	1.777(9)
N(2A)-Ta(1A)-N(3A)	95.9(2)	C(3A)-C(2A)-Ta(1A)	72.0(3)	B(11A)-B(6A)-Ta(1A)	128.3(4)
N(2A)-Ta(1A)-N(1A)	96.0(2)	B(6A)-C(2A)-Ta(1A)	68.9(3)	C(2A)-B(7A)-C(3A)	54.1(3)
N(3A)-Ta(1A)-N(1A)	106.4(2)	B(11A)-C(2A)-Ta(1A)	130.5(4)	C(2A)-B(7A)-B(12A)	104.4(5)
N(2A)-Ta(1A)-B(6A)	103.1(2)	B(7A)-C(2A)-Ta(1A)	133.2(3)	C(3A)-B(7A)-B(12A)	104.4(5)
N(3A)-Ta(1A)-B(6A)	90.6(2)	C(2A)-C(3A)-B(4A)	111.5(5)	C(2A)-B(7A)-B(8A)	102.2(4)
N(1A)-Ta(1A)-B(6A)	153.0(2)	C(2A)-C(3A)-B(8A)	111.5(5)	C(3A)-B(7A)-B(8A)	58.3(3)
N(2A)-Ta(1A)-B(5A)	88.1(2)	B(4A)-C(3A)-B(8A)	63.5(4)	B(12A)-B(7A)-B(8A)	60.8(4)
N(3A)-Ta(1A)-B(5A)	131.3(2)	C(2A)-C(3A)-B(7A)	62.5(3)	C(2A)-B(7A)-B(11A)	58.7(3)
N(1A)-Ta(1A)-B(5A)	121.5(2)	B(4A)-C(3A)-B(7A)	114.5(5)	C(3A)-B(7A)-B(11A)	102.8(4)
B(6A)-Ta(1A)-B(5A)	41.8(2)	B(8A)-C(3A)-B(7A)	61.5(4)	B(12A)-B(7A)-B(11A)	60.9(4)
N(2A)-Ta(1A)-B(4A)	114.3(2)	C(2A)-C(3A)-Ta(1A)	71.2(3)	B(8A)-B(7A)-B(11A)	108.7(5)
N(3A)-Ta(1A)-B(4A)	146.5(2)	B(4A)-C(3A)-Ta(1A)	69.9(3)	C(3A)-B(8A)-B(7A)	60.2(4)
N(1A)-Ta(1A)-B(4A)	85.4(2)	B(8A)-C(3A)-Ta(1A)	130.6(4)	C(3A)-B(8A)-B(12A)	104.7(5)
B(6A)-Ta(1A)-B(4A)	69.5(2)	B(7A)-C(3A)-Ta(1A)	131.6(4)	B(7A)-B(8A)-B(12A)	59.4(4)
B(5A)-Ta(1A)-B(4A)	42.0(2)	C(3A)-B(4A)-B(5A)	105.2(4)	C(3A)-B(8A)-B(4A)	57.7(3)
N(2A)-Ta(1A)-C(2A)	142.3(2)	C(3A)-B(4A)-B(8A)	58.8(4)	B(7A)-B(8A)-B(4A)	108.6(4)
N(3A)-Ta(1A)-C(2A)	81.8(2)	B(5A)-B(4A)-B(8A)	108.9(5)	B(12A)-B(8A)-B(4A)	108.0(5)
N(1A)-Ta(1A)-C(2A)	120.8(2)	C(3A)-B(4A)-B(9A)	104.5(5)	C(3A)-B(8A)-B(9A)	103.3(5)
B(6A)-Ta(1A)-C(2A)	39.8(2)	B(5A)-B(4A)-B(9A)	59.7(4)	B(7A)-B(8A)-B(9A)	107.1(5)
B(5A)-Ta(1A)-C(2A)	67.1(2)	B(8A)-B(4A)-B(9A)	60.4(4)	B(12A)-B(8A)-B(9A)	59.5(4)
B(4A)-Ta(1A)-C(2A)	65.6(2)	C(3A)-B(4A)-Ta(1A)	70.7(3)	B(4A)-B(8A)-B(9A)	60.0(4)
N(2A)-Ta(1A)-C(3A)	153.1(2)	B(5A)-B(4A)-Ta(1A)	68.4(3)	B(10A)-B(9A)-B(12A)	61.2(4)
N(3A)-Ta(1A)-C(3A)	108.3(2)	B(8A)-B(4A)-Ta(1A)	127.0(4)	B(10A)-B(9A)-B(5A)	60.7(4)
N(1A)-Ta(1A)-C(3A)	88.5(2)	B(9A)-B(4A)-Ta(1A)	124.5(4)	B(12A)-B(9A)-B(5A)	110.0(5)
B(6A)-Ta(1A)-C(3A)	65.9(2)	B(6A)-B(5A)-B(10A)	60.4(4)	B(10A)-B(9A)-B(4A)	107.9(5)
B(5A)-Ta(1A)-C(3A)	67.2(2)	B(6A)-B(5A)-B(4A)	105.6(5)	B(12A)-B(9A)-B(4A)	107.8(5)
B(4A)-Ta(1A)-C(3A)	39.5(2)	B(10A)-B(5A)-B(4A)	106.6(5)	B(5A)-B(9A)-B(4A)	59.8(4)
C(2A)-Ta(1A)-C(3A)	36.8(2)	B(6A)-B(5A)-B(9A)	106.4(5)	B(10A)-B(9A)-B(8A)	108.4(5)
C(13A)-N(1A)-C(14A)	106.0(4)	B(10A)-B(5A)-B(9A)	58.3(4)	B(12A)-B(9A)-B(8A)	59.7(4)
C(13A)-N(1A)-Ta(1A)	132.2(4)	B(4A)-B(5A)-B(9A)	60.5(4)	B(5A)-B(9A)-B(8A)	108.4(5)
C(14A)-N(1A)-Ta(1A)	121.7(4)	B(6A)-B(5A)-Ta(1A)	68.6(3)	B(4A)-B(9A)-B(8A)	59.6(4)
C(16A)-N(2A)-C(15A)	110.8(5)	B(10A)-B(5A)-Ta(1A)	125.7(4)	B(9A)-B(10A)-B(5A)	60.9(4)
C(16A)-N(2A)-Ta(1A)	119.7(4)	B(4A)-B(5A)-Ta(1A)	69.5(3)	B(9A)-B(10A)-B(6A)	107.6(5)
C(15A)-N(2A)-Ta(1A)	128.4(4)	B(9A)-B(5A)-Ta(1A)	126.3(4)	B(5A)-B(10A)-B(6A)	59.3(3)
C(18A)-N(3A)-C(17A)	108.0(4)	C(2A)-B(6A)-B(5A)	105.9(4)	B(9A)-B(10A)-B(12A)	60.7(4)
C(18A)-N(3A)-Ta(1A)	135.7(4)	C(2A)-B(6A)-B(10A)	104.5(4)	B(5A)-B(10A)-B(12A)	109.8(5)
C(17A)-N(3A)-Ta(1A)	116.0(3)	B(5A)-B(6A)-B(10A)	60.3(4)	B(6A)-B(10A)-B(12A)	108.0(5)
C(3A)-C(2A)-B(6A)	111.7(4)	C(2A)-B(6A)-B(11A)	59.0(4)	B(9A)-B(10A)-B(11A)	108.7(5)
C(3A)-C(2A)-B(11A)	112.9(4)	B(5A)-B(6A)-B(11A)	109.5(4)	B(5A)-B(10A)-B(11A)	109.0(5)
B(6A)-C(2A)-B(11A)	63.7(4)	B(10A)-B(6A)-B(11A)	60.1(4)	B(6A)-B(10A)-B(11A)	60.4(4)
C(3A)-C(2A)-B(7A)	63.4(3)	C(2A)-B(6A)-Ta(1A)	71.3(3)	B(12A)-B(10A)-B(11A)	60.0(4)
B(6A)-C(2A)-B(7A)	114.9(5)	B(5A)-B(6A)-Ta(1A)	69.6(3)	C(2A)-B(11A)-B(7A)	59.4(3)
B(11A)-C(2A)-B(7A)	61.9(4)	B(10A)-B(6A)-Ta(1A)	126.5(4)	C(2A)-B(11A)-B(12A)	103.6(4)

Appendix A – Crystal Data

B(7A)-B(11A)-B(12A)	59.1(4)	C(3B)-C(2B)-B(6B)	112.5(4)	B(12B)-B(7B)-B(8B)	61.1(4)
C(2A)-B(11A)-B(10A)	102.7(4)	C(3B)-C(2B)-B(11B)	113.0(5)	C(3B)-B(7B)-B(11B)	102.6(4)
B(7A)-B(11A)-B(10A)	107.2(5)	B(6B)-C(2B)-B(11B)	63.6(4)	C(2B)-B(7B)-B(11B)	58.2(3)
B(12A)-B(11A)-B(10A)	60.0(4)	C(3B)-C(2B)-B(7B)	62.9(3)	B(12B)-B(7B)-B(11B)	60.7(4)
C(2A)-B(11A)-B(6A)	57.3(3)	B(6B)-C(2B)-B(7B)	115.4(5)	B(8B)-B(7B)-B(11B)	108.4(5)
B(7A)-B(11A)-B(6A)	107.6(4)	B(11B)-C(2B)-B(7B)	62.3(4)	C(3B)-B(8B)-B(9B)	104.4(4)
B(12A)-B(11A)-B(6A)	107.3(4)	C(3B)-C(2B)-Ta(1B)	71.2(3)	C(3B)-B(8B)-B(7B)	59.4(3)
B(10A)-B(11A)-B(6A)	59.5(4)	B(6B)-C(2B)-Ta(1B)	69.9(3)	B(9B)-B(8B)-B(7B)	108.0(4)
B(7A)-B(12A)-B(9A)	108.4(5)	B(11B)-C(2B)-Ta(1B)	131.0(4)	C(3B)-B(8B)-B(4B)	58.3(3)
B(7A)-B(12A)-B(8A)	59.8(4)	B(7B)-C(2B)-Ta(1B)	132.0(3)	B(9B)-B(8B)-B(4B)	60.0(4)
B(9A)-B(12A)-B(8A)	60.8(4)	C(2B)-C(3B)-B(4B)	110.7(4)	B(7B)-B(8B)-B(4B)	108.4(4)
B(7A)-B(12A)-B(11A)	60.0(4)	C(2B)-C(3B)-B(8B)	112.0(5)	C(3B)-B(8B)-B(12B)	103.8(4)
B(9A)-B(12A)-B(11A)	106.7(4)	B(4B)-C(3B)-B(8B)	62.7(4)	B(9B)-B(8B)-B(12B)	60.8(4)
B(8A)-B(12A)-B(11A)	107.2(5)	C(2B)-C(3B)-B(7B)	63.0(3)	B(7B)-B(8B)-B(12B)	58.6(4)
B(7A)-B(12A)-B(10A)	107.9(5)	B(4B)-C(3B)-B(7B)	114.3(5)	B(4B)-B(8B)-B(12B)	108.1(5)
B(9A)-B(12A)-B(10A)	58.1(4)	B(8B)-C(3B)-B(7B)	62.1(4)	B(8B)-B(9B)-B(4B)	60.4(4)
B(8A)-B(12A)-B(10A)	106.8(4)	C(2B)-C(3B)-Ta(1B)	71.9(3)	B(8B)-B(9B)-B(10B)	107.8(5)
B(11A)-B(12A)-B(10A)	60.1(4)	B(4B)-C(3B)-Ta(1B)	68.9(3)	B(4B)-B(9B)-B(10B)	106.6(4)
N(2B)-Ta(1B)-N(1B)	95.9(2)	B(8B)-C(3B)-Ta(1B)	129.5(4)	B(8B)-B(9B)-B(5B)	108.9(4)
N(2B)-Ta(1B)-N(3B)	96.9(2)	B(7B)-C(3B)-Ta(1B)	132.8(3)	B(4B)-B(9B)-B(5B)	59.6(3)
N(1B)-Ta(1B)-N(3B)	109.7(2)	C(3B)-B(4B)-B(9B)	104.5(4)	B(10B)-B(9B)-B(5B)	59.8(3)
N(2B)-Ta(1B)-B(4B)	103.1(2)	C(3B)-B(4B)-B(5B)	105.9(4)	B(8B)-B(9B)-B(12B)	60.3(4)
N(1B)-Ta(1B)-B(4B)	88.0(2)	B(9B)-B(4B)-B(5B)	60.8(3)	B(4B)-B(9B)-B(12B)	108.0(5)
N(3B)-Ta(1B)-B(4B)	151.8(2)	C(3B)-B(4B)-B(8B)	58.9(3)	B(10B)-B(9B)-B(12B)	59.9(3)
N(2B)-Ta(1B)-C(3B)	143.5(2)	B(9B)-B(4B)-B(8B)	59.6(4)	B(5B)-B(9B)-B(12B)	108.7(4)
N(1B)-Ta(1B)-C(3B)	82.6(2)	B(5B)-B(4B)-B(8B)	109.2(5)	B(11B)-B(10B)-B(6B)	60.8(4)
N(3B)-Ta(1B)-C(3B)	118.1(2)	C(3B)-B(4B)-Ta(1B)	70.6(3)	B(11B)-B(10B)-B(5B)	109.6(5)
B(4B)-Ta(1B)-C(3B)	40.5(2)	B(9B)-B(4B)-Ta(1B)	127.1(4)	B(6B)-B(10B)-B(5B)	59.9(3)
N(2B)-Ta(1B)-B(6B)	109.8(2)	B(5B)-B(4B)-Ta(1B)	70.0(3)	B(11B)-B(10B)-B(9B)	108.4(5)
N(1B)-Ta(1B)-B(6B)	149.0(2)	B(8B)-B(4B)-Ta(1B)	127.4(4)	B(6B)-B(10B)-B(9B)	107.5(4)
N(3B)-Ta(1B)-B(6B)	84.8(2)	B(6B)-B(5B)-B(4B)	105.5(4)	B(5B)-B(10B)-B(9B)	60.2(3)
B(4B)-Ta(1B)-B(6B)	69.9(2)	B(6B)-B(5B)-B(10B)	59.6(3)	B(11B)-B(10B)-B(12B)	60.1(4)
C(3B)-Ta(1B)-B(6B)	66.4(2)	B(4B)-B(5B)-B(10B)	106.6(4)	B(6B)-B(10B)-B(12B)	108.5(5)
N(2B)-Ta(1B)-B(5B)	85.4(2)	B(6B)-B(5B)-B(9B)	107.0(4)	B(5B)-B(10B)-B(12B)	109.5(5)
N(1B)-Ta(1B)-B(5B)	128.0(2)	B(4B)-B(5B)-B(9B)	59.6(3)	B(9B)-B(10B)-B(12B)	60.4(3)
N(3B)-Ta(1B)-B(5B)	121.9(2)	B(10B)-B(5B)-B(9B)	59.9(3)	C(2B)-B(11B)-B(10B)	103.0(4)
B(4B)-Ta(1B)-B(5B)	42.1(2)	B(6B)-B(5B)-Ta(1B)	68.9(3)	C(2B)-B(11B)-B(7B)	59.5(4)
C(3B)-Ta(1B)-B(5B)	68.0(2)	B(4B)-B(5B)-Ta(1B)	67.9(3)	B(10B)-B(11B)-B(7B)	107.4(5)
B(6B)-Ta(1B)-B(5B)	41.9(2)	B(10B)-B(5B)-Ta(1B)	124.7(4)	C(2B)-B(11B)-B(12B)	103.6(5)
N(2B)-Ta(1B)-C(2B)	149.2(2)	B(9B)-B(5B)-Ta(1B)	124.1(4)	B(10B)-B(11B)-B(12B)	60.5(4)
N(1B)-Ta(1B)-C(2B)	111.8(2)	C(2B)-B(6B)-B(10B)	103.8(4)	B(7B)-B(11B)-B(12B)	58.7(4)
N(3B)-Ta(1B)-C(2B)	86.5(2)	C(2B)-B(6B)-B(5B)	105.3(4)	C(2B)-B(11B)-B(6B)	57.7(3)
B(4B)-Ta(1B)-C(2B)	66.2(2)	B(10B)-B(6B)-B(5B)	60.5(3)	B(10B)-B(11B)-B(6B)	59.6(3)
C(3B)-Ta(1B)-C(2B)	37.0(2)	C(2B)-B(6B)-B(11B)	58.7(4)	B(7B)-B(11B)-B(6B)	108.2(4)
B(6B)-Ta(1B)-C(2B)	39.8(2)	B(10B)-B(6B)-B(11B)	59.6(4)	B(12B)-B(11B)-B(6B)	107.9(4)
B(5B)-Ta(1B)-C(2B)	67.3(2)	B(5B)-B(6B)-B(11B)	109.0(4)	B(7B)-B(12B)-B(11B)	60.6(4)
C(13B)-N(1B)-C(14B)	107.7(5)	C(2B)-B(6B)-Ta(1B)	70.3(3)	B(7B)-B(12B)-B(10B)	108.0(5)
C(13B)-N(1B)-Ta(1B)	116.9(4)	B(10B)-B(6B)-Ta(1B)	125.7(3)	B(11B)-B(12B)-B(10B)	59.4(4)
C(14B)-N(1B)-Ta(1B)	135.5(4)	B(5B)-B(6B)-Ta(1B)	69.2(3)	B(7B)-B(12B)-B(8B)	60.3(4)
C(15B)-N(2B)-C(16B)	110.4(5)	B(11B)-B(6B)-Ta(1B)	126.7(4)	B(11B)-B(12B)-B(8B)	107.6(5)
C(15B)-N(2B)-Ta(1B)	122.1(4)	C(3B)-B(7B)-C(2B)	54.1(3)	B(10B)-B(12B)-B(8B)	106.6(4)
C(16B)-N(2B)-Ta(1B)	124.5(4)	C(3B)-B(7B)-B(12B)	105.0(5)	B(7B)-B(12B)-B(9B)	107.9(5)
C(18B)-N(3B)-C(17B)	107.0(4)	C(2B)-B(7B)-B(12B)	104.1(5)	B(11B)-B(12B)-B(9B)	107.3(4)
C(18B)-N(3B)-Ta(1B)	134.2(4)	C(3B)-B(7B)-B(8B)	58.5(4)	B(10B)-B(12B)-B(9B)	59.7(3)
C(17B)-N(3B)-Ta(1B)	118.8(4)	C(2B)-B(7B)-B(8B)	101.9(4)	B(8B)-B(12B)-B(9B)	58.9(4)

Table 4. Anisotropic displacement parameters ($\text{\AA}^2 \times 10^3$) for (17). The anisotropic displacement factor exponent takes the form: $-2\pi^2 [h^2 a^{*2} U^{11} + \dots + 2 h k a^* b^* U^{12}]$

U^{11}	U^{22}	U^{33}	U^{23}	U^{13}	U^{12}
----------	----------	----------	----------	----------	----------

Appendix A – Crystal Data

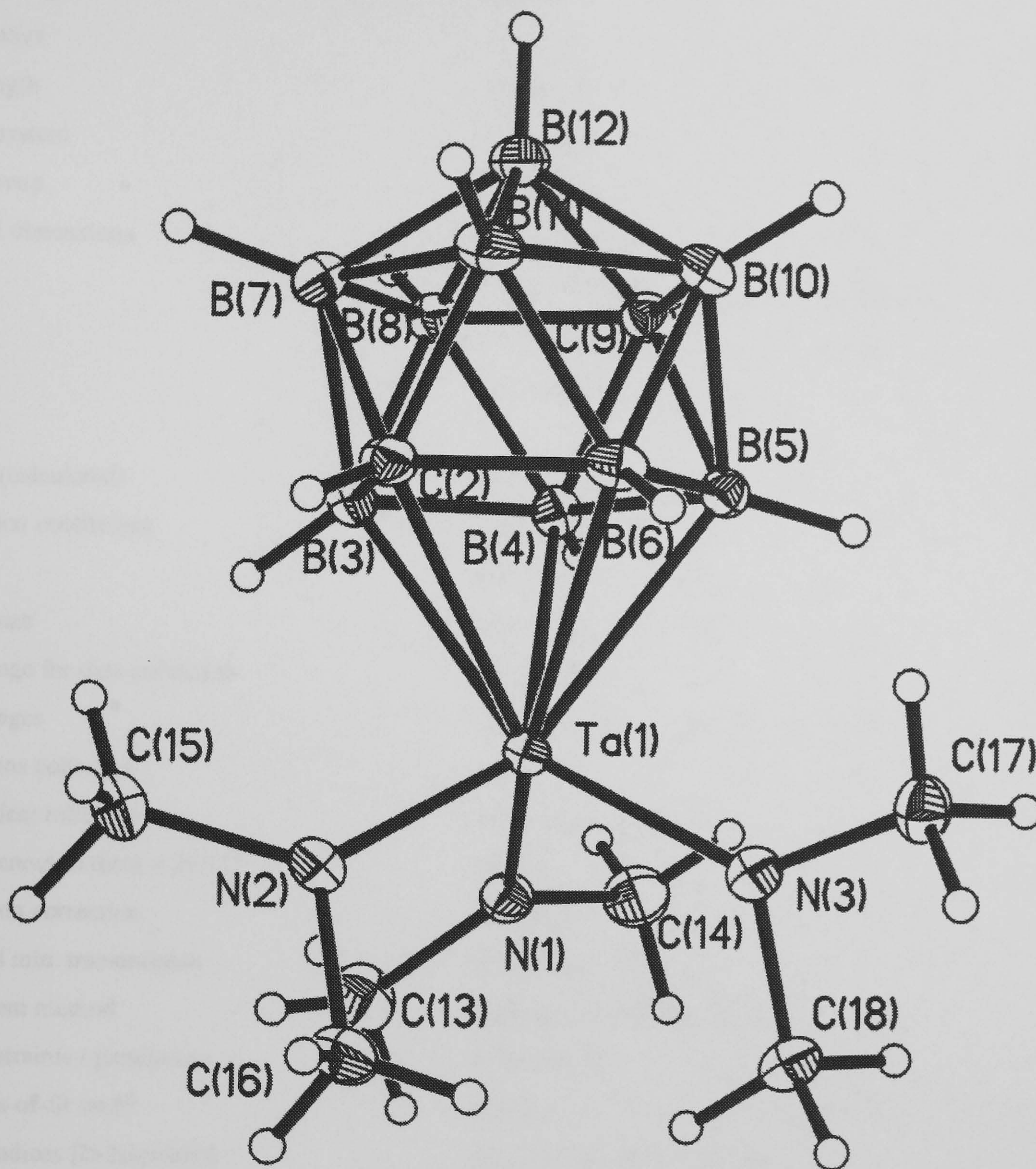
Ta(1A)	14(1)	13(1)	16(1)	1(1)	-1(1)	-1(1)
N(1A)	21(2)	21(2)	20(2)	1(2)	1(2)	1(2)
N(2A)	19(2)	19(2)	22(2)	6(2)	-1(2)	2(2)
N(3A)	19(2)	15(2)	23(2)	-4(2)	-3(2)	-3(2)
C(2A)	20(3)	16(2)	22(2)	1(2)	-1(2)	-4(2)
C(3A)	24(3)	17(2)	29(3)	-1(2)	-1(2)	-3(2)
B(4A)	33(4)	26(3)	26(3)	-3(3)	-7(3)	-7(3)
B(5A)	21(3)	30(3)	30(3)	7(3)	-9(3)	-8(3)
B(6A)	19(3)	23(3)	22(3)	4(2)	5(2)	1(2)
B(7A)	27(3)	20(3)	31(3)	7(2)	-4(3)	-2(3)
B(8A)	36(4)	18(3)	38(3)	-1(3)	2(3)	-7(3)
B(9A)	32(4)	29(3)	35(3)	3(3)	-8(3)	-12(3)
B(10A)	16(3)	34(3)	31(3)	10(2)	-3(3)	-6(3)
B(11A)	29(4)	25(3)	21(3)	6(2)	-1(3)	-6(3)
B(12A)	27(3)	26(3)	32(3)	11(3)	-1(3)	-8(3)
C(13A)	39(4)	33(3)	28(3)	-3(2)	9(3)	6(3)
C(14A)	33(3)	33(3)	27(3)	3(2)	6(2)	2(3)
C(15A)	49(4)	24(3)	32(3)	-2(2)	-2(3)	15(3)
C(16A)	30(3)	34(3)	28(3)	3(2)	-6(3)	2(3)
C(17A)	37(3)	24(3)	32(3)	-1(2)	-1(3)	-15(2)
C(18A)	29(3)	19(3)	27(3)	-4(2)	0(2)	-1(2)
Ta(1B)	14(1)	15(1)	17(1)	0(1)	0(1)	1(1)
N(1B)	21(3)	32(3)	23(2)	3(2)	1(2)	-2(2)
N(2B)	20(2)	24(2)	22(2)	-7(2)	-2(2)	-4(2)
N(3B)	21(2)	22(2)	26(2)	-1(2)	-3(2)	5(2)
C(2B)	18(3)	20(2)	27(3)	1(2)	-7(2)	0(2)
C(3B)	25(3)	16(2)	25(2)	3(2)	1(2)	-4(2)
B(4B)	26(3)	17(2)	27(3)	0(2)	-4(3)	2(2)
B(5B)	17(3)	17(3)	26(3)	-4(2)	-4(2)	3(2)
B(6B)	16(3)	23(3)	18(2)	-1(2)	2(2)	1(2)
B(7B)	29(4)	20(3)	32(3)	-6(2)	-8(3)	-1(3)
B(8B)	32(3)	17(3)	35(3)	-2(3)	-5(3)	-1(3)
B(9B)	17(3)	20(2)	28(3)	-2(2)	-4(3)	2(2)
B(10B)	27(3)	20(3)	27(3)	-5(2)	0(3)	5(3)
B(11B)	23(3)	27(3)	21(3)	-4(2)	-4(2)	3(2)
B(12B)	30(4)	21(3)	34(4)	-7(3)	-5(3)	3(3)
C(13B)	34(4)	56(5)	40(3)	1(3)	17(3)	5(3)
C(14B)	36(4)	40(4)	28(3)	8(3)	2(3)	-9(3)
C(15B)	40(4)	27(3)	35(3)	-8(2)	1(3)	-15(3)
C(16B)	35(4)	36(3)	32(3)	-5(3)	-7(3)	2(3)
C(17B)	47(4)	31(3)	35(3)	-2(3)	5(3)	22(3)
C(18B)	29(3)	26(3)	34(3)	3(2)	-5(3)	5(3)

Appendix A – Crystal Data

Table 5. Hydrogen coordinates (x 10⁴) and isotropic displacement parameters (Å²x 10³) for (17).

	x	y	z	U(eq)
H(2A)	848(44)	4465(36)	2459(32)	10(13)
H(3A)	512(40)	5471(32)	3478(28)	3(12)
H(4A)	2061(48)	5643(43)	4606(38)	33(18)
H(5A)	3730(43)	4397(38)	4027(33)	25(15)
H(6A)	2700(43)	3546(37)	2586(31)	17(15)
H(7A)	898(54)	5941(47)	2123(40)	43(20)
H(8A)	1746(54)	6852(46)	3436(40)	48(21)
H(9A)	3793(47)	6224(40)	3747(36)	36(17)
H(10A)	4112(51)	4918(40)	2441(40)	35(19)
H(11A)	2348(48)	4789(39)	1454(37)	30
H(12A)	3041(36)	6426(32)	2098(28)	5(12)
H(31A)	-516(27)	5034(7)	5066(25)	41(12)
H(32A)	282(26)	5524(19)	4652(21)	41(12)
H(33A)	358(24)	5364(17)	5514(23)	41(12)
H(41A)	852(35)	3267(28)	5529(16)	70(16)
H(42A)	-157(30)	3652(29)	5625(19)	70(16)
H(43A)	715(38)	4052(19)	6028(20)	70(16)
H(51A)	3238(30)	2204(5)	4207(26)	49(12)
H(52A)	2115(27)	2010(13)	4035(25)	49(12)
H(53A)	2540(33)	1884(16)	4886(19)	49(12)
H(61A)	2731(20)	4057(23)	5388(15)	27(10)
H(62A)	3654(25)	3434(22)	5096(10)	27(10)
H(63A)	2831(21)	3063(19)	5730(18)	27(10)
H(71A)	45(19)	2747(18)	4419(18)	23(9)
H(72A)	159(17)	1994(20)	3905(17)	23(9)
H(73A)	-583(22)	2655(19)	3723(15)	23(9)
H(81A)	1091(28)	3023(25)	2329(13)	39(12)
H(82A)	17(28)	2951(26)	2457(11)	39(12)
H(83A)	662(32)	2202(24)	2596(5)	39(12)
H(2B)	5854(54)	5437(46)	2534(40)	31(19)
H(3B)	5824(42)	4561(35)	3614(31)	11(13)
H(4B)	7581(43)	4611(37)	4515(33)	18(15)
H(5B)	8847(39)	6072(34)	3636(29)	14(13)
H(6B)	7282(44)	6656(40)	2363(33)	23(15)
H(7B)	6042(40)	3915(37)	2177(29)	14(13)
H(8B)	7264(43)	3261(38)	3420(33)	22(15)
H(9B)	9239(48)	4428(42)	3437(36)	31(17)
H(10B)	9099(43)	5544(38)	2078(33)	19(15)
H(11B)	7006(42)	5283(35)	1377(34)	19(15)
H(12B)	8254(43)	3760(36)	1999(32)	23(15)
H(31B)	5149(27)	6818(26)	4959(19)	58(14)
H(32B)	5330(23)	6252(24)	5758(25)	58(14)
H(33B)	4420(30)	6002(19)	5164(23)	58(14)
H(41B)	5856(33)	4759(8)	5591(24)	49(13)
H(42B)	6014(32)	4389(18)	4804(21)	49(13)
H(43B)	5003(29)	4612(15)	5066(25)	49(13)
H(51B)	7595(22)	7845(18)	3747(22)	37(11)
H(52B)	8605(27)	7506(10)	4195(22)	37(11)
H(53B)	7833(26)	8161(20)	4650(18)	37(11)
H(61B)	7371(25)	6196(26)	5548(14)	44(11)
H(62B)	7672(29)	7160(21)	5695(16)	44(11)
H(63B)	8428(28)	6522(27)	5307(6)	44(11)
H(71B)	5800(26)	7837(13)	4322(20)	35(11)
H(72B)	4806(26)	7858(13)	3895(20)	35(11)
H(73B)	5692(27)	8347(19)	3560(15)	35(11)
H(81B)	5640(32)	6746(26)	2249(16)	55(14)
H(82B)	5629(31)	7731(27)	2376(14)	55(14)
H(83B)	4712(31)	7187(32)	2589(5)	55(14)

A7 Crystal data for $[2\text{-Ta}(\text{NMe}_2)_3(1,12\text{-C}_2\text{B}_9\text{H}_{11})]$; (20).



Appendix A – Crystal Data

Table 1. Crystal data and structure refinement for (20).

Identification code	99srv207	
Empirical formula	C8 H29 B9 N3 Ta	
Formula weight	445.58	
Temperature	120(2) K	
Wavelength	0.71073 Å	
Crystal system	Monoclinic	
Space group	P2(1)/n	
Unit cell dimensions	a = 9.758(1) Å	α= 90°.
	b = 17.658(3) Å	β= 96.04(1)°.
	c = 10.326(1) Å	γ = 90°.
Volume	1769.4(4) Å ³	
Z	4	
Density (calculated)	1.673 Mg/m ³	
Absorption coefficient	6.201 mm ⁻¹	
F(000)	864	
Crystal size	0.40 x 0.28 x 0.22 mm ³	
Theta range for data collection	2.29 to 29.12°.	
Index ranges	-12<=h<=13, -24<=k<=23, -14<=l<=13	
Reflections collected	17446	
Independent reflections	4719 [R(int) = 0.0214]	
Completeness to theta = 29.12°	98.9 %	
Absorption correction	Multiscan	
Max. and min. transmission	0.3353 and 0.2338	
Refinement method	Full-matrix least-squares on F ²	
Data / restraints / parameters	4719 / 0 / 307	
Goodness-of-fit on F ²	1.123	
Final R indices [I>2sigma(I)]	R1 = 0.0164, wR2 = 0.0352	
R indices (all data)	R1 = 0.0223, wR2 = 0.0366	
Extinction coefficient	0.00275(10)	
Largest diff. peak and hole	0.885 and -0.639 e.Å ⁻³	

Appendix A – Crystal Data

Table 2. Atomic coordinates (x 10⁴) and equivalent isotropic displacement parameters (Å²x 10³) for (20). U(eq) is defined as one third of the trace of the orthogonalized U^{ij} tensor.

	x	y	z	U(eq)
Ta(1)	7689(1)	1257(1)	9455(1)	14(1)
N(1)	6443(2)	2100(1)	9779(2)	18(1)
N(2)	9446(2)	1824(1)	9787(2)	18(1)
N(3)	7449(2)	708(1)	11099(2)	18(1)
C(2)	8882(2)	741(1)	7621(2)	17(1)
B(3)	7636(3)	1364(1)	7089(2)	18(1)
B(4)	6064(3)	985(1)	7519(2)	16(1)
B(5)	6488(3)	137(1)	8416(2)	15(1)
B(6)	8309(3)	27(1)	8485(2)	17(1)
B(7)	8352(3)	727(2)	5989(2)	20(1)
B(8)	6552(3)	863(2)	5914(2)	18(1)
C(9)	5992(2)	123(1)	6777(2)	16(1)
B(10)	7222(3)	-510(1)	7348(3)	17(1)
B(11)	8760(3)	-125(2)	6876(3)	19(1)
B(12)	7246(3)	-65(2)	5789(2)	19(1)
C(13)	6760(3)	2908(1)	9805(3)	29(1)
C(14)	4972(3)	1979(2)	9915(3)	27(1)
C(15)	10396(3)	2153(2)	8933(3)	29(1)
C(16)	10001(3)	1967(2)	11153(2)	26(1)
C(17)	7460(3)	-99(1)	11462(2)	21(1)
C(18)	7075(3)	1135(2)	12245(2)	25(1)

Table 3. Bond lengths [Å] and angles [°] for (20).

Ta(1)-N(1)	1.9724(19)	B(4)-C(9)	1.702(3)	B(10)-H(10)	1.05(3)
Ta(1)-N(2)	1.9832(19)	B(4)-B(8)	1.785(4)	B(11)-B(12)	1.762(4)
Ta(1)-N(3)	1.9899(19)	B(4)-B(5)	1.786(3)	B(11)-H(11)	1.02(3)
Ta(1)-B(3)	2.446(3)	B(4)-H(4)	1.02(3)	B(12)-H(12)	1.01(3)
Ta(1)-B(4)	2.465(2)	B(5)-C(9)	1.711(3)	C(13)-H(131)	1.02(3)
Ta(1)-B(5)	2.484(2)	B(5)-B(6)	1.782(4)	C(13)-H(132)	0.93(3)
Ta(1)-B(6)	2.494(2)	B(5)-B(10)	1.789(4)	C(13)-H(133)	0.97(3)
Ta(1)-C(2)	2.497(2)	B(5)-H(5)	1.05(3)	C(14)-H(141)	0.97(3)
N(1)-C(13)	1.460(3)	B(6)-B(10)	1.772(4)	C(14)-H(142)	0.94(3)
N(1)-C(14)	1.472(3)	B(6)-B(11)	1.784(4)	C(14)-H(143)	0.98(3)
N(2)-C(15)	1.465(3)	B(6)-H(6)	1.05(3)	C(15)-H(151)	1.03(3)
N(2)-C(16)	1.479(3)	B(7)-B(12)	1.766(4)	C(15)-H(152)	0.92(3)
N(3)-C(17)	1.473(3)	B(7)-B(8)	1.766(4)	C(15)-H(153)	0.99(3)
N(3)-C(18)	1.480(3)	B(7)-B(11)	1.784(4)	C(16)-H(161)	1.01(3)
C(2)-B(6)	1.674(4)	B(7)-H(7)	1.10(3)	C(16)-H(162)	0.92(3)
C(2)-B(3)	1.688(3)	B(8)-C(9)	1.703(3)	C(16)-H(163)	0.94(4)
C(2)-B(7)	1.710(3)	B(8)-B(12)	1.783(4)	C(17)-H(171)	1.03(3)
C(2)-B(11)	1.711(3)	B(8)-H(8)	1.09(2)	C(17)-H(172)	0.93(3)
C(2)-H(2)	0.82(3)	C(9)-B(10)	1.699(3)	C(17)-H(173)	0.97(3)
B(3)-B(8)	1.762(4)	C(9)-B(12)	1.706(3)	C(18)-H(181)	1.03(3)
B(3)-B(4)	1.772(4)	C(9)-H(9)	0.94(3)	C(18)-H(182)	1.03(3)
B(3)-B(7)	1.792(4)	B(10)-B(11)	1.763(4)	C(18)-H(183)	0.98(3)
B(3)-H(3)	1.05(3)	B(10)-B(12)	1.793(4)		
N(1)-Ta(1)-N(2)	97.31(8)	B(6)-C(2)-H(2)	120(2)	B(4)-B(5)-H(5)	121.5(15)
N(1)-Ta(1)-N(3)	95.31(8)	B(3)-C(2)-H(2)	119(2)	B(10)-B(5)-H(5)	114.1(15)
N(2)-Ta(1)-N(3)	106.01(8)	B(7)-C(2)-H(2)	113(2)	Ta(1)-B(5)-H(5)	113.0(15)
N(1)-Ta(1)-B(3)	99.35(8)	B(11)-C(2)-H(2)	114(2)	C(2)-B(6)-B(10)	105.07(17)
N(2)-Ta(1)-B(3)	93.46(8)	Ta(1)-C(2)-H(2)	103(2)	C(2)-B(6)-B(5)	106.47(17)
N(3)-Ta(1)-B(3)	153.89(8)	C(2)-B(3)-B(8)	104.86(17)	B(10)-B(6)-B(5)	60.46(14)
N(1)-Ta(1)-B(4)	85.93(8)	C(2)-B(3)-B(4)	106.57(17)	C(2)-B(6)-B(11)	59.21(14)
N(2)-Ta(1)-B(4)	135.13(8)	B(8)-B(3)-B(4)	60.66(15)	B(10)-B(6)-B(11)	59.43(14)
N(3)-Ta(1)-B(4)	118.29(8)	C(2)-B(3)-B(7)	58.78(14)	B(5)-B(6)-B(11)	108.79(17)
B(3)-Ta(1)-B(4)	42.31(8)	B(8)-B(3)-B(7)	59.60(15)	C(2)-B(6)-Ta(1)	70.51(11)
N(1)-Ta(1)-B(5)	113.73(8)	B(4)-B(3)-B(7)	109.10(18)	B(10)-B(6)-Ta(1)	125.32(15)
N(2)-Ta(1)-B(5)	146.74(8)	C(2)-B(3)-Ta(1)	71.68(11)	B(5)-B(6)-Ta(1)	68.73(11)
N(3)-Ta(1)-B(5)	83.59(8)	B(8)-B(3)-Ta(1)	126.67(15)	B(11)-B(6)-Ta(1)	126.83(15)
B(3)-Ta(1)-B(5)	70.77(8)	B(4)-B(3)-Ta(1)	69.42(12)	C(2)-B(6)-H(6)	120.1(15)
B(4)-Ta(1)-B(5)	42.31(8)	B(7)-B(3)-Ta(1)	128.03(15)	B(10)-B(6)-H(6)	121.2(15)
N(1)-Ta(1)-B(6)	154.88(8)	C(2)-B(3)-H(3)	123.2(15)	B(5)-B(6)-H(6)	127.9(15)
N(2)-Ta(1)-B(6)	105.49(8)	B(8)-B(3)-H(3)	124.3(15)	B(11)-B(6)-H(6)	114.0(15)
N(3)-Ta(1)-B(6)	88.51(8)	B(4)-B(3)-H(3)	120.7(15)	Ta(1)-B(6)-H(6)	104.9(15)
B(3)-Ta(1)-B(6)	69.29(8)	B(7)-B(3)-H(3)	122.8(15)	C(2)-B(7)-B(12)	104.16(18)
B(4)-Ta(1)-B(6)	70.54(8)	Ta(1)-B(3)-H(3)	96.1(15)	C(2)-B(7)-B(8)	103.73(17)
B(5)-Ta(1)-B(6)	41.95(8)	C(9)-B(4)-B(3)	102.76(17)	B(12)-B(7)-B(8)	60.63(15)
N(1)-Ta(1)-C(2)	138.49(8)	C(9)-B(4)-B(8)	58.41(14)	C(2)-B(7)-B(11)	58.58(14)
N(2)-Ta(1)-C(2)	81.46(8)	B(3)-B(4)-B(8)	59.39(14)	B(12)-B(7)-B(11)	59.51(15)
N(3)-Ta(1)-C(2)	125.14(8)	C(9)-B(4)-B(5)	58.70(13)	B(8)-B(7)-B(11)	107.70(18)
B(3)-Ta(1)-C(2)	39.93(8)	B(3)-B(4)-B(5)	106.68(17)	C(2)-B(7)-B(3)	57.58(14)
B(4)-Ta(1)-C(2)	67.99(8)	B(8)-B(4)-B(5)	108.08(18)	B(12)-B(7)-B(3)	107.29(18)
B(5)-Ta(1)-C(2)	67.57(8)	C(9)-B(4)-Ta(1)	122.14(14)	B(8)-B(7)-B(3)	59.35(15)
B(6)-Ta(1)-C(2)	39.21(8)	B(3)-B(4)-Ta(1)	68.27(11)	B(11)-B(7)-B(3)	106.56(18)
C(13)-N(1)-C(14)	110.2(2)	B(8)-B(4)-Ta(1)	124.41(15)	C(2)-B(7)-H(7)	120.9(14)
C(13)-N(1)-Ta(1)	127.40(17)	B(5)-B(4)-Ta(1)	69.41(11)	B(12)-B(7)-H(7)	128.5(14)
C(14)-N(1)-Ta(1)	122.14(16)	C(9)-B(4)-H(4)	115.3(15)	B(8)-B(7)-H(7)	123.0(14)
C(15)-N(2)-C(16)	108.32(19)	B(3)-B(4)-H(4)	127.4(15)	B(11)-B(7)-H(7)	124.7(14)
C(15)-N(2)-Ta(1)	133.36(16)	B(8)-B(4)-H(4)	112.2(16)	B(3)-B(7)-H(7)	116.9(14)
C(16)-N(2)-Ta(1)	118.32(16)	B(5)-B(4)-H(4)	123.5(16)	C(9)-B(8)-B(3)	103.14(17)
C(17)-N(3)-C(18)	106.57(19)	Ta(1)-B(4)-H(4)	113.6(15)	C(9)-B(8)-B(7)	104.21(18)
C(17)-N(3)-Ta(1)	133.58(16)	C(9)-B(5)-B(6)	102.41(17)	B(3)-B(8)-B(7)	61.04(15)
C(18)-N(3)-Ta(1)	119.68(15)	C(9)-B(5)-B(4)	58.18(13)	C(9)-B(8)-B(12)	58.57(14)
B(6)-C(2)-B(3)	113.26(18)	B(6)-B(5)-B(4)	106.75(17)	B(3)-B(8)-B(12)	107.86(18)
B(6)-C(2)-B(7)	115.51(18)	C(9)-B(5)-B(10)	58.04(14)	B(7)-B(8)-B(12)	59.67(15)
B(3)-C(2)-B(7)	63.64(15)	B(6)-B(5)-B(10)	59.51(14)	C(9)-B(8)-B(4)	58.36(14)
B(6)-C(2)-B(11)	63.58(15)	B(4)-B(5)-B(10)	107.52(17)	B(3)-B(8)-B(4)	59.95(14)
B(3)-C(2)-B(11)	114.98(18)	C(9)-B(5)-Ta(1)	120.68(14)	B(7)-B(8)-B(4)	109.69(17)
B(7)-C(2)-B(11)	62.87(15)	B(6)-B(5)-Ta(1)	69.32(11)	B(12)-B(8)-B(4)	108.61(18)
B(6)-C(2)-Ta(1)	70.28(11)	B(4)-B(5)-Ta(1)	68.28(11)	C(9)-B(8)-H(8)	121.2(13)
B(3)-C(2)-Ta(1)	68.39(11)	B(10)-B(5)-Ta(1)	125.00(15)	B(3)-B(8)-H(8)	127.4(13)
B(7)-C(2)-Ta(1)	129.48(15)	C(9)-B(5)-H(5)	115.4(15)	B(7)-B(8)-H(8)	124.3(13)
B(11)-C(2)-Ta(1)	130.66(15)	B(6)-B(5)-H(5)	129.2(15)	B(12)-B(8)-H(8)	118.4(13)

Appendix A – Crystal Data

B(4)-B(8)-H(8)	120.6(13)	B(12)-B(11)-B(10)	61.17(15)	H(132)-C(13)-H(133)	110(3)
B(10)-C(9)-B(4)	115.97(17)	C(2)-B(11)-B(6)	57.22(14)	N(1)-C(14)-H(141)	109.6(19)
B(10)-C(9)-B(8)	115.60(18)	B(12)-B(11)-B(6)	108.17(18)	N(1)-C(14)-H(142)	110.7(18)
B(4)-C(9)-B(8)	63.23(14)	B(10)-B(11)-B(6)	59.96(15)	H(141)-C(14)-H(142)	111(3)
B(10)-C(9)-B(12)	63.54(15)	C(2)-B(11)-B(7)	58.55(14)	N(1)-C(14)-H(143)	112(2)
B(4)-C(9)-B(12)	116.45(18)	B(12)-B(11)-B(7)	59.72(15)	H(141)-C(14)-H(143)	110(3)
B(8)-C(9)-B(12)	63.06(15)	B(10)-B(11)-B(7)	108.44(18)	H(142)-C(14)-H(143)	103(3)
B(10)-C(9)-B(5)	63.29(14)	B(6)-B(11)-B(7)	106.72(18)	N(2)-C(15)-H(151)	111.6(18)
B(4)-C(9)-B(5)	63.11(14)	C(2)-B(11)-H(11)	121.1(16)	N(2)-C(15)-H(152)	115(2)
B(8)-C(9)-B(5)	115.70(17)	B(12)-B(11)-H(11)	124.1(15)	H(151)-C(15)-H(152)	104(3)
B(12)-C(9)-B(5)	116.63(18)	B(10)-B(11)-H(11)	126.9(16)	N(2)-C(15)-H(153)	111.3(19)
B(10)-C(9)-H(9)	118.9(17)	B(6)-B(11)-H(11)	122.8(15)	H(151)-C(15)-H(153)	107(3)
B(4)-C(9)-H(9)	115.1(17)	B(7)-B(11)-H(11)	118.1(16)	H(152)-C(15)-H(153)	106(3)
B(8)-C(9)-H(9)	115.9(17)	C(9)-B(12)-B(11)	103.70(17)	N(2)-C(16)-H(161)	110.3(18)
B(12)-C(9)-H(9)	117.3(16)	C(9)-B(12)-B(7)	104.08(18)	N(2)-C(16)-H(162)	113(2)
B(5)-C(9)-H(9)	117.1(16)	B(11)-B(12)-B(7)	60.77(15)	H(161)-C(16)-H(162)	107(3)
C(9)-B(10)-B(11)	103.97(18)	C(9)-B(12)-B(8)	58.37(14)	N(2)-C(16)-H(163)	111(2)
C(9)-B(10)-B(6)	103.29(17)	B(11)-B(12)-B(8)	107.96(18)	H(161)-C(16)-H(163)	108(3)
B(11)-B(10)-B(6)	60.61(15)	B(7)-B(12)-B(8)	59.71(15)	H(162)-C(16)-H(163)	107(3)
C(9)-B(10)-B(5)	58.68(13)	C(9)-B(12)-B(10)	58.04(14)	N(3)-C(17)-H(171)	109.0(17)
B(11)-B(10)-B(5)	109.39(18)	B(11)-B(12)-B(10)	59.44(15)	N(3)-C(17)-H(172)	112.8(19)
B(6)-B(10)-B(5)	60.03(14)	B(7)-B(12)-B(10)	107.90(18)	H(171)-C(17)-H(172)	110(2)
C(9)-B(10)-B(12)	58.42(14)	B(8)-B(12)-B(10)	107.23(17)	N(3)-C(17)-H(173)	110.0(18)
B(11)-B(10)-B(12)	59.40(15)	C(9)-B(12)-H(12)	122.0(17)	H(171)-C(17)-H(173)	106(2)
B(6)-B(10)-B(12)	107.29(18)	B(11)-B(12)-H(12)	125.0(16)	H(172)-C(17)-H(173)	109(3)
B(5)-B(10)-B(12)	108.54(18)	B(7)-B(12)-H(12)	125.1(17)	N(3)-C(18)-H(181)	108.8(16)
C(9)-B(10)-H(10)	119.6(14)	B(8)-B(12)-H(12)	120.8(16)	N(3)-C(18)-H(182)	115.9(16)
B(11)-B(10)-H(10)	127.5(15)	B(10)-B(12)-H(12)	120.6(17)	H(181)-C(18)-H(182)	108(2)
B(6)-B(10)-H(10)	127.0(14)	N(1)-C(13)-H(131)	110.7(19)	N(3)-C(18)-H(183)	114.4(16)
B(5)-B(10)-H(10)	117.4(15)	N(1)-C(13)-H(132)	113(2)	H(181)-C(18)-H(183)	104(2)
B(12)-B(10)-H(10)	120.7(15)	H(131)-C(13)-H(132)	111(3)	H(182)-C(18)-H(183)	105(2)
C(2)-B(11)-B(12)	104.30(18)	N(1)-C(13)-H(133)	109.7(19)		
C(2)-B(11)-B(10)	103.94(18)	H(131)-C(13)-H(133)	102(3)		

Symmetry transformations used to generate equivalent atoms:

Appendix A – Crystal Data

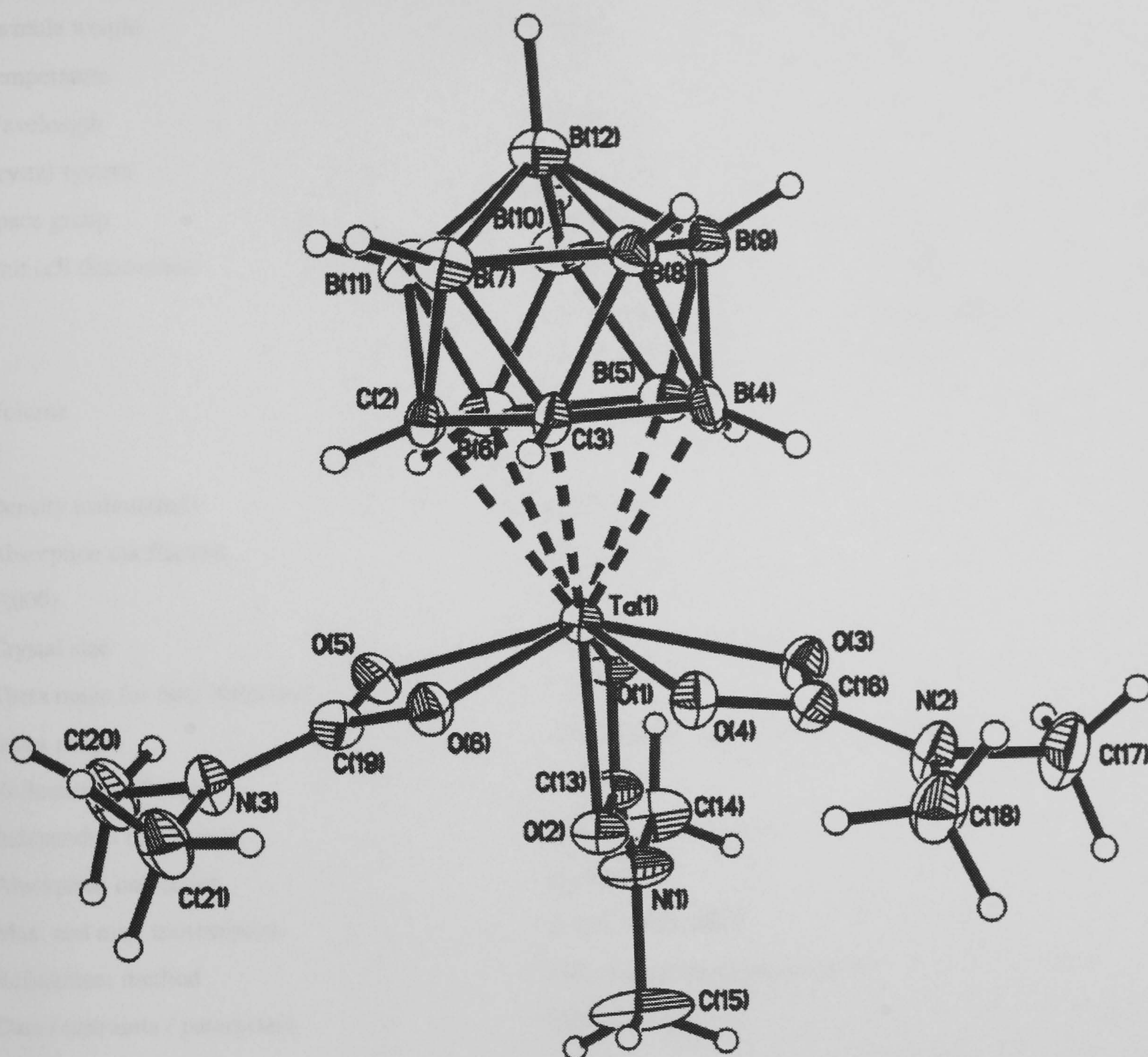
Table 4. Anisotropic displacement parameters ($\text{\AA}^2 \times 10^3$) for (20). The anisotropic displacement factor exponent takes the form: $-2\pi^2 [h^2 a^{*2} U^{11} + \dots + 2 h k a^* b^* U^{12}]$

	U ¹¹	U ²²	U ³³	U ²³	U ¹³	U ¹²
Ta(1)	16(1)	12(1)	13(1)	-1(1)	2(1)	-1(1)
N(1)	24(1)	14(1)	18(1)	-1(1)	5(1)	2(1)
N(2)	19(1)	17(1)	19(1)	-3(1)	2(1)	-4(1)
N(3)	21(1)	19(1)	16(1)	0(1)	2(1)	-1(1)
C(2)	13(1)	19(1)	18(1)	-5(1)	3(1)	-1(1)
B(3)	23(1)	14(1)	17(1)	0(1)	4(1)	-3(1)
B(4)	15(1)	15(1)	16(1)	2(1)	0(1)	1(1)
B(5)	17(1)	14(1)	14(1)	0(1)	1(1)	0(1)
B(6)	18(1)	16(1)	17(1)	-3(1)	-1(1)	3(1)
B(7)	22(1)	22(1)	16(1)	-2(1)	5(1)	-3(1)
B(8)	23(1)	17(1)	15(1)	-1(1)	3(1)	-1(1)
C(9)	17(1)	17(1)	15(1)	-1(1)	0(1)	-1(1)
B(10)	19(1)	13(1)	20(1)	-3(1)	1(1)	0(1)
B(11)	17(1)	19(1)	21(1)	-6(1)	2(1)	2(1)
B(12)	20(1)	19(1)	17(1)	-4(1)	3(1)	0(1)
C(13)	37(2)	16(1)	36(2)	2(1)	9(1)	3(1)
C(14)	26(1)	26(1)	30(1)	-4(1)	10(1)	4(1)
C(15)	31(1)	28(1)	27(1)	-3(1)	7(1)	-15(1)
C(16)	32(1)	25(1)	20(1)	-3(1)	-2(1)	-10(1)
C(17)	22(1)	20(1)	20(1)	5(1)	2(1)	0(1)
C(18)	36(1)	26(1)	14(1)	-1(1)	4(1)	-4(1)

Table 5. Hydrogen coordinates ($\times 10^4$) and isotropic displacement parameters ($\text{\AA}^2 \times 10^{-3}$) for (20).

	x	y	z	U(eq)
H(2)	9680(30)	892(16)	7790(30)	22(7)
H(3)	7790(30)	1951(15)	7070(30)	19(7)
H(4)	5150(30)	1257(15)	7520(30)	20(7)
H(5)	5790(30)	-114(16)	9000(30)	23(7)
H(6)	8970(30)	-237(15)	9210(30)	18(7)
H(7)	8990(30)	978(15)	5280(30)	18(7)
H(8)	5920(20)	1094(13)	5070(20)	9(6)
H(9)	5100(30)	-53(15)	6510(30)	19(7)
H(10)	6960(30)	-1083(15)	7420(30)	17(7)
H(11)	9620(30)	-418(16)	6690(30)	22(7)
H(12)	7060(30)	-369(16)	4960(30)	27(7)
H(131)	6160(30)	3190(20)	9080(30)	43(9)
H(132)	7690(30)	3008(19)	9760(30)	35(9)
H(133)	6460(30)	3135(18)	10580(30)	35(8)
H(141)	4740(30)	2215(18)	10710(30)	37(9)
H(142)	4760(30)	1460(17)	9910(30)	24(7)
H(143)	4380(30)	2175(19)	9160(30)	39(9)
H(151)	10550(30)	2723(19)	9110(30)	39(9)
H(152)	10110(30)	2125(18)	8060(30)	35(8)
H(153)	11310(30)	1905(18)	9060(30)	35(9)
H(161)	10970(30)	1772(18)	11320(30)	32(8)
H(162)	9500(30)	1739(19)	11750(30)	34(8)
H(163)	10020(30)	2490(20)	11330(30)	39(9)
H(171)	8090(30)	-171(17)	12320(30)	32(8)
H(172)	7740(30)	-411(18)	10820(30)	31(8)
H(173)	6540(30)	-255(17)	11650(30)	30(8)
H(181)	6090(30)	983(16)	12420(30)	23(7)
H(182)	7100(30)	1716(17)	12170(30)	24(7)
H(183)	7650(30)	1018(15)	13060(30)	22(7)

A8 *Crystal data for [3-Ta(O₂CNMe₂)₃(1,2-C₂B₉H₁₁):1/2C₇H₈; (22).*



Appendix A – Crystal Data

Table 1. Crystal data and structure refinement for (22).

Identification code	99srv026	
Empirical formula	C14.50 H33 B9 N3 O6 Ta	
Formula weight	623.68	
Temperature	150(2) K	
Wavelength	0.71073 Å	
Crystal system	Monoclinic	
Space group	P2(1)/c	
Unit cell dimensions	a = 12.297(2) Å	α= 90°.
	b = 17.424(3) Å	β= 111.34(5)°.
	c = 13.308(3) Å	γ= 90°.
Volume	2655.9(9) Å ³	
Z	4	
Density (calculated)	1.560 Mg/m ³	
Absorption coefficient	4.172 mm ⁻¹	
F(000)	1228	
Crystal size	0.36 x 0.20 x 0.08 mm ³	
Theta range for data collection	1.78 to 27.49°.	
Index ranges	-15<=h<=12, -22<=k<=19, -13<=l<=17	
Reflections collected	17271	
Independent reflections	6091 [R(int) = 0.0438]	
Absorption correction	Multiscan	
Max. and min. transmission	0.5630 and 0.2978	
Refinement method	Full-matrix least-squares on F ²	
Data / restraints / parameters	6082 / 0 / 340	
Goodness-of-fit on F ²	1.119	
Final R indices [I>2sigma(I)]	R1 = 0.0329, wR2 = 0.0858	
R indices (all data)	R1 = 0.0512, wR2 = 0.0978	
Extinction coefficient	not refined	
Largest diff. peak and hole	1.164 and -1.564 e.Å ⁻³	

Appendix A – Crystal Data

Table 2. Atomic coordinates ($\times 10^4$) and equivalent isotropic displacement parameters ($\text{\AA}^2 \times 10^3$) for (22). U(eq) is defined as one third of the trace of the orthogonalized U^{ij} tensor.

	x	y	z	U(eq)
Ta(1)	5643(1)	2446(1)	6222(1)	16(1)
C(2)	3841(4)	1694(2)	5838(4)	18(1)
C(3)	3685(5)	2483(2)	6369(4)	20(1)
B(4)	3788(5)	3223(3)	5625(5)	23(1)
B(5)	4046(5)	2829(3)	4497(5)	24(1)
B(6)	4103(5)	1825(3)	4699(5)	22(1)
B(7)	2452(5)	1932(3)	5794(5)	24(1)
B(8)	2409(5)	2923(3)	5603(5)	22(1)
B(9)	2613(6)	3129(3)	4375(5)	26(1)
B(10)	2794(5)	2248(4)	3797(5)	28(1)
B(11)	2718(6)	1505(3)	4681(5)	26(1)
B(12)	1775(5)	2316(4)	4481(5)	24(1)
O(1)	6504(3)	2391(2)	5128(3)	22(1)
O(2)	7524(3)	2468(2)	6848(3)	23(1)
N(1)	8483(4)	2440(3)	5650(4)	33(1)
C(13)	7528(5)	2430(3)	5878(4)	23(1)
C(14)	8423(6)	2412(4)	4533(5)	39(2)
C(15)	9650(6)	2491(4)	6512(6)	60(3)
O(3)	6134(3)	3647(2)	6082(3)	24(1)
O(4)	5904(3)	3209(2)	7517(3)	22(1)
N(2)	6430(4)	4468(2)	7515(4)	29(1)
C(16)	6166(5)	3785(3)	7037(4)	22(1)
C(17)	6656(6)	5127(3)	6948(5)	42(2)
C(18)	6454(6)	4570(3)	8611(5)	35(1)
O(5)	6180(3)	1231(2)	6291(3)	21(1)
O(6)	5930(3)	1798(2)	7645(3)	20(1)
N(3)	6573(4)	553(2)	7874(3)	25(1)
C(19)	6242(5)	1183(3)	7272(4)	22(1)
C(20)	6874(6)	-147(3)	7420(5)	37(2)
C(21)	6633(6)	546(3)	8992(4)	31(1)
C(1T)	15(11)	180(7)	8258(11)	159(12)
C(2T)	-472(15)	647(7)	7358(13)	148(11)
C(3T)	-423(16)	428(10)	6371(12)	154(12)
C(4T)	113(15)	-258(10)	6284(12)	102(7)
C(5T)	601(16)	-725(8)	7184(15)	146(11)
C(6T)	552(14)	-506(7)	8171(13)	134(10)
C(7T)	1(20)	349(12)	9394(13)	128(9)

Appendix A – Crystal Data

Table 3. Bond lengths [Å] and angles [°] for (22).

Ta(1)-O(1)	2.091(3)	B(4)-B(9)	1.770(9)	N(1)-C(14)	1.463(7)
Ta(1)-O(4)	2.106(3)	B(4)-B(5)	1.780(9)	N(1)-C(15)	1.478(8)
Ta(1)-O(6)	2.121(3)	B(5)-B(6)	1.768(8)	O(3)-C(16)	1.280(6)
Ta(1)-O(2)	2.156(4)	B(5)-B(9)	1.788(9)	O(4)-C(16)	1.292(6)
Ta(1)-O(3)	2.205(3)	B(5)-B(10)	1.794(9)	N(2)-C(16)	1.332(6)
Ta(1)-O(5)	2.208(3)	B(6)-B(10)	1.780(9)	N(2)-C(17)	1.454(7)
Ta(1)-C(2)	2.462(5)	B(6)-B(11)	1.784(9)	N(2)-C(18)	1.460(7)
Ta(1)-B(6)	2.464(6)	B(7)-B(8)	1.743(8)	O(5)-C(19)	1.282(6)
Ta(1)-C(3)	2.486(5)	B(7)-B(12)	1.771(8)	O(6)-C(19)	1.296(6)
Ta(1)-B(5)	2.508(6)	B(7)-B(11)	1.791(8)	N(3)-C(19)	1.333(6)
Ta(1)-B(4)	2.519(6)	B(8)-B(12)	1.763(8)	N(3)-C(21)	1.463(7)
Ta(1)-C(13)	2.521(5)	B(8)-B(9)	1.779(8)	N(3)-C(20)	1.466(6)
C(2)-C(3)	1.590(6)	B(9)-B(10)	1.768(9)	C(1T)-C(2T)	1.39
C(2)-B(6)	1.676(7)	B(9)-B(12)	1.789(9)	C(1T)-C(6T)	1.39
C(2)-B(11)	1.685(8)	B(10)-B(11)	1.775(9)	C(1T)-C(7T)	1.55
C(2)-B(7)	1.738(8)	B(10)-B(12)	1.802(8)	C(2T)-C(3T)	1.39
C(3)-B(4)	1.657(7)	B(11)-B(12)	1.786(9)	C(3T)-C(4T)	1.39
C(3)-B(8)	1.709(8)	O(1)-C(13)	1.292(6)	C(4T)-C(5T)	1.39
C(3)-B(7)	1.722(8)	O(2)-C(13)	1.294(6)	C(5T)-C(6T)	1.39
B(4)-B(8)	1.765(8)	N(1)-C(13)	1.316(7)	C(7T)-C(7T)#1	2.02(4)
O(1)-Ta(1)-O(4)	129.27(13)	O(5)-Ta(1)-B(4)	138.7(2)	B(4)-B(5)-B(10)	105.8(4)
O(1)-Ta(1)-O(6)	129.43(13)	C(2)-Ta(1)-B(4)	65.0(2)	B(9)-B(5)-B(10)	59.1(4)
O(4)-Ta(1)-O(6)	71.30(13)	B(6)-Ta(1)-B(4)	68.9(2)	B(6)-B(5)-Ta(1)	67.9(3)
O(1)-Ta(1)-O(2)	61.65(14)	C(3)-Ta(1)-B(4)	38.7(2)	B(4)-B(5)-Ta(1)	69.6(3)
O(4)-Ta(1)-O(2)	81.37(14)	B(5)-Ta(1)-B(4)	41.5(2)	B(9)-B(5)-Ta(1)	125.3(4)
O(6)-Ta(1)-O(2)	81.83(14)	O(1)-Ta(1)-C(13)	30.77(15)	B(10)-B(5)-Ta(1)	124.3(4)
O(1)-Ta(1)-O(3)	76.15(13)	O(4)-Ta(1)-C(13)	106.2(2)	C(2)-B(6)-B(5)	105.2(4)
O(4)-Ta(1)-O(3)	60.34(13)	O(6)-Ta(1)-C(13)	106.9(2)	C(2)-B(6)-B(10)	104.0(4)
O(6)-Ta(1)-O(3)	128.25(13)	O(2)-Ta(1)-C(13)	30.88(15)	B(5)-B(6)-B(10)	60.8(3)
O(2)-Ta(1)-O(3)	74.18(13)	O(3)-Ta(1)-C(13)	72.35(14)	C(2)-B(6)-B(11)	58.2(3)
O(1)-Ta(1)-O(5)	76.43(13)	O(5)-Ta(1)-C(13)	73.51(14)	B(5)-B(6)-B(11)	108.8(4)
O(4)-Ta(1)-O(5)	128.07(13)	C(2)-Ta(1)-C(13)	140.7(2)	B(10)-B(6)-B(11)	59.7(3)
O(6)-Ta(1)-O(5)	60.20(12)	B(6)-Ta(1)-C(13)	109.1(2)	C(2)-B(6)-Ta(1)	70.0(3)
O(2)-Ta(1)-O(5)	74.83(12)	C(3)-Ta(1)-C(13)	174.4(2)	B(5)-B(6)-Ta(1)	70.5(3)
O(3)-Ta(1)-O(5)	145.68(14)	B(5)-Ta(1)-C(13)	107.5(2)	B(10)-B(6)-Ta(1)	127.5(4)
O(1)-Ta(1)-C(2)	118.45(15)	B(4)-Ta(1)-C(13)	137.3(2)	B(11)-B(6)-Ta(1)	126.3(3)
O(4)-Ta(1)-C(2)	111.34(15)	C(3)-C(2)-B(6)	112.2(4)	C(3)-B(7)-C(2)	54.7(3)
O(6)-Ta(1)-C(2)	75.4(2)	C(3)-C(2)-B(11)	112.6(4)	C(3)-B(7)-B(8)	59.1(3)
O(2)-Ta(1)-C(2)	148.00(14)	B(6)-C(2)-B(11)	64.1(3)	C(2)-B(7)-B(8)	102.6(4)
O(3)-Ta(1)-C(2)	137.81(15)	C(3)-C(2)-B(7)	62.1(3)	C(3)-B(7)-B(12)	104.4(4)
O(5)-Ta(1)-C(2)	74.44(14)	B(6)-C(2)-B(7)	116.6(4)	C(2)-B(7)-B(12)	103.1(4)
O(1)-Ta(1)-B(6)	80.8(2)	B(11)-C(2)-B(7)	63.1(3)	B(8)-B(7)-B(12)	60.2(3)
O(4)-Ta(1)-B(6)	142.5(2)	C(3)-C(2)-Ta(1)	72.1(3)	C(3)-B(7)-B(11)	101.7(4)
O(6)-Ta(1)-B(6)	109.3(2)	B(6)-C(2)-Ta(1)	70.2(3)	C(2)-B(7)-B(11)	57.0(3)
O(2)-Ta(1)-B(6)	136.1(2)	B(11)-C(2)-Ta(1)	132.1(3)	B(8)-B(7)-B(11)	107.2(4)
O(3)-Ta(1)-B(6)	119.9(2)	B(7)-C(2)-Ta(1)	132.8(3)	B(12)-B(7)-B(11)	60.2(3)
O(5)-Ta(1)-B(6)	75.1(2)	C(2)-C(3)-B(4)	111.1(4)	C(3)-B(8)-B(7)	59.8(3)
C(2)-Ta(1)-B(6)	39.8(2)	C(2)-C(3)-B(8)	110.8(4)	C(3)-B(8)-B(12)	105.3(4)
O(1)-Ta(1)-C(3)	143.7(2)	B(4)-C(3)-B(8)	63.2(3)	B(7)-B(8)-B(12)	60.7(3)
O(4)-Ta(1)-C(3)	77.5(2)	C(2)-C(3)-B(7)	63.2(3)	C(3)-B(8)-B(4)	56.9(3)
O(6)-Ta(1)-C(3)	78.2(2)	B(4)-C(3)-B(7)	114.5(4)	B(7)-B(8)-B(4)	108.2(4)
O(2)-Ta(1)-C(3)	154.6(2)	B(8)-C(3)-B(7)	61.1(3)	B(12)-B(8)-B(4)	108.5(4)
O(3)-Ta(1)-C(3)	106.52(13)	C(2)-C(3)-Ta(1)	70.5(3)	C(3)-B(8)-B(9)	103.4(4)
O(5)-Ta(1)-C(3)	107.80(13)	B(4)-C(3)-Ta(1)	71.7(3)	B(7)-B(8)-B(9)	109.1(4)
C(2)-Ta(1)-C(3)	37.48(14)	B(8)-C(3)-Ta(1)	132.1(3)	B(12)-B(8)-B(9)	60.7(3)
B(6)-Ta(1)-C(3)	66.4(2)	B(7)-C(3)-Ta(1)	132.2(3)	B(4)-B(8)-B(9)	59.9(4)
O(1)-Ta(1)-B(5)	78.5(2)	C(3)-B(4)-B(8)	59.8(3)	B(10)-B(9)-B(4)	107.4(4)
O(4)-Ta(1)-B(5)	114.6(2)	C(3)-B(4)-B(9)	106.0(4)	B(10)-B(9)-B(8)	107.8(4)
O(6)-Ta(1)-B(5)	141.2(2)	B(8)-B(4)-B(9)	60.4(3)	B(4)-B(9)-B(8)	59.7(3)
O(2)-Ta(1)-B(5)	136.2(2)	C(3)-B(4)-B(5)	106.3(4)	B(10)-B(9)-B(5)	60.6(3)
O(3)-Ta(1)-B(5)	79.4(2)	B(8)-B(4)-B(5)	109.7(4)	B(4)-B(9)-B(5)	60.1(3)
O(5)-Ta(1)-B(5)	114.6(2)	B(9)-B(4)-B(5)	60.5(4)	B(8)-B(9)-B(5)	108.7(4)
C(2)-Ta(1)-B(5)	66.8(2)	C(3)-B(4)-Ta(1)	69.6(3)	B(10)-B(9)-B(12)	60.9(3)
B(6)-Ta(1)-B(5)	41.6(2)	B(8)-B(4)-Ta(1)	126.9(3)	B(4)-B(9)-B(12)	107.2(4)
C(3)-Ta(1)-B(5)	66.9(2)	B(9)-B(4)-Ta(1)	125.7(4)	B(8)-B(9)-B(12)	59.2(3)
O(1)-Ta(1)-B(4)	115.8(2)	B(5)-B(4)-Ta(1)	68.9(3)	B(5)-B(9)-B(12)	109.8(4)
O(4)-Ta(1)-B(4)	76.7(2)	B(6)-B(5)-B(4)	105.2(4)	B(9)-B(10)-B(11)	107.4(4)
O(6)-Ta(1)-B(4)	113.9(2)	B(6)-B(5)-B(9)	106.7(4)	B(9)-B(10)-B(6)	107.0(4)
O(2)-Ta(1)-B(4)	146.5(2)	B(4)-B(5)-B(9)	59.5(3)	B(11)-B(10)-B(6)	60.2(4)
O(3)-Ta(1)-B(4)	73.0(2)	B(6)-B(5)-B(10)	60.0(4)	B(9)-B(10)-B(5)	60.3(4)

Appendix A – Crystal Data

B(11)-B(10)-B(5)	108.0(4)	B(7)-B(12)-B(10)	108.0(4)	O(4)-C(16)-Ta(1)	55.3(2)
B(6)-B(10)-B(5)	59.3(3)	B(11)-B(12)-B(10)	59.3(3)	N(2)-C(16)-Ta(1)	176.6(4)
B(9)-B(10)-B(12)	60.1(3)	B(9)-B(12)-B(10)	59.0(3)	C(19)-O(5)-Ta(1)	90.6(3)
B(11)-B(10)-B(12)	59.9(3)	C(13)-O(1)-Ta(1)	93.3(3)	C(19)-O(6)-Ta(1)	94.2(3)
B(6)-B(10)-B(12)	108.1(4)	C(13)-O(2)-Ta(1)	90.4(3)	C(19)-N(3)-C(21)	120.6(4)
B(5)-B(10)-B(12)	108.9(4)	C(13)-N(1)-C(14)	121.0(5)	C(19)-N(3)-C(20)	120.4(4)
C(2)-B(11)-B(10)	103.9(4)	C(13)-N(1)-C(15)	121.2(5)	C(21)-N(3)-C(20)	119.0(4)
C(2)-B(11)-B(6)	57.7(3)	C(14)-N(1)-C(15)	117.8(5)	O(5)-C(19)-O(6)	114.8(4)
B(10)-B(11)-B(6)	60.0(3)	O(1)-C(13)-O(2)	114.6(5)	O(5)-C(19)-N(3)	123.9(4)
C(2)-B(11)-B(12)	104.7(4)	O(1)-C(13)-N(1)	121.6(5)	O(6)-C(19)-N(3)	121.2(5)
B(10)-B(11)-B(12)	60.8(3)	O(2)-C(13)-N(1)	123.8(5)	O(5)-C(19)-Ta(1)	59.4(2)
B(6)-B(11)-B(12)	108.7(4)	O(1)-C(13)-Ta(1)	55.9(3)	O(6)-C(19)-Ta(1)	55.5(2)
C(2)-B(11)-B(7)	59.9(3)	O(2)-C(13)-Ta(1)	58.7(3)	N(3)-C(19)-Ta(1)	176.4(4)
B(10)-B(11)-B(7)	108.4(4)	N(1)-C(13)-Ta(1)	177.0(4)	C(2T)-C(1T)-C(6T)	120.0
B(6)-B(11)-B(7)	108.7(4)	C(16)-O(3)-Ta(1)	90.2(3)	C(2T)-C(1T)-C(7T)	125.2
B(12)-B(11)-B(7)	59.4(3)	C(16)-O(4)-Ta(1)	94.5(3)	C(6T)-C(1T)-C(7T)	114.8
B(8)-B(12)-B(7)	59.1(3)	C(16)-N(2)-C(17)	121.2(5)	C(1T)-C(2T)-C(3T)	120.0
B(8)-B(12)-B(11)	106.6(4)	C(16)-N(2)-C(18)	119.9(4)	C(4T)-C(3T)-C(2T)	120.0
B(7)-B(12)-B(11)	60.5(3)	C(17)-N(2)-C(18)	118.9(4)	C(3T)-C(4T)-C(5T)	120.0
B(8)-B(12)-B(9)	60.1(3)	O(3)-C(16)-O(4)	115.0(4)	C(6T)-C(5T)-C(4T)	120.0
B(7)-B(12)-B(9)	107.4(4)	O(3)-C(16)-N(2)	123.7(4)	C(5T)-C(6T)-C(1T)	120.0
B(11)-B(12)-B(9)	106.1(4)	O(4)-C(16)-N(2)	121.3(5)	C(1T)-C(7T)-C(7T)#1	132.0(17)
B(8)-B(12)-B(10)	107.0(4)	O(3)-C(16)-Ta(1)	59.7(2)		

Symmetry transformations used to generate equivalent atoms:

#1 -x,-y,-z+2

Appendix A – Crystal Data

Table 4. Anisotropic displacement parameters ($\text{\AA}^2 \times 10^3$) for (22). The anisotropic displacement factor exponent takes the form: $-2\pi^2 [h^2 a^{*2}U^{11} + \dots + 2 h k a^* b^* U^{12}]$

	U ¹¹	U ²²	U ³³	U ²³	U ¹³	U ¹²
Ta(1)	20(1)	18(1)	12(1)	0(1)	7(1)	0(1)
C(2)	25(3)	14(2)	17(3)	-3(2)	9(2)	-2(2)
C(3)	25(3)	13(2)	21(3)	-2(2)	9(2)	-2(2)
B(4)	27(3)	14(2)	28(3)	6(2)	10(3)	4(2)
B(5)	23(3)	29(3)	18(3)	2(2)	7(2)	1(2)
B(6)	22(3)	30(3)	15(3)	-5(2)	9(2)	-1(2)
B(7)	24(3)	31(3)	20(3)	-1(2)	13(3)	2(2)
B(8)	20(3)	22(3)	23(3)	2(2)	9(2)	2(2)
B(9)	24(3)	34(3)	19(3)	10(2)	7(3)	2(2)
B(10)	24(3)	43(3)	17(3)	-2(3)	10(3)	-5(3)
B(11)	25(3)	28(3)	24(3)	-5(2)	10(3)	-7(2)
B(12)	20(3)	36(3)	19(3)	3(2)	10(2)	0(2)
O(1)	17(2)	33(2)	17(2)	1(1)	8(1)	-1(1)
O(2)	19(2)	33(2)	17(2)	-1(1)	7(1)	0(1)
N(1)	21(2)	61(3)	17(2)	-4(2)	6(2)	-4(2)
C(13)	21(2)	31(3)	14(2)	-2(2)	2(2)	-1(2)
C(14)	31(3)	69(4)	23(3)	-5(3)	16(3)	-5(3)
C(15)	21(3)	124(8)	29(4)	-7(4)	2(3)	-12(4)
O(3)	30(2)	22(2)	21(2)	-1(1)	11(2)	-5(2)
O(4)	31(2)	19(2)	15(2)	-3(1)	9(2)	-2(1)
N(2)	38(3)	20(2)	30(3)	-5(2)	13(2)	-8(2)
C(16)	24(3)	21(2)	21(3)	-1(2)	8(2)	-3(2)
C(17)	59(4)	26(3)	39(4)	1(2)	16(3)	-14(3)
C(18)	45(4)	27(3)	33(3)	-11(2)	13(3)	-5(2)
O(5)	25(2)	21(2)	18(2)	1(1)	9(2)	7(1)
O(6)	27(2)	17(2)	18(2)	-2(1)	8(2)	1(1)
N(3)	36(3)	19(2)	18(2)	0(2)	10(2)	3(2)
C(19)	22(3)	23(2)	21(3)	-3(2)	8(2)	2(2)
C(20)	53(4)	23(3)	33(4)	-1(2)	16(3)	13(3)
C(21)	46(4)	29(3)	20(3)	7(2)	13(3)	5(2)

Appendix A – Crystal Data

Table 5. Hydrogen coordinates (x 10⁴) and isotropic displacement parameters (Å²x 10³) for (22).

	x	y	z	U(eq)
H(2)	4044(46)	1254(30)	6318(42)	19(13)
H(3)	3757(47)	2474(23)	7138(47)	14(13)
H(4)	4026(45)	3740(29)	6088(40)	16(13)
H(5)	4506(51)	3141(33)	3989(49)	38(17)
H(6)	4636(41)	1335(25)	4507(40)	13(12)
H(7)	2084(56)	1626(34)	6401(54)	47(19)
H(8)	1956(49)	3280(30)	6026(46)	28(15)
H(9)	2219(45)	3610(28)	3960(43)	20(13)
H(10)	2511(47)	2129(32)	2916(47)	30(15)
H(11)	2521(45)	1007(30)	4571(43)	20(13)
H(12)	769(59)	2289(38)	4076(61)	54(20)
H(14A)	8786(32)	1937(11)	4415(10)	67(15)
H(14B)	8839(31)	2855(13)	4391(11)	67(15)
H(14C)	7605(6)	2428(24)	4043(5)	67(15)
H(15A)	10047(17)	2958(14)	6415(22)	88(19)
H(15B)	10115(15)	2040(13)	6482(24)	88(19)
H(15C)	9563(6)	2509(27)	7216(6)	88(19)
H(171)	7441(18)	5338(17)	7355(20)	73(15)
H(172)	6071(26)	5536(11)	6872(35)	73(15)
H(173)	6618(42)	4981(7)	6216(15)	73(15)
H(181)	7182(17)	4835(21)	9070(10)	53(12)
H(182)	6420(36)	4066(3)	8953(13)	53(12)
H(183)	5779(20)	4883(20)	8617(6)	53(12)
H(203)	6386(34)	-583(8)	7481(41)	90(17)
H(202)	7703(14)	-281(18)	7809(29)	90(17)
H(201)	6745(46)	-70(11)	6649(12)	90(17)
H(211)	7405(14)	359(24)	9480(6)	67(14)
H(212)	6023(25)	206(20)	9069(8)	67(14)
H(213)	6513(40)	1069(5)	9224(12)	67(14)
H(2T)	-843(24)	1121(10)	7419(18)	178
H(3T)	-760(24)	750(13)	5750(14)	185
H(4T)	147(21)	-409(13)	5602(14)	122
H(5T)	971(25)	-1198(10)	7124(20)	176
H(6T)	889(22)	-828(10)	8792(15)	161
H(71T)	-383(25)	830(13)	9384(17)	191
H(72T)	-411(23)	-53(14)	9599(15)	191
H(73T)	788(22)	375(15)	9905(11)	191

A9 Crystal data for $[3\text{-Nb}(\text{S}_2\text{CNMe}_2)_3(1,2\text{-C}_2\text{B}_9\text{H}_{11})]\text{:CD}_2\text{Cl}_2$; (23).

Identification code

Empirical formula

Formula weight

Temperature

Wavelength

Crystal system

Space group

Unit cell dimensions

Volume

Z

Density (calculated)

Absorption coefficient

$\mu(001)$

Crystal size

Temperature of measurement

Crystal description

Crystal growth

Crystal habit

Crystal color

Absorption (measured)

Max. and min. transmittance

Refinement method

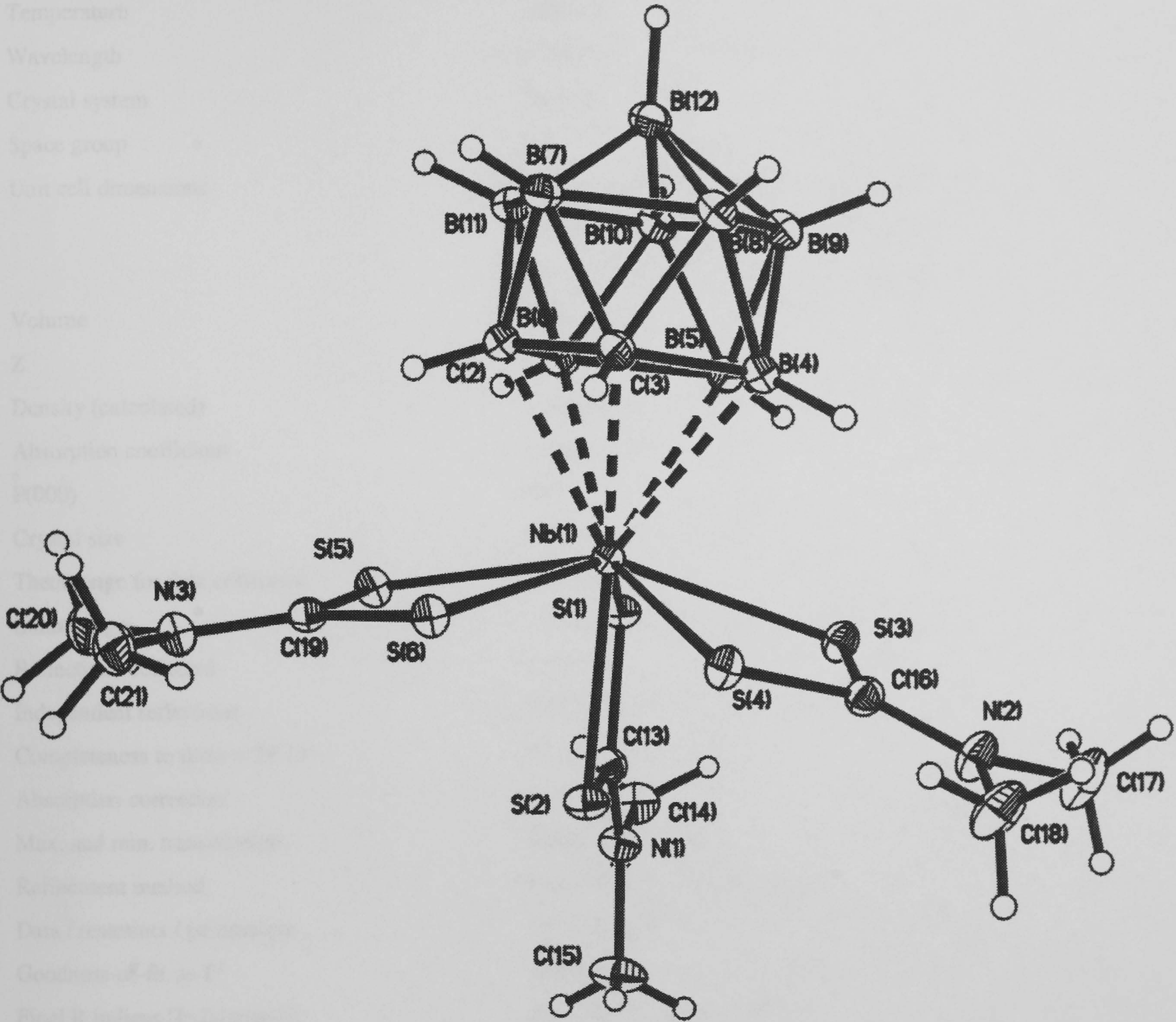
Data / observations / restraints

Goodness of fit on F^2

Final R indices / R_{int}

R indices (all data)

Largest diff. peak and hole



Appendix A – Crystal Data

Table 1. Crystal data and structure refinement for (23).

Identification code	99srv153	
Empirical formula	C12 H29 D2 B9 Cl2 N3 Nb S6	
Formula weight	672.87	
Temperature	120(2) K	
Wavelength	0.71073 Å	
Crystal system	Triclinic	
Space group	P-1	
Unit cell dimensions	a = 9.879(3) Å	α= 98.77(1)°.
	b = 11.637(3) Å	β= 97.42(1)°.
	c = 13.957(4) Å	γ= 113.04(1)°.
Volume	1427.5(7) Å ³	
Z	2	
Density (calculated)	1.566 Mg/m ³	
Absorption coefficient	1.058 mm ⁻¹	
F(000)	680	
Crystal size	0.40 x 0.15 x 0.13 mm ³	
Theta range for data collection	1.95 to 29.13°.	
Index ranges	-13<=h<=13, -15<=k<=15, -18<=l<=18	
Reflections collected	17790	
Independent reflections	7477 [R(int) = 0.0292]	
Completeness to theta = 29.13°	97.3 %	
Absorption correction	Integration	
Max. and min. transmission	0.9087 and 0.7849	
Refinement method	Full-matrix least-squares on F ²	
Data / restraints / parameters	7477 / 0 / 431	
Goodness-of-fit on F ²	1.040	
Final R indices [I>2sigma(I)]	R1 = 0.0220, wR2 = 0.0507	
R indices (all data)	R1 = 0.0286, wR2 = 0.0529	
Largest diff. peak and hole	0.310 and -0.429 e.Å ⁻³	

Appendix A – Crystal Data

Table 2. Atomic coordinates (x 10⁴) and equivalent isotropic displacement parameters (Å²x 10³) for rename. U(eq) is defined as one third of the trace of the orthogonalized U^{ij} tensor.

	x	y	z	U(eq)
Nb(1)	2285(1)	3622(1)	2485(1)	11(1)
S(2)	2534(1)	5971(1)	2777(1)	16(1)
S(1)	2039(1)	4464(1)	4240(1)	15(1)
S(3)	5033(1)	5052(1)	3506(1)	16(1)
S(4)	4221(1)	4657(1)	1415(1)	15(1)
S(5)	-501(1)	3406(1)	2351(1)	15(1)
S(6)	946(1)	3532(1)	715(1)	14(1)
N(3)	-1947(1)	3181(1)	509(1)	16(1)
N(1)	2509(2)	6925(1)	4661(1)	18(1)
N(2)	7063(2)	6122(1)	2428(1)	20(1)
C(3)	2198(2)	1585(1)	1505(1)	15(1)
C(2)	680(2)	1291(1)	1887(1)	15(1)
B(6)	983(2)	1669(2)	3134(1)	15(1)
B(5)	2955(2)	2233(2)	3554(1)	16(1)
B(4)	3684(2)	2193(2)	2451(1)	16(1)
B(7)	1000(2)	-18(2)	1389(1)	17(1)
B(11)	241(2)	41(2)	2467(1)	18(1)
B(10)	1722(2)	608(2)	3526(1)	17(1)
B(9)	3423(2)	937(2)	3096(1)	18(1)
B(8)	2972(2)	560(2)	1781(1)	18(1)
B(12)	1743(2)	-428(2)	2442(1)	18(1)
C(13)	2368(2)	5939(1)	3980(1)	15(1)
C(15)	2896(3)	8199(2)	4455(1)	28(1)
C(14)	2334(2)	6793(2)	5669(1)	23(1)
C(16)	5650(2)	5386(1)	2453(1)	16(1)
C(17)	8221(2)	6746(2)	3343(2)	32(1)
C(18)	7533(2)	6388(2)	1503(1)	28(1)
C(19)	-697(2)	3346(1)	1107(1)	14(1)
C(20)	-3307(2)	3013(2)	894(1)	23(1)
C(21)	-2087(2)	3033(2)	-564(1)	22(1)
C(22)	6552(2)	10103(2)	2178(1)	24(1)
Cl(1A)	6601(1)	9778(1)	897(1)	29(1)
Cl(2A)	5703(2)	8682(1)	2589(2)	36(1)
Cl(1B)	6380(20)	9460(20)	983(14)	55(5)
Cl(2B)	6073(18)	8865(11)	2942(14)	32(3)

Appendix A – Crystal Data

Table 3. Bond lengths [Å] and angles [°] for (23).

Nb(1)-C(2)	2.4841(16)	C(3)-B(7)	1.742(2)	B(9)-H(9)	1.090(18)
Nb(1)-B(6)	2.5058(17)	C(3)-H(3)	0.946(18)	B(8)-B(12)	1.780(3)
Nb(1)-C(3)	2.5137(16)	C(2)-B(6)	1.685(2)	B(8)-H(8)	1.066(19)
Nb(1)-B(4)	2.5438(17)	C(2)-B(11)	1.708(2)	B(12)-H(12)	1.032(19)
Nb(1)-B(5)	2.5674(17)	C(2)-B(7)	1.736(2)	C(15)-H(151)	0.94(3)
Nb(1)-S(1)	2.5734(8)	C(2)-H(2)	0.968(19)	C(15)-H(152)	0.94(3)
Nb(1)-S(2)	2.6087(8)	B(6)-B(5)	1.777(2)	C(15)-H(153)	0.88(3)
Nb(1)-S(4)	2.6119(7)	B(6)-B(10)	1.779(2)	C(14)-H(141)	0.95(3)
Nb(1)-S(6)	2.6149(8)	B(6)-B(11)	1.786(2)	C(14)-H(142)	0.91(3)
Nb(1)-S(3)	2.6287(8)	B(6)-H(6)	1.071(18)	C(14)-H(143)	0.95(3)
Nb(1)-S(5)	2.6423(9)	B(5)-B(4)	1.784(2)	C(17)-H(171)	0.88(3)
S(2)-C(13)	1.7126(16)	B(5)-B(10)	1.795(2)	C(17)-H(172)	0.87(4)
S(1)-C(13)	1.7227(15)	B(5)-B(9)	1.796(2)	C(17)-H(173)	0.96(4)
S(3)-C(16)	1.7035(16)	B(5)-H(5)	1.078(16)	C(18)-H(181)	0.94(2)
S(4)-C(16)	1.7237(16)	B(4)-B(9)	1.783(2)	C(18)-H(182)	0.94(3)
S(5)-C(19)	1.7087(16)	B(4)-B(8)	1.795(2)	C(18)-H(183)	0.92(3)
S(6)-C(19)	1.7240(16)	B(4)-H(4)	1.055(18)	C(20)-H(201)	0.95(2)
N(3)-C(19)	1.3257(19)	B(7)-B(8)	1.770(3)	C(20)-H(202)	1.01(2)
N(3)-C(21)	1.464(2)	B(7)-B(11)	1.770(3)	C(20)-H(203)	0.90(2)
N(3)-C(20)	1.464(2)	B(7)-B(12)	1.771(3)	C(21)-H(211)	0.91(3)
N(1)-C(13)	1.3226(19)	B(7)-H(7)	1.054(19)	C(21)-H(212)	0.95(3)
N(1)-C(14)	1.463(2)	B(11)-B(12)	1.772(3)	C(21)-H(213)	0.93(3)
N(1)-C(15)	1.464(2)	B(11)-B(10)	1.775(3)	C(22)-Cl(1B)	1.679(18)
N(2)-C(16)	1.330(2)	B(11)-H(11)	1.083(19)	C(22)-Cl(2A)	1.7593(19)
N(2)-C(18)	1.465(2)	B(10)-B(9)	1.777(3)	C(22)-Cl(1A)	1.782(2)
N(2)-C(17)	1.469(2)	B(10)-B(12)	1.793(3)	C(22)-Cl(2B)	1.872(11)
C(3)-C(2)	1.584(2)	B(10)-H(10)	1.127(19)	C(22)-D(222)	0.935(18)
C(3)-B(4)	1.674(2)	B(9)-B(8)	1.775(3)	C(22)-D(221)	0.90(2)
C(3)-B(8)	1.713(2)	B(9)-B(12)	1.793(3)		
C(2)-Nb(1)-B(6)	39.47(5)	S(1)-Nb(1)-S(3)	73.44(2)	B(8)-C(3)-H(3)	119.0(11)
C(2)-Nb(1)-C(3)	36.95(5)	S(2)-Nb(1)-S(3)	74.40(2)	B(7)-C(3)-H(3)	113.2(11)
B(6)-Nb(1)-C(3)	65.37(6)	S(4)-Nb(1)-S(3)	65.64(2)	Nb(1)-C(3)-H(3)	97.3(11)
C(2)-Nb(1)-B(4)	64.68(6)	S(6)-Nb(1)-S(3)	131.498(16)	C(3)-C(2)-B(6)	111.97(12)
B(6)-Nb(1)-B(4)	67.94(6)	C(2)-Nb(1)-S(5)	75.18(4)	C(3)-C(2)-B(11)	112.06(12)
C(3)-Nb(1)-B(4)	38.65(5)	B(6)-Nb(1)-S(5)	75.78(4)	B(6)-C(2)-B(11)	63.53(10)
C(2)-Nb(1)-B(5)	66.17(5)	C(3)-Nb(1)-S(5)	108.24(4)	C(3)-C(2)-B(7)	63.12(10)
B(6)-Nb(1)-B(5)	40.98(6)	B(4)-Nb(1)-S(5)	138.90(4)	B(6)-C(2)-B(7)	115.40(12)
C(3)-Nb(1)-B(5)	65.98(6)	B(5)-Nb(1)-S(5)	114.52(4)	B(11)-C(2)-B(7)	61.86(10)
B(4)-Nb(1)-B(5)	40.85(6)	S(1)-Nb(1)-S(5)	73.084(17)	C(3)-C(2)-Nb(1)	72.54(7)
C(2)-Nb(1)-S(1)	111.62(4)	S(2)-Nb(1)-S(5)	75.092(16)	B(6)-C(2)-Nb(1)	70.96(8)
B(6)-Nb(1)-S(1)	74.47(4)	S(4)-Nb(1)-S(5)	128.604(18)	B(11)-C(2)-Nb(1)	132.44(10)
C(3)-Nb(1)-S(1)	137.52(4)	S(6)-Nb(1)-S(5)	65.361(17)	B(7)-C(2)-Nb(1)	134.29(10)
B(4)-Nb(1)-S(1)	113.22(4)	S(3)-Nb(1)-S(5)	141.336(18)	C(3)-C(2)-H(2)	116.6(11)
B(5)-Nb(1)-S(1)	74.93(4)	C(13)-S(2)-Nb(1)	89.72(5)	B(6)-C(2)-H(2)	125.0(11)
C(2)-Nb(1)-S(2)	149.09(4)	C(13)-S(1)-Nb(1)	90.67(5)	B(11)-C(2)-H(2)	116.2(11)
B(6)-Nb(1)-S(2)	136.77(4)	C(16)-S(3)-Nb(1)	91.14(6)	B(7)-C(2)-H(2)	108.5(11)
C(3)-Nb(1)-S(2)	155.57(4)	C(16)-S(4)-Nb(1)	91.26(6)	Nb(1)-C(2)-H(2)	100.4(11)
B(4)-Nb(1)-S(2)	145.86(4)	C(19)-S(5)-Nb(1)	91.19(5)	C(2)-B(6)-B(5)	105.61(12)
B(5)-Nb(1)-S(2)	135.84(4)	C(19)-S(6)-Nb(1)	91.77(5)	C(2)-B(6)-B(10)	104.57(12)
S(1)-Nb(1)-S(2)	66.910(16)	C(19)-N(3)-C(21)	122.42(13)	B(5)-B(6)-B(10)	60.65(10)
C(2)-Nb(1)-S(4)	115.94(4)	C(19)-N(3)-C(20)	120.53(13)	C(2)-B(6)-B(11)	58.87(9)
B(6)-Nb(1)-S(4)	145.55(4)	C(21)-N(3)-C(20)	116.78(13)	B(5)-B(6)-B(11)	108.98(12)
C(3)-Nb(1)-S(4)	82.37(4)	C(13)-N(1)-C(14)	120.98(13)	B(10)-B(6)-B(11)	59.70(10)
B(4)-Nb(1)-S(4)	79.47(4)	C(13)-N(1)-C(15)	121.84(14)	C(2)-B(6)-Nb(1)	69.57(8)
B(5)-Nb(1)-S(4)	115.55(4)	C(14)-N(1)-C(15)	117.15(13)	B(5)-B(6)-Nb(1)	71.37(8)
S(1)-Nb(1)-S(4)	131.326(19)	C(16)-N(2)-C(18)	122.27(14)	B(10)-B(6)-Nb(1)	128.18(10)
S(2)-Nb(1)-S(4)	77.393(18)	C(16)-N(2)-C(17)	121.00(14)	B(11)-B(6)-Nb(1)	126.66(10)
C(2)-Nb(1)-S(6)	78.52(4)	C(18)-N(2)-C(17)	116.70(14)	C(2)-B(6)-H(6)	120.8(10)
B(6)-Nb(1)-S(6)	113.60(4)	C(2)-C(3)-B(4)	111.27(12)	B(5)-B(6)-H(6)	130.0(10)
C(3)-Nb(1)-S(6)	78.25(4)	C(2)-C(3)-B(8)	111.42(12)	B(10)-B(6)-H(6)	118.1(10)
B(4)-Nb(1)-S(6)	112.39(4)	B(4)-C(3)-B(8)	63.98(10)	B(11)-B(6)-H(6)	110.1(10)
B(5)-Nb(1)-S(6)	142.42(4)	C(2)-C(3)-B(7)	62.69(10)	Nb(1)-B(6)-H(6)	107.0(9)
S(1)-Nb(1)-S(6)	132.98(2)	B(4)-C(3)-B(7)	115.27(12)	B(6)-B(5)-B(4)	104.84(12)
S(2)-Nb(1)-S(6)	81.628(17)	B(8)-C(3)-B(7)	61.63(10)	B(6)-B(5)-B(10)	59.74(9)
S(4)-Nb(1)-S(6)	68.32(2)	C(2)-C(3)-Nb(1)	70.51(7)	B(4)-B(5)-B(10)	106.37(12)
C(2)-Nb(1)-S(3)	136.12(4)	B(4)-C(3)-Nb(1)	71.65(8)	B(6)-B(5)-B(9)	106.21(12)
B(6)-Nb(1)-S(3)	112.76(4)	B(8)-C(3)-Nb(1)	132.92(10)	B(4)-B(5)-B(9)	59.75(10)
C(3)-Nb(1)-S(3)	109.40(4)	B(7)-C(3)-Nb(1)	131.91(10)	B(10)-B(5)-B(9)	59.32(10)
B(4)-Nb(1)-S(3)	73.31(4)	C(2)-C(3)-H(3)	117.5(11)	B(6)-B(5)-Nb(1)	67.65(8)
B(5)-Nb(1)-S(3)	74.12(4)	B(4)-C(3)-H(3)	122.4(11)	B(4)-B(5)-Nb(1)	68.87(8)

Appendix A – Crystal Data

B(10)-B(5)-Nb(1)	123.90(10)	B(11)-B(10)-B(12)	59.55(10)	B(9)-B(12)-H(12)	124.2(11)
B(9)-B(5)-Nb(1)	124.70(10)	B(9)-B(10)-B(12)	60.27(10)	B(10)-B(12)-H(12)	125.0(11)
B(6)-B(5)-H(5)	125.2(9)	B(6)-B(10)-B(12)	107.97(12)	N(1)-C(13)-S(2)	125.31(12)
B(4)-B(5)-H(5)	124.4(9)	B(11)-B(10)-B(5)	108.68(12)	N(1)-C(13)-S(1)	122.13(12)
B(10)-B(5)-H(5)	118.2(9)	B(9)-B(10)-B(5)	60.35(10)	S(2)-C(13)-S(1)	112.54(8)
B(9)-B(5)-H(5)	117.8(9)	B(6)-B(10)-B(5)	59.61(10)	N(1)-C(15)-H(151)	113.0(16)
Nb(1)-B(5)-H(5)	106.9(9)	B(12)-B(10)-B(5)	109.44(12)	N(1)-C(15)-H(152)	109.8(17)
C(3)-B(4)-B(9)	104.71(12)	B(11)-B(10)-H(10)	119.0(10)	H(151)-C(15)-H(152)	111(2)
C(3)-B(4)-B(5)	106.25(12)	B(9)-B(10)-H(10)	125.5(10)	N(1)-C(15)-H(153)	110(2)
B(9)-B(4)-B(5)	60.46(10)	B(6)-B(10)-H(10)	119.8(10)	H(151)-C(15)-H(153)	112(2)
C(3)-B(4)-B(8)	59.07(9)	B(12)-B(10)-H(10)	121.9(10)	H(152)-C(15)-H(153)	100(2)
B(9)-B(4)-B(8)	59.47(10)	B(5)-B(10)-H(10)	122.0(10)	N(1)-C(14)-H(141)	111.0(17)
B(5)-B(4)-B(8)	108.93(12)	B(8)-B(9)-B(10)	107.97(12)	N(1)-C(14)-H(142)	111.7(19)
C(3)-B(4)-Nb(1)	69.70(8)	B(8)-B(9)-B(4)	60.59(10)	H(141)-C(14)-H(142)	102(2)
B(9)-B(4)-Nb(1)	126.66(10)	B(10)-B(9)-B(4)	107.18(12)	N(1)-C(14)-H(143)	110.8(17)
B(5)-B(4)-Nb(1)	70.29(8)	B(8)-B(9)-B(12)	59.87(10)	H(141)-C(14)-H(143)	105(2)
B(8)-B(4)-Nb(1)	126.47(10)	B(10)-B(9)-B(12)	60.31(10)	H(142)-C(14)-H(143)	116(2)
C(3)-B(4)-H(4)	121.6(10)	B(4)-B(9)-B(12)	108.15(12)	N(2)-C(16)-S(3)	124.41(12)
B(9)-B(4)-H(4)	119.6(10)	B(8)-B(9)-B(5)	109.28(12)	N(2)-C(16)-S(4)	123.64(12)
B(5)-B(4)-H(4)	127.5(10)	B(10)-B(9)-B(5)	60.33(10)	S(3)-C(16)-S(4)	111.95(9)
B(8)-B(4)-H(4)	113.2(10)	B(4)-B(9)-B(5)	59.78(10)	N(2)-C(17)-H(171)	114(2)
Nb(1)-B(4)-H(4)	105.7(10)	B(12)-B(9)-B(5)	109.45(12)	N(2)-C(17)-H(172)	113(2)
C(2)-B(7)-C(3)	54.19(9)	B(8)-B(9)-H(9)	120.7(10)	H(171)-C(17)-H(172)	109(3)
C(2)-B(7)-B(8)	102.02(11)	B(10)-B(9)-H(9)	122.8(10)	N(2)-C(17)-H(173)	107(2)
C(3)-B(7)-B(8)	58.37(9)	B(4)-B(9)-H(9)	121.5(10)	H(171)-C(17)-H(173)	99(3)
C(2)-B(7)-B(11)	58.31(9)	B(12)-B(9)-H(9)	121.4(10)	H(172)-C(17)-H(173)	114(3)
C(3)-B(7)-B(11)	102.08(11)	B(5)-B(9)-H(9)	120.9(10)	N(2)-C(18)-H(181)	111.9(13)
B(8)-B(7)-B(11)	107.29(13)	C(3)-B(8)-B(7)	60.00(9)	N(2)-C(18)-H(182)	110.0(18)
C(2)-B(7)-B(12)	103.73(12)	C(3)-B(8)-B(9)	103.44(12)	H(181)-C(18)-H(182)	100(2)
C(3)-B(7)-B(12)	103.98(12)	B(7)-B(8)-B(9)	108.51(13)	N(2)-C(18)-H(183)	108.8(19)
B(8)-B(7)-B(12)	60.35(10)	C(3)-B(8)-B(12)	104.82(12)	H(181)-C(18)-H(183)	114(2)
B(11)-B(7)-B(12)	60.05(10)	B(7)-B(8)-B(12)	59.85(10)	H(182)-C(18)-H(183)	112(2)
C(2)-B(7)-H(7)	118.0(10)	B(9)-B(8)-B(12)	60.56(10)	N(3)-C(19)-S(5)	124.86(11)
C(3)-B(7)-H(7)	119.6(10)	C(3)-B(8)-B(4)	56.95(9)	N(3)-C(19)-S(6)	123.56(11)
B(8)-B(7)-H(7)	126.5(11)	B(7)-B(8)-B(4)	108.10(12)	S(5)-C(19)-S(6)	111.58(8)
B(11)-B(7)-H(7)	123.2(10)	B(9)-B(8)-B(4)	59.94(10)	N(3)-C(20)-H(201)	110.4(14)
B(12)-B(7)-H(7)	131.6(10)	B(12)-B(8)-B(4)	108.19(12)	N(3)-C(20)-H(202)	107.8(13)
C(2)-B(11)-B(7)	59.83(9)	C(3)-B(8)-H(8)	119.6(10)	H(201)-C(20)-H(202)	110.1(19)
C(2)-B(11)-B(12)	104.84(12)	B(7)-B(8)-H(8)	118.6(10)	N(3)-C(20)-H(203)	108.1(14)
B(7)-B(11)-B(12)	60.00(10)	B(9)-B(8)-H(8)	127.2(10)	H(201)-C(20)-H(203)	113.6(19)
C(2)-B(11)-B(10)	103.80(12)	B(12)-B(8)-H(8)	126.5(10)	H(202)-C(20)-H(203)	106.6(19)
B(7)-B(11)-B(10)	108.94(13)	B(4)-B(8)-H(8)	120.1(10)	N(3)-C(21)-H(211)	111.0(17)
B(12)-B(11)-B(10)	60.74(10)	B(7)-B(12)-B(11)	59.96(10)	N(3)-C(21)-H(212)	106.7(17)
C(2)-B(11)-B(6)	57.61(9)	B(7)-B(12)-B(8)	59.80(10)	H(211)-C(21)-H(212)	104(2)
B(7)-B(11)-B(6)	108.78(12)	B(11)-B(12)-B(8)	106.79(12)	N(3)-C(21)-H(213)	110.4(16)
B(12)-B(11)-B(6)	108.59(12)	B(7)-B(12)-B(9)	107.67(12)	H(211)-C(21)-H(213)	112(2)
B(10)-B(11)-B(6)	59.95(10)	B(11)-B(12)-B(9)	106.72(12)	H(212)-C(21)-H(213)	113(2)
C(2)-B(11)-H(11)	118.5(10)	B(8)-B(12)-B(9)	59.56(10)	Cl(2A)-C(22)-Cl(1A)	111.50(10)
B(7)-B(11)-H(11)	117.4(10)	B(7)-B(12)-B(10)	108.07(12)	Cl(1B)-C(22)-Cl(2B)	112.0(6)
B(12)-B(11)-H(11)	126.8(10)	B(11)-B(12)-B(10)	59.70(10)	Cl(2A)-C(22)-D(222)	108.6(11)
B(10)-B(11)-H(11)	128.2(10)	B(8)-B(12)-B(10)	107.02(12)	Cl(1A)-C(22)-D(222)	109.2(11)
B(6)-B(11)-H(11)	119.8(10)	B(9)-B(12)-B(10)	59.42(10)	Cl(2A)-C(22)-D(221)	109.6(13)
B(11)-B(10)-B(9)	107.27(13)	B(7)-B(12)-H(12)	118.5(11)	Cl(1A)-C(22)-D(221)	105.6(13)
B(11)-B(10)-B(6)	60.35(10)	B(11)-B(12)-H(12)	122.4(11)	D(222)-C(22)-D(221)	112.3(17)
B(9)-B(10)-B(6)	106.92(12)	B(8)-B(12)-H(12)	120.6(11)		

Table 4. Anisotropic displacement parameters ($\text{\AA}^2 \times 10^3$) for (23). The anisotropic displacement factor exponent takes the form: $-2\pi^2 [h^2 a^{*2} U^{11} + \dots + 2 h k a^* b^* U^{12}]$

Appendix A – Crystal Data

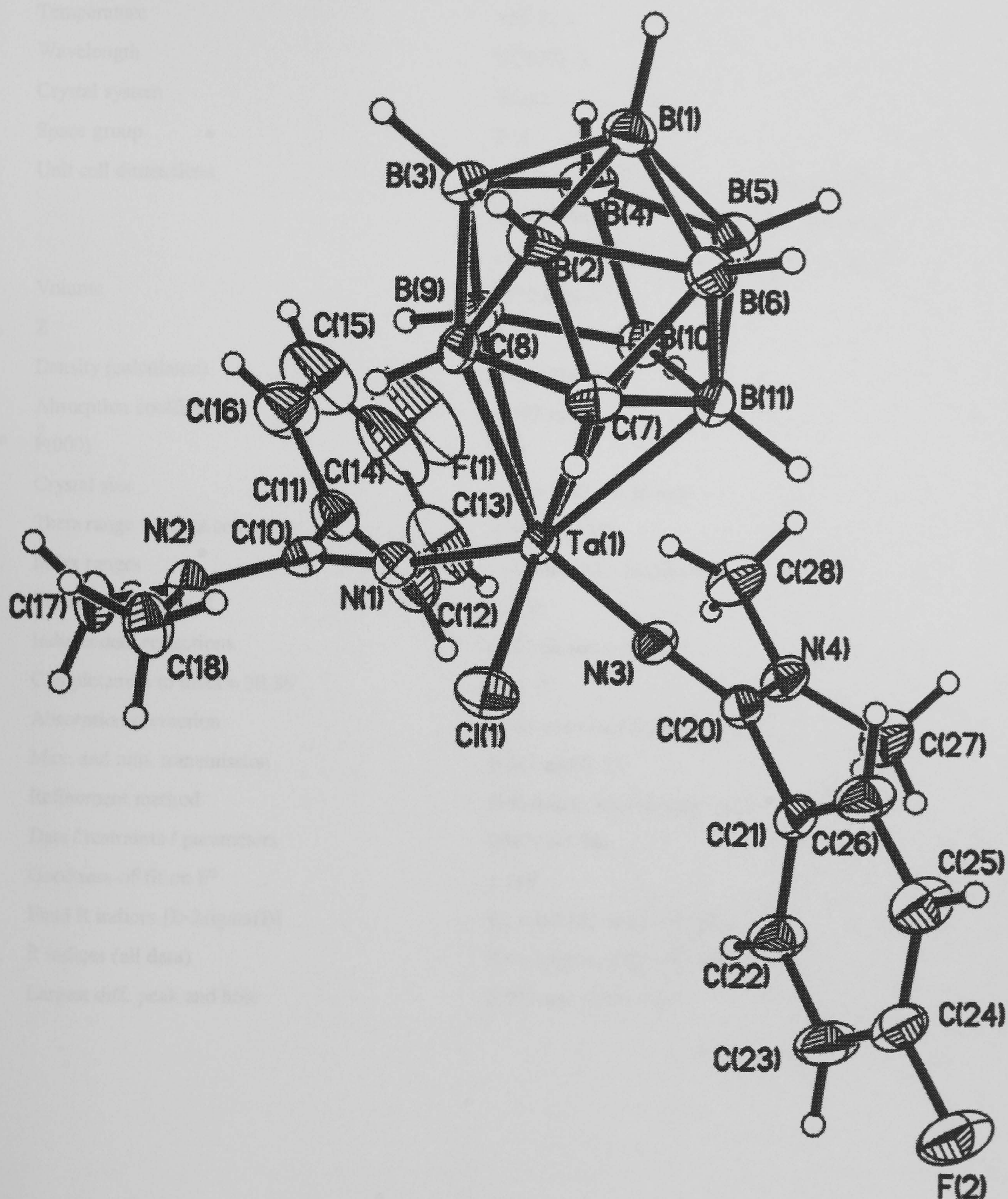
	U ¹¹	U ²²	U ³³	U ²³	U ¹³	U ¹²
Nb(1)	12(1)	12(1)	10(1)	3(1)	3(1)	5(1)
S(2)	22(1)	14(1)	12(1)	4(1)	5(1)	7(1)
S(1)	19(1)	14(1)	12(1)	4(1)	4(1)	7(1)
S(3)	14(1)	17(1)	13(1)	3(1)	2(1)	4(1)
S(4)	14(1)	18(1)	13(1)	4(1)	4(1)	5(1)
S(5)	15(1)	19(1)	13(1)	5(1)	5(1)	8(1)
S(6)	14(1)	18(1)	12(1)	4(1)	4(1)	7(1)
N(3)	15(1)	19(1)	15(1)	4(1)	2(1)	9(1)
N(1)	24(1)	17(1)	14(1)	3(1)	5(1)	10(1)
N(2)	15(1)	22(1)	18(1)	5(1)	4(1)	1(1)
C(3)	16(1)	16(1)	15(1)	3(1)	4(1)	8(1)
C(2)	14(1)	13(1)	17(1)	3(1)	2(1)	5(1)
B(6)	15(1)	15(1)	17(1)	6(1)	5(1)	6(1)
B(5)	16(1)	15(1)	16(1)	5(1)	3(1)	7(1)
B(4)	15(1)	17(1)	16(1)	4(1)	3(1)	8(1)
B(7)	19(1)	14(1)	19(1)	2(1)	2(1)	8(1)
B(11)	18(1)	13(1)	21(1)	5(1)	4(1)	6(1)
B(10)	19(1)	16(1)	18(1)	6(1)	4(1)	10(1)
B(9)	18(1)	19(1)	19(1)	5(1)	3(1)	10(1)
B(8)	19(1)	19(1)	19(1)	5(1)	4(1)	11(1)
B(12)	21(1)	15(1)	20(1)	4(1)	4(1)	9(1)
C(13)	15(1)	17(1)	13(1)	3(1)	2(1)	7(1)
C(15)	46(1)	17(1)	22(1)	4(1)	5(1)	16(1)
C(14)	32(1)	23(1)	14(1)	3(1)	7(1)	11(1)
C(16)	15(1)	15(1)	18(1)	4(1)	4(1)	6(1)
C(17)	19(1)	35(1)	26(1)	9(1)	-1(1)	-4(1)
C(18)	24(1)	28(1)	23(1)	8(1)	10(1)	-1(1)
C(19)	16(1)	12(1)	14(1)	2(1)	4(1)	6(1)
C(20)	16(1)	28(1)	26(1)	4(1)	5(1)	11(1)
C(21)	23(1)	27(1)	16(1)	4(1)	0(1)	11(1)
C(22)	19(1)	23(1)	29(1)	4(1)	6(1)	8(1)
Cl(1A)	26(1)	33(1)	24(1)	1(1)	2(1)	11(1)
Cl(2A)	31(1)	31(1)	45(1)	15(1)	13(1)	8(1)

Appendix A – Crystal Data

Table 5. Hydrogen coordinates (x 10⁴) and isotropic displacement parameters (Å²x 10³) for (23).

	x	y	z	U(eq)
H(3)	2250(20)	1830(17)	889(14)	18(4)
H(2)	-140(20)	1308(17)	1441(14)	18(4)
H(6)	160(20)	1829(17)	3499(13)	18(4)
H(5)	3591(18)	2855(15)	4262(12)	10(4)
H(4)	4770(20)	2765(17)	2362(14)	21(5)
H(7)	350(20)	-579(18)	687(14)	24(5)
H(11)	-930(20)	-582(18)	2401(14)	24(5)
H(10)	1480(20)	264(18)	4224(14)	26(5)
H(9)	4370(20)	829(17)	3494(14)	19(5)
H(8)	3590(20)	280(18)	1291(14)	23(5)
H(12)	1590(20)	-1365(18)	2393(14)	25(5)
H(151)	3080(30)	8240(20)	3810(20)	60(8)
H(152)	3720(30)	8810(30)	4940(20)	64(8)
H(153)	2200(30)	8460(30)	4570(20)	76(10)
H(141)	1440(30)	6070(30)	5660(20)	71(9)
H(142)	2180(30)	7450(30)	6000(20)	80(10)
H(143)	3120(30)	6620(30)	6000(20)	68(8)
H(171)	7910(30)	6500(30)	3870(20)	72(9)
H(172)	8610(40)	7580(30)	3450(20)	90(11)
H(173)	8950(40)	6390(30)	3310(30)	103(12)
H(181)	6800(30)	5830(20)	943(17)	36(6)
H(182)	8330(30)	6160(30)	1420(20)	69(9)
H(183)	7800(30)	7240(30)	1520(20)	80(10)
H(201)	-3890(30)	2130(20)	859(17)	45(7)
H(202)	-3900(30)	3360(20)	477(17)	41(6)
H(203)	-3030(20)	3510(20)	1512(17)	35(6)
H(211)	-1170(30)	3370(30)	-722(19)	59(8)
H(212)	-2550(30)	3560(30)	-750(20)	67(8)
H(213)	-2640(30)	2170(30)	-890(20)	60(8)
D(222)	7530(20)	10559(17)	2548(13)	15(4)
D(221)	6000(20)	10559(19)	2233(15)	29(5)

A10 Crystal data for $[3\text{-Ta}(\text{N}=\text{C}(\text{C}_6\text{H}_4\text{F})\text{NMe}_2)_2\text{Cl}(1,2\text{-C}_2\text{B}_9\text{H}_{11})]:2\text{CCl}_2\text{H}_2$;
(26).



Appendix A – Crystal Data

Table 1. Crystal data and structure refinement for (26).

Identification code	99srv158	
Empirical formula	C22 H35 B9 Cl5 F2 N4 Ta	
Formula weight	849.03	
Temperature	150(2) K	
Wavelength	0.71073 Å	
Crystal system	Triclinic	
Space group	P -1	
Unit cell dimensions	a = 10.122(2) Å	α= 90.21(1)°.
	b = 12.074(2) Å	β= 105.49(1)°.
	c = 15.206(3) Å	γ= 104.14(1)°.
Volume	1732.0(6) Å ³	
Z	2	
Density (calculated)	1.628 Mg/m ³	
Absorption coefficient	3.592 mm ⁻¹	
F(000)	832	
Crystal size	0.42 x 0.42 x 0.36 mm ³	
Theta range for data collection	1.39 to 30.38°.	
Index ranges	-14<=h<=14, -16<=k<=16, -20<=l<=20	
Reflections collected	22150	
Independent reflections	9387 [R(int) = 0.0221]	
Completeness to theta = 30.38°	89.7 %	
Absorption correction	Semi-empirical from equivalents	
Max. and min. transmission	0.381 and 0.307	
Refinement method	Full-matrix least-squares on F ²	
Data / restraints / parameters	9387 / 0 / 396	
Goodness-of-fit on F ²	1.118	
Final R indices [I>2sigma(I)]	R1 = 0.0330, wR2 = 0.0871	
R indices (all data)	R1 = 0.0364, wR2 = 0.0900	
Largest diff. peak and hole	2.892 and -2.243 e.Å ⁻³	

Appendix A – Crystal Data

Table 2. Atomic coordinates ($\times 10^4$) and equivalent isotropic displacement parameters ($\text{\AA}^2 \times 10^3$) for (26). U(eq) is defined as one third of the trace of the orthogonalized U^{ij} tensor.

	x	y	z	U(eq)
Ta(1)	644(1)	3293(1)	3452(1)	18(1)
Cl(1)	724(1)	3447(1)	5039(1)	31(1)
B(1)	3068(5)	6530(3)	2627(3)	27(1)
B(2)	2465(5)	6526(4)	3610(3)	29(1)
B(3)	1233(4)	6280(3)	2522(3)	26(1)
B(4)	1799(5)	5444(4)	1813(3)	29(1)
B(5)	3409(5)	5163(4)	2470(3)	31(1)
B(6)	3812(4)	5835(4)	3579(3)	31(1)
C(7)	2399(4)	5163(3)	3960(2)	25(1)
C(8)	961(4)	5407(3)	3372(2)	23(1)
B(9)	444(4)	4776(3)	2316(3)	25(1)
B(10)	1782(5)	4075(3)	2267(3)	26(1)
B(11)	3017(4)	4342(4)	3371(3)	26(1)
N(1)	-1322(3)	2877(3)	2949(2)	23(1)
C(10)	-2624(4)	2665(3)	2446(2)	22(1)
C(11)	-2973(4)	2142(4)	1495(3)	29(1)
C(12)	-2750(5)	1072(4)	1366(3)	41(1)
C(13)	-3048(6)	567(6)	485(4)	60(2)
C(14)	-3536(6)	1172(7)	-239(4)	67(2)
F(1)	-3833(5)	678(5)	-1092(3)	104(2)
C(15)	-3742(7)	2240(8)	-134(4)	68(2)
C(16)	-3464(5)	2738(5)	747(3)	47(1)
N(2)	-3657(3)	2895(3)	2753(2)	26(1)
C(17)	-5169(4)	2469(4)	2287(3)	33(1)
C(18)	-3323(4)	3457(4)	3664(3)	35(1)
N(3)	1106(3)	1900(3)	3402(2)	24(1)
C(20)	1594(4)	992(3)	3423(2)	23(1)
C(21)	2228(4)	618(3)	4344(3)	24(1)
C(22)	1587(5)	-400(4)	4656(3)	36(1)
C(23)	2187(5)	-706(4)	5520(3)	41(1)
C(24)	3425(5)	6(4)	6048(3)	34(1)
F(2)	4035(3)	-301(3)	6890(2)	49(1)
C(25)	4084(5)	1010(4)	5764(3)	38(1)
C(26)	3456(4)	1330(3)	4903(3)	33(1)
N(4)	1567(4)	406(3)	2675(2)	27(1)
C(27)	2246(5)	-542(4)	2690(3)	38(1)
C(28)	922(5)	718(4)	1764(3)	35(1)
C(30)	1395(7)	3351(6)	-280(4)	56(1)
Cl(2)	2966(3)	2944(4)	-46(2)	147(2)
Cl(3)	-36(3)	2155(2)	-276(1)	90(1)
C(31)	7076(6)	-2807(5)	2786(4)	50(1)
Cl(4)	8262(2)	-1553(1)	2588(1)	62(1)
Cl(5)	7476(1)	-4049(1)	2441(1)	49(1)

Appendix A – Crystal Data

Table 3. Bond lengths [Å] and angles [°] for (26).

Ta(1)-N(3)	1.859(3)	B(6)-B(11)	1.774(6)	C(18)-H(18B)	0.9600
Ta(1)-N(1)	1.870(3)	B(6)-H(6)	1.1000	C(18)-H(18C)	0.9600
Ta(1)-Cl(1)	2.3975(10)	C(7)-C(8)	1.588(5)	N(3)-C(20)	1.304(4)
Ta(1)-B(10)	2.461(4)	C(7)-B(11)	1.665(6)	C(20)-N(4)	1.328(5)
Ta(1)-B(11)	2.462(4)	C(7)-H(7)	0.99(5)	C(20)-C(21)	1.498(5)
Ta(1)-C(7)	2.479(4)	C(8)-B(9)	1.667(6)	C(21)-C(26)	1.384(5)
Ta(1)-B(9)	2.499(4)	C(8)-H(8)	0.96(5)	C(21)-C(22)	1.391(5)
Ta(1)-C(8)	2.501(3)	B(9)-B(10)	1.781(6)	C(22)-C(23)	1.386(6)
B(1)-B(2)	1.758(6)	B(9)-H(9)	1.1000	C(22)-H(22A)	0.9300
B(1)-B(6)	1.762(6)	B(10)-B(11)	1.779(6)	C(23)-C(24)	1.372(6)
B(1)-B(3)	1.771(6)	B(10)-H(10)	1.1000	C(23)-H(23A)	0.9300
B(1)-B(4)	1.794(6)	B(11)-H(11)	1.1000	C(24)-F(2)	1.360(5)
B(1)-B(5)	1.794(6)	N(1)-C(10)	1.297(5)	C(24)-C(25)	1.366(6)
B(1)-H(1)	1.1000	C(10)-N(2)	1.337(5)	C(25)-C(26)	1.395(6)
B(2)-C(7)	1.723(6)	C(10)-C(11)	1.493(5)	C(25)-H(25A)	0.9300
B(2)-C(8)	1.723(6)	C(11)-C(12)	1.386(6)	C(26)-H(26A)	0.9300
B(2)-B(3)	1.758(6)	C(11)-C(16)	1.393(6)	N(4)-C(28)	1.459(5)
B(2)-B(6)	1.774(7)	C(12)-C(13)	1.396(7)	N(4)-C(27)	1.470(5)
B(2)-H(2)	1.1000	C(12)-H(12A)	0.9300	C(27)-H(27A)	0.9600
B(3)-C(8)	1.706(5)	C(13)-C(14)	1.372(11)	C(27)-H(27B)	0.9600
B(3)-B(4)	1.765(6)	C(13)-H(13A)	0.9300	C(27)-H(27C)	0.9600
B(3)-B(9)	1.785(6)	C(14)-F(1)	1.352(6)	C(28)-H(28A)	0.9600
B(3)-H(3)	1.1000	C(14)-C(15)	1.371(11)	C(28)-H(28B)	0.9600
B(4)-B(9)	1.772(6)	C(15)-C(16)	1.394(8)	C(28)-H(28C)	0.9600
B(4)-B(5)	1.781(7)	C(15)-H(15A)	0.9300	C(30)-Cl(2)	1.726(6)
B(4)-B(10)	1.791(6)	C(16)-H(16A)	0.9300	C(30)-Cl(3)	1.779(7)
B(4)-H(4)	1.1000	N(2)-C(18)	1.457(5)	C(30)-H(30A)	0.9700
B(5)-B(11)	1.769(6)	N(2)-C(17)	1.463(5)	C(30)-H(30B)	0.9700
B(5)-B(6)	1.770(7)	C(17)-H(17A)	0.9600	C(31)-Cl(5)	1.758(6)
B(5)-B(10)	1.790(6)	C(17)-H(17B)	0.9600	C(31)-Cl(4)	1.770(6)
B(5)-H(5)	1.1000	C(17)-H(17C)	0.9600	C(31)-H(31A)	0.9700
B(6)-C(7)	1.708(6)	C(18)-H(18A)	0.9600	C(31)-H(31B)	0.9700
N(3)-Ta(1)-N(1)	102.25(14)	B(2)-B(1)-H(1)	121.6	B(3)-B(4)-B(10)	108.9(3)
N(3)-Ta(1)-Cl(1)	99.38(10)	B(6)-B(1)-H(1)	121.8	B(9)-B(4)-B(10)	60.0(2)
N(1)-Ta(1)-Cl(1)	98.91(10)	B(3)-B(1)-H(1)	122.3	B(5)-B(4)-B(10)	60.1(2)
N(3)-Ta(1)-B(10)	93.92(14)	B(4)-B(1)-H(1)	122.5	B(3)-B(4)-B(1)	59.7(2)
N(1)-Ta(1)-B(10)	109.18(14)	B(5)-B(1)-H(1)	122.1	B(9)-B(4)-B(1)	108.1(3)
Cl(1)-Ta(1)-B(10)	145.51(11)	C(7)-B(2)-C(8)	54.9(2)	B(5)-B(4)-B(1)	60.2(3)
N(3)-Ta(1)-B(11)	91.16(14)	C(7)-B(2)-B(3)	102.9(3)	B(10)-B(4)-B(1)	108.8(3)
N(1)-Ta(1)-B(11)	149.97(14)	C(8)-B(2)-B(3)	58.7(2)	B(3)-B(4)-H(4)	121.4
Cl(1)-Ta(1)-B(11)	105.31(11)	C(7)-B(2)-B(1)	103.8(3)	B(9)-B(4)-H(4)	121.8
B(10)-Ta(1)-B(11)	42.38(15)	C(8)-B(2)-B(1)	104.3(3)	B(5)-B(4)-H(4)	121.9
N(3)-Ta(1)-C(7)	124.50(13)	B(3)-B(2)-B(1)	60.5(2)	B(10)-B(4)-H(4)	121.1
N(1)-Ta(1)-C(7)	133.05(13)	C(7)-B(2)-B(6)	58.4(2)	B(1)-B(4)-H(4)	121.5
Cl(1)-Ta(1)-C(7)	79.16(9)	C(8)-B(2)-B(6)	102.8(3)	B(11)-B(5)-B(6)	60.2(3)
B(10)-Ta(1)-C(7)	67.14(13)	B(3)-B(2)-B(6)	107.7(3)	B(11)-B(5)-B(4)	107.3(3)
B(11)-Ta(1)-C(7)	39.40(14)	B(1)-B(2)-B(6)	59.8(3)	B(6)-B(5)-B(4)	107.4(3)
N(3)-Ta(1)-B(9)	131.26(14)	C(7)-B(2)-H(2)	126.0	B(11)-B(5)-B(10)	60.0(2)
N(1)-Ta(1)-B(9)	81.21(13)	C(8)-B(2)-H(2)	125.7	B(6)-B(5)-B(10)	108.7(3)
Cl(1)-Ta(1)-B(9)	128.48(10)	B(3)-B(2)-H(2)	122.2	B(4)-B(5)-B(10)	60.2(2)
B(10)-Ta(1)-B(9)	42.06(14)	B(1)-B(2)-H(2)	122.8	B(11)-B(5)-B(1)	107.4(3)
B(11)-Ta(1)-B(9)	69.91(14)	B(6)-B(2)-H(2)	122.6	B(6)-B(5)-B(1)	59.2(3)
C(7)-Ta(1)-B(9)	65.67(13)	C(8)-B(3)-B(2)	59.6(2)	B(4)-B(5)-B(1)	60.2(2)
N(3)-Ta(1)-C(8)	156.78(13)	C(8)-B(3)-B(4)	103.2(3)	B(10)-B(5)-B(1)	108.9(3)
N(1)-Ta(1)-C(8)	96.62(13)	B(2)-B(3)-B(4)	108.6(3)	B(11)-B(5)-H(5)	122.2
Cl(1)-Ta(1)-C(8)	90.85(9)	C(8)-B(3)-B(1)	104.5(3)	B(6)-B(5)-H(5)	121.9
B(10)-Ta(1)-C(8)	66.88(13)	B(2)-B(3)-B(1)	59.8(2)	B(4)-B(5)-H(5)	122.1
B(11)-Ta(1)-C(8)	65.95(12)	B(4)-B(3)-B(1)	61.0(2)	B(10)-B(5)-H(5)	120.9
C(7)-Ta(1)-C(8)	37.19(12)	C(8)-B(3)-B(9)	57.0(2)	B(1)-B(5)-H(5)	121.7
B(9)-Ta(1)-C(8)	38.96(13)	B(2)-B(3)-B(9)	108.1(3)	C(7)-B(6)-B(1)	104.3(3)
B(2)-B(1)-B(6)	60.5(3)	B(4)-B(3)-B(9)	59.9(2)	C(7)-B(6)-B(5)	103.1(3)
B(2)-B(1)-B(3)	59.8(2)	B(1)-B(3)-B(9)	108.6(3)	B(1)-B(6)-B(5)	61.1(3)
B(6)-B(1)-B(3)	107.7(3)	C(8)-B(3)-H(3)	125.8	C(7)-B(6)-B(2)	59.3(2)
B(2)-B(1)-B(4)	107.3(3)	B(2)-B(3)-H(3)	120.8	B(1)-B(6)-B(2)	59.7(2)
B(6)-B(1)-B(4)	107.2(3)	B(4)-B(3)-H(3)	122.4	B(5)-B(6)-B(2)	108.4(3)
B(3)-B(1)-B(4)	59.3(3)	B(1)-B(3)-H(3)	121.9	C(7)-B(6)-B(11)	57.1(2)
B(2)-B(1)-B(5)	108.0(3)	B(9)-B(3)-H(3)	121.8	B(1)-B(6)-B(11)	108.7(3)
B(6)-B(1)-B(5)	59.7(3)	B(3)-B(4)-B(9)	60.6(2)	B(5)-B(6)-B(11)	59.9(3)
B(3)-B(1)-B(5)	107.1(3)	B(3)-B(4)-B(5)	107.9(3)	B(2)-B(6)-B(11)	107.8(3)
B(4)-B(1)-B(5)	59.5(3)	B(9)-B(4)-B(5)	107.6(3)	C(7)-B(6)-H(6)	125.9

Appendix A – Crystal Data

B(1)-B(6)-H(6)	121.9	B(11)-B(10)-Ta(1)	68.83(19)	N(2)-C(18)-H(18A)	109.5
B(5)-B(6)-H(6)	122.4	B(9)-B(10)-Ta(1)	70.11(19)	N(2)-C(18)-H(18B)	109.5
B(2)-B(6)-H(6)	121.2	B(5)-B(10)-Ta(1)	125.2(3)	H(18A)-C(18)-H(18B)	109.5
B(11)-B(6)-H(6)	121.8	B(4)-B(10)-Ta(1)	126.0(2)	N(2)-C(18)-H(18C)	109.5
C(8)-C(7)-B(11)	112.2(3)	B(11)-B(10)-H(10)	124.3	H(18A)-C(18)-H(18C)	109.5
C(8)-C(7)-B(6)	112.1(3)	B(9)-B(10)-H(10)	123.4	H(18B)-C(18)-H(18C)	109.5
B(11)-C(7)-B(6)	63.5(3)	B(5)-B(10)-H(10)	119.5	C(20)-N(3)-Ta(1)	172.7(3)
C(8)-C(7)-B(2)	62.6(2)	B(4)-B(10)-H(10)	119.4	N(3)-C(20)-N(4)	123.3(3)
B(11)-C(7)-B(2)	115.6(3)	Ta(1)-B(10)-H(10)	103.4	N(3)-C(20)-C(21)	117.4(3)
B(6)-C(7)-B(2)	62.3(3)	C(7)-B(11)-B(5)	104.9(3)	N(4)-C(20)-C(21)	119.4(3)
C(8)-C(7)-Ta(1)	72.17(18)	C(7)-B(11)-B(6)	59.4(2)	C(26)-C(21)-C(22)	119.8(4)
B(11)-C(7)-Ta(1)	69.75(19)	B(5)-B(11)-B(6)	59.9(3)	C(26)-C(21)-C(20)	118.5(3)
B(6)-C(7)-Ta(1)	130.8(3)	C(7)-B(11)-B(10)	104.9(3)	C(22)-C(21)-C(20)	121.6(3)
B(2)-C(7)-Ta(1)	133.0(2)	B(5)-B(11)-B(10)	60.6(3)	C(23)-C(22)-C(21)	120.0(4)
C(8)-C(7)-H(7)	110(3)	B(6)-B(11)-B(10)	108.9(3)	C(23)-C(22)-H(22A)	120.0
B(11)-C(7)-H(7)	129(3)	C(7)-B(11)-Ta(1)	70.85(19)	C(21)-C(22)-H(22A)	120.0
B(6)-C(7)-H(7)	123(3)	B(5)-B(11)-Ta(1)	126.2(3)	C(24)-C(23)-C(22)	118.6(4)
B(2)-C(7)-H(7)	109(3)	B(6)-B(11)-Ta(1)	128.0(3)	C(24)-C(23)-H(23A)	120.7
Ta(1)-C(7)-H(7)	98(3)	B(10)-B(11)-Ta(1)	68.79(19)	C(22)-C(23)-H(23A)	120.7
C(7)-C(8)-B(9)	112.0(3)	C(7)-B(11)-H(11)	125.1	F(2)-C(24)-C(25)	118.1(4)
C(7)-C(8)-B(3)	111.4(3)	B(5)-B(11)-H(11)	119.8	F(2)-C(24)-C(23)	118.9(4)
B(9)-C(8)-B(3)	63.9(2)	B(6)-B(11)-H(11)	117.7	C(25)-C(24)-C(23)	123.0(4)
C(7)-C(8)-B(2)	62.5(2)	B(10)-B(11)-H(11)	123.6	C(24)-C(25)-C(26)	118.2(4)
B(9)-C(8)-B(2)	115.5(3)	Ta(1)-B(11)-H(11)	102.1	C(24)-C(25)-H(25A)	120.9
B(3)-C(8)-B(2)	61.7(2)	C(10)-N(1)-Ta(1)	168.1(3)	C(26)-C(25)-H(25A)	120.9
C(7)-C(8)-Ta(1)	70.64(18)	N(1)-C(10)-N(2)	122.3(3)	C(21)-C(26)-C(25)	120.3(4)
B(9)-C(8)-Ta(1)	70.46(18)	N(1)-C(10)-C(11)	118.5(3)	C(21)-C(26)-H(26A)	119.8
B(3)-C(8)-Ta(1)	131.2(2)	N(2)-C(10)-C(11)	119.3(3)	C(25)-C(26)-H(26A)	119.8
B(2)-C(8)-Ta(1)	131.4(2)	C(12)-C(11)-C(16)	120.5(4)	C(20)-N(4)-C(28)	121.3(3)
C(7)-C(8)-H(8)	117(3)	C(12)-C(11)-C(10)	119.0(4)	C(20)-N(4)-C(27)	123.6(3)
B(9)-C(8)-H(8)	123(3)	C(16)-C(11)-C(10)	120.5(4)	C(28)-N(4)-C(27)	115.0(3)
B(3)-C(8)-H(8)	118(3)	C(11)-C(12)-C(13)	120.4(5)	N(4)-C(27)-H(27A)	109.5
B(2)-C(8)-H(8)	111(3)	C(11)-C(12)-H(12A)	119.8	N(4)-C(27)-H(27B)	109.5
Ta(1)-C(8)-H(8)	100(3)	C(13)-C(12)-H(12A)	119.8	H(27A)-C(27)-H(27B)	109.5
C(8)-B(9)-B(4)	104.5(3)	C(14)-C(13)-C(12)	117.8(6)	N(4)-C(27)-H(27C)	109.5
C(8)-B(9)-B(10)	104.9(3)	C(14)-C(13)-H(13A)	121.1	H(27A)-C(27)-H(27C)	109.5
B(4)-B(9)-B(10)	60.5(2)	C(12)-C(13)-H(13A)	121.1	H(27B)-C(27)-H(27C)	109.5
C(8)-B(9)-B(3)	59.1(2)	F(1)-C(14)-C(15)	119.1(7)	N(4)-C(28)-H(28A)	109.5
B(4)-B(9)-B(3)	59.5(2)	F(1)-C(14)-C(13)	117.7(7)	N(4)-C(28)-H(28B)	109.5
B(10)-B(9)-B(3)	108.5(3)	C(15)-C(14)-C(13)	123.2(5)	H(28A)-C(28)-H(28B)	109.5
C(8)-B(9)-Ta(1)	70.58(18)	C(14)-C(15)-C(16)	119.0(6)	N(4)-C(28)-H(28C)	109.5
B(4)-B(9)-Ta(1)	124.8(2)	C(14)-C(15)-H(15A)	120.5	H(28A)-C(28)-H(28C)	109.5
B(10)-B(9)-Ta(1)	67.82(18)	C(16)-C(15)-H(15A)	120.5	H(28B)-C(28)-H(28C)	109.5
B(3)-B(9)-Ta(1)	126.9(2)	C(11)-C(16)-C(15)	119.1(6)	Cl(2)-C(30)-Cl(3)	110.3(4)
C(8)-B(9)-H(9)	125.0	C(11)-C(16)-H(16A)	120.4	Cl(2)-C(30)-H(30A)	109.6
B(4)-B(9)-H(9)	120.3	C(15)-C(16)-H(16A)	120.4	Cl(3)-C(30)-H(30A)	109.6
B(10)-B(9)-H(9)	123.7	C(10)-N(2)-C(18)	119.9(3)	Cl(2)-C(30)-H(30B)	109.6
B(3)-B(9)-H(9)	118.2	C(10)-N(2)-C(17)	124.0(3)	Cl(3)-C(30)-H(30B)	109.6
Ta(1)-B(9)-H(9)	103.3	C(18)-N(2)-C(17)	115.4(3)	H(30A)-C(30)-H(30B)	108.1
B(11)-B(10)-B(9)	106.0(3)	N(2)-C(17)-H(17A)	109.5	Cl(5)-C(31)-Cl(4)	111.4(3)
B(11)-B(10)-B(5)	59.4(3)	N(2)-C(17)-H(17B)	109.5	Cl(5)-C(31)-H(31A)	109.4
B(9)-B(10)-B(5)	106.9(3)	H(17A)-C(17)-H(17B)	109.5	Cl(4)-C(31)-H(31A)	109.4
B(11)-B(10)-B(4)	106.4(3)	N(2)-C(17)-H(17C)	109.5	Cl(5)-C(31)-H(31B)	109.4
B(9)-B(10)-B(4)	59.5(2)	H(17A)-C(17)-H(17C)	109.5	Cl(4)-C(31)-H(31B)	109.4
B(5)-B(10)-B(4)	59.7(2)	H(17B)-C(17)-H(17C)	109.5	H(31A)-C(31)-H(31B)	108.0

Table 4. Anisotropic displacement parameters ($\text{\AA}^2 \times 10^3$) for (26). The anisotropic displacement factor exponent takes the form: $-2\pi^2 [h^2 a^{*2} U^{11} + \dots + 2 h k a^* b^* U^{12}]$

Appendix A – Crystal Data

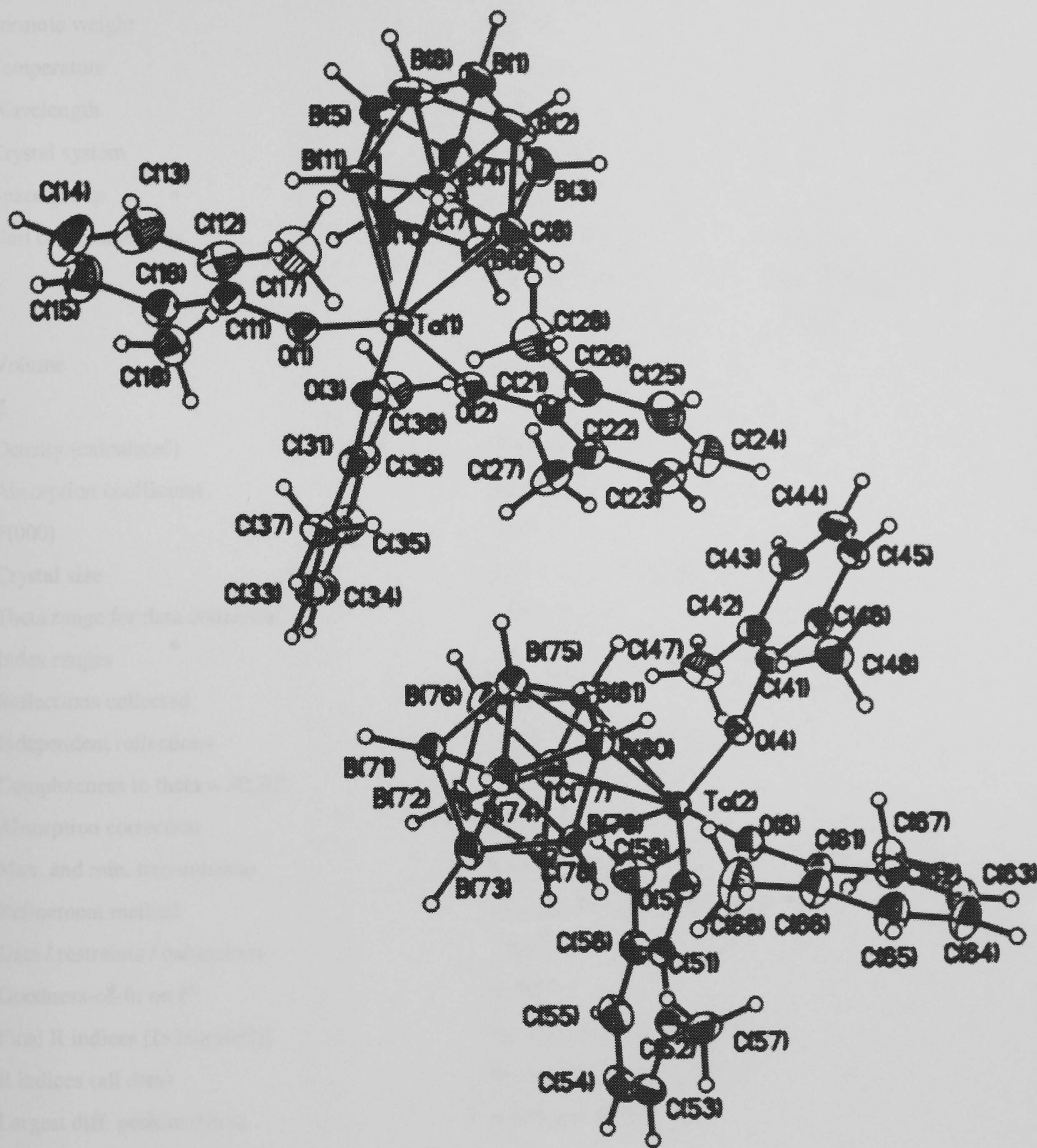
	U ¹¹	U ²²	U ³³	U ²³	U ¹³	U ¹²
Ta(1)	19(1)	16(1)	20(1)	2(1)	6(1)	7(1)
Cl(1)	39(1)	31(1)	22(1)	0(1)	11(1)	4(1)
B(1)	29(2)	21(2)	31(2)	3(1)	12(2)	4(1)
B(2)	35(2)	20(2)	31(2)	-3(1)	10(2)	3(2)
B(3)	28(2)	19(2)	34(2)	9(2)	11(2)	8(1)
B(4)	39(2)	21(2)	26(2)	4(1)	11(2)	6(2)
B(5)	32(2)	26(2)	44(2)	9(2)	21(2)	11(2)
B(6)	21(2)	27(2)	39(2)	7(2)	4(2)	2(2)
C(7)	28(2)	21(2)	23(2)	0(1)	5(1)	3(1)
C(8)	25(2)	20(1)	29(2)	1(1)	11(1)	11(1)
B(9)	24(2)	21(2)	28(2)	4(1)	4(1)	6(1)
B(10)	35(2)	22(2)	26(2)	2(1)	15(2)	10(2)
B(11)	21(2)	23(2)	37(2)	7(2)	8(2)	9(1)
N(1)	23(1)	23(1)	25(1)	3(1)	7(1)	7(1)
C(10)	25(2)	19(1)	26(2)	6(1)	9(1)	7(1)
C(11)	22(2)	36(2)	27(2)	1(1)	7(1)	4(1)
C(12)	41(2)	39(2)	45(2)	-8(2)	18(2)	8(2)
C(13)	55(3)	62(4)	59(3)	-28(3)	26(3)	-3(3)
C(14)	46(3)	107(6)	35(3)	-24(3)	19(2)	-12(3)
F(1)	88(3)	155(5)	46(2)	-47(3)	32(2)	-23(3)
C(15)	49(3)	117(6)	26(2)	9(3)	5(2)	7(3)
C(16)	40(2)	66(3)	32(2)	14(2)	6(2)	9(2)
N(2)	22(1)	29(2)	28(1)	0(1)	5(1)	9(1)
C(17)	19(2)	40(2)	40(2)	-1(2)	6(1)	9(2)
C(18)	31(2)	42(2)	32(2)	-6(2)	10(2)	10(2)
N(3)	28(1)	20(1)	26(1)	4(1)	9(1)	9(1)
C(20)	22(1)	20(1)	27(2)	3(1)	8(1)	6(1)
C(21)	25(2)	19(2)	30(2)	5(1)	8(1)	9(1)
C(22)	31(2)	30(2)	39(2)	12(2)	4(2)	0(2)
C(23)	38(2)	34(2)	43(2)	20(2)	6(2)	1(2)
C(24)	38(2)	33(2)	32(2)	13(2)	6(2)	14(2)
F(2)	52(2)	47(2)	38(1)	19(1)	-2(1)	9(1)
C(25)	35(2)	28(2)	40(2)	6(2)	-2(2)	1(2)
C(26)	35(2)	23(2)	36(2)	8(1)	4(2)	1(1)
N(4)	34(2)	21(1)	29(2)	3(1)	9(1)	12(1)
C(27)	50(2)	27(2)	44(2)	-1(2)	16(2)	21(2)
C(28)	50(2)	28(2)	27(2)	0(1)	7(2)	14(2)
C(30)	66(4)	73(4)	36(2)	5(2)	10(2)	33(3)
Cl(2)	97(2)	315(5)	61(1)	30(2)	11(1)	123(3)
Cl(3)	115(2)	67(1)	56(1)	15(1)	-3(1)	-7(1)
C(31)	38(2)	53(3)	69(3)	12(3)	23(2)	19(2)
Cl(4)	60(1)	49(1)	76(1)	11(1)	21(1)	9(1)
Cl(5)	42(1)	49(1)	60(1)	7(1)	20(1)	14(1)

Appendix A – Crystal Data

Table 5. Hydrogen coordinates (x 10⁴) and isotropic displacement parameters (Å²x 10⁻³) for (26).

	x	y	z	U(eq)
H(1)	3680	7320	2420	32
H(2)	2666	7303	4056	35
H(3)	637	6912	2254	31
H(4)	1581	5536	1072	34
H(5)	4245	5069	2159	38
H(6)	4907	6173	4006	37
H(7)	2420(50)	5170(40)	4620(30)	30
H(8)	310(50)	5530(40)	3700(30)	27
H(9)	-663	4489	1895	30
H(10)	1593	3321	1799	31
H(11)	3668	3756	3671	32
H(12A)	-2400	689	1871	49
H(13A)	-2919	-157	392	72
H(15A)	-4063	2627	-643	81
H(16A)	-3605	3459	833	57
H(17A)	-5289	1972	1762	50
H(17B)	-5564	3104	2095	50
H(17C)	-5644	2053	2699	50
H(18A)	-2319	3782	3885	52
H(18B)	-3622	2905	4070	52
H(18C)	-3808	4052	3636	52
H(22A)	754	-875	4284	43
H(23A)	1761	-1380	5738	50
H(25A)	4930	1469	6134	46
H(26A)	3864	2025	4705	40
H(27A)	2646	-686	3313	57
H(27B)	2984	-341	2389	57
H(27C)	1553	-1218	2380	57
H(28A)	504	1339	1816	52
H(28B)	203	70	1429	52
H(28C)	1636	949	1446	52
H(30A)	1220	3666	-874	67
H(30B)	1465	3942	176	67
H(31A)	7130	-2808	3433	61
H(31B)	6115	-2808	2451	61

A11 *Crystal data for [3-Ta(OC₆H₃-Me₂-2,6)₃](1,2-C₂B₉H₁₁)] ; (28).*



Appendix A – Crystal Data

Table 1. Crystal data and structure refinement for (28).

Identification code	99srv167	
Empirical formula	C26 H38 B9 O3 Ta	
Formula weight	676.80	
Temperature	150(2) K	
Wavelength	0.71073 Å	
Crystal system	Monoclinic	
Space group	P2(1)/c	
Unit cell dimensions	a = 18.732(3) Å	α= 90°.
	b = 19.920(3) Å	β= 95.108(4)°.
	c = 15.986(3) Å	γ= 90°.
Volume	5941.4(17) Å ³	
Z	8	
Density (calculated)	1.513 Mg/m ³	
Absorption coefficient	3.727 mm ⁻¹	
F(000)	2688	
Crystal size	0.44 x 0.42 x 0.14 mm ³	
Theta range for data collection	1.09 to 30.50°.	
Index ranges	-25<=h<=26, -28<=k<=26, -22<=l<=21	
Reflections collected	71190	
Independent reflections	16897 [R(int) = 0.0329]	
Completeness to theta = 30.50°	93.2 %	
Absorption correction	Integration	
Max. and min. transmission	0.608 and 0.252	
Refinement method	Full-matrix least-squares on F ²	
Data / restraints / parameters	16897 / 0 / 715	
Goodness-of-fit on F ²	1.059	
Final R indices [I>2sigma(I)]	R1 = 0.0240, wR2 = 0.0510	
R indices (all data)	R1 = 0.0423, wR2 = 0.0575	
Largest diff. peak and hole	0.908 and -0.991 e.Å ⁻³	

Appendix A – Crystal Data

Table 2. Atomic coordinates ($\times 10^4$) and equivalent isotropic displacement parameters ($\text{\AA}^2 \times 10^3$) for (28). U(eq) is defined as one third of the trace of the orthogonalized U^{ij} tensor.

	x	y	z	U(eq)
Ta(1)	4966(1)	6321(1)	2318(1)	22(1)
B(1)	6593(2)	7889(2)	2785(3)	41(1)
B(2)	5941(2)	7945(2)	1915(3)	50(1)
B(3)	5682(2)	8018(2)	2953(3)	46(1)
B(4)	6207(2)	7451(2)	3604(2)	35(1)
B(5)	6787(2)	7026(2)	2953(2)	31(1)
B(6)	6619(2)	7335(2)	1918(3)	42(1)
C(7)	5743(2)	7131(2)	1670(2)	33(1)
C(8)	5200(2)	7526(2)	2224(2)	41(1)
B(9)	5316(2)	7239(2)	3236(2)	33(1)
B(10)	6003(2)	6621(2)	3241(2)	26(1)
B(11)	6228(2)	6590(2)	2222(2)	27(1)
O(1)	5213(1)	5626(1)	1604(1)	27(1)
C(11)	5701(2)	5196(1)	1275(2)	29(1)
C(12)	5885(2)	5311(2)	458(2)	38(1)
C(13)	6372(2)	4867(2)	151(2)	52(1)
C(14)	6649(2)	4335(2)	623(2)	55(1)
C(15)	6448(2)	4232(2)	1422(2)	48(1)
C(16)	5967(2)	4662(2)	1769(2)	35(1)
C(17)	5582(2)	5884(2)	-64(2)	52(1)
C(18)	5759(2)	4561(2)	2643(2)	40(1)
O(2)	4103(1)	6612(1)	1740(1)	26(1)
C(21)	3587(2)	7097(1)	1561(2)	29(1)
C(22)	3121(2)	7248(2)	2169(2)	33(1)
C(23)	2611(2)	7743(2)	1975(2)	44(1)
C(24)	2564(2)	8064(2)	1213(3)	54(1)
C(25)	3021(2)	7895(2)	618(3)	51(1)
C(26)	3546(2)	7405(2)	776(2)	37(1)
C(27)	3157(2)	6878(2)	2993(2)	40(1)
C(28)	4056(2)	7214(2)	140(2)	45(1)
O(3)	4596(1)	5834(1)	3161(1)	27(1)
C(31)	4183(1)	5433(1)	3625(2)	24(1)
C(32)	3720(1)	4974(1)	3197(2)	26(1)
C(33)	3314(2)	4571(1)	3672(2)	33(1)
C(34)	3355(2)	4623(2)	4535(2)	41(1)
C(35)	3805(2)	5093(2)	4940(2)	39(1)
C(36)	4236(2)	5511(1)	4494(2)	29(1)
C(37)	3645(2)	4934(2)	2254(2)	33(1)
C(38)	4723(2)	6020(2)	4940(2)	39(1)
Ta(2)	-43(1)	6518(1)	2332(1)	20(1)
B(71)	1433(2)	4902(2)	1778(3)	37(1)
B(72)	927(2)	4860(2)	2658(3)	42(1)
B(73)	494(2)	4797(2)	1633(3)	39(1)
B(74)	925(2)	5354(2)	980(2)	35(1)
B(75)	1622(2)	5767(2)	1597(2)	34(1)
B(76)	1622(2)	5457(2)	2640(3)	40(1)
C(77)	798(2)	5693(2)	2971(2)	36(1)
C(78)	174(2)	5316(1)	2359(2)	32(1)
B(79)	146(2)	5589(2)	1412(2)	23(1)
B(80)	795(2)	6186(2)	1347(2)	28(1)
B(81)	1236(2)	6252(2)	2370(2)	29(1)
O(4)	301(1)	7290(1)	2873(1)	24(1)
C(41)	735(1)	7830(1)	3095(2)	23(1)
C(42)	1056(2)	7857(1)	3914(2)	30(1)
C(43)	1466(2)	8425(2)	4136(2)	39(1)
C(44)	1547(2)	8932(2)	3571(2)	39(1)
C(45)	1232(2)	8883(1)	2759(2)	34(1)
C(46)	819(1)	8329(1)	2497(2)	27(1)
C(47)	962(2)	7297(2)	4520(2)	42(1)
C(48)	495(2)	8268(2)	1609(2)	37(1)
O(5)	-736(1)	6256(1)	3051(1)	25(1)
C(51)	-1195(1)	5798(1)	3368(2)	29(1)
C(52)	-1782(2)	5580(1)	2838(2)	35(1)
C(53)	-2254(2)	5134(2)	3181(3)	46(1)
C(54)	-2143(2)	4923(2)	3996(3)	51(1)
C(55)	-1562(2)	5150(2)	4503(2)	46(1)
C(56)	-1071(2)	5600(2)	4203(2)	35(1)
C(57)	-1908(2)	5816(2)	1946(2)	43(1)
C(58)	-470(2)	5883(2)	4775(2)	48(1)
O(6)	-629(1)	6893(1)	1456(1)	27(1)
C(61)	-1093(1)	7301(1)	969(2)	23(1)
C(62)	-1445(1)	7818(1)	1365(2)	24(1)
C(63)	-1900(2)	8223(1)	856(2)	31(1)
C(64)	-2015(2)	8114(2)	1(2)	37(1)
C(65)	-1670(2)	7593(2)	-366(2)	36(1)
C(66)	-1196(2)	7176(1)	112(2)	30(1)
C(67)	-1355(2)	7917(1)	2296(2)	31(1)
C(68)	-821(2)	6608(2)	-293(2)	45(1)

Appendix A – Crystal Data

Table 3. Bond lengths [Å] and angles [°] for (28).

<hr/>					
Ta(1)-O(3)	1.8443(18)	C(22)-C(23)	1.388(4)	B(76)-H(76)	1.1200
Ta(1)-O(1)	1.8778(18)	C(22)-C(27)	1.505(5)	C(77)-C(78)	1.638(4)
Ta(1)-O(2)	1.8799(19)	C(23)-C(24)	1.372(5)	C(77)-B(81)	1.726(5)
Ta(1)-B(9)	2.400(3)	C(23)-H(23A)	0.9500	C(77)-H(77)	1.16(3)
Ta(1)-B(10)	2.408(3)	C(24)-C(25)	1.376(6)	C(78)-B(79)	1.605(4)
Ta(1)-B(11)	2.443(3)	C(24)-H(24A)	0.9500	C(78)-H(78)	0.94(3)
Ta(1)-C(8)	2.447(3)	C(25)-C(26)	1.393(5)	B(79)-B(80)	1.710(4)
Ta(1)-C(7)	2.462(3)	C(25)-H(25A)	0.9500	B(79)-H(79)	1.1200
B(1)-B(3)	1.769(6)	C(26)-C(28)	1.505(5)	B(80)-B(81)	1.770(5)
B(1)-B(2)	1.771(5)	C(27)-H(27A)	0.9800	B(80)-H(80)	1.1200
B(1)-B(5)	1.772(5)	C(27)-H(27B)	0.9800	B(81)-H(81)	1.1200
B(1)-B(6)	1.776(6)	C(27)-H(27C)	0.9800	O(4)-C(41)	1.375(3)
B(1)-B(4)	1.780(6)	C(28)-H(28A)	0.9800	C(41)-C(42)	1.392(4)
B(1)-H(1)	1.1200	C(28)-H(28B)	0.9800	C(41)-C(46)	1.399(4)
B(2)-C(7)	1.702(5)	C(28)-H(28C)	0.9800	C(42)-C(43)	1.396(4)
B(2)-C(8)	1.729(5)	O(3)-C(31)	1.375(3)	C(42)-C(47)	1.497(4)
B(2)-B(6)	1.759(6)	C(31)-C(36)	1.393(4)	C(43)-C(44)	1.372(5)
B(2)-B(3)	1.774(7)	C(31)-C(32)	1.397(4)	C(43)-H(43A)	0.9500
B(2)-H(2)	1.1200	C(32)-C(33)	1.380(4)	C(44)-C(45)	1.380(5)
B(3)-C(8)	1.717(5)	C(32)-C(37)	1.504(4)	C(44)-H(44A)	0.9500
B(3)-B(9)	1.772(5)	C(33)-C(34)	1.379(4)	C(45)-C(46)	1.390(4)
B(3)-B(4)	1.774(5)	C(33)-H(33A)	0.9500	C(45)-H(45A)	0.9500
B(3)-H(3)	1.1200	C(34)-C(35)	1.381(5)	C(46)-C(48)	1.498(4)
B(4)-B(9)	1.771(5)	C(34)-H(34A)	0.9500	C(47)-H(47A)	0.9800
B(4)-B(5)	1.782(5)	C(35)-C(36)	1.398(4)	C(47)-H(47B)	0.9800
B(4)-B(10)	1.782(4)	C(35)-H(35A)	0.9500	C(47)-H(47C)	0.9800
B(4)-H(4)	1.1200	C(36)-C(38)	1.501(4)	C(48)-H(48A)	0.9800
B(5)-B(11)	1.731(4)	C(37)-H(37A)	0.9800	C(48)-H(48B)	0.9800
B(5)-B(6)	1.766(5)	C(37)-H(37B)	0.9800	C(48)-H(48C)	0.9800
B(5)-B(10)	1.772(4)	C(37)-H(37C)	0.9800	O(5)-C(51)	1.381(3)
B(5)-H(5)	1.1200	C(38)-H(38A)	0.9800	C(51)-C(56)	1.392(4)
B(6)-C(7)	1.704(5)	C(38)-H(38B)	0.9800	C(51)-C(52)	1.396(4)
B(6)-B(11)	1.742(5)	C(38)-H(38C)	0.9800	C(52)-C(53)	1.400(4)
B(6)-H(6)	1.1200	Ta(2)-O(4)	1.8526(17)	C(52)-C(57)	1.500(5)
C(7)-C(8)	1.612(5)	Ta(2)-O(6)	1.8574(18)	C(53)-C(54)	1.367(6)
C(7)-B(11)	1.620(4)	Ta(2)-O(5)	1.8818(19)	C(53)-H(53A)	0.9500
C(7)-H(7)	0.91(3)	Ta(2)-B(79)	2.409(3)	C(54)-C(55)	1.376(5)
C(8)-B(9)	1.712(5)	Ta(2)-B(80)	2.413(3)	C(54)-H(54A)	0.9500
C(8)-H(8)	1.06(4)	Ta(2)-C(78)	2.428(3)	C(55)-C(56)	1.399(4)
B(9)-B(10)	1.781(5)	Ta(2)-C(77)	2.438(3)	C(55)-H(55A)	0.9500
B(9)-H(9)	1.1200	Ta(2)-B(81)	2.449(3)	C(56)-C(58)	1.497(5)
B(10)-B(11)	1.720(5)	B(71)-B(73)	1.766(5)	C(57)-H(57A)	0.9800
B(10)-H(10)	1.1200	B(71)-B(72)	1.766(5)	C(57)-H(57B)	0.9800
B(11)-H(11)	1.1200	B(71)-B(74)	1.769(5)	C(57)-H(57C)	0.9800
O(1)-C(11)	1.390(3)	B(71)-B(76)	1.777(5)	C(58)-H(58A)	0.9800
C(11)-C(16)	1.392(4)	B(71)-B(75)	1.789(5)	C(58)-H(58B)	0.9800
C(11)-C(12)	1.398(4)	B(71)-H(71)	1.1200	C(58)-H(58C)	0.9800
C(12)-C(13)	1.391(5)	B(72)-C(78)	1.708(5)	O(6)-C(61)	1.379(3)
C(12)-C(17)	1.497(5)	B(72)-C(77)	1.755(5)	C(61)-C(66)	1.389(4)
C(13)-C(14)	1.375(6)	B(72)-B(76)	1.766(6)	C(61)-C(62)	1.403(3)
C(13)-H(13A)	0.9500	B(72)-B(73)	1.767(6)	C(62)-C(63)	1.384(4)
C(14)-C(15)	1.380(5)	B(72)-H(72)	1.1200	C(62)-C(67)	1.496(4)
C(14)-H(14A)	0.9500	B(73)-C(78)	1.703(4)	C(63)-C(64)	1.381(4)
C(15)-C(16)	1.393(4)	B(73)-B(79)	1.732(4)	C(63)-H(63A)	0.9500
C(15)-H(15A)	0.9500	B(73)-B(74)	1.769(5)	C(64)-C(65)	1.381(4)
C(16)-C(18)	1.496(5)	B(73)-H(73)	1.1200	C(64)-H(64A)	0.9500
C(17)-H(17A)	0.9800	B(74)-B(79)	1.733(4)	C(65)-C(66)	1.393(4)
C(17)-H(17B)	0.9800	B(74)-B(75)	1.768(5)	C(65)-H(65A)	0.9500
C(17)-H(17C)	0.9800	B(74)-B(80)	1.782(4)	C(66)-C(68)	1.508(4)
C(18)-H(18A)	0.9800	B(74)-H(74)	1.1200	C(67)-H(67A)	0.9800
C(18)-H(18B)	0.9800	B(75)-B(81)	1.773(5)	C(67)-H(67B)	0.9800
C(18)-H(18C)	0.9800	B(75)-B(80)	1.774(5)	C(67)-H(67C)	0.9800
O(2)-C(21)	1.378(3)	B(75)-B(76)	1.778(5)	C(68)-H(68A)	0.9800
C(21)-C(26)	1.394(4)	B(75)-H(75)	1.1200	C(68)-H(68B)	0.9800
C(21)-C(22)	1.396(4)	B(76)-C(77)	1.739(5)	C(68)-H(68C)	0.9800
		B(76)-B(81)	1.778(5)		
<hr/>					
O(3)-Ta(1)-O(1)	100.67(9)	O(2)-Ta(1)-B(9)	103.96(10)	O(3)-Ta(1)-B(11)	126.12(10)
O(3)-Ta(1)-O(2)	99.16(8)	O(3)-Ta(1)-B(10)	90.99(10)	O(1)-Ta(1)-B(11)	80.27(9)
O(1)-Ta(1)-O(2)	100.21(8)	O(1)-Ta(1)-B(10)	109.00(9)	O(2)-Ta(1)-B(11)	134.10(10)
O(3)-Ta(1)-B(9)	93.06(11)	O(2)-Ta(1)-B(10)	146.69(9)	B(9)-Ta(1)-B(11)	69.99(11)
O(1)-Ta(1)-B(9)	149.84(10)	B(9)-Ta(1)-B(10)	43.49(11)	B(10)-Ta(1)-B(11)	41.52(11)

Appendix A – Crystal Data

O(3)-Ta(1)-C(8)	129.90(11)	B(10)-B(5)-B(1)	108.6(2)	B(9)-B(10)-Ta(1)	68.01(14)
O(1)-Ta(1)-C(8)	129.09(11)	B(11)-B(5)-B(4)	105.6(2)	B(4)-B(10)-Ta(1)	124.59(19)
O(2)-Ta(1)-C(8)	79.50(9)	B(6)-B(5)-B(4)	108.4(3)	B(11)-B(10)-H(10)	124.1
B(9)-Ta(1)-C(8)	41.36(12)	B(10)-B(5)-B(4)	60.18(18)	B(5)-B(10)-H(10)	118.4
B(10)-Ta(1)-C(8)	69.84(11)	B(1)-B(5)-B(4)	60.1(2)	B(9)-B(10)-H(10)	124.5
B(11)-Ta(1)-C(8)	66.50(11)	B(11)-B(5)-H(5)	123.7	B(4)-B(10)-H(10)	119.7
O(3)-Ta(1)-C(7)	157.86(9)	B(6)-B(5)-H(5)	121.0	Ta(1)-B(10)-H(10)	103.6
O(1)-Ta(1)-C(7)	92.32(10)	B(10)-B(5)-H(5)	121.3	C(7)-B(11)-B(10)	108.6(2)
O(2)-Ta(1)-C(7)	96.04(9)	B(1)-B(5)-H(5)	121.8	C(7)-B(11)-B(5)	108.1(2)
B(9)-Ta(1)-C(7)	67.58(12)	B(4)-B(5)-H(5)	122.2	B(10)-B(11)-B(5)	61.80(19)
B(10)-Ta(1)-C(7)	67.70(11)	C(7)-B(6)-B(11)	56.07(18)	C(7)-B(11)-B(6)	60.77(19)
B(11)-Ta(1)-C(7)	38.58(10)	C(7)-B(6)-B(2)	58.9(2)	B(10)-B(11)-B(6)	112.3(2)
C(8)-Ta(1)-C(7)	38.33(12)	B(11)-B(6)-B(2)	105.5(2)	B(5)-B(11)-B(6)	61.1(2)
B(3)-B(1)-B(2)	60.2(2)	C(7)-B(6)-B(5)	102.8(2)	C(7)-B(11)-Ta(1)	71.35(15)
B(3)-B(1)-B(5)	107.7(3)	B(11)-B(6)-B(5)	59.11(19)	B(10)-B(11)-Ta(1)	68.14(14)
B(2)-B(1)-B(5)	107.3(2)	B(2)-B(6)-B(5)	108.1(3)	B(5)-B(11)-Ta(1)	126.7(2)
B(3)-B(1)-B(6)	107.6(3)	C(7)-B(6)-B(1)	103.7(3)	B(6)-B(11)-Ta(1)	129.6(2)
B(2)-B(1)-B(6)	59.5(2)	B(11)-B(6)-B(1)	105.7(3)	C(7)-B(11)-H(11)	122.6
B(5)-B(1)-B(6)	59.7(2)	B(2)-B(6)-B(1)	60.1(2)	B(10)-B(11)-H(11)	121.6
B(3)-B(1)-B(4)	60.0(2)	B(5)-B(6)-B(1)	60.0(2)	B(5)-B(11)-H(11)	118.6
B(2)-B(1)-B(4)	108.1(3)	C(7)-B(6)-H(6)	126.0	B(6)-B(11)-H(11)	115.9
B(5)-B(1)-B(4)	60.2(2)	B(11)-B(6)-H(6)	123.9	Ta(1)-B(11)-H(11)	102.0
B(6)-B(1)-B(4)	108.1(2)	B(2)-B(6)-H(6)	121.5	C(11)-O(1)-Ta(1)	152.99(17)
B(3)-B(1)-H(1)	121.8	B(5)-B(6)-H(6)	122.6	O(1)-C(11)-C(16)	118.0(3)
B(2)-B(1)-H(1)	122.0	B(1)-B(6)-H(6)	122.8	O(1)-C(11)-C(12)	118.6(3)
B(5)-B(1)-H(1)	122.0	C(8)-C(7)-B(11)	112.1(2)	C(16)-C(11)-C(12)	123.4(3)
B(6)-B(1)-H(1)	122.0	C(8)-C(7)-B(2)	62.9(2)	C(13)-C(12)-C(11)	116.7(3)
B(4)-B(1)-H(1)	121.4	B(11)-C(7)-B(2)	114.0(2)	C(13)-C(12)-C(17)	121.1(3)
C(7)-B(2)-C(8)	56.02(19)	C(8)-C(7)-B(6)	113.5(3)	C(11)-C(12)-C(17)	122.2(3)
C(7)-B(2)-B(6)	59.0(2)	B(11)-C(7)-B(6)	63.2(2)	C(14)-C(13)-C(12)	121.5(3)
C(8)-B(2)-B(6)	105.3(2)	B(2)-C(7)-B(6)	62.2(2)	C(14)-C(13)-H(13A)	119.2
C(7)-B(2)-B(1)	104.0(3)	C(8)-C(7)-Ta(1)	70.33(15)	C(12)-C(13)-H(13A)	119.2
C(8)-B(2)-B(1)	105.1(3)	B(11)-C(7)-Ta(1)	70.08(14)	C(13)-C(14)-C(15)	120.2(3)
B(6)-B(2)-B(1)	60.4(2)	B(2)-C(7)-Ta(1)	130.7(2)	C(13)-C(14)-H(14A)	119.9
C(7)-B(2)-B(3)	102.8(3)	B(6)-C(7)-Ta(1)	130.6(2)	C(15)-C(14)-H(14A)	119.9
C(8)-B(2)-B(3)	58.7(2)	C(8)-C(7)-H(7)	115(2)	C(14)-C(15)-C(16)	121.1(3)
B(6)-B(2)-B(3)	108.2(3)	B(11)-C(7)-H(7)	125(2)	C(14)-C(15)-H(15A)	119.4
B(1)-B(2)-B(3)	59.9(2)	B(2)-C(7)-H(7)	112(2)	C(16)-C(15)-H(15A)	119.4
C(7)-B(2)-H(2)	125.8	B(6)-C(7)-H(7)	119(2)	C(11)-C(16)-C(15)	117.1(3)
C(8)-B(2)-H(2)	124.4	Ta(1)-C(7)-H(7)	100(2)	C(11)-C(16)-C(18)	121.5(3)
B(6)-B(2)-H(2)	121.4	C(7)-C(8)-B(9)	108.9(2)	C(15)-C(16)-C(18)	121.3(3)
B(1)-B(2)-H(2)	122.8	C(7)-C(8)-B(3)	109.4(3)	C(12)-C(17)-H(17A)	109.5
B(3)-B(2)-H(2)	122.7	B(9)-C(8)-B(3)	62.2(2)	C(12)-C(17)-H(17B)	109.5
C(8)-B(3)-B(1)	105.7(3)	C(7)-C(8)-B(2)	61.1(2)	H(17A)-C(17)-H(17B)	109.5
C(8)-B(3)-B(9)	58.7(2)	B(9)-C(8)-B(2)	113.2(3)	C(12)-C(17)-H(17C)	109.5
B(1)-B(3)-B(9)	108.2(2)	B(3)-C(8)-B(2)	62.0(2)	H(17A)-C(17)-H(17C)	109.5
C(8)-B(3)-B(2)	59.4(2)	C(7)-C(8)-Ta(1)	71.35(15)	H(17B)-C(17)-H(17C)	109.5
B(1)-B(3)-B(2)	60.0(2)	B(9)-C(8)-Ta(1)	67.83(15)	C(16)-C(18)-H(18A)	109.5
B(9)-B(3)-B(2)	108.2(3)	B(3)-C(8)-Ta(1)	127.2(2)	C(16)-C(18)-H(18B)	109.5
C(8)-B(3)-B(4)	105.4(2)	B(2)-C(8)-Ta(1)	130.1(2)	H(18A)-C(18)-H(18B)	109.5
B(1)-B(3)-B(4)	60.3(2)	C(7)-C(8)-H(8)	117(2)	C(16)-C(18)-H(18C)	109.5
B(9)-B(3)-B(4)	59.9(2)	B(9)-C(8)-H(8)	127(2)	H(18A)-C(18)-H(18C)	109.5
B(2)-B(3)-B(4)	108.3(3)	B(3)-C(8)-H(8)	119.9(19)	H(18B)-C(18)-H(18C)	109.5
C(8)-B(3)-H(3)	124.0	B(2)-C(8)-H(8)	111.2(19)	C(21)-O(2)-Ta(1)	151.03(17)
B(1)-B(3)-H(3)	122.0	Ta(1)-C(8)-H(8)	103.0(19)	O(2)-C(21)-C(26)	118.5(3)
B(9)-B(3)-H(3)	121.6	C(8)-B(9)-B(4)	105.7(3)	O(2)-C(21)-C(22)	118.5(3)
B(2)-B(3)-H(3)	121.3	C(8)-B(9)-B(3)	59.0(2)	C(26)-C(21)-C(22)	123.0(3)
B(4)-B(3)-H(3)	122.1	B(4)-B(9)-B(3)	60.1(2)	C(23)-C(22)-C(21)	117.3(3)
B(9)-B(4)-B(3)	60.0(2)	C(8)-B(9)-B(10)	105.4(2)	C(23)-C(22)-C(27)	121.3(3)
B(9)-B(4)-B(1)	107.8(3)	B(4)-B(9)-B(10)	60.22(18)	C(21)-C(22)-C(27)	121.4(3)
B(3)-B(4)-B(1)	59.7(2)	B(3)-B(9)-B(10)	108.1(2)	C(24)-C(23)-C(22)	121.2(3)
B(9)-B(4)-B(5)	107.4(2)	C(8)-B(9)-Ta(1)	70.81(15)	C(24)-C(23)-H(23A)	119.4
B(3)-B(4)-B(5)	107.1(3)	B(4)-B(9)-Ta(1)	125.6(2)	C(22)-C(23)-H(23A)	119.4
B(1)-B(4)-B(5)	59.7(2)	B(3)-B(9)-Ta(1)	127.0(2)	C(23)-C(24)-C(25)	120.4(3)
B(9)-B(4)-B(10)	60.16(18)	B(10)-B(9)-Ta(1)	68.50(14)	C(23)-C(24)-H(24A)	119.8
B(3)-B(4)-B(10)	108.0(2)	C(8)-B(9)-H(9)	124.4	C(25)-C(24)-H(24A)	119.8
B(1)-B(4)-B(10)	107.8(3)	B(4)-B(9)-H(9)	119.6	C(24)-C(25)-C(26)	121.2(3)
B(5)-B(4)-B(10)	59.63(18)	B(3)-B(9)-H(9)	118.5	C(24)-C(25)-H(25A)	119.4
B(9)-B(4)-H(4)	121.8	B(10)-B(9)-H(9)	123.8	C(26)-C(25)-H(25A)	119.4
B(3)-B(4)-H(4)	122.0	Ta(1)-B(9)-H(9)	102.8	C(25)-C(26)-C(21)	117.0(3)
B(1)-B(4)-H(4)	121.9	B(11)-B(10)-B(5)	59.41(18)	C(25)-C(26)-C(28)	122.4(3)
B(5)-B(4)-H(4)	122.4	B(11)-B(10)-B(9)	105.0(2)	C(21)-C(26)-C(28)	120.6(3)
B(10)-B(4)-H(4)	121.7	B(5)-B(10)-B(9)	107.4(2)	C(22)-C(27)-H(27A)	109.5
B(11)-B(5)-B(6)	59.76(19)	B(11)-B(10)-B(4)	106.1(2)	C(22)-C(27)-H(27B)	109.5
B(11)-B(5)-B(10)	58.79(18)	B(5)-B(10)-B(4)	60.19(19)	H(27A)-C(27)-H(27B)	109.5
B(6)-B(5)-B(10)	108.7(2)	B(9)-B(10)-B(4)	59.61(18)	C(22)-C(27)-H(27C)	109.5
B(11)-B(5)-B(1)	106.3(2)	B(11)-B(10)-Ta(1)	70.34(14)	H(27A)-C(27)-H(27C)	109.5
B(6)-B(5)-B(1)	60.3(2)	B(5)-B(10)-Ta(1)	126.6(2)	H(27B)-C(27)-H(27C)	109.5

Appendix A – Crystal Data

C(26)-C(28)-H(28A)	109.5	B(76)-B(71)-H(71)	122.1	C(78)-C(77)-B(76)	107.4(2)
C(26)-C(28)-H(28B)	109.5	B(75)-B(71)-H(71)	122.0	B(81)-C(77)-B(76)	61.7(2)
H(28A)-C(28)-H(28B)	109.5	C(78)-B(72)-C(77)	56.43(18)	C(78)-C(77)-B(72)	60.3(2)
C(26)-C(28)-H(28C)	109.5	C(78)-B(72)-B(76)	103.2(2)	B(81)-C(77)-B(72)	111.6(2)
H(28A)-C(28)-H(28C)	109.5	C(77)-B(72)-B(76)	59.2(2)	B(76)-C(77)-B(72)	60.7(2)
H(28B)-C(28)-H(28C)	109.5	C(78)-B(72)-B(73)	58.6(2)	C(78)-C(77)-Ta(2)	70.02(14)
C(31)-O(3)-Ta(1)	164.96(18)	C(77)-B(72)-B(73)	105.6(2)	B(81)-C(77)-Ta(2)	69.67(15)
O(3)-C(31)-C(36)	118.7(2)	B(76)-B(72)-B(73)	108.1(3)	B(76)-C(77)-Ta(2)	127.7(2)
O(3)-C(31)-C(32)	118.1(2)	C(78)-B(72)-B(71)	103.9(3)	B(72)-C(77)-Ta(2)	128.1(2)
C(36)-C(31)-C(32)	123.2(2)	C(77)-B(72)-B(71)	106.2(2)	C(78)-C(77)-H(77)	117.1(17)
C(33)-C(32)-C(31)	117.4(3)	B(76)-B(72)-B(71)	60.4(2)	B(81)-C(77)-H(77)	127.9(17)
C(33)-C(32)-C(37)	120.9(3)	B(73)-B(72)-B(71)	60.0(2)	B(76)-C(77)-H(77)	121.7(17)
C(31)-C(32)-C(37)	121.6(2)	C(78)-B(72)-H(72)	125.9	B(72)-C(77)-H(77)	112.3(17)
C(34)-C(33)-C(32)	121.4(3)	C(77)-B(72)-H(72)	123.6	Ta(2)-C(77)-H(77)	102.5(17)
C(34)-C(33)-H(33A)	119.3	B(76)-B(72)-H(72)	122.4	B(79)-C(78)-C(77)	111.7(2)
C(32)-C(33)-H(33A)	119.3	B(73)-B(72)-H(72)	121.7	B(79)-C(78)-B(73)	63.1(2)
C(33)-C(34)-C(35)	119.9(3)	B(71)-B(72)-H(72)	122.6	C(77)-C(78)-B(73)	114.2(2)
C(33)-C(34)-H(34A)	120.1	C(78)-B(73)-B(79)	55.73(17)	B(79)-C(78)-B(72)	113.6(2)
C(35)-C(34)-H(34A)	120.1	C(78)-B(73)-B(71)	104.1(3)	C(77)-C(78)-B(72)	63.2(2)
C(34)-C(35)-C(36)	121.4(3)	B(79)-B(73)-B(71)	105.7(2)	B(73)-C(78)-B(72)	62.4(2)
C(34)-C(35)-H(35A)	119.3	C(78)-B(73)-B(72)	58.9(2)	B(79)-C(78)-Ta(2)	69.96(14)
C(36)-C(35)-H(35A)	119.3	B(79)-B(73)-B(72)	104.9(2)	C(77)-C(78)-Ta(2)	70.64(14)
C(31)-C(36)-C(35)	116.7(3)	B(71)-B(73)-B(72)	60.0(2)	B(73)-C(78)-Ta(2)	130.9(2)
C(31)-C(36)-C(38)	122.4(3)	C(78)-B(73)-B(74)	103.2(2)	B(72)-C(78)-Ta(2)	131.5(2)
C(35)-C(36)-C(38)	120.9(3)	B(79)-B(73)-B(74)	59.35(19)	B(79)-C(78)-H(78)	121(2)
C(32)-C(37)-H(37A)	109.5	B(71)-B(73)-B(74)	60.1(2)	C(77)-C(78)-H(78)	120(2)
C(32)-C(37)-H(37B)	109.5	B(72)-B(73)-B(74)	107.8(3)	B(73)-C(78)-H(78)	114(2)
H(37A)-C(37)-H(37B)	109.5	C(78)-B(73)-H(73)	125.8	B(72)-C(78)-H(78)	114(2)
C(32)-C(37)-H(37C)	109.5	B(79)-B(73)-H(73)	124.2	Ta(2)-C(78)-H(78)	101(2)
H(37A)-C(37)-H(37C)	109.5	B(71)-B(73)-H(73)	122.7	C(78)-B(79)-B(80)	109.3(2)
H(37B)-C(37)-H(37C)	109.5	B(72)-B(73)-H(73)	121.9	C(78)-B(79)-B(73)	61.22(19)
C(36)-C(38)-H(38A)	109.5	B(74)-B(73)-H(73)	122.4	B(80)-B(79)-B(73)	113.0(2)
C(36)-C(38)-H(38B)	109.5	B(79)-B(74)-B(75)	105.0(2)	C(78)-B(79)-B(74)	109.1(2)
H(38A)-C(38)-H(38B)	109.5	B(79)-B(74)-B(73)	59.27(19)	B(80)-B(79)-B(74)	62.33(18)
C(36)-C(38)-H(38C)	109.5	B(75)-B(74)-B(73)	108.5(3)	B(73)-B(79)-B(74)	61.38(19)
H(38A)-C(38)-H(38C)	109.5	B(79)-B(74)-B(71)	105.5(2)	C(78)-B(79)-Ta(2)	71.27(14)
H(38B)-C(38)-H(38C)	109.5	B(75)-B(74)-B(71)	60.8(2)	B(80)-B(79)-Ta(2)	69.35(14)
O(4)-Ta(2)-O(6)	100.08(8)	B(73)-B(74)-B(71)	59.9(2)	B(73)-B(79)-Ta(2)	130.4(2)
O(4)-Ta(2)-O(5)	100.05(8)	B(79)-B(74)-B(80)	58.21(18)	B(74)-B(79)-Ta(2)	128.73(19)
O(6)-Ta(2)-O(5)	100.27(8)	B(75)-B(74)-B(80)	59.97(19)	C(78)-B(79)-H(79)	122.5
O(4)-Ta(2)-B(79)	149.20(9)	B(73)-B(74)-B(80)	107.9(2)	B(80)-B(79)-H(79)	120.9
O(6)-Ta(2)-B(79)	87.60(9)	B(71)-B(74)-B(80)	108.5(3)	B(73)-B(79)-H(79)	115.6
O(5)-Ta(2)-B(79)	107.91(9)	B(79)-B(74)-H(74)	124.5	B(74)-B(79)-H(79)	117.7
O(4)-Ta(2)-B(80)	108.23(10)	B(75)-B(74)-H(74)	122.0	Ta(2)-B(79)-H(79)	100.8
O(6)-Ta(2)-B(80)	89.61(10)	B(73)-B(74)-H(74)	121.4	B(79)-B(80)-B(81)	105.7(2)
O(5)-Ta(2)-B(80)	147.90(9)	B(71)-B(74)-H(74)	121.8	B(79)-B(80)-B(75)	105.7(2)
B(79)-Ta(2)-B(80)	41.55(10)	B(80)-B(74)-H(74)	121.7	B(81)-B(80)-B(75)	60.04(19)
O(4)-Ta(2)-C(78)	139.46(10)	B(74)-B(75)-B(81)	108.4(2)	B(79)-B(80)-B(74)	59.47(18)
O(6)-Ta(2)-C(78)	119.81(10)	B(74)-B(75)-B(80)	60.42(19)	B(81)-B(80)-B(74)	107.9(2)
O(5)-Ta(2)-C(78)	80.80(9)	B(81)-B(75)-B(80)	59.86(18)	B(75)-B(80)-B(74)	59.61(19)
B(79)-Ta(2)-C(78)	38.76(10)	B(74)-B(75)-B(76)	107.4(3)	B(79)-B(80)-Ta(2)	69.10(14)
B(80)-Ta(2)-C(78)	67.92(10)	B(81)-B(75)-B(76)	60.08(19)	B(81)-B(80)-Ta(2)	69.75(15)
O(4)-Ta(2)-C(77)	100.35(10)	B(80)-B(75)-B(76)	107.5(2)	B(75)-B(80)-Ta(2)	126.0(2)
O(6)-Ta(2)-C(77)	154.67(9)	B(74)-B(75)-B(71)	59.6(2)	B(74)-B(80)-Ta(2)	125.8(2)
O(5)-Ta(2)-C(77)	90.74(10)	B(81)-B(75)-B(71)	108.2(2)	B(79)-B(80)-H(80)	124.8
B(79)-Ta(2)-C(77)	67.25(10)	B(80)-B(75)-B(71)	107.9(2)	B(81)-B(80)-H(80)	123.1
B(80)-Ta(2)-C(77)	69.82(11)	B(76)-B(75)-B(71)	59.8(2)	B(75)-B(80)-H(80)	119.6
C(78)-Ta(2)-C(77)	39.34(11)	B(74)-B(75)-H(75)	121.7	B(74)-B(80)-H(80)	118.9
O(4)-Ta(2)-B(81)	82.50(9)	B(81)-B(75)-H(75)	121.4	Ta(2)-B(80)-H(80)	103.2
O(6)-Ta(2)-B(81)	128.06(10)	B(80)-B(75)-H(75)	121.8	C(77)-B(81)-B(80)	105.1(2)
O(5)-Ta(2)-B(81)	130.66(10)	B(76)-B(75)-H(75)	122.2	C(77)-B(81)-B(75)	106.3(2)
B(79)-Ta(2)-B(81)	69.65(10)	B(71)-B(75)-H(75)	121.8	B(80)-B(81)-B(75)	60.10(19)
B(80)-Ta(2)-B(81)	42.69(12)	C(77)-B(76)-B(72)	60.1(2)	C(77)-B(81)-B(76)	59.50(19)
C(78)-Ta(2)-B(81)	67.94(10)	C(77)-B(76)-B(71)	106.4(3)	B(80)-B(81)-B(76)	107.7(2)
C(77)-Ta(2)-B(81)	41.36(11)	B(72)-B(76)-B(71)	59.8(2)	B(75)-B(81)-B(76)	60.1(2)
B(73)-B(71)-B(72)	60.0(2)	C(77)-B(76)-B(75)	105.5(2)	C(77)-B(81)-Ta(2)	68.97(14)
B(73)-B(71)-B(74)	60.0(2)	B(72)-B(76)-B(75)	108.1(3)	B(80)-B(81)-Ta(2)	67.57(14)
B(72)-B(71)-B(74)	107.9(2)	B(71)-B(76)-B(75)	60.4(2)	B(75)-B(81)-Ta(2)	124.0(2)
B(73)-B(71)-B(76)	107.7(2)	C(77)-B(76)-B(81)	58.76(18)	B(76)-B(81)-Ta(2)	125.0(2)
B(72)-B(71)-B(76)	59.8(2)	B(72)-B(76)-B(81)	108.6(2)	C(77)-B(81)-H(81)	124.3
B(74)-B(71)-B(76)	107.4(2)	B(71)-B(76)-B(81)	108.5(3)	B(80)-B(81)-H(81)	124.0
B(73)-B(71)-B(75)	107.6(2)	B(75)-B(76)-B(81)	59.8(2)	B(75)-B(81)-H(81)	119.5
B(72)-B(71)-B(75)	107.7(2)	C(77)-B(76)-H(76)	123.6	B(76)-B(81)-H(81)	118.7
B(74)-B(71)-B(75)	59.6(2)	B(72)-B(76)-H(76)	121.1	Ta(2)-B(81)-H(81)	105.0
B(76)-B(71)-B(75)	59.8(2)	B(71)-B(76)-H(76)	121.8	C(41)-O(4)-Ta(2)	160.53(17)
B(73)-B(71)-H(71)	121.8	B(75)-B(76)-H(76)	122.3	O(4)-C(41)-C(42)	118.0(2)
B(72)-B(71)-H(71)	121.8	B(81)-B(76)-H(76)	121.4	O(4)-C(41)-C(46)	118.6(2)
B(74)-B(71)-H(71)	122.0	C(78)-C(77)-B(81)	108.2(2)	C(42)-C(41)-C(46)	123.3(2)

Appendix A – Crystal Data

C(41)-C(42)-C(43)	116.9(3)	C(56)-C(51)-C(52)	123.3(3)	O(6)-C(61)-C(62)	118.4(2)
C(41)-C(42)-C(47)	120.8(2)	C(51)-C(52)-C(53)	116.8(3)	C(66)-C(61)-C(62)	123.1(2)
C(43)-C(42)-C(47)	122.2(3)	C(51)-C(52)-C(57)	121.9(3)	C(63)-C(62)-C(61)	116.9(2)
C(44)-C(43)-C(42)	121.3(3)	C(53)-C(52)-C(57)	121.3(3)	C(63)-C(62)-C(67)	121.1(2)
C(44)-C(43)-H(43A)	119.3	C(54)-C(53)-C(52)	121.4(3)	C(61)-C(62)-C(67)	122.0(2)
C(42)-C(43)-H(43A)	119.3	C(54)-C(53)-H(53A)	119.3	C(64)-C(63)-C(62)	121.6(3)
C(43)-C(44)-C(45)	120.3(3)	C(52)-C(53)-H(53A)	119.3	C(64)-C(63)-H(63A)	119.2
C(43)-C(44)-H(44A)	119.8	C(53)-C(54)-C(55)	120.3(3)	C(62)-C(63)-H(63A)	119.2
C(45)-C(44)-H(44A)	119.8	C(53)-C(54)-H(54A)	119.8	C(65)-C(64)-C(63)	120.0(3)
C(44)-C(45)-C(46)	121.2(3)	C(55)-C(54)-H(54A)	119.8	C(65)-C(64)-H(64A)	120.0
C(44)-C(45)-H(45A)	119.4	C(54)-C(55)-C(56)	121.2(4)	C(63)-C(64)-H(64A)	120.0
C(46)-C(45)-H(45A)	119.4	C(54)-C(55)-H(55A)	119.4	C(64)-C(65)-C(66)	120.9(3)
C(45)-C(46)-C(41)	116.9(3)	C(56)-C(55)-H(55A)	119.4	C(64)-C(65)-H(65A)	119.5
C(45)-C(46)-C(48)	121.1(3)	C(51)-C(56)-C(55)	116.9(3)	C(66)-C(65)-H(65A)	119.5
C(41)-C(46)-C(48)	122.0(2)	C(51)-C(56)-C(58)	122.1(3)	C(61)-C(66)-C(65)	117.4(3)
C(42)-C(47)-H(47A)	109.5	C(55)-C(56)-C(58)	120.9(3)	C(61)-C(66)-C(68)	121.9(3)
C(42)-C(47)-H(47B)	109.5	C(52)-C(57)-H(57A)	109.5	C(65)-C(66)-C(68)	120.7(3)
H(47A)-C(47)-H(47B)	109.5	C(52)-C(57)-H(57B)	109.5	C(62)-C(67)-H(67A)	109.5
C(42)-C(47)-H(47C)	109.5	H(57A)-C(57)-H(57B)	109.5	C(62)-C(67)-H(67B)	109.5
H(47A)-C(47)-H(47C)	109.5	C(52)-C(57)-H(57C)	109.5	H(67A)-C(67)-H(67B)	109.5
H(47B)-C(47)-H(47C)	109.5	H(57A)-C(57)-H(57C)	109.5	C(62)-C(67)-H(67C)	109.5
C(46)-C(48)-H(48A)	109.5	H(57B)-C(57)-H(57C)	109.5	H(67A)-C(67)-H(67C)	109.5
C(46)-C(48)-H(48B)	109.5	C(56)-C(58)-H(58A)	109.5	H(67B)-C(67)-H(67C)	109.5
H(48A)-C(48)-H(48B)	109.5	C(56)-C(58)-H(58B)	109.5	C(66)-C(68)-H(68A)	109.5
C(46)-C(48)-H(48C)	109.5	H(58A)-C(58)-H(58B)	109.5	C(66)-C(68)-H(68B)	109.5
H(48A)-C(48)-H(48C)	109.5	C(56)-C(58)-H(58C)	109.5	H(68A)-C(68)-H(68B)	109.5
H(48B)-C(48)-H(48C)	109.5	H(58A)-C(58)-H(58C)	109.5	C(66)-C(68)-H(68C)	109.5
C(51)-O(5)-Ta(2)	153.19(17)	H(58B)-C(58)-H(58C)	109.5	H(68A)-C(68)-H(68C)	109.5
O(5)-C(51)-C(56)	118.9(3)	C(61)-O(6)-Ta(2)	164.41(17)	H(68B)-C(68)-H(68C)	109.5
O(5)-C(51)-C(52)	117.8(3)	O(6)-C(61)-C(66)	118.5(2)		

Appendix A – Crystal Data

Table 4. Anisotropic displacement parameters ($\text{\AA}^2 \times 10^3$) for (28). The anisotropic displacement factor exponent takes the form: $-2\pi^2 [h^2 a^{*2} U^{11} + \dots + 2 h k a^* b^* U^{12}]$

	U ¹¹	U ²²	U ³³	U ²³	U ¹³	U ¹²
Ta(1)	21(1)	25(1)	20(1)	0(1)	2(1)	-5(1)
B(1)	34(2)	27(2)	60(3)	2(2)	-11(2)	-8(1)
B(2)	43(2)	33(2)	69(3)	17(2)	-19(2)	-17(2)
B(3)	34(2)	27(2)	73(3)	-11(2)	-17(2)	1(1)
B(4)	29(2)	32(2)	43(2)	-11(1)	-5(1)	0(1)
B(5)	23(2)	31(2)	38(2)	-3(1)	-4(1)	-4(1)
B(6)	30(2)	50(2)	45(2)	8(2)	-1(2)	-19(2)
C(7)	32(2)	36(2)	31(2)	8(1)	-3(1)	-15(1)
C(8)	34(2)	25(1)	59(2)	1(1)	-12(2)	-6(1)
B(9)	26(2)	35(2)	39(2)	-12(1)	1(1)	1(1)
B(10)	23(1)	26(2)	29(2)	-2(1)	-3(1)	-2(1)
B(11)	20(1)	30(2)	31(2)	-2(1)	1(1)	-6(1)
O(1)	24(1)	28(1)	27(1)	-5(1)	2(1)	-2(1)
C(11)	24(1)	34(2)	30(2)	-10(1)	2(1)	-2(1)
C(12)	35(2)	53(2)	28(2)	-11(1)	6(1)	-4(1)
C(13)	44(2)	78(3)	37(2)	-20(2)	12(2)	-1(2)
C(14)	36(2)	75(3)	53(2)	-28(2)	0(2)	16(2)
C(15)	39(2)	50(2)	53(2)	-16(2)	-11(2)	13(2)
C(16)	29(2)	40(2)	35(2)	-9(1)	-5(1)	1(1)
C(17)	68(3)	57(2)	31(2)	-1(2)	14(2)	-5(2)
C(18)	44(2)	38(2)	38(2)	2(1)	-3(1)	2(1)
O(2)	22(1)	27(1)	29(1)	0(1)	1(1)	-2(1)
C(21)	25(1)	22(1)	38(2)	0(1)	-3(1)	-3(1)
C(22)	24(1)	31(2)	42(2)	-6(1)	-1(1)	-4(1)
C(23)	31(2)	34(2)	68(3)	-7(2)	7(2)	0(1)
C(24)	38(2)	36(2)	87(3)	10(2)	2(2)	9(2)
C(25)	47(2)	41(2)	63(2)	21(2)	-6(2)	1(2)
C(26)	35(2)	32(2)	43(2)	7(1)	-3(1)	-3(1)
C(27)	27(2)	56(2)	38(2)	-6(1)	5(1)	1(1)
C(28)	51(2)	48(2)	36(2)	12(1)	2(2)	1(2)
O(3)	27(1)	31(1)	23(1)	3(1)	4(1)	-7(1)
C(31)	24(1)	25(1)	25(1)	5(1)	7(1)	2(1)
C(32)	24(1)	25(1)	30(1)	1(1)	6(1)	2(1)
C(33)	31(2)	29(1)	40(2)	3(1)	11(1)	-3(1)
C(34)	40(2)	42(2)	43(2)	11(1)	15(1)	-4(1)
C(35)	43(2)	49(2)	27(2)	6(1)	13(1)	3(1)
C(36)	27(1)	33(2)	26(1)	2(1)	4(1)	4(1)
C(37)	33(2)	32(2)	33(2)	-2(1)	2(1)	-7(1)
C(38)	46(2)	43(2)	28(2)	-2(1)	2(1)	0(1)
Ta(2)	21(1)	18(1)	22(1)	0(1)	1(1)	1(1)
B(71)	30(2)	25(2)	57(2)	0(1)	14(2)	6(1)
B(72)	50(2)	25(2)	53(2)	8(2)	19(2)	13(2)
B(73)	36(2)	23(2)	61(3)	-11(2)	18(2)	3(1)
B(74)	36(2)	30(2)	41(2)	-7(1)	12(2)	4(1)
B(75)	27(2)	29(2)	46(2)	2(1)	9(1)	3(1)
B(76)	34(2)	38(2)	47(2)	2(2)	0(2)	13(2)
C(77)	38(2)	35(2)	34(2)	1(1)	-3(1)	10(1)
C(78)	31(1)	19(1)	48(2)	-1(1)	14(1)	1(1)
B(79)	20(1)	26(1)	22(1)	-8(1)	-1(1)	5(1)
B(80)	30(2)	25(2)	31(2)	3(1)	7(1)	6(1)
B(81)	20(1)	26(2)	41(2)	-3(1)	2(1)	-2(1)
O(4)	27(1)	20(1)	25(1)	-2(1)	2(1)	-2(1)
C(41)	21(1)	21(1)	29(1)	-4(1)	6(1)	-2(1)
C(42)	29(1)	33(2)	29(2)	-6(1)	4(1)	-5(1)
C(43)	35(2)	43(2)	39(2)	-13(1)	3(1)	-9(1)
C(44)	32(2)	32(2)	55(2)	-11(1)	8(1)	-9(1)
C(45)	29(2)	23(1)	51(2)	1(1)	12(1)	-2(1)
C(46)	25(1)	23(1)	33(2)	1(1)	9(1)	2(1)
C(47)	50(2)	47(2)	28(2)	2(1)	-5(1)	-10(2)
C(48)	41(2)	36(2)	34(2)	8(1)	6(1)	-3(1)
O(5)	22(1)	25(1)	29(1)	-2(1)	4(1)	-1(1)
C(51)	23(1)	21(1)	44(2)	-5(1)	12(1)	1(1)
C(52)	25(1)	25(1)	55(2)	-15(1)	9(1)	1(1)
C(53)	29(2)	33(2)	79(3)	-22(2)	19(2)	-6(1)
C(54)	45(2)	29(2)	85(3)	-12(2)	39(2)	-9(1)
C(55)	50(2)	35(2)	56(2)	1(1)	28(2)	-3(2)
C(56)	35(2)	31(2)	43(2)	0(1)	15(1)	-1(1)
C(57)	26(2)	46(2)	56(2)	-16(2)	-5(1)	-1(1)
C(58)	46(2)	61(2)	37(2)	10(2)	6(2)	-10(2)
O(6)	30(1)	25(1)	24(1)	-3(1)	-4(1)	4(1)
C(61)	22(1)	23(1)	23(1)	-1(1)	-3(1)	2(1)

Appendix A – Crystal Data

C(62)	24(1)	26(1)	23(1)	-2(1)	3(1)	0(1)
C(63)	31(1)	28(1)	34(2)	-2(1)	6(1)	7(1)
C(64)	37(2)	37(2)	34(2)	3(1)	-5(1)	14(1)
C(65)	40(2)	41(2)	25(1)	-1(1)	-4(1)	11(1)
C(66)	33(2)	33(1)	23(1)	-5(1)	-3(1)	7(1)
C(67)	37(2)	32(1)	24(1)	-4(1)	7(1)	5(1)
C(68)	56(2)	48(2)	28(2)	-13(1)	-9(2)	24(2)

Appendix A – Crystal Data

Table 5. Hydrogen coordinates (x 10⁴) and isotropic displacement parameters (Å²x 10³) for (28).

	x	y	z	U(eq)
H(1)	7008	8289	2925	50
H(2)	5915	8376	1463	60
H(3)	5485	8506	3195	55
H(4)	6365	7559	4283	42
H(5)	7334	6849	3196	37
H(6)	7045	7360	1469	50
H(7)	5583(18)	7081(17)	1120(20)	40
H(8)	4720(20)	7713(18)	1900(20)	49
H(9)	4889	7240	3684	40
H(10)	6065	6189	3691	32
H(11)	6434	6119	1946	32
H(13A)	6518	4933	-398	63
H(14A)	6979	4037	397	66
H(15A)	6641	3862	1742	58
H(17A)	5084	5961	53	77
H(17B)	5598	5777	-661	77
H(17C)	5865	6289	72	77
H(18A)	6017	4173	2897	60
H(18B)	5241	4479	2624	60
H(18C)	5880	4963	2978	60
H(23A)	2289	7861	2378	53
H(24A)	2215	8404	1096	65
H(25A)	2976	8117	90	61
H(27A)	2797	7061	3340	60
H(27B)	3635	6931	3286	60
H(27C)	3061	6400	2888	60
H(28A)	4129	6727	152	68
H(28B)	4517	7441	275	68
H(28C)	3855	7350	-421	68
H(33A)	2999	4249	3398	39
H(34A)	3075	4336	4850	49
H(35A)	3821	5134	5533	47
H(37A)	3318	4567	2074	49
H(37B)	4116	4849	2052	49
H(37C)	3453	5359	2020	49
H(38A)	4745	5942	5547	58
H(38B)	4537	6472	4814	58
H(38C)	5204	5979	4751	58
H(71)	1811	4492	1631	44
H(72)	959	4424	3102	50
H(73)	236	4319	1392	47
H(74)	961	5243	298	42
H(75)	2126	5929	1327	41
H(76)	2124	5412	3071	48
H(77)	709(18)	5733(17)	3680(20)	44
H(78)	-241(18)	5158(17)	2580(20)	38
H(79)	-362	5604	986	28
H(80)	765	6610	884	34
H(81)	1517	6716	2622	35
H(43A)	1693	8462	4690	47
H(44A)	1821	9318	3739	47
H(45A)	1299	9234	2372	41
H(47A)	1138	6878	4293	63
H(47B)	452	7250	4605	63
H(47C)	1233	7398	5058	63
H(48A)	672	8634	1272	55
H(48B)	-28	8296	1597	55
H(48C)	630	7836	1377	55
H(53A)	-2659	4973	2840	55
H(54A)	-2469	4617	4213	61
H(55A)	-1492	4999	5068	55
H(57A)	-1944	6306	1934	65
H(57B)	-2354	5620	1687	65
H(57C)	-1507	5674	1633	65
H(58A)	-495	6375	4765	72
H(58B)	-11	5737	4586	72
H(58C)	-510	5723	5349	72
H(63A)	-2138	8585	1100	37
H(64A)	-2332	8397	-334	44
H(65A)	-1756	7518	-953	43

Appendix A – Crystal Data

H(67A)	-1695	8257	2456	46
H(67B)	-865	8066	2464	46
H(67C)	-1445	7492	2577	46
H(68A)	-898	6648	-905	67
H(68B)	-1014	6179	-116	67
H(68C)	-306	6627	-120	67

A12 Crystal data for $[3\text{-Ta}(\text{SC}_6\text{H}_5)_4(9\text{-NHMe}_2\text{-1,2-C}_2\text{B}_9\text{H}_{10})]$; (29).

Identification code

Empirical formula

Formula weight

Temperature

Wavelength

Crystal system

Space group

Unit cell

Volume

Z

Density (calcd)

Absorption coefficient

F(000)

Crystal size

Theta range

Index range

Reflections

Index

Completeness

Absorption correction

Max. mu

Refinement method

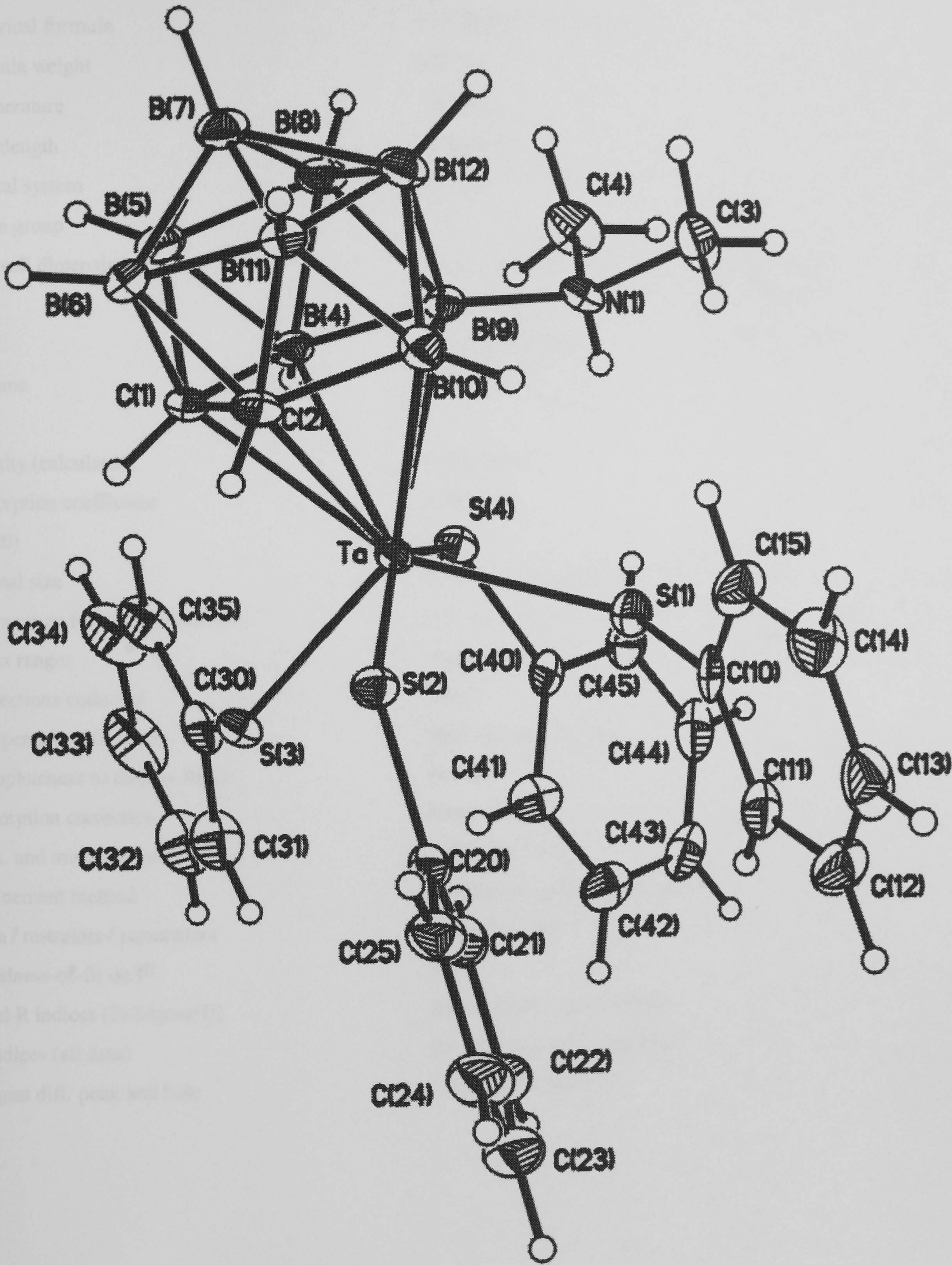
Data / restraints

Goodness-of-fit on F²

Final R indices

R indices (all data)

Largest diff. peak and hole



Appendix A – Crystal Data

Table 1. Crystal data and structure refinement for (29).

Identification code	99srv243		
Empirical formula	C31.50 H37 B9 N S4 Ta		
Formula weight	836.10		
Temperature	120(2) K		
Wavelength	0.71073 Å		
Crystal system	Triclinic		
Space group	P-1		
Unit cell dimensions	a = 11.236(1) Å	α= 110.016(3)°.	
	b = 11.950(1) Å	β= 96.548(2)°.	
	c = 15.081(2) Å	γ = 102.996(2)°.	
Volume	1813.1(3) Å ³		
Z	2		
Density (calculated)	1.532 Mg/m ³		
Absorption coefficient	3.286 mm ⁻¹		
F(000)	830		
Crystal size	0.24 x 0.08 x 0.04 mm ³		
Theta range for data collection	1.47 to 30.33°.		
Index ranges	-15<=h<=15, -16<=k<=16, -20<=l<=20		
Reflections collected	21823		
Independent reflections	9807 [R(int) = 0.0864]		
Completeness to theta = 30.33°	90.1 %		
Absorption correction	Integration		
Max. and min. transmission	0.885 and 0.512		
Refinement method	Full-matrix least-squares on F ²		
Data / restraints / parameters	9807 / 75 / 398		
Goodness-of-fit on F ²	0.913		
Final R indices [I>2sigma(I)]	R1 = 0.0497, wR2 = 0.0783		
R indices (all data)	R1 = 0.1092, wR2 = 0.0896		
Largest diff. peak and hole	1.390 and -1.564 e.Å ⁻³		

Appendix A – Crystal Data

Table 2. Atomic coordinates ($\times 10^4$) and equivalent isotropic displacement parameters ($\text{\AA}^2 \times 10^3$) for (29). U(eq) is defined as one third of the trace of the orthogonalized U^{ij} tensor.

	x	y	z	U(eq)
C(1)	5535(5)	7321(5)	6665(4)	18(1)
C(2)	4102(5)	6831(5)	6631(4)	18(1)
Ta	5126(1)	5516(1)	7196(1)	14(1)
B(4)	6389(7)	7776(6)	7780(5)	19(2)
B(5)	6109(7)	8875(6)	7296(5)	23(2)
B(6)	4639(7)	8250(6)	6516(5)	22(2)
B(7)	4813(7)	9357(7)	7687(5)	23(2)
B(8)	5903(7)	9074(6)	8469(5)	21(2)
B(9)	5256(6)	7589(6)	8515(4)	14(1)
B(10)	3797(7)	6932(6)	7713(5)	22(2)
B(11)	3520(7)	8016(6)	7217(5)	21(2)
B(12)	4291(6)	8561(6)	8429(5)	21(2)
N(1)	5558(5)	7451(5)	9514(3)	20(1)
C(3)	4512(1)	7431(1)	10043(1)	30(2)
C(4)	6749(1)	8328(1)	10163(1)	31(2)
S(1)	4499(1)	4388(1)	8210(1)	20(1)
C(10)	2922(1)	3471(1)	7914(1)	19(1)
C(11)	2684(1)	2187(1)	7632(1)	28(2)
C(12)	1461(7)	1428(6)	7450(5)	36(2)
C(13)	498(7)	1959(7)	7561(5)	37(2)
C(14)	716(6)	3208(6)	7849(5)	33(2)
C(15)	1911(6)	3971(6)	8031(4)	28(2)
S(2)	3252(1)	4151(1)	6019(1)	18(1)
C(20)	2981(6)	2524(5)	5591(4)	20(1)
C(21)	3833(6)	1900(6)	5747(4)	27(1)
C(22)	3493(6)	603(6)	5367(4)	30(1)
C(23)	2310(7)	-60(6)	4832(5)	37(2)
C(24)	1471(7)	566(6)	4679(5)	37(2)
C(25)	1778(6)	1837(5)	5036(4)	27(1)
S(3)	6005(1)	4514(1)	5852(1)	17(1)
C(30)	7663(6)	4850(6)	6063(4)	22(1)
C(31)	8175(6)	3857(6)	5828(4)	32(1)
C(32)	9453(6)	4067(7)	5933(5)	38(2)
C(33)	10222(6)	5256(7)	6244(5)	41(2)
C(34)	9717(6)	6257(7)	6442(5)	41(2)
C(35)	8441(6)	6057(6)	6357(4)	31(1)
S(4)	7103(1)	5810(1)	8249(1)	19(1)
C(40)	7372(5)	4466(5)	8395(4)	17(1)
C(41)	6975(5)	3289(5)	7680(5)	24(2)
C(42)	7257(6)	2305(6)	7858(5)	30(2)
C(43)	7916(6)	2483(6)	8740(5)	32(2)
C(44)	8331(6)	3670(6)	9463(5)	33(2)
C(45)	8062(6)	4647(6)	9277(4)	25(2)
C(1T)	9570(30)	1735(15)	10885(12)	102(3)
C(2T)	9760(20)	588(12)	10257(10)	102(3)
C(3T)	9852(18)	-328(13)	10611(9)	102(3)
C(4T)	10118(16)	-1392(12)	10036(11)	102(3)
C(5T)	10288(17)	-1540(12)	9108(11)	102(3)
C(6T)	10191(16)	-624(14)	8755(8)	102(3)
C(7T)	9925(16)	439(13)	9329(9)	102(3)

Appendix A – Crystal Data

Table 3. Bond lengths [Å] and angles [°] for (29).

C(1)-C(2)	1.573(8)	B(12)-H(12)	1.1000	C(34)-H(34C)	0.9300
C(1)-B(4)	1.677(9)	N(1)-C(4)	1.489(5)	C(35)-H(35C)	0.9300
C(1)-B(5)	1.697(8)	N(1)-C(3)	1.494(5)	S(4)-C(40)	1.779(6)
C(1)-B(6)	1.708(9)	N(1)-H(1N)	0.74(5)	C(40)-C(41)	1.382(8)
C(1)-Ta	2.515(6)	C(3)-H(3A)	0.9600	C(40)-C(45)	1.382(8)
C(1)-H(1)	1.0001	C(3)-H(3B)	0.9600	C(41)-C(42)	1.386(8)
C(2)-B(10)	1.674(9)	C(3)-H(3C)	0.9600	C(41)-H(41C)	0.9300
C(2)-B(11)	1.706(8)	C(4)-H(4A)	0.9600	C(42)-C(43)	1.369(9)
C(2)-B(6)	1.742(9)	C(4)-H(4B)	0.9600	C(42)-H(42C)	0.9300
C(2)-Ta	2.454(6)	C(4)-H(4C)	0.9600	C(43)-C(44)	1.395(9)
C(2)-H(2)	1.0001	S(1)-C(10)	1.7753	C(43)-H(43C)	0.9300
Ta-S(3)	2.4177(14)	C(10)-C(11)	1.3960	C(44)-C(45)	1.376(8)
Ta-S(2)	2.4224(15)	C(10)-C(15)	1.399(7)	C(44)-H(44C)	0.9300
Ta-S(1)	2.4255(14)	C(11)-C(12)	1.403(7)	C(45)-H(45C)	0.9300
Ta-S(4)	2.4580(16)	C(11)-H(11C)	0.9300	C(1T)-C(5T)#1	0.31(3)
Ta-B(10)	2.489(7)	C(12)-C(13)	1.371(9)	C(1T)-C(4T)#1	1.42(3)
Ta-B(4)	2.539(6)	C(12)-H(12C)	0.9300	C(1T)-C(2T)	1.4499
Ta-B(9)	2.552(6)	C(13)-C(14)	1.357(9)	C(1T)-C(6T)#1	1.66(3)
B(4)-B(5)	1.774(10)	C(13)-H(13C)	0.9300	C(2T)-C(4T)#1	1.18(3)
B(4)-B(8)	1.787(9)	C(14)-C(15)	1.379(8)	C(2T)-C(5T)#1	1.23(2)
B(4)-B(9)	1.807(10)	C(14)-H(14C)	0.9300	C(2T)-C(3T)#1	1.39(2)
B(4)-H(4)	1.1000	C(15)-H(15C)	0.9300	C(2T)-C(3T)	1.3900
B(5)-B(6)	1.752(10)	S(2)-C(20)	1.766(6)	C(2T)-C(7T)	1.3900
B(5)-B(8)	1.752(10)	C(20)-C(21)	1.385(8)	C(2T)-C(6T)#1	1.47(3)
B(5)-B(7)	1.772(10)	C(20)-C(25)	1.405(8)	C(2T)-C(2T)#1	1.60(2)
B(5)-H(5)	1.1000	C(21)-C(22)	1.398(8)	C(2T)-C(7T)#1	1.64(3)
B(6)-B(7)	1.764(10)	C(21)-H(21C)	0.9300	C(3T)-C(7T)#1	0.33(3)
B(6)-B(11)	1.768(10)	C(22)-C(23)	1.375(9)	C(3T)-C(6T)#1	1.23(2)
B(6)-H(6)	1.1000	C(22)-H(22C)	0.9300	C(3T)-C(2T)#1	1.39(2)
B(7)-B(11)	1.767(10)	C(23)-C(24)	1.373(9)	C(3T)-C(4T)	1.3900
B(7)-B(12)	1.768(10)	C(23)-H(23C)	0.9300	C(4T)-C(2T)#1	1.18(2)
B(7)-B(8)	1.770(11)	C(24)-C(25)	1.370(8)	C(4T)-C(7T)#1	1.23(3)
B(7)-H(7)	1.1000	C(24)-H(24C)	0.9300	C(4T)-C(5T)	1.3900
B(8)-B(12)	1.763(10)	C(25)-H(25C)	0.9300	C(4T)-C(1T)#1	1.42(2)
B(8)-B(9)	1.788(9)	S(3)-C(30)	1.781(6)	C(5T)-C(1T)#1	0.31(3)
B(8)-H(8)	1.1000	C(30)-C(31)	1.389(8)	C(5T)-C(2T)#1	1.23(2)
B(9)-N(1)	1.577(8)	C(30)-C(35)	1.396(8)	C(5T)-C(6T)	1.3900
B(9)-B(10)	1.757(9)	C(31)-C(32)	1.383(9)	C(6T)-C(3T)#1	1.23(2)
B(9)-B(12)	1.783(9)	C(31)-H(31C)	0.9300	C(6T)-C(7T)	1.3900
B(10)-B(11)	1.768(10)	C(32)-C(33)	1.373(9)	C(6T)-C(2T)#1	1.47(2)
B(10)-B(12)	1.789(9)	C(32)-H(32C)	0.9300	C(6T)-C(1T)#1	1.66(2)
B(10)-H(10)	1.1000	C(33)-C(34)	1.393(9)	C(7T)-C(3T)#1	0.33(3)
B(11)-B(12)	1.756(10)	C(33)-H(33C)	0.9300	C(7T)-C(4T)#1	1.23(3)
B(11)-H(11)	1.1000	C(34)-C(35)	1.383(8)	C(7T)-C(2T)#1	1.64(2)
C(2)-C(1)-B(4)	111.5(5)	B(10)-C(2)-H(2)	119.1	S(2)-Ta-B(4)	137.40(17)
C(2)-C(1)-B(5)	112.4(4)	B(11)-C(2)-H(2)	116.9	S(1)-Ta-B(4)	126.03(15)
B(4)-C(1)-B(5)	63.4(4)	B(6)-C(2)-H(2)	114.8	C(2)-Ta-B(4)	65.1(2)
C(2)-C(1)-B(6)	64.0(4)	Ta-C(2)-H(2)	96.8	S(4)-Ta-B(4)	71.46(17)
B(4)-C(1)-B(6)	115.6(4)	S(3)-Ta-S(2)	78.96(5)	B(10)-Ta-B(4)	68.7(2)
B(5)-C(1)-B(6)	61.9(4)	S(3)-Ta-S(1)	117.56(5)	C(1)-Ta-B(4)	38.8(2)
C(2)-C(1)-Ta	69.5(3)	S(2)-Ta-S(1)	86.76(5)	S(3)-Ta-B(9)	144.48(16)
B(4)-C(1)-Ta	71.4(3)	S(3)-Ta-C(2)	103.43(13)	S(2)-Ta-B(9)	124.85(15)
B(5)-C(1)-Ta	131.9(4)	S(2)-Ta-C(2)	73.04(13)	S(1)-Ta-B(9)	91.93(15)
B(6)-C(1)-Ta	132.0(4)	S(1)-Ta-C(2)	129.61(14)	C(2)-Ta-B(9)	66.03(19)
C(2)-C(1)-H(1)	121.3	S(3)-Ta-S(4)	87.04(5)	S(4)-Ta-B(9)	80.94(15)
B(4)-C(1)-H(1)	118.9	S(2)-Ta-S(4)	150.00(5)	B(10)-Ta-B(9)	40.8(2)
B(5)-C(1)-H(1)	115.7	S(1)-Ta-S(4)	76.36(5)	C(1)-Ta-B(9)	66.01(19)
B(6)-C(1)-H(1)	113.8	C(2)-Ta-S(4)	136.53(14)	B(4)-Ta-B(9)	41.6(2)
Ta-C(1)-H(1)	99.6	S(3)-Ta-B(10)	142.85(16)	C(1)-B(4)-B(5)	58.8(4)
C(1)-C(2)-B(10)	112.8(5)	S(2)-Ta-B(10)	84.28(17)	C(1)-B(4)-B(8)	103.6(5)
C(1)-C(2)-B(11)	111.1(4)	S(1)-Ta-B(10)	94.06(17)	B(5)-B(4)-B(8)	59.0(4)
B(10)-C(2)-B(11)	63.0(4)	C(2)-Ta-B(10)	39.6(2)	C(1)-B(4)-B(9)	104.7(5)
C(1)-C(2)-B(6)	61.8(4)	S(4)-Ta-B(10)	121.03(16)	B(5)-B(4)-B(9)	107.5(5)
B(10)-C(2)-B(6)	114.9(4)	S(3)-Ta-C(1)	85.26(13)	B(8)-B(4)-B(9)	59.7(4)
B(11)-C(2)-B(6)	61.7(4)	S(2)-Ta-C(1)	100.52(13)	C(1)-B(4)-Ta	69.8(3)
C(1)-C(2)-Ta	73.7(3)	S(1)-Ta-C(1)	157.09(13)	B(5)-B(4)-Ta	126.2(4)
B(10)-C(2)-Ta	71.4(3)	C(2)-Ta-C(1)	36.88(18)	B(8)-B(4)-Ta	125.3(4)
B(11)-C(2)-Ta	132.2(4)	S(4)-Ta-C(1)	104.64(14)	B(9)-B(4)-Ta	69.6(3)
B(6)-C(2)-Ta	134.0(4)	B(10)-Ta-C(1)	65.5(2)	C(1)-B(4)-H(4)	125.7
C(1)-C(2)-H(2)	120.5	S(3)-Ta-B(4)	102.90(15)	B(5)-B(4)-H(4)	119.0

Appendix A – Crystal Data

B(8)-B(4)-H(4)	120.9	C(2)-B(10)-B(9)	105.3(5)	C(15)-C(14)-H(14C)	119.6
B(9)-B(4)-H(4)	123.5	C(2)-B(10)-B(11)	59.3(4)	C(14)-C(15)-C(10)	120.6(5)
Ta-B(4)-H(4)	102.9	B(9)-B(10)-B(11)	108.3(5)	C(14)-C(15)-H(15C)	119.7
C(1)-B(5)-B(6)	59.4(4)	C(2)-B(10)-B(12)	104.5(5)	C(10)-C(15)-H(15C)	119.7
C(1)-B(5)-B(8)	104.2(5)	B(9)-B(10)-B(12)	60.4(4)	C(20)-S(2)-Ta	120.5(2)
B(6)-B(5)-B(8)	108.5(5)	B(11)-B(10)-B(12)	59.2(4)	C(21)-C(20)-C(25)	119.2(6)
C(1)-B(5)-B(7)	104.8(5)	C(2)-B(10)-Ta	69.1(3)	C(21)-C(20)-S(2)	126.2(5)
B(6)-B(5)-B(7)	60.1(4)	B(9)-B(10)-Ta	71.5(3)	C(25)-C(20)-S(2)	114.6(5)
B(8)-B(5)-B(7)	60.3(4)	B(11)-B(10)-Ta	126.5(4)	C(20)-C(21)-C(22)	120.3(6)
C(1)-B(5)-B(4)	57.7(4)	B(12)-B(10)-Ta	127.9(4)	C(20)-C(21)-H(21C)	119.9
B(6)-B(5)-B(4)	108.7(5)	C(2)-B(10)-H(10)	126.0	C(22)-C(21)-H(21C)	119.9
B(8)-B(5)-B(4)	60.9(4)	B(9)-B(10)-H(10)	122.4	C(23)-C(22)-C(21)	120.0(7)
B(7)-B(5)-B(4)	109.2(5)	B(11)-B(10)-H(10)	118.9	C(23)-C(22)-H(22C)	120.0
C(1)-B(5)-H(5)	125.3	B(12)-B(10)-H(10)	119.7	C(21)-C(22)-H(22C)	120.0
B(6)-B(5)-H(5)	120.9	Ta-B(10)-H(10)	101.6	C(24)-C(23)-C(22)	119.3(6)
B(8)-B(5)-H(5)	122.1	C(2)-B(11)-B(12)	104.6(5)	C(24)-C(23)-H(23C)	120.3
B(7)-B(5)-H(5)	121.9	C(2)-B(11)-B(7)	105.3(5)	C(22)-C(23)-H(23C)	120.3
B(4)-B(5)-H(5)	120.9	B(12)-B(11)-B(7)	60.3(4)	C(25)-C(24)-C(23)	122.1(7)
C(1)-B(6)-C(2)	54.2(3)	C(2)-B(11)-B(10)	57.6(4)	C(25)-C(24)-H(24C)	118.9
C(1)-B(6)-B(5)	58.7(4)	B(12)-B(11)-B(10)	61.0(4)	C(23)-C(24)-H(24C)	118.9
C(2)-B(6)-B(5)	102.1(5)	B(7)-B(11)-B(10)	109.2(5)	C(24)-C(25)-C(20)	119.1(6)
C(1)-B(6)-B(7)	104.6(5)	C(2)-B(11)-B(6)	60.2(4)	C(24)-C(25)-H(25C)	120.5
C(2)-B(6)-B(7)	103.9(5)	B(12)-B(11)-B(6)	108.7(5)	C(20)-C(25)-H(25C)	120.5
B(5)-B(6)-B(7)	60.5(4)	B(7)-B(11)-B(6)	59.9(4)	C(30)-S(3)-Ta	116.62(19)
C(1)-B(6)-B(11)	102.1(5)	B(10)-B(11)-B(6)	109.1(5)	C(31)-C(30)-C(35)	119.6(6)
C(2)-B(6)-B(11)	58.2(4)	C(2)-B(11)-H(11)	124.9	C(31)-C(30)-S(3)	118.0(5)
B(5)-B(6)-B(11)	107.2(5)	B(12)-B(11)-H(11)	122.0	C(35)-C(30)-S(3)	122.1(5)
B(7)-B(6)-B(11)	60.0(4)	B(7)-B(11)-H(11)	122.0	C(32)-C(31)-C(30)	120.2(7)
C(1)-B(6)-H(6)	125.9	B(10)-B(11)-H(11)	120.9	C(32)-C(31)-H(31C)	119.9
C(2)-B(6)-H(6)	126.5	B(6)-B(11)-H(11)	120.6	C(30)-C(31)-H(31C)	119.9
B(5)-B(6)-H(6)	122.6	B(11)-B(12)-B(8)	107.2(5)	C(33)-C(32)-C(31)	120.2(7)
B(7)-B(6)-H(6)	122.4	B(11)-B(12)-B(7)	60.2(4)	C(33)-C(32)-H(32C)	119.9
B(11)-B(6)-H(6)	122.9	B(8)-B(12)-B(7)	60.2(4)	C(31)-C(32)-H(32C)	119.9
B(6)-B(7)-B(11)	60.1(4)	B(11)-B(12)-B(9)	107.7(4)	C(32)-C(33)-C(34)	120.2(7)
B(6)-B(7)-B(12)	108.3(5)	B(8)-B(12)-B(9)	60.6(4)	C(32)-C(33)-H(33C)	119.9
B(11)-B(7)-B(12)	59.6(4)	B(7)-B(12)-B(9)	109.5(5)	C(34)-C(33)-H(33C)	119.9
B(6)-B(7)-B(8)	107.2(5)	B(11)-B(12)-B(10)	59.8(4)	C(35)-C(34)-C(33)	120.0(7)
B(11)-B(7)-B(8)	106.4(5)	B(8)-B(12)-B(10)	106.6(5)	C(35)-C(34)-H(34C)	120.0
B(12)-B(7)-B(8)	59.8(4)	B(7)-B(12)-B(10)	108.2(5)	C(33)-C(34)-H(34C)	120.0
B(6)-B(7)-B(5)	59.4(4)	B(9)-B(12)-B(10)	58.9(4)	C(34)-C(35)-C(30)	119.8(6)
B(11)-B(7)-B(5)	106.4(5)	B(11)-B(12)-H(12)	122.1	C(34)-C(35)-H(35C)	120.1
B(12)-B(7)-B(5)	107.2(5)	B(8)-B(12)-H(12)	122.3	C(30)-C(35)-H(35C)	120.1
B(8)-B(7)-B(5)	59.3(4)	B(7)-B(12)-H(12)	120.8	C(40)-S(4)-Ta	116.8(2)
B(6)-B(7)-H(7)	121.6	B(9)-B(12)-H(12)	121.3	C(41)-C(40)-C(45)	119.3(6)
B(11)-B(7)-H(7)	122.7	B(10)-B(12)-H(12)	122.6	C(41)-C(40)-S(4)	124.2(5)
B(12)-B(7)-H(7)	121.7	C(4)-N(1)-C(3)	111.2(3)	C(45)-C(40)-S(4)	116.5(4)
B(8)-B(7)-H(7)	122.6	C(4)-N(1)-B(9)	114.4(4)	C(40)-C(41)-C(42)	119.9(6)
B(5)-B(7)-H(7)	122.7	C(3)-N(1)-B(9)	114.9(4)	C(40)-C(41)-H(41C)	120.1
B(5)-B(8)-B(12)	108.3(5)	C(4)-N(1)-H(1N)	101(4)	C(42)-C(41)-H(41C)	120.1
B(5)-B(8)-B(7)	60.4(4)	C(3)-N(1)-H(1N)	107(4)	C(43)-C(42)-C(41)	120.6(6)
B(12)-B(8)-B(7)	60.1(4)	B(9)-N(1)-H(1N)	107(4)	C(43)-C(42)-H(42C)	119.7
B(5)-B(8)-B(4)	60.2(4)	N(1)-C(3)-H(3A)	109.5	C(41)-C(42)-H(42C)	119.7
B(12)-B(8)-B(4)	108.4(5)	N(1)-C(3)-H(3B)	109.5	C(42)-C(43)-C(44)	119.9(6)
B(7)-B(8)-B(4)	108.7(5)	H(3A)-C(3)-H(3B)	109.5	C(42)-C(43)-H(43C)	120.1
B(5)-B(8)-B(9)	109.3(5)	N(1)-C(3)-H(3C)	109.5	C(44)-C(43)-H(43C)	120.1
B(12)-B(8)-B(9)	60.3(4)	H(3A)-C(3)-H(3C)	109.5	C(45)-C(44)-C(43)	119.2(6)
B(7)-B(8)-B(9)	109.2(5)	H(3B)-C(3)-H(3C)	109.5	C(45)-C(44)-H(44C)	120.4
B(4)-B(8)-B(9)	60.7(4)	N(1)-C(4)-H(4A)	109.5	C(43)-C(44)-H(44C)	120.4
B(5)-B(8)-H(8)	121.3	N(1)-C(4)-H(4B)	109.5	C(44)-C(45)-C(40)	121.1(6)
B(12)-B(8)-H(8)	121.7	H(4A)-C(4)-H(4B)	109.5	C(44)-C(45)-H(45C)	119.4
B(7)-B(8)-H(8)	121.2	N(1)-C(4)-H(4C)	109.5	C(40)-C(45)-H(45C)	119.4
B(4)-B(8)-H(8)	121.4	H(4A)-C(4)-H(4C)	109.5	C(5T)#1-C(1T)-C(4T)#1	79(5)
B(9)-B(8)-H(8)	120.7	H(4B)-C(4)-H(4C)	109.5	C(5T)#1-C(1T)-C(2T)	40(6)
N(1)-B(9)-B(10)	124.9(5)	C(10)-S(1)-Ta	117.3	C(4T)#1-C(1T)-C(2T)	48.4(10)
N(1)-B(9)-B(12)	117.5(5)	C(11)-C(10)-C(15)	117.9(3)	C(5T)#1-C(1T)-C(6T)#1	28(6)
B(10)-B(9)-B(12)	60.7(4)	C(11)-C(10)-S(1)	118.3	C(4T)#1-C(1T)-C(6T)#1	102.8(13)
N(1)-B(9)-B(8)	117.5(5)	C(15)-C(10)-S(1)	123.6(3)	C(2T)-C(1T)-C(6T)#1	56.0(8)
B(10)-B(9)-B(8)	106.9(5)	C(10)-C(11)-C(12)	120.5(3)	C(4T)#1-C(2T)-C(5T)#1	70.7(13)
B(12)-B(9)-B(8)	59.2(4)	C(10)-C(11)-H(11C)	119.7	C(4T)#1-C(2T)-C(3T)#1	65.1(13)
N(1)-B(9)-B(4)	124.1(5)	C(12)-C(11)-H(11C)	119.7	C(5T)#1-C(2T)-C(3T)#1	134(2)
B(10)-B(9)-B(4)	105.5(4)	C(13)-C(12)-C(11)	119.4(6)	C(4T)#1-C(2T)-C(3T)	169(2)
B(12)-B(9)-B(4)	106.6(5)	C(13)-C(12)-H(12C)	120.3	C(5T)#1-C(2T)-C(3T)	112.0(17)
B(8)-B(9)-B(4)	59.6(4)	C(11)-C(12)-H(12C)	120.3	C(3T)#1-C(2T)-C(3T)	109.3(11)
N(1)-B(9)-Ta	107.2(4)	C(14)-C(13)-C(12)	120.8(6)	C(4T)#1-C(2T)-C(7T)	56.3(14)
B(10)-B(9)-Ta	67.7(3)	C(14)-C(13)-H(13C)	119.6	C(5T)#1-C(2T)-C(7T)	127.0(17)
B(12)-B(9)-Ta	124.7(4)	C(12)-C(13)-H(13C)	119.6	C(3T)#1-C(2T)-C(7T)	13.5(12)
B(8)-B(9)-Ta	124.5(4)	C(13)-C(14)-C(15)	120.7(6)	C(3T)-C(2T)-C(7T)	120.0
B(4)-B(9)-Ta	68.8(3)	C(13)-C(14)-H(14C)	119.6	C(4T)#1-C(2T)-C(1T)	64.3(14)

Appendix A – Crystal Data

C(5T)#1-C(2T)-C(1T)	9.3(17)	C(2T)#1-C(2T)-C(7T)#1	50.7(9)	C(1T)#1-C(5T)-C(6T)	146(6)
C(3T)#1-C(2T)-C(1T)	129.3(12)	C(7T)#1-C(3T)-C(6T)#1	114(6)	C(2T)#1-C(5T)-C(6T)	68.0(12)
C(3T)-C(2T)-C(1T)	119.6(3)	C(7T)#1-C(3T)-C(2T)#1	84(5)	C(4T)-C(5T)-C(6T)	120.0
C(7T)-C(2T)-C(1T)	120.2(3)	C(6T)#1-C(3T)-C(2T)#1	134(2)	C(3T)#1-C(6T)-C(5T)	112.0(12)
C(4T)#1-C(2T)-C(6T)#1	130.7(19)	C(7T)#1-C(3T)-C(4T)	54(5)	C(3T)#1-C(6T)-C(7T)	12.4(14)
C(5T)#1-C(2T)-C(6T)#1	61.3(11)	C(6T)#1-C(3T)-C(4T)	168(2)	C(5T)-C(6T)-C(7T)	120.0
C(3T)#1-C(2T)-C(6T)#1	154(3)	C(2T)#1-C(3T)-C(4T)	50.1(10)	C(3T)#1-C(6T)-C(2T)#1	61.3(10)
C(3T)-C(2T)-C(6T)#1	50.7(12)	C(7T)#1-C(3T)-C(2T)	136(6)	C(5T)-C(6T)-C(2T)#1	50.7(9)
C(7T)-C(2T)-C(6T)#1	167.3(18)	C(6T)#1-C(3T)-C(2T)	68.0(15)	C(7T)-C(6T)-C(2T)#1	70.0(9)
C(1T)-C(2T)-C(6T)#1	69.2(12)	C(2T)#1-C(3T)-C(2T)	70.7(10)	C(3T)#1-C(6T)-C(1T)#1	116.0(16)
C(4T)#1-C(2T)-C(2T)#1	119(2)	C(4T)-C(3T)-C(2T)	120.0	C(5T)-C(6T)-C(1T)#1	6.1(11)
C(5T)#1-C(2T)-C(2T)#1	158(3)	C(2T)#1-C(4T)-C(7T)#1	70.7(13)	C(7T)-C(6T)-C(1T)#1	124.7(7)
C(3T)#1-C(2T)-C(2T)#1	54.8(9)	C(2T)#1-C(4T)-C(5T)	56.3(10)	C(2T)#1-C(6T)-C(1T)#1	54.9(9)
C(3T)-C(2T)-C(2T)#1	54.5(9)	C(7T)#1-C(4T)-C(5T)	127.0(12)	C(3T)#1-C(7T)-C(4T)#1	114(6)
C(7T)-C(2T)-C(2T)#1	66.0(9)	C(2T)#1-C(4T)-C(3T)	64.7(11)	C(3T)#1-C(7T)-C(6T)	54(4)
C(1T)-C(2T)-C(2T)#1	167(2)	C(7T)#1-C(4T)-C(3T)	12.4(16)	C(4T)#1-C(7T)-C(6T)	168(2)
C(6T)#1-C(2T)-C(2T)#1	103.0(18)	C(5T)-C(4T)-C(3T)	120.0	C(3T)#1-C(7T)-C(2T)	82(4)
C(4T)#1-C(2T)-C(7T)#1	161(3)	C(2T)#1-C(4T)-C(1T)#1	67.3(12)	C(4T)#1-C(7T)-C(2T)	53.0(14)
C(5T)#1-C(2T)-C(7T)#1	113.4(19)	C(7T)#1-C(4T)-C(1T)#1	137(2)	C(6T)-C(7T)-C(2T)	120.0
C(3T)#1-C(2T)-C(7T)#1	105.1(14)	C(5T)-C(4T)-C(1T)#1	12.7(11)	C(3T)#1-C(7T)-C(2T)#1	36(4)
C(3T)-C(2T)-C(7T)#1	7.9(13)	C(3T)-C(4T)-C(1T)#1	131.8(10)	C(4T)#1-C(7T)-C(2T)#1	113.4(18)
C(7T)-C(2T)-C(7T)#1	116.7(9)	C(1T)#1-C(5T)-C(2T)#1	131(6)	C(6T)-C(7T)-C(2T)#1	57.3(7)
C(1T)-C(2T)-C(7T)#1	121.8(9)	C(1T)#1-C(5T)-C(4T)	88(4)	C(2T)-C(7T)-C(2T)#1	63.3(8)
C(6T)#1-C(2T)-C(7T)#1	52.7(9)	C(2T)#1-C(5T)-C(4T)	53.0(12)		

Symmetry transformations used to generate equivalent atoms:

#1 -x+2,-y,-z+2

Appendix A – Crystal Data

Table 4. Anisotropic displacement parameters ($\text{\AA}^2 \times 10^3$) for (29). The anisotropic displacement factor exponent takes the form: $-2\pi^2 [h^2 a^{*2} U^{11} + \dots + 2 h k a^* b^* U^{12}]$

	U ¹¹	U ²²	U ³³	U ²³	U ¹³	U ¹²
C(1)	23(4)	13(3)	19(3)	5(2)	8(3)	9(3)
C(2)	18(3)	12(3)	18(3)	0(2)	1(3)	2(2)
Ta	14(1)	12(1)	14(1)	3(1)	5(1)	3(1)
B(4)	21(4)	11(3)	24(4)	5(3)	9(3)	2(3)
B(5)	28(5)	15(4)	30(4)	9(3)	11(3)	10(3)
B(6)	32(5)	16(4)	24(4)	10(3)	11(3)	9(3)
B(7)	24(4)	17(4)	34(4)	10(3)	14(3)	10(3)
B(8)	20(4)	12(4)	27(4)	2(3)	7(3)	2(3)
B(9)	15(4)	13(3)	13(3)	4(3)	0(3)	6(3)
B(10)	24(4)	21(4)	23(4)	7(3)	10(3)	7(3)
B(11)	26(4)	15(4)	22(4)	6(3)	7(3)	7(3)
B(12)	22(4)	19(4)	21(4)	4(3)	9(3)	9(3)
N(1)	26(3)	17(3)	16(3)	3(2)	9(2)	10(3)
C(3)	31(4)	37(4)	23(3)	11(3)	12(3)	7(3)
C(4)	26(4)	34(4)	21(3)	2(3)	-3(3)	4(3)
S(1)	18(1)	21(1)	20(1)	10(1)	5(1)	4(1)
C(10)	17(3)	27(3)	16(3)	15(3)	7(3)	2(3)
C(11)	35(4)	31(4)	22(3)	16(3)	9(3)	7(3)
C(12)	42(5)	23(4)	33(4)	10(3)	6(3)	-5(3)
C(13)	25(4)	47(5)	32(4)	14(3)	12(3)	-3(3)
C(14)	24(4)	40(4)	38(4)	17(3)	13(3)	10(3)
C(15)	23(4)	23(4)	35(4)	12(3)	7(3)	-1(3)
S(2)	17(1)	16(1)	19(1)	5(1)	4(1)	4(1)
C(20)	21(3)	18(3)	19(2)	5(2)	10(2)	3(2)
C(21)	28(3)	25(3)	25(3)	8(2)	10(2)	3(2)
C(22)	37(3)	23(3)	33(3)	12(2)	13(2)	9(2)
C(23)	43(3)	22(3)	36(3)	5(2)	14(3)	-1(2)
C(24)	35(3)	25(3)	34(3)	-1(2)	10(3)	-8(2)
C(25)	25(3)	22(3)	27(3)	3(2)	6(2)	3(2)
S(3)	17(1)	18(1)	16(1)	3(1)	5(1)	6(1)
C(30)	17(3)	35(3)	21(3)	12(2)	12(2)	14(2)
C(31)	25(3)	43(3)	35(3)	18(2)	11(2)	16(2)
C(32)	28(3)	58(3)	40(3)	21(3)	13(3)	26(3)
C(33)	16(3)	66(4)	37(3)	13(3)	11(2)	15(3)
C(34)	21(3)	53(3)	38(3)	5(3)	10(3)	4(3)
C(35)	19(3)	41(3)	31(3)	8(2)	11(2)	9(2)
S(4)	18(1)	18(1)	18(1)	4(1)	3(1)	4(1)
C(40)	10(3)	23(3)	23(3)	13(3)	8(3)	4(2)
C(41)	13(3)	25(4)	34(4)	10(3)	6(3)	8(3)
C(42)	22(4)	25(4)	47(4)	15(3)	19(3)	6(3)
C(43)	30(4)	37(4)	52(5)	33(4)	26(4)	21(3)
C(44)	30(4)	48(5)	36(4)	29(4)	16(3)	16(4)
C(45)	21(4)	28(4)	28(4)	15(3)	8(3)	3(3)

Appendix A – Crystal Data

Table 5. Hydrogen coordinates (x 10⁴) and isotropic displacement parameters (Å²x 10³) for (29).

	x	y	z	U(eq)
H(1)	5910	6972	6098	21
H(2)	3542	6151	6038	22
H(4)	7353	7738	7954	23(16)
H(5)	6879	9496	7153	19(15)
H(6)	4433	8449	5864	13(14)
H(7)	4722	10292	7807	50(20)
H(8)	6539	9837	9102	11(14)
H(10)	3002	6326	7844	13(14)
H(11)	2565	8061	7012	6(13)
H(12)	3859	8988	9029	4(13)
H(1N)	5700(50)	6850(50)	9410(40)	2(16)
H(3A)	4768	7331	10634	46
H(3B)	3800	6751	9649	46
H(3C)	4295	8197	10185	46
H(4A)	6872	8180	10749	47
H(4B)	6713	9166	10311	47
H(4C)	7431	8204	9848	47
H(11C)	3342	1832	7565	33
H(12C)	1305	572	7256	43
H(13C)	-314	1458	7437	44
H(14C)	52	3553	7925	39
H(15C)	2045	4825	8234	33
H(21C)	4636	2347	6106	32
H(22C)	4067	188	5476	36
H(23C)	2080	-923	4575	44
H(24C)	669	113	4322	45
H(25C)	1198	2239	4913	33
H(31C)	7656	3049	5600	38
H(32C)	9794	3401	5792	46
H(33C)	11082	5394	6323	49
H(34C)	10238	7059	6631	50
H(35C)	8102	6724	6495	38
H(41C)	6519	3158	7081	29
H(42C)	6996	1515	7373	36
H(43C)	8087	1814	8857	38
H(44C)	8784	3801	10063	39
H(45C)	8349	5442	9754	30

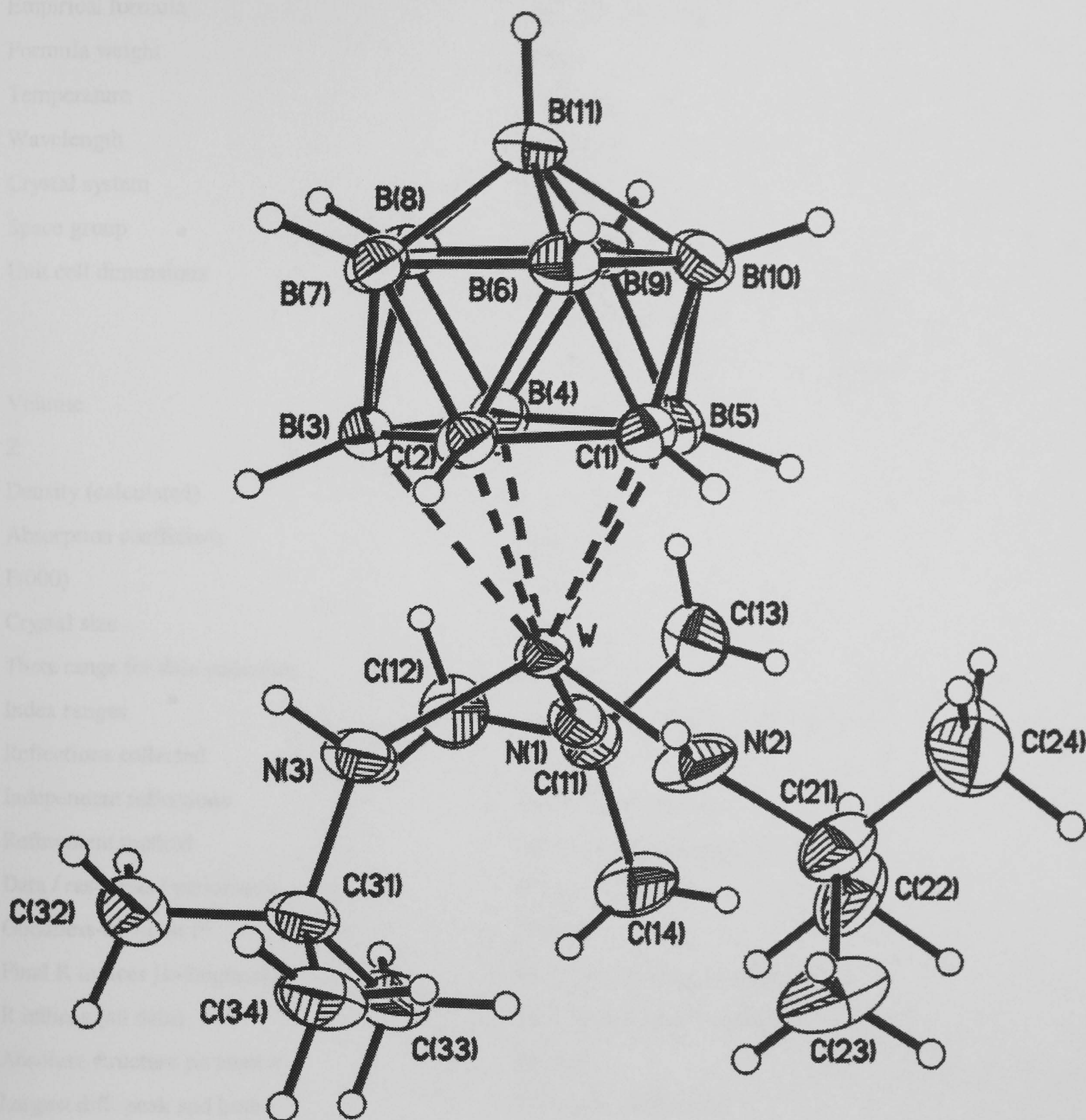
A13 *Crystal data for [3-W(NC₄H₉)(NHC₄H₉)₂(1,2-C₂B₉H₁₁)]:[C₇H₈] ; (31).*

10

C1321 

1

0



Appendix A – Crystal Data

Table 1. Crystal data and structure refinement for (30).

Identification code	99srv062	
Empirical formula	C21 H48 B9 N3 W	
Formula weight	623.76	
Temperature	150(2) K	
Wavelength	0.71073 Å	
Crystal system	Orthorombic	
Space group	P2(1)2(1)2(1)	
Unit cell dimensions	a = 11.4040(10) Å	α= 90°.
	b = 11.5010(10) Å	β= 90°.
	c = 22.6960(10) Å	γ= 90°.
Volume	2976.7(4) Å ³	
Z	4	
Density (calculated)	1.392 Mg/m ³	
Absorption coefficient	3.895 mm ⁻¹	
F(000)	1256	
Crystal size	0.45 x 0.30 x 0.25 mm ³	
Theta range for data collection	1.79 to 30.35°.	
Index ranges	-14<=h<=15, -16<=k<=15, -30<=l<=31	
Reflections collected	25039	
Independent reflections	8084 [R(int) = 0.0306]	
Refinement method	Full-matrix least-squares on F ²	
Data / restraints / parameters	8059 / 7 / 434	
Goodness-of-fit on F ²	1.140	
Final R indices [I>2sigma(I)]	R1 = 0.0237, wR2 = 0.0543	
R indices (all data)	R1 = 0.0273, wR2 = 0.0603	
Absolute structure parameter	0.077(9)	
Largest diff. peak and hole	1.541 and -0.950 e.Å ⁻³	

Table 2. Atomic coordinates (x 10⁴) and equivalent isotropic displacement parameters (Å²x 10³) for (30). U(eq) is defined as one third of the trace of the orthogonalized U^{ij} tensor.

	x	y	z	U(eq)
W	4094(1)	2122(1)	1505(1)	27(1)
N(1)	3829(3)	3011(3)	909(1)	33(1)
N(2)	3764(3)	591(4)	1176(2)	41(1)
N(3)	2726(3)	2287(4)	2017(2)	46(1)
C(1)	5813(4)	974(3)	1904(2)	29(1)
C(2)	5143(3)	1469(4)	2452(2)	27(1)
B(3)	5009(3)	2931(5)	2422(2)	27(1)
B(4)	5734(4)	3373(4)	1773(2)	30(1)
B(5)	6185(3)	2049(4)	1429(2)	31(1)
B(6)	6559(4)	950(4)	2560(2)	32(1)
B(7)	6055(4)	2242(4)	2899(2)	29(1)
B(8)	6487(4)	3439(4)	2464(2)	30(1)
B(9)	7227(4)	2887(5)	1830(2)	32(1)
B(10)	7246(4)	1345(5)	1891(2)	34(1)
B(11)	7432(3)	2209(4)	2530(2)	32(1)
C(11)	3831(3)	3958(4)	473(2)	36(1)
C(12)	3574(5)	5102(5)	790(2)	49(1)
C(13)	5038(5)	3991(5)	184(2)	46(1)
C(14)	2891(5)	3748(5)	-1(2)	52(1)
C(21)	3666(4)	-26(4)	610(2)	43(1)
C(22)	3459(6)	794(5)	109(2)	55(1)
C(23)	2598(6)	-836(6)	661(3)	70(2)
C(24)	4751(6)	-752(7)	530(3)	72(2)
C(31)	1428(3)	2316(5)	1921(2)	46(1)
C(32)	920(5)	3234(5)	2331(2)	57(1)
C(33)	1134(4)	2619(6)	1282(2)	56(2)
C(34)	959(5)	1125(6)	2072(3)	60(1)
C(51)	4072(8)	-1343(8)	-1204(3)	99(3)
C(52)	4536(7)	-2471(11)	-1051(3)	113(4)
C(53)	3832(7)	-3298(10)	-967(3)	110(4)
C(54)	2643(7)	-3231(6)	-1048(3)	79(2)
C(55)	2140(5)	-2166(6)	-1196(2)	62(1)
C(56)	2884(7)	-1236(6)	-1279(3)	75(2)
C(57)	4979(10)	-500(10)	-1259(5)	105(4)
C(58)	5749(13)	-2288(27)	-936(10)	118(20)

Table 3. Bond lengths [Å] and angles [°] for (30).

W-N(1)	1.721(3)	B(6)-B(7)	1.769(7)	C(24)-H(241)	1.12(6)
W-N(2)	1.949(4)	B(6)-H(6)	1.05(4)	C(24)-H(242)	1.12(6)
W-N(3)	1.955(3)	B(7)-B(8)	1.763(6)	C(24)-H(243)	1.06(6)
W-B(5)	2.392(4)	B(7)-B(11)	1.779(6)	C(31)-C(34)	1.509(9)
W-B(4)	2.437(4)	B(7)-H(7)	1.09(4)	C(31)-C(32)	1.521(7)
W-B(3)	2.507(4)	B(8)-B(11)	1.785(7)	C(31)-C(33)	1.530(7)
W-C(1)	2.531(4)	B(8)-B(9)	1.786(7)	C(32)-H(321)	0.99(5)
W-C(2)	2.572(4)	B(8)-H(8)	1.17(5)	C(32)-H(322)	1.02(5)
N(1)-C(11)	1.472(5)	B(9)-B(10)	1.780(7)	C(32)-H(323)	0.95(5)
N(2)-C(21)	1.472(6)	B(9)-B(11)	1.787(6)	C(33)-H(331)	1.00(5)
N(2)-H(2N)	0.88(5)	B(9)-H(9)	1.03(6)	C(33)-H(332)	1.07(5)
N(3)-C(31)	1.496(5)	B(10)-B(11)	1.772(7)	C(33)-H(333)	0.96(5)
N(3)-H(3N)	0.94(6)	B(10)-H(10)	1.10(4)	C(34)-H(341)	0.95(5)
C(1)-C(2)	1.567(5)	B(11)-H(11)	1.02(4)	C(34)-H(342)	0.99(5)
C(1)-B(10)	1.689(6)	C(11)-C(13)	1.525(6)	C(34)-H(343)	0.89(5)
C(1)-B(5)	1.693(6)	C(11)-C(12)	1.529(7)	C(51)-C(56)	1.371(12)
C(1)-B(6)	1.715(6)	C(11)-C(14)	1.538(6)	C(51)-C(57)	1.423(10)
C(1)-H(1)	0.94(5)	C(12)-H(121)	0.93(4)	C(51)-C(52)	1.444(14)
C(2)-B(3)	1.690(6)	C(12)-H(122)	1.00(4)	C(52)-C(53)	1.259(12)
C(2)-B(7)	1.703(5)	C(12)-H(123)	0.95(4)	C(52)-C(58)	1.42(2)
C(2)-B(6)	1.739(6)	C(13)-H(131)	0.94(5)	C(53)-C(54)	1.369(10)
C(2)-H(2)	0.96(4)	C(13)-H(132)	0.93(5)	C(53)-H(53)	0.95
B(3)-B(4)	1.764(6)	C(13)-H(133)	0.94(5)	C(54)-C(55)	1.394(9)
B(3)-B(8)	1.787(6)	C(14)-H(141)	0.99(4)	C(54)-H(54)	0.95
B(3)-B(7)	1.796(6)	C(14)-H(142)	0.96(4)	C(55)-C(56)	1.378(9)
B(3)-H(3)	1.13(4)	C(14)-H(143)	0.97(5)	C(55)-H(55)	0.95
B(4)-B(5)	1.787(6)	C(21)-C(22)	1.495(7)	C(56)-H(56)	0.95
B(4)-B(8)	1.790(6)	C(21)-C(24)	1.504(8)	C(57)-H(57A)	0.98
B(4)-B(9)	1.796(6)	C(21)-C(23)	1.538(8)	C(57)-H(57B)	0.98
B(4)-H(4)	1.10(4)	C(22)-H(221)	1.12(5)	C(57)-H(57C)	0.98
B(5)-B(9)	1.780(6)	C(22)-H(222)	1.07(5)	C(58)-H(58A)	0.98
B(5)-B(10)	1.795(6)	C(22)-H(223)	1.09(5)	C(58)-H(58B)	0.98
B(5)-H(5)	1.16(4)	C(23)-H(23A)	0.98	C(58)-H(58C)	0.98
B(6)-B(11)	1.758(7)	C(23)-H(23B)	0.98		
B(6)-B(10)	1.767(7)	C(23)-H(23C)	0.98		
N(1)-W-N(2)	101.7(2)	W-N(3)-H(3N)	119.9(33)	C(2)-B(3)-B(7)	58.4(2)
N(1)-W-N(3)	105.6(2)	C(2)-C(1)-B(10)	113.2(3)	B(4)-B(3)-B(7)	108.6(3)
N(2)-W-N(3)	99.2(2)	C(2)-C(1)-B(5)	111.2(3)	B(8)-B(3)-B(7)	59.0(2)
N(1)-W-B(5)	98.04(14)	B(10)-C(1)-B(5)	64.1(3)	C(2)-B(3)-W	72.7(2)
N(2)-W-B(5)	97.7(2)	C(2)-C(1)-B(6)	63.8(2)	B(4)-B(3)-W	67.0(2)
N(3)-W-B(5)	147.30(13)	B(10)-C(1)-B(6)	62.5(3)	B(8)-B(3)-W	124.0(2)
N(1)-W-B(4)	88.90(15)	B(5)-C(1)-B(6)	116.1(3)	B(7)-B(3)-W	127.8(3)
N(2)-W-B(4)	141.0(2)	C(2)-C(1)-W	73.6(2)	C(2)-B(3)-H(3)	120.4(21)
N(3)-W-B(4)	114.0(2)	B(10)-C(1)-W	127.7(3)	B(4)-B(3)-H(3)	128.2(21)
B(5)-W-B(4)	43.4(2)	B(5)-C(1)-W	65.5(2)	B(8)-B(3)-H(3)	121.8(22)
N(1)-W-B(3)	120.3(2)	B(6)-C(1)-W	134.7(3)	B(7)-B(3)-H(3)	114.2(21)
N(2)-W-B(3)	137.2(2)	C(2)-C(1)-H(1)	116.6(28)	W-B(3)-H(3)	105.1(22)
N(3)-W-B(3)	78.58(13)	B(10)-C(1)-H(1)	118.9(28)	B(3)-B(4)-B(5)	104.7(3)
B(5)-W-B(3)	70.01(13)	B(5)-C(1)-H(1)	122.3(28)	B(3)-B(4)-B(8)	60.4(2)
B(4)-W-B(3)	41.77(14)	B(6)-C(1)-H(1)	112.8(27)	B(5)-B(4)-B(8)	106.3(3)
N(1)-W-C(1)	136.63(13)	W-C(1)-H(1)	99.0(27)	B(3)-B(4)-B(9)	107.2(3)
N(2)-W-C(1)	79.37(14)	C(1)-C(2)-B(3)	111.9(3)	B(5)-B(4)-B(9)	59.6(3)
N(3)-W-C(1)	117.11(14)	C(1)-C(2)-B(7)	111.3(3)	B(8)-B(4)-B(9)	59.8(2)
B(5)-W-C(1)	40.11(14)	B(3)-C(2)-B(7)	63.9(2)	B(3)-B(4)-W	71.2(2)
B(4)-W-C(1)	67.91(13)	C(1)-C(2)-B(6)	62.2(3)	B(5)-B(4)-W	66.9(2)
B(3)-W-C(1)	64.80(13)	B(3)-C(2)-B(6)	115.5(3)	B(8)-B(4)-W	127.8(3)
N(1)-W-C(2)	155.70(14)	B(7)-C(2)-B(6)	61.8(3)	B(9)-B(4)-W	124.2(3)
N(2)-W-C(2)	98.38(14)	C(1)-C(2)-W	70.7(2)	B(3)-B(4)-H(4)	133.2(21)
N(3)-W-C(2)	84.38(13)	B(3)-C(2)-W	68.5(2)	B(5)-B(4)-H(4)	117.2(22)
B(5)-W-C(2)	65.56(13)	B(7)-C(2)-W	129.0(3)	B(8)-B(4)-H(4)	120.7(21)
B(4)-W-C(2)	66.84(13)	B(6)-C(2)-W	130.5(3)	B(9)-B(4)-H(4)	111.3(20)
B(3)-W-C(2)	38.84(13)	C(1)-C(2)-H(2)	118.7(25)	W-B(4)-H(4)	106.0(20)
C(1)-W-C(2)	35.75(12)	B(3)-C(2)-H(2)	123.7(25)	C(1)-B(5)-B(9)	103.7(3)
C(11)-N(1)-W	165.3(3)	B(7)-C(2)-H(2)	114.5(26)	C(1)-B(5)-B(4)	105.8(3)
C(21)-N(2)-W	141.6(3)	B(6)-C(2)-H(2)	108.8(26)	B(9)-B(5)-B(4)	60.5(3)
C(21)-N(2)-H(2N)	114.3(30)	W-C(2)-H(2)	106.3(26)	C(1)-B(5)-B(10)	57.8(3)
W-N(2)-H(2N)	102.7(29)	C(2)-B(3)-B(4)	106.1(3)	B(9)-B(5)-B(10)	59.7(2)
C(31)-N(3)-W	134.8(3)	C(2)-B(3)-B(8)	103.7(3)	B(4)-B(5)-B(10)	108.9(3)
C(31)-N(3)-H(3N)	105.2(33)	B(4)-B(3)-B(8)	60.5(2)	C(1)-B(5)-W	74.4(2)

Appendix A – Crystal Data

B(9)-B(5)-W	127.6(3)	B(4)-B(9)-H(9)	120.8(31)	C(21)-C(23)-H(23A)	109.5(3)
B(4)-B(5)-W	69.6(2)	C(1)-B(10)-B(6)	59.5(2)	C(21)-C(23)-H(23B)	109.5(3)
B(10)-B(5)-W	130.3(3)	C(1)-B(10)-B(11)	104.1(3)	H(23A)-C(23)-H(23B)	109.5
C(1)-B(5)-H(5)	112.4(20)	B(6)-B(10)-B(11)	59.6(3)	C(21)-C(23)-H(23C)	109.5(3)
B(9)-B(5)-H(5)	124.6(20)	C(1)-B(10)-B(9)	103.9(3)	H(23A)-C(23)-H(23C)	109.5
B(4)-B(5)-H(5)	137.1(20)	B(6)-B(10)-B(9)	108.5(3)	H(23B)-C(23)-H(23C)	109.5
B(10)-B(5)-H(5)	107.6(20)	B(11)-B(10)-B(9)	60.4(3)	C(21)-C(24)-H(241)	104.7(38)
W-B(5)-H(5)	102.3(20)	C(1)-B(10)-B(5)	58.1(2)	C(21)-C(24)-H(242)	115.0(39)
C(1)-B(6)-C(2)	53.9(2)	B(6)-B(10)-B(5)	108.6(3)	H(241)-C(24)-H(242)	106.5(42)
C(1)-B(6)-B(11)	103.5(3)	B(11)-B(10)-B(5)	107.8(3)	C(21)-C(24)-H(243)	109.0(41)
C(2)-B(6)-B(11)	103.8(3)	B(9)-B(10)-B(5)	59.7(3)	H(241)-C(24)-H(243)	110.9(45)
C(1)-B(6)-B(10)	58.0(3)	C(1)-B(10)-H(10)	119.3(21)	H(242)-C(24)-H(243)	110.6(43)
C(2)-B(6)-B(10)	101.7(3)	B(6)-B(10)-H(10)	122.8(21)	N(3)-C(31)-C(34)	107.3(5)
B(11)-B(6)-B(10)	60.3(3)	B(11)-B(10)-H(10)	129.9(21)	N(3)-C(31)-C(32)	107.7(4)
C(1)-B(6)-B(7)	101.7(3)	B(9)-B(10)-H(10)	124.2(21)	C(34)-C(31)-C(32)	110.9(4)
C(2)-B(6)-B(7)	58.1(2)	B(5)-B(10)-H(10)	115.6(21)	N(3)-C(31)-C(33)	111.1(3)
B(11)-B(6)-B(7)	60.6(3)	B(6)-B(11)-B(10)	60.1(3)	C(34)-C(31)-C(33)	110.1(4)
B(10)-B(6)-B(7)	107.6(3)	B(6)-B(11)-B(7)	60.0(3)	C(32)-C(31)-C(33)	109.7(5)
C(1)-B(6)-H(6)	121.2(23)	B(10)-B(11)-B(7)	106.9(3)	C(31)-C(32)-H(321)	112.8(32)
C(2)-B(6)-H(6)	119.0(23)	B(6)-B(11)-B(8)	108.3(3)	C(31)-C(32)-H(322)	110.4(32)
B(11)-B(6)-H(6)	130.4(22)	B(10)-B(11)-B(8)	107.7(3)	H(321)-C(32)-H(322)	104.4(35)
B(10)-B(6)-H(6)	126.5(23)	B(7)-B(11)-B(8)	59.3(2)	C(31)-C(32)-H(323)	110.3(35)
B(7)-B(6)-H(6)	122.6(23)	B(6)-B(11)-B(9)	108.6(3)	H(321)-C(32)-H(323)	110.4(38)
C(2)-B(7)-B(8)	104.2(3)	B(10)-B(11)-B(9)	60.0(3)	H(322)-C(32)-H(323)	108.2(38)
C(2)-B(7)-B(6)	60.1(2)	B(7)-B(11)-B(9)	107.0(3)	C(31)-C(33)-H(331)	103.0(34)
B(8)-B(7)-B(6)	108.8(3)	B(8)-B(11)-B(9)	60.0(3)	C(31)-C(33)-H(332)	110.4(33)
C(2)-B(7)-B(11)	104.4(3)	B(6)-B(11)-H(11)	120.8(25)	H(331)-C(33)-H(332)	106.2(34)
B(8)-B(7)-B(11)	60.5(3)	B(10)-B(11)-H(11)	123.2(23)	C(31)-C(33)-H(333)	113.2(37)
B(6)-B(7)-B(11)	59.4(3)	B(7)-B(11)-H(11)	121.3(22)	H(331)-C(33)-H(333)	115.0(39)
C(2)-B(7)-B(3)	57.7(2)	B(8)-B(11)-H(11)	121.3(25)	H(332)-C(33)-H(333)	108.8(36)
B(8)-B(7)-B(3)	60.3(2)	B(9)-B(11)-H(11)	122.7(23)	C(31)-C(34)-H(341)	113.3(37)
B(6)-B(7)-B(3)	109.0(3)	N(1)-C(11)-C(13)	108.0(3)	C(31)-C(34)-H(342)	106.3(34)
B(11)-B(7)-B(3)	108.3(3)	N(1)-C(11)-C(12)	108.6(3)	H(341)-C(34)-H(342)	104.4(39)
C(2)-B(7)-H(7)	122.1(25)	C(13)-C(11)-C(12)	110.8(4)	C(31)-C(34)-H(343)	109.5(40)
B(8)-B(7)-H(7)	124.6(24)	N(1)-C(11)-C(14)	110.7(4)	H(341)-C(34)-H(343)	113.2(44)
B(6)-B(7)-H(7)	119.5(24)	C(13)-C(11)-C(14)	109.4(4)	H(342)-C(34)-H(343)	109.8(42)
B(11)-B(7)-H(7)	124.9(25)	C(12)-C(11)-C(14)	109.4(4)	C(56)-C(51)-C(57)	130.3(10)
B(3)-B(7)-H(7)	120.5(25)	C(11)-C(12)-H(121)	113.3(32)	C(56)-C(51)-C(52)	118.2(6)
B(7)-B(8)-B(11)	60.2(2)	C(11)-C(12)-H(122)	110.8(27)	C(57)-C(51)-C(52)	111.5(9)
B(7)-B(8)-B(9)	107.8(3)	H(121)-C(12)-H(122)	106.7(30)	C(53)-C(52)-C(58)	134.8(14)
B(11)-B(8)-B(9)	60.1(3)	C(11)-C(12)-H(123)	110.2(31)	C(53)-C(52)-C(51)	118.8(8)
B(7)-B(8)-B(3)	60.8(2)	H(121)-C(12)-H(123)	110.4(35)	C(58)-C(52)-C(51)	105.5(13)
B(11)-B(8)-B(3)	108.4(3)	H(122)-C(12)-H(123)	105.0(32)	C(52)-C(53)-C(54)	124.7(9)
B(9)-B(8)-B(3)	106.6(3)	C(11)-C(13)-H(131)	108.7(34)	C(52)-C(53)-H(53)	117.4(6)
B(7)-B(8)-B(4)	108.8(3)	C(11)-C(13)-H(132)	104.5(35)	C(54)-C(53)-H(53)	117.9(5)
B(11)-B(8)-B(4)	109.2(3)	H(131)-C(13)-H(132)	108.8(38)	C(53)-C(54)-C(55)	119.2(7)
B(9)-B(8)-B(4)	60.3(2)	C(11)-C(13)-H(133)	116.9(35)	C(53)-C(54)-H(54)	120.4(5)
B(3)-B(8)-B(4)	59.1(2)	H(131)-C(13)-H(133)	108.4(37)	C(55)-C(54)-H(54)	120.4(4)
B(7)-B(8)-H(8)	122.7(23)	H(132)-C(13)-H(133)	109.3(38)	C(56)-C(55)-C(54)	117.5(6)
B(11)-B(8)-H(8)	127.4(23)	C(11)-C(14)-H(141)	106.3(32)	C(56)-C(55)-H(55)	121.3(4)
B(9)-B(8)-H(8)	124.4(23)	C(11)-C(14)-H(142)	106.4(31)	C(54)-C(55)-H(55)	121.2(4)
B(3)-B(8)-H(8)	116.9(23)	H(141)-C(14)-H(142)	111.5(35)	C(51)-C(56)-C(55)	121.5(7)
B(4)-B(8)-H(8)	116.1(23)	C(11)-C(14)-H(143)	108.4(31)	C(51)-C(56)-H(56)	119.4(5)
B(10)-B(9)-B(5)	60.6(3)	H(141)-C(14)-H(143)	110.7(32)	C(55)-C(56)-H(56)	119.2(4)
B(10)-B(9)-B(8)	107.3(3)	H(142)-C(14)-H(143)	113.1(37)	C(51)-C(57)-H(57A)	109.6(7)
B(5)-B(9)-B(8)	106.8(3)	N(2)-C(21)-C(22)	111.8(4)	C(51)-C(57)-H(57B)	109.4(5)
B(10)-B(9)-B(11)	59.6(3)	N(2)-C(21)-C(24)	108.1(4)	H(57A)-C(57)-H(57B)	109.5
B(5)-B(9)-B(11)	107.8(3)	C(22)-C(21)-C(24)	112.9(5)	C(51)-C(57)-H(57C)	109.4(6)
B(8)-B(9)-B(11)	59.9(3)	N(2)-C(21)-C(23)	106.6(4)	H(57A)-C(57)-H(57C)	109.5
B(10)-B(9)-B(4)	109.1(3)	C(22)-C(21)-C(23)	108.3(4)	H(57B)-C(57)-H(57C)	109.5
B(5)-B(9)-B(4)	60.0(2)	C(24)-C(21)-C(23)	108.9(5)	C(52)-C(58)-H(58A)	109.7(12)
B(8)-B(9)-B(4)	59.9(2)	C(21)-C(22)-H(221)	111.8(34)	C(52)-C(58)-H(58B)	109.7(12)
B(11)-B(9)-B(4)	108.9(3)	C(21)-C(22)-H(222)	114.1(34)	H(58A)-C(58)-H(58B)	109.5
B(10)-B(9)-H(9)	122.8(31)	H(221)-C(22)-H(222)	108.7(36)	C(52)-C(58)-H(58C)	109.0(10)
B(5)-B(9)-H(9)	124.3(33)	C(21)-C(22)-H(223)	103.4(33)	H(58A)-C(58)-H(58C)	109.5
B(8)-B(9)-H(9)	120.4(32)	H(221)-C(22)-H(223)	107.4(36)	H(58B)-C(58)-H(58C)	109.5
B(11)-B(9)-H(9)	120.3(32)	H(222)-C(22)-H(223)	111.1(37)		

Appendix A – Crystal Data

Table 4. Anisotropic displacement parameters ($\text{\AA}^2 \times 10^3$) for (30). The anisotropic displacement factor exponent takes the form: $-2\pi^2 [h^2 a^{*2} U^{11} + \dots + 2 h k a^* b^* U^{12}]$

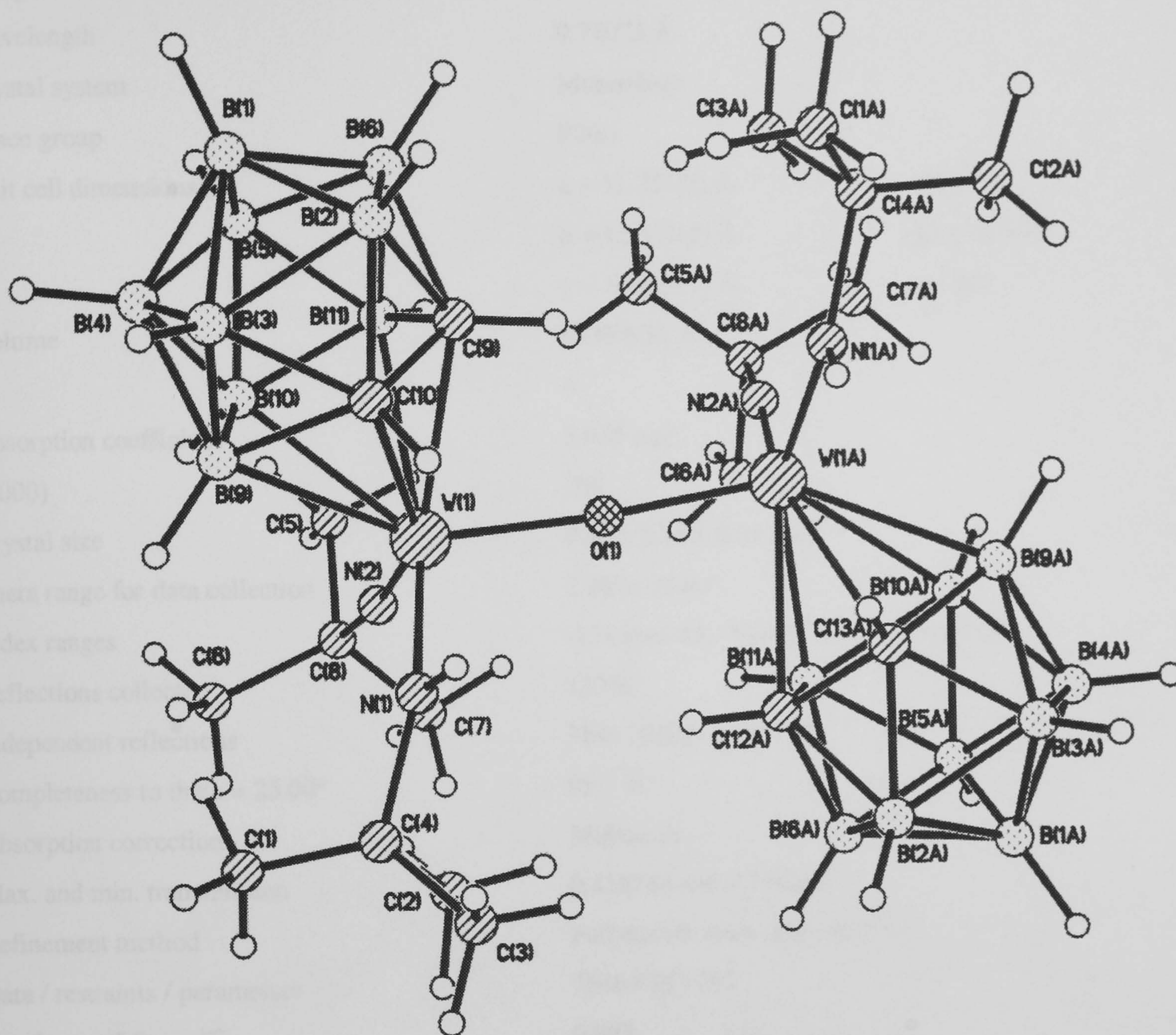
	U ¹¹	U ²²	U ³³	U ²³	U ¹³	U ¹²
W	20(1)	46(1)	17(1)	-1(1)	-1(1)	-3(1)
N(1)	24(1)	54(2)	20(1)	0(1)	-1(1)	4(1)
N(2)	41(2)	59(2)	24(2)	4(2)	-11(1)	-16(2)
N(3)	23(1)	91(3)	24(2)	0(2)	0(1)	-10(2)
C(1)	26(2)	35(2)	26(2)	-2(1)	-2(2)	-1(2)
C(2)	26(2)	35(2)	21(2)	0(1)	-2(1)	-5(2)
B(3)	22(2)	35(2)	23(2)	-2(2)	-2(1)	2(2)
B(4)	26(2)	38(2)	26(2)	1(2)	0(2)	-2(2)
B(5)	24(2)	44(2)	24(2)	-1(2)	4(1)	0(2)
B(6)	30(2)	35(2)	32(2)	2(2)	-6(2)	3(2)
B(7)	29(2)	37(2)	22(2)	-2(2)	-5(1)	-4(2)
B(8)	26(2)	34(2)	30(2)	2(2)	-5(2)	-3(2)
B(9)	23(2)	40(2)	33(2)	1(2)	0(2)	-2(2)
B(10)	22(2)	43(2)	36(2)	1(2)	2(2)	4(2)
B(11)	21(2)	39(2)	37(2)	1(2)	-6(2)	-3(2)
C(11)	35(2)	52(2)	21(2)	3(2)	-2(2)	2(2)
C(12)	54(3)	52(3)	40(2)	5(2)	-5(2)	14(2)
C(13)	47(3)	60(3)	30(2)	9(2)	8(2)	-1(2)
C(14)	56(3)	67(3)	34(2)	13(2)	-19(2)	-4(3)
C(21)	51(3)	43(2)	35(2)	-3(2)	-15(2)	-2(2)
C(22)	78(4)	58(3)	29(2)	-9(2)	-11(2)	4(3)
C(23)	70(4)	69(4)	70(4)	-1(3)	-33(3)	-15(3)
C(24)	77(4)	82(4)	59(4)	-4(3)	-11(3)	29(4)
C(31)	21(2)	90(4)	28(2)	-3(2)	-1(1)	-9(2)
C(32)	34(2)	91(4)	44(2)	-10(2)	5(2)	-4(3)
C(33)	27(2)	105(5)	37(2)	-8(2)	-6(2)	4(2)
C(34)	28(2)	91(4)	60(3)	-7(3)	-1(3)	-14(3)
C(51)	113(6)	140(7)	45(3)	-39(4)	32(4)	-94(6)
C(52)	69(4)	221(14)	48(4)	22(5)	-9(3)	-25(6)
C(53)	72(5)	180(10)	79(5)	71(6)	3(4)	8(5)
C(54)	74(4)	81(5)	81(5)	27(4)	11(4)	-9(4)
C(55)	50(3)	79(4)	56(3)	6(3)	-7(2)	-12(3)
C(56)	117(6)	60(4)	49(3)	-10(3)	15(4)	-16(4)
C(57)	118(9)	105(8)	94(7)	-20(6)	26(7)	-41(7)
C(58)	7(8)	316(63)	31(11)	-13(22)	-1(7)	18(19)

Appendix A – Crystal Data

Table 5. Hydrogen coordinates (x 10⁴) and isotropic displacement parameters (Å²x 10³) for (30).

	x	y	z	U(eq)
H(2N)	3835(37)	134(36)	1483(22)	33(11)
H(3N)	2827(47)	2377(45)	2424(25)	57(16)
H(1)	5592(39)	225(40)	1774(20)	34(12)
H(2)	4604(38)	972(37)	2657(19)	26(11)
H(3)	4271(40)	3382(35)	2661(18)	31(11)
H(4)	5663(32)	4147(31)	1492(19)	24(9)
H(5)	6322(35)	1709(34)	952(18)	22(11)
H(6)	6680(36)	168(36)	2795(18)	18(10)
H(7)	5941(41)	2266(38)	3374(20)	41(12)
H(8)	6632(40)	4369(40)	2661(20)	31(12)
H(9)	7895(49)	3351(47)	1640(26)	61(18)
H(10)	7873(36)	779(34)	1663(18)	24(11)
H(11)	8202(35)	2256(38)	2758(17)	25(10)
H(121)	3585(37)	5745(42)	542(20)	40(7)
H(122)	4165(39)	5252(38)	1104(18)	40(7)
H(123)	2844(36)	5056(41)	992(20)	40(7)
H(131)	5034(47)	4564(42)	-114(22)	57(9)
H(132)	5118(47)	3260(40)	8(23)	57(9)
H(133)	5681(49)	4128(41)	432(22)	57(9)
H(141)	2920(43)	4426(40)	-268(22)	50(9)
H(142)	2154(43)	3701(43)	202(21)	50(9)
H(143)	3088(41)	3039(42)	-212(21)	50(9)
H(221)	3313(49)	322(51)	-315(27)	75(11)
H(222)	4143(49)	1418(50)	47(25)	75(11)
H(223)	2639(47)	1216(53)	227(25)	75(11)
H(23A)	2515(33)	-1287(40)	297(11)	139(21)
H(23B)	1889(10)	-371(7)	725(27)	139(21)
H(23C)	2709(26)	-1367(37)	994(17)	139(21)
H(241)	4531(60)	-1361(61)	162(28)	98(14)
H(242)	4990(62)	-1308(63)	917(28)	98(14)
H(243)	5458(63)	-202(56)	412(30)	98(14)
H(321)	53(41)	3304(44)	2298(23)	59(10)
H(322)	1227(42)	4039(46)	2219(23)	59(10)
H(323)	1140(42)	3081(46)	2725(23)	59(10)
H(331)	267(44)	2525(43)	1267(25)	65(11)
H(332)	1486(42)	1980(46)	991(26)	65(11)
H(333)	1417(44)	3371(43)	1165(27)	65(11)
H(341)	128(44)	1069(52)	2039(24)	64(11)
H(342)	1117(47)	1006(49)	2497(23)	64(11)
H(343)	1336(44)	593(53)	1863(23)	64(11)
H(53)	4151(7)	-4021(10)	-843(3)	132
H(54)	2167(7)	-3902(6)	-999(3)	95
H(55)	1316(5)	-2086(6)	-1241(2)	74
H(56)	2565(7)	-504(6)	-1387(3)	90
H(57A)	5738(10)	-863(10)	-1175(5)	158
H(57B)	4840(10)	134(10)	-979(5)	158
H(57C)	4982(10)	-190(10)	-1661(5)	158
H(58A)	5977(13)	-1510(27)	-1069(10)	177
H(58B)	6215(13)	-2872(27)	-1146(10)	177
H(58C)	5889(13)	-2357(27)	-511(10)	177

A14 *Crystal data for $[\{3\text{-W}(\text{NC}_4\text{H}_9)(\text{NHC}_4\text{H}_9)(1,2\text{-C}_2\text{B}_9\text{H}_{11})\}_2(\square\text{-O})]:[\text{C}_7\text{H}_8]$; (32).*



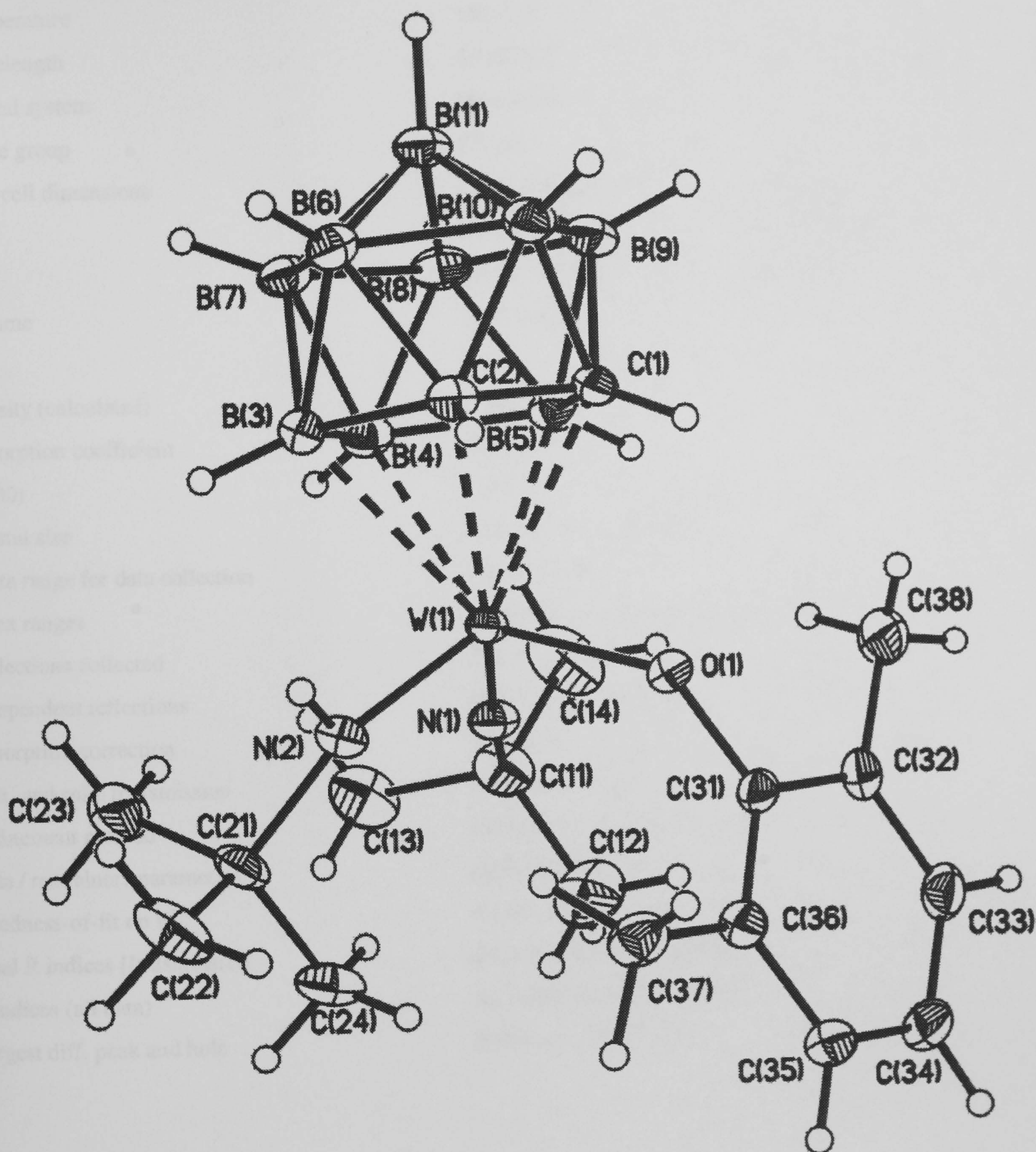
Appendix A – Crystal Data

Table 1. Crystal data and structure refinement for (32).

Identification code	99srv202. (NOT_SUITIBLE_FOR_PUBLISHING)	
Empirical formula	C10.54 H31.08 B9 Cl1.08 N2 O0.50 W	
Temperature	150(2) K	
Wavelength	0.71073 Å	
Crystal system	Monoclinic	
Space group	P2(c)	
Unit cell dimensions	a = 11.253(2) Å	α= 90°.
	b = 12.561(3) Å	β= 94.74(3)°.
	c = 16.609(3) Å	γ= 90°.
Volume	2339.6(8) Å ³	
Z	4	
Absorption coefficient	5.058 mm ⁻¹	
F(000)	998	
Crystal size	0.45 x 0.15 x 0.05 mm ³	
Theta range for data collection	2.28 to 25.00°.	
Index ranges	-13<=h<=13, -14<=k<=14, -17<=l<=19	
Reflections collected	13356	
Independent reflections	7646 [R(int) = 0.0546]	
Completeness to theta = 25.00°	99.7 %	
Absorption correction	Multiscan	
Max. and min. transmission	0.458288 and 0.340468	
Refinement method	Full-matrix least-squares on F ²	
Data / restraints / parameters	7646 / 18 / 257	
Goodness-of-fit on F ²	0.993	
Final R indices [I>2sigma(I)]	R1 = 0.0508, wR2 = 0.1176	
R indices (all data)	R1 = 0.0701, wR2 = 0.1249	
Absolute structure parameter	0.04(2)	
Extinction coefficient	not refined	
Largest diff. peak and hole	1.763 and -0.870 e.Å ⁻³	

NB: Due poor crystal diffraction quality, inadequate data was collected, resulting in poor solution to the final data.

A15 Crystal data for $[3\text{-W}(\text{NC}_4\text{H}_9)(\text{NHC}_4\text{H}_9)(\text{OC}_6\text{H}_3\text{-Me}_2)(1,2\text{-C}_2\text{B}_9\text{H}_{11})]$;
(33).



Appendix A – Crystal Data

Table 1. Crystal data and structure refinement for (33).

Identification code	98srv113	
Empirical formula	C18 H39 B9 N2 O W	
Formula weight	580.65	
Temperature	150(2) K	
Wavelength	0.71073 Å	
Crystal system	Monoclinic	
Space group	P2(1)/c	
Unit cell dimensions	a = 11.053(2) Å	α= 90°.
	b = 11.859(2) Å	β= 90.016(4)°.
	c = 20.074(4) Å	γ = 90°.
Volume	2631.3(8) Å ³	
Z	4	
Density (calculated)	1.466 Mg/m ³	
Absorption coefficient	4.403 mm ⁻¹	
F(000)	1152	
Crystal size	0.26 x 0.14 x 0.12 mm ³	
Theta range for data collection	1.84 to 27.49°.	
Index ranges	-14<=h<=14, -15<=k<=15, -26<=l<=25	
Reflections collected	29490	
Independent reflections	6033 [R(int) = 0.0306]	
Absorption correction	Multiscan	
Max. and min. transmission	0.526 and 0.420	
Refinement method	Full-matrix least-squares on F ²	
Data / restraints / parameters	6026 / 0 / 436	
Goodness-of-fit on F ²	1.145	
Final R indices [I>2sigma(I)]	R1 = 0.0184, wR2 = 0.0365	
R indices (all data)	R1 = 0.0252, wR2 = 0.0397	
Largest diff. peak and hole	0.485 and -1.282 e.Å ⁻³	

Table 2. Atomic coordinates ($\times 10^4$) and equivalent isotropic displacement parameters ($\text{\AA}^2 \times 10^3$) for (33). U(eq) is defined as one third of the trace of the orthogonalized U^{ij} tensor.

	x	y	z	U(eq)
W(1)	6355(1)	7742(1)	6433(1)	14(1)
O(1)	6092(1)	8994(1)	5832(1)	19(1)
N(1)	7206(2)	6804(2)	5977(1)	21(1)
N(2)	7548(2)	8323(2)	7042(1)	20(1)
C(1)	4150(2)	8083(2)	6453(1)	20(1)
C(2)	4656(2)	8435(2)	7159(1)	17(1)
B(3)	5389(2)	7376(2)	7532(1)	19(1)
B(4)	5301(2)	6219(2)	6965(2)	20(1)
B(5)	4497(2)	6752(3)	6256(1)	21(1)
B(6)	3891(2)	7759(3)	7786(1)	20(1)
B(7)	4272(2)	6339(2)	7656(2)	20(1)
B(8)	3721(3)	5927(3)	6858(2)	24(1)
B(9)	3009(2)	7133(3)	6500(2)	25(1)
B(10)	3110(2)	8257(3)	7083(2)	23(1)
B(11)	2853(2)	6865(3)	7367(2)	22(1)
C(11)	7718(2)	5867(2)	5580(2)	30(1)
C(12)	8485(4)	6370(4)	5027(2)	47(1)
C(13)	8467(3)	5109(3)	6036(2)	39(1)
C(14)	6663(3)	5179(3)	5293(2)	46(1)
C(21)	8847(2)	8101(2)	7208(1)	24(1)
C(22)	9302(3)	9095(3)	7623(2)	39(1)
C(23)	8914(3)	7015(3)	7614(2)	38(1)
C(24)	9590(3)	8014(3)	6577(2)	32(1)
C(31)	6759(2)	9287(2)	5273(1)	18(1)
C(32)	6383(2)	8870(2)	4654(1)	22(1)
C(33)	7081(2)	9143(2)	4097(1)	26(1)
C(34)	8105(2)	9809(3)	4154(1)	29(1)
C(35)	8409(2)	10267(2)	4764(1)	26(1)
C(36)	7734(2)	10036(2)	5333(1)	21(1)
C(37)	8008(3)	10622(2)	5980(1)	27(1)
C(38)	5257(3)	8173(3)	4590(2)	30(1)

Table 3. Bond lengths [Å] and angles [°] for (33).

W(1)-N(1)	1.720(2)	B(5)-B(8)	1.776(4)	C(21)-C(24)	1.513(4)
W(1)-N(2)	1.926(2)	B(5)-H(5)	1.06(3)	C(21)-C(23)	1.526(4)
W(1)-O(1)	1.934(2)	B(6)-B(7)	1.755(4)	C(21)-C(22)	1.529(4)
W(1)-B(5)	2.392(3)	B(6)-B(10)	1.757(4)	C(22)-H(22A)	0.97(3)
W(1)-B(4)	2.401(3)	B(6)-B(11)	1.773(4)	C(22)-H(22B)	0.96(4)
W(1)-C(1)	2.471(2)	B(6)-H(6)	1.07(3)	C(22)-H(22C)	0.98(4)
W(1)-B(3)	2.491(3)	B(7)-B(8)	1.783(4)	C(23)-H(23A)	0.96(4)
W(1)-C(2)	2.516(2)	B(7)-B(11)	1.785(4)	C(23)-H(23B)	0.91(4)
O(1)-C(31)	1.387(3)	B(7)-H(7)	1.09(3)	C(23)-H(23C)	1.00(4)
N(1)-C(11)	1.481(3)	B(8)-B(9)	1.783(5)	C(24)-H(24A)	0.90(3)
N(2)-C(21)	1.497(3)	B(8)-B(11)	1.790(4)	C(24)-H(24B)	0.95(4)
N(2)-H(2N)	0.86(3)	B(8)-H(8)	1.10(3)	C(24)-H(24C)	1.00(4)
C(1)-C(2)	1.580(3)	B(9)-B(10)	1.777(5)	C(31)-C(32)	1.402(3)
C(1)-B(5)	1.672(4)	B(9)-B(11)	1.777(4)	C(31)-C(36)	1.402(3)
C(1)-B(9)	1.693(4)	B(9)-H(9)	1.09(3)	C(32)-C(33)	1.396(4)
C(1)-B(10)	1.722(4)	B(10)-B(11)	1.770(4)	C(32)-C(38)	1.499(4)
C(1)-H(1)	0.94(3)	B(10)-H(10)	1.08(3)	C(33)-C(34)	1.385(4)
C(2)-B(3)	1.672(4)	B(11)-H(11)	1.09(3)	C(33)-H(33)	0.93(3)
C(2)-B(6)	1.715(4)	C(11)-C(12)	1.518(5)	C(34)-C(35)	1.381(4)
C(2)-B(10)	1.728(4)	C(11)-C(13)	1.527(4)	C(34)-H(34)	0.92(3)
C(2)-H(2)	0.93(3)	C(11)-C(14)	1.534(4)	C(35)-C(36)	1.391(4)
B(3)-B(7)	1.760(4)	C(12)-H(12A)	1.01(4)	C(35)-H(35)	0.95(3)
B(3)-B(4)	1.786(4)	C(12)-H(12B)	0.95(4)	C(36)-C(37)	1.504(4)
B(3)-B(6)	1.791(4)	C(12)-H(12C)	0.97(4)	C(37)-H(37A)	1.02(4)
B(3)-H(3)	1.09(3)	C(13)-H(13A)	0.96(4)	C(37)-H(37B)	0.98(3)
B(4)-B(5)	1.792(4)	C(13)-H(13B)	0.96(3)	C(37)-H(37C)	0.96(4)
B(4)-B(8)	1.794(4)	C(13)-H(13C)	0.93(4)	C(38)-H(38A)	0.91(4)
B(4)-B(7)	1.799(4)	C(14)-H(14A)	0.97(3)	C(38)-H(38B)	0.97(5)
B(4)-H(4)	1.06(3)	C(14)-H(14B)	0.99(3)	C(38)-H(38C)	0.91(4)
B(5)-B(9)	1.775(4)	C(14)-H(14C)	0.98(4)		
N(1)-W(1)-N(2)	101.25(9)	B(5)-C(1)-W(1)	67.36(12)	B(5)-B(4)-B(8)	59.4(2)
N(1)-W(1)-O(1)	104.30(9)	B(9)-C(1)-W(1)	128.8(2)	B(3)-B(4)-B(7)	58.8(2)
N(2)-W(1)-O(1)	102.99(8)	B(10)-C(1)-W(1)	133.7(2)	B(5)-B(4)-B(7)	105.7(2)
N(1)-W(1)-B(5)	94.19(10)	C(2)-C(1)-H(1)	116.7(17)	B(8)-B(4)-B(7)	59.5(2)
N(2)-W(1)-B(5)	148.99(9)	B(5)-C(1)-H(1)	121.6(17)	B(3)-B(4)-W(1)	71.29(13)
O(1)-W(1)-B(5)	98.94(9)	B(9)-C(1)-H(1)	118.8(16)	B(5)-B(4)-W(1)	67.77(13)
N(1)-W(1)-B(4)	90.90(10)	B(10)-C(1)-H(1)	113.1(17)	B(8)-B(4)-W(1)	124.4(2)
N(2)-W(1)-B(4)	108.55(10)	W(1)-C(1)-H(1)	98.7(16)	B(7)-B(4)-W(1)	126.2(2)
O(1)-W(1)-B(4)	141.43(8)	C(1)-C(2)-B(3)	112.0(2)	B(3)-B(4)-H(4)	124.4(15)
B(5)-W(1)-B(4)	43.92(10)	C(1)-C(2)-B(6)	111.1(2)	B(5)-B(4)-H(4)	126.2(15)
N(1)-W(1)-C(1)	130.82(9)	B(3)-C(2)-B(6)	63.8(2)	B(8)-B(4)-H(4)	116.6(15)
N(2)-W(1)-C(1)	127.31(9)	C(1)-C(2)-B(10)	62.5(2)	B(7)-B(4)-H(4)	116.3(15)
O(1)-W(1)-C(1)	74.72(8)	B(3)-C(2)-B(10)	115.3(2)	W(1)-B(4)-H(4)	107.4(15)
B(5)-W(1)-C(1)	40.17(9)	B(6)-C(2)-B(10)	61.3(2)	C(1)-B(5)-B(9)	58.8(2)
B(4)-W(1)-C(1)	68.70(9)	C(1)-C(2)-W(1)	69.98(12)	C(1)-B(5)-B(8)	104.4(2)
N(1)-W(1)-B(3)	126.38(10)	B(3)-C(2)-W(1)	69.66(12)	B(9)-B(5)-B(8)	60.3(2)
N(2)-W(1)-B(3)	78.02(9)	B(6)-C(2)-W(1)	129.8(2)	C(1)-B(5)-B(4)	105.0(2)
O(1)-W(1)-B(3)	128.44(8)	B(10)-C(2)-W(1)	130.3(2)	B(9)-B(5)-B(4)	109.2(2)
B(5)-W(1)-B(3)	71.18(10)	C(1)-C(2)-H(2)	115.7(18)	B(8)-B(5)-B(4)	60.3(2)
B(4)-W(1)-B(3)	42.77(10)	B(3)-C(2)-H(2)	125.3(18)	C(1)-B(5)-W(1)	72.47(13)
C(1)-W(1)-B(3)	65.85(9)	B(6)-C(2)-H(2)	118.1(19)	B(9)-B(5)-W(1)	129.0(2)
N(1)-W(1)-C(2)	158.08(9)	B(10)-C(2)-H(2)	109.4(18)	B(8)-B(5)-W(1)	125.8(2)
N(2)-W(1)-C(2)	91.48(9)	W(1)-C(2)-H(2)	103.4(19)	B(4)-B(5)-W(1)	68.31(12)
O(1)-W(1)-C(2)	89.89(7)	C(2)-B(3)-B(7)	104.4(2)	C(1)-B(5)-H(5)	119.7(14)
B(5)-W(1)-C(2)	66.75(9)	C(2)-B(3)-B(4)	105.4(2)	B(9)-B(5)-H(5)	113.6(14)
B(4)-W(1)-C(2)	67.99(9)	B(7)-B(3)-B(4)	61.0(2)	B(8)-B(5)-H(5)	122.8(14)
C(1)-W(1)-C(2)	36.93(8)	C(2)-B(3)-B(6)	59.24(15)	B(4)-B(5)-H(5)	129.3(14)
B(3)-W(1)-C(2)	39.02(8)	B(7)-B(3)-B(6)	59.2(2)	W(1)-B(5)-H(5)	102.2(14)
C(31)-O(1)-W(1)	128.03(14)	B(4)-B(3)-B(6)	109.0(2)	C(2)-B(6)-B(7)	102.8(2)
C(11)-N(1)-W(1)	168.8(2)	C(2)-B(3)-W(1)	71.32(13)	C(2)-B(6)-B(10)	59.7(2)
C(21)-N(2)-W(1)	137.3(2)	B(7)-B(3)-W(1)	123.2(2)	B(7)-B(6)-B(10)	108.8(2)
C(21)-N(2)-H(2N)	105.4(19)	B(4)-B(3)-W(1)	65.94(13)	C(2)-B(6)-B(11)	104.5(2)
W(1)-N(2)-H(2N)	114.9(19)	B(6)-B(3)-W(1)	127.2(2)	B(7)-B(6)-B(11)	60.8(2)
C(2)-C(1)-B(5)	112.4(2)	C(2)-B(3)-H(3)	119.5(15)	B(10)-B(6)-B(11)	60.2(2)
C(2)-C(1)-B(9)	112.9(2)	B(7)-B(3)-H(3)	119.9(15)	C(2)-B(6)-B(3)	56.93(14)
B(5)-C(1)-B(9)	63.7(2)	B(4)-B(3)-H(3)	130.9(15)	B(7)-B(6)-B(3)	59.5(2)
C(2)-C(1)-B(10)	63.0(2)	B(6)-B(3)-H(3)	110.4(15)	B(10)-B(6)-B(3)	108.1(2)
B(5)-C(1)-B(10)	116.1(2)	W(1)-B(3)-H(3)	109.2(16)	B(11)-B(6)-B(3)	108.2(2)
B(9)-C(1)-B(10)	62.7(2)	B(3)-B(4)-B(5)	105.2(2)	C(2)-B(6)-H(6)	117.1(15)
C(2)-C(1)-W(1)	73.08(12)	B(3)-B(4)-B(8)	106.2(2)	B(7)-B(6)-H(6)	128.4(14)

Appendix A – Crystal Data

B(10)-B(6)-H(6)	118.9(14)	C(2)-B(10)-B(11)	104.1(2)	C(24)-C(21)-C(23)	111.3(3)
B(11)-B(6)-H(6)	129.7(14)	B(6)-B(10)-B(11)	60.4(2)	N(2)-C(21)-C(22)	107.5(2)
B(3)-B(6)-H(6)	117.5(14)	C(1)-B(10)-B(9)	57.9(2)	C(24)-C(21)-C(22)	109.3(2)
B(6)-B(7)-B(3)	61.3(2)	C(2)-B(10)-B(9)	102.2(2)	C(23)-C(21)-C(22)	110.1(3)
B(6)-B(7)-B(8)	108.3(2)	B(6)-B(10)-B(9)	107.9(2)	C(21)-C(22)-H(22A)	110.8(20)
B(3)-B(7)-B(8)	107.7(2)	B(11)-B(10)-B(9)	60.1(2)	C(21)-C(22)-H(22B)	109.0(21)
B(6)-B(7)-B(11)	60.1(2)	C(1)-B(10)-H(10)	120.8(14)	H(22A)-C(22)-H(22B)	104.8(27)
B(3)-B(7)-B(11)	109.1(2)	C(2)-B(10)-H(10)	118.5(14)	C(21)-C(22)-H(22C)	110.9(22)
B(8)-B(7)-B(11)	60.2(2)	B(6)-B(10)-H(10)	122.3(14)	H(22A)-C(22)-H(22C)	112.6(30)
B(6)-B(7)-B(4)	110.0(2)	B(11)-B(10)-H(10)	130.6(14)	H(22B)-C(22)-H(22C)	108.5(29)
B(3)-B(7)-B(4)	60.2(2)	B(9)-B(10)-H(10)	126.3(14)	C(21)-C(23)-H(23A)	109.9(21)
B(8)-B(7)-B(4)	60.1(2)	B(10)-B(11)-B(6)	59.4(2)	C(21)-C(23)-H(23B)	112.2(23)
B(11)-B(7)-B(4)	109.4(2)	B(10)-B(11)-B(9)	60.1(2)	H(23A)-C(23)-H(23B)	109.4(30)
B(6)-B(7)-H(7)	121.6(15)	B(6)-B(11)-B(9)	107.1(2)	C(21)-C(23)-H(23C)	111.0(20)
B(3)-B(7)-H(7)	121.7(15)	B(10)-B(11)-B(7)	106.8(2)	H(23A)-C(23)-H(23C)	108.8(28)
B(8)-B(7)-H(7)	121.3(15)	B(6)-B(11)-B(7)	59.1(2)	H(23B)-C(23)-H(23C)	105.4(29)
B(11)-B(7)-H(7)	121.3(15)	B(9)-B(11)-B(7)	107.2(2)	C(21)-C(24)-H(24A)	105.1(21)
B(4)-B(7)-H(7)	120.0(15)	B(10)-B(11)-B(8)	108.0(2)	C(21)-C(24)-H(24B)	108.5(21)
B(5)-B(8)-B(7)	107.1(2)	B(6)-B(11)-B(8)	107.2(2)	H(24A)-C(24)-H(24B)	109.2(28)
B(5)-B(8)-B(9)	59.8(2)	B(9)-B(11)-B(8)	60.0(2)	C(21)-C(24)-H(24C)	110.9(22)
B(7)-B(8)-B(9)	107.0(2)	B(7)-B(11)-B(8)	59.8(2)	H(24A)-C(24)-H(24C)	110.0(29)
B(5)-B(8)-B(11)	107.8(2)	B(10)-B(11)-H(11)	116.9(16)	H(24B)-C(24)-H(24C)	112.7(30)
B(7)-B(8)-B(11)	59.9(2)	B(6)-B(11)-H(11)	123.1(16)	O(1)-C(31)-C(32)	118.2(2)
B(9)-B(8)-B(11)	59.6(2)	B(9)-B(11)-H(11)	118.2(16)	O(1)-C(31)-C(36)	119.9(2)
B(5)-B(8)-B(4)	60.3(2)	B(7)-B(11)-H(11)	127.9(16)	C(32)-C(31)-C(36)	121.8(2)
B(7)-B(8)-B(4)	60.4(2)	B(8)-B(11)-H(11)	124.3(16)	C(33)-C(32)-C(31)	117.7(2)
B(9)-B(8)-B(4)	108.8(2)	N(1)-C(11)-C(12)	108.1(2)	C(33)-C(32)-C(38)	121.2(2)
B(11)-B(8)-B(4)	109.5(2)	N(1)-C(11)-C(13)	109.1(2)	C(31)-C(32)-C(38)	121.1(2)
B(5)-B(8)-H(8)	122.4(15)	C(12)-C(11)-C(13)	111.5(3)	C(34)-C(33)-C(32)	121.2(3)
B(7)-B(8)-H(8)	122.1(15)	N(1)-C(11)-C(14)	108.1(2)	C(34)-C(33)-H(33)	121.4(18)
B(9)-B(8)-H(8)	122.4(15)	C(12)-C(11)-C(14)	111.1(3)	C(32)-C(33)-H(33)	117.4(18)
B(11)-B(8)-H(8)	121.4(15)	C(13)-C(11)-C(14)	108.9(3)	C(35)-C(34)-C(33)	119.7(3)
B(4)-B(8)-H(8)	120.3(15)	C(11)-C(12)-H(12A)	111.9(22)	C(35)-C(34)-H(34)	119.5(19)
C(1)-B(9)-B(5)	57.6(2)	C(11)-C(12)-H(12B)	110.7(21)	C(33)-C(34)-H(34)	120.8(18)
C(1)-B(9)-B(10)	59.4(2)	H(12A)-C(12)-H(12B)	104.4(29)	C(34)-C(35)-C(36)	121.4(2)
B(5)-B(9)-B(10)	108.3(2)	C(11)-C(12)-H(12C)	111.0(23)	C(34)-C(35)-H(35)	120.1(19)
C(1)-B(9)-B(11)	104.3(2)	H(12A)-C(12)-H(12C)	111.5(31)	C(36)-C(35)-H(35)	118.5(19)
B(5)-B(9)-B(11)	108.4(2)	H(12B)-C(12)-H(12C)	107.1(31)	C(35)-C(36)-C(31)	117.8(2)
B(10)-B(9)-B(11)	59.7(2)	C(11)-C(13)-H(13A)	107.9(20)	C(35)-C(36)-C(37)	120.7(2)
C(1)-B(9)-B(8)	103.2(2)	C(11)-C(13)-H(13B)	111.2(20)	C(31)-C(36)-C(37)	121.4(2)
B(5)-B(9)-B(8)	59.9(2)	H(13A)-C(13)-H(13B)	108.2(28)	C(36)-C(37)-H(37A)	108.6(20)
B(10)-B(9)-B(8)	108.0(2)	C(11)-C(13)-H(13C)	110.3(21)	C(36)-C(37)-H(37B)	111.4(19)
B(11)-B(9)-B(8)	60.4(2)	H(13A)-C(13)-H(13C)	109.7(29)	H(37A)-C(37)-H(37B)	109.6(26)
C(1)-B(9)-H(9)	121.9(16)	H(13B)-C(13)-H(13C)	109.6(29)	C(36)-C(37)-H(37C)	111.9(20)
B(5)-B(9)-H(9)	119.4(17)	C(11)-C(14)-H(14A)	111.6(19)	H(37A)-C(37)-H(37C)	104.7(28)
B(10)-B(9)-H(9)	120.6(16)	C(11)-C(14)-H(14B)	108.9(19)	H(37B)-C(37)-H(37C)	110.3(27)
B(11)-B(9)-H(9)	125.7(17)	H(14A)-C(14)-H(14B)	103.7(26)	C(32)-C(38)-H(38A)	109.2(23)
B(8)-B(9)-H(9)	125.2(16)	C(11)-C(14)-H(14C)	114.1(23)	C(32)-C(38)-H(38B)	112.0(26)
C(1)-B(10)-C(2)	54.53(14)	H(14A)-C(14)-H(14C)	108.7(29)	H(38A)-C(38)-H(38B)	112.0(34)
C(1)-B(10)-B(6)	102.8(2)	H(14B)-C(14)-H(14C)	109.3(29)	C(32)-C(38)-H(38C)	112.1(24)
C(2)-B(10)-B(6)	58.95(15)	N(2)-C(21)-C(24)	110.3(2)	H(38A)-C(38)-H(38C)	109.5(32)
C(1)-B(10)-B(11)	103.4(2)	N(2)-C(21)-C(23)	108.2(2)	H(38B)-C(38)-H(38C)	101.9(33)

Table 4. Anisotropic displacement parameters ($\text{\AA}^2 \times 10^3$) for (33). The anisotropic displacement factor exponent takes the form: $-2\pi^2 [h^2 a^{*2} U^{11} + \dots + 2 h k a^* b^* U^{12}]$

Appendix A – Crystal Data

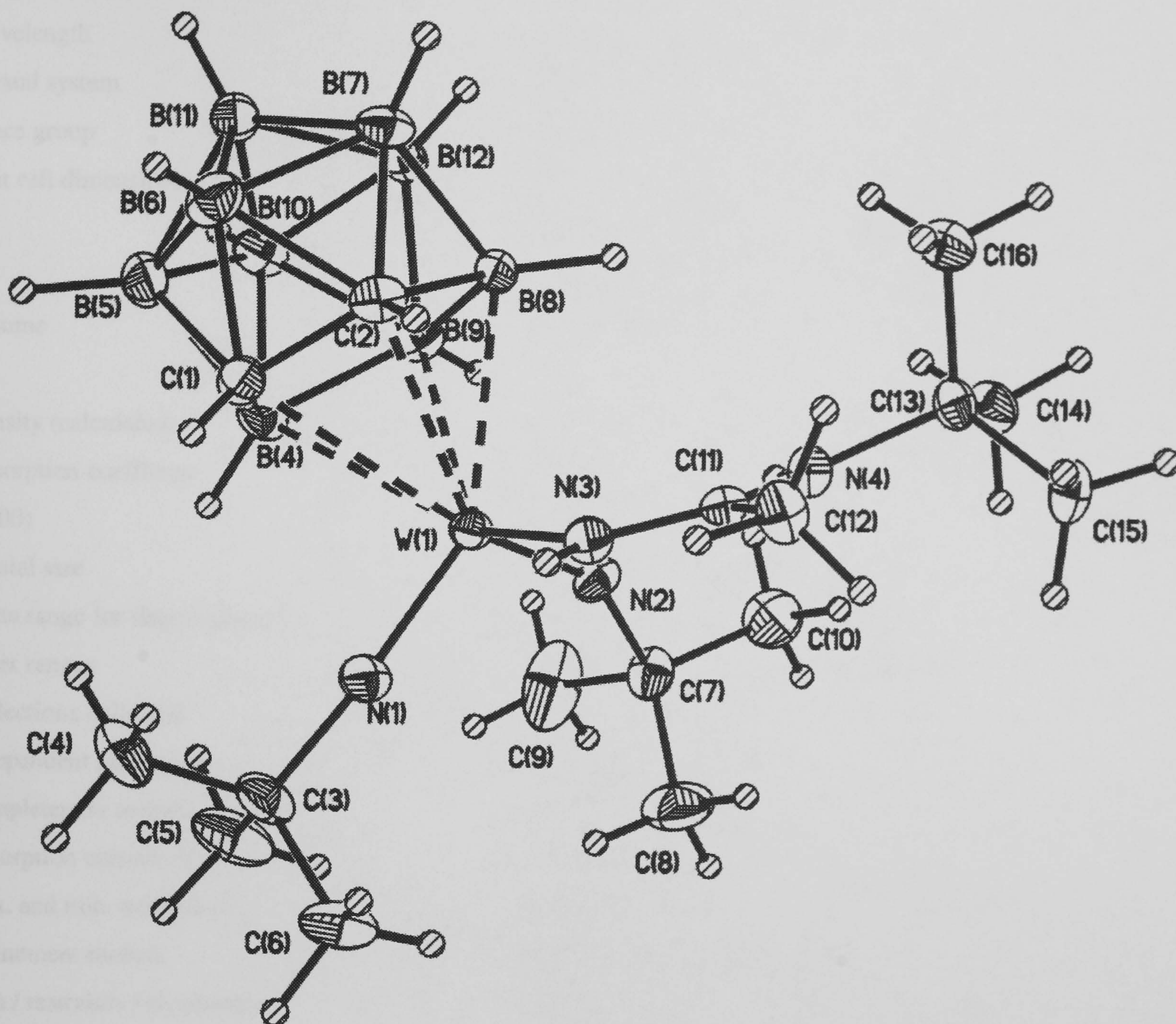
	U ¹¹	U ²²	U ³³	U ²³	U ¹³	U ¹²
W(1)	11(1)	15(1)	17(1)	1(1)	1(1)	0(1)
O(1)	17(1)	21(1)	18(1)	3(1)	3(1)	-1(1)
N(1)	16(1)	21(1)	24(1)	1(1)	4(1)	0(1)
N(2)	14(1)	22(1)	24(1)	-1(1)	1(1)	-1(1)
C(1)	13(1)	23(1)	23(1)	7(1)	1(1)	1(1)
C(2)	17(1)	13(1)	22(1)	0(1)	3(1)	1(1)
B(3)	17(1)	22(1)	19(1)	3(1)	0(1)	0(1)
B(4)	18(1)	15(1)	26(2)	3(1)	6(1)	1(1)
B(5)	18(1)	23(1)	22(2)	-2(1)	2(1)	-5(1)
B(6)	20(1)	18(1)	22(1)	2(1)	5(1)	2(1)
B(7)	18(1)	17(1)	26(2)	5(1)	6(1)	1(1)
B(8)	22(1)	21(2)	31(2)	-3(1)	7(1)	-7(1)
B(9)	15(1)	32(2)	27(2)	1(1)	1(1)	-5(1)
B(10)	17(1)	24(2)	28(2)	6(1)	5(1)	4(1)
B(11)	16(1)	23(1)	28(2)	2(1)	5(1)	-3(1)
C(11)	27(1)	29(2)	34(2)	-10(1)	3(1)	7(1)
C(12)	49(2)	52(2)	38(2)	-4(2)	18(2)	14(2)
C(13)	34(2)	29(2)	56(2)	-7(2)	1(2)	13(1)
C(14)	39(2)	41(2)	58(2)	-28(2)	-7(2)	10(2)
C(21)	12(1)	29(1)	30(1)	1(1)	-3(1)	0(1)
C(22)	22(2)	45(2)	49(2)	-15(2)	-10(1)	-2(1)
C(23)	25(2)	43(2)	46(2)	17(2)	-4(1)	4(1)
C(24)	15(1)	38(2)	44(2)	-1(1)	6(1)	-2(1)
C(31)	17(1)	19(1)	18(1)	5(1)	2(1)	3(1)
C(32)	22(1)	24(1)	20(1)	4(1)	-3(1)	3(1)
C(33)	30(1)	32(2)	17(1)	3(1)	-1(1)	4(1)
C(34)	25(1)	38(2)	22(1)	8(1)	7(1)	3(1)
C(35)	21(1)	27(1)	29(2)	8(1)	1(1)	-3(1)
C(36)	19(1)	21(1)	22(1)	4(1)	0(1)	0(1)
C(37)	29(1)	25(2)	26(2)	0(1)	2(1)	-8(1)
C(38)	31(2)	37(2)	23(2)	1(1)	-6(1)	-7(1)

Appendix A – Crystal Data

Table 5. Hydrogen coordinates ($\times 10^4$) and isotropic displacement parameters ($\text{\AA}^2 \times 10^{-3}$) for (33).

	x	y	z	U(eq)
H(2N)	7259(26)	8669(25)	7382(15)	25(8)
H(1)	4110(24)	8653(23)	6127(13)	20(7)
H(2)	4829(27)	9198(27)	7213(15)	33(8)
H(3)	6035(26)	7561(23)	7926(15)	29(8)
H(4)	5892(24)	5514(23)	6971(14)	23(7)
H(5)	4566(23)	6515(22)	5750(13)	18(7)
H(6)	3795(23)	8199(23)	8246(13)	19(7)
H(7)	4324(25)	5743(24)	8066(14)	28(8)
H(8)	3412(25)	5061(24)	6755(14)	26(8)
H(9)	2279(28)	7109(25)	6134(16)	37(9)
H(10)	2536(24)	8997(23)	7100(13)	21(7)
H(11)	1956(26)	6677(25)	7559(15)	32(8)
H(12A)	8905(34)	5771(32)	4757(19)	57(11)
H(12B)	9128(33)	6810(31)	5209(17)	46(10)
H(12C)	8009(34)	6865(33)	4749(19)	57(11)
H(13A)	8741(30)	4476(29)	5778(17)	43(9)
H(13B)	7991(30)	4829(28)	6397(17)	39(9)
H(13C)	9130(32)	5502(29)	6201(17)	45(10)
H(14A)	6949(29)	4555(28)	5021(16)	39(9)
H(14B)	6209(29)	5655(27)	4976(16)	36(9)
H(14C)	6105(36)	4883(32)	5631(20)	59(12)
H(22A)	10129(32)	8970(28)	7768(16)	46(10)
H(22B)	8840(31)	9137(28)	8027(18)	43(10)
H(22C)	9205(33)	9806(33)	7381(19)	56(11)
H(23A)	9738(33)	6846(29)	7719(17)	48(10)
H(23B)	8580(32)	6422(30)	7396(18)	45(10)
H(23C)	8443(33)	7087(29)	8039(18)	49(10)
H(24A)	10358(31)	7927(26)	6716(16)	36(9)
H(24B)	9521(30)	8702(30)	6340(17)	43(10)
H(24C)	9337(34)	7349(31)	6307(19)	55(11)
H(33)	6825(26)	8872(24)	3688(15)	27(8)
H(34)	8576(26)	9965(25)	3788(15)	29(8)
H(35)	9100(28)	10740(26)	4804(15)	33(8)
H(37A)	8881(32)	10898(29)	5969(17)	50(10)
H(37B)	7895(27)	10119(27)	6360(16)	36(9)
H(37C)	7535(31)	11291(30)	6035(17)	47(10)
H(38A)	4627(34)	8549(31)	4782(18)	52(11)
H(38B)	5361(39)	7420(38)	4775(22)	76(14)
H(38C)	5076(34)	8018(31)	4158(20)	57(11)

A16 Crystal data for $[3\text{-W}(\text{NC}_4\text{H}_9)_2(\text{N}(\text{H})\text{C}(\text{CH}_3)\text{NH}(\text{C}_4\text{H}_9)(1,2\text{-C}_2\text{B}_9\text{H}_{11}))]$; (35).



Appendix A – Crystal Data

Table 1. Crystal data and structure refinement for (35).

Identification code	00srv007	
Empirical formula	C16 H43 B9 N4 W	
Formula weight	572.68	
Temperature	120(2) K	
Wavelength	0.71073 Å	
Crystal system	Monoclinic	
Space group	P2(1)/c	
Unit cell dimensions	a = 17.825(3) Å	α= 90°.
	b = 10.920(2) Å	β= 95.333(4)°.
	c = 13.523(3) Å	γ= 90°.
Volume	2620.7(8) Å ³	
Z	4	
Density (calculated)	1.451 Mg/m ³	
Absorption coefficient	4.418 mm ⁻¹	
F(000)	1144	
Crystal size	0.24 x 0.09 x 0.05 mm ³	
Theta range for data collection	1.15 to 30.50°.	
Index ranges	-24<=h<=24, -15<=k<=13, -19<=l<=17	
Reflections collected	21485	
Independent reflections	7346 [R(int) = 0.0526]	
Completeness to theta = 30.50°	91.8 %	
Absorption correction	Integration	
Max. and min. transmission	0.803 and 0.475	
Refinement method	Full-matrix least-squares on F ²	
Data / restraints / parameters	7346 / 0 / 333	
Goodness-of-fit on F ²	0.980	
Final R indices [I>2sigma(I)]	R1 = 0.0311, wR2 = 0.0505	
R indices (all data)	R1 = 0.0616, wR2 = 0.0560	
Largest diff. peak and hole	0.774 and -0.851 e.Å ⁻³	

Appendix A – Crystal Data

Table 2. Atomic coordinates (x 10⁴) and equivalent isotropic displacement parameters (Å²x 10³) for (35). U(eq) is defined as one third of the trace of the orthogonalized U^{ij} tensor.

	x	y	z	U(eq)
W(1)	2750(1)	4198(1)	1657(1)	16(1)
N(1)	3597(2)	4300(3)	2419(2)	23(1)
N(2)	2754(2)	5378(3)	773(2)	21(1)
N(3)	2079(2)	5011(3)	2668(2)	19(1)
N(4)	1230(2)	6143(3)	1685(2)	19(1)
C(1)	2748(2)	1901(3)	2217(3)	24(1)
C(2)	1925(2)	2391(3)	2119(3)	21(1)
B(4)	3153(2)	2146(4)	1172(3)	24(1)
B(5)	2853(2)	637(4)	1528(4)	31(1)
B(6)	2053(2)	819(4)	2180(3)	29(1)
B(7)	1341(2)	1502(4)	1359(3)	24(1)
B(8)	1657(2)	2961(4)	996(3)	18(1)
B(9)	2434(2)	2760(4)	287(3)	21(1)
B(10)	2629(2)	1163(4)	299(3)	26(1)
B(11)	1940(2)	367(4)	932(3)	24(1)
B(12)	1683(2)	1676(4)	187(3)	20(1)
C(3)	4335(2)	4282(4)	2987(3)	29(1)
C(4)	4406(2)	3124(4)	3630(3)	39(1)
C(5)	4933(2)	4286(5)	2249(3)	44(1)
C(6)	4405(2)	5426(4)	3637(3)	39(1)
C(7)	3140(2)	6355(3)	271(3)	25(1)
C(8)	3453(2)	7272(4)	1039(3)	44(1)
C(9)	3763(3)	5759(5)	-261(4)	58(2)
C(10)	2584(2)	6979(4)	-489(3)	39(1)
C(11)	1473(2)	5708(3)	2568(2)	19(1)
C(12)	1086(2)	6027(3)	3468(2)	23(1)
C(13)	493(2)	6751(3)	1347(3)	20(1)
C(14)	570(2)	7144(3)	287(3)	26(1)
C(15)	345(2)	7898(3)	1950(3)	26(1)
C(16)	-145(2)	5816(4)	1368(3)	25(1)

Appendix A – Crystal Data

Table 3. Bond lengths [Å] and angles [°] for (35).

W(1)-N(1)	1.750(3)	B(5)-H(5)	1.16(3)	C(6)-H(6C)	0.9800
W(1)-N(2)	1.759(3)	B(6)-B(11)	1.751(6)	C(7)-C(8)	1.512(6)
W(1)-N(3)	2.094(3)	B(6)-B(7)	1.771(6)	C(7)-C(10)	1.521(5)
W(1)-B(9)	2.455(4)	B(6)-H(6)	1.06(3)	C(7)-C(9)	1.525(5)
W(1)-B(4)	2.461(4)	B(7)-B(12)	1.761(6)	C(8)-H(8A)	0.9800
W(1)-B(8)	2.469(4)	B(7)-B(11)	1.768(6)	C(8)-H(8B)	0.9800
W(1)-C(2)	2.573(3)	B(7)-B(8)	1.775(6)	C(8)-H(8C)	0.9800
W(1)-C(1)	2.620(4)	B(7)-H(7)	1.10(4)	C(9)-H(9A)	0.9800
N(1)-C(3)	1.461(4)	B(8)-B(9)	1.770(5)	C(9)-H(9B)	0.9800
N(2)-C(7)	1.469(4)	B(8)-B(12)	1.783(5)	C(9)-H(9C)	0.9800
N(3)-C(11)	1.318(4)	B(8)-H(8)	1.17(3)	C(10)-H(10A)	0.9800
N(3)-H(3N)	0.71(4)	B(9)-B(10)	1.778(6)	C(10)-H(10B)	0.9800
N(4)-C(11)	1.320(4)	B(9)-B(12)	1.782(6)	C(10)-H(10C)	0.9800
N(4)-C(13)	1.504(4)	B(9)-H(9)	1.16(3)	C(11)-C(12)	1.496(4)
N(4)-H(4N)	0.91(4)	B(10)-B(12)	1.770(6)	C(12)-H(12A)	0.9800
C(1)-C(2)	1.556(5)	B(10)-B(11)	1.787(6)	C(12)-H(12B)	0.9800
C(1)-B(4)	1.668(6)	B(10)-H(10)	1.18(4)	C(12)-H(12C)	0.9800
C(1)-B(5)	1.686(6)	B(11)-B(12)	1.785(6)	C(13)-C(14)	1.515(5)
C(1)-B(6)	1.709(6)	B(11)-H(11)	1.03(4)	C(13)-C(15)	1.530(5)
C(1)-H(1)	0.81(4)	B(12)-H(12)	1.10(3)	C(13)-C(16)	1.530(5)
C(2)-B(8)	1.669(5)	C(3)-C(6)	1.526(5)	C(14)-H(14A)	0.9800
C(2)-B(7)	1.698(5)	C(3)-C(5)	1.526(5)	C(14)-H(14B)	0.9800
C(2)-B(6)	1.733(6)	C(3)-C(4)	1.534(6)	C(14)-H(14C)	0.9800
C(2)-H(2)	0.99(3)	C(4)-H(4A)	0.9800	C(15)-H(15A)	0.9800
B(4)-B(10)	1.792(6)	C(4)-H(4B)	0.9800	C(15)-H(15B)	0.9800
B(4)-B(9)	1.801(6)	C(4)-H(4C)	0.9800	C(15)-H(15C)	0.9800
B(4)-B(5)	1.811(6)	C(5)-H(5A)	0.9800	C(16)-H(16A)	0.9800
B(4)-H(4)	1.11(3)	C(5)-H(5B)	0.9800	C(16)-H(16B)	0.9800
B(5)-B(6)	1.756(6)	C(5)-H(5C)	0.9800	C(16)-H(16C)	0.9800
B(5)-B(10)	1.768(7)	C(6)-H(6A)	0.9800		
B(5)-B(11)	1.772(6)	C(6)-H(6B)	0.9800		
N(1)-W(1)-N(2)	107.21(14)	C(2)-C(1)-B(6)	63.9(2)	B(9)-B(4)-H(4)	129.4(18)
N(1)-W(1)-N(3)	95.89(12)	B(4)-C(1)-B(6)	117.1(3)	B(5)-B(4)-H(4)	113.3(19)
N(2)-W(1)-N(3)	99.90(13)	B(5)-C(1)-B(6)	62.3(2)	W(1)-B(4)-H(4)	102.8(19)
N(1)-W(1)-B(9)	127.59(13)	C(2)-C(1)-W(1)	70.91(19)	C(1)-B(5)-B(6)	59.5(3)
N(2)-W(1)-B(9)	88.29(14)	B(4)-C(1)-W(1)	65.76(19)	C(1)-B(5)-B(10)	103.1(3)
N(3)-W(1)-B(9)	131.20(12)	B(5)-C(1)-W(1)	128.4(3)	B(6)-B(5)-B(10)	108.2(3)
N(1)-W(1)-B(4)	87.55(14)	B(6)-C(1)-W(1)	132.4(2)	C(1)-B(5)-B(11)	104.1(3)
N(2)-W(1)-B(4)	117.77(14)	C(2)-C(1)-H(1)	122(3)	B(6)-B(5)-B(11)	59.5(2)
N(3)-W(1)-B(4)	139.32(13)	B(4)-C(1)-H(1)	120(3)	B(10)-B(5)-B(11)	60.6(3)
B(9)-W(1)-B(4)	42.99(14)	B(5)-C(1)-H(1)	113(3)	C(1)-B(5)-B(4)	56.8(2)
N(1)-W(1)-B(8)	148.90(14)	B(6)-C(1)-H(1)	111(3)	B(6)-B(5)-B(4)	107.7(3)
N(2)-W(1)-B(8)	101.98(13)	W(1)-C(1)-H(1)	105(3)	B(10)-B(5)-B(4)	60.1(2)
N(3)-W(1)-B(8)	89.38(12)	C(1)-C(2)-B(8)	113.2(3)	B(11)-B(5)-B(4)	108.2(3)
B(9)-W(1)-B(8)	42.13(13)	C(1)-C(2)-B(7)	112.1(3)	C(1)-B(5)-H(5)	119.4(17)
B(4)-W(1)-B(8)	69.23(13)	B(8)-C(2)-B(7)	63.6(2)	B(6)-B(5)-H(5)	114.9(17)
N(1)-W(1)-C(2)	112.79(13)	C(1)-C(2)-B(6)	62.4(2)	B(10)-B(5)-H(5)	130.3(17)
N(2)-W(1)-C(2)	139.96(12)	B(8)-C(2)-B(6)	116.0(3)	B(11)-B(5)-H(5)	124.5(17)
N(3)-W(1)-C(2)	78.07(11)	B(7)-C(2)-B(6)	62.2(2)	B(4)-B(5)-H(5)	123.6(17)
B(9)-W(1)-C(2)	66.17(12)	C(1)-C(2)-W(1)	74.24(18)	C(1)-B(6)-C(2)	53.7(2)
B(4)-W(1)-C(2)	63.50(13)	B(8)-C(2)-W(1)	67.34(18)	C(1)-B(6)-B(11)	104.0(3)
B(8)-W(1)-C(2)	38.59(12)	B(7)-C(2)-W(1)	128.6(2)	C(2)-B(6)-B(11)	103.3(3)
N(1)-W(1)-C(1)	85.13(13)	B(6)-C(2)-W(1)	134.1(2)	C(1)-B(6)-B(5)	58.2(2)
N(2)-W(1)-C(1)	153.90(13)	C(1)-C(2)-H(2)	118.5(18)	C(2)-B(6)-B(5)	101.4(3)
N(3)-W(1)-C(1)	101.60(12)	B(8)-C(2)-H(2)	119.1(18)	B(11)-B(6)-B(5)	60.7(3)
B(9)-W(1)-C(1)	66.38(13)	B(7)-C(2)-H(2)	118.5(17)	C(1)-B(6)-B(7)	101.7(3)
B(4)-W(1)-C(1)	38.15(13)	B(6)-C(2)-H(2)	115.1(18)	C(2)-B(6)-B(7)	57.9(2)
B(8)-W(1)-C(1)	63.80(12)	W(1)-C(2)-H(2)	97.8(17)	B(11)-B(6)-B(7)	60.2(2)
C(2)-W(1)-C(1)	34.85(11)	C(1)-B(4)-B(10)	102.8(3)	B(5)-B(6)-B(7)	107.5(3)
C(3)-N(1)-W(1)	173.8(3)	C(1)-B(4)-B(9)	106.6(3)	C(1)-B(6)-H(6)	119.2(19)
C(7)-N(2)-W(1)	151.4(3)	B(10)-B(4)-B(9)	59.3(2)	C(2)-B(6)-H(6)	117.3(19)
C(11)-N(3)-W(1)	133.6(3)	C(1)-B(4)-B(5)	57.8(2)	B(11)-B(6)-H(6)	132.5(19)
C(11)-N(3)-H(3N)	112(3)	B(10)-B(4)-B(5)	58.8(3)	B(5)-B(6)-H(6)	127.2(18)
W(1)-N(3)-H(3N)	114(3)	B(9)-B(4)-B(5)	107.8(3)	B(7)-B(6)-H(6)	122.9(19)
C(11)-N(4)-C(13)	129.7(3)	C(1)-B(4)-W(1)	76.09(19)	C(2)-B(7)-B(12)	103.8(3)
C(11)-N(4)-H(4N)	119(2)	B(10)-B(4)-W(1)	125.0(2)	C(2)-B(7)-B(11)	104.1(3)
C(13)-N(4)-H(4N)	111(2)	B(9)-B(4)-W(1)	68.31(18)	B(12)-B(7)-B(11)	60.7(2)
C(2)-C(1)-B(4)	110.6(3)	B(5)-B(4)-W(1)	131.0(3)	C(2)-B(7)-B(6)	59.9(2)
C(2)-C(1)-B(5)	112.7(3)	C(1)-B(4)-H(4)	119.8(18)	B(12)-B(7)-B(6)	108.7(3)
B(4)-C(1)-B(5)	65.4(3)	B(10)-B(4)-H(4)	122.4(18)	B(11)-B(7)-B(6)	59.3(2)

Appendix A – Crystal Data

C(2)-B(7)-B(8)	57.4(2)	B(6)-B(11)-B(5)	59.8(3)	C(8)-C(7)-C(10)	110.0(3)
B(12)-B(7)-B(8)	60.6(2)	B(7)-B(11)-B(5)	107.0(3)	N(2)-C(7)-C(9)	107.5(3)
B(11)-B(7)-B(8)	108.8(3)	B(6)-B(11)-B(12)	108.6(3)	C(8)-C(7)-C(9)	111.6(4)
B(6)-B(7)-B(8)	108.9(3)	B(7)-B(11)-B(12)	59.4(2)	C(10)-C(7)-C(9)	109.3(4)
C(2)-B(7)-H(7)	118(2)	B(5)-B(11)-B(12)	107.5(3)	C(7)-C(8)-H(8A)	109.5
B(12)-B(7)-H(7)	131(2)	B(6)-B(11)-B(10)	107.6(3)	C(7)-C(8)-H(8B)	109.5
B(11)-B(7)-H(7)	126(2)	B(7)-B(11)-B(10)	106.2(3)	H(8A)-C(8)-H(8B)	109.5
B(6)-B(7)-H(7)	114(2)	B(5)-B(11)-B(10)	59.6(3)	C(7)-C(8)-H(8C)	109.5
B(8)-B(7)-H(7)	122(2)	B(12)-B(11)-B(10)	59.4(2)	H(8A)-C(8)-H(8C)	109.5
C(2)-B(8)-B(9)	106.0(3)	B(6)-B(11)-H(11)	125(2)	H(8B)-C(8)-H(8C)	109.5
C(2)-B(8)-B(7)	59.0(2)	B(7)-B(11)-H(11)	125(2)	C(7)-C(9)-H(9A)	109.5
B(9)-B(8)-B(7)	108.9(3)	B(5)-B(11)-H(11)	122(2)	C(7)-C(9)-H(9B)	109.5
C(2)-B(8)-B(12)	104.1(3)	B(12)-B(11)-H(11)	120(2)	H(9A)-C(9)-H(9B)	109.5
B(9)-B(8)-B(12)	60.2(2)	B(10)-B(11)-H(11)	119(2)	C(7)-C(9)-H(9C)	109.5
B(7)-B(8)-B(12)	59.3(2)	B(7)-B(12)-B(10)	107.2(3)	H(9A)-C(9)-H(9C)	109.5
C(2)-B(8)-W(1)	74.08(18)	B(7)-B(12)-B(9)	108.9(3)	H(9B)-C(9)-H(9C)	109.5
B(9)-B(8)-W(1)	68.51(18)	B(10)-B(12)-B(9)	60.1(2)	C(7)-C(10)-H(10A)	109.5
B(7)-B(8)-W(1)	130.7(2)	B(7)-B(12)-B(8)	60.1(2)	C(7)-C(10)-H(10B)	109.5
B(12)-B(8)-W(1)	126.0(2)	B(10)-B(12)-B(8)	106.0(3)	H(10A)-C(10)-H(10B)	109.5
C(2)-B(8)-H(8)	117.9(17)	B(9)-B(12)-B(8)	59.5(2)	C(7)-C(10)-H(10C)	109.5
B(9)-B(8)-H(8)	130.7(17)	B(7)-B(12)-B(11)	59.8(2)	H(10A)-C(10)-H(10C)	109.5
B(7)-B(8)-H(8)	112.3(17)	B(10)-B(12)-B(11)	60.4(2)	H(10B)-C(10)-H(10C)	109.5
B(12)-B(8)-H(8)	123.3(17)	B(9)-B(12)-B(11)	109.8(3)	N(3)-C(11)-N(4)	119.9(3)
W(1)-B(8)-H(8)	102.0(17)	B(8)-B(12)-B(11)	107.7(3)	N(3)-C(11)-C(12)	119.1(3)
B(8)-B(9)-B(10)	106.2(3)	B(7)-B(12)-H(12)	119.1(18)	N(4)-C(11)-C(12)	121.0(3)
B(8)-B(9)-B(12)	60.3(2)	B(10)-B(12)-H(12)	127.6(18)	C(11)-C(12)-H(12A)	109.5
B(10)-B(9)-B(12)	59.6(2)	B(9)-B(12)-H(12)	119.5(18)	C(11)-C(12)-H(12B)	109.5
B(8)-B(9)-B(4)	103.3(3)	B(8)-B(12)-H(12)	117.3(18)	H(12A)-C(12)-H(12B)	109.5
B(10)-B(9)-B(4)	60.1(2)	B(11)-B(12)-H(12)	124.9(18)	C(11)-C(12)-H(12C)	109.5
B(12)-B(9)-B(4)	106.6(3)	N(1)-C(3)-C(6)	108.3(3)	H(12A)-C(12)-H(12C)	109.5
B(8)-B(9)-W(1)	69.36(18)	N(1)-C(3)-C(5)	107.9(3)	H(12B)-C(12)-H(12C)	109.5
B(10)-B(9)-W(1)	126.1(3)	C(6)-C(3)-C(5)	110.5(3)	N(4)-C(13)-C(14)	105.0(3)
B(12)-B(9)-W(1)	126.9(2)	N(1)-C(3)-C(4)	109.4(3)	N(4)-C(13)-C(15)	112.8(3)
B(4)-B(9)-W(1)	68.71(18)	C(6)-C(3)-C(4)	110.5(3)	C(14)-C(13)-C(15)	107.9(3)
B(8)-B(9)-H(9)	125.3(16)	C(5)-C(3)-C(4)	110.3(3)	N(4)-C(13)-C(16)	109.2(3)
B(10)-B(9)-H(9)	119.1(16)	C(3)-C(4)-H(4A)	109.5	C(14)-C(13)-C(16)	109.9(3)
B(12)-B(9)-H(9)	119.0(16)	C(3)-C(4)-H(4B)	109.5	C(15)-C(13)-C(16)	111.8(3)
B(4)-B(9)-H(9)	124.6(16)	H(4A)-C(4)-H(4B)	109.5	C(13)-C(14)-H(14A)	109.5
W(1)-B(9)-H(9)	102.7(16)	C(3)-C(4)-H(4C)	109.5	C(13)-C(14)-H(14B)	109.5
B(5)-B(10)-B(12)	108.3(3)	H(4A)-C(4)-H(4C)	109.5	H(14A)-C(14)-H(14B)	109.5
B(5)-B(10)-B(9)	110.8(3)	H(4B)-C(4)-H(4C)	109.5	C(13)-C(14)-H(14C)	109.5
B(12)-B(10)-B(9)	60.3(2)	C(3)-C(5)-H(5A)	109.5	H(14A)-C(14)-H(14C)	109.5
B(5)-B(10)-B(11)	59.8(2)	C(3)-C(5)-H(5B)	109.5	H(14B)-C(14)-H(14C)	109.5
B(12)-B(10)-B(11)	60.2(2)	H(5A)-C(5)-H(5B)	109.5	C(13)-C(15)-H(15A)	109.5
B(9)-B(10)-B(11)	109.8(3)	C(3)-C(5)-H(5C)	109.5	C(13)-C(15)-H(15B)	109.5
B(5)-B(10)-B(4)	61.2(2)	H(5A)-C(5)-H(5C)	109.5	H(15A)-C(15)-H(15B)	109.5
B(12)-B(10)-B(4)	107.6(3)	H(5B)-C(5)-H(5C)	109.5	C(13)-C(15)-H(15C)	109.5
B(9)-B(10)-B(4)	60.6(2)	C(3)-C(6)-H(6A)	109.5	H(15A)-C(15)-H(15C)	109.5
B(11)-B(10)-B(4)	108.4(3)	C(3)-C(6)-H(6B)	109.5	H(15B)-C(15)-H(15C)	109.5
B(5)-B(10)-H(10)	120.0(18)	H(6A)-C(6)-H(6B)	109.5	C(13)-C(16)-H(16A)	109.5
B(12)-B(10)-H(10)	119.9(18)	C(3)-C(6)-H(6C)	109.5	C(13)-C(16)-H(16B)	109.5
B(9)-B(10)-H(10)	122.9(18)	H(6A)-C(6)-H(6C)	109.5	H(16A)-C(16)-H(16B)	109.5
B(11)-B(10)-H(10)	117.0(18)	H(6B)-C(6)-H(6C)	109.5	C(13)-C(16)-H(16C)	109.5
B(4)-B(10)-H(10)	125.7(18)	N(2)-C(7)-C(8)	108.8(3)	H(16A)-C(16)-H(16C)	109.5
B(6)-B(11)-B(7)	60.4(3)	N(2)-C(7)-C(10)	109.5(3)	H(16B)-C(16)-H(16C)	109.5

Table 4. Anisotropic displacement parameters ($\text{\AA}^2 \times 10^3$) for (35). The anisotropic

Appendix A – Crystal Data

displacement factor exponent takes the form: $-2\pi^2[h^2 a^{*2}U^{11} + \dots + 2 h k a^* b^* U^{12}]$

	U ¹¹	U ²²	U ³³	U ²³	U ¹³	U ¹²
W(1)	14(1)	17(1)	18(1)	-3(1)	2(1)	-1(1)
N(1)	16(1)	25(2)	28(2)	-6(1)	6(1)	0(1)
N(2)	24(2)	16(2)	25(2)	-4(1)	7(1)	-2(1)
N(3)	20(2)	20(2)	16(2)	-2(1)	2(1)	0(1)
N(4)	21(2)	21(2)	16(2)	1(1)	3(1)	3(1)
C(1)	33(2)	19(2)	19(2)	0(2)	-11(2)	-1(2)
C(2)	24(2)	23(2)	18(2)	-4(2)	6(1)	-5(2)
B(4)	16(2)	27(2)	29(2)	-10(2)	1(2)	3(2)
B(5)	32(2)	23(2)	35(3)	-5(2)	-11(2)	5(2)
B(6)	39(2)	23(2)	23(2)	1(2)	-3(2)	-4(2)
B(7)	21(2)	26(2)	23(2)	-7(2)	0(2)	-6(2)
B(8)	18(2)	18(2)	18(2)	-1(2)	-1(2)	0(2)
B(9)	26(2)	21(2)	17(2)	-2(2)	2(2)	-3(2)
B(10)	21(2)	30(2)	29(2)	-14(2)	2(2)	1(2)
B(11)	27(2)	20(2)	24(2)	-5(2)	-6(2)	1(2)
B(12)	21(2)	21(2)	17(2)	-5(2)	-3(2)	1(2)
C(3)	15(2)	39(2)	33(2)	-6(2)	-1(1)	2(2)
C(4)	23(2)	45(3)	46(3)	2(2)	-6(2)	8(2)
C(5)	17(2)	73(3)	42(3)	-10(3)	7(2)	-9(2)
C(6)	36(2)	47(3)	33(2)	-11(2)	-7(2)	-12(2)
C(7)	26(2)	23(2)	28(2)	5(2)	9(2)	0(2)
C(8)	45(3)	36(3)	51(3)	3(2)	0(2)	-21(2)
C(9)	56(3)	46(3)	79(4)	20(3)	49(3)	15(3)
C(10)	40(2)	36(3)	41(3)	11(2)	6(2)	-6(2)
C(11)	19(2)	16(2)	21(2)	-3(2)	-1(1)	-4(1)
C(12)	26(2)	30(2)	15(2)	-3(2)	3(1)	7(2)
C(13)	21(2)	21(2)	18(2)	4(1)	-1(1)	3(1)
C(14)	25(2)	30(2)	22(2)	6(2)	-2(2)	0(2)
C(15)	32(2)	20(2)	26(2)	5(2)	2(2)	9(2)
C(16)	23(2)	30(2)	22(2)	1(2)	0(1)	-3(2)

Appendix A – Crystal Data

Table 5. Hydrogen coordinates ($\times 10^4$) and isotropic displacement parameters ($\text{\AA}^2 \times 10^{-3}$) for (35).

	x	y	z	U(eq)
H(3N)	2180(20)	4840(30)	3170(30)	16(11)
H(4N)	1500(20)	6000(30)	1160(30)	29(11)
H(1)	3000(20)	1880(40)	2750(30)	35(12)
H(2)	1725(16)	2770(30)	2710(20)	7(8)
H(4)	3777(19)	2240(30)	1200(30)	26(10)
H(5)	3266(19)	-130(30)	1830(30)	18(9)
H(6)	1939(18)	370(30)	2850(30)	19(9)
H(7)	770(20)	1350(40)	1570(30)	37(11)
H(8)	1175(19)	3690(30)	930(30)	20(9)
H(9)	2549(17)	3330(30)	-400(20)	12(8)
H(10)	2870(20)	650(30)	-370(30)	32(11)
H(11)	1770(20)	-490(40)	690(30)	35(11)
H(12)	1283(18)	1670(30)	-480(30)	19(9)
H(4A)	3994	3100	4062	58
H(4B)	4890	3133	4038	58
H(4C)	4379	2399	3201	58
H(5A)	4899	5050	1867	66
H(5B)	4851	3589	1796	66
H(5C)	5434	4223	2611	66
H(6A)	4314	6155	3220	59
H(6B)	4913	5466	3982	59
H(6C)	4033	5392	4126	59
H(8A)	3038	7641	1362	67
H(8B)	3726	7914	714	67
H(8C)	3797	6857	1538	67
H(9A)	4139	5399	230	87
H(9B)	4005	6379	-648	87
H(9C)	3547	5116	-706	87
H(10A)	2181	7359	-149	58
H(10B)	2366	6370	-965	58
H(10C)	2846	7609	-842	58
H(12A)	1337	5609	4049	35
H(12B)	558	5768	3371	35
H(12C)	1110	6915	3575	35
H(14A)	704	6434	-103	39
H(14B)	966	7767	281	39
H(14C)	91	7487	-3	39
H(15A)	812	8371	2069	39
H(15B)	168	7657	2586	39
H(15C)	-41	8401	1579	39
H(16A)	-24	5086	992	38
H(16B)	-616	6176	1069	38
H(16C)	-203	5586	2058	38

Table 6. Hydrogen bonds for (35) [\AA and $^\circ$].

D-H...A	d(D-H)	d(H...A)	d(D...A)	$\angle(\text{DHA})$
N(4)-H(4N)...N(2)	0.91(4)	2.43(4)	3.199(4)	142(3)

Appendix B

Courses, Lectures, Colloquia and Conferences Attended

B1 FIRST YEAR INTRODUCTION COURSES: OCTOBER 1996

The courses consist of one hour lectures on the services available in the department.

1. Department Safety
2. Safety Matters
3. Electrical appliances and Infrared Spectroscopy
4. Chromatography and Microanalysis
5. Atomic Absorption and Inorganic Analysis
6. Library Facilities
7. Mass Spectroscopy
8. Nuclear Magnetic Resonance
9. Glass Blowing Techniques
10. Introduction to Computing Facilities

B2 EXAMINED LECTURE COURSES: OCTOBER 1996 TO APRIL 1997

Three courses were attended consisting of one hour lectures followed by a written examination in each.

1. “Diffraction and Scattering Methods”, Dr C. Lehmann (6 hours)
2. “NMR Techniques”, Dr. A. Kenwright (6 hours)
3. “Molecular Modelling”, Dr. C. Lehmann (6 hours)

**B3 RESEARCH COLLOQUIA, SEMINARS AND LECTURES ORGANISED BY THE
DEPARTMENT OF CHEMISTRY**

Only lectures attended by the author are shown

During the Period 1996 - 1997 (August 1 - July 31)

- October 9 Professor G. Bowmaker, University Auckland, NZ
Coordination and Materials Chemistry of the Group 11 and Group 12 Metals:
Some Recent Vibrational and Solid State NMR Studies
- October 22 Professor Lutz Gade, Univ. Wurzburg, Germany
Organic Transformations with Early-Late Heterobimetallics: Synergism and
Selectivity
- October 22 Professor B. J. Tighe, Department of Molecular Sciences and Chemistry,
University of Aston
Making Polymers for Biomedical Application - can we meet Nature's
Challenge?
- October 23 Professor H. Ringsdorf (Perkin Centenary Lecture), Johannes Gutenberg-
Universitat, Mainz,
Germany
Function Based on Organisation
- October 29 Professor D. M. Knight, Department of Philosophy, University of Durham.
The Purpose of Experiment - A Look at Davy and Faraday
- October 30 Dr Phillip Mountford, Nottingham University
Recent Developments in Group IV Imido Chemistry
- November 12 Professor R. J. Young, Manchester Materials Centre, UMIST
New Materials - Fact or Fantasy?

Appendix B – Courses, Lectures, Colloquia and Conferences Attended

November 13 Dr G. Resnati, Milan

Perfluorinated Oxaziridines: Mild Yet Powerful Oxidising Agents

November 18 Professor G. A. Olah, University of Southern California, USA

Crossing Conventional Lines in my Chemistry of the Elements

November 19 Professor R. E. Grigg, University of Leeds

Assembly of Complex Molecules by Palladium-Catalysed Queueing Processes

November 27 Dr Richard Templer, Imperial College, London

Molecular Tubes and Sponges

December 3 Professor D. Phillips, Imperial College, London

"A Little Light Relief"

December 11 Dr Chris Richards, Cardiff University

Stereochemical Games with Metallocenes

January 15 Dr V. K. Aggarwal, University of Sheffield

Sulfur Mediated Asymmetric Synthesis

January 16 Dr Sally Brooker, University of Otago, NZ

Macrocycles: Exciting yet Controlled Thiolate Coordination Chemistry

January 22 Dr Neil Cooley, BP Chemicals, Sunbury

Synthesis and Properties of Alternating Polyketones

February 4 Dr A. J. Banister, University of Durham

From Runways to Non-metallic Metals - A New Chemistry Based on Sulphur

February 5 Dr A. Haynes, University of Sheffield

Mechanism in Homogeneous Catalytic Carbonylation

February 18 Professor Sir James Black, Foundation/King's College London

My Dialogues with Medicinal Chemists

Appendix B – Courses, Lectures, Colloquia and Conferences Attended

- February 19 Professor Brian Hayden, University of Southampton
The Dynamics of Dissociation at Surfaces and Fuel Cell Catalysts
- February 25 Professor A. G. Sykes, University of Newcastle
The Synthesis, Structures and Properties of Blue Copper Proteins
- February 26 Dr Tony Ryan, UMIST
Making Hairpins from Rings and Chains
- March 4 Professor C. W. Rees, Imperial College
Some Very Heterocyclic Chemistry
- March 19 Dr Katharine Reid, University of Nottingham
Probing Dynamical Processes with Photoelectrons

1997 - 1998 (August 1 - July 31)

- October 15 Dr R. M. Ormerod, Department of Chemistry, Keele University
Studying Catalysts in Action
- October 21 Professor A. F. Johnson, IRC, Leeds
Reactive Processing of Polymers: Science and Technology
- October 22 Professor R. J. Puddephatt (RSC Endowed Lecture), University of Western
Ontario
Organoplatinum Chemistry and Catalysis
- October 23 Professor M. R. Bryce, University of Durham, Inaugural Lecture
New Tetrathiafulvalene Derivatives in Molecular, Supramolecular and
Macromolecular Chemistry: Controlling the Electronic Properties of Organic
Solids
- November 5 Dr M. Hii, Oxford University
Studies of the Heck reaction

Appendix B – Courses, Lectures, Colloquia and Conferences Attended

- November 11 Professor V. Gibson, Imperial College, London
Metallocene Polymerisation
- November 19 Dr G. Morris, Department of Chemistry, Manchester Univ.
Pulsed Field Gradient NMR Techniques: Good News for the Lazy and DOSY
- November 20 Dr L. Spiccia, Monash University, Melbourne, Australia
Polynuclear Metal Complexes
- November 26 Professor R. W. Richards, University of Durham, Inaugural Lecture
A Random Walk in Polymer Science
- December 2 Dr C. J. Ludman, University of Durham
Explosions
- October 27 Professor W. Roper FRS. University of Auckland, New Zealand
Boryl Complexes of Ruthenium and Osmium
- January 20 Professor J. Brooke, University of Lancaster
What's in a Formula?: Some Chemical Controversies of the 19th Century
- January 21 Professor D. Cardin, University of Reading
Sterically Encumbered Tin Clusters
- January 27 Professor R. Jordan, Dept. of Chemistry, Univ. of Iowa, USA.
Cationic Transition Metal and Main Group Metal Alkyl Complexes in Olefin
Polymerisation
- February 3 Dr J. Beacham, ICI Technology
The Chemical Industry in the 21st Century
- February 4 Professor P. Fowler, Department of Chemistry, Exeter University
Classical and Non-Classical Fullerenes

Appendix B – Courses, Lectures, Colloquia and Conferences Attended

February 25 Dr C. Jones, Swansea University

Low Coordination Arsenic and Antimony Chemistry

March 18 Dr J. S. O. Evans, Oxford University

Materials which Contract on Heating (from Shrinking Ceramics to Bullet Proof Vests)

1998 - 1999 (August 1 - July 31)

October 9 Professor M. F. Hawthorne, Department Chemistry & Biochemistry, UCLA, USA

Camouflaged Boranes and Carboranes

October 26 Dr W. Peirs, University of Calgary, Alberta, Canada

Reactions of the Highly Electrophilic Boranes $\text{HB}(\text{C}_6\text{F}_5)_2$ and $\text{B}(\text{C}_6\text{F}_5)_3$ with Zirconium and Tantalum Based Metallocenes

November 4 Dr N. Kaltsoyannis, Department of Chemistry, UCL, London

Computational Adventures in d & f Element Chemistry

November 10 Dr J. S. O. Evans, Chemistry Department, University of Durham

Shrinking Materials

November 12 Professor S. Loeb, University of Windsor, Ontario, Canada

From Macrocycles to Metallo-Supramolecular Chemistry

November 24 Dr B. G. Davis, Department of Chemistry, University of Durham

Sugars and Enzymes

December 1 Professor N. Billingham, University of Sussex

Plastics in the Environment - Boon or Bane

(In association with The North-East Polymer Association)

Appendix B – Courses, Lectures, Colloquia and Conferences Attended

- February 9 Professor D. J. Cole-Hamilton, St. Andrews University
Chemistry and the Future of Life on Earth
- February 10 Dr C. Bain, University of Oxford
Surfactant Adsorption and Marangoni Flow at Expanding Liquid Surfaces
- May 12 Dr Duncan Bruce, Exeter University
The Synthesis and Characterisation of Liquid-Crystalline Transition Metal
Complexes

B4 CONFERENCES AND SYMPOSIA ATTENDED

Posters[†] and papers[‡] presented

‡“Intraboron 17”, Fimbush Point Field Centre, University Of Edinburgh, 1st-3rd September, 1997.

†“Anglo German Conference on Inorganic and Organometallic Chemistry”, Marburg University, Marburg, Germany, 14st–17th September, 1997.

†“The Chemistry of Group 13, 14, and 15 Discussion Group” King’s College, Kensington Campus, London. 17th April, 1998.

‡“Intraboron 18”, University of Bangor, Bangor, September, 1998.

†“Organometallic Chemistry in the South Pacific”, University of Auckland, Auckland, New Zealand, 24th-28th January, 1999.

‡“Inorganic Chemistry ‘99”, Victoria University, Wellington, New Zealand, 31st January-4th February, 1999.

“The Seventh BCA Intensive Teaching School in X-ray Structure Analysis”, University of Durham, Durham, 7th-15th April, 1999.

†“Tenth International Conference On Boron Chemistry”, University of Durham, Durham, 11th-15th July, 1999.

*“Ladies and Gentlemen,
Elvis has left the building”*

